

METHODS IN MOLECULAR BIOLOGY™

Volume 380

# Immunological Tolerance

*Methods and Protocols*

*Edited by*

**Paul J. Fairchild**

 HUMANA PRESS

# **Immunological Tolerance**

# METHODS IN MOLECULAR BIOLOGY™

*John M. Walker, SERIES EDITOR*

422. **Phylogenomics**, edited by *William J. Murphy, 2008*
421. **Affinity Chromatography: Methods and Protocols**, *Second Edition*, edited by *Michael Zachariou, 2008*
420. **Drosophila: Methods and Protocols**, edited by *Christian Dahmann, 2008*
419. **Post-Transcriptional Gene Regulation**, edited by *Jeffrey Wilusz, 2008*
418. **Avidin-Biotin Interactions: Methods and Applications**, edited by *Robert J. McMahon, 2008*
417. **Tissue Engineering, Second Edition**, edited by *Hansjörg Hauser and Martin Fussenegger, 2007*
416. **Gene Essentiality: Protocols and Bioinformatics**, edited by *Andrei L. Osterman, 2008*
415. **Innate Immunity**, edited by *Jonathan Ewbank and Eric Vivier, 2007*
414. **Apoptosis in Cancer: Methods and Protocols**, edited by *Gil Mor and Ayesha Alvero, 2008*
413. **Protein Structure Prediction, Second Edition**, edited by *Mohammed Zaki and Chris Bystroff, 2008*
412. **Neutrophil Methods and Protocols**, edited by *Mark T. Quinn, Frank R. DeLeo, and Gary M. Bokoch, 2007*
411. **Reporter Genes for Mammalian Systems**, edited by *Don Anson, 2007*
410. **Environmental Genomics**, edited by *Cristofre C. Martin, 2007*
409. **Immunoinformatics: Predicting Immunogenicity In Silico**, edited by *Darren R. Flower, 2007*
408. **Gene Function Analysis**, edited by *Michael Ochs, 2007*
407. **Stem Cell Assays**, edited by *Vemuri C. Mohan, 2007*
406. **Plant Bioinformatics: Methods and Protocols**, edited by *David Edwards, 2007*
405. **Telomerase Inhibition: Strategies and Protocols**, edited by *Lucy Andrews and Trygve O. Tollefsbol, 2007*
404. **Topics in Biostatistics**, edited by *Walter T. Ambrosius, 2007*
403. **Patch-Clamp Methods and Protocols**, edited by *Peter Molnar and James J. Hickman, 2007*
402. **PCR Primer Design**, edited by *Anton Yuryev, 2007*
401. **Neuroinformatics**, edited by *Chiquito J. Crasto, 2007*
400. **Methods in Lipid Membranes**, edited by *Alex Dopico, 2007*
399. **Neuroprotection Methods and Protocols**, edited by *Tiziana Borsello, 2007*
398. **Lipid Rafts**, edited by *Thomas J. McIntosh, 2007*
397. **Hedgehog Signaling Protocols**, edited by *Jamila I. Horabin, 2007*
396. **Comparative Genomics, Volume 2**, edited by *Nicholas H. Bergman, 2007*
395. **Comparative Genomics, Volume 1**, edited by *Nicholas H. Bergman, 2007*
394. **Salmonella: Methods and Protocols**, edited by *Heide Schatten and Abe Eisenstark, 2007*
393. **Plant Secondary Metabolites**, edited by *Harinder P. S. Makkar, P. Siddhuraju, and Klaus Becker, 2007*
392. **Molecular Motors: Methods and Protocols**, edited by *Ann O. Sperry, 2007*
391. **MRSA Protocols**, edited by *Yinduo Ji, 2007*
390. **Protein Targeting Protocols, Second Edition**, edited by *Mark van der Giezen, 2007*
389. **Pichia Protocols, Second Edition**, edited by *James M. Cregg, 2007*
388. **Baculovirus and Insect Cell Expression Protocols, Second Edition**, edited by *David W. Murhammer, 2007*
387. **Serial Analysis of Gene Expression (SAGE): Digital Gene Expression Profiling**, edited by *Kare Lehmann Nielsen, 2007*
386. **Peptide Characterization and Application Protocols**, edited by *Gregg B. Fields, 2007*
385. **Microchip-Based Assay Systems: Methods and Applications**, edited by *Pierre N. Floriano, 2007*
384. **Capillary Electrophoresis: Methods and Protocols**, edited by *Philippe Schmitt-Kopplin, 2007*
383. **Cancer Genomics and Proteomics: Methods and Protocols**, edited by *Paul B. Fisher, 2007*
382. **Microarrays, Second Edition: Volume 2, Applications and Data Analysis**, edited by *Jang B. Rampal, 2007*
381. **Microarrays, Second Edition: Volume 1, Synthesis Methods**, edited by *Jang B. Rampal, 2007*
380. **Immunological Tolerance: Methods and Protocols**, edited by *Paul J. Fairchild, 2007*
379. **Glycoviroplogy Protocols**, edited by *Richard J. Sugrue, 2007*
378. **Monoclonal Antibodies: Methods and Protocols**, edited by *Maher Albitar, 2007*
377. **Microarray Data Analysis: Methods and Applications**, edited by *Michael J. Korenberg, 2007*
376. **Linkage Disequilibrium and Association Mapping: Analysis and Application**, edited by *Andrew R. Collins, 2007*
375. **In Vitro Transcription and Translation Protocols: Second Edition**, edited by *Guido Grandi, 2007*
374. **Quantum Dots: Applications in Biology**, edited by *Marcel Bruchez and Charles Z. Hotz, 2007*
373. **Pyrosequencing® Protocols**, edited by *Sharon Marsh, 2007*
372. **Mitochondria: Practical Protocols**, edited by *Dario Leister and Johannes Herrmann, 2007*
371. **Biological Aging: Methods and Protocols**, edited by *Trygve O. Tollefsbol, 2007*

METHODS IN MOLECULAR BIOLOGY™

# Immunological Tolerance

*Methods and Protocols*

Edited by

**Paul J. Fairchild**

*Sir William Dunn School of Pathology, University of Oxford  
Oxford, UK*

HUMANA PRESS  TOTOWA, NEW JERSEY




© 2007 Humana Press Inc.  
999 Riverview Drive, Suite 208  
Totowa, New Jersey 07512

**www.humanapress.com**

All rights reserved. No part of this book may be reproduced, stored in a retrieval system, or transmitted in any form or by any means, electronic, mechanical, photocopying, microfilming, recording, or otherwise without written permission from the Publisher. Methods in Molecular Biology™ is a trademark of The Humana Press Inc.

All papers, comments, opinions, conclusions, or recommendations are those of the author(s), and do not necessarily reflect the views of the publisher.

This publication is printed on acid-free paper.   
ANSI Z39.48-1984 (American Standards Institute)

Permanence of Paper for Printed Library Materials.

Cover: Karen Schulz

For additional copies, pricing for bulk purchases, and/or information about other Humana titles, contact Humana at the above address or at any of the following numbers: Tel.: 973-256-1699; Fax: 973-256-8341; E-mail: orders@humanapr.com; or visit our Website: www.humanapress.com

**Photocopy Authorization Policy:**

Authorization to photocopy items for internal or personal use, or the internal or personal use of specific clients, is granted by Humana Press Inc., provided that the base fee of US \$30.00 per copy is paid directly to the Copyright Clearance Center at 222 Rosewood Drive, Danvers, MA 01923. For those organizations that have been granted a photocopy license from the CCC, a separate system of payment has been arranged and is acceptable to Humana Press Inc. The fee code for users of the Transactional Reporting Service is: [978-1-58829-652-8/07 \$30.00 ].

Printed in the United States of America. 10 9 8 7 6 5 4 3 2 1

eISBN 978-1-59745-395-0

**Library of Congress Cataloging-in-Publication Data**

Immunological tolerance : methods and protocols / edited by Paul J. Fairchild.

p. ; cm. — (Methods in molecular biology ; v. 380)

Includes bibliographical references.

ISBN 978-1-58829-652-8 (alk. paper)

1. Immunological tolerance—Laboratory manuals. 2. Dendritic cells—Immunology—Laboratory manuals. 3. Immunosuppression—Laboratory manuals. I. Fairchild, Paul J. II.

Series: Methods in molecular biology (Clifton, N.J.) ; v. 380.

[DNLM: 1. Immune Tolerance—Laboratory Manuals. 2. Dendritic Cells—immunology—Laboratory Manuals. 3. Laboratory Techniques and Procedures—Laboratory Manuals. 4. Models, Animal—Laboratory Manuals. 5. T-Lymphocytes—immunology—Laboratory Manuals.

W1 ME9616J v.380 2007 / QW 525 I324905 2007]

QR188.4.I462 2007

616.07'9—dc22

2006024123

---

# Preface

Recent advances in our understanding of immunological tolerance and the processes that lead to its breakdown have helped to illuminate the etiology of many of the autoimmune diseases that affect up to 1 in 20 members of the population. The prospect of reestablishing a state of self-tolerance in the face of progressive autoimmunity is no longer the distant possibility it once seemed: various strategies have proven successful in animal models of disease, raising hopes for their eventual application in the clinic. Furthermore, the demonstration that tolerance may be extended from self to foreign tissues offers tangible alternatives for the treatment of transplant rejection, which may one day avoid the need for immunosuppression with its attendant risks and long-term side effects. Such an exciting transition phase in the field of immunological tolerance requires rigorous analysis to gauge the effectiveness of novel approaches to its induction. *Immunological Tolerance: Methods and Protocols* seeks to address this need by providing a comprehensive guide to the techniques currently used for culturing and characterizing the cell types responsible for imposing self-tolerance and the experimental models employed to study their function both in vitro and in vivo.

*Immunological Tolerance: Methods and Protocols* has been divided into four sections, each of which is introduced by one or more overview chapters intended to place the material in context and highlight relevant questions that remain to be addressed. Part I focuses on the those cell types whose contribution to the induction of tolerance is unequivocal: while thymic epithelial cells are instrumental to central tolerance and regulatory T cells to dominant tolerance in the periphery, dendritic cells may influence the T cell repertoire in either context, whether imposing negative selection in the thymus or polarizing responding T cells in the periphery towards a regulatory phenotype. This section therefore documents methods for the generation and culture of each of these critical cell types and approaches to their subsequent characterization. Part II describes protocols for the study of tolerance in vitro either by gene expression profiling of the relevant cell types or by recreating the specialized microenvironments in which the necessary cell-cell interactions may occur. While fetal thymus organ cultures and reagggregates of thymic stromal cells have historically illuminated the mechanisms of T cell repertoire selection, the use of three-dimensional collagen matrices represents a recent development which has begun to address the inadequacy of conventional in vitro approaches to the study of immune cell dynamics.

Part III explores issues related to the study of tolerance *in vivo* by describing animal models of autoimmunity, inflammatory disease and transplantation while documenting recent techniques for monitoring the outcome of therapeutic intervention. Finally, Part IV outlines novel and established strategies for the induction of tolerance experimentally through mixed chimerism, the adoptive transfer of regulatory T cells or the administration of biologicals such as monoclonal antibodies or exosomes derived from tolerogenic dendritic cells. Needless to say, many of the protocols in these sections involve procedures on live animals: since the regulatory framework surrounding such experiments varies considerably between countries, it is important to ensure that local ethical committee approval and the necessary licenses have been obtained before implementing the protocols described. With this proviso in mind, may I wish all readers success in applying the insights described in this volume within their chosen field of study.

I am, of course, most grateful for the efforts and dedication of all the authors who have contributed, not only the protocols they have developed or modified for the study of tolerance, but also for their first-hand experiences of immunology, gained from many years at the bench. I am also deeply indebted to my mentors, both past and present, who have instilled in me their enthusiasm and passion for the study of tolerance: to Jonathan Austyn, who first introduced me to the fascination and foibles of dendritic cells; to David Wraith, with whom I spent several fond years in Cambridge, grappling with autoimmunity, and to Herman Waldmann, whose immeasurable contribution to the field of tolerance I can only dream of emulating.

Finally, my heart-felt thanks go to Jackie, my wife, and Richard, my son, for their unfaltering love and support throughout the preparation of this volume, even when their own immunological tolerance had undoubtedly been pushed to the limit!

*Paul J. Fairchild*

---

# Contents

Preface .....	v
Contributors .....	xi
1 Frontiers of Immunological Tolerance <i>Giorgio Raimondi, Hèth R. Turnquist, and Angus W. Thomson</i> .....	1
<b>PART I CELL TYPES CONTRIBUTING TO IMMUNOLOGICAL TOLERANCE</b>	
2 Balancing Tolerance and Immunity: <i>The Role of Dendritic Cell and T Cell Subsets</i> <i>Elena Shklovskaya and Barbara Fazekas de St. Groth</i> .....	25
3 Differentiation of Dendritic Cell Subsets from Mouse Bone Marrow <i>Ludovica Bruno</i> .....	47
4 Genetic Modification of Dendritic Cells Through the Directed Differentiation of Embryonic Stem Cells <i>Paul J. Fairchild, Kathleen F. Nolan, and Herman Waldmann</i> .....	59
5 Generation of Immunocompetent T Cells from Embryonic Stem Cells <i>Renée F. de Pooter and Juan Carlos Zúñiga-Pflücker</i> .....	73
6 Isolation, Expansion, and Characterization of Human Natural and Adaptive Regulatory T Cells <i>Silvia Gregori, Rosa Bacchetta, Laura Passerini,        Megan K. Levings, and Maria Grazia Roncarolo</i> .....	83
7 Derivation, Culture, and Characterization of Thymic Epithelial Cell Lines <i>Michiyuki Kasai and Toshiaki Mizuochi</i> .....	107
<b>PART II THE STUDY OF IMMUNOLOGICAL TOLERANCE IN VITRO</b>	
8 Thymus Organogenesis and Development of the Thymic Stroma <i>Craig S. Nowell, Alison M. Farley,        and C. Clare Blackburn</i> .....	125
9 Generation of a Tissue-Engineered Thymic Organoid <i>Fabrizio Vianello and Mark C. Poznansky</i> .....	163
10 Studying T-Cell Repertoire Selection Using Fetal Thymus Organ Cultures <i>Philip G. Ashton-Rickardt</i> .....	171

- 11 Investigating Central Tolerance with Reaggregate  
Thymus Organ Cultures  
**Graham Anderson and Eric J. Jenkinson ..... 185**
- 12 Estimating Thymic Function Through Quantification  
of T-Cell Receptor Excision Circles  
**Marie-Lise Dion, Rafick-Pierre Sékaly, and Rémi Cheynier ..... 197**
- 13 Gene Expression Profiling of Dendritic Cells by Microarray  
**Maria Foti, Paola Ricciardi-Castagnoli, and Francesca Granucci ... 215**
- 14 SAGE Analysis of Cell Types Involved in Tolerance Induction  
**Kathleen F. Nolan, Stephen P. Cobbold, and Herman Waldmann . 225**
- 15 Analyzing the Physicodynamics of Immune Cells  
in a Three-Dimensional Collagen Matrix  
**Peter Reichardt, Frank Gunzer, and Matthias Gunzer ..... 253**

### **PART III THE STUDY OF IMMUNOLOGICAL TOLERANCE IN VIVO**

- 16 Etiology of Autoimmune Disease:  
*How T Cells Escape Self-Tolerance*  
**Eli Sercarz and Claudia Raja-Gabaglia ..... 271**
- 17 Animal Models of Spontaneous Autoimmune Disease:  
*Type 1 Diabetes in the Nonobese Diabetic Mouse*  
**Nadia Giaratana, Giuseppe Penna, and Luciano Adorini ..... 285**
- 18 Antigen-Based Therapy and Immune Regulation  
in Experimental Autoimmune Encephalomyelitis  
**Mandy J. McGeachy, Richard O'Connor, Leigh A. Stephens,  
and Stephen M. Anderton ..... 313**
- 19 Induction and Regulation of Inflammatory Bowel Disease  
in Immunodeficient Mice by Distinct CD4<sup>+</sup> T-Cell Subsets  
**Kevin J. Maloy ..... 327**
- 20 In Vivo Models for the Study of Transplantation Tolerance  
**Hannah Stewart, Rommel Ravanan, and Richard Smith ..... 337**
- 21 Ectopic Transplantation of Tissues Under the Kidney Capsule  
**Nathan J. Robertson, Paul J. Fairchild,  
and Herman Waldmann ..... 347**
- 22 Intravital Two-Photon Imaging of T-Cell Priming  
and Tolerance in the Lymph Node  
**Susanna Celli and Philippe Bousso ..... 355**
- 23 Tracing Tolerance and Immunity In Vivo by CFSE-Labeling  
of Administered Cells  
**Elizabeth Ingulli ..... 365**



**PART IV METHODS FOR INDUCING AND BREAKING IMMUNOLOGICAL TOLERANCE**

24 Thymic Involution: *Implications for Self-Tolerance*  
**Frances T. Hakim and Ronald E. Gress ..... 377**

25 Inducing Mixed Chimerism and Transplantation  
 Tolerance Through Allogeneic Bone Marrow  
 Transplantation with Costimulation Blockade  
**Ines Pree and Thomas Wekerle ..... 391**

26 Induction of Dominant Tolerance  
 Using Monoclonal Antibodies  
**Ana Água-Doce and Luis Graça ..... 405**

27 Induction of Tolerance by Adoptive Transfer of Treg Cells  
**Kanji Nagahama, Eiji Nishimura, and Shimon Sakaguchi ..... 431**

28 Modulation of the Immune Response  
 Using Dendritic Cell–Derived Exosomes  
**Nicole R. Bianco, Seon-Hee Kim, Adrian E. Morelli,  
 and Paul D. Robbins ..... 443**

29 Breaking Self-Tolerance to Tumor-Associated Antigens  
 by In Vivo Manipulation of Dendritic Cells  
**Ines Mende and Edgar G. Engleman ..... 457**

Index ..... 469



---

## Contributors

LUCIANO ADORINI • *BioXell, Milan, Italy*

ANA ÁGUA-DOCE • *Instituto de Medicina Molecular, Universidade de Lisboa, Lisboa, Portugal*

GRAHAM ANDERSON • *MRC Centre for Immune Regulation, Department of Anatomy, University of Birmingham, Birmingham, UK*

STEPHEN M. ANDERTON • *Institute of Immunology and Infection Research, University of Edinburgh, Edinburgh, UK*

PHILIP G. ASHTON-RICKARDT • *Department of Pathology & Ben May Institute for Cancer Research, University of Chicago, Chicago, IL*

ROSA BACCHETTA • *San Raffaele Telethon Institute for Gene Therapy, Milan, Italy*

NICOLE R. BIANCO • *Department of Molecular Genetics and Biochemistry, University of Pittsburgh School of Medicine, Pittsburgh, PA*

C. CLARE BLACKBURN • *Institute for Stem Cell Research, University of Edinburgh, Edinburgh, UK*

PHILIPPE BOUSSO • *Département d'Immunologie, Institut Pasteur, Paris, France*

LUDOVICA BRUNO • *The Institute of Cancer Research, London, UK*

SUSANNA CELLI • *Département d'Immunologie, Institut Pasteur, Paris, France*

RÉMI CHEYNIER • *Unité des Virus Lents, Institut Pasteur, Paris, France*

STEPHEN P. COBBOLD • *Sir William Dunn School of Pathology, University of Oxford, Oxford, UK*

RENÉE F. DE POOTER • *Department of Immunology, University of Toronto, Sunnybrook Research Institute, Toronto, Canada*

MARIE-LISE DION • *Laboratoire d'Immunologie, Centre de Recherches du CHUM, Montréal, Canada and Department of Microbiology and Immunology, McGill University, Montréal, Canada*

EDGAR G. ENGLEMAN • *Department of Pathology, Stanford University School of Medicine, Palo Alto, CA*

PAUL J. FAIRCHILD • *Sir William Dunn School of Pathology, University of Oxford, Oxford, UK*

ALISON M. FARLEY • *Institute for Stem Cell Research, University of Edinburgh, Edinburgh, UK*

BARBARA FAZEKAS DE ST GROTH • *Centenary Institute of Cancer Medicine and Cell Biology, University of Sydney, Sydney, Australia*

- MARIA FOTI • *Department of Biotechnology and Bioscience, University of Milano-Bicocca, Milan, Italy*
- NADIA GIARRATANA • *BioXell, Milan, Italy*
- LUIS GRAÇA • *Instituto de Medicina Molecular, Universidade de Lisboa, Lisboa, Portugal*
- FRANCESCA GRANUCCI • *Department of Biotechnology and Bioscience, University of Milano-Bicocca, Milan, Italy*
- SILVIA GREGORI • *San Raffaele Telethon Institute for Gene Therapy, Milan, Italy*
- RONALD E. GRESS • *Experimental Transplantation & Immunology Branch, National Cancer Institute, Bethesda, Maryland, MD*
- FRANK GUNZER • *The German University of Cairo – GUC, Department of Physics, New Cairo City, Egypt*
- MATTHIAS GUNZER • *Helmholtz Centre for Infection Research, Braunschweig, Germany*
- FRANCES T. HAKIM • *Experimental Transplantation & Immunology Branch, National Cancer Institute, Bethesda, Maryland, MD*
- ELIZABETH INGULLI • *Center for Immunology and Department of Pediatrics, University of Minnesota Medical School, Minneapolis, MN*
- ERIC J. JENKINSON • *MRC Centre for Immune Regulation, Department of Anatomy, University of Birmingham, Birmingham, UK*
- MICHIYUKI KASAI • *Dept of Research on Blood & Biological Product, National Institute of Infectious Diseases, Tokyo, Japan*
- SEON-HEE KIM • *Department of Molecular Genetics and Biochemistry, University of Pittsburgh School of Medicine, Pittsburgh, PA*
- MEGAN K. LEVINGS • *Department of Surgery, University of British Columbia, Vancouver, Canada*
- KEVIN J. MALOY • *Sir William Dunn School of Pathology, University of Oxford, Oxford, UK*
- MANDY J. MCGEACHY • *Institute of Immunology and Infection Research, University of Edinburgh, Edinburgh, UK*
- INES MENDE • *Department of Pathology, Stanford University School of Medicine, Palo Alto, CA*
- TOSHIAKI MIZUOCHI • *Department of Research on Blood & Biological Product, National Institute of Infectious Diseases, Tokyo, Japan*
- ADRIAN E. MORELLI • *Department of Surgery & Thomas E. Stazl Transplantation Institute, University of Pittsburgh School of Medicine, Pittsburgh, PA*
- KANJI NAGAHAMA • *Department of Experimental Pathology, Institute for Frontier Medical Sciences, Kyoto University, Kyoto, Japan*

- EIJI NISHIMURA • *Department of Experimental Pathology, Institute for Frontier Medical Sciences, Kyoto University, Kyoto, Japan*
- KATHLEEN F. NOLAN • *Sir William Dunn School of Pathology, University of Oxford, Oxford, UK*
- CRAIG S. NOWELL • *Institute for Stem Cell Research, University of Edinburgh, Edinburgh, UK*
- RICHARD O'CONNOR • *Institute of Immunology and Infection Research, University of Edinburgh, Edinburgh, UK*
- LAURA PASSERINI • *San Raffaele Telethon Institute for Gene Therapy, Milan, Italy*
- GIUSEPPE PENNA • *BioXell, Milan, Italy*
- MARK C. POZNANSKY • *Infectious Diseases Division & Partners AIDS Research Center, Harvard Medical School, Charlestown, MA*
- INES PREE • *Division of Transplantation, Department of Surgery, Medical University of Vienna, Vienna, Austria*
- GIORGIO RAIMONDI • *University of Pittsburgh School of Medicine, Thomas E. Starzl Transplantation Institute, Pittsburgh, PA*
- CLAUDIA RAJA-GABAGLIA • *Torrey Pines Institute for Molecular Studies, San Diego, CA*
- ROMMEL RAVANAN • *Academic Renal Unit, Southmead Hospital, Bristol, UK*
- PETER REICHARDT • *Helmholtz Centre for Infection Research, Braunschweig, Germany*
- PAOLA RICCIARDI-CASTAGNOLI • *Department of Biotechnology and Bioscience, University of Milano-Bicocca, Milan, Italy*
- PAUL D. ROBBINS • *Department of Molecular Genetics and Biochemistry, University of Pittsburgh School of Medicine, Pittsburgh, PA*
- NATHAN J. ROBERTSON • *Sir William Dunn School of Pathology, University of Oxford, Oxford, UK*
- MARIA GRAZIA RONCAROLO • *San Raffaele Telethon Institute for Gene Therapy, Milan, Italy and Vita Salute San Raffaele University, Milan, Italy*
- SHIMON SAKAGUCHI • *Department of Experimental Pathology, Institute for Frontier Medical Sciences, Kyoto University, Kyoto, Japan*
- RAFICK-PIERRE SÉKALY • *Laboratoire d'Immunologie, Centre de Recherches du CHUM, Montréal, Canada and Department of Microbiology and Immunology, McGill University, Montréal, Canada and Département de Microbiologie et Immunologie, Université de Montréal, Montréal, Canada*
- ELI SERCARZ • *Torrey Pines Institute for Molecular Studies, San Diego, CA*
- ELENA SHKLOVSKAYA • *Centenary Institute of Cancer Medicine & Cell Biology, University of Sydney, Sydney, Australia*



- RICHARD SMITH • *Academic Renal Unit, Southmead Hospital, Bristol, UK*
- LEIGH A. STEPHENS • *Institute of Immunology and Infection Research,  
University of Edinburgh, Edinburgh, UK*
- HANNAH STEWART • *Academic Renal Unit, Southmead Hospital, Bristol, UK*
- ANGUS W. THOMSON • *University of Pittsburgh School of Medicine, Thomas  
E. Starzl Transplantation Institute, Pittsburgh, PA*
- HÉTH TURNQUIST • *University of Pittsburgh School of Medicine, Thomas E.  
Starzl Transplantation Institute, Pittsburgh, PA*
- FABRIZIO VIANELLO • *Department of Hematology, University Medical School  
of Padova, Italy*
- HERMAN WALDMANN • *Sir William Dunn School of Pathology, University of  
Oxford, Oxford, UK*
- THOMAS WEKERLE • *Division of Transplantation, Department of Surgery,  
Medical University of Vienna, Vienna, Austria*
- JUAN CARLOS ZÚÑIGA-PFLÜCKER • *Department of Immunology, University of  
Toronto, Sunnybrook Research Institute, Toronto, Canada*

# Frontiers of Immunological Tolerance

Giorgio Raimondi, Hēth R. Turnquist, and Angus W. Thomson

## Summary

Herein, we succinctly review mechanisms underlying self-tolerance and the roles of dendritic leukocytes (DCs) in T-cell tolerance to self and foreign antigens. We also consider the properties of naturally arising and other populations of regulatory T cells (Treg), together with growing evidence that interplay between DCs and Treg cells can sustain antigen-specific tolerance. B-cell tolerance and the role of hematopoietic cell chimerism in the induction and maintenance of tolerance are also discussed, as is the impact of cosignaling pathway manipulation on tolerance induction. This overview also surveys prospects for technological advances in the monitoring and prediction of tolerance and the application of genomic and proteomic analysis. In addition, we consider potential novel therapeutic targets for promotion of tolerance induction.

**Key Words:** Tolerance; dendritic cells; T cells; regulatory T cells; B cells; costimulation blockade; chimerism; monitoring of tolerance.

## 1. Introduction

Improved understanding of the cellular and molecular regulation of immunological tolerance is of fundamental importance in basic immunology. It is also of major significance in the clinic, as we pursue mechanisms that underlie the breaking of self-tolerance in various autoimmune disorders and design strategies to restore tolerance to self-antigens (Ags). In transplantation, as in autoimmune diseases, the ability to induce or to restore and maintain tolerance to donor tissue-specific Ags would eliminate dependency on nonspecific immunosuppressive agents, the use of which, is often associated with serious morbidity. The ability to promote Ag-specific tolerance is also the goal of many investigators seeking to eliminate adverse immune reactions in patients with allergic hypersensitivity. On another immunological front, for researchers and clinicians battling cancer and infectious disease, the breaking of tolerance to tumor or viral

Ag, with restoration of immune effector mechanisms capable of disease eradication, are important, keenly sought-after goals. Although tolerance can be induced with comparative ease using a variety of approaches in small animal models, it has proved difficult to achieve in human disease. At the same time, although there are many well-established, laboratory-based assays and *in vivo* tests for monitoring immunity (1) there are no reliable “tolerance assays” in the clinic. In this short review chapter, we highlight several current conceptual and technologic “frontiers” in immunological tolerance as an overture to more detailed treatment of these topics in subsequent chapters of this book.

## **2. Regulation of Self Tolerance**

There has been considerable progress in understanding how sets of gene products coordinate self tolerance mechanisms and how failure of these controls can predispose to autoimmune disease (2). Many of the genes and proteins involved are conserved between commonly used experimental animals and humans, allowing extrapolation between mechanisms defined in animals and clinical investigations. The strategies used to regulate self-reactive receptors during T- or B-lymphocyte differentiation are (1) cell deletion, (2) “editing” of the offending receptor to reduce binding to self Ag (3), (3) use of intrinsic mechanisms that result in clonal anergy or biochemical “tuning” and, should the cells evade these mechanisms, (4) extrinsic controls that limit the supply of crucial growth factors, costimulatory molecules (CD40 ligand [CD154], B7 family ligands and Toll-like receptor [TLR] ligands), inflammatory mediators, and other factors. These extrinsic controls also include active suppression by regulatory T cells (Treg) through mechanisms that are as yet poorly understood (4).

It appears that these successive mechanisms can provide “back-up” to control all but a few exceptional forbidden receptors. Many genes, such the autoimmune regulator gene (5), BIM (BCL-2-interacting mediator of cell death), the tyrosine kinase ZAP70, and FAS are involved in these “checkpoints.” Because the rate at which new autoimmunity genes are being discovered is high, it is very likely that most of the candidate genes have yet to be identified. Therapeutic strategies designed to prevent or treat autoimmune disease will need to correct weak checkpoints, reinforce back-up mechanisms and avoid interference with mechanisms that could allow breakthrough of forbidden clones. Effective approaches will require a more comprehensive map of both the genes and cellular mechanisms that regulate self tolerance, in addition to improved means of identifying individual variation and personal risk factors (e.g., HLA complex and associated genes [6]).

## **3. Dendritic Cells and Tolerance**

Dendritic cell (DC) biology has recently shifted focus from the role that these uniquely well-equipped Ag-presenting cells play in the induction of

immunity, to their pivotal role in immune tolerance (7,8). The tolerizing function of both classic myeloid DC (mDC) and more recently identified plasmacytoid DC (pDC) subsets has become apparent, as has the fact that both immature and mature DC can be tolerogenic. Moreover, the tolerizing properties of DCs appear to be linked to effects on Treg. Furthermore, the unique ability of DCs to capture and cross-present exogenous Ag on major histocompatibility complex (MHC) class I molecules can be used to induce Ag-specific CD8<sup>+</sup> T-cell tolerance under noninflammatory conditions. Immature mDCs, that express low surface levels of MHC class II and costimulatory molecules (CD40, CD80, CD86), can induce Ag-specific T-cell tolerance, whereas mature mDCs that express much higher levels of these molecules, induce T-cell immunity. This paradigm has been widely supported by data from experimental animal models, including observations that immature DCs of either donor or host origin can promote transplant tolerance induction. For example, one injection of immature, donor-derived DC, 7 d before organ transplant, extends (9) or prolongs indefinitely (10) mouse MHC-mismatched heart allograft survival in a donor-specific manner. This effect is markedly potentiated by blockade of the CD40–CD154 costimulatory pathway (11). “Alternatively activated” or “regulatory” DCs, that also exhibit very low costimulatory ability, can protect mice from lethal, acute graft-vs-host disease (12) and, if administered 7 d before transplant, prolong the survival of fully MHC-mismatched skin grafts (13). Similarly, heart allograft survival is prolonged significantly in rats when immature DC of *host* origin are given 1 d before transplantation (14). Moreover, impressive synergistic effects and indefinite (>100 d) donor-specific heart graft survival are achieved, when these immature DCs are combined with suboptimal immunosuppression (15).

Notably, there is also evidence that mature DCs can promote tolerance. In a cell culture system in which human monocyte-derived DCs cross-presented Ag to CD8<sup>+</sup> T cells in the absence of CD4<sup>+</sup> T-cell help, maturation of DCs with tumor necrosis factor (TNF)- $\alpha$  and prostaglandin E<sub>2</sub> led to proliferation of T cells with tolerogenic properties (16). In separate studies using human autologous DCs and T cells in the absence of Ag, mature but not immature DC induced CD4<sup>+</sup> T cells expressing the transcriptional repressor Forkhead winged helix protein-3 (Foxp3) (Treg) that inhibited allogeneic mixed leukocyte reactions (17). In vivo, bone marrow-derived DCs matured with TNF $\alpha$ , but not lipopolysaccharide or anti-CD40 Ab, protected mice from CD4<sup>+</sup> T cell-mediated experimental autoimmune encephalomyelitis, despite strong expression of MHC class II and costimulatory molecules (18). It also is evident that immature or mature DC can prime Treg that prevent autoimmunity (19–21), as discussed below.

As the molecular basis of tolerance induction becomes better defined, it may become possible to use DCs derived from embryonic stem cells (22) to “reprogram” the immune system to tolerate grafted therapeutic tissues derived from the same embryonic stem cell line.

#### 4. Plasmacytoid DCs and Tolerance Induction

There is growing evidence of the role of pDCs in immune tolerance. Defined originally by their capacity to secrete large amounts of type I interferons in response to viruses (23), pDCs also play an essential role in protection against inflammatory responses to harmless (inhaled) Ags (24). As discussed below, mature DCs can induce Treg responses in vitro (25,26), whereas in mice, pre-pDCs appear to be the principal cell type that facilitates allogeneic hematopoietic stem cell engraftment and the consequent induction of donor-specific skin graft tolerance (27). Moreover, donor-derived pre-pDCs infused 7 d before vascularized heart transplantation, significantly prolong subsequent graft survival in the absence of immunosuppressive therapy (28). As with mDCs (11), this effect is markedly enhanced by anti-CD154 monoclonal antibody (MAb) administration (29). Thus, it appears that both mDCs and pDCs can function as tolerogenic antigen-presenting cells (APC), and that maturation by itself is not the feature that distinguishes their immunogenic from their tolerogenic function. Indeed, maturation is more of a continuum than an “on-off” switch, and a “semi-mature” state, in which DCs are phenotypically mature, but remain poor producers or proinflammatory cytokines, has also been linked to tolerogenic function (18,30).

#### 5. Regulatory T Cells

Regulatory T cells comprise many subpopulations: naturally arising CD4<sup>+</sup>CD25<sup>+</sup> Treg; CD4<sup>+</sup> type 1 (interleukin [IL]-10-producing) regulatory cells (Tr1); transforming growth factor (TGF)- $\beta$ -secreting T cells (Th3); CD8<sup>+</sup> suppressor cells (that include Qa-1-restricted CD8<sup>+</sup> T cells and non-Qa-1-restricted CD8<sup>+</sup>CD28<sup>-</sup> T cells), and NKT cells. Treg are the most investigated by far, but definitive answers to questions related to their ontogeny/selection, lineage markers, Ag specificity, mechanisms of action, and regulation of suppression are still lacking.

##### 5.1. Naturally-Arising Treg

Treg develop in the thymus through a selection process that generates a T-cell receptor (TCR) repertoire (31) with the ability to interact more efficiently with MHC class II-bound self peptides than normal CD4 T cells (32). The importance of this population in the control of self reactivity has been demonstrated extensively: thus, (1) neonatal thymectomy (around d 5) leads to overt autoimmune reactivity, associated with the absence of Treg, that can be



prevented by their adoptive transfer; and (2) depletion of Treg (with depleting antibodies) results in uncontrolled anti-self reactivity of T cells that can be reversed by injection of new Treg. These experiments have been made possible by the identification of Treg as cells that constitutively express the  $\alpha$ -chain of the IL-2 receptor (CD25). However, the same molecule is expressed by activated T cells, restricting Treg isolation to animals with no ongoing immune reactions. The identification/isolation/purification of Treg remains a challenging issue as no specific surface markers have been discovered (all proposed candidates are also expressed by activated T cells). However, an important discovery has been the association between mutation of the transcriptional regulator forkhead box P3 (Foxp3; formerly *scurfin*), that causes a severe lymphoproliferative autoimmune syndrome in mice and humans, and Treg deficiency. This has led to the demonstration that Foxp3 controls the development and function of Treg. Moreover, its expression (intracellular) is associated with suppressive function (33). The recent generation of Foxp3<sup>gfp</sup> mice with a Foxp3 knock-in allele, encoding a green fluorescence protein (gfp)-Foxp3 fusion protein, allows direct analysis of Foxp3 expression at the single cell level (33). This model is being used to unravel the developmental and functional cytokine regulation of Treg (34,35), and will be a valuable model in future work continuing to assess the role of Treg in immunological tolerance.

Treg Ag-specificity is a challenging need that must be met to convert these cells into therapeutic agents. Although it has been demonstrated that the regulatory activity of Treg is initiated by TCR engagement (36), there is also evidence that Treg function in a nonspecific manner once activated, leading to questions as to how these cells contribute to the maintenance of tolerance in vivo, without compromising immunity to pathogens. This issue is made more complex by our lack of detailed insight into the molecular mechanisms that control unwanted immune reactions. Cell-cell contact is required for suppression in vitro (36), but the molecules at the Treg-T cell interface that are involved in this activity have not been identified. A role for cytotoxic T lymphocyte Ag-4 has been proposed (as mAb-mediated blockade prevents suppression), but the process of “reverse-signaling” via CD80/CD86 (or other, unknown molecules) that should prevent activation, has not been elucidated (37). Inhibition of IL-2 production (that generally characterizes T-cell activation) in vitro, has been ascribed to transcriptional control, but it has never been demonstrated whether this represents the main target of Treg suppressive activity, or whether it simply represents the outcome of a series of molecular events that prevent T-cell activation. IL-10 and TGF- $\beta$  produced by Treg (in particular surface-bound TGF- $\beta$ ) could also play important roles, but contrasting results obtained in vitro and in vivo have not confirmed these roles. More recently, cytolytic ability, targeted mainly toward activated T cells and mediated by granzyme A/B expression, has been attributed to Treg (38).

## 5.2. Natural Killer T Cells

NKT cells are another, naturally occurring population that possesses regulatory properties. These cells express receptors of the natural killer (NK) lineage, as well as a TCR (a defined “invariant”  $\alpha$  chain, paired with a limited number of possible  $\beta$  chains). The TCR recognizes lipid Ags presented by the MHC class Ib molecule CD1d (39). Although identified originally as cells able to lyse a variety of tumor cells (40), NKT cells were later implicated in the regulation of autoimmune diseases (41–43). This role is thought to be linked to the fact that, following Ag stimulation (via the TCR), NKT cells secrete large amounts of IL-4 and interferon (IFN)- $\gamma$ , as well as TGF- $\beta$ , IL-13, and IL-10 (43,44), that influence activation of cell types important in mediating both innate immunity and Th2-type adaptive immunity. In support of this hypothesis, it has been shown that NKT cells affect the course of experimental autoimmune disease, in particular the type-1 diabetes (nonobese diabetic) mouse model and the EAE model of multiple sclerosis. A reduction in number or altered function of NKT cells has also been correlated with autoimmune disease in humans (45).

## 5.3. Tr1 Cells

In addition to “natural arising” cells with suppressor activity, it has been shown clearly that other types of regulatory T cells can develop under specific (but yet not completely defined) conditions. Tr1 represent probably the most widely investigated population of this genre. Upon TCR-mediated activation, these cells produce high levels of IL-10 and TGF- $\beta$ , IFN- $\gamma$ , and IL-5 (a unique pattern of cytokine production). Tr1 cells were defined initially as able to prevent inflammatory bowel disease in vivo (46). They can be generated in vitro by activation (e.g., interaction with allogeneic monocytes) in the presence of exogenous IL-10 that causes the development of long-lasting, Ag-specific anergic cells. Tr1 cells exert their suppressive function partially via IL-10 and TGF- $\beta$ , but other mechanisms, including cell–cell contact-dependent mechanisms have been suggested (47,48). As with Treg, no specific membrane marker has been identified that allows unequivocal isolation of Tr1, but this has not hampered the identification of Tr1 cells in patients (49), confirming that these cells can be generated in vivo by processes that still have to be clarified. It is significant that stable, long-term acceptance of pancreatic islet allografts can be achieved following the induction of Tr1 cells in diabetic mice treated with a combination of rapamycin and IL-10. Roncarolo et al. (50), have shown that it is possible to isolate Tr1 cells from the spleens of these tolerant animals and that CD4<sup>+</sup> T cells are sufficient to transfer Ag-specific tolerance to “new” recipients.

#### 5.4. CD8<sup>+</sup> Regulatory T Cells

CD8<sup>+</sup> T cells were the first suppressor cells identified. Qa-1-restricted regulatory CD8<sup>+</sup> T cells (51,52) are specific for self Ag (not yet identified) presented by nonclassical MHC class Ib molecules (Qa-1). Interestingly, Qa-1 is expressed preferentially on activated, but not resting T cells and its surface expression is short-lived. This pattern is compatible with the observation (44) that the role of Qa-1 on regulatory CD8<sup>+</sup> T cells in the control of autoimmune disease is evident during secondary, but not primary, immune responses. This supports the idea that initial stimulation of the immune system can promote the generation/activation of Qa-1-restricted CD8<sup>+</sup> T cells (recognizing self peptides) that can then control successive activation of T cells. Even for Qa-1 restricted CD8<sup>+</sup> T cells, the mechanisms involved in their suppressive activity have not been delineated (differentiation into specific CTL and/or secretion of inhibitory lymphokines have been suggested). In addition to Qa-1-dependent regulatory CD8<sup>+</sup> cells, another population has been recently described: CD8<sup>+</sup>CD28<sup>-</sup> T cells. These cells, isolated from peripheral blood of transplant recipients, can suppress immune responses by interacting directly with Ag-presenting DC and rendering these cells tolerogenic (53–55). Many aspects of CD8<sup>+</sup>CD28<sup>-</sup> T-cell generation and their mechanisms of action remain obscure.

Thus, multiple T-cell subsets can exert suppressive effects and are employed by the immune system in different phases/conditions to maintain a healthy state of self tolerance. Autoimmunity may not reflect deficiency in a single subset of regulatory cells, but instead a defect in an integrated system of immunoregulation, mediated at different levels by distinct T-cell subsets. Successful manipulation of this complex system for the induction (or alteration) of tolerance will only be possible when various challenging questions are answered. The identification of specific markers to allow purification of regulatory cells remains one of the highest priorities, as, once purified, these cells (generally present in low number) can be expanded with appropriate protocols that have already been delineated (56). Moreover, clarification of the Ag-specificities of these cells, together with elucidation of the molecular mechanisms of suppression, will be key to the design of approaches that will target (promote or repress) their regulatory functions. Furthermore, comprehension of the interactions between the subsets of regulatory T cells described above, and their interactions with other immune cells, will be of fundamental importance for identification of the parameters that it will be necessary to manipulate to induce a self-sustained (robust) state (of tolerance or immunity). This aspect is of particular relevance, as it is evident that APC can control the suppressive properties of regulatory T cells. Identification of the molecular mediators involved will reveal new targets for innovative therapies. In conclusion, although many questionmarks

characterize current knowledge of regulatory T-cell subsets, there is considerable expectation that therapeutic approaches employing/targeting these cells will soon be available.

## 6. Interplay Between Tolerogenic DCs and Regulatory T Cells

Regulatory T cells are emerging as key players in the downstream effects of tolerogenic DCs. In mice, CD4<sup>+</sup> CD25<sup>+</sup> Treg expand following stimulation by Ag-loaded mature DC, a process that is dependent, in part, on costimulation, and can be used to block autoimmune diabetes in nonobese diabetic mice (20,21). In vitro maturation of human pDCs with cytosine-poly-guanine oligodeoxynucleotides promotes their ability to prime CD4<sup>+</sup> CD25<sup>+</sup> Treg (26). Similarly, CD154-stimulated mature human pDCs, but not mDCs, prime naive CD8<sup>+</sup> T cells to become IL-10-producing regulatory T cells (57). On the other hand, repeated exposure of human naïve peripheral blood CD4<sup>+</sup> T cells to immature, allogeneic monocyte-derived DCs induces Treg (58). Large numbers of alloAg-specific Tr1 cells can be generated in this manner for potential clinical use (59). Recent efforts to render stably immature, human monocyte-derived DCs for the generation of regulatory T cells have focused on inhibition of nuclear factor- $\kappa$ B and oxidative pathways (60). An innovative approach is the creation of tolerogenic human DCs via intracellular cytotoxic T lymphocyte Ag-4 (that prevents CD80/CD86 expression) (60). Consistent with the ability of immature DCs to generate Treg in vitro, administration of immature DCs is effective in promoting Treg responses and graft survival in rodent models. Taner et al. (61) reported that immature host DCs pulsed with donor alloAg induced Ag-specific T-cell regulation, associated with alloAg-specific heart transplant survival in the mouse. The DCs were maintained in an immature state before infusion, by exposure to the immunophilin ligand, rapamycin, one of numerous anti-inflammatory and immunosuppressive drugs that inhibit the functional maturation of DCs and enhance their tolerogenicity (62). In rats, pretransplant infusion of immature donor (F<sub>1</sub>)-derived DCs prolongs kidney allograft survival and most notably, prevents the development of transplant vasculopathy, associated with the induction of indirect pathway CD4<sup>+</sup> Treg (63). In these studies, immaturity of the DCs was sustained by exposure to dexamethasone and IL-10. Similarly, allogeneic rat DC rendered immature by transfection with a dominant negative form of IKK2 (to block nuclear factor- $\kappa$ B activation), induce potent CD4<sup>+</sup> Treg in vitro (19). Interestingly, inhibition of murine DC maturation in vivo by vitamin D3 and mycophenolate mofetil is associated with increased frequency of CD4<sup>+</sup> CD25<sup>+</sup> Treg, which can adoptively transfer transplant tolerance (64). Alternatively, use of a 15-deoxyspergualin analog, combined with induction of CD4<sup>+</sup> CD25<sup>+</sup> Treg through administration of Ab to CD45RB, is associated with long-term heart allograft acceptance in mice (65). Evidence of a positive feedback

loop between immature DCs and Treg (65), suggests that targeting both of these cells may ultimately be the most effective means to achieve indefinite graft survival. Notably, marked inhibition of DC maturation in secondary lymphoid tissue is associated with the induction of stable renal transplant tolerance in rhesus monkeys (66). Overall, the evidence suggests that harnessing the tolerogenic properties of immature DC (at least of immature myeloid/monocytoid DC) may be key to achieving their tolerogenic potential in organ transplantation.

Although there have been compelling demonstrations of the therapeutic potential of “DC therapy” and of *in situ* targeting of Ag to DCs in small animal transplantation or autoimmune disease models, the challenge now is to ascertain the safety and efficacy of these approaches for human application, and the clinical conditions under which they can be tested. Proof of principle that immature human DC can induce Ag-specific regulatory T cells (CD8<sup>+</sup>) and inhibit effector T-cell function in humans has already been documented in healthy volunteers (67). The challenge now is to ascertain the safety and efficacy of these approaches for human application, and the clinical conditions under which they can be tested, and hopefully utilized successfully to regulate allo- and autoAg responses in transplantation and autoimmunity.

## 7. B-Cell Tolerance

Historically, the principal association between B lymphocytes and tolerance has concerned the capacity of plasmablasts and plasma cells (the end products of B-cell differentiation) to produce self-damaging Abs. These autoreactive Abs bind self-Ags and interfere with normal cell functions, as well as harness immune effector mechanisms to generate autoimmune pathology. Analysis of transgenic mice that generate a restricted repertoire of Ag-specific B cells has permitted identification of cellular events responsible for the control of self-reactivity. A process of V(D)J recombination, similar to that which generates TCR genes in T cells during their differentiation in the thymus, is responsible for the assembly of unique B-cell receptors (BCR) in the bone marrow. As with T cells, this process generates a significant proportion of receptors that bind to one or more self-components. Four different strategies employed by the immune system, to keep those potential auto-reactive B cells at bay, have been delineated by recent discoveries.

As alluded to above, a first “checkpoint” is activated during the development of B cells in the bone marrow. If intracellular signals generated by a self-reactive BCR on an immature B cell exceed a certain threshold, then the cell rapidly internalizes the “offending” BCR. This is followed by arrest of maturation characterized by: (1) the absence of homing receptors necessary to enter lymphoid organs, (2) an increased dependence on B-cell survival factors,



(3) the rearrangement of a new BCR light chain to replace the original. If a B cell expressing a forbidden receptor fails to edit to a less self-reactive receptor, cell death occurs within 1–2 d. Although the molecular mechanisms that characterize these processes are currently being elucidated, there is no clear evidence as yet that defects in BCR editing or deletion contribute to human autoimmunity.

A second regulatory “checkpoint” can occur both in primary and secondary lymphoid tissues and is represented by a series of intrinsic biochemical changes in cells displaying self-reactive BCR. Several intrinsic mechanisms of anergy (reversible unresponsiveness to BCR stimulation) are well documented in autoreactive B cells (68–70). This state can be induced by decreased surface expression of the self-reactive BCR, or by biochemical “tuning” that involves alteration of the level/function of proteins that increase the threshold for B-cell activation. A third strategy is the “survival of the fittest,” a process that selects on the basis of subtle differences in affinity for self Ags and relates to the dependency of B cells on the molecule BAFF, a member of the TNF cytokine family, to survive. The engagement of a self-reactive BCR below the threshold required to trigger maturation arrest in the bone marrow is sufficient to induce an elevated requirement for BAFF. This system allows the existence, in the periphery, of a certain number of B cells with intermediate affinity for self-Ags that could be highly specific for microbial Ags. Their potential as auto-reactive cells is controlled by the fact that (unless stimulated during infection or other pathological conditions that cause levels of BAFF to increase) their survival under homeostatic conditions is limited by competition with a large number of circulating B cells that sequester the available BAFF resulting in their death (71). The final checkpoint is determined by the requirement for two signals in short succession that must be received by the B cell to generate an Ab response, signal one from Ag binding to the BCR and signal two from T helper cells. The existence of tolerance mechanisms that control T cell self reactivity should guarantee that autoreactive B cells are not stimulated. However, it is possible that signal two from T helper cells responding to foreign Ag could be misdirected to B cells that recognize self components associated with microbial components.

A second pathway of B-cell activation involves the recognition of microbial-derived products by specific receptors normally associated with the innate immune response (e.g., TLR), that can substitute for T-cell help (probably to allow Ab control of microorganisms, even in T-cell-deficient individuals). However, relatively little is known about how TLR signaling is dampened to ensure that the threshold for stimulation is high enough to stop activation of self-reactive B cells. Each of the aforementioned checkpoints has been demonstrated in control of the auto-reactivity generated by V(D)J recombination in primary lymphoid organs; however, self-reactive BCRs are also generated in a second wave of receptor-gene diversification through somatic hypermutation

in germinal-center follicles of peripheral lymphoid tissues (2). One of the current challenges to our understanding of B-cell tolerance is comprehension of the mechanisms that normally deal with self-reactive BCRs that arise in germinal centers, and how the same mechanisms are altered in human autoimmunity.

Besides the production of autoAbs, B cells play a role in alteration of self reactivity through other functions, i.e., secretion of inflammatory cytokines, Ag presentation, augmentation of T-cell activation, and generation of ectopic lymphogenesis (72,73). This has led to growing interest in therapeutic approaches for the re-establishment of tolerance based on depletion of B cells. Three strategies constitute the mainstay approaches: (1) use of depleting Ab against B-cell surface proteins, (2) generation of fusion proteins or Abs that block B-cell survival signals, and (3) generation of Abs that activate proapoptotic signals. Based on the notion that surface immunoglobulin crosslinking, in the absence of coreceptor engagement, can induce apoptosis in mature B cells (74–76), a protocol employing mAbs directed against surface IgD has been developed. This approach reduces circulating B cells, but is likely to have limited therapeutic use because most pathogenic cells have switched isotypes and do not express surface IgD. Other targets have been investigated. Abs against human CD20 are the most advanced among the B cell-depleting armamentarium in autoimmune disorders. Anti-CD20 mAbs successfully deplete human peripheral B lymphocytes for periods ranging from 3 mo to more than 1 yr, through mechanisms involving Fc- and complement-dependent killing, as well as possible proapoptotic and other signals. CamPath® is a humanized mAb directed against CD52, an Ag expressed on normal as well as malignant B and T cells, a subset of CD34<sup>+</sup> bone marrow cells, NK cells, monocytes, macrophages, and tissues within the male reproductive system (77). Ongoing development of therapies directed against additional B-cell targets, including CD23, CD80, and HLA-DR, will provide greater insights into the principles of cellular immunotherapy.

Although preliminary results from testing of these agents indicate promising potential, two important aspects remain unresolved. The first concerns translation from animal models to humans, a phase during which many promising potential therapies have failed. The second is the absence of specificity for all of the developed therapeutics that could compromise the ability of the immune system to respond adequately to pathogens. A possible solution could derive from the previously mentioned dependency of B-cell survival on the availability of BAFF, and the discovery that potential self-reactive B cells are more dependent on this factor than normal cells. Partial antagonism of BAFF may be a particularly powerful approach to enhance autoimmune B-cell sensitivity to natural tolerance mechanisms. Furthermore, it may also be a valuable adjunct to B cell-depleting therapies that might otherwise increase BAFF availability and favor the survival of self-reactive B cells.

In addition to their role in autoimmunity, B cells are involved in the allograft rejection response. Their role is particularly evident during hyperacute rejection, which occurs in presensitized patients that possess preformed, donor-specific Abs. As with autoimmunity, selective targeting of B cells that produce antidonor Ab would be most beneficial. Promising results (that also indicate potential in cases of autoimmunity) derive from work on transplant tolerance induction. Studies in animal models indicate that induction of mixed chimerism (*see* below) is a promising approach to simultaneously tolerize T cells and both preexisting and newly developing B cells (78). Another intriguing approach derives from the susceptibility of immature B cells to apoptosis induced by stimulation of the BCR. Specific treatments of mature B cells can result in their adopting an immature B-cell response phenotype (79). It will be of great value to verify whether manipulation can be achieved *in vivo*, and whether it might represent a “magic bullet” for the elimination of B-cells responsive to alloAgs, as well those involved in autoimmune reactions.

Finally, B cells are APC with potential as tools for tolerance induction. Small resting B cells can induce robust tolerance to defined Ags *in vivo* (80). Even more interestingly, it has been shown recently that persistence of Ag presentation function by B cells plays a dominant role in their ability to induce T-cell tolerance as it can even override the activation state of the presenting cell (81,82). This could represent an important advantage over DCs that could render B cells more attractive therapeutic tools in at least some forms of autoimmunity, however further experimentation is necessary to test this concept.

Targeting autoreactive B cells or using B cells for tolerance induction represents a challenging frontier that still has to be confronted. Well-targeted interventions will require the development of a complete map of the cellular mechanisms and genes underpinning self tolerance, but recent advances and the development of more sophisticated techniques may allow rapid progress in this direction.

## 8. Hematopoietic Cell Chimerism in Immunological Tolerance

The significance of donor cell chimerism in transplant tolerance has been recognized both clinically and experimentally for the past half century (83), and the establishment of donor hematopoietic cells in graft recipients as a means to tolerize the recipient to donor alloAgs remains at the forefront of basic and translational immune tolerance research. Hematopoietic chimerism appears to represent a key mechanism for maintenance of specific cytotoxic T-cell unresponsiveness (84) and persistence of donor cells, even at the microchimeric level (<1%), appears to be an important goal in optimizing allograft acceptance, even under minimal immunosuppression. To date, the establishment of hematopoietic mixed chimerism, defined as the coexistence of hematopoietic cells from the donor with those of a recipient, has been demonstrated to be one of the most

successful and consistent methods to induce T- and B-cell tolerance to allo- and xenografts in rodent models, and possibly in both nonhuman primates (NHP) and humans (78,85,86). Although these developments are impressive, there remain several barriers and questions that currently limit the widespread application of the induction of hematopoietic chimerism in allograft and autoimmune tolerance induction (87,88). To date, experiments involving NHP and limited clinical trials, have established that even rigorous induction regimens, including use of cyclophosphamide, total body irradiation, thymic irradiation, and anti-thymocyte globulin, may only establish a transient state of mixed chimerism following bone marrow cell infusion. Less severe protocols must be established to safely and more widely exploit chimerism induction as a means to reduce immunosuppressive drug treatment of patients for allograft rejection and autoimmunity. Furthermore, it is critical that these protocols (at least with respect to transplantation) are tested in NHP models, as an accurate assessment of the level of donor cell engraftment necessary to establish clinically relevant tolerance to alloAgs in the presence of possible cross-reactive T cells may only be obtained in animal models with heterologous immunity through previous exposure to diverse Ags and pathogens (89).

Furthermore, it is understood that the major mechanisms operating to establish donor-specific tolerant states following establishment of chimerism are central deletion and clonal exhaustion of reactive T cells, especially CD8<sup>+</sup> T cells (83,84). However, the recent development of reagents (e.g., Abs to Foxp3 or glucocorticoid-induced TNF family related receptor and CD25<sup>+</sup>-depleting Abs) are beginning to allow better assessment of the role of regulatory T cells in the process of T-cell deletion and the establishment of donor cell chimerism (90). Graft-vs-host disease remains a very significant risk factor following chimerism induction after hematopoietic stem cell transplant. Accumulating findings suggest that DCs and regulatory cells both play active and determining roles in its manifestation, but also may offer potential therapeutic means to prevent and/or regulate graft-vs-host disease (91–94).

The role of naturally arising microchimerism (<1% chimerism), a small number of cells or DNA persisting from one individual in another (e.g., fetal cells in a mother), has drawn attention as a possible basis for induction of autoimmunity and is another area of chimerism-related research. Limited studies, driven by the observation that autoimmune diseases are more common in women and increase in incidence following childbirth, have suggested a possible etiological association between microchimerism and the development of autoimmune responses. However, microchimerism is widely detected in healthy individuals and in organs not prone to autoimmune responses. Thus, the negative or positive outcome from the establishment of divergent HLA microchimerism is yet to be fully elucidated (95).

## 9. Manipulation of Cosignaling Pathways

A balance between stimulatory and inhibitory molecular signals is necessary for maintaining tolerance. Signaling through both the original and newer members of the B7-CD28 pathway provides second signals that can regulate the activation, inhibition and “fine tuning” of T-cell responses (96). The five new B7 family members, PD-L1 (B7-H1), PD-L2 (B7-DC), B7-H3, B7-H4, and ICOS ligand, are expressed on professional APC and regulate T-cell activation and tolerance. The novel CD28 family members, PD-1, ICOS, and BTLA are expressed inducibly on T cells and regulate previously activated T cells. PD-1 and BTLA are also expressed on B cells. The PD-1:PD-L1/PD-L2 pathway plays a critical role in regulation of T-cell activation and tolerance, whereas the ICOS-ICOSL pathway appears to be important in stimulating effector T-cell responses, T cell-dependent B-cell responses, and in regulation of T-cell tolerance. As recently discussed (96), manipulation of the PD-L1:PD-1 and ICOSL:ICOS pathways in autoimmune disease and transplantation models offers considerable therapeutic potential for controlling T-cell responses.

Acquired immune responses are dependent on signaling via the CD40-CD40 ligand (CD154) pathway, blockade of which can prevent and inhibit cell- and Ab-mediated autoimmune disease and promote transplant tolerance in experimental models (97). Blockade of this pathway is particularly effective if anti-CD154 is administered together with donor Ag to the quiescent immune system before the inflammatory response caused by organ transplantation. Thus, as demonstrated recently, infusion of donor alloAg (apoptotic cells) plus anti-CD154 before transplant can induce indefinite survival of vascularized heart grafts free of transplant vasculopathy linked to the deletion of allospecific T cells and induction of regulatory T cells (98). Studies such as these are providing remarkable insights into the process of allospecific tolerance.

## 10. Frontiers in Monitoring and Predicting States of Tolerance and Therapeutic Targets to Influence Self- and Allo-Responsiveness

Basic and clinical research findings continue to provide insight into the specific cells, including specific subsets of DCs, Treg, and NK cells, in addition to the soluble factors and genes, that are directly responsible for the regulation of immunological tolerance. As such, developing avenues of study seek to apply this knowledge and to improve our capacities to both dynamically assess, and then regulate or adjust patient treatment based on immunologic indices of responsiveness/tolerance to the relevant Ag(s). A conceptual framework for the application of in vitro and in vivo assays to assess donor-specific unresponsiveness in organ (liver) transplant patients has been discussed in detail (99). Recent

analysis of circulating DC subsets was found to correlate with clinical unresponsiveness to donor Ags in stable liver transplant patients off all immunosuppression and thus (in conjunction with other assays) may help facilitate the future direction of patient selection for weaning off immunosuppression (*100,101*). Interestingly, analysis of circulating Treg (CD4<sup>+</sup>CD25<sup>hi</sup>) in operationally tolerant, human pediatric live donor liver transplant recipients revealed significantly elevated levels of these cells compared with controls (*102*). In a separate vein, assessment of both the cellular composition of hematopoietic stem cell transplants and the resultant circulating recipient and donor immune cells has been utilized recently to establish clinical correlates that may predict disease-free outcomes or transplant-related complications (e.g., acute or chronic graft-vs-host disease [*103–105*]).

Through their constant interaction with other immune cells and the local environment, DCs, T cells and B cells are altered biochemically, both temporarily (e.g., cellular signaling cascades and transient gene expression following receptor ligation) and more permanently (e.g., functional gene expression and protein production following lymphocyte differentiation or DC maturation). As new technologies evolve, they allow probing of these internal molecular records. As one example, current analysis utilizing phospho-specific Abs in combination with multiparameter flow cytometric analysis, is beginning to demonstrate the value of quantitative, real-time dissection of single cell-type signaling pathways, particularly in T cells (*106,107*). Thus, it can be envisaged that this type of analysis, when combined with the determination of immune cell composition (*100,101*), will provide an indication (based on both the level of cells and their detected activated signaling pathways) of the extent of functioning cells and, thus their potential to influence immunological tolerance. The further recent advancement of “humanized” mice, in which severe combined immune deficiency mice are used to establish a surrogate of the human immune system, offers an important model to rapidly test these and other new assays. These mice are not new, however recent models, incorporating transplanted fetal thymus and liver with CD34<sup>+</sup> cell transplants, are the first to demonstrate the ability of these “humanized” mice to mount an adaptive immune response as well as to reject xenotransplants (*108,109*). Thus, it is expected that these mice will be valuable models to both correlate clinical conditions and test novel therapies.

## 11. Genomic and Proteomic Analysis of Immune Tolerance

Historically, the assessment of graft function, presence of autoimmune-related pathology and analysis of circulating immune cell components and function, the latter through quantification of serum proteins (such as allo- and autoAbs, complement or cytokines), have been used as biomarkers to assess the

level of immune responses related to tolerance and immunity. However, earlier and more informative indicators and prognosticators of the pathological or tolerant states in graft rejection and autoimmunity are now being sought via proteomic approaches, such as protein arrays, surface-enhanced laser desorption ionization/time-of-flight mass spectrometry, and two-dimensional gel electrophoresis combined with mass spectrometry ([110,111](#)). Although these technologies are in their infancy with regards to applications in immunological systems, they have potential, in the long-term, for greater sensitivity and provision of information than is currently available using enzyme immunoassay and other clinical or laboratory measures.

Likewise, microarray analysis continues to evolve as a broadly applicable and powerful method to identify candidate genes, expression levels of which are altered during diverse biological processes. Recent studies have aimed, through array analysis, to dissect the processes underlying allograft changes during surgery and transplant rejection or acceptance ([112–114](#)), as well as in organ-specific autoimmune responses ([115](#)). Furthermore, the central importance of DCs to tolerance regulation has led to focused examination of their gene regulation following exposure to tolerogenic (e.g., IL-10, vitamin D3) ([116,117](#)) or inflammatory stimuli (e.g., TLR ligands) ([118](#)). Similarly, peripheral blood mononuclear cells possess global patterns of gene expression dictated by their exposure to immunomodulatory cytokines and other factors, and as such, the resultant molecular signature of these cells may disclose the condition of the body. Bennett et al. ([119](#)) demonstrated the power of microarray analysis of peripheral blood mononuclear cells when they confirmed the role of IFN- $\gamma$  in the pathogenesis of systemic lupus erythematosus, based on a pattern of upregulated IFN-induced genes, which was lost upon successful steroid treatment of the disease. These array data also established a possible role for immature granulocytes in systemic lupus erythematosus ([119](#)). As these data clearly indicate, informative gene expression patterns are contained in the circulating leukocyte population. As continued, focused analysis of DC, T-, and B-cell populations in various tolerant or reactive states of transplant, cancer, and autoimmunity are completed, a more precise and comprehensive picture of the immune vs tolerant state will emerge.

As these phenotypic, genomic, and proteomic analytic and diagnostic tools continue to evolve and become standardized, their use as (potentially powerful) clinical tools to rapidly and broadly assess patterns of immune reactivity or tolerance, and their utilization to distinguish patients who may be “predisposed” to tolerance, or require immunosuppressive therapy, can be envisaged. Similarly, their value in rapid, real-time assessment of the impact of novel therapeutic strategies aimed at modifying the immune response to self, tumor-associated or alloAgs, is likely to be realized.



## Acknowledgments

The work of the authors' laboratory is supported by grants from the National Institutes of Health, The American Heart Association, and the Roche Organ Transplantation Research Foundation. GR is in receipt of a fellowship from The Transplantation Society and HRT is in receipt of a fellowship from The American Society of Transplantation. We thank Ms. Miriam Meade for skilled administrative support.

## References

1. Lotze, M. T. and Thomson, A. W. (2005) *Monitoring Immunity*. Elsevier-Academic Press, New York. pp. 1–722.
2. Goodnow, C. C., Sprent, J., Fazekas de St. Groth, B., and Vinuesa, C. G. (2005) Cellular and genetic mechanisms of self tolerance and autoimmunity. *Nature* **435**, 590–597.
3. Nemazee, D. and Hogquist, K. A. (2003) Antigen receptor selection by editing or downregulation of V(D)J recombination. *Curr. Opin. Immunol.* **15**, 182–189.
4. Kronenberg, M. and Rudensky, A. (2005) Regulation of immunity by self-reactive T cells. *Nature* **435**, 598–604.
5. Liston, A., Lesage, S., Wilson, J., Peltonen, L., and Goodnow, C. C. (2003) Aire regulates negative selection of organ-specific T cells. *Nat. Immunol.* **4**, 350–354.
6. Thorsby, E. and Lie, B. A. (2005) HLA associated genetic predisposition to autoimmune diseases: genes involved and possible mechanisms. *Transpl. Immunol.* **14**, 175–182.
7. Steinman, R. M., Hawiger, D., and Nussenzweig, M. C. (2003) Tolerogenic dendritic cells. *Annu. Rev. Immunol.* **21**, 685–711.
8. Morelli, A. E. and Thomson, A. W. (2003) Dendritic cells: regulators of alloimmunity and opportunities for tolerance induction. *Immunol. Rev.* **196**, 125–146.
9. Fu, F., Li, Y., Qian, S., et al. (1996) Costimulatory molecule-deficient dendritic cell progenitors (MHC class II<sup>+</sup>, CD80<sup>dim</sup>, CD86<sup>-</sup>) prolong cardiac allograft survival in nonimmunosuppressed recipients. *Transplantation* **62**, 659–665.
10. Lutz, M. B., Suri, R. M., Niimi, M., et al. (2000) Immature dendritic cells generated with low doses of GM-CSF in the absence of IL-4 are maturation resistant and prolong allograft survival in vivo. *Eur. J. Immunol.* **30**, 1813–1822.
11. Lu, L., Li, W., Fu, F., et al. (1997) Blockade of the CD40-CD40 ligand pathway potentiates the capacity of donor-derived dendritic cell progenitors to induce long-term cardiac allograft survival. *Transplantation* **64**, 1808–1815.
12. Sato, K., Yamashita, N., Yamashita, N., Baba, M., and Matsuyama, T. (2003) Regulatory dendritic cells protect mice from murine acute graft-versus-host disease and leukemia relapse. *Immunity* **18**, 367–379.
13. Roelen, D. L., Schuurhuis, D. H., van den Boogaardt, D. E., et al. (2003) Prolongation of skin graft survival by modulation of the alloimmune response with alternatively activated dendritic cells. *Transplantation* **76**, 1608–1615.



14. Peche, H., Trinite, B., Martinet, B., and Cuturi, M. C. (2005) Prolongation of heart allograft survival by immature dendritic cells generated from recipient type bone marrow progenitors. *Am. J. Transplant.* **5**, 255–267.
15. Beriou, G., Peche, H., Guillonneau, C., Merieau, E., and Cuturi, M. C. (2005) Donor-specific allograft tolerance by administration of recipient-derived immature dendritic cells and suboptimal immunosuppression. *Transplantation* **79**, 969–972.
16. Albert, M. L., Jegathesan, M., and Darnell, R. B. (2001) Dendritic cell maturation is required for the cross-tolerization of CD8+ T cells. *Nat. Immunol.* **2**, 1010–1017.
17. Verhasselt, V., Vosters, O., Beuneu, C., Nicaise, C., Stordeur, P., and Goldman, M. (2004) Induction of FOXP3-expressing regulatory CD4pos T cells by human mature autologous dendritic cells. *Eur. J. Immunol.* **34**, 762–772.
18. Menges, M., Rossner, S., Voigtlander, C., et al. (2002) Repetitive injections of dendritic cells matured with tumor necrosis factor alpha induce antigen-specific protection of mice from autoimmunity. *J. Exp. Med.* **195**, 15–21.
19. Tomasoni, S., Aiello, S., Cassis, L., et al. (2005) Dendritic cells genetically engineered with adenoviral vector encoding dnIKK2 induce the formation of potent CD4+ T-regulatory cells. *Transplantation* **79**, 1056–1061.
20. Tarbell, K. V., Yamazaki, S., Olson, K., Toy, P., and Steinman, R. M. (2004) CD25+ CD4+ T cells, expanded with dendritic cells presenting a single autoantigenic peptide, suppress autoimmune diabetes. *J. Exp. Med.* **199**, 1467–1477.
21. Yamazaki, S., Iyoda, T., Tarbell, K., et al. (2003) Direct expansion of functional CD25+ CD4+ regulatory T cells by antigen-processing dendritic cells. *J. Exp. Med.* **198**, 235–247.
22. Fairchild, P. J., Nolan, K. F., Cartland, S., and Waldmann, H. (2005) Embryonic stem cells: a novel source of dendritic cells for clinical applications. *Int. Immunopharmacol.* **5**, 13–21.
23. Colonna, M., Trinchieri, G., and Liu, Y. J. (2004) Plasmacytoid dendritic cells in immunity. *Nat. Immunol.* **5**, 1219–1226.
24. De Heer, H. J., Hammad, H., Soullie, T., et al. (2004) Essential role of lung plasmacytoid dendritic cells in preventing asthmatic reactions to harmless inhaled antigen. *J. Exp. Med.* **200**, 89–98.
25. Gilliet, M., Boonstra, A., Paturel, C., et al. (2002) The development of murine plasmacytoid dendritic cell precursors is differentially regulated by FLT3-ligand and granulocyte/macrophage colony-stimulating factor. *J. Exp. Med.* **195**, 953–958.
26. Moseman, E. A., Liang, X., Dawson, A. J., et al. (2004) Human plasmacytoid dendritic cells activated by CpG oligodeoxynucleotides induce the generation of CD4+CD25+ regulatory T cells. *J. Immunol.* **173**, 4433–4442.
27. Fugier-Vivier, I. J., Rezzoug, F., Huang, Y., et al. (2005) Plasmacytoid precursor dendritic cells facilitate allogeneic hematopoietic stem cell engraftment. *J. Exp. Med.* **201**, 373–383.
28. Abe, M., Wang, Z., De Creus, A., and Thomson, A. W. (2005) Plasmacytoid dendritic cell precursors induce allogeneic T cell hyporesponsiveness and prolong heart graft survival. *Am. J. Transplant.* **5**, 1808–1819.

29. Bjorck, P., Coates, P. T., Wang, Z., Duncan, F. J., and Thomson, A. W. (2005) Promotion of long-term heart allograft survival by combination of mobilized donor plasmacytoid dendritic cells and anti-CD154 monoclonal antibody. *J. Heart Lung Transplant.* **24**, 1118–1120.
30. Lutz, M. B. and Schuler, G. (2002) Immature, semi-mature and fully mature dendritic cells: which signals induce tolerance or immunity? *Trends Immunol.* **23**, 445–449.
31. Bluestone, J. A. and Abbas, A. K. (2003) Natural versus adaptive regulatory T cells. *Nat. Rev. Immunol.* **3**, 253–257.
32. Hsieh, C. S., Liang, Y., Tzysnik, A. J., Self, S. G., Liggitt, D., and Rudensky, A. Y. (2004) Recognition of the peripheral self by naturally arising CD25+ CD4+ T cell receptors. *Immunity* **21**, 267–277.
33. Fontenot, J. D., Rasmussen, J. P., Williams, L. M., Dooley, J. L., Farr, A. G., and Rudensky, A. Y. (2005) Regulatory T cell lineage specification by the forkhead transcription factor foxp3. *Immunity* **22**, 329–341.
34. Fontenot, J. D., Rasmussen, J. P., Gavin, M. A., and Rudensky, A. Y. (2005) A function for interleukin 2 in Foxp3-expressing regulatory T cells. *Nat. Immunol.* **6**, 1142–1151.
35. Fontenot, J. D., Dooley, J. L., Farr, A. G., and Rudensky, A. Y. (2005) Developmental regulation of Foxp3 expression during ontogeny. *J. Exp. Med.* **202**, 901–906.
36. Shevach, E. M. (2002) CD4+ CD25+ suppressor T cells: more questions than answers. *Nat. Rev. Immunol.* **2**, 389–400.
37. von Boehmer, H. (2005) Mechanisms of suppression by suppressor T cells. *Nat. Immunol.* **6**, 338–344.
38. Grossman, W. J., Verbsky, J. W., Barchet, W., Colonna, M., Atkinson, J. P., and Ley, T. J. (2004) Human T regulatory cells can use the perforin pathway to cause autologous target cell death. *Immunity* **21**, 589–601.
39. Bendelac, A. (1995) Mouse NK1+ T cells. *Curr. Opin. Immunol.* **7**, 367–374.
40. Cui, J., Shin, T., Kawano, T., et al. (1997) Requirement for Valpha14 NKT cells in IL-12-mediated rejection of tumors. *Science* **278**, 1623–1626.
41. Gombert, J. M., Herbelin, A., Tancrede-Bohin, E., Dy, M., Carnaud, C., and Bach, J. F. (1996) Early quantitative and functional deficiency of NK1+ like thymocytes in the NOD mouse. *Eur. J. Immunol.* **26**, 2989–2998.
42. Godfrey, D. I., Hammond, K. J., Poulton, L. D., Smyth, M. J., and Baxter, A. G. (2000) NKT cells: facts, functions and fallacies. *Immunol. Today* **21**, 573–583.
43. Wilson, S. B. and Delovitch, T. L. (2003) Janus-like role of regulatory iNKT cells in autoimmune disease and tumour immunity. *Nat. Rev. Immunol.* **3**, 211–222.
44. Jiang, H. and Chess, L. (2004) An integrated view of suppressor T cell subsets in immunoregulation. *J. Clin. Invest.* **114**, 1198–1208.
45. Wilson, S. B., Kent, S. C., Patton, K. T., et al. (1998) Extreme Th1 bias of invariant Valpha24JalphaQ T cells in type 1 diabetes. *Nature* **391**, 177–181.

46. Groux, H., O'Garra, A., Bigler, M., et al. (1997) A CD4<sup>+</sup> T-cell subset inhibits antigen-specific T-cell responses and prevents colitis. *Nature* **389**, 737–742.
47. Hawrylowicz, C. M. and O'Garra, A. (2005) Potential role of interleukin-10-secreting regulatory T cells in allergy and asthma. *Nat. Rev. Immunol.* **5**, 271–283.
48. Roncarolo, M. G., Bacchetta, R., Bordignon, C., Narula, S., and Levings, M. K. (2001) Type 1 T regulatory cells. *Immunol. Rev.* **182**, 68–79.
49. Gregori, S., Bacchetta, R., Hauben, E., Battaglia, M., and Roncarolo, M. G. (2005) Regulatory T cells: prospective for clinical application in hematopoietic stem cell transplantation. *Curr. Opin. Hematol.* **12**, 451–456.
50. Battaglia, M., Stabilini, A., Draghici, E., et al. (2006) Rapamycin and interleukin-10 treatment induces T regulatory type 1 cells that mediate antigen-specific transplantation tolerance. *Diabetes* **55**, 40–49.
51. Sarantopoulos, S., Lu, L., and Cantor, H. (2004) Qa-1 restriction of CD8<sup>+</sup> suppressor T cells. *J. Clin. Invest.* **114**, 1218–1221.
52. Kumar, V. (2004) Homeostatic control of immunity by TCR peptide-specific Tregs. *J. Clin. Invest.* **114**, 1222–1226.
53. Jiang, S., Tugulea, S., Pennesi, G., et al. (1998) Induction of MHC-class I restricted human suppressor T cells by peptide priming in vitro. *Hum. Immunol.* **59**, 690–699.
54. Chang, C. C., Ciubotariu, R., Manavalan, J. S., et al. (2002) Tolerization of dendritic cells by T(S) cells: the crucial role of inhibitory receptors ILT3 and ILT4. *Nat. Immunol.* **3**, 237–243.
55. Najafian, N., Chitnis, T., Salama, A. D., et al. (2003) Regulatory functions of CD8<sup>+</sup>CD28<sup>-</sup> T cells in an autoimmune disease model. *J. Clin. Invest.* **112**, 1037–1048.
56. Bluestone, J. A. (2005) Regulatory T-cell therapy: is it ready for the clinic? *Nat. Rev. Immunol.* **5**, 343–349.
57. Gilliet, M. and Liu, Y. J. (2002) Generation of human CD8 T regulatory cells by CD40 ligand-activated plasmacytoid dendritic cells. *J. Exp. Med.* **195**, 695–704.
58. Jonuleit, H., Schmitt, E., Schuler, G., Knop, J., and Enk, A. H. (2000) Induction of interleukin 10-producing, nonproliferating CD4<sup>+</sup> T cells with regulatory properties by repetitive stimulation with allogeneic immature human dendritic cells. *J. Exp. Med.* **192**, 1213–1222.
59. Levings, M. K., Gregori, S., Tresoldi, E., Cazzaniga, S., Bonini, C., and Roncarolo, M. G. (2005) Differentiation of Tr1 cells by immature dendritic cells requires IL-10 but not CD25<sup>+</sup>CD4<sup>+</sup> Tr cells. *Blood* **105**, 1162–1169.
60. Tan, P. H., Sagoo, P., Chan, C., et al. (2005) Inhibition of NF-kappaB and oxidative pathways in human dendritic cells by antioxidative vitamins generates regulatory T cells. *J. Immunol.* **174**, 7633–7644.
61. Taner, T., Hackstein, H., Wang, Z., Morelli, A. E., and Thomson, A. W. (2005) Rapamycin-treated, alloantigen-pulsed host dendritic cells induce Ag-specific T cell regulation and prolong graft survival. *Am. J. Transplant.* **5**, 228–236.

62. Hackstein, H. and Thomson, A. W. (2004) Dendritic cells: emerging pharmacological targets of immunosuppressive drugs. *Nat. Rev. Immunol.* **4**, 24–35.
63. Mirenda, V., Berton, I., Read, J., et al. (2004) Modified dendritic cells coexpressing self and allogeneic major histocompatibility complex molecules: an efficient way to induce indirect pathway regulation. *J. Am. Soc. Nephrol.* **15**, 987–997.
64. Gregori, S., Casorati, M., Amuchastegui, S., Smiroldo, S., Davalli, A. M., and Adorini, L. (2001) Regulatory T cells induced by 1 alpha,25-dihydroxyvitamin D3 and mycophenolate mofetil treatment mediate transplantation tolerance. *J. Immunol.* **167**, 1945–1953.
65. Min, W. P., Zhou, D., Ichim, T. E., et al. (2003) Inhibitory feedback loop between tolerogenic dendritic cells and regulatory T cells in transplant tolerance. *J. Immunol.* **170**, 1304–1312.
66. Thomas, J. M., Contreras, J. L., Jiang, X. L., et al. (1999) Peritransplant tolerance induction in macaques: early events reflecting the unique synergy between immunotoxin and deoxyspergualin. *Transplantation* **68**, 1660–1673.
67. Dhodapkar, M. V. and Steinman, R. M. (2002) Antigen-bearing immature dendritic cells induce peptide-specific CD8(+) regulatory T cells in vivo in humans. *Blood* **100**, 174–177.
68. Healy, J. I. and Goodnow, C. C. (1998) Positive versus negative signaling by lymphocyte antigen receptors. *Annu. Rev. Immunol.* **16**, 645–670.
69. Fields, M. L. and Erikson, J. (2003) The regulation of lupus-associated autoantibodies: immunoglobulin transgenic models. *Curr. Opin. Immunol.* **15**, 709–717.
70. Benschop, R. J., Aviszus, K., Zhang, X., Manser, T., Cambier, J. C., and Wysocki, L. J. (2001) Activation and anergy in bone marrow B cells of a novel immunoglobulin transgenic mouse that is both hapten specific and autoreactive. *Immunity* **14**, 33–43.
71. Lesley, R., Xu, Y., Kalled, S. L., et al. (2004) Reduced competitiveness of autoantigen-engaged B cells due to increased dependence on BAFF. *Immunity* **20**, 441–453.
72. Martin, F. and Chan, A. C. (2004) Pathogenic roles of B cells in human autoimmunity; insights from the clinic. *Immunity* **20**, 517–527.
73. Silverman, G. J. and Carson, D. A. (2003) Roles of B cells in rheumatoid arthritis. *Arthritis Res. Ther.* **5**, S1–S6.
74. Chentoufi, A. A., Nizet, Y., Havaux, X., et al. (1999) Differential effects of injections of anti-mu and anti-delta monoclonal antibodies on B-cell populations in adult mice: regulation of xenoreactive natural antibody-producing cells. *Transplantation* **68**, 1728–1736.
75. Chentoufi, A. A., Nizet, Y., Havaux, X., Nisol, F., Bazin, H., and Latinne, D. (2000) B-Cell suppression in adult mice injected with anti-delta followed by anti-mu mAb. *Cell. Immunol.* **205**, 40–51.
76. Finkelman, F. D., Holmes, J. M., Dukhanina, O. I., and Morris, S. C. (1995) Cross-linking of membrane immunoglobulin D, in the absence of T cell help, kills mature B cells in vivo. *J. Exp. Med.* **181**, 515–525.

77. Flynn, J. M. and Byrd, J. C. (2000) Campath-1H monoclonal antibody therapy. *Curr. Opin. Oncol.* **12**, 574–581.
78. Sykes, M., Shimizu, I., and Kawahara, T. (2005) Mixed hematopoietic chimerism for the simultaneous induction of T and B cell tolerance. *Transplantation* **79**, S28–S29.
79. Monroe, J. G. (2005) Molecular mechanisms regulating B cell responsiveness and tolerance. *Transplantation* **79**, S12–S13.
80. Fuchs, E. J. and Matzinger, P. (1992) B cells turn off virgin but not memory T cells. *Science* **258**, 1156–1159.
81. Raimondi, G., Zanoni, I., Citterio, S., Ricciardi-Castagnoli, P., and Granucci, F. (2006) Induction of peripheral T cell tolerance by antigen presenting B cells. I. Relevance of antigen presentation persistence. *J. Immunol.* **176**, 4012–4020.
82. Raimondi, G., Zanoni, I., Citterio, S., Ricciardi-Castagnoli, P., and Granucci, F. (2006) Induction of peripheral T cell tolerance by antigen presenting B cells. II Chronic antigen presentation overrules antigen presenting B cell activation. *J. Immunol.* **176**, 4021–4028.
83. Starzl, T. E. (2004) Chimerism and tolerance in transplantation. *Proc. Natl. Acad. Sci. USA* **101**, 14,607–14,614.
84. Bonilla, W. V., Geuking, M. B., Aichele, P., Ludewig, B., Hengartner, H., and Zinkernagel, R. M. (2006) Microchimerism maintains deletion of the donor cell-specific CD8 T cell repertoire. *J. Clin. Invest.* **116**, 156–162.
85. Fehr, T. and Sykes, M. (2004) Tolerance induction in clinical transplantation. *Transpl. Immunol.* **13**, 117–130.
86. Bruno, D. A., Dhanireddy, K. K., and Kirk, A. D. (2005) Challenges in therapeutic strategies for transplantation: where now from here? *Transpl. Immunol.* **15**, 149–155.
87. Claas, F. (2004) Chimerism as a tool to induce clinical transplantation tolerance. *Curr. Opin. Immunol.* **16**, 578–583.
88. Sykes, M. and Nikolic, B. (2005) Treatment of severe autoimmune disease by stem-cell transplantation. *Nature* **435**, 620–627.
89. Adams, A. B., Pearson, T. C., and Larsen, C. P. (2003) Heterologous immunity: an overlooked barrier to tolerance. *Immunol. Rev.* **196**, 147–160.
90. Kurtz, J., Wekerle, T., and Sykes, M. (2004) Tolerance in mixed chimerism: a role for regulatory cells? *Trends Immunol.* **25**, 518–523.
91. Hess, A. D. (2006) Modulation of graft-versus-host disease: role of regulatory T lymphocytes. *Biol. Blood Marrow Transplant.* **12**, 13–21.
92. Porta, M. D., Rigolin, G. M., Alessandrino, E. P., et al. (2004) Dendritic cell recovery after allogeneic stem-cell transplantation in acute leukemia: correlations with clinical and transplant characteristics. *Eur. J. Haematol.* **72**, 18–25.
93. Reddy, V., Iturraspe, J. A., Tzolas, A. C., Meier-Kriesche, H. U., Schold, J., and Wingard, J. R. (2004) Low dendritic cell count after allogeneic hematopoietic stem cell transplantation predicts relapse, death, and acute graft-versus-host disease. *Blood* **103**, 4330–4335.
94. Nachbaur, D. and Kircher, B. (2005) Dendritic cells in allogeneic hematopoietic stem cell transplantation. *Leuk. Lymphoma* **46**, 1387–1396.

95. Lambert, N. and Nelson, J. L. (2003) Microchimerism in autoimmune disease: more questions than answers? *Autoimmun. Rev.* **2**, 133–139.
96. Greenwald, R. J., Freeman, G. J., and Sharpe, A. H. (2005) The B7 family revisited. *Annu. Rev. Immunol.* **23**, 515–548.
97. Quezada, S. A., Jarvinen, L. Z., Lind, E. F., and Noelle, R. J. (2004) CD40/CD154 interactions at the interface of tolerance and immunity. *Annu. Rev. Immunol.* **22**, 307–328.
98. Wang, Z., Larregina, A., Shufesky, W., et al. (2006) Use of the inhibitory effect of apoptotic cells on dendritic cells for graft survival via T cell deletion and regulatory T cells. *Am. J. Transplant.* **6**, 1297–1231.
99. Thomson, A. W., Mazariegos, G. V., Reyes, J., et al. (2001) Monitoring the patient off immunosuppression. Conceptual framework for a proposed tolerance assay study in liver transplant recipients. *Transplantation* **72**, S13–S22.
100. Mazariegos, G. V., Zahorchak, A. F., Reyes, J., Chapman, H., Zeevi, A., and Thomson, A. W. (2005) Dendritic cell subset ratio in tolerant, weaning and non-tolerant liver recipients is not affected by extent of immunosuppression. *Am. J. Transplant.* **5**, 314–322.
101. Mazariegos, G. V., Zahorchak, A. F., Reyes, J., et al. (2003) Dendritic cell subset ratio in peripheral blood correlates with successful withdrawal of immunosuppression in liver transplant patients. *Am. J. Transplant.* **3**, 689–696.
102. Tanaka, M., Zwierzchoniowska, M., Mokhtari, G. K., et al. (2005) Progression of alloresponse and tissue-specific immunity during graft coronary artery disease. *Am. J. Transplant.* **5**, 1286–1296.
103. Vela-Ojeda, J., Garcia-Ruiz Esparza, M. A., Reyes-Maldonado, E., et al. (2006) Clinical relevance of NK, NKT, and dendritic cell dose in patients receiving G-CSF-mobilized peripheral blood allogeneic stem cell transplantation. *Ann. Hematol.* **85**, 113–120.
104. Vakkila, J., Thomson, A. W., Hovi, L., Vetteranta, K., and Saarinen-Pihkala, U. M. (2005) Circulating dendritic cell subset levels after allogeneic stem cell transplantation in children correlate with time post transplant and severity of acute graft-versus-host disease. *Bone Marrow Transplant.* **35**, 501–507.
105. Panse, J. P., Heimfeld, S., Guthrie, K. A., et al. (2005) Allogeneic peripheral blood stem cell graft composition affects early T-cell chimaerism and later clinical outcomes after non-myeloablative conditioning. *Br. J. Haematol.* **128**, 659–667.
106. Danna, E. A. and Nolan, G. P. (2006) Transcending the biomarker mindset: deciphering disease mechanisms at the single cell level. *Curr. Opin. Chem. Biol.* **10**, 20–27.
107. Krutzik, P. O., Hale, M. B., and Nolan, G. P. (2005) Characterization of the murine immunological signaling network with phosphospecific flow cytometry. *J. Immunol.* **175**, 2366–2373.
108. Traggiai, E., Chicha, L., Mazzucchelli, L., et al. (2004) Development of a human adaptive immune system in cord blood cell-transplanted mice. *Science* **304**, 104–107.

109. Lan, P., Tonomura, N., Shimizu, A., Wang, S., and Yang, Y. G. (2006) Reconstitution of a functional human immune system in immunodeficient mice through combined human fetal thymus/liver and CD34+ cell transplantation. *Blood* **108**, 487–492.
110. Utz, P. J. (2005) Protein arrays for studying blood cells and their secreted products. *Immunol. Rev.* **204**, 264–282.
111. Voshol, H., Brendlen, N., Muller, D., et al. (2005) Evaluation of biomarker discovery approaches to detect protein biomarkers of acute renal allograft rejection. *J. Proteome Res.* **4**, 1192–1199.
112. Mansfield, E. S. and Sarwal, M. M. (2004) Arraying the orchestration of allograft pathology. *Am. J. Transplant.* **4**, 853–862.
113. Kurian, S. M., Flechner, S. M., Kaouk, J., et al. (2005) Laparoscopic donor nephrectomy gene expression profiling reveals upregulation of stress and ischemia associated genes compared to control kidneys. *Transplantation* **80**, 1067–1071.
114. Matsui, Y., Saiura, A., Sugawara, Y., et al. (2003) Identification of gene expression profile in tolerizing murine cardiac allograft by costimulatory blockade. *Physiol. Genomics* **15**, 199–208.
115. Oertelt, S., Selmi, C., Invernizzi, P., Podda, M., and Gershwin, M. E. (2005) Genes and goals: an approach to microarray analysis in autoimmunity. *Autoimmun. Rev.* **4**, 414–422.
116. Perrier, P., Martinez, F. O., Locati, M., et al. (2004) Distinct transcriptional programs activated by interleukin-10 with or without lipopolysaccharide in dendritic cells: induction of the B cell-activating chemokine, CXC chemokine ligand 13. *J. Immunol.* **172**, 7031–7042.
117. Griffin, M. D., Xing, N., and Kumar, R. (2004) Gene expression profiles in dendritic cells conditioned by 1 $\alpha$ ,25-dihydroxyvitamin D3 analog. *J. Steroid Biochem. Mol. Biol.* **89–90**, 443–448.
118. Napolitani, G., Rinaldi, A., Bertoni, F., Sallusto, F., and Lanzavecchia, A. (2005) Selected Toll-like receptor agonist combinations synergistically trigger a T helper type 1-polarizing program in dendritic cells. *Nat. Immunol.* **6**, 769–776.
119. Bennett, L., Palucka, A. K., Arce, E., et al. (2003) Interferon and granulopoiesis signatures in systemic lupus erythematosus blood. *J. Exp. Med.* **197**, 711–723.

## Balancing Tolerance and Immunity

### *The Role of Dendritic Cell and T Cell Subsets*

Elena Shklovskaya and Barbara Fazekas de St. Groth

#### Summary

The interaction between dendritic cells and T cells is crucial for the regulation of immunological tolerance and immunity. Although our understanding of the mechanisms responsible for these phenomena has advanced significantly in recent years, we are still lacking a fully integrated model of how dendritic cell phenotype correlates with function, and how complex interactions with multiple dendritic and T cell subpopulations shape the course of the immune response *in vivo*. In this review, we summarize the current state of knowledge in the field, highlighting the areas where further investigation is likely to advance our understanding of this fundamental immunological interaction.

**Key Words:** Dendritic cell; T cell; tolerance; immunity.

#### 1. Introduction

Maintaining an appropriate balance between tolerance and immunity is at the heart of the interaction between the adaptive and innate immune systems. Dendritic cells (DCs) serve as interpreters between the two systems, by integrating environmental signals both directly (via surface receptors such as those in the Toll-like receptor [TLR] family) and indirectly (via interactions with cells such as natural killer [NK] and natural killer T [NKT] cells). The principal targets of DCs are T cells, and it can be argued that the final arbiter of the decision between tolerance and immunity is the CD4<sup>+</sup> T cell subset, which in turn controls the responses of both CD8<sup>+</sup> T and B cells (*1*). Dendritic cells in secondary lymphoid tissues are unique in their ability to activate naïve CD4<sup>+</sup> T cells via high level expression of major histocompatibility complex (MHC) class II and costimulatory molecules, driving and controlling both primary and



secondary immune responses. Decisions between tolerance and immunity are thus confined to the professional lymphoid tissues where maximum control can be exerted to ensure that self-reactive responses are not permitted.

The role of individual DC and T cell subsets in the decision between tolerance and immunity remains highly controversial. Many factors have made this one of the most challenging areas of immunological investigation, but one of the most important has been our inability to successfully recapitulate induction of the tolerant state *ex vivo*. Development of *in vivo* models of DC function has also been severely hampered, in comparison to those aimed at understanding T and B cells, by the difficulty of DC reconstitution *in vivo*. Unlike lymphocytes, DCs home very poorly to their original location after harvesting, so that correlation of phenotype and function requires sophisticated experimental models such as those using transgenic and “knock-in” technology.

## 2. Dendritic Cell Subsets *In Vivo*

DCs are defined functionally by their ability to stimulate naïve T cells, a property that requires antigen uptake, processing, and presentation in association with MHC, together with expression of costimulatory molecules. DCs have been classified according to a number of different schemes, based on tissue distribution, surface phenotype, maturation state, hematopoietic lineage, and function. In general, the relationship between phenotype, lineage, and *in vivo* function remains highly controversial. In addition, the expression of the currently characterized DC surface molecules differs between mouse and man, making it difficult to draw parallels between the two species.

### 2.1. *Basic Terminology: Immature, Mature, and Activated DCs*

Much of our understanding of DC biology comes from *in vitro* studies of DC differentiation from bone marrow (BM) precursors (2) or blood monocytes (3). In culture, newly differentiated DCs are identified by virtue of their expression of MHC class II and ability to stimulate T cells in an antigen-specific manner. At this “immature” stage they have the capacity to capture soluble and particulate antigens and/or pathogens through several mechanisms including macropinocytosis, receptor-mediated endocytosis, and phagocytosis. Immature DCs are poor stimulators of T cells as cell surface antigen–MHC class II complexes are short-lived and expression of costimulatory molecules is low (reviewed in **ref. 4**). When immature DCs are exposed in culture to CD40 ligand (CD40L) or lipopolysaccharide (LPS), they rearrange their antigen processing machinery from “antigen uptake” mode to “antigen presentation” mode in which they express stable peptide-loaded MHC class II and I molecules on the cell surface and upregulate expression of costimulatory molecules

(5). These changes in the ability to present antigen have been termed “maturation,” and are associated with the ability to stimulate potent responses by naïve T cells.

By analogy to the *in vitro* studies, DCs with “immature” and “mature” phenotype have been identified *in vivo* and it has been suggested that they are also linked by a precursor–product relationship. Thus BM-derived DC precursors that migrate through blood to peripheral tissues are believed to give rise to immature DCs, which then move to the draining lymph nodes (LN) after antigen/pathogen capture. This migration is chemokine-driven and therefore associated with changes in chemokine receptor expression, as well as maturation *en route* (4). Mature DCs localize in the T cell area of the LN where they are potent inducers of primary T cell responses and drive the generation of immunological memory (6,7). In addition to DCs that migrate from nonlymphoid sites, blood-borne DC precursors are also believed to migrate into lymphoid tissues such as LN and spleen, and to generate immature DCs *in situ*. Thus, the mature and immature DCs in the LN are presumed to correspond to migrated and resident DCs, respectively (8).

However, this model does not account for all the properties of DCs *in vivo*. In addition to migration and maturation induced by capture of pathogens such as bacteria, at least some subsets of DCs in peripheral nonlymphoid tissues are capable of steady-state migration. Mucosal- and epidermal-derived DCs that migrate in the steady state, without exposure to pathogens, also display changes characteristic of “mature” DCs once they reach a draining LN (8–10). However, antigen presentation by these DCs is associated with tolerance rather than immunity, indicating that not all mature DCs induce immunity (11–13). Moreover, LPS and CD40L, which are employed *in vitro* to induce “maturation,” produce “activation” of DCs *in vivo*, a process associated with high expression of costimulatory molecules, interleukin [IL]-12 production, and generation of immunity rather than tolerance (14–16). Thus the terms “mature” and “activated” are used to refer to analogous processes *in vitro* and *in vivo*, respectively. This difference between terminology in the two experimental systems is not solely an issue of semantics, but highlights a major problem in our understanding of the biology of DCs. By using the term “mature” to describe activated DCs *in vitro*, we are glossing over the fact that mature nonactivated DCs equivalent to those that induce immunological tolerance *in vivo* have not yet been generated *in vitro*. So far, *in vitro* models have been unable to recapitulate the crucial process of tolerance induction in naïve T cells.

## 2.2. Distribution and Phenotype of DCs

DCs are strategically located at places where they can capture antigen and/or meet T cells for antigen presentation—body surfaces (epithelia of skin, airways,

and gut), interstitial spaces of many organs, central and secondary lymphoid organs as well as blood and afferent lymphatics. Most peripheral DCs have a short life span (3–5 d) and are therefore continuously replaced from blood-borne precursors (17). A circulating population of committed DC precursors has been defined in human (18,19) and mouse blood (20,21). DCs at epithelial surfaces can position themselves between epithelial cells. Thus epidermal Langerhans cells are held in place by E-cadherin-mediated adhesion to keratinocytes (10). DCs can also reside just beneath the epithelial layer, protruding dendrites through the junctions between epithelial cells into the intestinal or airway lumen to sample antigens (22,23). DCs are also abundant within gut-associated lymphoid tissue where they can access antigens transported by M-cells. After antigen sampling, epithelial DCs migrate to the draining LNs in response to chemokines CCL19 and CCL21; once in the LN, they are quickly immobilized within the network of LN resident DCs (7).

In the mouse, most DCs within secondary lymphoid organs belong to one of three major subpopulations displaying the “immature” phenotype  $CD11c^+MHC$  class II<sup>int</sup>  $CD80/86^{low}$ . Best characterized in the spleen, the three subpopulations comprise  $CD8^+DEC205^+$  DCs, principally located in the T-cell areas, and  $CD8^-DEC205^-CD4^-$  and  $CD8^-DEC205^-CD4^+$  DCs that are concentrated within the marginal zone (24,25). Importantly, exposure to a “danger” signal such as LPS changes this localization and induces relocation of  $CD8^-DEC205^-$  DCs into the T cell area (26,27). In addition to the  $CD11c^+$  DCs previously described, a murine homologue of human interferon (IFN)- $\alpha$ -producing DCs (IDC) has been identified (28). Mouse IDCs, which are  $B220^+CD11c^{low}CD4^+Ly6C^+$ , are also the principal producers of type I interferons in response to viral infections. In contrast to human IDCs, mouse IDCs also produce IL-12 (28). Most likely, IDCs are not involved in stimulating antigen-specific T cells as they express relatively low levels of MHC class II and costimulatory molecules (29).

Although mouse DCs have been phenotyped extensively, lack of human DC-specific markers has thus far prevented detailed characterization of human DC subsets and tissue distribution. In addition, DC phenotyping efforts have been concentrated on blood rather than tissues, making interspecies comparisons difficult. Human blood DC precursors (termed preDC) comprise two subpopulations, preDC1 ( $Lin^-CD11c^+MHC$  class II<sup>+</sup>) with monocyte-like morphology and preDC2 ( $Lin^-CD11c^{low}IL-3R\alpha^+$ ) with plasmacytoid morphology (19,30). When isolated from blood, preDC1 respond to granulocyte-macrophage colony-stimulating factor (GM-CSF) *in vitro* and stimulate Th1 responses, whereas preDC2 respond to IL-3 and stimulate Th2 responses (30). PreDC1 are believed to represent an analogue of mouse DC precursors that differentiate into tissue DCs, sample antigens in the periphery and migrate to LNs (4). PreDC2

migrate to secondary lymphoid organs via the blood stream and develop into type 1 interferon-producing IDCs that are homologous to murine IDCs (31,32). Recently, use of phage antibody libraries allowed characterization of a new DC-specific marker, nectin-like protein 2, whose expression is paralleled in human splenic T-zone DCs and mouse splenic CD8 $\alpha^+$  DCs (33). The use of the phage approach by Galibert et al. was predicated on the assumption that some subset-specific DC markers are highly conserved and thus specific monoclonal antibodies (mAbs) against these molecules will not be raised using traditional immunization techniques. It is anticipated that the discovery of further parallels between human and mouse DC subsets will require additional non-mAb-based techniques.

### 2.3. DC Development In Vivo and In Vitro

DC development in vivo has been studied extensively in the mouse. Both BM myeloid-committed precursors (common myeloid precursors [CMPs], lineage [Lin]<sup>-</sup>CD34<sup>+</sup>Sca-1<sup>-</sup>IL-7R $\alpha$ <sup>-</sup>ckit<sup>+</sup>Fc $\gamma$ RII/III<sup>lo</sup>) and lymphoid-committed precursors (common lymphoid precursors [CLPs], Lin<sup>-</sup>Thy1<sup>-</sup>Sca-1<sup>int</sup>IL-7R $\alpha$ <sup>+</sup>ckit<sup>int</sup>) can give rise to DCs upon transfer into lethally irradiated animals (34,35). In addition, thymic precursors that are committed to the lymphoid lineage (CD4<sup>low</sup>Thy1<sup>high</sup>ckit<sup>+</sup>) can provide transient DC reconstitution after transfer into irradiated hosts (34–36). It is remarkable that, after lethal irradiation and reconstitution, all three populations of precursors can give rise to DCs with all the phenotypes so far described, including IDCs (37) and Langerhans cells (38,39), although lymphoid restricted progenitors generally give rise to a higher proportion of CD8<sup>+</sup> DCs. Importantly, only the subpopulation of CMPs or CLPs that expresses flt3 receptor has DC reconstitution potential in vivo (37,40), which is in line with the activity of flt3 ligand as an in vivo DC expanding agent (41,42).

In humans, DCs can be generated in vitro from CD34<sup>+</sup> BM or cord blood precursors in the presence of tumor necrosis factor- $\alpha$  and GM-CSF (2,43,44). Once again, flt3 ligand induces human DC expansion in vivo, confirming its primary role in regulating development of DCs (45). In vivo reconstitution studies using human myeloid and lymphoid-restricted progenitors have not been performed to test whether both can give rise to DCs. Although such experiments remain of scientific interest, most human studies have concentrated on sources of DC precursors for clinical scale DC propagation. For this purpose, the fact that monocytes can differentiate into DCs in vitro in the presence of cytokines such as GM-CSF and IL-4 has proven very useful (3). In addition, monocytes acquire DC characteristics upon migration through the endothelial cell monolayer, suggesting that this differentiation pathway may also be of physiological relevance (46).

The ability of committed murine progenitors from two distinct hematopoietic lineages to generate what appears to be the same spectrum of DCs suggests a highly unusual case of convergent evolution; alternatively, it may indicate that DC precursors in lethally irradiated hosts may display unusual differentiative plasticity, or that we have not yet discovered phenotypic markers that correlate with important functional differences between DC subsets. We have previously proposed that the DCs generated from lymphoid- and myeloid-restricted progenitors may differ in one crucial property—the ability to induce tolerance or immunity (27). According to this model, lymphoid-derived DCs are the constitutive antigen-presenting cells to which naïve T cells are exposed in the T cell zones of lymphoid tissues, whereas myeloid-derived DCs are segregated in the marginal and interfollicular regions where they wait for the pathogen-derived signals that will cause them to become activated, to relocate to the T cell zones, and to generate an immunogenic response from the resident T cells. This model is satisfying from an evolutionary standpoint, as it explains why a new type of DC was required at the time the lymphoid system arose (27). In addition, it fits neatly with the binary nature of the *in vivo* decision between tolerance and immunity (47).

There are currently no known markers that distinguish murine DCs of lymphoid and myeloid origin. It was previously assumed that expression of CD8 by peripheral DCs correlated with lymphoid origin, so that CD8<sup>+</sup>DEC205<sup>+</sup> DCs were often referred to as “lymphoid,” in contrast to CD8<sup>-</sup>DEC205<sup>-</sup> “myeloid” DCs. This distinction was based on the assumption that thymic and peripheral CD8<sup>+</sup> DCs were developmentally related. Thymic CD8<sup>+</sup> DCs, which are involved in negative selection (and therefore tolerance), can be generated *in situ* from intrathymic lymphoid-committed precursors (48), and approx 25% of steady-state thymic CD8<sup>+</sup> DCs contain lymphoid-specific mRNA rearrangements suggestive of lymphoid origin (49). Although the same thymic precursor can generate CD8<sup>+</sup> DCs in the periphery when transferred into irradiated animals (48), in general, peripheral DCs do not contain mRNA transcripts specific for the lymphoid lineage (49). Moreover, as previously mentioned, all peripheral DC subsets, and in particular CD8<sup>+</sup> DCs, can be generated from CMP, CLP, and thymic progenitors. Some experimental evidence suggests that CD8<sup>+</sup> DCs can induce peripheral tolerance to tissue-associated antigens (50), although the same subset has also been implicated in priming CTL immunity to viruses (11,51).

There is an additional level of complexity to the *in vivo* DC network: DCs may exchange captured material via a number of mechanisms including cross-presentation (52), exosome secretion (53,54), and membrane exchange (55); as a result, peptide–MHC complexes may be presented to the T cell by a DC that did not participate directly in antigen capture (56).

### 3. Interactions Between T Cells and DCs

#### 3.1. Role of DCs in Central Tolerance

The primary site where self-tolerance is imposed on the T cell repertoire is the thymus. Here, developing T cells are exposed to self-antigen presented by BM-derived DCs in the thymic medulla under conditions that ensure deletion of high affinity TCRs (reviewed in **ref. 57**), either by deletion of the cells bearing them (negative selection) or by editing of the TCR to an acceptable specificity (**58**). Although it has long been recognized that TCRs reactive with antigens expressed ubiquitously, or accessible via the circulation, will be purged from the repertoire, recent studies of “ectopic” antigen synthesis in the thymus have indicated that a number of peripheral tissue-specific self-antigens appear to be synthesised there expressly to ensure negative selection of the TCR repertoire (**59**). A particular subset of thymic epithelial cells (TECs) present in the thymic medulla appears to be responsible for synthesis of these self-antigens, and the process is driven by a dedicated transcriptional regulator, the autoimmune regulator (AIRE) gene (**60**). TEC-mediated central tolerance can occur via direct recognition of self-peptide–MHC complexes displayed by TECs themselves or after transfer of these complexes to BM-derived DCs (**61**). Patients with mutations in the autoimmune regulator gene show increased susceptibility to a number of autoimmune conditions, indicating the importance of central tolerance in preventing autoimmune disease. However, the clinical syndrome usually does not manifest until adolescence or early adulthood, showing that peripheral regulatory mechanisms directed against high affinity anti-self T cells are also highly effective in the short and medium term.

The important role of BM-derived elements for the induction of central tolerance was recognized by Owen 60 yr ago (**62**) and has subsequently been utilized in the mixed hematopoietic chimerism approach to solid organ transplantation (reviewed in **ref. 63**). Although long-term mixed hematopoietic chimerism is a highly effective approach to maintaining transplantation tolerance, it remains unacceptable in a clinical setting as preparative regimen for solid organ transplantation, mainly because of high risk of life-threatening graft-vs-host disease (**63**). Nonmyeloablative strategies of chimerism induction that exclusively target T cells and therefore pose a lesser risk of graft-vs-host disease are now being developed (**63**).

#### 3.2. Peripheral Mechanisms of T-Cell Tolerance

According to Burnet’s theory of tolerance, lymphocytes pass through a stage at which contact with antigen induces obligatory tolerance, after which antigen recognition always leads to immunity (**64**). Although the induction of obligatory tolerance to self-antigen in the thymus is consistent with the theory, it is

clear that tolerance can also be induced in the mature peripheral T-cell compartment, either by administration of foreign antigen via a tolerogenic route (65,66), or by experimentally induced contact with self-antigen in the periphery (67). Several different mechanisms have been invoked to explain how tolerance can be induced in the periphery, including deletion of responding cells, induction of a state of unresponsiveness termed anergy, and differentiation of regulatory or suppressor cells that prevent other cells from responding to antigen. In addition, the active immune response may be deviated toward a functional phenotype that avoids pathology. Under many experimental conditions, multiple mechanisms operate simultaneously, increasing the difficulty of unravelling the underlying biochemistry.

It has often been assumed that the administration of tolerogenic foreign antigen, or the manipulation of experimental models so that naive T cells first contact high affinity self-antigen in the periphery, recapitulates a process whereby self-tolerance is induced and maintained *in vivo*. However, comparison of the TCR repertoire to tissue-specific self-antigens in normal animals vs those in which the antigen is absent as a result of a genetic lesion (68) shows that they are not equivalent. Thus, normal animals have deleted the highest affinity tissue antigen-specific cells in the thymus and the residual repertoire of self-reactive T cells in the periphery is of lower average affinity than an unselected repertoire exposed to that self-antigen for the first time. On the other hand, when a foreign antigen is administered in a tolerogenic fashion to mimic the induction of self-tolerance, it is recognized by an unselected repertoire that will include TCRs of high affinity. This difference is important for our understanding of peripheral tolerance to exogenous antigen (high affinity) vs self-antigen (low affinity).

### ***3.3. Role of DCs in Peripheral Tolerance to High Affinity Antigen***

In general, protein antigens administered in the absence of adjuvant (or any substances that bind to TLRs) are tolerogenic. In particular, the intravenous, inhalational, and oral routes are well characterized means of inducing tolerance to foreign antigens (66). The intravenous route is postulated to target DCs in a resting or “immature” state in the T cell zones of secondary lymphoid tissues. This phenomenon has led to the idea that contact between naive T cells and “immature” DCs is tolerogenic. There is considerable experimental evidence in support of this model. For example, administration of high doses of soluble antigen results in presentation of the antigen by steady state peripheral DCs as well as thymic DCs, which leads to simultaneous central and peripheral deletion of antigen-specific T cells (69,70). Antigen delivery to the DC endocytic compartment by targeting the DEC205 receptor results in peripheral tolerance through deletion of the majority of adoptively transferred antigen-specific



CD4<sup>+</sup> or CD8<sup>+</sup> T cells and induction of anergy in the remaining cells (71,72). Targeting of DC-SIGN, another endocytic receptor important for uptake of some mycobacteria species and HIV-1, has been shown to induce immunosuppression by interfering with LPS-induced DC maturation (73). Another means of antigen targeting that does not result in DC maturation or activation is uptake of apoptotic cells by DCs (74). Antigens expressed by apoptotic cells can be presented to specific CD4<sup>+</sup> and CD8<sup>+</sup> T cells via direct or cross-presentation (74–77). In contrast, phagocytosis of necrotic cells results in DC activation, probably via concomitant release of inflammatory cytokines that activate DCs (74).

These findings support a model in which DCs that present antigen without receiving an activation signal are tolerogenic. However, the precise phenotypic and functional characteristics of the DCs that induce tolerance in these models are not clear, nor are the molecular mechanisms that they use to signal tolerance to T cells. Moreover, their origin (lymphoid and/or myeloid) is also unknown at this time.

### **3.4. Conversion of High Affinity Peripheral Tolerance to Immunity**

Activation of DCs *in vivo* is associated with the induction of primary T-cell immunity and the generation of memory. A number of different stimuli can activate DCs and induce immunogenic responses. Activated NKT cells responding to ligands presented by CD1d molecules on DCs can transmit activation signals (78). Pathogens can directly stimulate DCs via production of ligands that bind to TLRs expressed either on the DC surface (TLR 2,4) or intracellularly (TLR 3,7,9) (reviewed in ref. 79). Importantly, the activation state of the DC, rather than its maturation status, is important for the priming of memory. Thus immature DCs incubated with agents such as dexamethasone (80), vitamin D3 (81), or the Rel-B inhibitor Bay 11-7082 (82) can induce peripheral tolerance, despite expressing levels of CD86 equivalent to those of mature DCs. The tolerogenic effect is due to inhibition of the CD40L-CD40 DC activation pathway, and can be mimicked by use of DCs generated from CD40<sup>-/-</sup> mice or RelB<sup>-/-</sup> mice (82,83). A DC that has received a CD40 activation signal from the CD4<sup>+</sup> T cell is considered “licensed” to fully activate CD8 T cells (15,16,84). Thus presentation of a viral epitope *in vivo* by resting DCs induces antigen-specific CD8<sup>+</sup> T-cell tolerance unless the DCs are activated by administration of anti-CD40 (85). Similarly, mature DCs induce CD8<sup>+</sup> T-cell tolerance to the cross-presented influenza virus antigen unless they are activated via the CD40 pathway (86).

It is often assumed that the effect of DC activating agents is to convert tolerogenic DCs into immunogenic DCs by changing their phenotypic and functional characteristics. For example, one of the proposed mechanisms of CD40-dependent DC activation is release of DCs from steady state inhibitory interaction



with regulatory T cells (*see below*) (87). Consequently, DCs stop producing indoleamine 2,3-dioxygenase, an enzyme involved in catabolism of tryptophan required by proliferating T cells (88). However, DC activating agents are also capable of inducing the movement of DCs from the periphery of lymphoid organs into the central T cell zones, raising the alternative possibility that the movement of a subset of specialized immunogenic DCs into contact with naïve T cells is responsible for the conversion of tolerogenic to immunogenic responses. Distinguishing between these two possibilities is technically difficult, especially because of the lack of an *in vitro* model for peripheral naïve T cell tolerance. Restriction of antigen-presentation to defined subsets of DCs *in vivo* is an experimental maneuver that we are currently applying to this problem (47).

### 3.5. Are There Specialized Subpopulations of Regulatory DCs?

As discussed above, antigen presentation by resting DCs (*i.e.*, in the absence of a CD40 signal) leads to peripheral tolerance, suggesting that steady state contact between DCs and naïve T cells is, by default, tolerogenic (50,85,89). Similarly, DCs that acquire antigen upon mucosal exposure generally mediate antigen-specific tolerance (12). There is some evidence that IDC exert regulatory functions. Thus, acute depletion of IDC resulted in an asthmatic reaction to otherwise harmless inhaled antigen (90). Conversely, administration of mobilized stem cell preparations containing higher numbers of plasmacytoid preDCs was associated with lower risk of graft-vs-host disease in the posttransplant period (91).

In addition, two recently described mouse DC subsets can regulate ongoing T cell responses via production of IL-10. The first is a CD11c<sup>low</sup>CD11b<sup>+</sup>CD45RB<sup>+</sup> subset of regulatory DCs (DCreg) with plasmacytoid morphology, present in normal spleen and LN and enriched in IL-10 transgenic or *Leishmania*-infected mice (92,93). DCreg differ from IDCs in phenotype (B220<sup>-</sup>Gr1<sup>-</sup>DEC205<sup>int</sup>CD4<sup>int</sup>CD8<sup>-</sup>) and function, producing IL-10 rather than IFN- $\alpha$ . They inhibit antigen-dependent proliferation and Th1 cytokine production of CD4<sup>+</sup> T cells *in vitro* and *in vivo* and B-cell antibody isotype switching *in vivo* (92,93), in addition to driving the differentiation of IL-10-producing regulatory Tr1 cells (*see below*).

A second population of regulatory DC, termed differentiated DC (diffDC), can be generated by means of cell division of fully matured bone-marrow derived DCs cocultured with splenic stromal cells. They exhibit a CD11c<sup>low</sup>MHC class II<sup>low</sup>CD86<sup>low</sup>CD40<sup>hi</sup>CD80<sup>hi</sup>CD11b<sup>hi</sup> phenotype (94). Most strikingly, diffDC generation requires a direct cell-cell contact and is partially TGF $\beta$ -dependent. DiffDC inhibit antigen-dependent proliferation of CD4<sup>+</sup> T cells *in vitro* and *in vivo* in a nitric oxide- and IL-10-dependent manner.

### 3.6. Peripheral Tolerance to Low Affinity (Self) Antigen

In contrast to the high affinity T cell repertoire described above, the self-reactive T cell repertoire is of relatively low affinity. Insufficient self-antigen is generally available in the periphery to provide an activation signal for these cells and they remain naïve. However, they can, under defined circumstances, make significant anti-self-responses that have the potential to develop into full-blown autoimmune disease. This implies that the threshold at which the thymus imposes deletional tolerance must be quite close to the normal activation threshold in the periphery. Why the thymic threshold is not set lower remains an interesting question, but it is reasonable to assume that preservation of a sufficiently large repertoire of anti-foreign specificities requires that purging for anti-self-reactivity be limited.

What are the circumstances in which activation of low affinity anti-self T cells will generate autoimmune pathology? Although it has long been held that infection with a pathogen expressing a cross-reactive epitope is sufficient to break self-tolerance, there is little experimental support for this notion. Indeed, in early experiments designed to induce autoimmune disease, gross disturbance of the T-cell compartment (for example, via adult thymectomy combined with irradiation, treatment with anti-lymphocyte globulin, or use of cyclophosphamide) was necessary (reviewed in [ref. 1](#)). Models in which gross disturbance of the T-cell compartment is required usually induce a state of CD4<sup>+</sup> T cell lymphopenia. Indeed, it was by studying one of these lymphopenic models that Sakaguchi first realized the importance of CD4<sup>+</sup>CD25<sup>+</sup> regulatory cells (Treg) in maintaining self-tolerance ([95](#)).

## 4. Regulatory T Cells

### 4.1. CD4<sup>+</sup> Regulatory T Cells Constitutively Expressing CD25

The evidence in support of a role for CD4<sup>+</sup>CD25<sup>+</sup> regulatory T cells (Treg) in the maintenance of self-tolerance in the normal, low affinity self-reactive T cell compartment is now well accepted. Not only is a deficit in Treg associated with development of spontaneous autoimmune disease, but reconstitution of this T cell subpopulation can prevent disease in animal models ([95](#)). Treg are selected by their specificity for self-antigen in the thymus, and the currently available evidence suggests that they represent those cells with the highest anti-self-affinity among the population that escapes negative selection, i.e., that they have an anti-self affinity intermediate between that of cells that are deleted and cells that undergo conventional positive selection ([96,97](#)). In one experimental model, it has been demonstrated that thymic epithelium is the source of the selecting antigen ([98](#)). However, the process of selection is dependent on CD28-B7 interactions, suggesting that antigen is probably transferred to a

thymic DC for presentation to Treg (99). Like positive selection, selection of Treg is stochastic, because not every T cell with a permissive TCR is selected into the Treg compartment (100). Treg display an activated phenotype in the thymus, consistent with exposure to a TCR signal-mediated selective event (96). Once in the periphery, their phenotype reflects the degree to which they continue to receive TCR-mediated signals from self-antigen and any environmental antigens that cross-react with self.

The master regulator transcription factor Foxp3 is essential for Treg selection and function. Mice with defective Foxp3 develop multisystem inflammatory disease and succumb at an early age (101,102). In humans, Foxp3 mutations have been found in patients with the severe IPEX syndrome (103,104). Interestingly, this syndrome is more akin to Metchnikoff's "horror autotoxicus" than the APECED syndrome in which negative selection in the thymus is defective because of decreased expression of self-antigen, indicating the relative importance of thymic vs peripheral mechanisms in the maintenance of self-tolerance.

The mechanism of action of Treg is controversial. In vitro studies have indicated that a cell-surface interaction with conventional T cells is required to suppress the proliferation of the latter cells. No candidate molecules have been identified, apart from surface TGF- $\beta$ , a result that has been disputed by several investigators (105,106). However, evidence from in vivo studies suggests that the in vitro assay may not mimic the in vivo situation. In lymphopenic mice, the development of autoimmune disease is dependent on proliferation of self-reactive CD4<sup>+</sup> T cells that would not normally undergo any proliferation at all. Thus, Treg appear to prevent the recruitment of T cells into division, rather than reducing the division rate as they do in vitro. Second, in vitro assays are not dependent on the presence of DCs, but reflect the ratio of Treg to conventional T cells. In vivo, on the other hand, the ratio of Treg to conventional T cells appears to be preserved in many of the lymphopenic models in which spontaneous autoimmune disease develops, whereas the ratio of Treg to DCs is decreased.

Direct confirmation of the importance of interactions between Treg and DCs has come from recently published studies using intravital microscopy to track Treg in living lymphoid tissue, in which Treg formed stable associations not with conventional T cells but with DCs (107). Our own unpublished studies of the interaction between Treg and DCs in vivo indicate that Treg control expression of costimulatory molecules by DCs (Koh, W. -P., Power, C., and Fazekas de St. Groth, B., unpublished observations). Evidence for this model also comes from in vitro studies in which Treg were able to reduce expression of CD86 by DCs isolated from the spleen (108). By reducing the level of costimulation, Treg have a relatively greater effect on low affinity responses such as those to self-antigen, as the requirement for costimulation is greater when antigen availability and affinity are low. Thus the function of Treg may be differentially

focused on anti-self-responses not only because of the self-reactivity of their TCR repertoire, but also because of their enhanced effectiveness in suppressing low rather than high affinity responses.

Interestingly, soluble mediators such as IL-10 and TGF- $\beta$  have been implicated in Treg function in vivo, although it is not clear whether Treg actually rely on these suppressive cytokines for functional activity. Recent data indicate that Treg express high levels of receptors for IL-10 and TGF- $\beta$  (109), so the in vivo data indicating a requirement for these molecules in Treg function may relate to their effects on Treg themselves, rather than on conventional T cells or DCs.

Studies from the laboratory of von Boehmer have indicated that Treg can differentiate from conventional CD25<sup>-</sup> T cells in the periphery under conditions of very low avidity signaling (110). Thus the signaling requirements for Treg development in the thymus and periphery are similar (96). Peripheral Treg express many of the same molecules as Treg selected in the thymus, including CTLA-4 and Foxp3. However, they may also manifest as yet undefined differences. Interestingly, although some investigators have shown that transfection with Foxp3 or treatment with TGF- $\beta$  (which drives expression of Foxp3) can confer suppressive activity in vitro (111), others have not reproduced these results (112). Given the avidity constraints on the TCR repertoire of Treg selected in vivo, these results may indicate that only cells of intermediate affinity can exert regulatory function.

#### **4.2. Regulatory T Cells Generated in Response to Foreign Antigen**

In contrast to Treg, Tr1 are derived from conventional naive CD4<sup>+</sup> T cells after peripheral contact with high doses of foreign antigen. They produce high levels of IL-10 and mediate IL-10-dependent suppression in vitro and in vivo (113). In vivo they may develop under the influence of IL-10-producing DCs such as the DCreg and diffDC mentioned above. In vitro, Tr1 cells are usually generated in the presence of pharmacological levels of IL-10, and their place within the spectrum of in vivo regulatory mechanisms is unclear. Although cells producing large amounts of IL-10 have been isolated ex vivo from patients with highly abnormal immune systems (114), spontaneous pathology in IL-10-deficient mice is limited to inflammation of the bowel (115), indicating that the function of IL-10 at other sites may be redundant.

A third subset of regulatory T cells is the Th3 cells that produce TGF- $\beta$ . These are particularly associated with mucosal surfaces where TGF- $\beta$  levels are high. Like Tr1, they arise after stimulation of conventional naive CD4<sup>+</sup> T cells with foreign antigen (116). There is some evidence that DCs derived from mucosal sites have the ability to drive T-cell differentiation toward a Th3 phenotype (117). TGF- $\beta$  has a wide range of activities apart from its immunosuppressive properties and, once again, a detailed analysis of its effects on individual T cell and DC subsets in vivo has not been performed.

## 5. Tolerance Induction Using DC Vaccines: Current Approaches

Human DCs generated *ex vivo* have so far been used for induction of immunity rather than tolerance, particularly in the field of clinical cancer immunotherapy. An understanding of how DCs induce immunity vs tolerance is crucial not only for the development of such vaccines (118,119), but for expanding their use in autoimmune diseases and in solid organ transplantation. Several approaches have been trialed, including prevention of DC activation *in vivo* after transfer of immature DCs by use of nuclear factor- $\kappa$ B deficient DCs or coinjection of anti-CD40L mAb, and generation of tolerogenic DCs by pharmacological treatment *in vitro*, using cytokines such as IL-10, TGF- $\beta$ 1, PgE2, vitamin D3 metabolites, specific nuclear factor- $\kappa$ B inhibitors, rapamycin, and other immunosuppressive drugs. In addition, targeting resting DCs through the administration of apoptotic cells is a possible means of inducing donor-specific tolerance in organ transplantation (reviewed in **ref. 120**).

## 6. Conclusions

Maintenance of tolerance is a complex and demanding role for the adaptive immune system. The generation of a semirandom repertoire of antigen-receptors, while providing the means to develop antigen-specific memory for virtually every possible epitope, brings with it the daunting task of controlling the inherent self-reactivity of the system. At the heart of this control is the interaction between the DC and the T cell. As we learn about these interactions in more detail, using *in vivo* models that can adequately mimic the normal decision-making process between tolerance and immunity, we will gain insights that can improve the translation of experimental immune manipulation into the clinical setting.

## Acknowledgments

Barbara Fazekas de St. Groth is supported by a Principal Research Fellowship from the National Health and Medical Research Council of Australia. This work was funded by a Program Grant from the National Health and Medical Research Council of Australia. The support of the New South Wales Health Department through its research and infrastructure grants program is gratefully acknowledged.

## References

1. Fazekas de St. Groth, B. (1995) Regulation of the immune response: lessons from transgenic models. *Aust. N. Z. J. Med.* **25**, 761–767.
2. Caux, C., Dezutter-Dambuyant, C., Schmitt, D., and Banchereau, J. (1992) GM-CSF and TNF co-operate in the generation of dendritic Langerhans cells. *Nature* **360**, 258–261.

3. Sallusto, F. and Lanzavecchia, A. (1994) Efficient presentation of soluble antigen by cultured human dendritic cells is maintained by granulocyte/macrophage colony-stimulating factor plus interleukin 4 and downregulated by tumor necrosis factor  $\alpha$ . *J. Exp. Med.* **179**, 1109–1118.
4. Banchereau, J., Briere, F., Caux, C., et al. (2000) Immunobiology of dendritic cells. *Annu. Rev. Immunol.* **18**, 767–811.
5. Trombetta, E. S. and Mellman, I. (2005) Cell biology of antigen processing in vitro and in vivo. *Annu. Rev. Immunol.* **23**, 975–1028.
6. Inaba, K., Pack, M., Inaba, M., Sakuta, H., Isdell, F., and Steinman, R. M. (1997) High levels of a major histocompatibility complex II-self peptide complex on dendritic cells from the T cell areas of lymph nodes. *J. Exp. Med.* **186**, 665–672.
7. Lindquist, R. L., Shakhar, G., Dudziak, D., et al. (2004) Visualizing dendritic cell networks in vivo. *Nat. Immunol.* **5**, 1243–1250.
8. Wilson, N., El-Sukkari, D., Belz, G. T., et al. (2003) Most lymphoid organ dendritic cell types are phenotypically and functionally immature. *Blood* **102**, 2187–2194.
9. Liu, L., Zhang, M., Jenkins, C., and MacPherson, G. G. (1998) Dendritic cell heterogeneity in vivo: two functionally different dendritic cell populations in rat intestinal lymph can be distinguished by CD4 expression. *J. Immunol.* **161**, 1146–1155.
10. Jakob, T., Ring, J., and Udey, M. C. (2001) Multistep navigation of Langerhans/dendritic cells in and out of the skin. *J. Allergy Clin. Immunol.* **108**, 688–696.
11. Allan, R. S., Smith, C. M., Belz, G. T., et al. (2003) Epidermal viral immunity induced by CD8alpha+ dendritic cells but not by Langerhans cells. *Science* **301**, 1925–1928.
12. Akbari, O., DeKruyff, R. H., and Umetsu, D. T. (2001) Pulmonary dendritic cells producing IL-10 mediate tolerance induced by respiratory exposure to antigen. *Nat. Immunol.* **2**, 725–731.
13. Steinman, R. M., Turley, S., Mellman, I., and Inaba, K. (2000) The induction of tolerance by dendritic cells that have captured apoptotic cells. *J. Exp. Med.* **191**, 411–416.
14. Matzinger, P. (1994) Tolerance, danger, and the extended family. *Annu. Rev. Immunol.* **12**, 991–1045.
15. Ridge, J. P., Di Rosa, F., and Matzinger, P. (1998) A conditioned dendritic cell can be a temporal bridge between a CD4<sup>+</sup> T-helper and a T-killer cell. *Nature* **393**, 474–478.
16. Bennett, S. R. M., Carbone, F. R., Karamalis, F., Flavell, R. A., Miller, J. F. A. P., and Heath, W. R. (1998) Help for cytotoxic-T-cell responses is mediated by CD40 signalling. *Nature* **393**, 478–480.
17. Kamath, A. T., Pooley, J., O’Keeffe, M. A., et al. (2000) The development, maturation, and turnover rate of mouse spleen dendritic cell populations. *J. Immunol.* **165**, 6762–6770.
18. Romani, N., Gruner, S., Brang, D., et al. (1994) Proliferating dendritic cell progenitors in human blood. *J. Exp. Med.* **180**, 83–93.

19. Grouard, G., Rissoan, M. -C., Filgueira, L., Durand, I., Banchereau, J., and Liu, Y. -J. (1997) The enigmatic plasmacytoid T cells develop into dendritic cells with interleukin (IL)-3 and CD40-ligand. *J. Exp. Med.* **185**, 1101–1111.
20. Inaba, K., Steinman, R. M., Pack, M. W., et al. (1992) Identification of proliferating dendritic cell precursors in mouse blood. *J. Exp. Med.* **175**, 1157–1167.
21. del Hoyo, G. M., Martin, P., Vargas, H. H., Ruiz, S., Arias, C. F., and Ardavin, C. (2002) Characterization of a common precursor population for dendritic cells. *Nature* **415**, 1043–1047.
22. von Garnier, C., Filgueira, L., Wikstrom, M., et al. (2005) Anatomical location determines the distribution and function of dendritic cells and other APCs in the respiratory tract. *J. Immunol.* **175**, 1609–1618.
23. Niess, J. H., Brand, S., Gu, X., et al. (2005) CX3CR1-mediated dendritic cell access to the intestinal lumen and bacterial clearance. *Science* **307**, 254–258.
24. Vremec, D. and Shortman, K. (1997) Dendritic cell subtypes in mouse lymphoid organs. Cross-correlation of surface markers, changes with incubation and differences among thymus, spleen and lymph nodes. *J. Immunol.* **159**, 565–573.
25. Steinman, R. M., Pack, M., and Inaba, K. (1997) Dendritic cells in the T-cell areas of lymphoid organs. *Immunol. Rev.* **156**, 25–37.
26. De Smedt, T., Pajak, B., Muraille, E., et al. (1996) Regulation of dendritic cell numbers and maturation by lipopolysaccharide in vivo. *J. Exp. Med.* **184**, 1413–1424.
27. Fazekas de St. Groth, B. (1998) The evolution of self tolerance: a new cell is required to meet the challenge of self-reactivity. *Immunol. Today* **19**, 448–454.
28. Asselin-Paturel, C., Boonstra, A., Dalod, M., et al. (2001) Mouse type I IFN-producing cells are immature APCs with plasmacytoid morphology. *Nat. Immunol.* **2**, 1144–1150.
29. Liu, Y. J. (2005) IPC: professional type 1 interferon-producing cells and plasmacytoid dendritic cell precursors. *Annu. Rev. Immunol.* **23**, 275–306.
30. Rissoan, M. -C., Soumelis, V., Kadowaki, N., et al. (1999) Reciprocal control of T helper cell and dendritic cell differentiation. *Science* **283**, 1183–1186.
31. Cella, M., Jarrossay, D., Facchetti, F., et al. (1999) Plasmacytoid monocytes migrate to inflamed lymph nodes and produce large amounts of type I interferon. *Nat. Med.* **5**, 919–923.
32. Siegal, F. P., Kadowaki, N., Shodell, M., et al. (1999) The nature of the principal type 1 interferon-producing cells in human blood. *Science* **284**, 1835–1837.
33. Galibert, L., Diemer, G. S., Liu, Z., et al. (2005) Nectin-like protein 2 defines a subset of T-cell zone dendritic cells and is a ligand for class-I-restricted T-cell-associated molecule. *J. Biol. Chem.* **280**, 21,955–21,964.
34. Wu, L., D'Amico, A., Hochrein, H., O'Keeffe, M., Shortman, K., and Lucas, K. (2001) Development of thymic and splenic dendritic cell populations from different hemopoietic precursors. *Blood* **98**, 3376–3382.
35. Manz, M. G., Traver, D., Miyamoto, T., Weissman, I. L., and Akashi, K. (2001) Dendritic cell potentials of early lymphoid and myeloid progenitors. *Blood* **97**, 3333–3341.

36. Martin, P., Martinez del Hoyo, G., Anjuere, F., et al. (2000) Concept of lymphoid versus myeloid dendritic cell lineages revisited: both CD8 $\alpha$ <sup>-</sup> and CD8 $\alpha$ <sup>+</sup> dendritic cells are generated from CD4<sup>low</sup> lymphoid-committed precursors. *Blood* **96**, 2511–2519.
37. D'Amico, A. and Wu, L. (2003) The early progenitors of mouse dendritic cells and plasmacytoid predendritic cells are within the bone marrow hemopoietic precursors expressing Flt3. *J. Exp. Med.* **198**, 293–303.
38. Merad, M., Manz, M. G., Karsunky, H., et al. (2002) Langerhans cells renew in the skin throughout life under steady-state conditions. *Nat. Immunol.* **3**, 1135–1141.
39. Anjuere, F., Martinez del Hoyo, G., Martin, P., and Ardavin, C. (2000) Langerhans cells develop from a lymphoid-committed precursor. *Blood* **96**, 1633–1637.
40. Karsunky, H., Merad, M., Cozzio, A., Weissman, I. L., and Manz, M. G. (2003) Flt3 ligand regulates dendritic cell development from Flt3<sup>+</sup> lymphoid and myeloid-committed progenitors to Flt3<sup>+</sup> dendritic cells in vivo. *J. Exp. Med.* **198**, 305–313.
41. Maraskovsky, E., Brasel, K., Teepe, M., et al. (1996) Dramatic increase in the numbers of functionally mature dendritic cells in Flt3 ligand-treated mice: multiple dendritic cell subpopulations identified. *J. Exp. Med.* **184**, 1953–1962.
42. Pulendran, B., Lingappa, J., Kennedy, M., et al. (1997) Developmental pathways of dendritic cells in vivo: Distinct function, phenotype, and localization of dendritic cell subsets in FLT3 ligand-treated mice. *J. Immunol.* **159**, 2222–2231.
43. Bernhard, H., Disis, M. L., Heimfeld, S., Hand, S., Gralow, J. R., and Cheever, M. A. (1995) Generation of immunostimulatory dendritic cells from human CD34<sup>+</sup> hematopoietic progenitor cells of the bone marrow and peripheral blood. *Cancer Res.* **55**, 1099–1104.
44. Caux, C., Massacrier, C., Vanbervliet, B., et al. (1997) CD34<sup>+</sup> hematopoietic progenitors from human cord blood differentiate along two independent dendritic cell pathways in response to granulocyte-macrophage colony-stimulating factor plus tumor necrosis factor  $\alpha$ : II. Functional analysis. *Blood* **90**, 1458–1470.
45. Maraskovsky, E., Daro, E., Roux, E., et al. (2000) In vivo generation of human dendritic cell subsets by Flt3 ligand. *Blood* **96**, 878–884.
46. Randolph, G. J., Beaulieu, S., Lebecque, S., Steinman, R. M., and Muller, W. A. (1998) Differentiation of monocytes into dendritic cells in a model of transendothelial trafficking. *Science* **282**, 480–483.
47. Fazekas de St. Groth, B., Smith, A. L., Bosco, J., Sze, D. M. -Y., Power, C. A., and Austen, F. I. (2002) Experimental models linking dendritic cell lineage, phenotype and function. *Immunol. Cell Biol.* **80**, 469–476.
48. Ardavin, C., Wu, L., Li, C. -L., and Shortman, K. (1993) Thymic dendritic cells and T cells develop simultaneously in the thymus from a common precursor population. *Nature* **362**, 761–763.
49. Corcoran, L., Ferrero, I., Vremec, D., et al. (2003) The lymphoid past of mouse plasmacytoid cells and thymic dendritic cells. *J. Immunol.* **170**, 4926–4932.



50. Belz, G. T., Behrens, G. M., Smith, C. M., et al. (2002) The CD8alpha<sup>+</sup> dendritic cell is responsible for inducing peripheral self-tolerance to tissue-associated antigens. *J. Exp. Med.* **196**, 1099–1104.
51. Belz, G. T., Smith, C. M., Eichner, D., et al. (2004) Conventional CD8 alpha<sup>+</sup> dendritic cells are generally involved in priming CTL immunity to viruses. *J. Immunol.* **172**, 1996–2000.
52. Carbone, F. R., Belz, G. T., and Heath, W. R. (2004) Transfer of antigen between migrating and lymph node-resident DCs in peripheral T-cell tolerance and immunity. *Trends Immunol.* **25**, 655–658.
53. Thery, C., Regnault, A., Garin, J., et al. (1999) Molecular characterization of dendritic cell-derived exosomes. Selective accumulation of the heat shock protein hsc73. *J. Cell Biol.* **147**, 599–610.
54. Thery, C., Duban, L., Segura, E., Veron, P., Lantz, O., and Amigorena, S. (2002) Indirect activation of naive CD4<sup>+</sup> T cells by dendritic cell-derived exosomes. *Nat. Immunol.* **3**, 1156–1162.
55. Smith, A. L. and Fazekas de St. Groth, B. (1999) Antigen-pulsed CD8α<sup>+</sup> dendritic cells generate an immune response without homing to the draining lymph node. *J. Exp. Med.* **189**, 593–598.
56. Itano, A. A., McSorley, S. J., Reinhardt, R. L., et al. (2003) Distinct dendritic cell populations sequentially present antigen to CD4 T cells and stimulate different aspects of cell-mediated immunity. *Immunity* **19**, 47–57.
57. Stockinger, B. (1999) T lymphocyte tolerance: from thymic deletion to peripheral control mechanisms. *Adv. Immunol.* **71**, 229–265.
58. McGargill, M. A., Derbinski, J. M., and Hogquist, K. A. (2000) Receptor editing in developing T cells. *Nat. Immunol.* **1**, 336–341.
59. Derbinski, J., Schulte, A., Kyewski, B., and Klein, L. (2001) Promiscuous gene expression in medullary thymic epithelial cells mirrors the peripheral self. *Nat. Immunol.* **2**, 1032–1039.
60. Anderson, M. S., Venzani, E. S., Klein, L., et al. (2002) Projection of an immunological self shadow within the thymus by the aire protein. *Science* **298**, 1395–1401.
61. Gallegos, A. M. and Bevan, M. J. (2004) Central tolerance to tissue-specific antigens mediated by direct and indirect antigen presentation. *J. Exp. Med.* **200**, 1039–1049.
62. Owen, R. D. (1945) Immunogenetic consequences of vascular anastomoses between bovine twins. *Science* **102**, 400–401.
63. Lechler, R. I., Sykes, M., Thomson, A. W., and Turka, L. A. (2005) Organ transplantation-how much of the promise has been realized? *Nat. Med.* **11**, 605–613.
64. Burnet, F. M. and Fenner, F. (1949) *The Production of Antibodies*. Macmillan, New York.
65. Smith, R. T. (1961) Immunological tolerance of nonliving antigens. *Adv. Immunol.* **1**, 67–129.
66. Weigle, W. O. (1973) Immunological unresponsiveness. *Adv. Immunol.* **16**, 61–123.
67. Rocha, B. and von Boehmer, H. (1991) Peripheral selection of the T cell repertoire. *Science* **251**, 1225–1228.

68. Targoni, O. S. and Lehmann, P. V. (1998) Endogenous myelin basic protein inactivates the high avidity T cell repertoire. *J. Exp. Med.* **187**, 2055–2063.
69. Smith, A. L., Wikstrom, M. E., and Fazekas de St. Groth, B. (2000) Visualizing T cell competition for peptide/MHC complexes: a specific mechanism to minimize the effect of precursor frequency. *Immunity* **13**, 783–794.
70. Zhong, G., Reis e Sousa, C., and Germain, R. N. (1997) Antigen-unspecific B cells and lymphoid dendritic cells both show extensive surface expression of processed antigen-major histocompatibility complex class II complexes after soluble protein exposure in vivo or in vitro. *J. Exp. Med.* **186**, 673–682.
71. Hawiger, D., Inaba, K., Dorsett, Y., et al. (2001) Dendritic cells induce peripheral T cell unresponsiveness under steady state conditions in vivo. *J. Exp. Med.* **194**, 769–779.
72. Bonifaz, L., Bonnyay, D., Mahnke, K., Rivera, M., Nussenzweig, M. C., and Steinman, R. M. (2002) Efficient targeting of protein antigen to the dendritic cell receptor DEC-205 in the steady state leads to antigen presentation on major histocompatibility complex class I products and peripheral CD8<sup>+</sup> T cell tolerance. *J. Exp. Med.* **196**, 1627–1638.
73. Geijtenbeek, T. B., Van Vliet, S. J., Koppel, E. A., et al. (2003) Mycobacteria target DC-SIGN to suppress dendritic cell function. *J. Exp. Med.* **197**, 7–17.
74. Sauter, B., Albert, M. L., Francisco, L., Larsson, M., Somersan, S., and Bhardwaj, N. (2000) Consequences of cell death: exposure to necrotic tumor cells, but not primary tissue cells or apoptotic cells, induces the maturation of immunostimulatory dendritic cells. *J. Exp. Med.* **191**, 423–433.
75. Albert, M. L., Sauter, B., and Bhardwaj, N. (1998) Dendritic cells acquire antigen from apoptotic cells and induce class I-restricted CTLs. *Nature* **392**, 86–87.
76. Albert, M. L., Pearce, S. F., Francisco, L. M., et al. (1998) Immature dendritic cells phagocytose apoptotic cells via  $\alpha_v\beta_5$  and CD36, and cross-present antigens to cytotoxic T lymphocytes. *J. Exp. Med.* **188**, 1359–1368.
77. Huang, F. P., Platt, N., Wykes, M., et al. (2000) A discrete subpopulation of dendritic cells transports apoptotic intestinal epithelial cells to T cell areas of mesenteric lymph nodes. *J. Exp. Med.* **191**, 435–444.
78. Fujii, S. -I., Shimizu, K., Smith, C., Bonifaz, L., and Steinman, R. M. (2003) Activation of natural killer T cells by  $\alpha$ -galactosylceramide rapidly induces the full maturation of dendritic cells in vivo and thereby acts as an adjuvant for combined CD4 and CD8 T cell immunity to a coadministered protein. *J. Exp. Med.* **198**, 267–279.
79. Rifkin, I. R., Leadbetter, E. A., Busconi, L., Viglianti, G., and Marshak-Rothstein, A. (2005) Toll-like receptors, endogenous ligands, and systemic autoimmune disease. *Immunol. Rev.* **204**, 27–42.
80. Rea, D., van Kooten, C., van Meijgaarden, K. E., Ottenhoff, T. H., Melief, C. J., and Offringa, R. (2000) Glucocorticoids transform CD40-triggering of dendritic cells into an alternative activation pathway resulting in antigen-presenting cells that secrete IL-10. *Blood* **95**, 3162–3167.

81. Adorini, L., Penna, G., Giarratana, N., and Uskokovic, M. (2003) Tolerogenic dendritic cells induced by vitamin D receptor ligands enhance regulatory T cells inhibiting allograft rejection and autoimmune diseases. *J. Cell. Biochem.* **88**, 227–233.
82. Martin, E., O'Sullivan, B., Low, P., and Thomas, R. (2003) Antigen-specific suppression of a primed immune response by dendritic cells mediated by regulatory T cells secreting interleukin-10. *Immunity* **18**, 155–167.
83. Hochweller, K. and Anderton, S. M. (2004) Systemic administration of antigen-loaded CD40-deficient dendritic cells mimics soluble antigen administration. *Eur. J. Immunol.* **34**, 990–998.
84. Smith, C. M., Wilson, N. S., Waithman, J., et al. (2004) Cognate CD4<sup>+</sup> T cell licensing of dendritic cells in CD8<sup>+</sup> T cell immunity. *Nat. Immunol.* **5**, 1143–1148.
85. Probst, H. C., Lagnel, J., Kollias, G., and van den Broek, M. (2003) Inducible transgenic mice reveal resting dendritic cells as potent inducers of CD8<sup>+</sup> T cell tolerance. *Immunity* **18**, 713–720.
86. Albert, M. L., Jegathesan, M., and Darnell, R. B. (2001) Dendritic cell maturation is required for the cross-tolerization of CD8<sup>+</sup> T cells. *Nat. Immunol.* **2**, 1010–1017.
87. Serra, P., Amrani, A., Yamanouchi, J., et al. (2003) CD40 ligation releases immature dendritic cells from the control of regulatory CD4<sup>+</sup>CD25<sup>+</sup> T cells. *Immunity* **19**, 877–889.
88. Fallarino, F., Grohmann, U., Hwang, K. W., et al. (2003) Modulation of tryptophan catabolism by regulatory T cells. *Nat. Immunol.* **4**, 1206–1212.
89. Martin, P., Del Hoyo, G. M., Anjuere, F., et al. (2002) Characterization of a new subpopulation of mouse CD8 $\alpha$ <sup>+</sup> B220<sup>+</sup> dendritic cells endowed with type 1 interferon production capacity and tolerogenic potential. *Blood* **100**, 383–390.
90. de Heer, H. J., Hammad, H., Soullie, T., et al. (2004) Essential role of lung plasmacytoid dendritic cells in preventing asthmatic reactions to harmless inhaled antigen. *J. Exp. Med.* **200**, 89–98.
91. Arpinati, M., Green, C. L., Heimfeld, S., Heuser, J. E., and Anasetti, C. (2000) Granulocyte-colony stimulating factor mobilizes T helper 2-inducing dendritic cells. *Blood* **95**, 2484–2490.
92. Wakkach, A., Fournier, N., Brun, V., Breitmayer, J. P., Cottrez, F., and Groux, H. (2003) Characterization of dendritic cells that induce tolerance and T regulatory 1 cell differentiation in vivo. *Immunity* **18**, 605–617.
93. Svensson, M., Maroof, A., Ato, M., and Kaye, P. M. (2004) Stromal cells direct local differentiation of regulatory dendritic cells. *Immunity* **21**, 805–816.
94. Zhang, M., Tang, H., Guo, Z., et al. (2004) Splenic stroma drives mature dendritic cells to differentiate into regulatory dendritic cells. *Nat. Immunol.* **5**, 1124–1133.
95. Sakaguchi, S., Sakaguchi, N., Asano, M., Itoh, M., and Toda, M. (1995) Immunologic self-tolerance maintained by activated T cells expressing IL-2 receptor  $\alpha$ -chains (CD25). *J. Immunol.* **155**, 1151–1164.

96. Fazekas de St Groth, B., Smith, A. L., and Higgins, C. A. (2004) T cell activation: in vivo veritas. *Immunol. Cell. Biol.* **82**, 260–268.
97. Sakaguchi, S. (2004) Naturally arising CD4<sup>+</sup> regulatory T cells for immunologic self-tolerance and negative control of immune responses. *Annu. Rev. Immunol.* **22**, 531–562.
98. Jordan, M. S., Boesteanu, A., Reed, A. J., et al. (2001) Thymic selection of CD4(+)CD25(+) regulatory T cells induced by an agonist self-peptide. *Nat. Immunol.* **2**, 301–306.
99. Salomon, B., Lenschow, D. J., Rhee, L., et al. (2000) B7/CD28 costimulation is essential for the homeostasis of the CD4<sup>+</sup>CD25<sup>+</sup> immunoregulatory T cells that control autoimmune diabetes. *Immunity* **12**, 431–440.
100. Apostolou, I., Sarukhan, A., Klein, L., and von Boehmer, H. (2002) Origins of regulatory T cells with known specificity for antigen. *Nat. Immunol.* **3**, 756–763.
101. Hori, S., Nomura, T., and Sakaguchi, S. (2003) Control of regulatory T cell development by the transcription factor Foxp3. *Science* **299**, 1057–1061.
102. Khattri, R., Cox, T., Yasayko, S. A., and Ramsdell, F. (2003) An essential role for Scurfin in CD4<sup>+</sup>CD25<sup>+</sup> T regulatory cells. *Nat. Immunol.* **4**, 337–342.
103. Bennett, C. L., Christie, J., Ramsdell, F., et al. (2001) The immune dysregulation, polyendocrinopathy, enteropathy, X-linked syndrome (IPEX) is caused by mutations of FOXP3. *Nat. Genet.* **27**, 20–21.
104. Wildin, R. S., Ramsdell, F., Peake, J., et al. (2001) X-linked neonatal diabetes mellitus, enteropathy and endocrinopathy syndrome is the human equivalent of mouse scurfy. *Nat. Genet.* **27**, 18–20.
105. Nakamura, K., Kitani, A., and Strober, W. (2000) Cell contact-dependent immunosuppression by CD4<sup>+</sup>CD25<sup>+</sup> regulatory T cells is mediated by cell-surface-bound transforming growth factor  $\beta$ . *J. Exp. Med.* **194**, 629–644.
106. Piccirillo, C. A., Letterio, J. J., Thornton, A. M., et al. (2002) CD4<sup>+</sup>CD25<sup>+</sup> regulatory T cells can mediate suppressor function in the absence of transforming growth factor beta1 production and responsiveness. *J. Exp. Med.* **196**, 237–246.
107. Tang, Q., Adams, J. Y., Tooley, A. J., et al. (2006) Visualizing regulatory T cell control of autoimmune responses in nonobese diabetic mice. *Nat. Immunol.* **7**, 83–92.
108. Cederbom, L., Hall, H., and Ivars, F. (2000) CD4<sup>+</sup>CD25<sup>+</sup> regulatory T cells down-regulate co-stimulatory molecules on antigen-presenting cells. *Eur. J. Immunol.* **30**, 1538–1543.
109. Marie, J. C., Letterio, J. J., Gavin, M., and Rudensky, A. Y. (2005) TGF-beta1 maintains suppressor function and Foxp3 expression in CD4<sup>+</sup>CD25<sup>+</sup> regulatory T cells. *J. Exp. Med.* **201**, 1061–1067.
110. Kretschmer, K., Apostolou, I., Hawiger, D., Khazaie, K., Nussenzweig, M. C., and von Boehmer, H. (2005) Inducing and expanding regulatory T cell populations by foreign antigen. *Nat. Immunol.* **6**, 1219–1227.
111. Fontenot, J. D. (2003) Foxp3 programs the development and function of CD4<sup>+</sup>CD25<sup>+</sup> regulatory T cells. *Nat. Immunol.* **4**, 330–336.

112. Allan, S. E., Passerini, L., Bacchetta, R., et al. (2005) The role of 2 FOXP3 isoforms in the generation of human CD4 Tregs. *J. Clin. Invest.* **115**, 3276–3284.
113. Groux, H., O’Garra, A., Bigler, M., et al. (1997) A CD4<sup>+</sup> T-cell subset inhibits antigen-specific T-cell responses and prevents colitis. *Nature* **389**, 737–742.
114. Bacchetta, R., Bigler, M., Touraine, J. L., et al. (1994) High levels of interleukin 10 production in vivo are associated with tolerance in SCID patients transplanted with HLA mismatched hematopoietic stem cells. *J. Exp. Med.* **179**, 493–502.
115. Kühn, R., Löhler, J., Rennick, D., Rajewsky, K., and Müller, W. (1993) Interleukin-10-deficient mice develop chronic enterocolitis. *Cell* **75**, 263–274.
116. Chen, Y., Kuchroo, V. K., Inobe, J., Hafler, D. A., and Weiner, H. L. (1994) Regulatory T cell clones induced by oral tolerance: suppression of autoimmune encephalomyelitis. *Science* **265**, 1237–1240.
117. Faria, A. M. and Weiner, H. L. (2005) Oral tolerance. *Immunol. Rev.* **206**, 232–259.
118. Figdor, C. G., de Vries, I. J., Lesterhuis, W. J., and Melief, C. J. (2004) Dendritic cell immunotherapy: mapping the way. *Nat. Med.* **10**, 475–480.
119. Schuler, G., Schuler-Thurner, B., and Steinman, R. M. (2003) The use of dendritic cells in cancer immunotherapy. *Curr. Opin. Immunol.* **15**, 138–147.
120. Morelli, A. E. and Thomson, A. W. (2003) Dendritic cells: regulators of alloimmunity and opportunities for tolerance induction. *Immunol. Rev.* **196**, 125–146.

## Differentiation of Dendritic Cell Subsets from Mouse Bone Marrow

Ludovica Bruno

### Summary

Dendritic cells (DC) are key regulators of the immune system. They are capable of stimulating lymphocytes to generate potent cell-mediated and humoral immune responses against pathogens and tumor cells. DC not only activate lymphocytes, but can also educate T cells to tolerate self-antigens, thereby minimizing autoimmune reactions. Another peculiarity of the DC system is the large variety of subsets described, both in the human and in the mouse, according to surface phenotype and organ distribution. Different protocols have been developed to differentiate DC from total mouse bone marrow *in vitro*. Here, we describe the isolation of a specific DC progenitor population, referred to as preimmunocytes, and document protocols for their differentiation into various DC subsets.

**Key Words:** Hematopoiesis; dendritic cell; macrophage; interferon producing cell; preimmunocyte; differentiation; GM-CSF.

### 1. Introduction

Dendritic cells (DC) are professional antigen-presenting cells (APCs) that play an essential role in the activation of T lymphocytes and modulation of responses by B and natural killer cells. Compared to the two other types of APCs, B cells, and macrophages, DC are the only cells able to prime naïve T cells (*1*). This functional competence derives from the capacity of DC to capture antigen, process it and present antigenic peptides associated with major histocompatibility complex (MHC) class I and II complexes to specific T cells. DC live an extremely dynamic life. They reside in peripheral tissues in a quiescent, immature state, awaiting encounter with antigen (Ag). Upon Ag encounter, DC undergo a maturation process that renders them highly immunogenic and

they then migrate to T-cell areas of secondary lymphoid tissues where they can induce activation and proliferation of specific naïve CD4<sup>+</sup> T helper cells and CD8<sup>+</sup> cytotoxic T lymphocytes (2,3). DC not only prime T cells, but are also able to tolerize them toward self-antigens (4–8).

DC originate from hematopoietic precursors in the bone marrow (BM) (9,10) and are the only blood cell type known to originate from two distinct differentiation pathways: lymphoid and myeloid (11,12). In particular, in vivo experiments have shown that DC can originate from both the common lymphoid progenitor and the common myeloid progenitor (13,14). Another peculiarity of the DC system is the large variety of subsets described, both in the human and in the mouse systems, according to surface phenotype and organ distribution (6,11). In the mouse, all DC subsets described until now express the integrin CD11c. What distinguishes each subset, is its particular combination of surface markers and its anatomical location. A simplified distinction that can be made for the different mouse DC subsets according to their surface phenotype and location, is to divide them into CD11c<sup>+</sup>CD8 $\alpha$ <sup>-</sup> and CD11c<sup>+</sup>CD8 $\alpha$ <sup>+</sup> DC, present in thymus, lymph nodes and spleen, Langerhans cells in the epidermis, and plasmacytoid pre-DC (pDC) detectable in spleen, BM, blood, thymus, and lymph nodes. The latter subset, the plasmacytoid pre-DC, express B220 and Gr-1 on the cell surface and secrete large amounts of type I interferon (IFN) in response to viral stimulation (15,16). Different protocols have been published describing the differentiation of DC from total BM in vitro. In these protocols, total mouse BM is cultured in the presence of granulocyte/macrophage colony stimulating factor (GM-CSF) either alone (17–19) or in combination with tumor necrosis factor- $\alpha$  or transforming growth factor- $\beta$  (20) to generate CD11c<sup>+</sup>CD8 $\alpha$ <sup>-</sup> DC, or cultured in the presence of Flt3 ligand (21,22), to give rise to plasmacytoid pre-DC.

DC are rare in all body tissues and isolation procedures are not only time consuming, but also generate low cell yields. For this reason, culturing total BM in vitro in the presence of different cytokines allows the generation of a large number of DC that can be further used for molecular or cell biology studies. Because the starting precursor population used in these protocols is poorly defined, the DC obtained are at different stages of differentiation and are not a homogenous population. Moreover, mixed colonies of DC, granulocytes, and macrophages are ultimately generated. Therefore, these protocols are very efficient at producing a relatively large number of DC from total mouse BM ( $5 \times 10^6$  per mouse in one study [23] and  $1-3 \times 10^6$  per mouse in another [18]).

In contrast to the protocols previously described, we set out to differentiate the main DC subsets from a defined BM precursor population. For this reason, we characterized a novel subset of precursor cells present in mouse BM that can give rise, under appropriate conditions, to most accessory types of the immune

system, a population we, therefore, referred to as preimmunocytes (24). In particular, under the aegis of M-CSF or GM-CSF these cells rapidly differentiate into either macrophages or immature DC, which can be further induced to mature by lipopolysaccharide (LPS) stimulation. Using fetal thymus organ culture (FTOC) the same population differentiates to both CD11c<sup>+</sup>CD8 $\alpha$ <sup>-</sup>, and CD11c<sup>+</sup>CD8 $\alpha$ <sup>+</sup> DC, and when injected in vivo they differentiate to all conventional DC subsets (Seidl, T., unpublished data). Moreover, following stimulation with influenza virus, they rapidly express high levels of type I IFN mRNA, characteristic of plasmacytoid pre-DC. Although in this chapter, we describe the different systems used to differentiate this particular progenitor population into DC, the same protocols can be used to study the differentiation potential of any progenitor population of interest, because relatively few cells are required to perform the assays.

## 2. Materials

### 2.1. Mice

1. Balb/c and C57BL/6 (B6) obtained from suppliers such as IFFA-Credo (France) and Harlan Olac (UK).
2. Fetal B6 mice obtained from timed matings of B6 females and males. The date of finding a vaginal plug is regarded as day 0 of embryonic development.

### 2.2. Flow-Cytometric Analysis

1. FACS staining buffer: phosphate buffered saline (PBS) supplemented with 2% FCS (Invitrogen-Gibco).
2. Digestion solution for isolating DC from fetal thymi: PBS supplemented with 5% FCS, 1 mg/mL collagenase D (Roche Molecular Biochemicals, cat. no. 1088 866) and DNase I (Sigma, cat. no DN-25) (*see Note 1*).
3. Monoclonal antibodies (MAbs) used for sorting preimmunocytes from bone marrow: CD31-PE, Ly6-C-bio, CD11c-FITC (BD-Pharmingen).
4. MAbs used to specifically stain DC present in FTOC: CD16/CD32 (Fc $\gamma$  III/II), H-2A<sup>b</sup>-PE, CD11c-FITC, CD8 $\alpha$ -APC, (BD-Pharmingen), and anti-H-2<sup>d</sup>-FITC (Hammerling, G. J., unpublished).
5. Streptavidin-APC as a secondary reagent for biotin-conjugated MAbs.
6. A FACStar Plus (Becton Dickinson) or Moflo high-speed sorter (Cytomation) for cell sorting and a FACS-Calibur (Becton Dickinson) for analysis of samples.

### 2.3. Preimmunocyte Enrichment From Total Bone Marrow

1. MACS buffer: PBS supplemented with 1% FCS and 2 mM EDTA.
2. CD11c-coupled magnetic beads (MACS, Miltenyi Biotec) for labeling CD11c<sup>+</sup> cells in total BM that are subsequently isolated by positive selection with specific LS<sup>+</sup> columns (Miltenyi Biotec).
3. Cell strainers with pore size of 40  $\mu$ m (BD Falcon, cat. no. 352340).



## 2.4. $CD4^-CD8^-$ Double Negative Thymocytes

$CD4^-CD8^-$  double negative thymocytes (DN) are obtained by depleting  $CD4^+$  and  $CD8^+$  thymocytes from 3 to 4 wk old B6 thymi using the following reagents:

1. Supernatants containing MAbs to CD4 (clone RL.172) and CD8 (clone 3.168.8.1 [31 M]) (a kind gift from Ceredig, R.).
2. Rabbit complement (Low Tox-M Rabbit Complement, Cedarlane).
3. Ficoll for recovery of live cells by density-gradient centrifugation.

## 2.5. Cell Culture

The following are required for the culture of sorted BM preimmunocytes:

1. Flat-bottom 96-well plates (Nunc, cat. no. 167008).
2. Iscove's modified Dulbecco's medium (Invitrogen-Gibco) supplemented with 10% FCS (Invitrogen-Gibco) and 25 ng/mL of recombinant GM-CSF (R&D Systems) (*see Note 2*).
3. LPS (Sigma) at a final concentration of 1  $\mu\text{g/mL}$  for maturation of DC.
4. Influenza virus ( $10^6$  PFU/mL) for viral stimulation experiments.

## 2.6. FTOC

1. Embryonic material is obtained from mating of B6 (H-2<sup>b</sup>) mice.
2. Dissecting microscope (Leica MZ8) for isolation of fetal thymi.
3. Iscove's modified Dulbecco's medium supplemented with 10% FCS,  $5 \times 10^{-5}$  M 2-mercaptoethanol, and 1X glutamine, nonessential amino acids, sodium pyruvate, penicillin, and streptomycin from 100X stocks (Invitrogen-Gibco).
4. 2-deoxyguanosine (2-dGuo) (Sigma, cat. no. D-0901) at a final concentration of 1.35 mM for thymocyte depletion.
5. Terasaki plates supplied by Greiner Bio-One.
6. Nitrocellulose filters (0.2  $\mu\text{m}$  pore size) (Millipore) placed on 1 mL of medium in 24-well plates (Nunc, cat. no. 142475) or 4 mL of medium in 6-well plates (Falcon, cat. no. 3046, Becton Dickinson).

## 3. Methods

### 3.1. Cell Preparation and Staining

#### 3.1.1. Bone Marrow Samples

1. Flush BM from the femurs and tibia bones with FACS buffer using a 25-gauge  $\times$  0.5-mm needle attached to a 2-mL syringe.
2. Briefly resuspend cell aggregates with a Pasteur pipet before centrifuging at 200g for 10 min.

#### 3.1.2. Bone Marrow CD11c Enrichment

When larger numbers of preimmunocytes are needed, we enrich BM samples by using CD11c-coupled magnetic beads according to the manufacturer's instructions, with the following adaptations:

1. Flush BM from the femurs and tibias of four mice (approx  $1.6 \times 10^8$  cells).
2. Filter the cell suspension through a cell strainer into a 50-mL falcon tube (*see Note 3*) and centrifuge at 200g for 10 min.
3. Carefully resuspend the pellet in 100  $\mu$ L of MACS buffer. Dilute 10  $\mu$ L of CD11c beads in 100  $\mu$ L of MACS buffer and add to the cell suspension.
4. Place the sample in the door of a 4°C fridge for 15 min and shake the sample gently every 5 min.
5. Add 40 mL of MACS buffer to the 200  $\mu$ L of cell suspension and filter into a fresh 50-mL falcon tube before centrifugation.
6. Resuspend the pelleted cells in 1 mL of MACS buffer and apply on the column previously washed three times with 1 mL of MACS buffer. A 25-gauge 0.5-mm needle may be applied to the column to control the flow of the fluid.
7. After the cell sample has passed through, the column is washed twice with MACS buffer before the CD11c<sup>+</sup> cells are eluted by removing the column from the magnetic field.

### 3.1.3. Isolation of Double Negative Thymocytes

1. A maximum of  $200 \times 10^6$  thymocytes are required for a 10-mL depletion mixture.
2. Resuspend the cells in 7 mL of unsupplemented DMEM in a 15-mL tube.
3. Add 1 mL of supernatant containing CD4 MAb (RL.172) and CD8 MAb (31 M) and incubate the tube at 37°C for 10 min.
4. Make up a bottle of rabbit complement with 1 mL of deionized water and add immediately to the cells. Gently resuspend the mixture every 10 min using a Pasteur pipet.
5. After 45 min, underlay the cell suspension with 3 mL of Ficoll (equilibrated to room temperature) and centrifuge for 20 min at room temperature.
6. DN cells are recovered at the interface between the medium and Ficoll.  $3\text{--}5 \times 10^6$  DN thymocytes are typically obtained.

### 3.1.4. FTOC Staining

1. Transfer fetal thymus lobes that have been cultured with sorted cells to 1 mL of collagenase–DNase digestion mixture in 4-mL tubes (8–10 lobes/tube).
2. Place samples in a shaker at 37°C for 1 h (30 min + 30 min, *see below*).
3. After 30 min, resuspend the lobes with a P1000 Gilson pipet to encourage their disaggregation. Transfer loose cells to a fresh Eppendorf tube and leave on ice while fresh collagenase–DNase mixture is added to the undigested tissue, which is incubated for a further 30 min at 37°C with continual shaking.

## 3.2. Cell Sorting

1. Stain single cell suspensions in FACS buffer with different combinations of MAbs, as described in **Subheading 2.**, following standard procedures.
2. Using MAbs specific for CD31, Ly6C and CD11c and gating on total cells (*see Fig. 1A*) the BM of Balb/c mice can be divided into five subpopulations (*see Fig. 1B* and **Note 4**). A distinct subset can be identified based on the expression of CD11c (*see Fig. 1C*) and defined levels of CD31 and Ly6C (gate R2 in **Fig. 1B**)

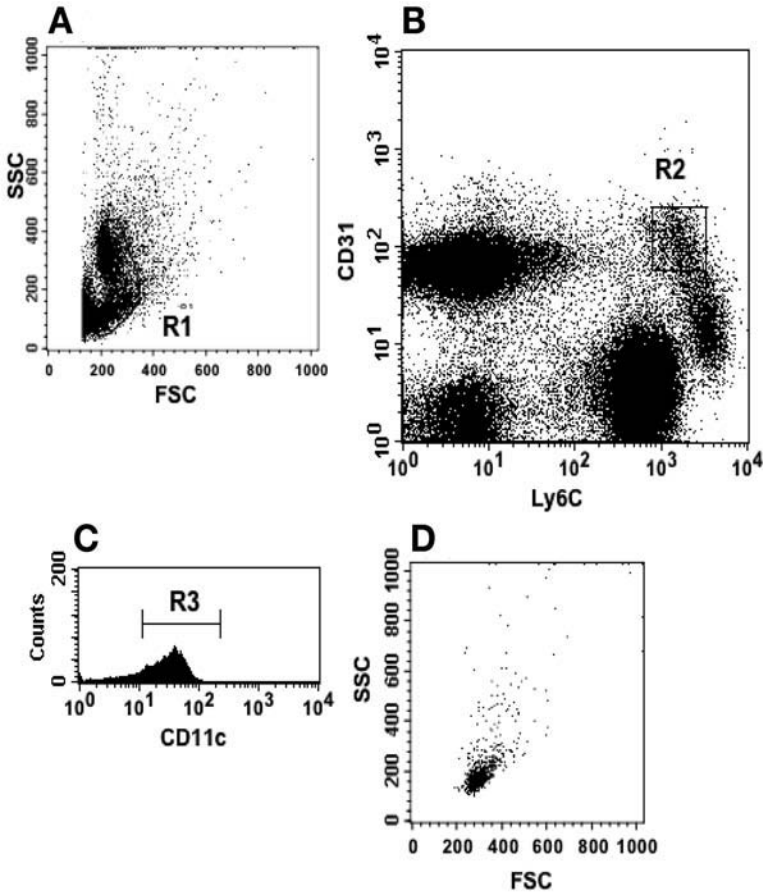


Fig. 1. Characterization of preimmunocytes in total mouse bone marrow (BM). (A) Gate R1 used on total BM cells. (B) Dot plot of BM cells, gated on R1, from Balb/c mice stained with monoclonal antibodies to CD31, Ly6C, and CD11c. (C) Analysis of CD11c expression by R2-gated cells. (D) Analysis of the physical parameters of preimmunocytes (gated in R2 + R3).

as well as physical criteria (FSC vs SSC in **Fig. 1D**). We define these cells as preimmunocytes which represent only a small fraction of total BM cells (0.5–1%), and have a homogenous size and granularity (FSC vs SSC), intermediate between that of lymphocytes and granulocytes. **Figure 2** shows FACS analysis, using the same MAb combination, of BM samples after enrichment with CD11c magnetic beads.

### 3.3. Cell Culture

1. Culture  $5\text{--}7 \times 10^4$  sorted BM-derived preimmunocytes in flat-bottom 96-well plates in 200  $\mu\text{L}$  of medium supplemented with either GM-CSF or M-CSF.

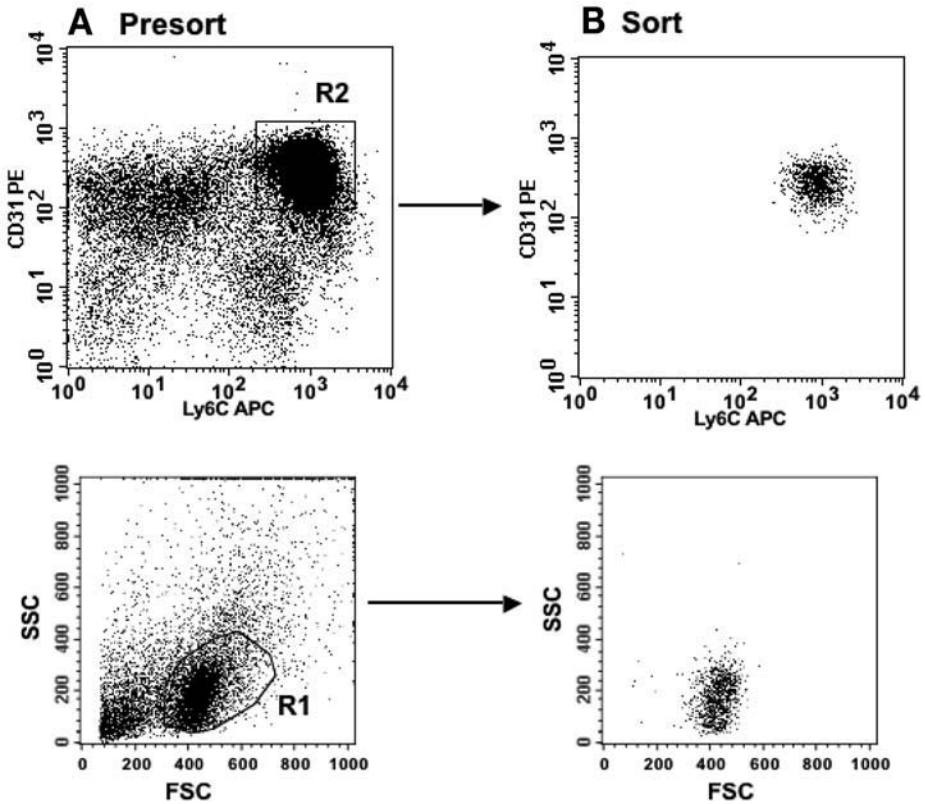


Fig. 2. Bone marrow (BM) preparation enriched with CD11c magnetic beads. (A) Presorted CD11c-enriched BM sample stained as in Fig. 1. (B) Reanalysis of the sorted population of cells stained as in A.

2. Add LPS on day 4 of culture and leave for 40 h to mature before harvesting.
3. For viral stimulation, culture  $1 \times 10^5$  cells in the presence of influenza virus ( $10^6$  PFU/mL) for 7–8 h before assessing the secretion of type I IFN.

### 3.4. FTOC

1. B6 male and female mice are caged together overnight and checked for vaginal plugs the next morning. The day on which a vaginal plug is observed is designated d 0 of gestation.
2. For FTOC, dissect fetal thymi from embryos of B6 time-mated females on day 14.5 of gestation. Remove the head and the lower body containing the liver so as to leave the thoracic segment. Open the rib cage superficially and longitudinally with the tip of fine forceps. Two distinct thymus lobes can be identified above the heart. Thymus lobes are precultured for 5 d in the presence of 1.35 mM 2-dGuo. This treatment kills all rapidly dividing thymocytes, leaving intact the thymic

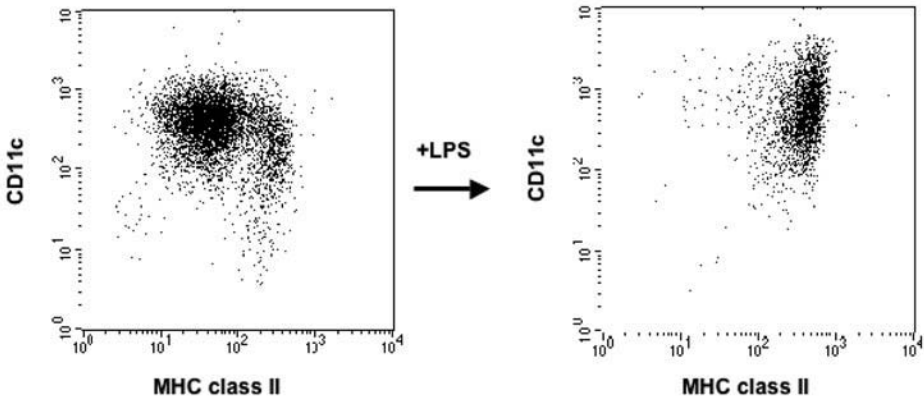


Fig. 3. Bone marrow derived preimmunocytes differentiate to immature dendritic cells (DC) that further mature upon lipopolysaccharide (LPS) stimulation. Bone marrow-derived preimmunocytes, sorted as shown in Fig. 1A are cultured with granulocyte/macrophage colony stimulating factor (GM-CSF) and analyzed for the expression of surface molecules, which are characteristic of DC (CD11c, MHC class II). GM-CSF-dependent cultures are stimulated with LPS for 40 h.

stroma, which acts as an ideal environment in which to assess the differentiation potential of precursor cells. A maximum of eight lobes may be placed on a nucleopore filter, floating on medium in a 24-well plate.

3. After the 2-dGuo treatment, wash the B6 (H-2<sup>b</sup>) thymus lobes and coculture in hanging drops in the wells of a Terasaki plate containing sorted BM cells from Balb/c mice (H-2<sup>d</sup>) together with DN thymocytes from B6 (H-2<sup>b</sup>) thymi. Carefully place the thymus lobes onto the surface of a 20- $\mu$ L drop of medium in the wells of a Terasaki plate, each containing  $1-5 \times 10^3$  sorted preimmunocytes and  $0.5 \times 10^3$  DN cells (*see Note 5*). DN thymocytes are used to reconstitute the thymocyte population and recreate a T cell-stromal environment suitable for the developing preimmunocytes. The plates are inverted for 2 d, after which the reconstituted thymi are transferred to nucleopore filters (Millipore) floating on medium in six-well plates for a further 4-6 d.

### 3.5. Analyzing DC Differentiation by Flow Cytometry

1. After 4-5 d of in vitro culture, add LPS to appropriate wells and leave for 40 h. Figure 3 shows the profile of FTOC stained with the specific DC marker combination of CD11c and MHC class II.
2. To detect DC in FTOC, carefully remove thymus lobes from the filters and prepare a single cell suspension by treatment with collagenase-DNase.
3. Block Fc receptors by means of CD16/CD32 MAbs.
4. Stain with MAbs specific for CD8, MHC class II, CD11c, and H-2<sup>b</sup>.
5. Identify cells derived from preimmunocytes by gating on H-2<sup>d+</sup> cells in the appropriate histogram (*see Fig. 4*).

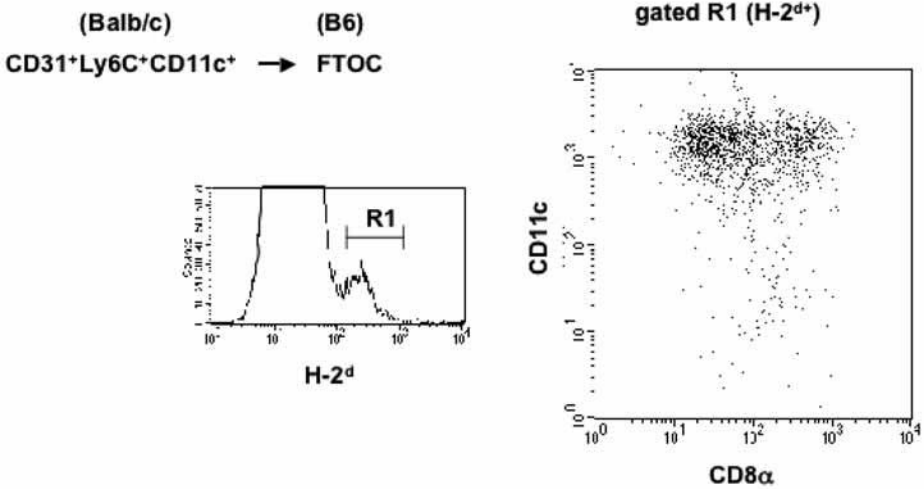


Fig. 4. Mouse preimmunocytes give rise to both CD8 $\alpha$ <sup>+</sup> and CD8 $\alpha$ <sup>-</sup> DC in fetal thymus organ culture. Sorted Balb/c preimmunocytes are cocultured for 5 d in 2-dGuo-treated thymi together with B6 DN thymocytes to allow efficient reconstitution of the T cell compartment. The profile of CD8 $\alpha$  and CD11c is shown after gating on H-2<sup>d</sup><sup>+</sup> cells.

#### 4. Notes

1. Cell surface expression of CD8 $\alpha$  is resistant to this treatment.
2. FCS must be endotoxin-free to prevent DC maturation. Different batches of FCS are tested on total BM grown in the presence of GM-CSF (18). After 10 d, cells are stained with CD11c and H-2A<sup>b</sup> MAbs to select the FCS producing DC with low class II surface expression, when compared to the same cells stimulated with LPS.
3. During isolation of DC from organs, all lab wear, from tubes used during the collagenase-DNase treatment to the ones used for staining or sorting purposes, should be made from polypropylene to prevent DC from adhering to the plastic.
4. We find that Balb/c mice have a more distinct population of preimmunocytes compared to B6 mice.
5. Thymus lobes should float on the drop rather than sink to the bottom of the well.

#### Acknowledgments

The author would like to thank Antonio Lanzavecchia for his help and support.

#### References

1. Lanzavecchia, A. and Sallusto, F. (2001) Regulation of T cell immunity by dendritic cells. *Cell* **106**, 263–266.
2. Banchereau, J., Briere, F., Caux, C., et al. (2000) Immunobiology of dendritic cells. *Annu. Rev. Immunol.* **18**, 767–811.

3. Banchereau, J. and Steinman, R. M. (1998) Dendritic cells and the control of immunity. *Nature* **392**, 245–252.
4. Brocker, T., Riedinger, M., and Karjalainen, K. (1997) Targeted expression of major histocompatibility complex (MHC) class II molecules demonstrates that dendritic cells can induce negative but not positive selection of thymocytes in vivo. *J. Exp. Med.* **185**, 541–550.
5. Shortman, K. and Heath, W. R. (2001) Immunity or tolerance? That is the question for dendritic cells. *Nat. Immunol.* **2**, 988–989.
6. Shortman, K. and Liu, Y. J. (2002) Mouse and human dendritic cell subtypes. *Nat. Rev. Immunol.* **2**, 151–161.
7. Steinman, R. M., Turley, S., Mellman, I., and Inaba, K. (2000) The induction of tolerance by dendritic cells that have captured apoptotic cells. *J. Exp. Med.* **191**, 411–416.
8. Suss, G. and Shortman, K. (1996) A subclass of dendritic cells kills CD4 T cells via Fas/Fas-ligand-induced apoptosis. *J. Exp. Med.* **183**, 1789–1796.
9. Cella, M., Sallusto, F., and Lanzavecchia, A. (1997) Origin, maturation and antigen presenting function of dendritic cells. *Curr. Opin. Immunol.* **9**, 10–16.
10. Steinman, R. M. (1991) The dendritic cell system and its role in immunogenicity. *Annu. Rev. Immunol.* **9**, 271–296.
11. Ardavin, C. (2003) Origin, precursors and differentiation of mouse dendritic cells. *Nat. Rev. Immunol.* **3**, 582–590.
12. Ardavin, C., Wu, L., Li, C. L., and Shortman, K. (1993) Thymic dendritic cells and T cells develop simultaneously in the thymus from a common precursor population. *Nature* **362**, 761–763.
13. Manz, M. G., Traver, D., Miyamoto, T., Weissman, I. L., and Akashi, K. (2001) Dendritic cell potentials of early lymphoid and myeloid progenitors. *Blood* **97**, 3333–3341.
14. Traver, D., Akashi, K., Manz, M., et al. (2000) Development of CD8alpha-positive dendritic cells from a common myeloid progenitor. *Science* **290**, 2152–2154.
15. Asselin-Paturel, C., Boonstra, A., Dalod, M., et al. (2001) Mouse type I IFN-producing cells are immature APCs with plasmacytoid morphology. *Nat. Immunol.* **2**, 1144–1150.
16. Grouard, G., Risoan, M. C., Filgueira, L., Durand, I., Banchereau, J., and Liu, Y. J. (1997) The enigmatic plasmacytoid T cells develop into dendritic cells with interleukin (IL)-3 and CD40-ligand. *J. Exp. Med.* **185**, 1101–1111.
17. Inaba, K., Inaba, M., Romani, N., et al. (1992) Generation of large numbers of dendritic cells from mouse bone marrow cultures supplemented with granulocyte/macrophage colony-stimulating factor. *J. Exp. Med.* **176**, 1693–1702.
18. Lutz, M. B., Kukutsch, N., Ogilvie, A. L., et al. (1999) An advanced culture method for generating large quantities of highly pure dendritic cells from mouse bone marrow. *J. Immunol. Methods* **223**, 77–92.
19. Scheicher, C., Mehlig, M., Zecher, R., and Reske, K. (1992) Dendritic cells from mouse bone marrow: in vitro differentiation using low doses of recombinant granulocyte-macrophage colony-stimulating factor. *J. Immunol. Methods* **154**, 253–264.

20. Yamaguchi, Y., Tsumura, H., Miwa, M., and Inaba, K. (1997) Contrasting effects of TGF-beta 1 and TNF-alpha on the development of dendritic cells from progenitors in mouse bone marrow. *Stem Cells* **15**, 144–153.
21. Brawand, P., Fitzpatrick, D. R., Greenfield, B. W., Brasel, K., Maliszewski, C. R., and De Smedt, T. (2002) Murine plasmacytoid pre-dendritic cells generated from Flt3 ligand-supplemented bone marrow cultures are immature APCs. *J. Immunol.* **169**, 6711–6719.
22. Gilliet, M., Boonstra, A., Paturel, C., et al. (2002) The development of murine plasmacytoid dendritic cell precursors is differentially regulated by FLT3-ligand and granulocyte/macrophage colony-stimulating factor. *J. Exp. Med.* **195**, 953–958.
23. Inaba, K., Inaba, M., Romani, N., et al. (1992) Generation of large numbers of dendritic cells from mouse bone marrow cultures supplemented with granulocyte/macrophage colony-stimulating factor. *J. Exp. Med.* **176**, 1693–1702.
24. Bruno, L., Seidl, T., and Lanzavecchia, A. (2001) Mouse pre-immunocytes as non-proliferating multipotent precursors of macrophages, interferon-producing cells, CD8alpha(+) and CD8alpha(-) dendritic cells. *Eur. J. Immunol.* **31**, 3403–3412.





## Genetic Modification of Dendritic Cells Through the Directed Differentiation of Embryonic Stem Cells

Paul J. Fairchild, Kathleen F. Nolan, and Herman Waldmann

### Summary

Recent years have witnessed a progressive acceptance of the dual role played by dendritic cells (DC) in the initiation of immune responses and their specific attenuation through the induction of immunological tolerance. Nevertheless, as terminally differentiated cells of the myeloid lineage, DC share with macrophages an inherent resistance to genetic modification, greatly restricting strategies available for studying their physiology and function. Consequently, little is known of the molecular interactions provided by DC that underlie the critical decision between tolerance and immunity. Embryonic stem (ES) cells are, by contrast, relatively amenable to genetic modification. Furthermore, their propensity for self-renewal, one of the cardinal features of a stem cell, permits cloning at the single cell level and the rational design of ES cell lines, uniformly expressing a desired, mutant phenotype. Here, we describe how another defining property of ES cells, their demonstrable pluripotency, may be harnessed for their directed differentiation along the DC pathway, enabling the generation of limitless numbers of DC faithfully expressing candidate genes of interest. The protocols we outline in this chapter may, therefore, offer new opportunities for dissecting the biology of DC and the molecular basis of their unique properties.

**Key Words:** Dendritic cell; embryonic stem cell; directed differentiation; tolerance; genetic modification.

### 1. Introduction

During the past decade, numerous lines of evidence have converged on dendritic cells (DC) as playing a critical role in the establishment and ongoing maintenance of immunological tolerance (1,2). Although originally considered to be restricted to the induction of central tolerance (3), their remit is now known to extend beyond negative selection in the thymus to the imposition of dominant tolerance in the periphery, though the polarization of naïve T cells toward a regulatory phenotype (4). Various studies have suggested that recognition

of antigen by naïve T cells in the absence of full activation signals is the critical parameter in driving their commitment to the regulatory lineage (5), a scenario epitomized by antigen presentation by immature DC (6,7). In contrast, other studies have provided evidence consistent with the need for expression by DC of molecules such as B7-H1, inducible costimulator ligand or the enzyme indoleamine 2,3-dioxygenase (8–10) to set in place a regulatory network. These findings imply that DC play a proactive role in the decision-making process, inducing regulatory T cell development solely through the provision of specific signals. Systematic attempts to resolve this ambiguity have, however, been confounded by the innate resistance of terminally differentiated DC to genetic modification. Although electroporation and lipid-based protocols have proven to be of little value when applied to this cell type, the use of viral vectors has enjoyed some measure of success (11). Nevertheless, their use has been widely reported to adversely affect the maturation status of DC, either impairing their activation in response to pathogen-associated molecules (11) or prompting their premature maturation and significantly reducing their life span (12).

In the light of these limitations, we have devised an alternative approach to the study of DC by deciphering their differentiation pathways from pluripotent embryonic stem (ES) cells through the formation of embryoid bodies (EB), macroscopic structures that recapitulate some of the early events of embryogenesis *in vitro* (13,14). The relative ease with which ES cells may be transfected with heterologous genes, together with opportunities for cloning at the single cell level, pave the way for the generation of ES cell lines, constitutively expressing defined transgenes or silencing constructs. Such a permanent resource may serve as a prelude to the directed differentiation of copious DC uniformly expressing the same mutant phenotype (15). Such an approach may greatly facilitate a systematic investigation of the role played by specific genes in DC function and the capacity of this cell type to refine the balance between tolerance and immunity in response to changes in circumstance. Furthermore, the recent advent of pluripotent ES cell lines of human origin (16,17) offers prospects for adapting these protocols for the genetic modification of human DC, thereby helping to bridge the species barrier between mouse and man.

## 2. Materials

### 2.1. Preparation of Embryonic Fibroblasts

1. Female C57Bl/6 or Rosa 26 mice at day 13 of gestation (*see Note 1*).
2. Standard dissection instruments.
3. Scalpel fitted with a sterile no. 23 surgical blade.
4. Water bath warmed to 37°C.
5. Inverted phase-contrast microscope.
6. Phosphate buffered saline (PBS).

7. B6 medium: Dulbecco's modified Eagle's medium (DMEM) (Invitrogen), 10% (v/v) fetal calf serum (FCS), 2 mM L-glutamine (Invitrogen), 50 U/mL penicillin, 50 µg/mL streptomycin (Invitrogen),  $5 \times 10^{-5}$  M 2-mercaptoethanol (Promega).
8. Sterile trypsin-EDTA solution: PBS, 0.125% trypsin (v/v) (Invitrogen), 0.02% EDTA (w/v).
9. Dimethyl sulfoxide Hybri-Max<sup>®</sup> (DMSO) (Sigma).
10. Sterile 90-mm diameter Petri dishes.
11. Sterile 75- and 150-cm<sup>2</sup> tissue culture flasks.
12. Sterile Universal tubes.

## 2.2. Routine Maintenance of ES Cells

1. Two 75-cm<sup>2</sup> flasks of confluent primary embryonic fibroblasts.
2. ES medium: DMEM, 15% FCS (v/v) (*see Note 2*), 2 mM L-glutamine, 1 mM sodium pyruvate (Invitrogen),  $5 \times 10^{-5}$  M 2-mercaptoethanol.
3. PBS and trypsin-EDTA solution.
4. Stock mitomycin C (MMC, Sigma) dissolved in PBS at 1 mg/mL. Being toxic, MMC should be handled carefully and a risk assessment performed.
5. Sterile 25-cm<sup>2</sup> tissue culture flasks.

## 2.3. Genetic Modification of ES Cells

1. 24-Well plates and 96-well flat-bottomed plates seeded with MMC-treated Rosa 26 embryonic fibroblasts.
2. Inverted phase-contrast microscope.
3. P200 Gilson pipet.
4. Multi-12-channel pipet.
5. Fresh B6 medium (*see Subheading 2.1., item 7*).
6. ES medium supplemented with 1000 U/mL of recombinant murine leukemia inhibitory factor (rLIF) (Chemicon).
7. Sterile PBS and trypsin-EDTA solution.
8. Sterile PBS containing 0.1% (w/v) gelatin Type A (Sigma).
9. Endotoxin-free preparation of plasmid DNA.
10. LipofectAMINE Plus<sup>™</sup> (Life Technologies) or equivalent transfection reagent.
11. Stock solution of the neomycin analog G418-sulfate (Geneticin; Invitrogen) at 250 mg/mL in DMEM, or an appropriate alternative selection reagent.
12. Trypan blue (Sigma).
13. Six-well plates gelatinized by incubating with 0.1% gelatin (w/v) in PBS for 30 min at 37°C and washing twice with sterile PBS before overlaying with PBS before use.
14. Gelatinized 12- and 25-cm<sup>2</sup> flasks.
15. Polystyrene reagent reservoirs (Corning).

## 2.4. Directed Differentiation of ES Cells

1. EB maintained in suspension culture for 14 d.
2. P1000 Gilson pipet.
3. Fresh ES medium (*see Subheading 2.2., item 2*).

4. Sterile EDTA, 0.2% (w/v) in PBS.
5. Recombinant murine granulocyte/macrophage colony stimulating factor (rmGM-CSF) (R&D Systems) and recombinant murine interleukin-3 (rmIL-3) (R&D Systems).
6. G418-sulfate or an appropriate alternative antibiotic for selection purposes.
7. Lipopolysaccharide (LPS: *Escherichia coli* Serotype 0127:B8) (Sigma).
8. Leukopor tape<sup>®</sup> (Beiersdorf AG Hamburg, Germany).
9. Sterile 90-mm diameter tissue culture plates (Corning).

### 3. Methods

#### 3.1. Preparation of Primary Embryonic Fibroblasts

1. To prepare a stock of fibroblasts, arrange timed matings of C57Bl/6 mice, defining the day on which a vaginal plug is observed as d 0 of gestation.
2. Sacrifice the mother on d 13 and carefully remove the embryos, dissecting them from the uterus and surrounding extraembryonic tissues into a Petri dish of ice cold PBS.
3. Decapitate and carefully remove the liver, which serves as the principle hematopoietic organ at this stage of ontogeny.
4. Remove the PBS and replace with 10 mL of trypsin-EDTA. Finely macerate the embryonic tissues using a scalpel fitted with a sterile no. 23 surgical blade.
5. Transfer the tissue to a Universal tube. Rinse the Petri dish with a further 5 mL of trypsin-EDTA and combine with the original suspension.
6. Place in a water bath for 5 min at 37°C.
7. Shake the tube vigorously to mechanically disrupt the tissue and leave for 3 min to allow lipids to rise to the surface and any remaining tissue to sediment under unit gravity.
8. Carefully collect 5–10 mL of cell suspension between the pellet and lipid layer and transfer to a 50-mL conical tube containing 10 mL of complete B6 medium as a source of FCS proteins to inactivate the trypsin.
9. Replace the volume removed with an equivalent volume of trypsin-EDTA and return the Universal to the water bath for a further 5 min.
10. Repeat the extraction protocol two further times (**steps 7–9**), pooling the material obtained from each extraction. When complete, allow the cell suspension to stand briefly and remove any fragments of tissue that settle to the bottom of the tube using a sterile Pasteur pipet. Likewise, carefully remove any fatty deposits from the air-liquid interface and discard them.
11. Spin the tube at 200g to pellet the cells and resuspend in fresh B6 medium. Distribute equally among 75-cm<sup>2</sup> tissue culture flasks. Although the number of flasks will vary according to the size of the litter, we routinely seed one flask for every two embryos used.
12. After culture for 1–2 d, the fibroblasts should have produced a near-confluent monolayer of cells. Remove any debris and floating cells by gently pipetting over the surface and replacing with fresh medium (*see Note 3*).

13. Once the cells reach confluency, passage them into an equivalent number of 150-cm<sup>2</sup> flasks to provide room for expansion. To do so, remove the overlying medium and replace with 20 mL of PBS. Gently swirl the flask to exclude any traces of medium and FCS, which might inhibit the action of proteases. Replace with 10 mL of trypsin–EDTA and return to the incubator for 3 min. Shake the flask vigorously to release the adherent cells and transfer to a 50-mL conical tube containing 10 mL of B6 medium.
14. Centrifuge for 5 min at 200g and resuspend in fresh B6 medium before seeding the appropriate number of flasks.
15. Although the fibroblasts are still subconfluent and are not, therefore, susceptible to contact inhibition, harvest and pool the cells from all flasks. Centrifuge and resuspend in medium supplemented with 10% DMSO (v/v). Prepare vials of feeder cells at 10<sup>7</sup> cells per vial and freeze rapidly on dry ice before storing long-term under liquid nitrogen (*see Note 4*).

### 3.2. Routine Passage of Mouse ES Cell Lines

1. Although different mouse ES cell lines may vary subtly in their properties, we find that they invariably require passaging every third day of culture.
2. Because primary embryonic fibroblasts are required as feeder cells, these must be passaged in parallel. Therefore, thaw a vial of stock fibroblasts in advance and expand to form two confluent 75-cm<sup>2</sup> flasks.
3. The day before passaging the ES cell line, remove the medium from one of the flasks of fibroblasts and replace it with 10 mL of fresh B6 medium, supplemented with MMC at a final concentration of 10 µg/mL. Incubate for 2 h at 37°C to ensure that the cells are mitotically inactivated (*see Note 5*).
4. During this period, passage the remaining flask of fibroblasts into two 75-cm<sup>2</sup> flasks so as to encourage expansion and the replenishment of stocks for subsequent use.
5. After 2 h, harvest the MMC-treated cells using trypsin–EDTA (*see Subheading 2.1., item 8*), spin and resuspend in fresh B6 medium. Distribute equally among two 25-cm<sup>2</sup> flasks and incubate overnight to encourage the formation of confluent monolayers onto which the ES cells may be passaged.
6. On the day of passaging, the ES cell line should appear as discrete, compact colonies in which the borders of individual cells are difficult to discern (*see Fig. 1A*). Prepare a single cell suspension of the ES cell line by removing the medium and replacing with 10 mL of PBS. Swirl the flask and replace with 5 mL of trypsin–EDTA.
7. Return the flask to the incubator for 3–4 min. Shake vigorously to disaggregate the colonies of ES cells and transfer the cell suspension to a 15-mL conical tube containing 5 mL of complete B6 medium. Centrifuge at 200g for 5 min and resuspend in 10 mL of complete ES medium.
8. Seed the two 25-cm<sup>2</sup> flasks with ES cells at two different densities. Although the extent to which the cells should be diluted will need to be determined empirically, we routinely perform a 1:3 and 1:10 dilution. Preparation of stocks of ES cells at two different densities increases the likelihood of ensuring optimal growth conditions.

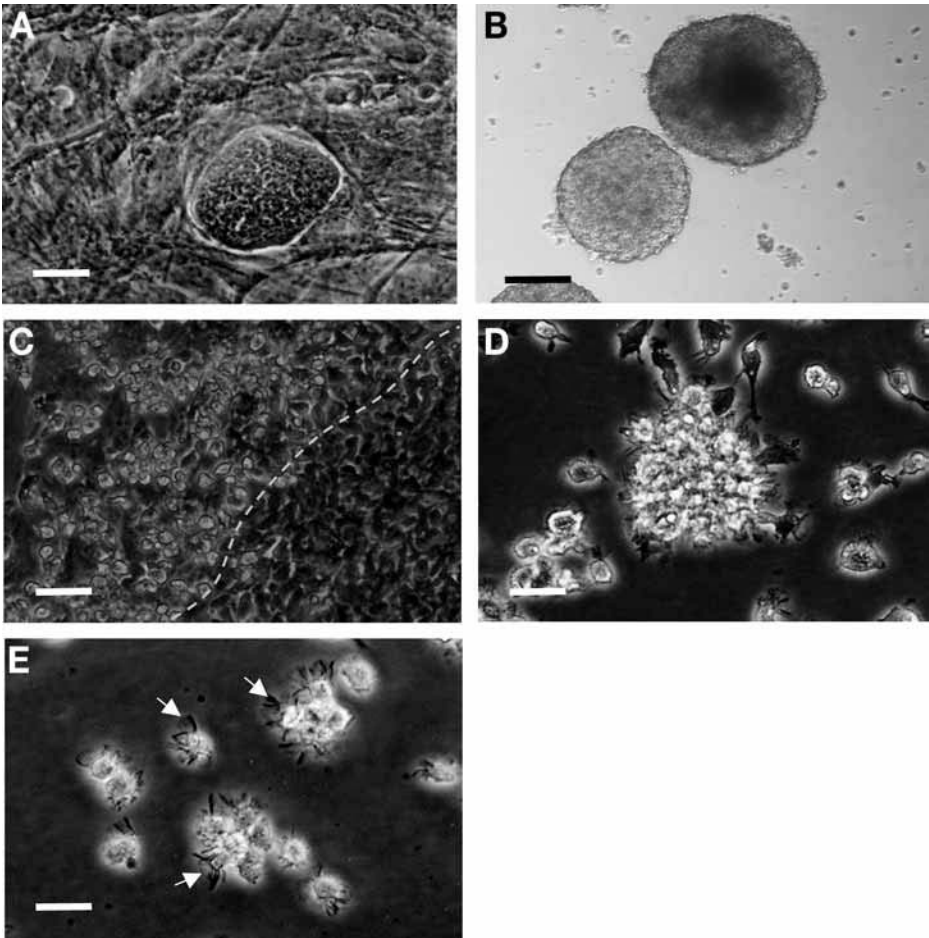


Fig. 1. Sequential stages during the directed differentiation of embryonic stem (ES) cells along the dendritic cell pathway. **(A)** Colony of undifferentiated ES cells cultured on a monolayer of primary embryonic fibroblasts. Bar = 30  $\mu\text{m}$ . **(B)** EB formed from the proliferation of ES cells cultured in single cell suspension for 14 d. Bar = 500  $\mu\text{m}$ . **(C)** Immature dendritic cells (DC) accumulating around the edge of an EB (indicated by the broken line). Bar = 30  $\mu\text{m}$ . **(D)** Typical cluster of immature DC, lightly adherent to tissue culture plastic. Bar = 10  $\mu\text{m}$ . **(E)** DC induced to mature following transient exposure to lipopolysaccharide. Note the many dendrites and veils of cytoplasm (arrows). Bar = 10  $\mu\text{m}$ .

### 3.3. Transfection of ES Cells

Although various methods may be used for the stable transfection of mouse ES cells, we prefer the use of lipid-based approaches, which do not place the cells under detectable stress and have obtained good results with both

LipofectAMINE Plus and Fugene. Whichever reagent is chosen, however, preparatory titration of the plasmid DNA and adherence to the manufacturer's instructions throughout is strongly recommended. The choice of selection system is largely restricted to the use of the neomycin resistance gene due to the availability of embryonic fibroblasts from Rosa 26 mice that are inherently neomycin resistant and which may, therefore, be used for the routine passage of stable transfectants.

1. In preparation for transfection, it is necessary to determine the optimal concentration of the neomycin analog, G418, that will select for transfectants while not compromising the viability of Rosa 26 fibroblasts. Although the sensitivity of ES cell lines to G418 may vary, we have found 600  $\mu\text{g}/\text{mL}$  to be optimal for all lines tested so far.
2. In advance of transfection, the ES cells should be weaned away from primary embryonic fibroblasts by serial passage onto gelatinized flasks in complete ES medium, further supplemented with 1000 U/mL of rLIF to maintain their pluripotency. This results in the progressive dilution of the fibroblasts and preferential expansion of the ES cell line.
3. Harvest the cells with trypsin-EDTA and plate  $10^5$  cells into each well of a gelatinized six-well tissue culture plate in 4 mL of ES medium containing rLIF.
4. Incubate for 48 h to permit adherence of the cells and the formation of colonies. Monitor carefully until the ES cells reach approx 40% confluency (*see Note 6*).
5. Perform the transfection using the preferred reagent according the manufacturer's instructions, designating a single well for "mock" transfection in which the plasmid DNA is omitted. Incubate the ES cells in ES medium supplemented with rLIF for 24–48 h before adding G418 at a predetermined concentration.
6. Monitor the cultures over the ensuing few days until no viable cells remain in the mock transfected well. Screen the remaining wells for colonies of ES cells that have survived selection as evidence of their incorporation of the plasmid DNA.
7. When the surviving colonies have become established, harvest all wells using trypsin-EDTA and pool to form a polyclonal cell line, which may be expanded in a gelatinized 25-cm<sup>2</sup> flask in ES medium supplemented with G418 and rLIF.
8. When ready for passaging, prepare frozen stocks of the transfected cell line for future use and screen for expression of the transgene using an appropriate assay. In the event that monoclonal antibodies are available specific for the gene product, this may involve the use of flow cytometry or the development of a specific enzyme-linked immunosorbent assay. Alternatively, functional assays or an appropriate PCR-based strategy may be required. Once expression of the transgene has been confirmed, the polyclonal cell line may be used for cloning at the single cell level.

### 3.4. Cloning of ES Cells

Although ES cell lines may be maintained in gelatinized dishes in medium supplemented with rLIF, it is inadvisable to culture them long-term in this way because they have a tendency to become teratocarcinoma cells, which lose any



capacity for subsequent differentiation. We therefore recommend transferring stable transfectants of the ES cell line onto primary embryonic fibroblasts at the first opportunity.

1. In preparation for cloning the ES cell line, prepare MMC-treated Rosa 26 fibroblasts (*see above*) and distribute into the wells of 96-well flat-bottomed plates. We find that a confluent 75-cm<sup>2</sup> flask of feeder cells is sufficient for seeding two 96-well plates, which should be incubated overnight in B6 medium to promote the formation of monolayers.
2. Remove the medium by aspiration and overlay each well with 50  $\mu\text{L}$  of ES medium.
3. Harvest the polyclonal ES cell line that has been cultured in gelatinized flasks and prepare a single cell suspension. Perform a viability count using trypan blue exclusion as an appropriate readout and resuspend the cells to  $2 \times 10^5$  cells per milliliter in ES medium.
4. Transfer 100  $\mu\text{L}$  of cell suspension (approx  $2 \times 10^3$  cells) to a tube containing 900  $\mu\text{L}$  of medium, mix thoroughly and transfer 150  $\mu\text{L}$  of this suspension (approx 300 cells) to a polystyrene reservoir containing 30 mL of ES medium.
5. Using a 12-channel multipipet, transfer 100  $\mu\text{L}$  to each well of the two 96-well plates seeded with fibroblasts, such that each well receives, on average, a single ES cell.
6. Prepare 20 mL of ES medium containing 2.4 mg/mL of G418 and distribute 50  $\mu\text{L}$  to each well, thereby yielding a final concentration of G418 of 600  $\mu\text{g/mL}$ .
7. Culture the plates for 4 d before screening individual wells for colonies using inverted phase contrast microscopy. Exclude any wells containing multiple colonies.
8. Once colonies have become established, expand into 24-well plates seeded with MMC-treated Rosa 26 fibroblasts. To harvest individual colonies, remove medium from the relevant wells by aspiration and overlay with 100  $\mu\text{L}$  of PBS. Replace with 50  $\mu\text{L}$  of trypsin–EDTA and incubate at 37°C for 3 min.
9. Harvest the cells by gentle pipetting with a P200 Gilson pipet and transfer the entire cell suspension to a designated well of the 24-well plate, containing 2 mL of complete ES medium to neutralize the effect of the trypsin. The wholesale transfer of the contents of individual wells is preferable to centrifugation, which risks losing a significant proportion of the small number of ES cells in each colony.
10. Once individual clones have become established, they may be expanded to prepare frozen stock and screened for expression of the transgene (*see Fig. 2*). Ultimately, those clones proving positive should be tested for their capacity to sustain DC differentiation.

### **3.5. Production of Embryoid Bodies**

1. As a prelude to the production of EB, the ES cells should be weaned away from primary embryonic fibroblasts by serial passage onto gelatinized 12-cm<sup>2</sup> flasks in

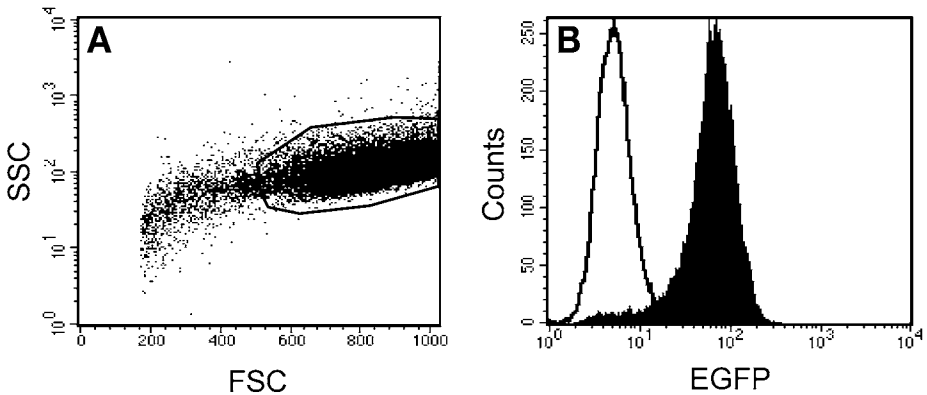


Fig. 2. Expression of the reporter gene (EGFP) by mouse embryonic stem (ES) cells following cloning at the single cell level. (A) Scatter profile of ES cells showing the gating procedure adopted. (B) EGFP expression by transfected (filled histogram) compared with mock transfected ES cell line (open histogram).

complete ES medium, further supplemented with G418 and 1000 U/mL of rLIF to maintain their pluripotency (*see Note 7*). This results in the progressive dilution of the fibroblasts, which might otherwise interfere with the formation of EBs.

2. Once the burden of fibroblasts has been significantly reduced, prepare a single cell suspension of the ES cells and determine their number and viability using trypan blue exclusion.
3. Resuspend the cells in ES medium containing G418 to a density of  $4 \times 10^5$  cell/mL and transfer 1 mL of cell suspension to two 90-mm diameter dishes of bacteriological plastic in a total of 20 mL of medium lacking an exogenous source of rLIF. This low density of cells is intended to prevent their aggregation, thereby ensuring that each EB is derived from the proliferation and differentiation of a single ES cell.
4. Return cultures to the incubator for a total of 14 d. EBs may be observed with the naked eye as early as 4 d after seeding the dish with ES cells and appear as small spherical structures, floating freely in the medium. By day 14 of culture, EBs may become large macroscopic structures, often several millimeters in diameter (*see Fig. 1B* and *Note 8*).
5. Carefully monitor the medium for the depletion of nutrients during the course of the culture period. Should the medium become acidified, transfer the EB to a 15-mL conical tube and allow them to settle under unit gravity for 2 min. Carefully draw the EB into a sterile Pasteur pipet and transfer them to a dish containing fresh ES medium.

### 3.6. Directed Differentiation of Dendritic Cells

1. To further direct the differentiation of ES cells along the DC lineage pathway, prepare differentiation medium consisting of complete ES medium further supplemented

with 200 U/mL of rmIL-3 and 25 ng/mL of rmGM-CSF. An appropriate concentration of G418 should also be added to the medium to prevent loss of the transgene during differentiation.

2. Harvest the EB after 14 d in suspension culture (*see Note 9*), allowing them to settle in a 50-mL conical tube.
3. Gently draw the EB into a sterile Pasteur pipet and distribute approx 20–30 of these structures into 90-mm tissue culture dishes in 35 mL of differentiation medium (*see Note 10*).
4. Seal the dishes with Leukopor tape and incubate at 37°C, 5% CO<sub>2</sub> (*see Note 11*). Take care not to disturb the cultures for at least 48 h to encourage the adhesion of EB to the tissue culture plastic and the outgrowth of terminally differentiated cell types.
5. Regular observation of cultures will reveal the chaotic nature of the differentiation process, many different cell types becoming apparent over time, of which cardiomyocytes are undoubtedly the most easily identified by virtue of their propensity to contract rhythmically *in situ*. DC may become visible as early as day 4–5 of culture although the kinetics of their appearance may vary considerably between ES cell lines and even different passages of the same line. Typically DC appear around the very perimeter of the colonies derived from adherent EB (*see Fig. 1C*), frequently forming a distinctive “halo” of cells. Extensive proliferation results in their accumulation and the formation of clusters, highly reminiscent of immature DC differentiated from cultures of mouse bone marrow progenitors (*see Fig. 1D*). The terminally differentiated DC, which are stably immature at this stage, may eventually become confluent (*see Note 12*).
6. Care should be taken to ensure that cultures do not become depleted of nutrients. When feeding cultures, remove all exhausted medium, leaving behind the lightly adherent DC, and carefully replace with fresh differentiation medium.
7. Because DC differentiated from ES cells adhere strongly to one another when pelleted, forming clumps that are difficult to dissociate without harming the cells, we routinely centrifuge the cell suspension in PSB containing EDTA. To do so, discard the medium, removing the last traces using a Pasteur pipet, and overlay with 9 mL of PBS.
8. Use a 1-mL Gilson pipet and moderate force to expel medium over the surface of the dish and dislodge the lightly adherent cells, which may be seen as a “cloud” when tilting the dish forward (*see Note 13*).
9. Transfer the cell suspension to a 15-mL conical tube and add 1 mL of 0.2% EDTA in PBS to yield a final concentration of 0.02%. Centrifuge the cell suspension for 5 min at 200g before using the cells in immunological assays, designed to investigate the impact of transgene expression on DC function.

### 3.7. Maturation of Dendritic Cells

1. Although ES cell-derived DC are stably immature for prolonged periods in culture, they may be induced to mature by transient exposure to LPS. To initiate their

maturation program, harvest the DC and plate overnight onto fresh tissue culture plates in differentiation medium.

2. Add LPS (*E. coli* serotype 0127:B8) at a final concentration of 1  $\mu\text{g}/\text{mL}$  and return to the incubator.
3. After overnight culture, the majority of cells will have adhered strongly to the plastic and begun to spread out. Remove all medium and replace with fresh differentiation medium that lacks any traces of LPS, before incubating again overnight.
4. Observation under an inverted phase-contrast microscope the following day will reveal floating cells displaying highly dendritic morphology, a cardinal feature of mature DC (see Fig. 1E). To obtain a substantially pure population of mature DC, harvest the medium without pipetting over the surface of the dish and centrifuge. Because, upon maturation, the DC lose their propensity for aggregation, the addition of EDTA is unnecessary at this stage.
5. Feed cultures with fresh differentiation medium and return to the incubator, examining for the release of further cohorts of mature cells over the ensuing few days (see Note 14).

#### 4. Notes

1. We prefer C57Bl/6 mice as a source of embryonic fibroblasts except when culturing ES cells under selection conditions following transfection. When using the neomycin analog G418-sulfate, for selection purposes, it is necessary to use primary embryonic fibroblasts from Rosa 26 mice, because these are intrinsically neomycin-resistant.
2. Batches of FCS may vary enormously with respect to their capacity to support ES cell growth and directed differentiation of ES cells along the DC pathway. We recommend screening samples from different suppliers against both of these criteria and ordering the best batch in bulk.
3. At this stage of the protocol, embryonic fibroblasts are only lightly adherent. Care should be taken, therefore, when trying to dislodge debris by expelling medium onto the surface of the monolayer.
4. Batches of fibroblasts may vary enormously with respect to their viability after thawing, their doubling time and the total number of passages they can sustain. We recommend comparing batches by defining the length of time taken to reach confluency after seeding a 75-cm<sup>2</sup> flask with a single vial of fibroblasts and the number of passages they can undergo before falling quiescent. This information can be extremely valuable when planning the maintenance of ES cell lines and the best time to replace existing flasks of feeder cells from frozen stocks.
5. Although we favor the use of mitomycin C, the availability of a <sup>60</sup>Co radiation source provides an inexpensive alternative approach to rendering feeder cells mitotically inactive. The delivery of 30 Gy is sufficient to prevent their proliferation.
6. Although protocols for the use of other cell types frequently suggest performing transfection once cells have reached 80% confluency, we find that mouse ES cells, plated at this density, have a tendency to overgrow and die prematurely, before

succumbing to G418 toxicity. A cell density of 40% therefore provides adequate scope for expansion during the course of transfection and selection.

7. We recommend the use of 12-cm<sup>2</sup> tissue culture flasks at this stage of the protocol as a result of the need to supplement the culture medium with a source of rLIF, which constitutes a major expense. The use of 12-cm<sup>2</sup> flasks requires as little as 4 mL of complete medium but still yields sufficient ES cells for the generation of copious EB.
8. EB vary enormously in size and morphology, even when cultured from a homogenous suspension of ES cells. In general, however, EB may be characterized as either “simple” or “cystic,” the latter being distinguished by the development of a fluid-filled cavity, which may increase significantly in size, sometimes reaching up to 5 mm in diameter. Importantly, we have yet to observe any difference in the ability of either type of EB to sustain the differentiation of DC.
9. Although we have been able to generate DC from EB that have been cultured for as little as 4 d before plating, their appearance is significantly delayed and yields are comparatively low. Likewise, EB cultured in suspension for 21 d prior to plating may be permissive, but yields of DC decrease progressively beyond this time point. For this reason, we routinely use EB cultured for 14 d as the starting material for directed differentiation.
10. Given the inevitable investment of time and resources in the generation of genetically modified ES cells, there can be significant psychological pressure not to waste any material, with the result that too many EB may be seeded per plate. This temptation should, however, be strongly resisted, even if a significant proportion of the EB is discarded, because crowding of the EB provides too little space for DC to develop.
11. We find that sealing dishes with leukopor tape helps to maintain sterility during prolonged incubation periods of up to 1 mo. This is particularly important when repeatedly handling dishes, because even the most experienced worker will occasionally deposit medium around the rim of the dish during routine observation, which leaves the culture especially vulnerable to fungal infection.
12. Although ES cell-derived DC remain stably immature with time, showing none of the phenotypic changes associated with maturation, they appear to undergo predictable changes in morphology during prolonged periods in culture. In particular, the cells become enlarged, rounded, and highly vacuolated, as though actively sampling the surrounding milieu. Importantly, such morphological changes do not appear to affect the immunostimulatory function of the cells *in vitro*.
13. After harvesting DC, we routinely feed the culture with fresh medium supplemented with rmGM-CSF and rmIL-3, to permit the emergence of a further cohort of cells. It is, in fact, possible to obtain at least three batches of DC from the same culture before the cells fall quiescent.
14. When first challenged with LPS, the DC become uniformly and transiently adherent to tissue culture plastic before gradually releasing over the course of the

ensuing few days. These may be harvested in successive waves, or allowed to accumulate in the medium for several days before harvesting. For unexplained reasons, only a proportion of the original cells appears capable of assuming a classic nonadherent dendritic morphology, the majority remaining strongly adherent through out.

## References

1. Steinman, R. M., Hawiger, D., and Nussenzweig, M. C. (2003) Tolerogenic dendritic cells. *Annu. Rev. Immunol.* **21**, 767–811.
2. Morelli, A. E. and Thomson, A. W. (2003) Dendritic cells: regulators of alloimmunity and opportunities for tolerance induction. *Immunol. Rev.* **196**, 125–146.
3. Fairchild, P. J. and Austyn, J. M. (1990) Thymic dendritic cells: phenotype and function. *Int. Rev. Immunol.* **6**, 187–196.
4. Fairchild, P. J. and Waldmann, H. (2000) Dendritic cells and prospects for transplantation tolerance. *Curr. Opin. Immunol.* **12**, 528–535.
5. Waldmann, H., Chen, T. -C., Graca, L., et al. (2006) Regulatory T cells in transplantation. *Sem. Immunol.* **18**(2):111–119.
6. Jonuleit, H., Schmitt, E., Schuler, G., Knop, J., and Enk, E. H. (2000) Induction of IL-10-producing, non-proliferating CD4<sup>+</sup> T cells with regulatory properties by repetitive stimulation with allogeneic immature human dendritic cells. *J. Exp. Med.* **192**, 1213–1222.
7. Mahnke, K., Qian, Y., Knop, J., and Enk, A. H. (2003) Induction of CD4<sup>+</sup>CD25<sup>+</sup> regulatory T cells by targeting of antigens to immature dendritic cells. *Blood* **101**, 4862–4869.
8. Chen, L. (2004) Co-inhibitory molecules of the B7-CD28 family in the control of T-cell immunity. *Nat. Rev. Immunol.* **4**, 336–347.
9. Munn, D. H., Sharma, M. D., Lee, J. R., et al. (2002) Potential regulatory function of human dendritic cells expressing indoleamine 2,3-dioxygenase. *Science* **297**, 1867–1870.
10. Mellor, A. L. and Munn, D. H. (2004) IDO expression by dendritic cells: Tolerance and tryptophan catabolism. *Nat. Rev. Immunol.* **4**, 762–774.
11. Jenne, L., Schuler, G., and Steinkasserer, A. (2001) Viral vectors for dendritic cell-based immunotherapy. *Trends Immunol.* **22**, 102–102.
12. Morelli, A. E., Larregina, A. T., Ganster, et al. (2000) Recombinant adenovirus induces maturation of dendritic cells via an NF- $\kappa$ B-dependent pathway. *J. Virol.* **74**, 9617–9628.
13. Fairchild, P. J., Brook, F. A., Gardner, R. L., et al. (2000) Directed differentiation of dendritic cells from mouse embryonic stem cells. *Curr. Biol.* **10**, 1515–1518.
14. Fairchild, P. J., Nolan, K. F., and Waldmann, H. (2003) Probing dendritic cell function by guiding the differentiation of embryonic stem cells. *Meth. Enzymol.* **365**, 169–186.

15. Fairchild, P. J., Nolan, K. F., Graça, L., and Waldmann, H. (2003) Stable lines of genetically modified dendritic cells from embryonic stem cells. *Transplantation* **76**, 606–608.
16. Thomson, J. A., Itskovitz-Eldor, J., Shapiro, S. S., et al. (1998) Embryonic stem cell lines derived from human blastocysts. *Science* **282**, 1145–1147.
17. Reubinoff, B. E., Pera, M. F., Fong, C. Y., Trounson, A., and Bongso, A. (2000) Embryonic stem cell lines from human blastocysts: somatic differentiation in vitro. *Nat. Biotechnol.* **18**, 399–404.

## Generation of Immunocompetent T Cells from Embryonic Stem Cells

Renée F. de Pooter and Juan Carlos Zúñiga-Pflücker

### Summary

Mature hematopoietic cells, like all other terminally differentiated lineages, arise during ontogeny via a series of increasingly restricted intermediates. Hematopoietic progenitors derive from the mesoderm, which gives rise to hemangioblasts that can differentiate into endothelial or endocardial precursors, or hematopoietic stem cells (HSCs). These HSCs, in turn, may either self-renew or differentiate into lineage-restricted progenitors, and ultimately mature effector cells. The ability to generate most hematopoietic lineages in a two-dimensional *in vitro* environment has facilitated our study of this complex process. Until recently, T lymphocytes were the exception, and appeared to require the specific three-dimensional microenvironment of the thymus to develop. However, here we describe a protocol for the generation of immunocompetent T lymphocytes from embryonic stem cells (ESCs) *in vitro*, within the two-dimensional microenvironment provided by OP9 bone marrow stromal cells that have been transduced to express the Notch ligand Delta-like-1. This procedure will facilitate further study of T lymphocytes by providing a model system in which the effects of genetic and environmental manipulations of ESC-derived progenitors can be examined, and the mechanisms of tolerance potentially dissected, *in vitro*.

**Key Words:** Lymphocyte development; T-cell development; fetal thymic organ culture; hematopoiesis; hemangioblast; Flt-3L; IL-7; embryonic stem cells; stromal cells; Delta-like-1; Notch; OP9 stromal cells.

### 1. Introduction

Of the cells in the vertebrate hematopoietic system, the T and B lymphocytes, which comprise the effectors of the adaptive immune system, are arguably the most complex in their development, as both must pass developmental checkpoints that allow only cells with functional, nonautoreactive antigen receptors to survive to maturity.

From: *Methods in Molecular Biology*, vol. 380: *Immunological Tolerance: Methods and Protocols*  
Edited by: P. J. Fairchild © Humana Press Inc., Totowa, NJ



Although other protocols produce T cells from embryonic stem cells (ESCs) (1–4), the totipotent cells isolated from the inner cell mass of a blastocyst (5), they do not greatly facilitate the manipulation of the hematopoietic environment and progenitors required to gain a thorough understanding of the process of maturation itself. In the seminal work that led to development of our own system, Nakano et al. demonstrated that the in vitro differentiation of ESCs into B lymphocytes could be achieved using the bone marrow stromal cell line OP9 (6,7), which is derived from mice deficient in macrophage colony stimulating factor (M-CSF). The absence of M-CSF prevents macrophages from overwhelming other lineages in the coculture (8), and allows OP9 stromal cells to support the efficient differentiation of ESCs (ESC/OP9 coculture) into multiple hematopoietic lineages. Although initially the efficiency of B-cell generation in ESC/OP9 cocultures was low, Cho et al. demonstrated that the addition of exogenous Flt-3L and interleukin (IL)-7, cytokines known to potentiate B-cell production (9–14), allowed for the efficient and consistent production of B cells (15). T-cell potential, however, remained elusive, although transfer of prehematopoietic Flk-1<sup>+</sup>CD45<sup>-</sup> precursors from the ESC/OP9 cocultures to reaggregate thymic organ cultures, though inefficient, did allow the production of mature T cells from ESCs in vitro (16). Ultimately, the issue of efficiency of in vitro T-cell development was resolved by transducing OP9 stromal cells with the Notch ligand Delta-like-1 (Dll-1) (17).

The Notch signaling pathway had already been demonstrated to play an important role in commitment to the T- vs B-lymphocyte fate (18,19), and when OP9 stromal cells were retrovirally transduced to express Dll-1 (OP9-DL1), the resulting ESC/OP9-DL1 cocultures now supported robust T, but no longer B, lymphopoiesis, from fetal liver, bone marrow, and ESC-derived hematopoietic progenitors (17,20).

This system permits the efficient generation of mature, functional CD8<sup>+</sup> T cells, although mature CD4<sup>+</sup> T cells do not arise, presumably because the absence of MHC II expression on OP9 cells precludes their positive selection. The ESC/OP9-DL1 cocultures permit detailed molecular studies under various culture conditions, and facilitate the manipulation of ESCs throughout the stages of differentiation from progenitor to mature lymphocyte.

## 2. Materials

### 2.1. Cellular Components

#### 2.1.1. ESCs and Embryonic Fibroblast Cells

1. ESCs (R1, D3, E14K derived from 129/Sv mice and ESCs derived from BALB/c and C57BL/6, and [C57BL6/129]F2 mice have all been used to generate lymphocytes in vitro).
2. Mouse embryonic fibroblast (EF) cells (21).

3. Fetal bovine serum (FBS). Different sources required for ESC vs OP9/coculture media. Heat-inactivate at 56°C for 30 min and store at 4°C (*see Note 1*).
4. High glucose Dulbecco's modified Eagle's medium (Sigma, cat. no. D-5671). Store at 4°C.
5. 1X Phosphate buffered saline (PBS) without Ca<sup>2+</sup>/Mg<sup>2+</sup> (Gibco, cat. no. 14190-144). Store at room temperature.
6. HEPES, sodium pyruvate, gentamicin solution: 5 mL HEPES 100X or 1 M (Gibco, cat. no. 15630-08), 5 mL sodium pyruvate 100X or 100 mM (Gibco, cat. no. 11360-070), 0.5 mL Gentamicin 1000X or 50 mg/mL (Gibco, cat. no. 15750-060), aliquoted into 14-mL conical tubes. Store at 4°C, stable for approx 1 yr.
7. Penicillin/streptomycin, glutamax, 2(β)-mercaptoethanol solution: 5 mL penicillin/streptomycin 100X or 10,000 U/mL penicillin and 10,000 μg/mL streptomycin (Gibco, cat. no. 15140-122), 5 mL Glutamax 100X or 200 mM (Gibco, cat. no. 35050-061), 0.5 mL β-mercaptoethanol 1000X or 55 mM, (Gibco, cat. no. 21985-023), aliquoted into 14-mL conical tubes. Store at -20°C, stable for approx 1 yr.
8. ESC medium: 500 mL of high glucose Dulbecco's modified Eagle's medium supplemented with 15% heat-inactivated FBS (iFBS), 10.5 mL PGS solution and 10.5 mL HEPES, sodium pyruvate, gentamicin solution (one aliquot each).
9. 2.5% Trypsin (Gibco, cat. no. 15090-046). Dilute with PBS to 0.25% solution as needed and store at 4°C.
10. Mitomycin C solution: 1 mg/mL (100X) mitomycin C (Sigma, cat. no. M-4287) stock solution in PBS. Store in the dark at 4°C, stable for 2 wk.
11. Mouse leukemia inhibitory factor (LIF) (Sigma, cat. no. L5158). Dilute to 7.5 μg/mL (1000X). Aliquot and store at -80°C.
12. Freezing medium: 90% iFBS, 10% dimethyl sulfoxide.
13. Tissue culture ware, tissue culture treated (suggested suppliers: Sarstedt or Falcon).

### 2.1.2. OP9-DL1 Cells

1. OP9 cells (Riken cell repository, <http://www.brc.riken.jp/lab/cell/english/index.shtml>) retrovirally transduced to express Dll-1, as previously reported (*17*).
2. α-Modified Eagle's medium (Gibco, cat. no. 12561-056). Store at 4°C.
3. OP9 medium: α-modified Eagle's medium αMEM, supplemented with 20% iFBS and 1X of penicillin/streptomycin.

### 2.2. ESC/OP9-DL1 Coculture

1. Mouse IL-7 (R&D 407-ML). Reconstitute at 1 μg/mL (1000X). Aliquot and store at -80°C.
2. Human Flt-3L (R&D 308-FK). Reconstitute at 5 μg/mL (1000X). Aliquot and store at -80°C.

## 3. Methods

The methods described next outline (1) the maintenance of the required cell lines and (2) the coculture of ESCs on OP9-DL1 cells for the production of T cells. It should be noted that all incubations are performed in a standard,

humidified, cell culture incubator, at 37°C in 5% CO<sub>2</sub>, all tissue culture ware is tissue culture treated for adherent cells, and cells are pelleted by centrifuging at 300g for 5 min.

### 3.1. Cellular Components of the Coculture System

#### 3.1.1. ESCs and EF Cells

1. ESCs are maintained as adherent colonies on monolayers of growth-inactivated EF in ESC medium. EF inactivation may be performed by either irradiation (3000 cGy) or treatment with mitomycin C. In the case of treatment with mitomycin C, which is light-sensitive, EF are incubated for 2.5 h in ESC medium with 10 µg/mL of mitomycin C. Wash three times with PBS, and add fresh ESC medium. EF cells should be used within 5 d of either treatment.
2. For the maintenance of undifferentiated ESCs, Hyclone offers prescreened, characterized lots of FBS (*see Note 1*). ESCs should be thawed in a 37°C water bath and transferred to a 14-mL conical tube containing 10 mL of ESC medium. Pellet the cells, and resuspend in 3 mL of ESC medium to be plated on a 6-cm diameter dish of approx 80% confluent inactivated EF cells. Add 3 µL of LIF. Change the medium the next day, and passage to a fresh plate of inactivated EF the following day (*see below*), each time adding LIF. Maintain ESC by repeating this procedure, alternating media changes and passages, and allowing them to become no more than 80% confluent.
3. To passage the ESCs, remove the medium and wash the dish gently with 4 mL of PBS. Remove PBS and incubate the plate with 1 mL 0.25% trypsin for 5 min. Wash the cells from the plate by adding 2 mL of ESC medium and pipetting vigorously. If the plate has become over confluent, or large colonies with borders of flattened, nonrefractive cells have formed, small, undifferentiated colonies can sometimes be restored by passing the cells through 70-µm nylon mesh. Pellet the cells, and resuspend in 3 mL ESC medium with LIF. Remove the medium from a fresh 6-cm diameter dish of 80% confluent inactivated EF cells, and add the resuspended ESCs. Gently agitate the plate to disperse the cells and LIF.
4. To generate frozen stocks of ESCs, wash with PBS, treat with trypsin, and collect the cells as described above. Resuspend the ESCs in ice-cold freezing medium, and aliquot them into cryovials (two to four vials per confluent 6-cm plate of ESCs). Transfer the vials on ice to a -80°C freezer overnight, and the next day to liquid nitrogen for long-term storage.

#### 3.1.2. OP9-DL1 Cells

1. Thaw a vial of OP9-DL1 cells as described for ESCs, but substitute OP9 medium for ESC medium. Plate cells in a 10-cm diameter dish with 8–10 mL of fresh OP9 medium. Change the medium the next day. OP9-DL1 cells should not be allowed to become more than 80% confluent, and can generally be maintained by passaging 1:4 every 2 d.
2. To passage OP9-DL1 cells from a 10-cm plate, remove the medium, wash with 6 mL of PBS, remove the PBS, and incubate for 5 min with 4 mL of 0.25% trypsin.

Following trypsin treatment, prepare a 50-mL conical tube with 5 mL of OP9 medium. Add 4 mL of PBS to the trypsin-treated plate, pipet vigorously, and add the cells to the tube containing medium. OP9-DL1 cells, especially early passage cells, are very adherent. Rinse the plate again with 8 mL of PBS and pool this with the first wash. Pellet the cells, resuspend them, and divide them among four 10-cm plates, or four six-well plates. Gently agitate the plate to distribute the cells evenly (see **Notes 2** and **3**).

### **3.2. ESC/OP9-DL1 Coculture**

This section describes (1) the preparation of the cells for coculture and (2) the production of T cells.

#### **3.2.1. Coculture (see **Note 4**)**

##### **3.2.1.1. DAY -6 TO -2**

1. Thaw the ESCs onto inactivated EF cells 4–6 d before beginning the coculture (d -6 to d -4).
2. Maintain undifferentiated ESCs as described above.
3. Thaw OP9-DL1 stromal cells at d -4.
4. At d -2, passage a confluent plate of OP9-DL1 stromal cells onto 4 × 10-cm diameter plates.

##### **3.2.1.2. DAY 0**

1. Remove the media from 10-cm dishes of OP9-DL1 stromal cells that are no more than 80% confluent, and replace with 8 mL fresh OP9 medium.
2. Aspirate the medium from the ESCs and treat them with trypsin (described above).
3. Disaggregate the cells by vigorous pipetting and add 6 mL of ESC medium.
4. Transfer the cells to a new empty 10-cm dish, with no preexisting EF monolayer.
5. Incubate the cells for 30 min to allow the EF cells to settle and adhere to the plate (plate out).
6. Collect the nonadherent cells from the ESC plate and pellet them.
7. Resuspend the ESCs in 3 mL ESC medium to count.
8. Dilute  $5 \times 10^4$  ESCs into 2 mL of OP9 medium, and seed onto a 10-cm dish of 80% confluent OP9-DL1 stromal cells from **step 1**.

##### **3.2.1.3. DAY 3**

1. Aspirate the coculture medium without disturbing the cells or the monolayer.
2. Replace with 10 mL of fresh OP9 medium.

##### **3.2.1.4. DAY 5**

1. Fifty to one hundred percent of colonies should have mesoderm characteristics (**7**) (see **Note 5**). Aspirate the medium without disturbing the cells or the monolayer.
2. Wash with 10 mL of PBS and remove the PBS.

3. Add 4 mL of 0.25% trypsin to the plates, and incubate for 5 min.
4. Disaggregate the cells by vigorous pipetting to create a homogenous suspension.
5. Add 4 mL of OP9 medium and incubate the disaggregated cells for 30 min to plate out the OP9-DL1 cells.
6. Collect the nonadherent cells and pellet them.
7. Resuspend the cells in 2 mL of fresh OP9 medium and count them.
8. Seed  $6 \times 10^5$  cells per fresh 10-cm plate of 80% confluent OP9-DL1 stromal cells. If cells are to be analyzed by flow cytometry at later time points, a good guideline is to seed one 10-cm plate of OP9-DL1 stroma per anticipated time point (*see Note 6*).
9. Add Flt3-L to a final concentration of 5 ng/mL.

#### 3.2.1.5. DAY 8

1. Small clusters of 4–10 round, refractile blast-like cells should be visible. Transfer all the culture media into a 50-mL conical tube. Gently wash the surface of the plate using a 10-mL pipet with 8 mL of PBS, attempting not to disrupt the OP9-DL1 monolayer. Transfer the wash into the same 50-mL conical tube, passing the wash through a 70- $\mu$ m filter to exclude pieces of disrupted monolayer. The object is to collect all round, loosely adherent, blast-like cells. Determine whether this has been accomplished by observing the culture under an inverted phase-contrast microscope.
2. Pellet the collected cells and resuspend them in 2 mL of fresh OP9 medium.
3. Transfer the cells to fresh six-well plates of 80% confluent OP9-DL1 stromal cells: one 10-cm plate's worth of cells is transferred to one well of a six-well plate, in 3 mL of OP9 medium.
4. Add Flt3-L to a final concentration of 5 ng/mL.
5. For T cell differentiation, add IL-7 to a final concentration of 1 ng/mL.

#### 3.2.1.6. DAY 10

1. Change the medium by collecting culture media into a 14-mL tube and centrifuging.
2. Add 1 mL of fresh OP9 medium to the wells to prevent the cells from drying out.
3. Resuspend any pelleted cells with 2 mL of fresh OP9 medium per well of the six-well plate.
4. Gently pipet the resuspended cells onto the original well without disrupting the monolayer.
5. Add cytokines to the final concentrations described above.

#### 3.2.1.7. DAY 12

1. Passage the cells by vigorously pipetting to disrupt the monolayer, and pass through a 70- $\mu$ m mesh into a tube.
2. Pellet the cells, and resuspend them in 3 mL per well of fresh OP9 medium.
3. Transfer to the same number of wells in fresh six-well plates of 80% confluent OP9-DL1 stromal cells, with appropriate cytokines.

## 3.2.1.8. BEYOND DAY 12

To continue the cultures beyond d 12, transfer the cells to fresh OP9-DL1 stroma every 4–6 d, and change the medium every 2–3 d. Alternate the media change and passage protocols described for d 10 and 12, respectively. Although, for efficient hematopoiesis, it is best to leave the cocultures undisturbed as much as possible, overconfluent OP9-DL1 monolayers differentiate into adipocytic cells that no longer support hematopoiesis and may begin to detach from the culture dish and roll up from the edges (*see Note 6*).

**4. Notes**

1. Although Hyclone offers prescreened, characterized batches of FBS for the propagation of undifferentiated ESCs, prescreened lots of FBS for ESC/OP9-DL1 coculture are not yet commercially available. To screen FBS for this purpose, cocultures maintained in OP9 medium supplemented with different lots of heat-inactivated FBS must be tested in parallel. The outcome is assessed by the efficiency and cell number of resulting T cells, coexpressing the cell surface markers CD4 and CD8, at d 15–20 of coculture.
2. For differentiating ESCs, OP9-DL1 cells should not be kept in continuous culture for longer than 4 wk. OP9-DL1 cells that have been maintained in good condition are large flat cells with short dendritic protrusions and an overall star-like shape. OP9-DL1 cells will lose their ability to induce hematopoiesis from ESCs after prolonged culture, and allowing overconfluency will hasten this process. Noticeably increased or decreased rates of division, or an increased frequency of adipocytes (rounded OP9-DL1 cells with highly refractile fat droplets) are indications of OP9-DL1 stroma that may no longer support hematopoiesis from ESCs, but may still support hematopoiesis from fetal liver- or bone marrow-derived progenitors. Older stocks of OP9-DL1 cells that may no longer be suitable for initiating an ESC/OP9-DL1 coculture can still be used at later time points of a coculture, such as day 8 or 12. During the course of ESC/OP9-DL1 cocultures, cells are seeded onto 80% confluent OP9-DL1 monolayers, which quickly become overconfluent. Thus, the appearance of some adipocytes during a coculture is normal, but these should not predominate.
3. To preserve early passage stocks of OP9-DL1 stromal cells, once thawed OP9-DL1 cells have become 60–80% confluent, passage the 10-cm diameter dish into four more dishes, and continue until 16 or 32 plates are 60–80% confluent. Freeze one 80% confluent plate to one cryovial in freezing media, as described for ESCs. These stocks may be expanded to generate working stocks.
4. During the coculture, hematopoietic cells arise at day 5. Lymphopoiesis, producing DN2 (CD44<sup>+</sup>CD25<sup>+</sup>) thymocyte-like cells, may begin as early as day 12 and, in the presence of IL-7 and Flt3L should predominate up to day 16, and thereafter CD4<sup>+</sup>CD8<sup>+</sup> expressing cells should appear. When cocultures are maintained past day 20, only lymphoid cells are evident, indicating that multilineage potential does not persist during the coculture.

5. Mesoderm colonies contain tightly packed refractile cells. Early colonies are flat, and the cells may be arranged in somewhat concentric circles. Later colonies acquire pronounced three-dimensional structures, and resemble asymmetric “wagon wheels,” with spokes leading out to the rim from a central hub.
6. The kinetics of the coculture can be assessed by flow cytometry. Hematopoietic cells, defined by the expression of the pan-hematopoietic marker CD45 (leukocyte common antigen), can be detected as early as day 5 of coculture, but more readily by d 8 (15). Early T-cell progenitors, called DN2 cells, express CD44 and CD25. Expression of CD44 is lost as these progenitors mature to pre-T cells. Cells restricted to the T-cell lineage can be identified by their expression of CD90 and CD25, and later, by upregulation of first surface CD3 and TCR and then CD4 and CD8. Fluorescently labeled antibodies against the markers described can be purchased from either Pharmingen or eBiosciences.

## References

1. Chen, U., Kosco, M., and Staerz, U. (1992) Establishment and characterization of lymphoid and myeloid mixed-cell populations from mouse late embryoid bodies “embryonic-stem-cell fetuses.” *Proc. Natl. Acad. Sci. USA* **89**, 2541–2545.
2. Gutierrez-Ramos, J. C. and Palacios, R. (1992) In vitro differentiation of embryonic stem cells into lymphocyte precursors able to generate T and B lymphocytes in vivo. *Proc. Natl. Acad. Sci. USA* **89**, 9171–9175.
3. Potocnik, A. J., Nielsen, P. J., and Eichmann, K. (1994) In vitro generation of lymphoid precursors from embryonic stem cells. *EMBO J.* **13**, 5274–5283.
4. Burt, R. K., Verda, L., Kim, D. A., Oyama, Y., Luo, K., and Link, C. (2004) Embryonic stem cells as an alternate marrow donor source: engraftment without graft-versus-host disease. *J. Exp. Med.* **199**, 895–904.
5. Robertson, E. J. (1987) *Teratocarcinomas and Embryonic Stem Cells: A Practical Approach*. IRL Press, Oxford, UK.
6. Nakano, T. (1995) Lymphohematopoietic development from embryonic stem cells in vitro. *Semin. Immunol.* **7**, 197–203.
7. Nakano, T., Kodama, H., and Honjo, T. (1994) Generation of lymphohematopoietic cells from embryonic stem cells in culture. *Science* **265**, 1098–1101.
8. Yoshida, H., Hayashi, S., Kunisada, T., et al. (1990) The murine mutation osteopetrosis is in the coding region of the macrophage colony stimulating factor gene. *Nature* **345**, 442–444.
9. Hirayama, F., Lyman, S. D., Clark, S. C., and Ogawa, M. (1995) The flt3 ligand supports proliferation of lymphohematopoietic progenitors and early B-lymphoid progenitors. *Blood* **85**, 1762–1768.
10. Hudak, S., Hunte, B., Culpepper, J., et al. (1995) FLT3/FLK2 ligand promotes the growth of murine stem cells and the expansion of colony-forming cells and spleen colony-forming units. *Blood* **85**, 2747–2755.
11. Hunte, B. E., Hudak, S., Campbell, D., Xu, Y., and Rennick, D. (1996) *flk2/flt3* ligand is a potent cofactor for the growth of primitive B cell progenitors. *J. Immunol.* **156**, 489–496.

12. Jacobsen, S. E., Okkenhaug, C., Myklebust, J., Veiby, O. P., and Lyman, S. D. (1995) The FLT3 ligand potently and directly stimulates the growth and expansion of primitive murine bone marrow progenitor cells in vitro: synergistic interactions with interleukin (IL) 11, IL-12, and other hematopoietic growth factors. *J. Exp. Med.* **181**, 1357–1363.
13. Lyman, S. D. and Jacobsen, S. E. (1998) c-kit Ligand and Flt3 Ligand: stem/progenitor cell factors with overlapping yet distinct activities. *Blood* **91**, 1101–1134.
14. Veiby, O. P., Lyman, S. D. and Jacobsen, S. E. W. (1996) Combined signaling through interleukin-7 receptors and flt3 but not c-kit potently and selectively promotes B-cell commitment and differentiation from uncommitted murine bone marrow progenitor cells. *Blood* **88**, 1256–1265.
15. Cho, S. K., Webber, T. D., Carlyle, J. R., et al. (1999) Functional characterization of B lymphocytes generated in vitro from embryonic stem cells. *Proc. Natl. Acad. Sci. USA* **96**, 9797–9802.
16. de Pooter, R. F., Cho, S. K., Carlyle, J. R., and Zúñiga-Pflücker J. C. (2003) In vitro generation of T lymphocytes from embryonic stem cell-derived pre-hematopoietic progenitors. *Blood* **102**, 1649–1653.
17. Schmitt, T. M. and Zúñiga-Pflücker, T. M. (2002) Induction of T cell development from hematopoietic progenitor cells by Delta-like-1 in vitro. *Immunity* **17**, 749–756.
18. Pui, J.C., Allman, D., Xu, L., et al. (1999) Notch1 expression in early lymphopoiesis influences B versus T lineage determination. *Immunity* **11**, 299–308.
19. Radtke, F., Wilson, A., Stark, G., et al. (1999) Deficient T cell fate specification in mice with an induced inactivation of *Notch1*. *Immunity* **10**, 547–558.
20. Schmitt, T. M., de Pooter, R. F., Gronski, M. A., et al. (2004) Induction of T cell development and establishment of T cell competence from embryonic stem cells differentiated in vitro. *Nat. Immunol.* **5**, 410–417.
21. Robertson, E. J. (1997) Derivation and maintenance of embryonic stem cell cultures. *Methods Mol. Biol.* **75**, 173–184.
22. Carlyle, J. R., Michie, A. M., Cho, S. K., and Zúñiga-Pflücker, J. C. (1998) Natural killer cell development and function precede alpha beta T cell differentiation in mouse fetal thymic ontogeny. *J. Immunol.* **160**, 744–753.





## Isolation, Expansion, and Characterization of Human Natural and Adaptive Regulatory T Cells

Silvia Gregori, Rosa Bacchetta, Laura Passerini, Megan K. Levings, and Maria Grazia Roncarolo

### Summary

Regulatory T cells play a central role in controlling homeostasis, and in inducing and maintaining tolerance to both foreign and self-antigens. Several types of T cells with regulatory activity have been described both in mice and humans, and those within the CD4<sup>+</sup> subset have been extensively studied. Among them, the best characterized are the naturally occurring CD4<sup>+</sup>CD25<sup>+</sup> regulatory T (Treg) cells, and the adaptive type 1 regulatory T (Tr1) cells. Natural Treg cells can arise directly from the thymus, are characterized by the constitutive expression of the transcription factor Foxp3, and suppress T cell responses in a cell–cell contact mediated mechanism. On the contrary, adaptive Tr1 cells arise in the periphery upon encountering antigen in a tolerogenic environment, produce high levels of interleukin (IL)-10 and mediate suppression via IL-10. During the last decade, much effort has been placed on developing protocols to generate regulatory T-cell lines and clones, to further define the similarities and differences between various regulatory T-cell subsets. In this chapter, we will outline protocols to expand naturally occurring Treg cells, to differentiate homogeneous population of Tr1 cells in vitro, and to generate natural Treg and Tr1 cell clones and cell lines.

**Key Words:** CD4<sup>+</sup>CD25<sup>+</sup> regulatory T cells; Foxp3; type 1 regulatory T cells; immature DCs; IL-10.

### 1. Introduction

Peripheral tolerance is operational throughout life and controls immune responses to self-antigens that are not expressed in the thymus, and to foreign antigens that are encountered in peripheral tissues. Mechanisms of peripheral T-cell tolerance include cell death with consequent clonal deletion, development of a state of nonresponsiveness in T cells, and active suppression mediated by regulatory T cells. Cells with regulatory function exist within all major

T- and natural killer T (NKT)-cell subsets (1), although most attention has been focused on regulatory T cells with a CD4<sup>+</sup> phenotype. Among CD4<sup>+</sup> regulatory T cells the best characterized are the naturally occurring CD4<sup>+</sup>CD25<sup>+</sup> regulatory T (Treg) cells and the adaptive type 1 regulatory (Tr1) T cells. These two regulatory T-cell subsets share some common features such as suppressive function and low proliferative response in vitro. However, they also possess several differences that clearly demonstrate that they are two distinct regulatory T-cell subsets with different mechanisms of action (2,3).

Treg cells emerge from the thymus and constitutively express the  $\alpha$  chain of the interleukin (IL)-2R (CD25), intracellular cytotoxic T lymphocyte antigen (CTLA)-4, glucocorticoid-induced TNF receptor (GITR) (4), and the transcription factor Foxp3, which is involved in their development (5). CD25<sup>+</sup> T cells comprise a minor population of CD4<sup>+</sup> T cells: on average approx 10% in rodents and approx 13% in humans. Human CD25<sup>+</sup> T cells can be split into suppressive (CD25<sup>bright</sup>) and nonsuppressive (CD25<sup>low</sup>) T cells according to the level of expression of CD25 (6). Importantly, analysis at the clonal level revealed that even the small fraction of CD25<sup>bright</sup> cells is not a homogeneous population, which contains both suppressor cells and nonsuppressor cells (7). Treg cells are characterized by their inability to produce IL-2 (8), and are anergic in response to Ag-specific, allogeneic or polyclonal stimulation in vitro (6,7,9–12). This hyporesponsiveness can be reversed in vitro by stimulation via T-cell receptor (TCR) and high concentrations of IL-2. Indeed, exogenous IL-2 is required for expansion and suppressive function of Treg cells (13,14). Treg cells suppress proliferation and cytokine production by effector T cells (11) via a yet unidentified cell–cell contact dependent mechanism. The role of immunosuppressive cytokines, and in particular transforming growth factor (TGF)- $\beta$ , in this process remains controversial. Regulatory T cells, which are phenotypically and functionally similar to Treg cells, can also be induced in vitro. For example, in humans a certain fraction of activated CD4<sup>+</sup> T cells remains CD25 positive, begins to express Foxp3, and acquires suppressive capacity in vitro (15,16). The regulatory function of Treg cells has been demonstrated in vivo in several models of autoimmune pathology, including autoimmune diabetes in nonobese diabetic mice (17). In preclinical mouse models of bone marrow transplantation, both depletion of either recipient or donor Treg cells results in markedly accelerated graft-vs-host disease (GvHD) (18), and addition of freshly isolated Treg cells to the donor graft delays GvHD lethality (19,20).

In contrast to natural Treg cells, Tr1 cells are exclusively generated in the periphery, and are defined by a unique cytokine production profile: high levels

of IL-10 and TGF- $\beta$ , low amounts of interferon (IFN)- $\gamma$  and IL-2, and no IL-4 (21). Of note, Tr1 cells do not express high levels of Foxp3 (22–24). Tr1 cells are anergic, but proliferation can be restored by IL-2 and -15, independently from TCR-mediated activation (25). To date, no specific markers, which could allow isolation of Tr1 cells in the periphery, have been identified. Tr1 cells mediate their suppressive function mainly via production of the immunosuppressive cytokines IL-10 and TGF- $\beta$ . Differentiation of Tr1 cells is driven by IL-10 in the presence of TCR activation. Activation of human CD4<sup>+</sup> T cells with allogeneic monocytes in the presence of exogenous IL-10, results in a long-lasting Ag-specific anergy, and the generation of Tr1 cells which can be isolated in vitro (26). Even though IL-10 is essential for the generation of Tr1 cells, it is not sufficient for their *de novo* differentiation in vitro in high numbers. We found that IFN- $\alpha$ , a crucial cytokine for clearing viral infections and increasing IL-10 production by T cells (27), synergizes with IL-10 in vitro to promote the differentiation of human CD4<sup>+</sup> Tr1 cells (28). In vivo the induction of Tr1 cells is strictly dependent on the tolerogenic state of antigen-presenting cells (APCs) in the microenvironment (29). Tr1 cells specific for different antigens can be induced in vivo in both mice and humans, and they regulate immune responses in a number of different Th1- and Th2-mediated pathologies, including intestinal inflammatory diseases (21), airway hyper-reactivity (30), allograft rejection (31), and GvHD (26).

## 2. Materials

1. Lymphoprep (Axis-Shield, Oslo, Norway).
2. RPMI 1640 (Euroclone Life Sciences Division, Pero, Italy).
3. Fetal bovine serum (FBS) (Cambrex, East Rutherford, NJ).
4. Penicillin/streptomycin (Bristol-Myers Squibb, Sermoneta, Italy).
5. L-glutamine (Life Technologies, Milan, Italy).
6. FACS antibodies: anti-CD4 FITC conjugated, anti-CD25 PE conjugated, anti-CD69 FITC conjugated, anti-CD40L FITC conjugated, anti-CD28 PE conjugated (BD Bioscience, San Diego, CA), anti-GITR monoclonal antibody (MAb) (R&D Systems, Minneapolis, MN), anti-CTLA-4 biotin conjugated (BD Bioscience), anti-human Foxp3 PE conjugated (clone PCH 101) (e-bioscience, San Diego, CA).
7. X-VIVO 15 (Cambrex).
8. Human serum (AB) (Cambrex).
9. CD4 T cell isolation kit II (Miltenyi Biotech, Bergisch Gladbach, Germany).
10. CD25 microbeads (Miltenyi Biotech).
11. CD45RO microbeads (Miltenyi Biotech).
12. MACS buffer: PBS pH 7.2, 2 mM EDTA, 0.5% human serum (Cambrex).
13. PHA (Roche Diagnostic, Roche Applied Science, Mannheim, Germany).

14. Proleukin (IL-2) (Chiron Corporation, Emeryville, CA).
15. [<sup>3</sup>H]-thymidine deoxyribose ([<sup>3</sup>H]-TdR) (Amersham Biosciences, Uppsala, Sweden).
16. Anti-CD3 MAb (clone OKT3) (Orthoclone Janssen-Cilag, Cologno Monzese, Italy).
17. Anti-CD28 MAb (clone V5T CD28.05) (BD Bioscience).
18. Th1/Th2 Cytometric bead array (CBA) (BD Bioscience).
19. Trypsin-EDTA (Life Technologies).
20. Recombinant human IL-15 (rhIL-15) (R&D Systems).
21. Recombinant human IL-10 (rhIL-10) (BD Bioscience).
22. Recombinant human IFN (rhIFN)- $\alpha$  (PeproTech, Rocky Hill, NJ).
23. Recombinant human IL-4 (rhIL-4) (R&D Systems).
24. Recombinant human IL-12 (rhIL-12) (R&D Systems).
25. Anti-human IL-4 MAb (clone MP4-25D2) (BD Bioscience).
26. Anti-human IL-12 MAb (clone C8.6) (BD Bioscience).
27. CD3, CD8, CD14 and CD19 beads for depletion (Dynal, Oxoid, Milan, Italy).
28. 2-Mercaptoethanol (Bio-Rad Laboratories, CA).
29. Recombinant human granulocyte-macrophage colony-stimulating factor (rhGM-CSF) (Immunotools, Friesoythe, Germany).
30. Tetanus Toxoid (Calbiochem, Bioscience, Inc., La Jolla CA; Alexis Biochemicals, Switzerland).
31. Paraformaldehyde (Fluka Chemicals AG, Switzerland).
32. Saponin (Sigma Aldrich CO, St. Louis MO).
33. Brefeldin A (Sigma).
34. PE-labeled anti-hIL-4, anti-hIL-2, or anti-hIL-10, and FITC-coupled anti-hIFN- $\gamma$  (BD Bioscience).

### 3. Methods

The methods described below outline (1) isolation of naturally occurring CD4<sup>+</sup>CD25<sup>+</sup> Treg cells from peripheral blood, (2) in vitro expansion and cloning of Treg cells, (3) biological characterization of Treg cells, (4) in vitro induction of adaptive Tr1 cells upon different mode of activation, and (5) biological characterization of adaptive Tr1 cells.

#### **3.1. Isolation of Naturally Occurring CD4<sup>+</sup>CD25<sup>+</sup> Regulatory T Cells**

Peripheral blood mononuclear cells (PBMC) are obtained by centrifugation over Ficoll-Hypaque gradients. Treg cells can be isolated from purified PBMC based on the expression of the cell surface marker IL-2 receptor  $\alpha$  (CD25) either by FACS sorting or by magnetic sorting, as described next, depending on the desired use. Bead-sorted cells are only suitable for immediate in vitro suppression assays and should not be expanded in culture to generate T-cell lines as the purity is not sufficient for long-term maintenance of suppressive cells.

### 3.1.1. Isolation of CD4<sup>+</sup>CD25<sup>+</sup> Treg Cells by FACS Sorting

This method is particularly suitable for purifying Treg cells starting from small numbers of cells (i.e., a starting population of PBMC ranging from  $1 \times 10^7$  to  $5 \times 10^7$ ). For samples larger than  $5 \times 10^7$  PBMC, it is preferable to use the magnetic beads method **steps 1 and 2** (see **Subheading 3.1.2.**) or **step 1** for enrichment of CD4<sup>+</sup> T cells, followed by FACS sorting of the CD25<sup>+</sup> T cells as described here.

1. Resuspend total PBMC or CD4<sup>+</sup> T cells in RPMI supplemented with 1% FBS at a concentration of  $1 \times 10^7$  cells/mL.
2. Add anti-CD4 FITC and anti-CD25 PE conjugated MAb (50  $\mu$ L/ $10^7$  cells) to the PBMC cell suspension (see **Note 1**), or, if working with a CD4-enriched cell suspension, add only anti-CD25 PE conjugated MAb (50  $\mu$ L/ $10^7$  cells).
3. Incubate for 30 min at 4°C in the dark (see **Note 2**).
4. Wash the cells twice with RPMI containing 1% FBS, and resuspend them at a final concentration of  $2 \times 10^7$  cells/mL.
5. Pass the cells through a cell strainer before transferring them to a sterile FACS tube. Keep the cells on ice until the FACS sorter is ready for separation.
6. Prepare collection tubes for positive and negative fractions (see **Note 3**). Set the gate for positive selection to include only the CD4<sup>+</sup>CD25<sup>bright</sup> population (1–2% of PBMC) (see **Fig. 1A**) and collect the whole CD4<sup>+</sup>CD25<sup>-</sup> population in the negative fraction.
7. When separation is complete, centrifuge the two fractions, resuspend the cells in X-VIVO 15 medium supplemented with 5% HS, and 100 U/mL penicillin/streptomycin (hereafter referred to as complete medium) and count.
8. Check the purity of the collected fractions (see **Fig. 1A**). Expect yields of CD4<sup>+</sup>CD25<sup>bright</sup> cells to be less than 2% of the total PBMC and 5% of the CD4<sup>+</sup> T cells, and a purity of at least 90%.

### 3.1.2. Isolation of CD4<sup>+</sup>CD25<sup>+</sup> Treg Cells by Magnetic Beads Separation

For samples larger than  $5 \times 10^7$  PBMC, Treg cells can be isolated by magnetic beads. This procedure includes two successive steps: (1) isolation of total CD4<sup>+</sup> T cells by negative selection and (2) positive selection of CD25<sup>+</sup> T cells (see **Fig. 1B**).

1. Total CD4<sup>+</sup> T cells can be isolated using the CD4<sup>+</sup> T cell isolation kit II, strictly following the manufacturer's instructions (see **Note 4**). The CD4<sup>+</sup> T-cell fraction obtained in this first step is untouched and therefore allows the positive selection of CD25<sup>+</sup> T cells with magnetic beads directly coupled to anti-CD25 MAb.
2. Add 10  $\mu$ L of magnetic beads directly coupled to anti-CD25 MAb per  $1 \times 10^7$  cells to maximize purity of the CD4<sup>+</sup>CD25<sup>+</sup> fraction, strictly following the manufacturer's instructions for purification.
3. After incubation with magnetic beads directly coupled to anti-CD25 MAb, pass the cells over two successive positive selection columns usually (MS).



4. To obtain pure CD25<sup>-</sup> cells, pass the cells over a depletion column (LD) after removal of the CD25<sup>+</sup> cells.
5. Check the purity by FACS staining before proceeding to functional assays (see **Note 5**) (see **Fig. 1B**). Expect yields of CD25<sup>+</sup> cells should be less than 10% of the CD4<sup>+</sup> T cells, and the purity of least 80%.

### 3.2. In Vitro Expansion of CD4<sup>+</sup>CD25<sup>+</sup> Regulatory T Cells

Treg cells can be expanded in vitro using a protocol that preserves suppressive activity, as we previously described (9).

#### 3.2.1. Generation of CD4<sup>+</sup>CD25<sup>+</sup> Treg Cell Lines

1. Treg cells isolated by FACS sorting (see **Note 6**) are stimulated at the final concentration of  $2.5 \times 10^5$ /mL with 0.1  $\mu$ g/mL PHA and 20 U/mL of rhIL-2 in the presence of allogeneic feeder mixture containing  $1 \times 10^6$ /mL irradiated (6000 rad) allogeneic PBMC,  $1 \times 10^5$ /mL irradiated (10,000 rad) allogeneic EBV-LCL (JY), as previously described (26). All cultures are performed in complete medium.
2. Add 100 U/mL of rhIL-2 3 d after activation. Split the cells periodically as necessary and replenish with fresh medium containing rhIL-2 at the final concentration of 100 U/mL every 3 d.
3. Restimulate T-cell lines every 14 d, as previously described. Because Treg cells are known to grow very slowly (9) and in vitro culture favors the expansion of non-Treg cells present in the starting population, it is necessary to routinely check for CD25 and Foxp3 expression in the bulk population and possibly re-enrich for the CD4<sup>+</sup>CD25<sup>bright</sup> subset by FACS sorting before restimulation. All experimental assays should be performed on resting cells, at least 12 d after the last stimulation.

#### 3.2.2. Generation of CD4<sup>+</sup>CD25<sup>+</sup> Treg Cell Clones

Treg cell clones are obtained by limiting dilution of FACS-sorted CD4<sup>+</sup>CD25<sup>+</sup> T cells (7).

1. After purification (see **Note 6**), Treg cells are plated in 200  $\mu$ L of complete medium at 1 cell/well in 96-well round-bottom plates in the presence of allogeneic feeder mixture containing  $5 \times 10^5$  cells/mL of irradiated (6000 rad) allogeneic PBMC,  $5 \times 10^4$  cells/mL of irradiated (10,000 rad) allogeneic JY, 0.05  $\mu$ g/mL of PHA, and 40 U/mL of rhIL-2 in a final volume of 150  $\mu$ L.
2. Add rhIL-2 (100 U/mL) in 50  $\mu$ L after 3 d.
3. After 9 d, pulse one 96-well plate overnight with [<sup>3</sup>H]-TdR (1  $\mu$ Ci/well), to determine the total number of wells with proliferating cells (i.e., the cloning efficiency).
4. At d 14, growing wells are identified by eye, cells are transferred to a 48-well plate, and restimulated with a feeder mixture consisting of  $1 \times 10^6$  cells/mL of irradiated (6000 rad) allogeneic PBMC,  $1 \times 10^5$  cells/mL irradiated (10,000 rad) allogeneic JY, 0.1  $\mu$ g/mL of PHA, and 100 U/mL of rhIL-2.



- Clones are split as necessary and restimulated every 14 d. Fresh complete medium with rhIL-2 at a final concentration of 100 U/mL is added every 3 d. T-cell clones are used for experiments in the resting phase (10–14 d after restimulation).

---

#### Timing of the T-cell cloning

---

- Day 0: Cloning of freshly sorted cells.
- Day 3: Add rhIL-2.
- Day 7: Change medium: remove 80  $\mu$ L/well, and add 100  $\mu$ L/well of fresh medium containing 200 U/mL of rhIL-2.
- Day 9: Sacrifice one plate from each condition and add [ $^3$ H]TdR to all wells to calculate the cloning efficiency. These plates should have one row containing only feeder mixture to determine the background incorporation of [ $^3$ H]-TdR. The expected cloning efficiency must be approx 2–3% for Treg cells.
- Day 10: Change medium: remove 80  $\mu$ L/well and add 100  $\mu$ L/well of fresh medium containing 100 U/mL of rhIL-2.
- Day 14: Restimulation: remove 80  $\mu$ L/well and add 100  $\mu$ L/well of 2X feeder mixture. Between approximately day 10 and 14, growing T-cell clones are ready to be characterized.
- 

### 3.3. Biological Characterization of Naturally Occurring CD4<sup>+</sup>CD25<sup>+</sup> Regulatory T Cells

The human CD4<sup>+</sup>CD25<sup>+</sup> T-cell subset is a heterogeneous population composed of Treg cells displaying suppressive activity and activated cells (not suppressive) (6,7). Therefore, T-cell clones and lines generated from this bulk population need to be characterized based on the following parameters:

- Expression of Treg markers (*see Subheading 3.3.1.*)
- Cytokine production profile (*see Subheading 3.3.2.*)
- Proliferation in response to TCR stimulation (*see Subheading 3.3.3.*)
- In vitro suppressive activity (*see Subheading 3.3.4.*)

#### 3.3.1. CD4<sup>+</sup>CD25<sup>+</sup> Treg Markers Analysis

Treg cell clones and lines display a characteristic cell surface phenotype in the resting phase: they constitutively express high levels of CD25 (4), GITR (32), and intracellular CTLA-4 (33). All these markers can be easily followed by FACS analysis. Although these molecules are indicative of a Treg phenotype, they are also expressed by activated T cells and, thus, may not be useful for ex vivo analyses (2). To date, the only marker that is highly specific for Treg cells is Foxp3, a transcription factor involved in the differentiation of naturally occurring Treg cells (34,35). Very recently, new tools for the analysis of Foxp3 expression in human T cells by FACS have become commercially available (*see Fig. 2.*)

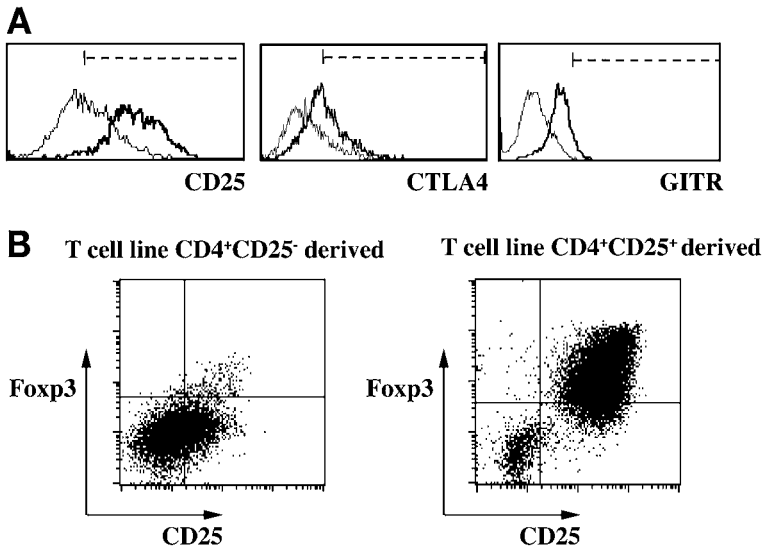


Fig. 2. Phenotype of CD4<sup>+</sup>CD25<sup>-</sup> and CD4<sup>+</sup>CD25<sup>bright</sup> T-cell lines. Phenotypic analysis of T-cell lines generated from CD4<sup>+</sup>CD25<sup>-</sup> (thin line) and CD4<sup>+</sup>CD25<sup>bright</sup> T cells (thick line). Surface expression of CD25, GITR, and intracellular expression of CTLA-4 are shown in (A); surface expression of CD25 and intracellular Foxp3 are shown in (B). Staining was performed on resting cells (at least 12 d postactivation). Regions of positive staining were set based on the isotype control (dashed line in A and quadrants in B).

### 3.3.2. Cytokine Production

Treg cell clones and lines are characterized by a typical cytokine production profile: upon TCR-mediated activation, suppressive Treg clones fail to produce IL-2, IL-10, IL-4, IL-5, and IFN- $\gamma$ . In contrast, Treg cells produce detectable levels of TGF- $\beta$  (7).

1. The cytokine production profile can be determined by activating T-cell lines or clones with immobilized anti-CD3 (10  $\mu$ g/mL) and soluble anti-CD28 (1  $\mu$ g/mL) MAbs.
2. Supernatants, collected after 24, 48, and 72 h, are tested for the presence of cytokines by ELISA or cytometric bead array (*see Note 7*).

### 3.3.3. Suppressive Activity

The suppressive activity of ex vivo freshly isolated or in vitro expanded CD4<sup>+</sup>CD25<sup>+</sup> Treg cells (4) can be tested in vitro by coculture with responder T cells. Responder cells may either be total CD4<sup>+</sup> T cells, or CD4<sup>+</sup>CD25<sup>-</sup> T cells, and may be autologous or allogeneic.

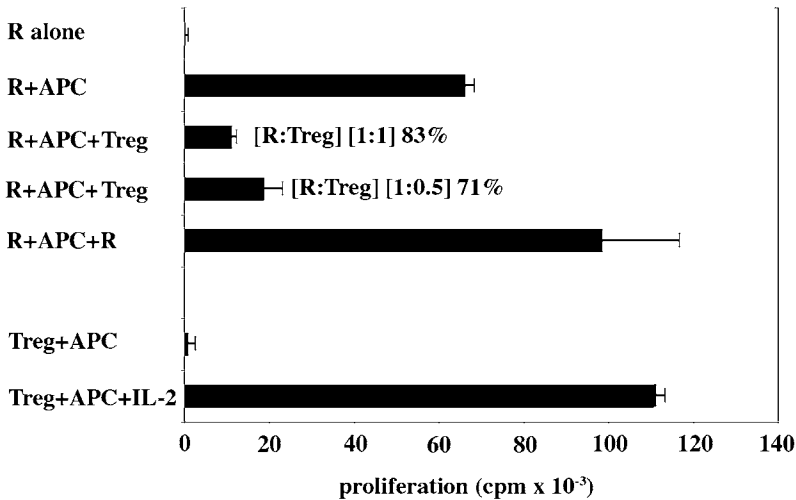


Fig. 3. Suppressive activity of CD4<sup>+</sup>CD25<sup>+</sup> Treg cells, isolated by magnetic separation. Responder cells (CD4<sup>+</sup>CD25<sup>-</sup> T cells) (R) were activated with irradiated APC and soluble anti-CD3 MAb (1  $\mu$ g/mL), as described. Suppressor cells (autologous CD4<sup>+</sup>CD25<sup>+</sup> Treg cells) (Treg) were added either at [1:1] or at [1:0.5] ratios. As a control, suppressor cells were substituted with an equal number of responder cells ([1:0.5] ratio). Anergy of Treg cells was tested by activating them with APC and anti-CD3 MAb, and was reversed in the presence of rhIL-2 (100 U/mL). Percentages indicate inhibition of proliferation.

1. Responder T cells ( $5 \times 10^4$  cells/well) are plated alone or in the presence of Treg cells at a variety of ratios, and stimulated with irradiated (6000 rad) CD3-depleted allogeneic PBMC (APC) and soluble anti-CD3 MAb (1  $\mu$ g/mL), in a final volume of 200  $\mu$ L of complete medium (*see Note 8*) (9). As a control to ensure suppression is not because of over growth and consequent consumption of IL2 in the medium, responder T cells should also be cocultured with the appropriate ratio(s) of CD4<sup>+</sup>CD25<sup>-</sup> T cells in parallel.
2. After 72 h, pulse wells for 16 h with 1  $\mu$ Ci/well of [<sup>3</sup>H]-TdR (*see Note 9*) (*see Fig. 3*). In parallel, supernatants can be harvested for analysis of cytokine production. Consistent suppression of IFN- $\gamma$  and TNF- $\alpha$  should be observed. The ratio of responder:suppressor cells is a critical parameter of this assay. If ex vivo freshly isolated Treg cells are being tested, start at a ratio of 1:2 (R:S) and ideally test at least three or four more dilutions (i.e., 1:0.5, 1:0.25, 1:0.125). If in vitro expanded Treg cells are being used, start at a 1:1 ratio. This dilution series will give a good indication of the real potency of the Treg cells in question.
3. To test the proliferative response of CD4<sup>+</sup>CD25<sup>+</sup> Treg cells to TCR-mediated stimulation,  $5 \times 10^4$  cells/well of CD4<sup>+</sup>CD25<sup>+</sup> Treg cells are cultured alone, or in the presence of APC and anti-CD3 MAb, with or without 100 U/mL of rhIL-2.

### 3.4. Induction of Tr1 Cells

#### 3.4.1. Naïve CD4<sup>+</sup> T-Cell Preparation

Naïve CD4<sup>+</sup> T cells can be isolated from either peripheral blood or umbilical cord blood. This procedure includes two successive steps: (1) isolation of total CD4<sup>+</sup> T cells by negative selection and (2) negative selection of CD45RA<sup>+</sup> T cells.

1. Cells are prepared by centrifugation over Ficoll-Hypaque gradients and CD4<sup>+</sup> T cells are purified as previously described using the CD4<sup>+</sup> T cell isolation kit II, according to the manufacturer's instructions. The CD4<sup>+</sup> T-cell fraction obtained in this first step is untouched (*see Note 10*) and therefore allows the negative selection of the CD45RO<sup>+</sup> T cells with magnetic beads directly coupled to anti-CD45RO MAb. Add 10  $\mu$ L of magnetic beads directly coupled to anti-CD45RO MAb per  $1 \times 10^7$  cells (*see Note 11*).
2. After incubation with magnetic beads directly coupled to anti-CD45RO MAb, pass the cells over negative selection columns (LD). The phenotype of the resulting cells is routinely greater than 90% CD4<sup>+</sup>CD45RO<sup>+</sup>CD45RA<sup>+</sup>.

#### 3.4.2. Differentiation of Polyclonal Tr1 Cell Lines

Polyclonal Tr1 cell lines can be generated using murine L-cells as surrogate APC. T cells are stimulated with anti-CD3 MAbs cross-linked on L-cells expressing costimulatory molecules, as previously described (28).

1. Murine L-cell transfectants expressing hCD32 (FCRII), hCD58 (LFA-3), and hCD80 are cultured in RPMI 1640 supplemented with 10% FBS, 100 U/mL of penicillin/streptomycin, and 2 mM glutamine.
2. Detach L-cells from the plastic by incubation with trypsin-EDTA and irradiate (7000 rad).
3. Following washing, plate the L-cells in 24-well plates in 500  $\mu$ L at an initial density of  $4 \times 10^5$  cells/mL in complete medium.
4. Incubate the L-cells for 1 h at 37°C.
5. After the L-cells have adhered, add 500  $\mu$ L of CD4<sup>+</sup> cord blood or CD4<sup>+</sup>CD45RO<sup>-</sup> peripheral blood T cells at an initial density of  $4 \times 10^5$  cells/mL in complete medium containing rhIL-2 (100 U/mL), rhIL-15 (1 ng/mL), 0.2  $\mu$ g/mL of anti-CD3 MAb.
6. The following polarizing conditions should be set up to obtain Th2, Th1, and Th0 cultures in parallel:
  - a. Tr1 polarizing condition: rhIL-10 (100 U/mL) and rhIFN- $\alpha$  (5 ng/mL).
  - b. Th2 polarizing condition: rhIL-4 (200 U/mL) and anti-human IL-12 MAb (10  $\mu$ g/mL).
  - c. Th1 polarizing condition: rhIL-12 (5 ng/mL) and anti-human IL-4 MAb (200 ng/mL).
  - d. Th0 polarizing condition: complete medium alone.

7. T cells are split as necessary and IL-2 and -15 are replenished in all cultures. Th2 cultures must also be replenished with IL-4 and Tr1 cultures with IL-10 and IFN $\alpha$ .
8. At d 7, collect, wash and count the T cells and restimulate them under identical conditions for an additional 7 d.
9. After a total of 14 d of in vitro culture, collect, wash, count the T cells, and analyze them for their profile of cytokine production and proliferative capacity. Note that the cells under Tr1 polarizing conditions will expand poorly and hence 5–10X more wells should be used for this condition.

---

#### Timing for differentiation of Tr1 cell lines

---

- Day 0: Plate naïve CD4<sup>+</sup> cord blood or CD4<sup>+</sup>CD45RO<sup>-</sup> peripheral blood T cells.  
 Day 7: Restimulate the T cells under identical conditions.  
 Day 14: Tr1 cells are differentiated.
- 

### 3.4.3. Differentiation of Alloantigen-Specific Tr1 Cell Lines Using Immature Dendritic Cells

#### 3.4.3.1. IMMATURE DENDRITIC CELL PREPARATION

1. Wash PBMC, isolated as previously described, but taking care to remove platelets (which interfere with monocyte adherence) by washing two times at 800 rpm for 10 min. A third wash may be necessary if a significant number of platelets remain.
2. To isolate the CD14<sup>+</sup> monocytes as the adherent fraction, plate  $10 \times 10^6$  PBMC/well in a six-well plate, in 2 mL of RPMI 1640 supplemented with 10% FBS, 100 U/mL of penicillin/streptomycin, and 50 mM 2-mercaptoethanol (DC medium) at 37°C.
3. Incubate at 37°C for 1–2 h (*see Note 12*).
4. After incubation, wash away the nonadherent cells by gently adding 2 mL of warm RPMI/well and swirling. Do this at least four times, or until all the nonadherent cells have been removed, as assessed under phase contrast microscopy.
5. Differentiate adherent monocytes into dendritic cells (DC) by culturing them in 2 mL of DC medium containing 10 ng/mL of rhIL-4 and 100 ng/mL rhGM-CSF.
6. At d 3, add 2 mL of fresh DC medium containing IL-4 (20 ng/mL) and GM-CSF (100 U/mL).
7. After an additional 2 d, leave the DC either unstimulated or transferred to wells containing irradiated (10,000 rads) 3T3 fibroblasts expressing human CD40L.
8. 3T3-CD40L cells are cultured in DMEM containing 10% FBS and 100 U/mL of penicillin/streptomycin.
9. Detach 3T3-CD40L cells from the plastic by incubation with trypsin-EDTA and irradiate (10,000 rad).
10. After washing, plate 3T3-CD40L cells in 24-well plates at an initial density of  $1.5 \times 10^5$  cells/mL in DC medium.
11. Incubate 3T3-CD40L cells for 1 h at 37°C (*see Note 13*).
12. Wash away the medium and transfer 2 mL of immature DC and 2 mL of fresh DC medium containing IL-4 (20 ng/mL) and GM-CSF (200 U/mL). Alternatively DC can be matured by addition of LPS (1  $\mu$ g/mL) (*see Note 14*).

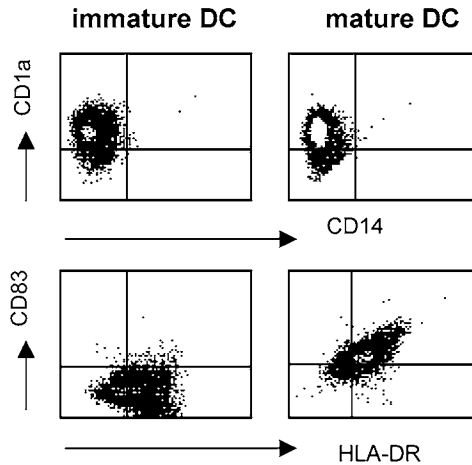


Fig. 4. Phenotype of monocyte-derived immature and mature dendritic leukocytes (DC). After 5 d of differentiation in IL-4 and GM-CSF, monocyte-derived DC were either left immature or matured for 48 h *via* activation of CD40. DC were then analyzed by flow cytometry to determine levels of expression of CD1a, CD14, CD83, and HLA-DR.

13. After an additional 2 d, collect and irradiate (6000 rads) immature and mature DC and use them to stimulate naïve CD4<sup>+</sup> T cells prepared as previously described. In parallel, freeze DC for subsequent restimulations and thaw them before each round of stimulation (*see Note 15*) (24). The purity and maturation state of DC are routinely checked by flow cytometric analysis to determine expression of CD1a, CD14, CD83, and HLA-DR (*see Fig. 4*).

---

#### Timing of DC preparation

---

Day 0: Begin DC differentiation.

Day 3: Add 2 mL of DC medium containing rhIL-4 and rhGM-CSF.

Day 5: Remove 2 mL of medium and add 2 mL of fresh DC medium containing rhIL-4 (20 ng/mL) and rhGM-CSF (200 U/mL) for immature DC. In parallel, mature DC on 3T3-CD40L cells or with 1 µg/mL of LPS.

Day 7: Immature and mature DC are ready to use.

---

#### 3.4.3.2. DIFFERENTIATION OF ALLOANTIGEN-SPECIFIC TR1 CELL LINES

1. DC ( $1 \times 10^5$ ) are cocultured with allogeneic CD4<sup>+</sup>CD45RO<sup>-</sup> T cells ( $1 \times 10^6$ ) in 1 mL of complete medium.
2. Add rhIL-2 (40 U/mL) after 6 or 7 d and expand the T cells for an additional 7–8 d.
3. 14 d after initiation of the culture, collect, and wash the T cells twice with HBSS supplemented with 2% HS.

4. Restimulate the T cells with immature or mature DC from the same allogeneic donor used in the primary culture at a 10:1 ratio.
5. Add rhIL-2 (40 U/mL) after 3 d.
6. One week after initiation of the second stimulation, collect and wash the T cells twice with HBSS supplemented with 2% HS. Test a portion of the T cells for their proliferative and suppressive capacity (*see below*) and restimulate the remaining T cells a third time. T cells cultured with immature DC typically expand 10-fold less in comparison to cultures stimulated with mature DC (24).

---

#### Timing of T-cell differentiation

---

- Day 0: Start cocultures ( $1 \times 10^5$  DC +  $1 \times 10^6$  allogeneic CD4<sup>+</sup>CD45RO<sup>-</sup> T cells).
- Day 6/7: Add rhIL-2.
- Day 14: Restimulation ( $1 \times 10^5$  DC +  $1 \times 10^6$  T-cell lines).
- Day 17: Add rhIL-2.
- Day 21: First read-out and restimulation.
- Day 24: Add rhIL-2.
- Day 28. T-cell lines are ready to be tested.
- 

#### 3.4.4. Generation of Tr1 Cell Lines

Tr1 cell clones can be generated from either polyclonal polarized Tr1 cell lines obtained using the protocol described in **Subheading 3.4.2.**, or antigen-specific Tr1 cell lines. Antigen-specific Tr1 cell clones are generated starting from an IL-10-energized population of CD4<sup>+</sup> T cells.

##### 3.4.4.1. POLYCLONAL TR1 CELL LINES

1. Polarized Tr1 cell lines differentiated in the presence of IL-10 and IFN- $\alpha$ , are cloned at 1 cell/well in the presence of a feeder cell mixture consisting of  $5 \times 10^5$  cells/mL of irradiated (6000 rad) allogeneic PBMC,  $5 \times 10^4$  cells/mL of irradiated (10,000 rad) allogeneic JY, and soluble anti-CD3 MAb (1  $\mu$ g/mL) in complete medium at the final volume of 150  $\mu$ L/well (25,26).
2. At d 3, add 50  $\mu$ L/well of rhIL-2 (40 U/mL).
3. Change medium at d 7 by removing 80  $\mu$ L/well and add 100  $\mu$ L/well of fresh medium containing rhIL-2 (40 U/mL).
4. Restimulate the clones every 14 d with the feeder cell mixture and soluble anti-CD3 (1  $\mu$ g/mL).
5. Add rhIL-2 (40 U/mL) 6–7 d after restimulation. Tr1 cell clones are usually slow growing and the cloning plates usually need a second stimulation before the Tr1 cell clones become visible. Th cell clones, which overgrow, can be removed from the original cloning plate, expanded separately, and kept as control clones.

##### 3.4.4.2. ALLOANTIGEN-SPECIFIC TR1 CELL CLONES

1. Alloantigen-specific Tr1 cell clones can be generated from IL-10-energized T cells obtained by stimulating PBMC from normal donors ( $5 \times 10^5$  cells/well) with

allogeneic CD3-depleted PBMC ( $5 \times 10^5$  cells/well, irradiated at 6000 rad) in the presence of rhIL-10 (10 ng/mL). Control PBMC, kept in the same culture conditions in the absence of IL-10, are usually performed in parallel.

2. After 10 d of culture, CD4<sup>+</sup> T cells are purified by depletion of CD8<sup>+</sup>/CD14<sup>+</sup>/CD19<sup>+</sup> cells using dynabeads and cloned at one cell per well with immobilized anti-CD3 MAb (1  $\mu$ g/mL) in the presence of feeder cell mixture, as described in **Subheading 3.2.2. (25,36)**. Usually before cloning, the CD4<sup>+</sup> T cells primed in the presence of IL-10 are tested for the acquisition of anergy by confirming the absence/very low proliferative response towards the same allogeneic cells, present during the priming. An anergy level of >75% (reduction of proliferation compared to the same cultures primed in the absence of IL-10) should be sufficient to generate Tr1 cell clones.
3. 3 d after cloning, add 50  $\mu$ L/well of rhIL-2 (100 U/mL), or rhIL-2 (100 U/mL) and rhIL-15 (10 ng/mL).
4. Change the medium at d 7 by removing 80  $\mu$ L/well and add 100  $\mu$ L/well of fresh medium containing rhIL-2 (40 U/mL).
5. Restimulate the clones every 14 d with the feeder cell mixture and soluble anti-CD3 MAb.
6. Between d 10 and 12 after the second restimulation with feeder cells, cloning plates are ready for screening to distinguish Tr1 from Th cell clones.
7. A first screening can be performed using half the amount of cells present in each well and plating them in a new plate precoated with anti-CD3 MAb (10  $\mu$ g/mL), in which anti-CD28 MAb (1  $\mu$ g/mL) will also be added in a final volume of 200  $\mu$ L/well.
8. After 48 h, supernatants are collected and IL-10, IL-4, and IFN- $\gamma$  are measured by ELISA to detect the clones with the highest IL-10/IL-4 production ratio.
9. High IL-10, low IL-4 T-cell clones, and all the controls that need to be retested, are expanded in a 48- and/or 24-well plate and retested by stimulating  $1 \times 10^6$  cell/mL with anti-CD3 and anti-CD28 MAbs. In this case, the pattern of production of cytokines will include IL-2 (collect supernatant after 20 h), IL-4, IL-5, IL-10, IFN- $\gamma$ , and TGF- $\beta$ . Either ELISA or CBA may be used as an appropriate detection method.

#### 3.4.4.3. ANTIGEN-SPECIFIC TR1 CELL CLONES

1. Tetanus toxoid (TT)-specific T-cell clones can be generated from IL-10-anergized cells obtained by restimulating in vitro PBMC from immunized subjects given an in vivo booster, with TT (25  $\mu$ g/mL) in the presence or absence of rhIL-10 (10 ng/mL). The TT used must be titrated using PBMC to identify the optimal dose to be used for each batch or brand available.
2. After 10 d of culture, CD4<sup>+</sup> T cells are purified by depletion of CD8<sup>+</sup>/CD14<sup>+</sup>/CD19<sup>+</sup> cells using dynabeads and cloned at one cell per well in the presence of TT (25  $\mu$ g/mL) and autologous PBMC as a source of APC ( $5 \times 10^4$  cells/well, irradiated at 6000 rad) in a final volume of 150  $\mu$ L/well. As previously described, before cloning, the CD4<sup>+</sup> T cells primed in the presence of IL-10, are



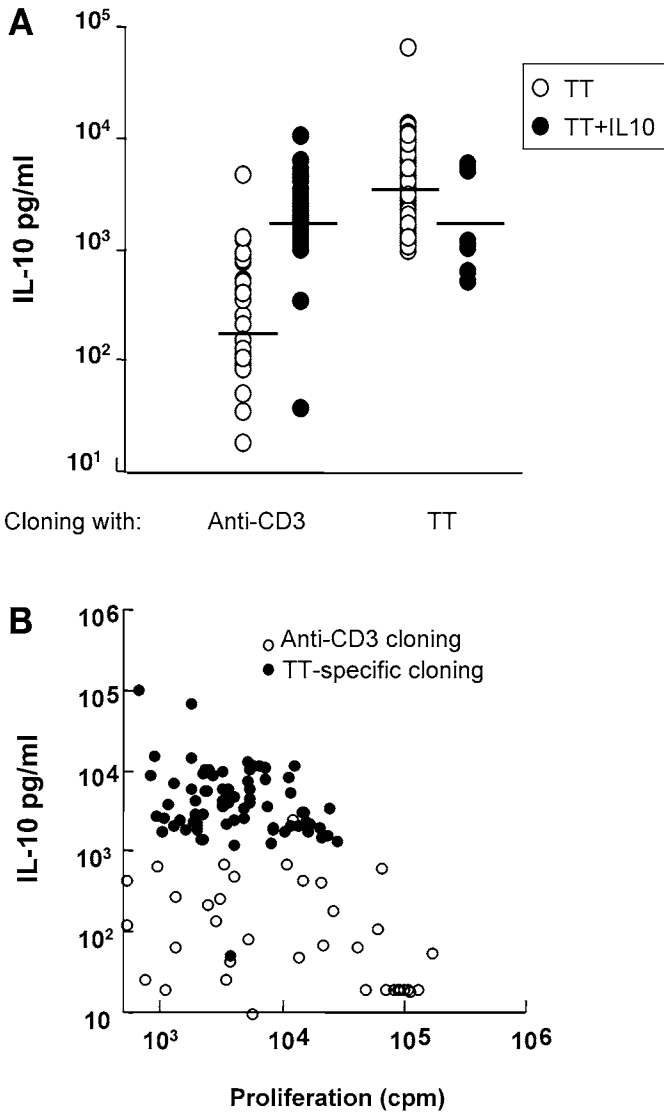


Fig. 5. Interleukin (IL)-10 production and proliferation of tetanus toxoid (TT)-specific Tr1 cell clones. TT-specific Tr1 cell clones were generated from peripheral blood mononuclear cells (PBMC) of immunized subjects collected after in vivo booster and restimulated in vitro, with TT (25 mg/mL) in the presence or absence of rhIL-10 (10 ng/mL). After 10 d of culture, CD4<sup>+</sup> T cells were purified and cloned either polyclonally with anti-CD3 monoclonal antibody (MAb) or in the presence of TT (25 mg/mL) and irradiated (6000 rad) autologous PBMC as antigen-presenting cells (APC). (A) The amount of IL-10 detectable at the first screening from TT-specific cloning in the different conditions. Repetitive stimulation with the TT and/or the presence of IL-10 during

tested for the acquisition of anergy toward autologous CD3-depleted PBMC pulsed with TT (25 µg/mL).

3. 3 d after cloning, add 50 µL/well of rhIL-2 (100 U/mL), or rhIL-2 (100 U/mL) and rhIL-15 (10 ng/mL).
4. Change the medium at d 7 by removing 80 µL/well and add 100 µL/well of fresh medium containing rhIL-2 (40 U/mL).
5. Restimulate the clones every 14 d with the feeder cell mixture and soluble anti-CD3 MAb (25).
6. As previously described, after the second restimulation, cloning plates are screened by activation and ELISA to distinguish Tr1 from Th cell clones (see Fig. 5). To identify bona fide Tr1 cell clones, each one should also be tested for the complete panel of cytokines in response to TCR-mediated activation and for antigen-specific suppression.

### 3.5. Biological Characterization of Adaptive Regulatory Type 1 Cells

#### 3.5.1. Phenotype of Tr1 Cells

Although to date, no specific markers of Tr1 cells have been described, Tr1 cells consistently express high levels of the  $\beta$ - and  $\gamma$ -chain of the IL-2 receptor (CD122 and CD132, respectively), which can be easily checked by FACS. In addition, Tr1 cells express the activation markers CD40L, CD69 (6 h after activation), CD25, CD28, and HLA-DR (24 h after activation) upon activation with anti-CD3 and anti-CD28 MAbs but are normally downregulated compared to Th cells.

#### 3.5.2. Cytokine Production Profile of Tr1 Cells

Once Tr1 clones are isolated, the characterization of their cytokine production pattern remains the primary method to distinguish them from Th cell clones (21). Upon TCR-mediated activation, Tr1 cells produce high levels of IL-10, TGF- $\beta$ , and IL-5, but low amounts of IFN- $\gamma$  and IL-2 and no IL-4. Cytokines are measured in culture supernatants by ELISA or CBA as described in **Subheading 3.4.4.1.**, or by intracytoplasmic staining, which allows the frequency of IL-10-producing cells to be evaluated. Intracellular cytokines are detected as follows:

1. Stimulate  $1 \times 10^6$  T cells/mL with immobilized anti-CD3 (1 µg/mL) and MAb TPA (10 ng/mL) in complete medium and centrifuge the plate at 1500 rpm for 5 min to maximize contact with the MAb.

---

Fig. 5. (Continued) the beginning of in vitro stimulation favors the presence of high IL-10-producing T-cell clones. (B) Cytokine pattern and proliferative capacity of Tr1 cell clones obtained either polyclonally (anti-CD3 MAb) or TT-specific after the first screening, showing inverse correlation between high IL-10 production and low proliferation in response to the specific antigen.

2. Add brefeldin A (10  $\mu\text{g}/\text{mL}$ ) after 3 h of activation.
3. Collect the T cells after a total of 6 h of activation.
4. Wash the cells and fix by incubation with 2% PFA medium for 20 min at room temperature (or overnight at 4°C).
5. Permeabilize the T cells by incubation in saponin buffer (PBS containing 2% FBS and 0.5% saponin) for 10 min.
6. Incubate permeabilized T cells with PE-labeled anti-hIL-4, anti-hIL-2, or anti-hIL-10, and FITC-coupled anti-hIFN- $\gamma$ .
7. After washing, analyze the T cells using a FACScan (28).

**ELISA:**

- a. To test cytokine production following antigen-specific activation (allogeneic monocytes or DC, TT presented by autologous monocytes or EBV-LCL), plate  $5 \times 10^5$  cells/mL of alloantigen-specific Tr1 cells with  $5 \times 10^5$  cells/mL of allogeneic monocytes or  $5 \times 10^4$  allogeneic DC, or  $5 \times 10^5$  cells/mL of autologous monocytes in the presence of TT (25  $\mu\text{g}/\text{mL}$ ) in a total volume of 200  $\mu\text{L}/\text{well}$ .
- b. Collect the supernatants after 24 h to determine the amount of IL-2 released, after 48 h to detect IL-4, IL-10, IFN- $\gamma$ , and TGF- $\beta$  and after 72 h to evaluate IFN- $\gamma$  and TGF- $\beta$  by CBA or ELISA, performed according to manufacturer's instructions (see Note 7).

### 3.5.3. Proliferation Assays

Even if very low, it is possible to detect a proliferative response specifically to the antigen used in the priming (allogeneic monocytes or DC, TT presented by autologous monocytes or EBV-LCL).

1. Plate  $5 \times 10^4$  Tr1 cells with  $5 \times 10^4$  irradiated (6000 rad) CD3-depleted cells in round-bottom 96-well plates or  $5 \times 10^3$  DC. For TCR-mediated polyclonal proliferation, stimulate  $5 \times 10^4$  Tr1 cells with immobilized anti-CD3 (10  $\mu\text{g}/\text{mL}$ ) with or without soluble anti-CD28 (1  $\mu\text{g}/\text{mL}$ ) MAbs (see Note 8).
2. Pulse the cultures after 2 d, for 14–16 h with 1  $\mu\text{Ci}/\text{well}$  of [ $^3\text{H}$ ]-TdR (see Note 9).

### 3.5.4. Suppressive Function of Tr1 Cells

1. Tr1 cells should be tested for their ability to suppress the proliferation of naïve CD4 $^+$  T cells in response to the relevant antigen.
  - a. Culture autologous CD4 $^+$  T cells ( $5 \times 10^4$  cells/well), which are either cryopreserved at the start of the experiment or obtained from an accessible donor, together with irradiated, allogeneic CD3-depleted PBMC ( $5 \times 10^4$  cells/well), in the absence or presence of Tr1 cells ( $5 \times 10^4$  cells/well), in a final volume of 200  $\mu\text{L}$  of complete medium (see Note 8). To test the ability of TT-specific Tr1 cells to suppress the proliferation of autologous TT-specific Th cells, coculture TT-specific Th cells ( $5 \times 10^4$  cells/well) together with irradiated, autologous CD3-depleted PBMCs ( $5 \times 10^4$  cells/well), in the absence or presence of TT-specific Tr1 cells ( $5 \times 10^4$  cells/well), in a final volume of 200  $\mu\text{L}$  of complete medium (see Note 8).

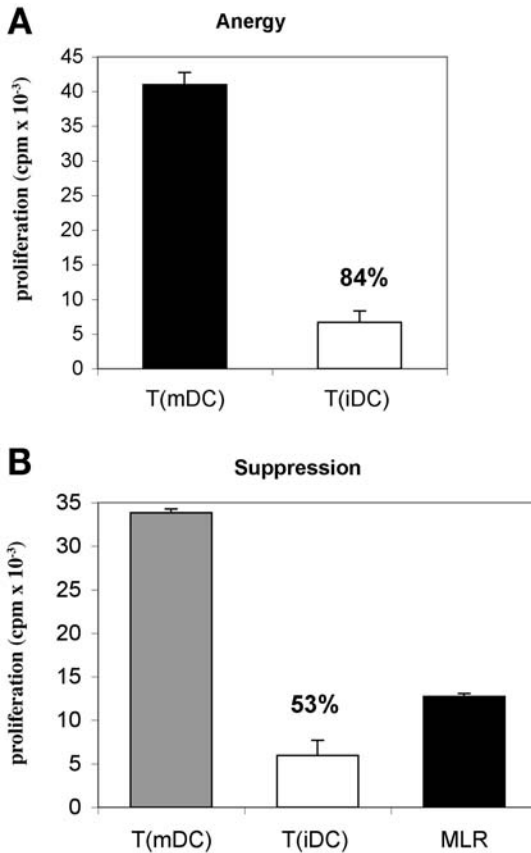


Fig. 6. Anergy and suppression of type 1 regulatory T (Tr1) cell lines generated by immature dendritic leukocytes (DC). Peripheral blood CD4<sup>+</sup>CD45RO<sup>-</sup> T cells were stimulated with immature T(iDC) or mature T(mDC) allogeneic DC three times. T-cell lines were tested for their ability to proliferate in response to mature allogeneic DC (mDC). **(A)** Proliferative responses were evaluated by [<sup>3</sup>H]-TdR incorporation after 48 h of culture. Number represents the percentage of anergy compared to mDC. **(B)** T cells were collected and tested for their ability to suppress responses of autologous CD4<sup>+</sup> T cells. Thawed CD4<sup>+</sup> T cells were stimulated with mDC alone (MLR) or in the presence of T(iDC) or T(mDC) cell lines at a 1:1 ratio. [<sup>3</sup>H]TdR was added after 72 h for an additional 16 h.

- b. Pulse the cultures after 2 d, for 14–16 h with 1 μCi/well of [<sup>3</sup>H]TdR (25) (see Note 9).
2. To test for the capacity of Tr1 cells generated with immature DC to suppress proliferation and/or cytokine production:
  - a. Culture autologous CD4<sup>+</sup> T cells (5 × 10<sup>4</sup> cells/well), which are cryopreserved at the start of the experiment, with allogeneic irradiated (6000 rads) mature DC

(10:1, T:DC). Stimulate naïve CD4<sup>+</sup> T cells alone, or in the presence of Tr1 cells (1:1 ratio) in a final volume of 200  $\mu$ L of complete medium in 96-well round-bottom plates (see **Note 8**).

- b. After 2, 3, or 4 d of culture, pulse for 14–16 h with 1  $\mu$ Ci/well of [<sup>3</sup>H] TdR (see **Note 9**) (see **Fig. 6**).
- c. Alternatively, collect supernatants for analysis of inhibition of IFN- $\gamma$  production (**24**).

#### 4. Notes

1. To properly set the gates for positive and negative fractions, keep a fraction of cells ( $5 \times 10^5$  cells) for staining with isotype controls.
2. Alternatively, incubate for 15 min at room temperature.
3. To avoid loss of cells, 15-mL V-bottom tubes are preferable.
4. To improve the purity of CD4<sup>+</sup> T cells, do not load more than  $1.5 \times 10^8$  cells per column.
5. Because the microbeads are coupled to a MAb specific for epitope A of the IL-2R $\alpha$  chain, always remember to use an anti-CD25 MAb specific for epitope B when checking the purity of the collected fractions. Expected purity of the samples is usually lower than that obtained by FACS sorting; samples with purity lower than 80% display minimal in vitro suppressive activity.
6. For the generation of Treg cell lines and clones, purification by FACS sorting is preferable because better purity and higher CD25 mean fluorescence intensity of the starting population is indicative of a higher percentage of Treg cells in the bulk population.
7. CBA analysis allows the detection of six cytokines in 50  $\mu$ L of supernatant; much larger volumes are required for ELISA. Therefore, when cell numbers are limiting, CBA is usually preferable. The limit of detection of the two methods is comparable.
8. Prepare triplicate wells for each condition.
9. Cells are harvested and counted in a scintillation counter.
10. To purify naïve CD4<sup>+</sup> T cells from peripheral blood, use LD columns (Miltenyi) for negative selection.
11. Once CD4<sup>+</sup> T cells are isolated, freeze at least two vials of  $10 \times 10^6$  CD4<sup>+</sup> T cells to be used as responder cells in future readouts.
12. Do not let the PBMC adhere for more than 2 h, as the monocytes will start to detach from the plastic.
13. 3T3-CD40L transfected cells can be prepared 1 d in advance and kept at 37°C.
14. Mature DC are routinely used to generate control effector T cells in parallel to Tr1 cell lines.
15. To generate Tr1 cell lines using immature DC, T cells need to be restimulated two to three times, therefore, freeze two vials of immature DC. In parallel, freeze three vials of mature DC: two of them are required to generate effector T cells and one is required to determine proliferative and suppressive functions of T-cell lines at the end of the differentiation.

## Acknowledgments

The authors thank Claudia Sartirana and Eleonora Tresoldi for technical help. The authors' own work is partially supported by grants from the Italian Telethon Foundation and the Canadian Institute for Health Research (MKL). MKL holds a Canada Research Chair in Transplantation and is a Michael Smith Foundation for Health Research Scholar.

## References

1. Roncarolo, M. G. and Levings, M. K. (2000) The role of different subsets of T regulatory cells in controlling autoimmunity. *Curr. Opin. Immunol.* **12**, 676–683.
2. Levings, M. K. and Roncarolo, M. G. (2005) Phenotypic and functional differences between human CD4+CD25+ and type 1 regulatory T cells. *Curr. Top. Microbiol. Immunol.* **293**, 303–326.
3. Hauben, E. and Roncarolo, M. G. (2005) Human CD4+ regulatory T cells and activation-induced tolerance. *Microbes Infect.* **7**, 1023–1032.
4. Sakaguchi, S. (2005) Naturally arising Foxp3-expressing CD25+CD4+ regulatory T cells in immunological tolerance to self and non-self. *Nat. Immunol.* **6**, 345–352.
5. Fontenot, J. D. and Rudensky, A. Y. (2005) A well adapted regulatory contrivance: regulatory T cell development and the forkhead family transcription factor Foxp3. *Nat. Immunol.* **6**, 331–337.
6. Baecher-Allan, C., Brown, J. A., Freeman, G. J., and Hafler, D. A. (2001) CD4+CD25high regulatory cells in human peripheral blood. *J. Immunol.* **167**, 1245–1253.
7. Levings, M. K., Sangregorio, R., Sartirana, C., et al. (2002) Human CD25+CD4+ T suppressor cell clones produce transforming growth factor beta, but not interleukin 10, and are distinct from type 1 T regulatory cells. *J. Exp. Med.* **196**, 1335–1346.
8. Su, L., Creusot, R. J., Gallo, E. M., et al. (2004) Murine CD4+CD25+ regulatory T cells fail to undergo chromatin remodeling across the proximal promoter region of the IL-2 gene. *J. Immunol.* **173**, 4994–5001.
9. Levings, M. K., Sangregorio, R., and Roncarolo, M. G. (2001) Human CD25+CD4+ T regulatory cells suppress naive and memory T-cell proliferation and can be expanded *in vitro* without loss of function. *J. Exp. Med.* **193**, 1295–1302.
10. Jonuleit, H., Schmitt, E., Stassen, M., Tuettenberg, A., Knop, J., and Enk, A. H. (2001) Identification and functional characterization of human CD4(+)/CD25(+) T cells with regulatory properties isolated from peripheral blood. *J. Exp. Med.* **193**, 1285–1294.
11. Dieckmann, D., Plottner, H., Berchtold, S., Berger, T., and Schuler, G. (2001) Ex vivo isolation and characterization of CD4(+)/CD25(+) T cells with regulatory properties from human blood. *J. Exp. Med.* **193**, 1303–1310.
12. Ng, W. F., Duggan, P. J., Ponchel, F., et al. (2001) Human CD4(+)/CD25(+) cells: a naturally occurring population of regulatory T cells. *Blood* **98**, 2736–2744.

13. Shevach, E. M. (2002) CD4+CD25+ suppressor T cells: more questions than answers. *Nat. Rev. Immunol.* **2**, 389–400.
14. Setoguchi, R., Hori, S., Takahashi, T., and Sakaguchi, S. (2005) Homeostatic maintenance of natural Foxp3+ CD25+ CD4+ regulatory T cells by interleukin (IL)-2 and induction of autoimmune disease by IL-2 neutralization. *J. Exp. Med.* **201**, 723–735.
15. Walker, M. R., Carson, B. D., Nepom, G. T., Ziegler, S. F., and Buckner, J. H. (2005) De novo generation of antigen-specific CD4+CD25+ regulatory T cells from human CD4+CD25- cells. *Proc. Natl. Acad. Sci. USA* **102**, 4103–4108.
16. Walker, M. R., Kaspirowicz, D. J., Gersuk, V. H., et al. (2003) Induction of FoxP3 and acquisition of T regulatory activity by stimulated human CD4+CD25- T cells. *J. Clin. Invest.* **112**, 1437–1443.
17. Salomon, B., Lenschow, D. J., Rhee, L., et al. (2000) B7/CD28 costimulation is essential for the homeostasis of the CD4+CD25+ immunoregulatory T cells that control autoimmune diabetes. *Immunity* **12**, 431–440.
18. Taylor, P. A., Lees, C. J., and Blazar, B. R. (2002) The infusion of ex vivo activated and expanded CD4(+)CD25(+) immune regulatory cells inhibits graft-versus-host disease lethality. *Blood* **99**, 3493–3499.
19. Taylor, P. A., Panoskaltis-Mortari, A., Swedin, J. M., et al. (2004) L-Selectin(hi) but not the L-selectin(lo) CD4+25+ T-regulatory cells are potent inhibitors of GVHD and BM graft rejection. *Blood* **104**, 3804–3812.
20. Ermann, J., Hoffmann, P., Edinger, M., et al. (2005) Only the CD62L+ subpopulation of CD4+CD25+ regulatory T cells protects from lethal acute GVHD. *Blood* **105**, 2220–2226.
21. Groux, H., O'Garra, A., Bigler, M., et al. (1997) A CD4+ T-cell subset inhibits antigen-specific T-cell responses and prevents colitis. *Nature* **389**, 737–742.
22. Vieira, P. L., Christensen, J. R., Minaee, S., et al. (2004) IL-10-secreting regulatory T cells do not express Foxp3 but have comparable regulatory function to naturally occurring CD4+CD25+ regulatory T cells. *J. Immunol.* **172**, 5986–5993.
23. Allan, S. E., Passerini, L., Bacchetta, R., et al. (2005) The role of 2 Foxp3 isoforms in the generation of human CD4 Tregs. *J. Clin. Invest.* **115**, 3276–3284.
24. Levings, M. K., Gregori, S., Tresoldi, E., Cazzaniga, S., Bonini, C., and Roncarolo, M. G. (2005) Differentiation of Tr1 cells by immature dendritic cells requires IL-10 but not CD25+CD4+ Tr cells. *Blood* **105**, 1162–1169.
25. Bacchetta, R., Sartirana, C., Levings, M. K., Bordignon, C., Narula, S., and Roncarolo, M. G. (2002) Growth and expansion of human T regulatory type 1 cells are independent from TCR activation but require exogenous cytokines. *Eur. J. Immunol.* **32**, 2237–2245.
26. Bacchetta, R., Bigler, M., Touraine, J. L., et al. (1994) High levels of interleukin 10 production in vivo are associated with tolerance in SCID patients transplanted with HLA mismatched hematopoietic stem cells. *J. Exp. Med.* **179**, 493–502.
27. McRae, B. L., Semnani, R. T., Hayes, M. P., and van Seventer, G. A. (1998) Type I IFNs inhibit human dendritic cell IL-12 production and Th1 cell development. *J. Immunol.* **160**, 4298–4304.

28. Levings, M. K., Sangregorio, R., Galbiati, F., Squadrone, S., de Waal Malefyt, R., and Roncarolo, M. G. (2001) IFN- $\alpha$  and IL-10 induce the differentiation of human type 1 T regulatory cells. *J. Immunol.* **166**, 5530–5539.
29. Roncarolo, M. G., Levings, M. K., and Traversari, C. (2001) Differentiation of T regulatory cells by immature dendritic cells. *J. Exp. Med.* **193**, F5–F9.
30. Akbari, O., Freeman, G. J., Meyer, E. H., et al. (2002) Antigen-specific regulatory T cells develop via the ICOS-ICOS-ligand pathway and inhibit allergen-induced airway hyperreactivity. *Nat. Med.* **8**, 1024–1032.
31. Battaglia, M., Stabilini, A., Draghici, E., et al. (2006) Induction of tolerance in type 1 diabetes via both CD4<sup>+</sup>CD25<sup>+</sup> T regulatory cells and T regulatory type 1 cells. *Diabetes* **6**, 1571–1580.
32. Shimizu, J., Yamazaki, S., Takahashi, T., Ishida, Y., and Sakaguchi, S. (2002) Stimulation of CD25(+)CD4(+) regulatory T cells through GITR breaks immunological self-tolerance. *Nat. Immunol.* **3**, 135–142.
33. Takahashi, T., Tagami, T., Yamazaki, S., et al. (2000) Immunologic self-tolerance maintained by CD25(+)CD4(+) regulatory T cells constitutively expressing cytotoxic T lymphocyte-associated antigen 4. *J. Exp. Med.* **192**, 303–310.
34. Hori, S., Nomura, T., and Sakaguchi, S. (2003) Control of regulatory T cell development by the transcription factor Foxp3. *Science* **299**, 1057–1061.
35. Khattry, R., Cox, T., Yasayko, S. A., and Ramsdell, F. (2003) An essential role for Scurfin in CD4<sup>+</sup>CD25<sup>+</sup> T regulatory cells. *Nat. Immunol.* **4**, 337–342.
36. Bacchetta, R., Parkman, R., McMahon, M., et al. (1995) Dysfunctional cytokine production by host-reactive T-cell clones isolated from a chimeric severe combined immunodeficiency patient transplanted with haploidentical bone marrow. *Blood* **85**, 1944–1953.





## Derivation, Culture, and Characterization of Thymic Epithelial Cell Lines

Michiyuki Kasai and Toshiaki Mizuochi

### Summary

The major histocompatibility complex (MHC)-restricted presentation of self-peptides, generated from tissue-specific antigens, by thymic epithelial cells (TECs) is essential for development of central tolerance and for generation of the regulatory T-cell repertoire in the thymus. However, the mechanisms by which self-peptides are generated in and presented by TECs have not been well defined. To elucidate the processes involved in MHC class II-restricted presentation of self-peptides by TECs, cortical and medullary TEC lines may be established from C57BL/6 mouse thymi. Localization of a variety of molecules, including the MHC class II molecules critically involved in the presentation of antigen by TECs, may be investigated by both immunofluorescence microscopy and Western blotting analyses. Our own studies using these approaches have demonstrated that such molecules are localized in the H2-DM<sup>+</sup> lysosomal compartments isolated from both cortical and medullary TECs.

**Key Words:** Thymus; thymic epithelial cells; antigen presentation; H2-DM; MHC class II molecules; endocytosis; autophagy; confocal immunofluorescence.

### 1. Introduction

The presentation of antigenic peptides by professional antigen presenting cells (APC) plays a critical role in induction of the adaptive immune response among naïve T cells. In APC, intracellular as well as extracellular antigens are processed, either by the ubiquitin/proteasome system or by the endosomal/lysosomal system, which degrades antigen into antigenic peptides for loading into either major histocompatibility complex (MHC) class I or class II molecules for activation of T cells (1). In contrast, in the thymus, such MHC-restricted presentation of self-peptides plays an important role in the establishment of central tolerance (2). Recent reports describing the establishment of central tolerance in

the thymus have indicated that autoimmune regulator (AIRE) promotes central tolerance by inducing the expression of tissue-specific antigens (TSAs) in medullary TEC (2,3). Unlike the MHC-restricted presentation of nominal antigens by professional APC, however, MHC-restricted presentation of self-peptides generated from thymic TSA by TEC is poorly understood.

In this chapter, we first present the method used to establish both cortical and medullary TEC lines from mouse thymus and then describe methods for investigating the localization of various molecules involved in MHC class II restricted self-antigen presentation in the endosomal/lysosomal compartments of TEC.

## 2. Materials

### 2.1. Cell Culture

1. Swiss mouse 3T3 cells: random-bred Swiss mouse 3T3 cells provide optimal feeder support for epithelial cells (4). The cells are maintained by weekly passage at a dilution of between 1:10 and 1:20. Use fresh cells within 6 mo after thawing, because the cells start to senesce or undergo spontaneous transformation with prolonged passages.
2. Dulbecco's modified Eagle's medium (DMEM) culture medium for Swiss mouse 3T3 cells and TECs: 500 mL of DMEM (Sigma, cat. no. D5796) is supplemented with 1.2 g of HEPES, 0.375 g of L-glutamine, 25 mg of gentamicin, 2  $\mu$ L of 2-mercaptoethanol, and 25–50 mL of fetal calf serum (FCS; 5.0–10%).
3. JMEM culture medium for TECs (*see Note 1*): 500 mL of minimal essential medium, Joktic modification (JMEM, Sigma, cat. no. M8028) is supplemented with 1.2 g of HEPES, 0.375 g of L-glutamine, 25 mg of gentamicin, 2  $\mu$ L of 2-mercaptoethanol, and 37.5–50 mL of FCS (7.5–10%).
4. Trypsin solution (0.25%): solutions of trypsin (0.25%) and ethylenediamine tetraacetic acid (EDTA) (1 mM) are purchased from Gibco/BRL.
5. Interferon (IFN)- $\gamma$  (PeproTech EC Ltd., cat. no. 315-05) is dissolved at  $10^6$  U/mL in 5.0% FCS-DMEM and stored in 50- $\mu$ L aliquots at  $-20^{\circ}\text{C}$ . To enhance the expression of MHC class II molecules on TEC, IFN- $\gamma$  is added to the 5.0% FCS-DMEM at 500 U/mL (*see Note 2*).
6. Plastic wares for cultivation of TEC: the use of 60-mm dishes (Falcon Primaria, cat. no. 353802) and six-well multiwell plates (Falcon Primaria, cat. no. 353846) or 60-mm gelatin-coated dishes (IWAKI, cat. no. 4010-020) supports both the growth and the colony formation of TEC during both the isolation and cloning procedures. After cloning, any other plastic ware for tissue culture, as well as the above, can be used to culture TEC.

### 2.2. Immunofluorescence Confocal Microscopy

1. Confocal microscope: A Zeiss LSM 510 confocal microscope, equipped with a x64/1.4 NA Plan-Apochromat oil-immersion lens. Ar-laser liner at 488 nm is used for excitation of fluorescein isothiocyanate (FITC) or Alexa 488. On the other hand, He-Ne laser liner at 545 nm is used for excitation of rhodamine or Alexa

543. Emission wavelengths are separated by band pass (505–530 nm) and long pass (585 nm) filters, respectively.
2. Glass slides: eight-hole heavy Teflon-coated slides (Bokusui Brown, New York, NY) are washed extensively with a neutral detergent, rinsed well with hot water and rinsed once with acetone; slides are sterilized by rinsing with 70% ethanol and are air-dried on a clean bench. Prior to use, place one drop of 10% FCS-DMEM on each hole of the slides and incubate them in a CO<sub>2</sub> incubator for over 24 h.
  3. Phosphate buffered saline (PBS): dissolve 9.6 g of PBS powder (Nissui, Japan, cat. no. 05913) in Milli-Q grade water and make up to a volume of 1 L. Sterilize by autoclaving.
  4. Stock PBS (2X): dissolve 9.6 g of the PBS powder in Milli-Q grade water and make up to a volume of 500 mL. Sterilize the stock PBS (2X) by autoclaving.
  5. Fixation solution: add 50 mL of Milli-Q grade water and 40 µL of 1 N NaOH to 4.0 g of paraformaldehyde (P001, TAAB Lab. Equip. Ltd.). The suspension is swirled and then carefully warmed in a microwave oven at intervals of 10 s. These procedures are repeated until the solution turns clear (*see Note 3*). Cool the solution to room temperature and then add 50 mL of 2X stock PBS. Check that the pH value of the solution is approx 7.0, by means of a pH-test paper (*see Note 4*).
  6. Tris-buffered saline (TBS): dissolve one package of TBS powder (TAKARA, Japan; cat. no. T903) in 1 L of Milli-Q grade water.
  7. Quenching solution: dissolve 3.75 g of glycine in 500 mL of Milli-Q grade water. Adjust the pH of the solution to pH 7.0 with 1 M Tris-HCl solution.
  8. Permeabilization solution: dissolve 25 mg of saponin (Sigma, cat. no. S-7900) in 50 mL of TBS to yield a 0.05% solution.
  9. Antibody dilution buffer: 1% BSA, 0.02% NaN<sub>3</sub>, TBS. Dissolve 1.0 g of BSA powder (Fraction V) and 20 mg of NaN<sub>3</sub> in 100 mL of TBS.
  10. Mounting medium: mix one volume of PBS with nine volumes of glycerin (MERCK, Germany; cat. no. 1.04095).

### **2.3. Antibodies for Use in Immunofluorescence and Western Blotting Analyses**

1. Anti-pan keratin antibody: a rabbit anti-human keratin antibody (A0575) is purchased from DAKO Co., CA.
2. Anti-keratin 5 antibody: a rabbit anti-mouse cytokeratin 5 (AF138) antibody is purchased from CONVANCE, Berkeley, CA.
3. Anti-keratin 8 antibody: a mouse anti-human cytokeratin 8 monoclonal antibody (MAB) is purchased from PROGEN Biotechnik GmbH, Heiderberg, Germany.
4. M5/114: a rat MAb specific for mouse I-A<sup>b</sup> (**5**). M5/114 has been purified from the culture supernatant of the hybridoma using a protein A-sepharose column, according to the manufacturer's instructions (Amersham Biosciences AB, Uppsala, Sweden). Determine the concentration of this MAb by the Bradford method according to the manufacturer's manual (Bio-Rad Lab., CA).
5. In1.1: a rat MAb specific for mouse invariant chain (**6**). In1.1 is supplied by Dr. G. J. Hämmerling (German Cancer Research Center, Germany). Add 326 g of

ammonium sulfate (55% of ammonium sulfate solution at 0°C) to 1 L of culture supernatant. After centrifugation at 15,000g for 15 min, the precipitate is dissolved in a small volume of PBS and dialyzed three times against 100 vol of PBS containing 0.02% NaN<sub>3</sub> at intervals of more than 4 h. Determine the concentration of the MAb by the Bradford method.

6. 30-2: a mouse MAb that reacts with the I-A<sup>b</sup> molecules associated with CLIP (7). 30-2 is supplied by Dr. A. Rudensky (Howard Hughes Medical Institute, University of Washington School of Medicine, Seattle, WA). 30-2 has been purified from the culture supernatant of the hybridoma with a protein A-sepharose column. Determine the MAb concentration by the Bradford method.
7. Anti-H2-DM antiserum: rabbit anti-sera to H2-DMβ2 chain has been raised against a KLH-coupled synthetic peptide derived from the cytoplasmic tail of H2-DMβ2 chain (CRKSHSSSYTPLPGSTYPEGRH) (8). As shown in the sequence of the synthetic peptide, a cysteine residue is added to the N-terminus. This cysteine is available for the conjugation of the synthetic peptide with both KLH for immunization and with epoxy-activated sepharose 6B for affinity purification of the antiserum, according to the manufacturer's instructions (Amersham Biosciences AB, Uppsala, Sweden). Determine the concentration of the antiserum by the Bradford method. The antibody is designated as anti-H2-DM antibody by immunofluorescence staining and Western blotting.
8. Anti-rab 5 MAb: a mouse MAb to rab 5 for immunofluorescence studies is purchased from Transduction Lab (Lexington, KY).
9. Anti-rab5 antiserum: a rabbit anti-serum to rab 5A for Western blot analysis is purchased from Santa Cruz Biotech, Inc. (Santa Cruz, CA).
10. Anti-cathepsin B antibody, anti-cathepsin D antibody, and anti-cathepsin L antibody: these antibodies are provided by Dr. E. Kominami (Department of Biochemistry, School of Medicine, Juntendo University, Tokyo, Japan).
11. Anti-cathepsin S antiserum: a goat anti-serum raised against a peptide corresponding to an amino acid sequence at the carboxy terminus of rat cathepsin S is purchased from Santa Cruz Biotech, Inc. (cat. no. sc-6505).
12. Anti-LC3 antiserum: a rabbit antiserum to LC3, a molecular marker peculiar to autophagy (9) is provided by Dr. T. Ueno (Department of Biochemistry, School of Medicine, Juntendo University).
13. FITC-conjugated rat anti-mouse CD107a (LAMP-1) MAb is purchased from BD PharMingen.
14. Fluorochrome-conjugated anti-immunoglobulin (IgG) antiserum: for single-color immunofluorescence studies, use an anti-IgG antiserum conjugated with Alexa 543 (Molecular Probes, Inc., Eugene, OR). For two-color immunofluorescence, use an anti-rabbit IgG anti-serum conjugated with TRITC (DAKO A/S, Denmark, cat. no. R 156) or Alexa 543 (Molecular Probes, Inc., cat. no. A11034) to probe the primary antibody and an anti-IgG antiserum conjugated with Alexa 488 (Molecular Probes, Inc.) to probe the secondary antibody. When using biotin-conjugated second antibodies, use avidin-conjugated Alexa 488 (Molecular Probes, Inc.) for visualization.

#### 2.4. Cell Lysis and Subcellular Fractionation

1. Dynabeads M-280 sheep anti-rabbit IgG (DYNAL, cat. no. 112.03) are purchased from Dynal Biotech (Oslo, Norway).
2. 0.25 M Sucrose solution: prepare 0.25 M sucrose solution containing 5 mM HEPES-KOH (pH 7.4) and 1 mM EDTA in Milli-Q grade water.
3. Protease inhibitors: 200 mM PMSF in dry ethanol, 20 mM TPCK in dry ethanol, 2 mM leupeptin in Milli-Q grade water, 10 mg/mL of aprotinin in Milli-Q grade water, 2 mg/mL of pepstatin in DMSO, 2 mg/mL of E64d in DMSO.
4. Sodium dodecyl sulfate-polyacrylamide gels (SDS-PAGE) sample buffer: 125 mM Tris-HCl (pH 6.8), 4% SDS, 35% (w/v) sucrose, 10% 2-mercaptoethanol, 0.01% bromophenol blue.

#### 2.5. SDS-PAGE

1. 1.5 M Tris-HCl, pH 8.8. Store at room temperature.
2. 0.5 M Tris-HCl, pH 6.8. Store at room temperature.
3. 10% SDS solution: dissolve 10 g of SDS powder in Milli-Q grade water and make up the volume to 100 mL. Store at room temperature.
4. 30% Acrylamide/0.8% bisacrylamide solution: dissolve 30 g of acrylamide and 0.8 g of N,N'-methylenebisacrylamide in Milli-Q grade water and make up the volume to 100 mL. Store at 8°C (in a refrigerator). These reagents are neurotoxins when unpolymerized; care should, therefore, be taken when handling.
5. 10% Ammonium persulfate solution: prepare a 10% (w/v) solution in Milli-Q grade water. Immediately freeze in single use (200 µL) aliquots and store at -20°C.
6. N,N,N,N'-Tetramethyl-ethylenediamine (TEMED; Bio-Rad, Hercules, CA).
7. Water-saturated isobutanol. Shake equal volumes of Milli-Q grade water and isobutanol in a glass bottle and allow to separate. Use the top layer. Store at room temperature.
8. Running buffer: dissolve 6.0 g of Trizma base, 28.8 g of glycine, and 2.0 g of SDS in Milli-Q grade water to make up to 2 L. Store at room temperature.
9. Prestained protein marker, broad range (BioLabs, New England).
10. Slab gel cassette consisting of a silicon rubber spacer 1.0-mm thick and a pair of glass plates. One of the plates is 160-mm wide and 160-mm high and has two 1.0-mm thick glass spacers. Another is 160-mm wide and 160-mm high and has a notch of 20-mm deep and 130-mm wide.

#### 2.6. Western Blotting for Analysis of Intracellular Compartments

1. Transfer buffer: dissolve 3.02 g of Trizma base (25 mM) and 14.42 g of glycine (192 mM) with Milli-Q grade water to make 500 mL. Add 200 mL of methanol (20% v/v) to the solution and make up the volume to 1 L with Milli-Q grade water. It is not necessary to adjust the pH. Store the transfer buffer in the transfer apparatus in a refrigerator.
2. Supported PVDF membrane from Millipore, Bedford, MA, and 3MM chromatography paper from Whatman, Maidstone, UK.

3. Tris-buffered saline with Tween-20 (TBS-T): add 0.25 g of Tween-20 (0.05%) to 500 mL of TBS.
4. Blocking buffer: dissolve 5.0 g of bovine serum albumin (BSA) fraction V (5% w/v) and 20 mg of  $\text{NaN}_3$  (0.02% w/v) in 100 mL of TBS.
5. Primary antibody dilution buffer is the same as the antibody dilution buffer (1% BSA, 0.02%  $\text{NaN}_3$ , TBS) described in **Subheading 2.2**.
6. Horseradish peroxidase-conjugated anti-IgG antiserum is purchased from CAPPEL Inc., Aurora, OH.
7. Dilution buffer for horseradish peroxidase-conjugated anti-IgG antisera: dissolve 1.0 g of bovine serum albumin (BSA) fraction V (1% w/v) in 100 mL of TBS.
8. SuperSignal West Dura Extended Duration Substrate is purchased from PIERCE, Rockford, IL.
9. Bio-Max ML film is purchased from Kodak, Rochester, NY.

### 3. Methods

The establishment of central tolerance in  $\text{CD4}^+$  T cells, as well as the development of Treg cells in the thymus, is closely associated with the MHC class II-restricted presentation of self-peptides by TEC. In contrast to the mechanism involved in the presentation of nominal antigens by APC, the presentation of self-peptides by TEC has been only poorly defined. To address this issue, the following three difficulties must be overcome: (1) establishment of TEC lines from the thymus, (2) isolation of endosomal/lysosomal compartments relevant to the formation of MHC class II complexes by TEC, and (3) identification of those tissue specific antigens (TSA) that serve as self antigens in TEC.

The first issue may be overcome by the culture of TEC on irradiated Swiss mouse 3T3 cells at  $35^\circ\text{C}$ . The irradiated Swiss mouse 3T3 cells support the growth of TEC and oppose the adherence of fibroblast cells derived from the thymus. The culture at  $35^\circ\text{C}$  does not affect the growth rate of TEC, but prevents the growth of fibroblast cells. The second issue may be resolved by the use of anti-H2-DM antibody for analyzing endosomal/lysosomal compartments within TEC by means of immunofluorescence confocal microscopy. It is well known that in endosomal/lysosomal compartments of APC, antigenic peptides, which are generated by lysosomal enzymes from not only extracellular antigens via endocytosis but also intracellular antigens via autophagy (1), are loaded on MHC class II heterodimers through the catalytic function of HLA-DM (human)/H2-DM (mouse). The H2-DM molecule is a nonpolymorphic MHC class II-like determinant, which is transported into the lysosomal compartments because the carboxy-terminal domain contains the YTPL motif known to mediate lysosomal targeting (10,11). We prepared the anti-H2-DM antibody against the carboxy-terminal domain of H2-DM by the modified method described by Karlsson et al. (8). As the antibody binds to the H2-DM molecules residing in the endosomal/lysosomal compartments, application of this antibody

enables isolation of the same endosomal/lysosomal compartments as those detected by immunofluorescence microscopy in TEC. The anti-H2-DM antibody is, therefore, useful for exploring the MHC class II-restricted presentation of self-antigens.

### 3.1. Establishment and Maintenance of TEC Lines

#### 3.1.1. Preparation of a Feeder Layer

1. Swiss mouse 3T3 cells are selected to support optimal growth of TECs isolated from mouse thymus. The cells are cultured with 5% FCS-DMEM at 37°C in 5% CO<sub>2</sub> and maintained by weekly passage at a 1:10 dilution.
2. Upon reaching confluency, remove the medium and rinse the cells once with 0.02% EDTA–PBS. The cells are then harvested with 0.25% trypsin, 0.02% EDTA. After centrifugation at 500g for 10 min, resuspend  $1 \times 10^7$  cells in 10 mL of 5% FCS–DMEM.
3. To irreversibly inhibit proliferation of the cells, irradiate the cell suspension at 40 Gy.
4. Plate  $7 \times 10^5$  irradiated cells per 4 mL of 7.5% FCS-DMEM into a 60-mm diameter dish and culture for 1–2 d.

#### 3.1.2. Establishment of TEC Lines From Mouse Thymus

1. Isolate thymic lobes from newborn mice or embryos at 15 d of gestation and disperse them in PBS containing 0.25% trypsin and 0.02% EDTA with gentle pipetting.
2. Add an equal volume of 10% FCS-DMEM into the cell suspension. After centrifugation at 500g for 10 min, resuspend the cell pellets in 2 mL of 10% FCS DMEM. Repeat this procedure once.
3. After centrifugation, resuspend the cell pellets at  $10^5$  per milliliter of 10% FCS-DMEM. Plate 1 mL of the cell suspension on Swiss 3T3 cells that are preirradiated at 40 Gy, plated at  $7 \times 10^5$  per 2 mL of 10% DMEM in a 60-mm dish and culture for 2 d in 5% CO<sub>2</sub> at 37°C.
4. Culture the cells in 5% CO<sub>2</sub> at 35°C (*see Note 5*). Remove half the volume of medium and add the same volume of 10% FCS–Jolik MEM (*see Note 1*) at intervals of 4–5 d.
5. The epithelial cells push aside feeder cells to form colonies (*see Fig. 1*). When colonies grow to a diameter of approx 10 mm, the epithelial cells are cloned as follows.
6. Wash the dish twice with 4 mL of PBS containing 0.02% EDTA to remove Swiss 3T3 cells and thymic nonepithelial cells. Add 2 mL of PBS containing 0.25% trypsin and 0.02% EDTA and incubate to remove the cells from the dish.
7. Add an equal volume of 10% FCS-DMEM and centrifuge the cell suspension at 500g for 10 min. Resuspend the cell pellet in 2 mL of 10% FCS-DMEM. Repeat this procedure once.
8. Resuspend the cells to a density of  $10^4$ /mL in 10% FCS-DMEM in a 60-mm dish. Under an inverted phase-contrast microscope, pick up a single cell or a



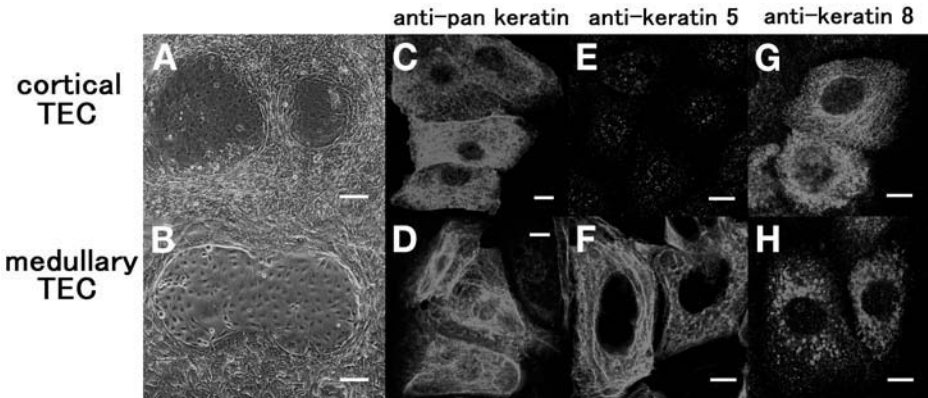


Fig. 1. Phase-contrast and immunofluorescence micrographs of thymic epithelial cell (TEC) lines established from C57/BL6 mouse thymus. TEC have been established on irradiated Swiss 3T3 feeder cells in 10% fetal calf serum (FCS) JMEM at 35°C. These cells form typical cobblestone-like colonies, as shown in phase-contrast micrographs (A,B). Bar = 100  $\mu$ m. After cloning, these TEC lines were cultured in the presence of interferon- $\gamma$  and characterized with respect to their expression of pan-keratin, keratin 5, and keratin 8 by the confocal microscopy. In the case of the TEC line shown in A,C,E,G, a part of the cells were stained in a fibrous manner with anti-pan keratin antibody (C) as well as anti-keratin 8 antibody (G), but only weakly stained in a dotted manner with anti-keratin 5 antibody (E). In the case of the other TEC line shown in B,D,F,H, cells stained brightly in a fibrous manner with anti-pan keratin antibody (D) as well as anti-keratin five antibody (F), and only weakly stained in a dotted manner with anti-keratin 8 antibody (H). In the thymus, the cortical region is stained with both anti-pan-keratin and anti-keratin 8 antibodies, whereas the medullary region is stained with both anti-pan-keratin and anti-keratin 5 antibodies. Although the staining pattern of TEC lines with a set of anti-keratin antibodies is not completely compatible with that in the thymus, the TEC lines stained in a fibrous manner with anti-pan-keratin and anti-keratin 8 antibodies could be assigned to the cortical TEC (cTEC), whereas the TEC lines stained in fibrous manner with anti-pan-keratin and anti-keratin 5 antibodies may be assigned to the medullary TEC (mTEC). (C–H). Bar = 10  $\mu$ m.

cluster of cells from the cell suspension by using a micropipet and transfer them to each well of a 24-well plate (Falcon, cat. no. 3847), coated with  $10^5$  40 Gy-irradiated Swiss 3T3 cells in 1 mL of 10% FCS-DMEM. The culture is maintained in 5%  $\text{CO}_2$  at 35°C, the medium being replaced with 0.5 mL of 10% FCS-Jolik MEM at intervals of 4 d. The cloning procedure is repeated once to obtain TEC lines.

### 3.1.3. Maintenance of TEC Lines

1. Once established, culture TEC lines in 10% FCS-JMEM at 35–37°C in 5%  $\text{CO}_2$ . Replace the cultured medium with fresh medium at intervals of 4 d. If the growth

of the TEC becomes slow or arrested, add  $10^5$  40 Gy-irradiated Swiss 3T3 cells per milliliter of 10% FCS-DMEM.

2. When the cell growth reaches confluency, cells are washed with PBS once and treated with PBS containing 0.25% trypsin and 0.02% EDTA at 37°C. Add 10% FCS-DMEM to inhibit the residual enzymatic activity of trypsin and then centrifuge at 500g for 10 min.
3. Resuspend the cell pellet in 10% FCS-JMEM and transfer a quarter of the cell suspension to a new dish supplemented with fresh medium and culture at 35–37°C in 5% CO<sub>2</sub>.

#### 3.1.4. Preservation of TEC Lines

Cells are washed with PBS once, treated with 0.25% trypsin at 37°C, and centrifuged at 500g for 10 min. Resuspend the cells to approx  $5 \times 10^6$  per milliliter of FCS containing 10% DMSO. The stock may be stored first at –70°C and then transferred to liquid nitrogen 2 d later.

### 3.2. Characterization of TEC Lines Using Ab to Keratins and Epithelial Cell Markers

1. Put one drop (approx 50  $\mu$ L) containing  $10^5$  TEC cells in 5% FCS-DMEM onto the wells of an eight-hole heavy Teflon-coated slide prepared as described in **Subheading 2.2.2.**, and incubate the slides at 35°C in 5% CO<sub>2</sub> for several days.
2. To enhance the expression of molecules, including MHC class II, involved in antigen presentation, TEC line cells are cultured in 5% FCS-DMEM containing 400 IU/mL of IFN- $\gamma$  at 37°C in 5% CO<sub>2</sub> for 72 h.
3. Wash the cells twice with FCS-free MEM for 10 min at room temperature.
4. Fix the cells with cold acetone (kept at 4°C) for 10 min on ice.
5. Wash the cells three times with cold TBS for 10 min.
6. Incubate the cells with 5  $\mu$ g/mL of the primary Ab in 1% BSA-TBS overnight in a refrigerator with gentle swinging.
7. Wash the cells three times with cold TBS for 10 min.
8. Incubate the cells with 5  $\mu$ g/mL of the secondary antibody in 1% BSA-TBS for 3 h at room temperature.
9. After washing the cells three times with cold TBS for 10 min, seal the slides with PBS-glycerin solution (1:9). The sealed slides can be stored at –20°C for at least 1 mo.
10. Immunofluorescence photographs may be taken on a Zeiss confocal laser scanning inverted-microscope, LSM 510. The typical staining patterns of cortical and medullary TEC line cells are shown in **Fig. 1**.

### 3.3. Immunofluorescence Staining of H2-DM<sup>+</sup> Compartments in TEC Lines

1. Put one drop of  $10^5$  TEC line cells in 10% FCS-DMEM onto the wells of an eight-well heavy Teflon-coated slide, prepared as described in **Subheading 2.2.2.** and incubate the slides at 35°C in 5% CO<sub>2</sub> for several days.

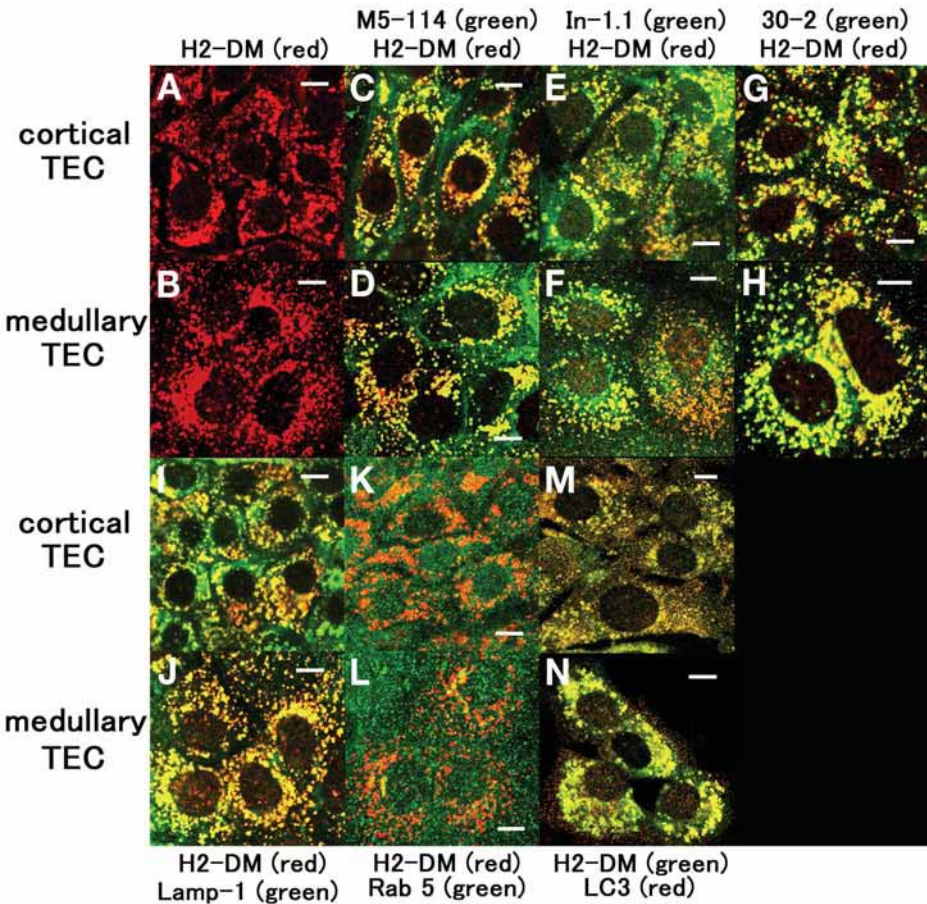


Fig. 2. Two-color immunofluorescent micrographs of the cortical and medullary thymic epithelial cell (TEC) lines costained with the anti-H2-DM antibody and various antibodies against molecules involved in major histocompatibility complex (MHC) class II-restricted antigen presentation. Both TEC lines were cultured with 6  $\mu\text{g}/\text{mL}$  of pepstatin A and 6  $\mu\text{g}/\text{mL}$  of E64d for 8 h, fixed, and then analyzed using confocal microscopy. The cytoplasm in the cortical TEC lines as well as the medullary TEC (mTEC) line is stained in a dotted manner with anti-H2-DM antibody (**A,B**). These H2-DM<sup>+</sup> compartments (red) in the cytoplasm of both the cortical TEC (cTEC) and the mTEC are stained with M5-114 for MHC class II molecules (green, **C,D**), In-1.1 for invariant chains (green, **E,F**) and 30-2 for MHC class II plus CLIP complexes (green, **G,H**). These results indicate that the formation of MHC class II complexes actually occurs in the H2-DM<sup>+</sup> compartments. In addition, these H2-DM<sup>+</sup> compartments colocalize with the endosomal marker, rab5 (green, **K,L**) as well as the lysosomal marker, LAMP-1 (green, **I,J**). Moreover, these H2-DM<sup>+</sup> compartments (green) are colocalized with a marker peculiar to the autophagosome, LC3 (red, **M,N**). The results shown (**K-N**) suggest that not only endosomes but also autophagosomes could access and fuse to the H2-DM compartments. Bar = 10  $\mu\text{m}$ .

2. To enhance the expression of molecules involved in the MHC class II-restricted presentation of antigen, TEC line cells are cultured in 5% FCS-DMEM containing 400 IU/mL of IFN- $\gamma$  at 37°C in 5% CO<sub>2</sub> for 72 h.
3. Half of the cells are further cultured in 5% FCS-DMEM containing 100 IU/mL of IFN- $\gamma$ , 6  $\mu$ g/mL of pepstatin A, and 6  $\mu$ g/mL of E64d at 37°C for 8 h (see **Note 6**). The remaining cells are further cultured in 5% FCS-DMEM containing 100 IU/mL of IFN- $\gamma$  without protease inhibitors.
4. Wash the cells once with FCS-free MEM for 10 min at room temperature.
5. Fix the cells with PBS (pH 7.0) containing 4% paraformaldehyde (PFA) for 10 min at room temperature, and then incubate in 0.1 M glycine solution (adjusted to pH 7.0 with 1 M Tris-HCl) to halt the reaction of the PFA.
6. After washing the cells twice with TBS for 10 min, permeabilize the cells with TBS containing 0.05% (w/v) saponin for 10 min at room temperature.
7. Wash the cells three times with TBS for 10 min, apply 5  $\mu$ g/mL of rabbit anti-H2-DM antibody or anti-LC3 antibody in 1% BSA-TBS and incubate the cells overnight in a refrigerator with gentle swinging.
8. Wash the cells three times with TBS for 10 min, incubate the cells with 5  $\mu$ g/mL of Alexa 543-conjugated anti-rabbit immunoglobulins in 1% BSA-TBS for 3 h at room temperature with gentle swinging.
9. Wash the cells three times with TBS for 10 min, incubate the cells with 5  $\mu$ g/mL of the secondary antibody in 1% BSA, TBS, 0.02% NaN<sub>3</sub> overnight in a refrigerator with gentle swinging.
10. Wash the cells three times with TBS for 10 min, incubate the cells with 5  $\mu$ g/mL of Alexa488-conjugated anti-IgG antiserum or Alexa488-conjugated avidin in 1% BSA, TBS, 0.02% NaN<sub>3</sub> for 3 h at room temperature with gentle swinging.
11. After washing the cells three times with TBS for 10 min, seal the stained samples with PBS/glycerin (1:9) and visualize using a Zeiss LSM 510 confocal microscope. The distribution of MHC class II and related molecules in TEC line cells is shown in **Fig. 2**.

### **3.4. Immunological Isolation of H2-DM<sup>+</sup> Compartments From TEC Lines**

#### *3.4.1. Preparation of Magnetic Beads Coated With Anti-H2-DM Antibody*

1. Place  $2.0 \times 10^8$  Dynabeads labeled with sheep anti-rabbit IgG (DYNAL, cat. no. 112.03) into a 1.5-mL Eppendorf tube.
2. Place the tube on a magnet for 2 min and remove the fluid portion.
3. Remove the tube from the magnet and resuspend the beads in 0.8 mL of 1% BSA, 0.02% NaN<sub>3</sub> in PBS.
4. Repeat **steps 2 and 3**.
5. Resuspend the beads in 60  $\mu$ g of anti-H2-DM antibody in PBS containing 0.02% NaN<sub>3</sub> (according to the manufacturer's protocol, approx 0.8–3.0  $\mu$ g of antibody per  $10^7$  beads will give the necessary concentration to effectively bind a specific target). Make the final volume up to 0.8 mL with 1% BSA, 0.02% NaN<sub>3</sub> in PBS.
6. Rotate the tube overnight in a refrigerator.
7. Place the tube on a magnet for 2 min and remove the fluid.

8. Remove the tube from the magnet and suspend the pellet in 0.8 mL of 1% BSA, 0.02% NaN<sub>3</sub> in PBS.
9. Repeat **step 8** and resuspend the beads in 0.5 mL of 1% BSA, 0.02% NaN<sub>3</sub> in PBS. The final concentration should be  $4.0 \times 10^8$  beads/mL.

### 3.4.2. Subcellular Fractionation of Vesicles Using Magnetic Beads Coated With Anti-H2-DM Antibody

1. Culture TEC line cells in 100-mm dishes with 10% FCS-JMEM.
2. Upon reaching confluency, culture the TEC line cells with 8 mL of 5% FCS-DMEM containing 100 IU/mL of IFN- $\gamma$  for 3 d. Replace the culture medium with the same volume of fresh medium every day.
3. After stimulation with IFN- $\gamma$ , remove the medium and rinse the dishes with 4 mL of 0.02% EDTA in PBS.
4. Remove the 0.02% EDTA and rinse with 4 mL of 0.25 M sucrose solution.
5. Remove the 0.25 M sucrose solution and replace with 0.8 mL of 0.25 M sucrose solution containing a protease inhibitor (1 mM PMSF, 0.1 mM TPCK, 10  $\mu$ g/mL of aprotinin, 0.1 mM leupeptin).
6. Remove the cells using a cell scraper.
7. Transfer the cell suspension into a 15-mL test tube.
8. Put 0.8 mL of 0.25 M sucrose solution containing protease inhibitors into the dishes, and scrape the cells again.
9. Transfer the cell suspension into a 15-mL test tube and homogenize the cells by passing 1.6 mL of the 0.25 M sucrose solution 20 times through a 23-gauge needle, attached to a disposable 1-mL plastic syringe.
10. Centrifuge the homogenate at 1000g for 10 min to eliminate large cell fragments and nuclei.
11. Divide the supernatant (postnuclear supernatant, PNS) into two aliquots. Put each aliquot into a 1.5-mL screw cap tube.
12. Add 50  $\mu$ L of the magnetic beads conjugated with the anti-H2-DM antibody ( $2 \times 10^7$  beads bound to approx 6  $\mu$ g of antibody) into each aliquot of the PNS.
13. Rotate the tubes gently in a refrigerator for 24 h.
14. Place the tubes on a magnet for 10 min at 2–8°C and carefully pipet off the fluid.
15. Resuspend the pellet in 0.4 mL of PBS and mix gently.
16. Repeat **steps 14** and **15**.
17. Place the tubes on a magnet for 10 min at 2–8°C and carefully remove the fluid.
18. Store the pellet at –80°C until use.

## 3.5. SDS-PAGE

### 3.5.1. Preparation of SDS Samples

1. Add 50  $\mu$ L of SDS sample buffer without 2-mercaptoethanol into the tubes containing the magnetic beads.
2. Transfer the contents into a filter-tube and centrifuge at 10,000g for 10 min.
3. Take off the filter unit and dilute 10  $\mu$ L of the filtrate 1:4 with dH<sub>2</sub>O. Then, estimate the protein concentrations in the diluted filtrate by means of the BCA



assay, according to the manufacturer's instructions (PIERCE, Rockford, IL) (see **Note 7**).

4. Add 40  $\mu\text{L}$  of SDS sample buffer with 2-mercaptoethanol into the remaining filtrate. Apply 10–50  $\mu\text{L}$  of the mixture on SDS-gel without boiling (i.e., under nonreducing conditions) or with boiling for 2 min (reducing conditions).

### 3.5.2. PAGE

1. Assemble the notched glass plate with the glass plate fitted with glass spacers (1.0-mm thick) and the 1.0-mm-thick silicon rubber spacer. Hold the assembled plates together with the aid of fold-back clamps.
2. Prepare the 12.5% acrylamide solution by mixing 7.5 mL of separating buffer, with 12.5 mL of acrylamide/bisacrylamide solution, 0.3 mL of 10% SDS solution, 9.7 mL of Milli-Q grade water, 100  $\mu\text{L}$  of ammonium persulfate solution, and 20  $\mu\text{L}$  of TEMED. Pour the gel, leaving space for a stacking gel, and overlay with water-saturated isobutanol. The gel should polymerize in approx 30 min.
3. Pour off the isobutanol and rinse the top of the gel twice with water.
4. Prepare the stacking gel by mixing 3 mL of stacking buffer with 2 mL of acrylamide/bisacrylamide solution, 0.12 mL of 10% SDS solution, 6.9 mL of Milli-Q grade water, 50  $\mu\text{L}$  of ammonium persulfate solution, and 10  $\mu\text{L}$  of TEMED. Use approx 0.5 mL of this mixture to quickly rinse the top of the gel and then pour the stack and insert the comb. The stacking gel should polymerize within 30 min.
5. Prepare the running buffer by diluting 200 mL of the 4X running buffer with 800 mL of Milli-Q grade water in a measuring cylinder. Cover with Parafilm and invert the cylinder to mix well.
6. Once the stacking gel has set, carefully remove the comb and clean the wells with a strip of Whatman 3MM paper or rinse the wells with Milli-Q grade water. Remove the clamps and the silicone rubber spacer, and clean the space between the two glass plates using a strip of Whatman 3MM paper.
7. Wet a Whatman 3MM paper 160-mm wide and 110-mm high with electrode buffer, and place it on the notched side of the gel plates and true up the bottom ends of the paper and the plates. Clamp the gel plates and the paper to the electrophoresis chambers, which have been prefilled with electrode buffer. Fill the upper chamber until the slots are submerged to a depth of 5 mm. Remove any air bubbles trapped at the bottom of the gel with electrode buffer using a syringe fitted with a bent needle.
8. Load the protein samples into the bottom of the wells using a micropipet fitted with a long narrow tip. Volumes of 10–50  $\mu\text{L}$  are acceptable for loading. Include one well for prestained molecular weight markers.
9. Attach the electrode wires. Apply 80–150 V at a constant current until the dye is 10 mm from the bottom of the gel. If the gel plates become hot, reduce the current. During normal operation, the gel plates will become warm to the touch.
10. Turn off the current. Remove the gel cassette, carefully take apart the plates with the use of a spatula and remove the gels for blotting.

### 3.6. Western Blotting for Analysis of H2-DM<sup>+</sup> Compartments From TEC Line Cells

1. Cut a filter paper (Whatman 3MM) and the PVDF membrane to the dimensions of the gel to be transferred.
2. Wet the PVDF membrane with methanol first. Then soak both the membrane and filter papers in transfer buffer and leave for 15 min.
3. Soak the filter paper, the membrane and four sheets of Whatman 3MM filter paper in transfer buffer for 10 min.
4. The fiber pads for the tank transfer should be soaked well in buffer and any air bubbles removed.
5. Assemble the materials in the following order from cathode side to anode side: fiber pad, two sheets of filter paper, gel, PVDF membrane, two sheets of filter paper, fiber pad.
6. Clamp this sandwich together in the cassette, according to the apparatus being used. Half fill the tank with buffer and insert the cassette, then quickly fill the tank with buffer to above the height of the cassette.
7. Transfer at 12 mA for 18–20 h at 4–8°C.
8. Following electrophoretic transfer, block any nonspecific binding sites with blocking buffer for 1 h at room temperature with agitation and then remove the buffer.
9. Incubate the blot in diluted primary antibody solution in incubation buffer, for 48 h at 4–8°C with agitation and then remove.
10. Wash the blot with T-TBS once for 30 min and then with TBS twice for 30 min at room temperature.
11. Incubate with secondary antibody in 1% skimmed milk in TBS at the recommended dilution (usually 1:2000–1:5000) for 2 h at room temperature with agitation and then remove.
12. Wash, as in **step 10**.
13. Leave the blot in the final washing buffer (TBS). During this period, 2-mL aliquots of each portion of the chemiluminescent solutions (supersignal, PIEACE) are warmed separately to room temperature and then mixed together. Incubate the blot in this solution for 1 min while rotating by hand.
14. Drain off the reagent and wrap the blot in plastic wrap.
15. The chemiluminescent signal on the blot can be measured digitally with a FujiFilm LAS 3000. Alternatively, expose the blot to conventional film, as required, and develop. Typical results obtained using this protocol are shown in **Fig. 3**.

### 4. Notes

1. This medium (JMEM) is a Ca<sup>2+</sup>-free form of MEM. The low concentration of Ca<sup>2+</sup> is recommended for establishment and maintenance of TEC lines.
2. The addition of IFN- $\gamma$  to the 5% FCS-DMEM is necessary for the expression of MHC class II molecules by TEC lines. To fully express MHC class II molecules, TEC lines should be cultured for 2 d in 5% FCS-DMEM with 500 IU/mL of IFN- $\gamma$ .

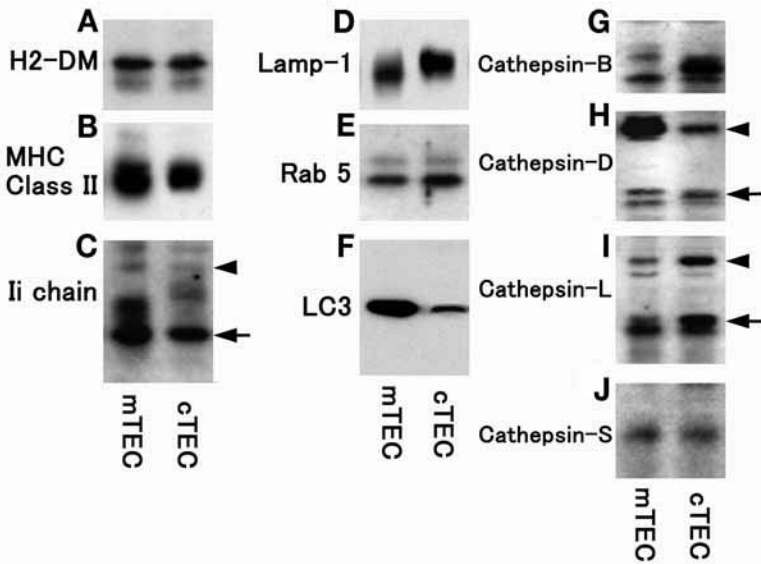


Fig. 3. Isolation and characterization of vesicles from the PNS of thymic epithelial cells (TECs) by utilizing magnetic beads coated with anti-H2-DM. After vesicles were isolated from the PNS of both cortical TECs (cTECs) and medullary TECs (mTECs) by means of magnetic beads coated with anti-H2-DM antibody, they were analyzed by Western blotting. The H2-DM molecules are detected in vesicles of both the cTEC and the mTEC (A). In these vesicles, major histocompatibility complex (MHC) class II heterodimers are probed by M5-114 (B) and 30 kDa-invariant chain (shown as an arrow in C) and 35 kDa-invariant chains (an arrow head in C) are probed by In-1.1. These results are concordant with the results shown in the immunofluorescence study (Fig. 2C–F). The typical lysosomal marker, LAMP-1 (D), the endosomal marker rab5A (E), and a marker peculiar to autophagosomes, LC3 (F) are also detected in these vesicles, suggesting that self-antigens could be transported into the H2-DM<sup>+</sup> compartments via autophagy as well as endocytosis. Moreover, a series of soluble endosomal/lysosomal proteases, i.e., cathepsin-B (G), -D (preforms: an arrow head, mature forms: an arrows in H), -L (preforms: an arrow head, mature forms: an arrows in I), and -S (J) are detected, suggesting that the integral vesicles have been isolated from the lysates and antigens and invariant chains are processed by the above proteases.

3. PFA is toxic. Wear gloves, face mask, and safety glasses. Do not boil the PFA solution in a microwave oven. If this should occur, however, immediately transfer the solution to a chemical fume hood.
4. It is better to fix cells with the PFA solution with a pH value of between pH 6.8 and 7.2. Upon fixation with acidic PFA solution (i.e., less than pH 6.5), antibodies fail to react efficiently with fixed cells. On the other hand, upon fixation with



basic PFA solution (i.e., more than pH 7.5), the extent of background in immunofluorescence staining could increase.

5. The irradiated Swiss mouse 3T3 cells secrete growth factors to support the growth of TEC and oppose the adherence of fibroblast cells derived from thymus. The culture of cells at 35°C does not affect the growth rate of TEC but diminishes the growth rate of the fibroblast cells.
6. E64d inhibits the activity of cysteine proteases, for example, cathepsin-B, -L, and -S. Pepstatin A inhibits the activity of aspartic proteases, for example, cathepsin-D. The inhibition of these lysosomal enzymes arrests the maturation of lysosomes and simultaneously accumulates the MHC class II molecules and associated molecules in lysosomes.
7. To assay the protein concentration without interference of SDS, Tris, and sucrose, make the concentration of SDS, Tris, and sucrose less than 1%, 100 mM, and 40%, respectively.

## Acknowledgments

The authors thank Professor Mitsuru Matsumoto for valuable suggestions, and Rieko Ohki for technical assistance.

## References

1. Crotzer, V. L. and Blum, J. S. (2005) Autophagy and intracellular surveillance: modulating MHC class II antigen presentation with stress. *Proc. Natl. Acad. Sci. USA* **22**, 7779–7780.
2. Kyewski, B. and Derbinski, J. (2004) Self-presentation in the thymus: an extended view. *Nat. Rev. Immunol.* **4**, 688–698.
3. Anderson, M. S., Venanzi, E. S., Chen, Z., Berzin, S. P., Benoist, C., and Mathis, D. (2005) The cellular mechanism of Aire control of T cell tolerance. *Immunity* **23**, 227–239.
4. Kasai, M. and Hirokawa, K. (1991) A novel cofactor produced by a thymic epithelial cell line: promotion of proliferation of immature thymic lymphocytes by the presence of interleukin-1 and various mitogens. *Cell. Immunol.* **132**, 662–667.
5. Bhattacharya, A., Dorf, M. E., and Springer, T. A. (1981) A shared alloantigenic determinant on Ia antigens encoded by I-A and I-E subregions: evidence for I region gene duplication. *J. Immunol.* **127**, 2488–2495.
6. Koch, N., Koch, S., and Hammerling, G. J. (1981) Ia invariant chain detected on lymphocyte surfaces by monoclonal antibody. *Nature* **299**, 644–645.
7. Eastman, S., Defetos, M., DeRoos, P. C., et al. (1996) A study of complexes of class II invariant chain peptide: major histocompatibility complex class II molecules using a new complex-specific monoclonal antibody. *Eur. J. Immunol.* **26**, 385–393.
8. Karlsson, L., Peleraux, A., Lindstedt, R., Liljedahl, M., and Peterson, P. A. (1994) Reconstitution of operational MHC class II compartment in nonantigen-presenting cells. *Science* **266**, 1569–1573.

9. Tanida, I., Ueno, T., and Kominami, E. (2004) LC3 conjugation system in mammalian autophagy. *Int. J. Biochem. Cell Biol.* **36**, 2503–2518.
10. Lindstedt, R., Liljedahl, M., Peleraux, A., Peterson, P. A., and Karlsson, L. (1995) The class II molecule H2-M is targeted to an endosomal compartment by a tyrosine-based targeting motif. *Immunity* **3**, 561–572.
11. Marks, M. S., Roche, P. A., von Donselaar, E., Woodruff, L., Peters, P. J., and Bonifacino, J. S. (1995) A lysosomal targeting signal in the cytoplasmic tail of the  $\beta$  chain directs HLA-DM to MHC class II compartments. *J. Cell Biol.* **131**, 351–369.



## Thymus Organogenesis and Development of the Thymic Stroma

Craig S. Nowell, Alison M. Farley, and C. Clare Blackburn

### Summary

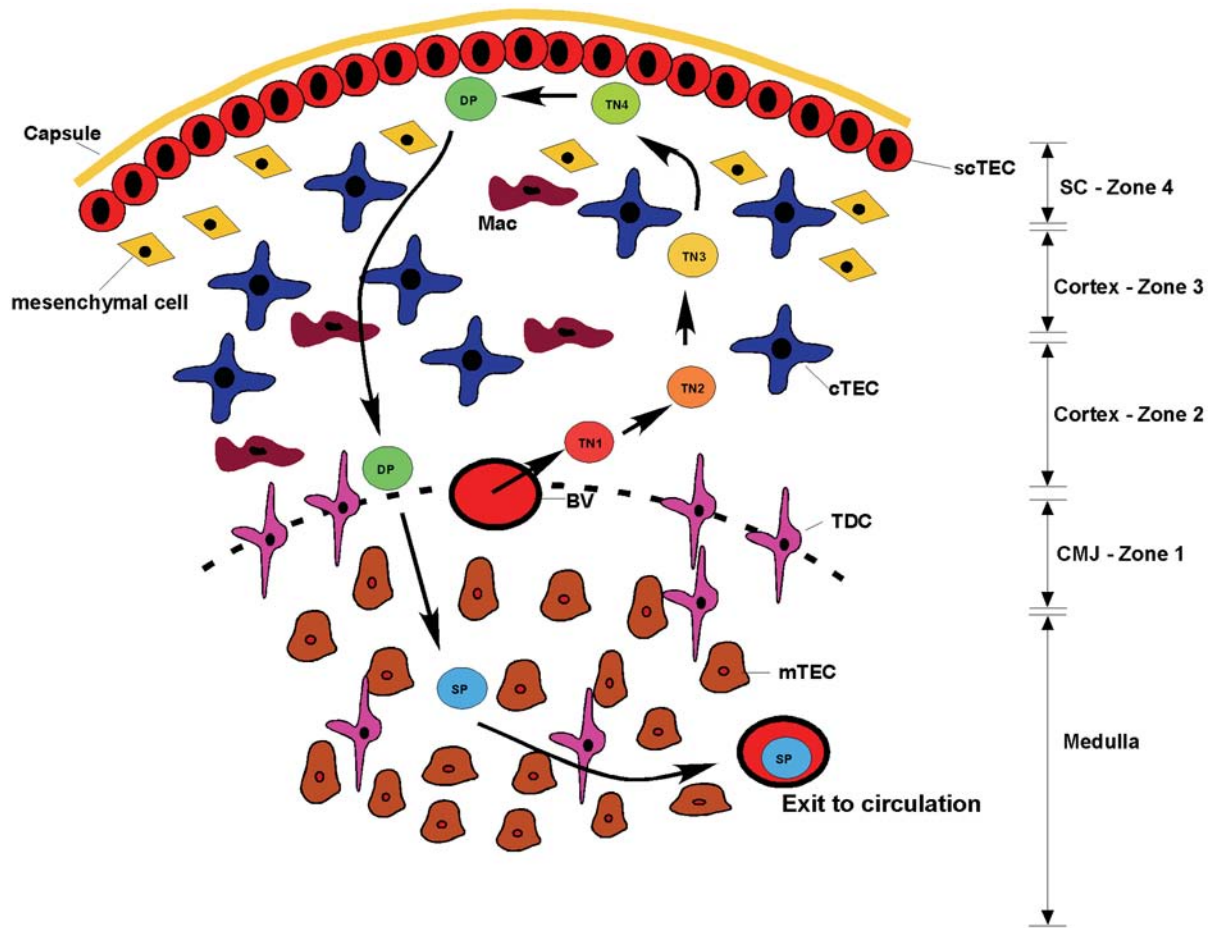
T-cell development occurs principally in the thymus. Here, immature progenitor cells are guided through the differentiation and selection steps required to generate a complex T-cell repertoire that is both self-tolerant and has propensity to bind self major histocompatibility complex. These processes depend on an array of functionally distinct epithelial cell types within the thymic stroma, which have a common developmental origin in the pharyngeal endoderm. Here, we describe the structural and phenotypic attributes of the thymic stroma, and review current cellular and molecular understanding of thymus organogenesis.

**Key Words:** Thymus; endoderm; thymic epithelium; epithelium; organogenesis; patterning; stem cell; progenitor cell; Foxn1.

### 1. The Thymic Microenvironment

#### 1.1. Structure and Morphology of the Thymus

The mature thymus is characterized by the presence of developing T lymphocytes (thymocytes), which make up more than 95% of its cellularity. Within the thymus, T-cell development is mediated by a range of stromal elements, including mesenchymal cells, bone marrow (BM)-derived stromal cells and vasculature, and the uniquely specialized thymic epithelium (1). The organ is divided histologically into two main regions, the cortex and medulla, and is surrounded by an outer capsule consisting of a thick layer of connective tissue (see Fig. 1). The capsule is separated from the cortex by a thin layer—the subcapsule—consisting of simple epithelium (1), whereas the cortex consists of three-dimensional networks of epithelial cells densely packed with developing thymocytes (1–3). The inner medullary region again consists of a three-dimensional network of epithelial cells populated with thymocytes, however, the ratio of



medullary epithelial cells to thymocytes is higher than in the cortex and this region is also densely populated with BM-derived stromal cells (1).

Intrathymic T-cell development is regulated so that thymocytes at different stages of development are found in different anatomical locations. Hematopoietic progenitors enter the postnatal thymus at the corticomedullary junction. T-cell development from the earliest postcolonization stages of thymocyte maturation (termed “triple negative” [TN] cells as they do not express CD3 or the coreceptors CD4 or CD8) through to the CD4<sup>+</sup>CD8<sup>+</sup> double positive (DP) stage occurs in the thymic cortex. Those DP cells selected to proceed to mature into CD4<sup>+</sup> or CD8<sup>+</sup> single positive (SP) cells subsequently migrate into the medulla, from where they exit into the peripheral immune system. The cortex itself can be subdivided into four regions based on the localization of different thymocyte populations: zone 1 contains the colonizing population of hematopoietic progenitor cells that are not yet committed to the T-cell lineage; these early thymocytes undergo proliferative expansion in zone 2; commitment to the T-cell lineage occurs in zone 3; and in zone 4, thymocytes differentiate to the DP stage of development, characterized by expression of both CD4 and CD8 coreceptors (4).

## 1.2. The Thymic Epithelium

Thymic epithelial cells (TEC) are broadly classified into three populations; subcapsular/subtrabecular epithelial cells, cortical thymic epithelial cells (cTEC), and medullary thymic epithelial cells (mTEC). Within these subdivisions ultrastructural and immunohistochemical analyses have revealed at least six

---

Fig. 1. (*Opposite page*) Histology of the postnatal thymus. The mature thymus is histologically divided into an outer cortex and an inner medulla. The main body of the cortex contains cortical thymic epithelial cells (cTEC), macrophages (MΦ) and developing thymocytes at the triple negative (TN) and double positive (DP) stages of differentiation. The cortex is surrounded by a mesenchymal capsule, under which lies a layer of subcapsular thymic epithelial cells (scTEC). Thymocytes are localized to four distinct regions of the cortex depending on their differentiation status: TN1 thymocytes reside in zone 1 at the cortico-medullary junction (CMJ), where they enter the thymus from blood vessels (BV). During their differentiation into TN2 and TN3 thymocytes they progressively migrate into zones 2 and 3. TN4 cells are located in zone 4, the subcapsule (SC), where they undergo the TN to DP transition. DP thymocytes then migrate through the cortex to the CMJ. Those thymocytes that successfully undergo positive selection into single positive (SP) thymocytes then migrate into the medulla, where medullary thymic epithelial cells (mTEC) mediate the final stages of T-cell differentiation, and aspects of tolerance induction. Thymic dendritic cells (TDC) found at the CMJ and in the medulla are also important mediators of negative selection. Mature SP thymocytes then exit the thymus via the vasculature to form the peripheral T-cell pool.

**Table 1**  
**TEC Subpopulations Defined by CTES MAbs**

Antibody	Staining pattern in adult thymus	CTES group	References
ER-TR3	Cortical and medullary TEC	I	69
MTS39	Pan-epithelial	I	8
ER-TR5	Medullary TEC	II	69
IVC4	Subcapsular and medullary TEC	II	162,163
MTS10	Medulla	II	8
CDR1	Cortical TEC	III	164
ER-TR4	Cortical and isolated medullary TEC	IIIB	69
MTS44	Cortex	IIIB	8
4F1	Cortical TEC	IIIB	162,163
MTS32	Cortical TEC and thymocytes	IIIC	165
MTS20	Isolated cells in medulla	IV	8
MTS29	Isolated medullary TEC	IV	8
MTS9	Medullary and some cortical TEC	XX	165
MTS37	Isolated cortical and medullary TEC and thymocytes	XX	166,167
MTS35	Minority of medullary TEC	XX	166,167

subsets of epithelial cells (5), which are assigned “clusters of thymic epithelial staining” (CTES) types I, II, III, IIIB, IIIC, and IV (6) (see Table 1) based on the different monoclonal antibodies (MAb) staining profiles observed.

The subcapsular/subtrabecular epithelium forms a barrier between the external and internal thymic microenvironments and consists of type I epithelial cells in a simple epithelial layer. These type I cells are major histocompatibility complex (MHC) class II negative (7) and are reactive to CTES II MAbs (8).

The thymic cortex lies directly beneath the subcapsular/subtrabecular epithelium. The outermost cortical subpopulations are type II epithelial cells, characterised by their pale appearance in electronmicrographs (9). Immediately adjacent to the type II epithelia are type III thymic epithelial cells, which show intermediate electron lucency (9), whereas the innermost cTEC are type IV cells that have high electron lucency and oval/spindle shaped nuclei (9). Ultrastructural analysis has also revealed large complexes of type II and type III cells and developing thymocytes (9), termed “thymic nurse cells,” which may be important in mediating positive selection of developing thymocytes (10,11). All cTEC stain with CTES III MAbs (9), and type II and III cells are strongly MHC class II<sup>+</sup> (1). However, no MAbs are currently known to identify individual subpopulations corresponding to the type II-IV cells described above.

The medullary thymic epithelium is also heterogeneous. mTEC predominantly express determinants reactive to CTES II and IV MAbs, with type III

cells also being identified by ultrastructural analysis (9). In addition, type V epithelia, classified as undifferentiated cells, exist in small isolated clusters at the cortico–medullary junction (9), along with type VI cells that have been proposed to be precursors of differentiated epithelial cells (12). All mTEC express MHC class I, whereas MHC class II expression is variable (13–16).

The thymic epithelium has also been defined by the expression of cytokeratins (K), which are expressed by epithelial cells in all tissues. In the cortex, two populations have been identified: a predominant  $K5^+K14^-K8^+K18^+$  subset and a minor subset also consisting of  $K5^+K14^-K8^+K18^+$  cells (17). Most mTEC display a  $K5^+K14^+K8^-K18^-$  phenotype (17) and express the antigen reactive to MAb MTS10 (8), and a minor  $K5^-K14^-K8^+K18^+$  MTS10<sup>-</sup> medullary subset is also present (17).

### 1.3. Nonepithelial Stromal Elements

In addition to epithelial cells the thymic stroma also contains BM-derived cells, principally macrophages and dendritic cells (1,7,18). Macrophages reside predominantly in the cortex and cortico–medullary junction regions and differ morphologically depending on their location (18,19). Although present throughout the thymus, dendritic cells are concentrated at the cortico–medullary junction and in the medulla (18,19); unlike thymic macrophages, which show varying levels of MHC class II expression, all thymic dendritic cells display strong expression of MHC class II (1).

The thymic stroma also contains mesenchymal cells, which, along with cTEC, secrete an extensive network of extracellular matrix (ECM) components (1). ECM exists in close association with the subcapsular epithelium and forms fine networks throughout the medulla, and is likely to support the growth and development of both thymocytes (20,21) and TEC (22,23). Consistent with this, both thymocytes and epithelial cells show differential expression of a wide array of ECM receptors (24–27).

### 1.4. TEC Subset Function

The high level of heterogeneity observed in the thymic epithelium has long suggested that individual TEC subpopulations are specialized to support specific stages of T-cell maturation, an idea reinforced by the observation that discrete stages of thymocyte maturation map to distinct intrathymic locations (4). Recently, functional evidence has confirmed that specific TEC subtypes mediate particular aspects of thymopoiesis (28–30).

TEC are likely to mediate thymocyte maturation via several mechanisms, including the provision of soluble growth factors. For instance, TEC secrete stem cell factor and interleukin (IL)-7 (31), whose receptors are expressed on early TN thymocytes (31). IL-7 is an important growth factor for TN thymocytes and



also drives the expansion of thymocytes that have successfully undergone positive selection (32). Although widely expressed in the thymic primordium during development, IL-7 expression is restricted to TEC subsets at the corticomedullary junction and in the medulla of the postnatal thymus (33). Confirming the indispensable role of IL-7 in T-cell development, IL-7<sup>-/-</sup> mice are lymphopenic, with severely reduced numbers of  $\alpha\beta$ T cells (34), as are mice deficient in the interleukin-7 receptor (IL-7R) (35). The soluble factors tumor necrosis factor  $\alpha$  and IL-1 $\alpha$ , both of which have been implicated in the generation of TN2 thymocytes from their TN1 precursors (36), are also secreted by TEC (31). TEC also secrete members of the chemokine family of soluble factors, which provide chemotactic cues that coordinate the migration of developing thymocytes through the thymic stroma with their differentiation (37). Chemokine–chemokine receptor interactions have been convincingly demonstrated to regulate the migration of thymocytes from the cortico–medullary junction to the cortex (28,38) and from the cortex to the subcapsular zone (39). These migratory patterns are mediated by CXCL12/CXCR4 and CCL25/CCR9, respectively. CXCL12/CXCR4 interactions are particularly important, as CXCR4 deficient thymocytes fail to differentiate beyond the TN stages of maturation (28).

Contact between TEC and thymocytes is also crucial for proper T-cell development. Anderson and colleagues demonstrated that maturation of CD4<sup>+</sup>CD8<sup>+</sup> DP thymocytes occurred in reaggregate thymus organ cultures in which the TEC were metabolically inactivated (29), whereas cultures consisting of MHC class II<sup>+</sup> epithelial cells from other tissues (e.g., salivary epithelium, gut epithelium, dendritic cells) could not support positive selection (29), suggesting that cell surface molecules other than MHC/peptide ligands are provided by TEC to support the maturation of CD4<sup>+</sup>CD8<sup>+</sup> DP thymocytes. Separate *in vivo* studies support an essential role of cTEC in positive selection; mice in which MHC class II expression is limited to particular stromal elements demonstrate that CD4<sup>+</sup> SP T cells are only produced when MHC class II/peptide ligands are directed to the cortex (40). Similarly, positive selection of restricted transgenic TCRs occurs only when the selecting MHC/peptide ligand is expressed by cTEC (41,42). The accessory signals provided by cTEC have yet to be elucidated, although involvement of Notch/Notch ligand interactions is plausible as Notch plays an important role in the earliest stages of thymocyte maturation, including commitment of hematopoietic progenitors to the T-cell fate (43,44). TEC express a range of Notch ligands, including Jagged1 and 2 and Delta-like 1 and Delta-like 4 (45), and can initiate and sustain Notch signaling in thymocytes *in vitro* (46). There is also evidence that Notch signaling is involved in the expansion of thymocytes during the DN to DP transition (47,48) and from the DP to SP stages of maturation (49,50).

Functional analysis of medullary TEC indicates that these cells play a critical role in tolerance induction, and specifically mediate tolerance to tissue

specific and temporally regulated antigens via expression of a wide variety of tissue-specific and temporally regulated genes (51,52). The ability of mTEC to express otherwise tissue-restricted genes appears to be a cell autonomous property acquired during the fetal period (51,53) and is partly regulated by the transcription factor *Aire* (autoimmune regulator). In the thymus, *Aire* is expressed specifically in mTEC (54,55), and analysis of *Aire*<sup>-/-</sup> mice indicates a direct role for *Aire* in the regulated expression of at least some otherwise peripheral antigens in the thymic medulla (54). Furthermore, absence of *Aire* leads to autoimmunity in mice and humans (54,56–59).

## 2. Thymus Organogenesis

### 2.1. Cellular Events in Thymus Organogenesis

#### 2.1.1. Cellular Regulation of Early Thymus Organogenesis

Thymus organogenesis occurs in the pharyngeal region of the developing embryo. This region is composed of a number of bilateral bulges known as pharyngeal arches, which are separated by structures known as pharyngeal pouches and pharyngeal clefts. The pharyngeal pouches are bilateral outpocketings of pharyngeal endoderm, which form sequentially in a rostral to caudal manner and initially comprise a single layer of simple epithelium, whereas the opposing pharyngeal clefts are invaginations of surface ectoderm also consisting of a layer of simple epithelium (see Fig. 2).

During embryogenesis, the thymus arises from the endoderm of the third pharyngeal pouch, in a common primordium with the parathyroid gland. Overt organogenesis is apparent from approximately day 10 of embryonic development (E10) in the mouse, when third pharyngeal pouch cells begin to proliferate to form the bilateral primordia. Each primordium is surrounded by a condensing population of mesenchymal cells that will eventually form the capsule (60,61). Further outgrowth of the primordia, which results in expansion of both epithelial and mesenchymal components, occurs until approx E12.5, at which point the primordia separate from the pharynx and begin to resolve into discrete thymus and parathyroid organs. These subsequently migrate to their final anatomical locations—at the midline and at the lateral margins of the thyroid respectively. Patterning of the common primordium into a prospective thymus domain located in the ventral aspect of the pouch, and prospective parathyroid domain located in the dorsal aspect, appears to be an early event in organogenesis, as the parathyroid domain is delineated by the transcription factor *glial cells missing-2* (*Gcm2*) as early as E9.5. Possible mechanisms regulating the establishment/maintenance of these domains are discussed in **Subheading 2.3**.

The mesenchymal capsule surrounding the thymus primordium is derived from the neural crest, a transient population formed between the neural tube and

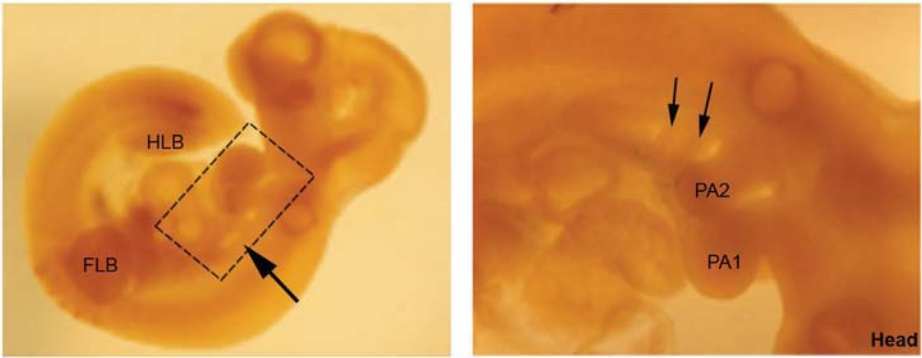
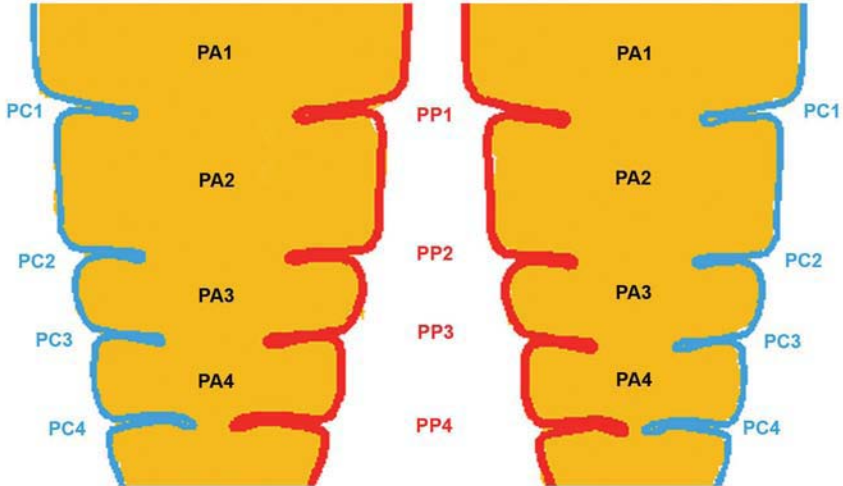
**A****B**

Fig. 2. Morphology of the pharyngeal region. **(A)** Lateral views of an E10 mouse embryo: left panel shows whole embryo (tip of the tail is missing), box indicates pharyngeal region, arrow points to the third pharyngeal pouch, FLB, fore limb bud; HLB, hind limb bud. Right panel shows detail of pharyngeal region—arrows point to third and fourth pharyngeal arches; PA, pharyngeal arch; dorsal is up and ventral down. Note that the orientation of the two embryos is different. **(B)** Cartoon representing coronal section through the same area. In mouse there are five pharyngeal arches (PA), which consist of mesenchymal and mesodermal cells (gold) bounded by an outer layer of surface ectoderm (turquoise) and inner layer of pharyngeal endoderm (168). The ectoderm forms four invaginations, the pharyngeal clefts (PC 1–4), which separate the arches, whereas the endoderm forms four opposing outpocketings, the pharyngeal pouches (PP 1–4).

the surface ectoderm. From E9.0, neural crest cells (NCC) migrate into the pharyngeal region and populate the pharyngeal arches. Studies using the chick–quail chimera system provided the first evidence that NCC are the exclusive source of mesenchymal cells in the thymus (60). This was confirmed more recently using a line of transgenic mice that expressed both a “silent LacZ” reporter from the ubiquitous Rosa26 promoter and *Cre*-recombinase under the control of the *Wnt1* promoter (61), such that LacZ was expressed in all cells derived from the neural crest. As expected, this analysis demonstrated that, in the fetus, thymic mesenchyme was derived from NCC, but a reduced contribution of NCC was unexpectedly indicated in neonatal animals. These data have been interpreted to indicate that the origin of the thymic mesenchyme may change during development, however, clarification of this point is required as an alternative explanation is transgene silencing.

Lymphocytes first seed the thymus at E11.5 (62–64). As vascularization has not occurred at this stage, the first colonizing cells leave the circulation and migrate through the peri-thymic mesenchyme into the thymic epithelium. Some evidence suggests that the first progenitor cells that colonise the thymic rudiment exhibit comparatively low T-cell progenitor activity, and that a second colonizing wave which arrives between E12 and E14 displays much higher levels of T-cell potential upon *in vivo* transfer (65).

Post-E12.5, epithelial cells within the thymic primordium continue to proliferate, at least partly in response to factors supplied by the mesenchymal capsule. Concomitantly, TEC differentiation commences: the first cortical and medullary TEC appear by E12.5 (66) and development of the two compartments proceeds in a lymphocyte independent manner until E15.5 (67,68). The expression of MHC class II on thymic epithelial cells is first detected at E13.5, with cell surface MHC class I expression occurring at approx E16 (16,69) and expression of both these antigens is followed by the appearance of CD4<sup>+</sup> and CD8<sup>+</sup> SP thymocytes at E15.5 and E17.5, respectively (16,69). Although a functional thymus is present in neonates, the full organization of the stroma characteristic of the mature organ is not achieved until 2–3 wk postnatally in the mouse.

### 2.1.2. Origin of Thymic Epithelial Cells

The embryonic origins of the thymic epithelium have been controversial, with conflicting hypotheses suggesting that the epithelium has a dual endodermal/ectodermal origin (63,70), or derives solely from the pharyngeal endoderm (71–74). However, a recent study has resolved this controversy by providing definitive evidence for a single endodermal origin in mice (72). This study used

three approaches to address the origins of the thymic epithelium. First, detailed histological analysis indicated that although there was contact between the endoderm and ectoderm at E10.5, the germ layers subsequently separated, with apoptosis occurring in the ectoderm that had previously resided in the contact region. Second, lineage tracing of pharyngeal surface ectoderm of E10.5 mouse embryos failed to find evidence for an ectodermal contribution to the thymic primordium and third, transplantation of pharyngeal endoderm isolated from E8.5 to E9.0 embryos (i.e., prior to initiation of overt thymus organogenesis) indicated that the grafted endoderm was sufficient for complete thymus organogenesis, similar to previous results obtained using chick-quail chimeras (71). These data collectively establish that pharyngeal endoderm alone is sufficient for the generation of both cortical and medullary thymic epithelial compartments.

### 2.1.3. Thymic Epithelial Progenitor Cells

The formation of complex multicellular organs from the relatively simple structures found in the developing embryo relies on the capacity of specified progenitor cells to expand and differentiate into the multiple cell types that constitute the functional organ. Thus, the early thymic rudiment contains thymic epithelial progenitor cells (TEPC) capable of giving rise to the highly diverse range of epithelial subtypes that mediate T-cell differentiation.

The phenotype of TEPC has been of considerable interest. Evidence suggestive of a progenitor/stem cell activity was initially provided by analysis of a subset of human thymic epithelial tumors: these were found to contain cells that could generate both cortical and medullary subpopulations, suggesting that the tumorigenic targets were epithelial progenitor/stem cells (75). However, the first indication of a TEPC phenotype was provided by a study addressing the nature of the defect in *nude* mice (76). Here, MHC mismatched *nude*-wild type aggregation chimeras were generated and analyzed to determine whether *nude*-derived cells could contribute to the thymic epithelium. As *nude*-derived cells were unable to contribute to the major thymic epithelial subsets, this study established that the *nude* gene product (*Foxn1*) is required cell-autonomously for the development and/or maintenance of all mature TEC. However, a few *nude* derived cells were present in the thymi of adult chimeras, and phenotypic analysis indicated that these cells expressed determinants reactive to MAbs MTS20 (77) and MTS24, but did not express markers associated with mature TEC including MHC class II. This suggested that in the absence of *Foxn1*, TEC lineage cells undergo maturational arrest and persist as MTS20<sup>+</sup>24<sup>+</sup> progenitors (76).

Further data regarding the phenotype of thymic epithelial progenitors was provided by analysis of mice with a secondary block in thymus development

resulting from a primary T-cell differentiation defect. The thymi of postnatal *CD3e26tg* mice, in which thymocyte development is blocked at the CD44<sup>+</sup>CD25<sup>-</sup>TN1 stage (78), principally contain epithelial cells that coexpress K5 and K8 (17), which, in the normal postnatal thymus, are predominantly restricted to the medulla and cortex, respectively, and are coexpressed by only a small population of cells at the cortico–medullary junction. In this study, Klug and colleagues demonstrated that transplantation of *CD3e26tg* thymi into *Rag1*<sup>-/-</sup> mice, which sustain a later block in T-cell differentiation, results in the development of K5<sup>+</sup>K8<sup>+</sup> cells, suggesting that the K5<sup>+</sup>K8<sup>+</sup> cells are progenitors of cTEC (17).

Ontogenic analysis subsequently demonstrated that the proportion of MTS20<sup>+</sup>24<sup>+</sup> cells in the thymic epithelium decreased from approx 50% at E12.5 to less than 1% in the postnatal thymus (66), consistent with the expression profile expected of markers of fetal tissue progenitor cells. Phenotypic analysis of the MTS20<sup>+</sup>24<sup>+</sup> and MTS20<sup>-</sup>24<sup>-</sup> populations of the E12.5 thymus indicated that all cells in the MTS20<sup>+</sup>24<sup>+</sup> population coexpressed K5 and K8, whereas none expressed TEC differentiation markers, including MHC class II (66). Importantly, the functional capacity of isolated MTS20<sup>+</sup>24<sup>+</sup> cells and MTS20<sup>-</sup>24<sup>-</sup> cells was then determined via ectopic transplantation. This analysis demonstrated that the MTS20<sup>+</sup>24<sup>+</sup> population was sufficient for establishment of a functional thymus containing both cortical and medullary TEC populations, whereas, in this assay, the MTS20<sup>-</sup>24<sup>-</sup> population fulfilled none of these functions (66,79). The MTS20<sup>+</sup>24<sup>+</sup> population thus contains TEPC; it is unclear at present if a single MTS20<sup>+</sup>24<sup>+</sup> cell can give rise to both cortex and medulla, or if distinct cortical and medullary progenitors are specified from an endodermal cell of wider potency (see Fig. 3). Although medullary islets in the adult thymus are clonally derived (80), this could be consistent with either of these scenarios and clarification of this issue will require clonal analysis of MTS20<sup>+</sup>24<sup>+</sup> cells. However, the demonstration that the thymic epithelium has a single endodermal origin (72) indicates that, at some level, cortical and medullary TEC share a common endodermal progenitor. Although in the models presented, the major cortical and medullary thymic epithelial cell types arise as separate “sublineages,” the best evidence supporting this model is the observation that in chimeric thymi, no correlation could be found to support a clonal origin for individual medullary islets and adjacent regions of cortical epithelium (80). However, because lineage tracing has not been reported for the adult thymic epithelium, it remains possible that a lineal relationship exists between cortical and medullary cell types.

#### 2.1.4. Thymic Epithelial Cell Differentiation

Thymic epithelial differentiation has been described principally via expression analysis of early and late differentiation markers. These include members of the cytokeratin family of intermediate filaments and markers associated



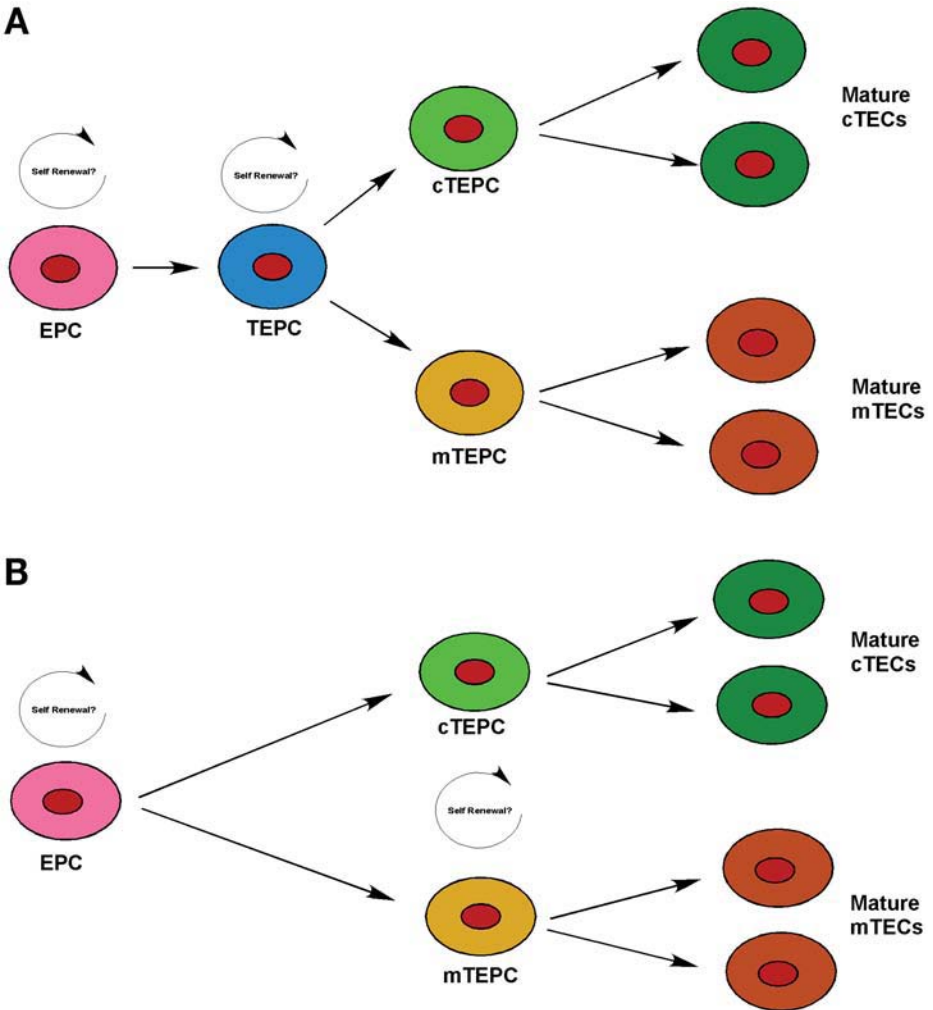


Fig. 3. Models of thymic epithelial cell differentiation. **(A)** A common thymic epithelial progenitor cell (TEPC) may arise from an endodermal progenitor cell (EPC). In this case TEPC will have the potential to generate both cortical thymic epithelial cells (cTEC) and medullary TEC (mTEC). **(B)** In the second model, an EPC gives rise directly to cortical TEPC (cTEPC) and medullary TEPC (mTEPC), which differentiate into mature cTEC and mTEC, respectively. In both cases the progenitor populations may contain self-renewing stem cells.

specifically with subsets of thymic epithelium, many of which are of unknown biochemical identity.

At E11.5, the MTS20 and MTS24 determinants are expressed throughout the common primordium by the majority of epithelial cells (66). K8 is also strongly

expressed throughout the primordium (66), and is reported by some investigators to colocalize with K5 expression in the *Foxn1* expressing domain (66). At this stage of development, the expression of other known TEC differentiation markers cannot be detected (66). Thus, at E11.5, the phenotype of epithelial cells within the thymic primordium appears to be MTS20<sup>+</sup>24<sup>+</sup>K5<sup>+</sup>K8<sup>+</sup>.

By E12.5, signs of early differentiation are apparent. Approximately 50% of TEC (66) remain MTS20<sup>+</sup>24<sup>+</sup>K5<sup>+</sup>K8<sup>+</sup>, and these MTS20<sup>+</sup>24<sup>+</sup> cells are now present as foci in the E12.5 thymic epithelium (66). K5 and K8 are also expressed in some MTS20<sup>-</sup>24<sup>-</sup> TEC, and flow cytometric analysis suggests considerable heterogeneity within this population (66). Analysis by immunohistochemistry indicates areas of the epithelium that retain costaining for K5 and K8. However, cells displaying the highest levels of K5 expression have often downregulated expression of K8 (66,67). These cells coexpress MTS10 (67), suggesting they are differentiating into medullary epithelial cells. In more peripheral areas, cells appear K8<sup>+</sup>K5<sup>-/lo</sup>, suggesting differentiation into cortical epithelium (66,67).

As fetal development proceeds, the proportion of epithelial cells expressing MTS20 and MTS24 declines, so that by E17.5 only 1–2% of epithelial cells within the thymus express these markers (66). Similarly, coexpression of K5 and K8 declines during ontogeny. Thus, by E15.5, smaller groups of K5<sup>+</sup>K8<sup>+</sup> TEC can be seen towards the periphery of the thymus, interspersed among K5<sup>-</sup>K8<sup>+</sup> TEC (67). The innermost cells within the K5<sup>+</sup>K8<sup>+</sup> clusters show strong expression of K5, whereas expression is much lower in those present at the boundary of these groups (67). By E17.5, a notable difference can be observed in the thymic architecture. A well-organized cortex is now apparent, consisting of K5<sup>-</sup>K8<sup>+</sup> TEC (67) which also express the late cortical marker 4F1 (66). Also, presumptive K5<sup>+</sup>K8<sup>-</sup> medullary regions are present, which display strong expression of MTS10 (67). At this stage, K5<sup>+</sup>K8<sup>+</sup> cells are still present although they no longer form central cores as they do during earlier stages of development (67).

Acquisition of the characteristic cortex-medulla structure of the thymus occurs by 3 wk of age in the mouse. At this stage, MTS20 and MTS24 expression is restricted to a small number of isolated cells in the medulla (66,76), and while the majority of epithelial cells express either K5 or K8, K5<sup>+</sup>K8<sup>+</sup> DP cells are present in reasonably high numbers at the cortico–medullary junction (17,67), where they persist in the postnatal thymus (17,81).

### 2.1.5. Human Thymus Development

As in the mouse, the human thymus develops from the third pharyngeal pouch. From early week 6 of fetal development, the endoderm of the third pouch forms a hollow tube-like lateral expansion from the pharynx, which



makes contact with the ectoderm of the third pharyngeal cleft (82,83). Although a single endodermal origin has not been formally demonstrated for the human thymic epithelium, it is reasonable to assume that this is the case given the demonstration of a single endodermal origin in mice and birds (71). Again, as in the mouse, the bilateral human primordia initially each comprise ventral thymic and dorsal parathyroid domains, and are encased in a neural crest derived mesenchymal capsule from the onset of development. From week 7 to mid-week 8 the thymic component of this primordium migrates ventrally, becoming stretched out in an elongated, highly lobulated cord-like structure. The upper part of this structure normally disappears, leaving the parathyroid in the location in which it will remain throughout adulthood (82). The two thymic structures meet and attach at the pericardium—their final location of the thymus into adulthood—by mid-week 8 (82). It is well documented that an accessory thymus can exist in the cervical region in humans, possibly as a result of inadequate detachment of the lobulated thymic cord from the parathyroid or development of thymic tissue left along the route of primordium migration (84), and similarly, the occurrence of cervical thymi in the mouse has recently been reported. (*See Note added in proof.*) The early human primordium appears to contain undifferentiated epithelial cells, as reported for the mouse (66), and some markers that are restricted to either cortical or medullary compartments in the postnatal thymus are expressed by all epithelial cells (85). Medullary development is seen from wk 8 and by wk 16, distinct cortical and medullary compartments are clearly evident. At wk 8 other cell types penetrate the thymus, including mesenchymal, vascular, and lymphoid cells. Between 14 and 16 wk, mature lymphocytes begin to leave the thymus to seed the peripheral immune tissues (84,86).

## 2.2. Cellular Interactions During Thymus Organogenesis

### 2.2.1. Epithelial/Mesenchymal Interactions

The essential role of NCC in thymus organogenesis was demonstrated by the perturbed development of TEC in E12.5 thymic lobes cultured in the absence of the mesenchymal capsule (87). In addition, ablation of the migratory capacity of NCC, by artificially induced lesions in chick embryos (88) results in thymic aplasia or hypoplasia. However, although NCC are likely to be important in early stages of thymus formation, no functional role has been demonstrated before E12.5. Thymic NCC are not unique in their ability to support thymus organogenesis, as illustrated by experiments in which thymic epithelial rudiments from E12.5 mouse embryos were cultured with mesenchyme from non-thymic sources, including kidney and lung (87). This study demonstrated that nonthymic mesenchymal cells could support the development of the thymic

epithelium, albeit not as effectively as pharyngeal NCC (87), and the chick–quail chimera study described above also indicated that the pharyngeal endoderm can induce nonpharyngeal mesenchyme to contribute to the thymus (71). Thus, during the initiation of thymus organogenesis, NCC mesenchyme may respond to patterning signals from the pharyngeal endoderm and then contribute to the development of the epithelial component of the thymus.

The mechanism by which mesenchymal cells influence thymus organogenesis is at least in part via the provision of soluble growth factors; Auerbach and colleagues demonstrated that the effects mediated by mesenchymal cells on the thymic epithelium could occur independently of cell-cell contact (87). In addition, the growth factors *Fgf7* and *Fgf10* are expressed by the mesenchymal cells surrounding the thymus, and TEC express their receptor, fibroblast growth factor receptor 2 IIIb (*FgfR2IIIb*). *FgfR2IIIb*<sup>-/-</sup> mice display a block in the growth of the thymic epithelium from E12.5, indicating that these factors play an important role during the development of the thymus (89). It has also been shown that insulin-like growth factor 1 (IGF-1) and epidermal growth factor (EGF) can support the *in vitro* growth and differentiation of E12.5 thymic lobes in the absence of the mesenchymal capsule (90) although the significance of IGF-1 and EGF in normal thymus development remains to be determined.

### 2.2.2. Lympho-Epithelial Cross-Talk

The requirement of lympho-stromal cross-talk for the expansion and maintenance of both cortical and medullary compartments is well established and has been reviewed extensively elsewhere (73,91,92). It is now clear that lympho-epithelial interactions are not required for initial epithelial differentiation, because the differentiation and patterning of the epithelium during embryonic development occurs normally until E15.5 in the absence of lymphoid cells committed to the T-cell lineage (67). Furthermore, TEC that differentiate in the absence of developing thymocytes retain their functional capacity (68). However, in the absence of thymocytes, the postnatal thymus is characterised by predominance of K5<sup>+</sup>K8<sup>+</sup> cells and a reduction in epithelial cell number (67). This suggests that lympho-epithelial cross-talk is required for maturation/expansion/maintenance of the cortical and medullary epithelial compartments and that, in the absence of cross-talk, immature TEC may revert to a TEPC phenotype or TEPC-like cells may persist at the expense of more differentiated TEC. Because the aberrant thymic epithelial phenotype associated with secondary effects is reversible in some models, at least some of these cells must retain thymic epithelial identity rather than adopting aberrant fates.

The dialog between TEC and developing thymocytes is likely to involve both soluble factors and intercellular adhesion molecules. Thus, several cell adhesion molecules and cytokines and their receptors are reciprocally expressed by TEC

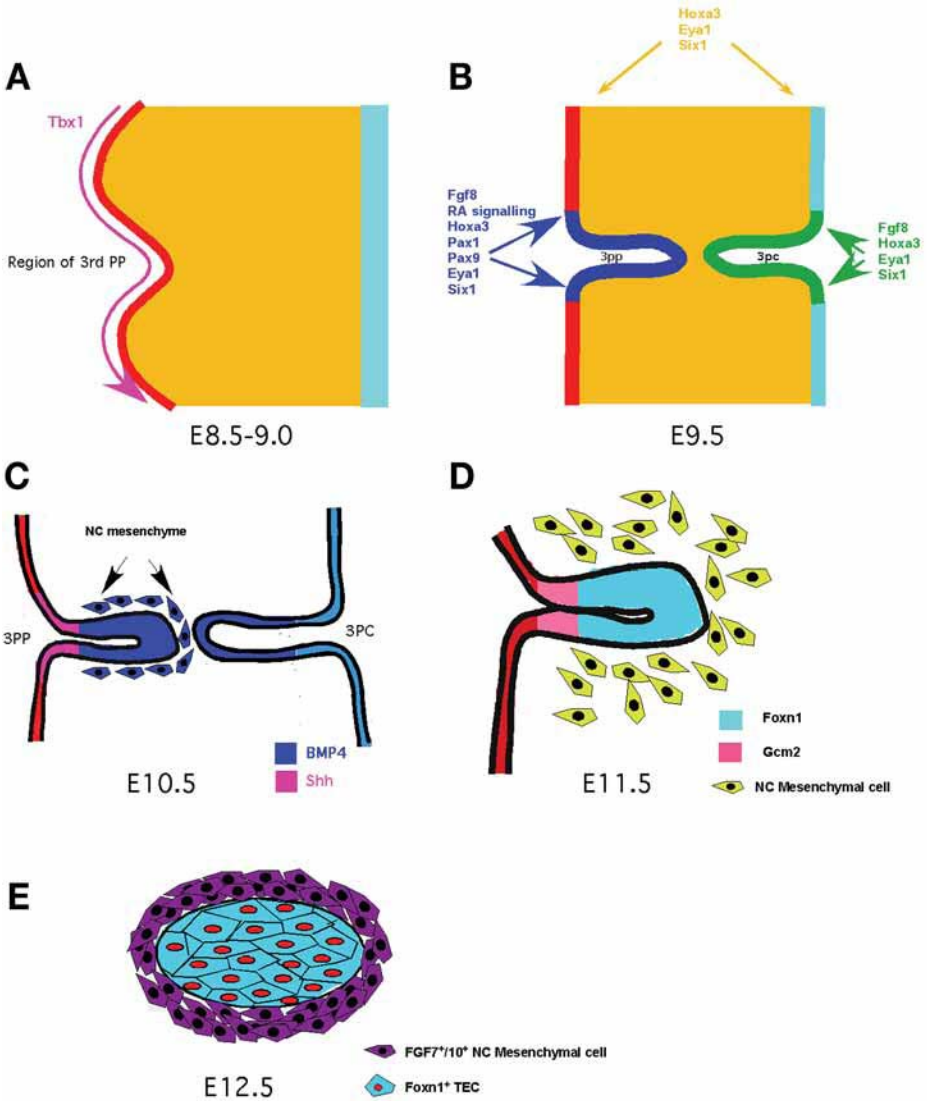


Fig. 4. Molecular regulation of early thymus development. (A) *Tbx1* expression (pink) is required in the pharyngeal endoderm (168) prior to E8.5 for formation of the third pharyngeal pouch (3pp). (B) E9.5—continued development of the 3pp is dependent on Fgf8, RA, Hoxa3, Pax1, Pax9, Eya1, and Six1, all of which are expressed in the endoderm (blue). *Hoxa3*, *Eya1*, and *Six1* are also expressed in the pharyngeal arch mesenchyme (gold), whereas the ectoderm of the third pharyngeal cleft (3pc) expresses *Fgf8*, *Hoxa3*, *Eya1*, and *Six1* (green). The tissue specific requirements for these factors have not been elucidated. (C) E10.5—the dorsal opening of the 3pp expresses *Shh*

and thymocytes. Examples include the adhesion molecules CD2 and CD58, CD54 and CD11a (92) and the cytokines IL-1, IL-4, IL-6, IL-7, and tumor necrosis factor  $\alpha$  (31,93–104). In addition, certain subpopulations of thymocytes have been shown to express *Fgf7* (105), a factor shown to be important in the growth and differentiation of the epithelium (89,105,106) although, as discussed previously, thymocytes are not the exclusive source of this growth factor.

Lymphotoxin  $\beta$  receptor (LT $\beta$ R) and its ligands lymphotoxin  $\beta$  (LT $\beta$ ) and LIGHT were recently shown to have an important role in the maintenance of the thymic architecture (53,55). Expression of LT $\beta$ R is found on mTEC, whereas LT $\beta$  is expressed by medullary thymocytes (53). Mice lacking functional LT $\beta$ R display a reduction in the number of mTEC, with those cells that persist existing as small isolated clusters instead of the organized network of epithelial cells typical of a normal medulla (53). Both LT $\beta$  and LT $\beta$ R deficient mice exhibit down-regulation of *Aire* expression in mTEC and develop autoimmune diseases (55), further indicating that this pathway is involved in the correct development of the medulla. In addition, the medulla of LT $\beta$ R<sup>-/-</sup> mice retains increased numbers of mature CD4<sup>+</sup> and CD8<sup>+</sup> thymocytes, which themselves display upregulated expression of LT $\beta$  (53). Thus, the LT $\beta$ R–LT $\beta$  interaction may operate in a regulatory loop and have a role in the export of functionally mature thymocytes.

### 2.3. Molecular Regulation of Thymus Development

Current understanding of the molecular mechanisms that govern the early stages of thymus organogenesis has come primarily from analysis of mice carrying classical or engineered mutations. The key molecules (see Fig. 4) identified via these studies are reviewed below.

#### 2.3.1. Transcription Factors

##### 2.3.1.1. TBX1

*Tbx1* is a T-box related transcription factor and is expressed from E7.5 to E12.5 in a variety of structures during development, including the pharyngeal

---

Fig. 4. (Continued) (pink), whereas the ventral region expresses *Bmp4* (blue), which is also expressed by the surrounding neural crest cells and the ectoderm of the 3pc. (D) E11.5—the ventral thymus domain expresses the transcription factor *Foxn1* (light blue), which is required for the continued development of thymic epithelial cells (TEC). The dorsal parathyroid region expresses *Gcm2* (pink). Communication between the 3pp and the surrounding neural crest cells (yellow nucleated polygons) continues via soluble factors including BMP4. (E) E12.5—differentiating TEC maintain expression of *Foxn1* (light blue) and proliferate, mediated in part by FGF7 and FGF10 (purple) secreted by the neural crest capsule surrounding the thymic epithelium.

endoderm and the core mesenchyme of the pharyngeal arches (107–109). The role of *Tbx1* in thymus organogenesis became apparent through analysis of *Dfl* mice, which carry a deletion of chromosome 16 (110): these mice were generated in an attempt to mimic a human disease known as 22q11.2 deletion syndrome (22q11.2DS—also known as DiGeorge syndrome) in which a large portion (usually 3 Mb) of chromosome 22 is deleted resulting in the loss of approx 30 genes (111). Mice heterozygous for the deletion (*Dfl*<sup>+/-</sup>) closely phenocopy 22q11.2DS, developing aortic arch defects, thymus and parathyroid hypoplasia, and neurobehavioral abnormalities (112,113), and further analysis identified *Tbx1* as the gene responsible for the cardiovascular and thymus phenotypes (114–116).

Lack of functional *Tbx1* results in severe defects in the pharyngeal region, with abnormal patterning of the first pharyngeal arch, hypoplasia of the second arch and absence of the third, fourth, and sixth arches and pouches (114). As a result of this, *Tbx1* has been suggested to play a role in the segmentation and development of the whole pharyngeal region. Not surprisingly, *Tbx1*<sup>-/-</sup> mutants display thymus and parathyroid aplasia, as well as a spectrum of cardiovascular abnormalities and craniofacial defects (114). However, *Tbx1* is haploinsufficient with respect to thymus development (115), suggesting an additional direct effect on thymus organogenesis. In keeping with this, an elegant study has recently addressed the temporal requirement for *Tbx1* in pharyngeal region development (117). These data indicate that the requirement for *Tbx1* in thymus organogenesis is most critical during formation of the third pharyngeal pouch, as deletion of functional *Tbx1* at E8.5 results in athymia as a result of defective third pouch formation. Fate mapping experiments presented in the same study indicate that cells that express *Tbx1* at E8.5 contribute significantly to the thymic primordium (117). *Tbx1* may also have a later role in thymus organogenesis, because deletion of functional *Tbx1* at E9.5/E10.5 results in morphological defects, albeit not as severe as the aplasia observed following deletion at E8.5 (117). However, as labeling of *Tbx1* expressing cells at around E9.5/E10.5 reveals a limited but consistent contribution to the thymus, it is likely that this effect is nonautonomous.

The function of *Tbx1* at a cellular level is unknown, although given that *Fgf10* and possibly *Fgf8* are *Tbx1* targets, it is possible that induction or maintenance of proliferation may be one mechanism by which it mediates its effects. In keeping with this idea, in the absence of *Tbx1* the pharyngeal endoderm shows reduced levels of proliferation (117).

### 2.3.1.2. *HoxA3*

*Hoxa3*, a member of the homeobox family of transcription factors that specify lineage identity (118), is also essential for thymus development. *Hoxa3*<sup>-/-</sup> mutants show multiple pharyngeal defects, including athymia, absence of

parathyroid glands, thyroid hypoplasia, and defects in ultimobranchial body migration (119,120). In the mouse embryo, *Hoxa3* is expressed from E9.5 in the endoderm of the third and fourth pharyngeal pouches, the NCC of the pharyngeal arches and the premigratory and migratory NCC of rhombomeres 4–6 (119,120). Initiation of overt thymus formation fails in *Hoxa3*<sup>-/-</sup> mutants. However, because *Hoxa3* is expressed in several tissues in the pharyngeal region it is unclear whether this phenotype results from an endoderm autonomous effect. *Hoxa3* also regulates the migration of the thymus/parathyroid primordia, because although *Hoxb3*<sup>-/-</sup>, *Hoxd3*<sup>-/-</sup>, and *Hoxb3*<sup>-/-</sup>*d3*<sup>-/-</sup> double mutants show no defects in thymus organogenesis, migration of the thymic primordia is impaired in *Hoxa3*<sup>+/-</sup>*b3*<sup>-/-</sup>*d3*<sup>-/-</sup> mice (119).

#### 2.3.1.3. *PAX1* AND *PAX9*

*Pax1* and *Pax9* are closely related members of the paired box family of transcription factors and are expressed in the pharyngeal endoderm from E8.5, and the third pharyngeal pouch from approximately E9.5 (121,122). *Pax1*<sup>-/-</sup> mice exhibit relatively mild thymus hypoplasia, resulting from reduced thymocyte numbers (122). This defect is likely to be owing to aberrant differentiation of thymic epithelial cells, because both the number of MHC class II<sup>+</sup> TEC and the level at which MHC class II is expressed are reduced in *Pax1*<sup>-/-</sup> animals (123,124). Mice deficient in *Pax9* show a more severe phenotype: initiation of thymus organogenesis occurs in these mice but the primordia fail to migrate to the mediastinum and from E14.5 onward, the *Pax9*<sup>-/-</sup> thymus is severely reduced in size, although it is vascularized and contains lymphocytes (125).

The observation that *Pax1* and *Pax9* expression is initiated in *Hoxa3*<sup>-/-</sup> mice but is not maintained at wildtype levels after E10.5 (120) indicates that *Hoxa3*, *Pax1*, and *Pax9* operate in synergy during early stages of thymus organogenesis. In keeping with this, *Hoxa3*<sup>+/-</sup>*Pax1*<sup>-/-</sup> compound mutants (124) show delayed separation of the common thymus/parathyroid primordium from the pharynx, leading to thymic ectopia, and exhibit a more severe thymic hypoplasia than that seen in *Pax1*<sup>-/-</sup> single mutants as a result of reduced proliferation and increased apoptosis of the thymic epithelium (124). In addition, these mutants show a complete lack of parathyroid glands. An interesting feature of the *Hoxa3*<sup>+/-</sup>*Pax1*<sup>-/-</sup> compound mutants is that they reveal a role for *Pax1* in the migration of the thymus/parathyroid primordium, a function not apparent in *Pax1*<sup>-/-</sup> single mutants. The fact that single mutants do not show this phenotype may indicate functional redundancy between *Pax1* and *Pax9* genes during early thymus organogenesis.

#### 2.3.1.4. *EYA1* AND *SIX1*

*Eya1*, the mouse homolog of the *Drosophila* gene *Eyes Absent* (126), is expressed in the second to fourth pharyngeal pouch endoderm, NCC and the



third and fourth pharyngeal cleft ectoderm between E9.5 and E10.5 (127). Both thymus and parathyroid primordia are absent in *Eya1*<sup>-/-</sup> embryos at E12.5 (127) and, in addition, there is general hypoplasia of the pharyngeal pouch endoderm (127). As with *Hoxa3*, the fact that *Eya1* is expressed in cells derived from multiple germ layers complicates interpretation of the null phenotype. However, although *Hoxa3*, *Pax1*, and *Pax9* expression are not detectably altered in endoderm or NCC prior to budding and outgrowth of the thymus, *Eya1*<sup>-/-</sup> embryos show reduced expression of *sine oculis 1* (*Six1*) in the third and fourth pouch endoderm and surface ectoderm of the second, third, and fourth pharyngeal arches (127). *Six1*, a transcriptional regulator often coexpressed with *Eya1* (128,129), has been shown to regulate proliferation and survival of precursor populations during the development of other organs including the kidney, and seems to act in a pathway involving *Eya1* and *Dach1* (130). The relationship between *Eya1* and *Six1* has recently been elucidated to some degree by Zi and colleagues (130), who demonstrate that *Eya1* has an intrinsic phosphatase activity and acts to convert *Six1* from a transcriptional repressor (a function promoted by *Dach1*) to a transcriptional activator (130).

Taken together, these data indicate that a genetic network including *Hoxa3/Pax1/Pax9/Eya1/Six1* operates during early thymus organogenesis to regulate initiation and migration of the thymic primordia, reminiscent of the *Pax-Eya-Six* cascade that operates in *Drosophila* to control proliferation and patterning of the eye (131). Interpretation of the indicated phenotypes is complicated by the fact that *Hoxa3*, *Eya1*, and *Six1* are all expressed in ectoderm and NCC as well as the endoderm. However, in the pharyngeal region, *Pax1* and *Pax9* are expressed exclusively in the endoderm and, therefore, if the *Pax-Eya-Six* regulatory network is conserved in the vertebrate thymus, it must act specifically in this germ layer.

#### 2.3.1.5. PAX3

*Pax3* encodes a transcription factor essential for the survival and migration of NCC (132,133). Mice that are homozygous for the mutant *Splotch* allele of *Pax3* have severe NCC defects and die by approximately E12.5 owing to malformation of the cardiac outflow tract. Although thymus organogenesis is reportedly impaired in *Splotch* mutants (reviewed in ref. 134), recent re-examination has revealed that *Pax3*<sup>Sp/Sp</sup> mice actually develop a large, albeit ectopic thymus rudiment due to a relative increase in the thymus-fated domain of the shared thymus/parathyroid primordium. This finding suggests that NCC cells play a previously unappreciated role in patterning the third pouch endoderm (E. Richie, manuscript in preparation).

### 2.3.1.6. *FOXP1* AND *GCM2*

The transcription factor *Foxn1*, a member of the forkhead family of transcription factors, is the gene mutated in the classical mouse mutant *nude* and as such is a central regulator of thymus organogenesis (135). The pleiotropic *nude* phenotype is characterised by congenital athymia and hairlessness. Thymus organogenesis is correctly initiated in *nude* mice and proceeds normally until E11.5–E12.0 (63,136,137). However, lymphocyte precursors fail to enter the thymic primordium and instead remain in the surrounding perithymic mesenchyme (138). In addition, the epithelial cells within the primordium fail to expand after E12.5 and vascularization of the primordium does not occur (138). A small, alymphoid thymic rudiment persists into adulthood resulting in a lack of functional T cells and severe immunodeficiency.

During development, *Foxn1* is expressed in the ventral posterior aspect of the third pharyngeal pouch endoderm from approximately E11.25 (137), although transcripts can be detected as early as E10.5 by RT-PCR (139). *Foxn1* is subsequently expressed in the thymic epithelium throughout development and into adulthood (140) and, in addition, is expressed in the epidermis and hair follicle, where it affects hair growth (141). Current data suggest that *Foxn1* acts in a separate genetic pathway to the *Hox/Pax/Eya/Six* cascade described above, as *Foxn1* expression appears unaffected in *Pax9*<sup>-/-</sup> mice (125) and in *Hoxa3*<sup>+/-</sup>*Pax1*<sup>-/-</sup> compound mutants (123).

*Gcm2* is a parathyroid specific transcription factor whose expression is initiated in the dorsal region of the third pouch endoderm from E9.5 onward. The absence of *Gcm2* results in a lack of parathyroids, although thymus development is completely normal. *Gcm2* expression is downregulated in *Hoxa3*<sup>-/-</sup> (73) and *Eya1*<sup>-/-</sup> embryos (127) and in *Hoxa3*<sup>+/-</sup>*Pax1*<sup>-/-</sup> compound mutants (124), indicating that it operates downstream of these transcription factors.

The roles of *Foxn1* and *Gcm2* in the specification of the thymus and parathyroid are not fully elucidated. *Foxn1* is unlikely to specify thymic epithelial identity. However, *Gcm2* may be the determining factor for parathyroid development, as *Gcm2*<sup>-/-</sup> embryos lack these structures but display completely normal thymus formation (142). Thymus may thus represent the default pathway for this region, with *Gcm2* expression overriding this pathway to allow parathyroid development. Alternatively, as yet unknown gene/genes may act upstream of *Foxn1* to actively specify thymus identity.

### 2.3.2. The Role of *Foxn1* in Thymic Epithelial Development

Once the rudimentary thymus primordium has formed, further development of all subtypes of thymic epithelial cell is dependent on the cell-autonomous



action of *Foxn1* (76). Precisely how *Foxn1* regulates the development of the thymic epithelium is not clear. Studies examining the *nude* phenotype in the epidermis suggest that in this tissue *Foxn1* regulates the balance between epithelial proliferation and terminal differentiation, as keratinocytes from *Foxn1*<sup>-/-</sup> mice express markers associated with terminal differentiation, whereas when *Foxn1* is overexpressed, markers associated with earlier stages of differentiation are upregulated and later markers are absent (143). A more recent publication found that transient expression of *Foxn1* in primary human epidermal keratinocytes initiated terminal differentiation, but end stage maturation was dependent on activated *Akt* (144). In this in vitro system, the levels of activated *Akt* appeared to be regulated by *Foxn1* (144). Thus, in the case of the epidermis, *Foxn1* may act to regulate the correct program of events required for the terminal differentiation of keratinocytes.

Some evidence suggests that in the thymus, *Foxn1* may be involved in cross-talk between the epithelium and the lymphoid cells seeding the thymus from the circulation (145,146). Support for this idea comes from comparative gene expression profiling of *Foxn1*<sup>-/-</sup> and wild-type embryos (145). One of the genes found to be downregulated in *nude* embryos was PD-1 ligand, whose receptor is expressed on TN thymocytes and has been implicated in thymocyte survival, proliferation, and positive selection (147,148). In addition, a recent paper found that a splice variant lacking the N-terminal domain of *Foxn1*, caused by a targeted insertion into exon 3, lead to a thymus specific defect in which epithelial development was delayed and suspended at a stage equivalent to E13.5 in wild-type embryos (146). The thymus in postnatal mice of this strain (designated *Foxn1*<sup>ΔΔ</sup>) was hypoplastic and contained epithelial cells that predominantly expressed both K5 and K8, a profile usually restricted to epithelial precursors and cells residing at the corticomedullary junction (17). In addition, no organized cortical or medullary regions were present, and there was a postnatal defect in thymocyte differentiation, although some T-cell development occurred. Because the stromal phenotype of these mice resembled that seen in mice sustaining early blocks in T-cell development, such as *hCD3ε26tg* or *Ikaros*<sup>-/-</sup> mice (i.e., predominance of K5<sup>+</sup>K8<sup>+</sup> TEC) (17,67), it was suggested that the N-terminal domain of *Foxn1* was required for lympho-stromal interactions necessary for the correct development of the thymus. However, the block in TEC differentiation was distinct from those observed in *hCD3ε 26tg* or *Ikaros*<sup>-/-</sup> mice, as TEC in the *Foxn1* hypomorphs show delayed expression of K5 during ontogeny, an effect not observed in mice sustaining developmental blocks in T-cell development (67). *Foxn1*<sup>ΔΔ</sup> mice also retained a reticular network of epithelial cells into adulthood, whereas *hCD3ε 26tg* mice revert to a nonreticular epithelial structure (17,78), suggesting that *Foxn1*<sup>ΔΔ</sup> TEC may be competent to participate in cross-talk. It is therefore unclear at present if *Foxn1* has a direct

role in lympho-stromal crosstalk or if the defects observed are a downstream consequence of aberrant differentiation of the epithelium.

#### **2.4. Signaling Molecules and Thymus Organogenesis**

Secreted factors play an important role in many organ systems during development. As with many other organs, bone morphogenic proteins (Bmps), fibroblast growth factors (Fgfs), wingless (Wnt), retinoic acid (RA), and the secreted glycoprotein sonic hedgehog homolog (Shh) all have apparent roles in thymus organogenesis.

##### *2.4.1. Bone Morphogenetic Proteins*

Bmps are members of the TGF- $\beta$  superfamily and act as morphogens in the development of many organ systems. During thymus organogenesis *Bmp4* shows a spatially and temporally dynamic expression pattern. At E9.5, expression is restricted to a small number of mesenchymal cells in the third pharyngeal arch and is absent from the third pouch endoderm and third cleft ectoderm. However, by E10.5 *Bmp4* expression is evident in the ventral aspect of the third pouch endoderm and the adjacent mesenchyme—but is absent from the anterior dorsal domain. This pattern is maintained in the third pouch at E11.5, and by E12.5 *Bmp4* expression is evident throughout the primordium and the surrounding mesenchymal capsule (149). This expression pattern suggests that *Bmp4* may be involved in specifying thymus identity in the ventral posterior domain of the third pouch. *Foxn1* is expressed in this region at approximately E11.25 and some *in vitro* evidence suggests that *Bmp4* may induce *Foxn1* expression in TEC (150). In keeping with this, the expression pattern of the Bmp inhibitor *Noggin* is restricted to the dorsal anterior aspect of the third pouch at both E10.5 and E11.5, in a complementary domain to *Bmp4* expression. *Noggin* may therefore allow specification of the *Gcm2*<sup>+</sup> parathyroid domain by inhibiting *Bmp4* expression in this region.

Direct *in vivo* evidence for a role of BMP4 in the development of the thymic stroma has been provided through analysis of a transgenic mouse in which *Noggin* expression is driven by the *Foxn1* promoter. These mice develop hypoplastic and cystic thymi, which fail to migrate to their normal position above the heart (151), apparently as a direct outcome of impaired Bmp signaling in the stroma, as defects are evident prior to the entry of lymphocytes and thymocyte development is unperturbed. The underlying mechanism is likely to concern epithelial/mesenchymal communication, because downstream mediators of Bmp signaling such as phosphorylated Smad proteins and the transcription factor *Msx1* are absent in both TEC and mesenchymal cells. Interestingly, the expression of *Foxn1* in these mice appears normal, at least when determined by *in situ* hybridisation, in apparent contradiction to reports that BMP4 regulates

*Foxn1* expression. However, as *Noggin* expression and therefore inhibition of BMP signaling, is driven by the *Foxn1* promoter, these data do not rule out a role for BMP4 in the initiation of *Foxn1* expression.

#### 2.4.2. Fibroblast Growth Factors

Fgfs are a family of approx 19 growth factors that can have both mitogenic and differentiative effects. Convincing evidence implicates some members of the Fgf family in development of the thymic stroma. *Fgf8* is expressed in the early gut endoderm and also in the endoderm and ectoderm of the pharyngeal region. Mice that express hypomorphic alleles of *Fgf8* show a consistent defect in thymus and parathyroid development, presenting as a spectrum ranging from thymic hypoplasia to aplasia in the most severe cases (152,153). This is part of a more complex phenotype, characterized by earlier defects in the development of the pharyngeal region, including hypoplastic first and second pharyngeal arches, abnormal ectodermal clefts, and severe hypoplasia/aplasia of the third and fourth pharyngeal arches and pouch endoderm (152,153). The phenotype of *Fgf8* hypomorphs closely resembles that of a spectrum of abnormalities found in experimental NCC ablation (88,154), suggesting that the glandular defects caused by *Fgf8* hypomorphs may result from a direct effect on NCC. In keeping with this hypothesis, NCC in E9.5 and E10.5 *Fgf8* hypomorphs show increased levels of apoptosis (152,153) and express reduced levels of *Fgf10* (153), a factor that may act on the epithelia of the pharyngeal endoderm (153). Whether the reduction in *Fgf10* expression is a consequence of the increased apoptosis of NCC or reflects aberrant differentiation of these cells is unclear. The migration and specification of NCC in E9.5 *Fgf8* hypomorphs appears normal with respect to *Crabp1* and *Ap2a* expression (155,156). However, a mild reduction in these factors is apparent at E10.5 (152), suggesting that the maintenance of NCC is perturbed. Thus, *Fgf8* secreted by the endoderm may act as a NCC survival/differentiation factor.

Analysis of a conditional allele of *Fgf8* has begun to delineate its role in different expression domains. Ectodermal *Fgf8* expression was ablated from the 10 somite stage (10ss) by utilizing double transgenic *Fgf8<sup>GFP</sup>/Ap2aIRESCre* mice. In these mice, *Cre* expression driven by the *Ap2a* promoter results in ectodermal ablation of *Fgf8* and concomitant activation of a green fluorescent protein (GFP) reporter. Endodermal and ectodermal ablation was achieved by utilizing *Fgf8<sup>GFP</sup>/Hoxa3IRESCre* mice, which carry the same conditional *Fgf8* allele but express *Cre* under control of the *Hoxa3* promoter and, thus, in the ectoderm of pharyngeal arches 1–3 and the endoderm of the third pharyngeal pouches. Ectoderm-specific ablation resulted in vascular and craniofacial defects, as seen in the global hypomorphs, however no pharyngeal glandular abnormalities were observed (157). Endodermal/ectodermal ablation gave rise

to thymus and parathyroid hypoplasia and ectopy, in addition to the vascular defects seen in *Fgf8* hypomorphs (157). The observed differences between ectodermal only and endodermal and ectodermal ablation of *Fgf8* function could not be ascribed to differential effects on migrating NCC, as the same defects were seen in both situations (157). This suggested that endodermally derived *Fgf8* had a specific effect on the development of the thymus and parathyroids. However, because of the combined ectodermal and endodermal ablation, it was unclear if the phenotypic differences described were due to tissue-specific requirements of *Fgf8* or if they reflected a dosage or range effect. Despite this, it is interesting that the defects in thymus formation resulting from ectodermal/endodermal *Fgf8* ablation do not approach the same severity seen in the hypomorphic mutants, which frequently display bilateral thymic and parathyroid aplasia. A possible explanation for this may be that the globally reduced levels of *Fgf8* in hypomorphic mutants affects endoderm development earlier than the *Hoxa3* driven endodermal ablation, which occurs from E9.5 (157).

Two other members of the *Fgf* family, *Fgf7* and *Fgf10*, also affect thymus development, although at a later stage of organogenesis. An in vitro study performed on E12 and E14 fetal thymic lobes suggested that *Fgf7* and *Fgf10*, which are expressed by the perithymic mesenchyme, stimulate the proliferation of epithelial precursors (158), resulting in the expansion of these cells. This study also inferred that although these factors were required for epithelial growth, they were not essential for epithelial differentiation, as this occurred in the absence of mesenchyme or exogenous *Fgf7/10*. In a separate study, administration of *Fgf7* to thymocyte depleted E16 lobes resulted in expansion of medullary epithelial cells, as well as increased expression of the chemokines macrophage-derived chemokine (MDC) and Epstein–Barr virus-induced molecule-1 induced ligand chemokine (ELC) (105), which are normally expressed in this compartment (159).

Mice null for *FgfR2IIIb*, the receptor for *Fgf7* and *Fgf10*, display severe thymic hypoplasia, although they are able to support T-cell differentiation (89). TEC differentiation is reported to occur in these mice, although a detailed study has not been presented. A similar degree of thymic hypoplasia is also seen in *Fgf10*<sup>-/-</sup> deficient mice (89), although the *Fgf7* signaling pathway is still functional in these animals. Thus, *Fgf10* may be the primary ligand for *FgfR2IIIb* during the development of the thymus.

#### 2.4.3. Retinoic Acid

A role for RA signaling in thymus development has been demonstrated in experiments investigating the effect of a RA antagonist on embryo development in in vitro culture (160). In this system, blockade of RA signal transduction at E8.0 led to abnormalities in the caudal pharyngeal region, including the absence of *Fgf8* and *Fgf3* expression in the third pouch endoderm. In addition,

*Pax9*, which is normally expressed in the endoderm of the first to fourth pharyngeal pouches between E9.5 and E10.5 (121), showed a much broader pattern of expression in the second pouch endoderm and an absence in the third pouch endoderm, and NCC appeared to migrate predominantly to the first and second branchial arches, by-passing the third and fourth arches completely. These data suggest that in the absence of appropriate RA signaling, the pharyngeal endoderm is not specified correctly and is not capable of initiating/supporting correct NCC migration into the caudal pharyngeal region. Disrupted RA signaling had differential effects on the first and second vs the third and fourth branchial arches, as development of the second branchial arch and pouch endoderm appeared to be enhanced, whereas development of the third and fourth branchial arches and pouches was severely disrupted. A role for retinoid signaling in thymus organogenesis was also revealed through analysis of fetal mice that are null for the  $\alpha$  and  $\beta$  retinoic acid receptors, which display thymus agenesis and ectopia despite retaining functional retinoic acid receptors- $\gamma$  (161).

#### 2.4.4. Sonic Hedgehog

Shh is a secreted glycoprotein expressed by many signaling centers during development. Functionally, Shh acts as a morphogen and can act over 80- to 300- $\mu\text{m}$  distances depending on the tissue. In the pharyngeal region, *Shh* is differentially expressed between the anterior and posterior pharyngeal arches. At E9.5 *Shh* is expressed in both the dorsal and ventral endoderm, but is absent from the first, second, and third pouches (33). By E10.5, the expression domain is expanded to include the first and second pouches, although the distal tips of these pouches do not express *Shh* (33) and at this stage, only the openings of the third and fourth pouches express *Shh* (33). At E11.5 *Shh* expression is expanded further into the first and second pouches but is still absent from the third and fourth pouches. *Patched 1*, the receptor for *Shh*, is expressed in the endoderm and mesenchyme in close proximity to the Shh expressing region (33).

The role of *Shh* in thymus organogenesis has been relatively difficult to determine because *Shh*<sup>-/-</sup> embryos have a severe phenotype affecting a number of organ systems. However, careful analysis of *Shh*<sup>-/-</sup> mutants has indicated that in the third pouch endoderm, *Shh* signaling is required for the correct specification of the thymus and parathyroid domains, as in the absence of *Shh*, *Bmp4* expression in the third pouch is expanded, resulting in expansion of the *Foxn1* expression domain and corresponding loss of *Gcm2* expression (33). Thus, in the absence of *Shh*, the entire third pouch adopts thymus identity and the parathyroids are absent, suggesting that in the pharyngeal region, *Shh* opposes BMP4 signaling to allow specification of the parathyroid lineage.

#### 2.4.5. Wnts

Wnts are a large family of secreted glycoproteins and regulate many aspects of cellular development including fate specification, migration, proliferation, polarity, and death. *Wnt1*, *Wnt4*, *Wnt5b*, and *Wnt10b* are expressed in the thymus by both stromal and lymphoid cells, although Wnt receptors appear to be exclusively expressed by TEC (139). The earliest stage at which *Wnt* expression can be detected is E10.5, when the epithelium of the third pharyngeal pouch and adjacent cells express *Wnt4* (139). A possible function of Wnt signaling in TEC may be to regulate *Foxn1* expression, as overexpression of *Wnt* in a cTEC line results in increased *Foxn1* expression (139).

### 3. Conclusion

The data discussed above indicate a network of transcription factors and signaling molecules that regulate thymus organogenesis (see Fig. 4). Although all of these factors are required for the formation of a fully functional thymus, many issues regarding the regulation of thymus organogenesis are unresolved. Notably, the molecular pathways controlling specification and patterning of thymic epithelial lineage cells have not been fully elucidated: in particular, improved understanding of the initiation and maintenance of *Foxn1* expression, and the role of *Foxn1* in regulating proliferation, differentiation, and/or maintenance of the different TEC subtypes is urgently required. In addition, a clear understanding of the lineage relationships within the thymic epithelium, and of the mechanism by which the TEC subtypes are generated and maintained in homeostasis, will be crucial for the development of regenerative or cell replacement strategies for clinical enhancement of thymus function.

*Note added in proof:* Evidence of a cervical thymus in mice has been published in the following papers. Cervical thymus in the mouse. *J. Immunol.* 2006, Jan 1; **176**(11): 648–690; Evidence for a function second thymus in mice. *Science* 2006, Apr. 14; **312**(5771): 284–287.

### Acknowledgments

The authors wish to thank Julie Sheridan and Lucy Morris for helpful discussions, Ellen Richie (University of Texas MD Anderson Cancer Center), and Andy Farr (University of Washington, Seattle, WA) for sharing unpublished data. Blackburn, C. C., Farley, A. M., and Nowell, C. S. are supported by the Leukaemia Research Fund, the MRC, and by the European Union FP6 integrated project “EuroStemCell.”



## References

1. Boyd, R. L., Tucek, C. L., Godfrey, D. I., et al. (1993) The thymic microenvironment. *Immunol. Today* **14**, 445–459.
2. van Ewijk, W., Shores, E. W., and Singer, A. (1994) Crosstalk in the mouse thymus. *Immunol. Today* **15**, 214–217.
3. Van Vliet, E., Jenkinson, E. J., Kingston, R., Owen, J. J., and Van Ewijk, W. (1985) Stromal cell types in the developing thymus of the normal and nude mouse embryo. *Eur. J. Immunol.* **15**, 675–681.
4. Lind, E. F., Prockop, S. E., Porritt, H. E., and Petrie, H. T. (2001) Mapping precursor movement through the postnatal thymus reveals specific microenvironments supporting defined stages of early lymphoid development. *J. Exp. Med.* **194**, 127–134.
5. van de Wijngaert, F. P., Rademakers, L. H., Schuurman, H. J., de Weger, R. A., and Kater, L. (1983) Identification and in situ localization of the “thymic nurse cell” in man. *J. Immunol.* **130**, 2348–2351.
6. Brekelmans, P. and van Ewijk, W. (1990) Phenotypic characterization of murine thymic microenvironments. *Semin. Immunol.* **2**, 13–24.
7. Boyd, R. L., Wilson, T. J., Bean, A. G., Ward, H. A., and Gershwin, M. E. (1992) Phenotypic characterization of chicken thymic stromal elements. *Dev. Immunol.* **2**, 51–66.
8. Godfrey, D. I., Izon, D. J., Tucek, C. L., Wilson, T. J., and Boyd, R. L. (1990) The phenotypic heterogeneity of mouse thymic stromal cells. *Immunol.* **70**, 66–74.
9. van de Wijngaert, F. P., Kendall, M. D., Schuurman, H. J., Rademakers, L. H., and Kater, L. (1984) Heterogeneity of epithelial cells in the human thymus. An ultrastructural study. *Cell Tissue Res.* **237**, 227–237.
10. Wekerle, H. and Ketelsen, U. P. (1980) Thymic nurse cells—Ia-bearing epithelium involved in T-lymphocyte differentiation? *Nature* **283**, 402–404.
11. Wekerle, H., Ketelsen, U. P., and Ernst, M. (1980) Thymic nurse cells. Lymphoepithelial cell complexes in murine thymuses: morphological and serological characterization. *J. Exp. Med.* **151**, 925–944.
12. von Gaudecker, B., Steinmann, G. G., Hansmann, M. L., Harpprecht, J., Milicevic, N. M., and Muller-Hermelink, H. K. (1986) Immunohistochemical characterization of the thymic microenvironment. A light-microscopic and ultrastructural immunocytochemical study. *Cell Tissue Res.* **244**, 403–412.
13. Bofill, M., Janossy, G., Willcox, N., Chilosi, M., Trejdosiewicz, L. K., and Newsom-Davis, J. (1985) Microenvironments in the normal thymus and the thymus in myasthenia gravis. *Am. J. Pathol.* **119**, 462–473.
14. Surh, C. D., Gao, E. K., Kosaka, H., et al. (1992) Two subsets of epithelial cells in the thymic medulla. *J. Exp. Med.* **176**, 495–505.
15. Farr, A. G. and Nakane, P. K. (1983) Cells bearing Ia antigens in the murine thymus. An ultrastructural study. *Am. J. Pathol.* **111**, 88–97.
16. Jenkinson, E. J., Van Ewijk, W., and Owen, J. J. (1981) Major histocompatibility complex antigen expression on the epithelium of the developing thymus in normal and nude mice. *J. Exp. Med.* **153**, 280–292.

17. Klug, D. B., Carter, C., Crouch, E., Roop, D., Conti, C. J., and Richie, E. R. (1998) Interdependence of cortical thymic epithelial cell differentiation and T-lineage commitment. *Proc. Natl. Acad. Sci. USA* **95**, 11,822–11,827.
18. Duijvestijn, A. M. and Hoefsmit, E. C. (1981) Ultrastructure of the rat thymus: the micro-environment of T-lymphocyte maturation. *Cell Tissue Res.* **218**, 279–292.
19. Milicevic, N. M., Milicevic, Z., Colic, M., and Mujovic, S. (1987) Ultrastructural study of macrophages in the rat thymus, with special reference to the cortico-medullary zone. *J. Anat.* **150**, 89–98.
20. Cardarelli, P. M., Crispe, I. N., and Pierschbacher, M. D. (1988) Preferential expression of fibronectin receptors on immature thymocytes. *J. Cell Biol.* **106**, 2183–2190.
21. Cardarelli, P. M. and Pierschbacher, M. D. (1986) T-lymphocyte differentiation and the extracellular matrix: identification of a thymocyte subset that attaches specifically to fibronectin. *Proc. Natl. Acad. Sci. USA* **83**, 2647–2651.
22. Schreiber, L., Eshel, I., Meilin, A., Sharabi, Y., and Shoham, J. (1991) Analysis of thymic stromal cell subpopulations grown in vitro on extracellular matrix in defined medium. III. Growth conditions of human thymic epithelial cells and immunomodulatory activities in their culture supernatant. *Immunol.* **74**, 621–629.
23. Watt, S. M., Thomas, J. A., Murdoch, S. J., Kearney, L., Chang, S. E., and Bartek, J. (1991) Human thymic epithelial cells are frequently transformed by retroviral vectors encoding simian virus 40. *Cell. Immunol.* **138**, 456–472.
24. Anderson, G., Anderson, K. L., Tchilian, E. Z., Owen, J. J., and Jenkinson, E. J. (1997) Fibroblast dependency during early thymocyte development maps to the CD25+ CD44+ stage and involves interactions with fibroblast matrix molecules. *Eur. J. Immunol.* **27**, 1200–1206.
25. Boyd, R. L. and Hugo, P. (1991) Towards an integrated view of thymopoiesis. *Immunol. Today* **12**, 71–79.
26. Savino, W., Villa-Verde, D. M. and Lannes-Vieira, J. (1993) Extracellular matrix proteins in intrathymic T-cell migration and differentiation? *Immunol. Today* **14**, 158–161.
27. Watt, S. M., Thomas, J. A., Edwards, A. J., Murdoch, S. J., and Horton, M. A. (1992) Adhesion receptors are differentially expressed on developing thymocytes and epithelium in human thymus. *Exp. Hematol.* **20**, 1101–1111.
28. Plotkin, J., Prockop, S. E., Lepique, A., and Petrie, H. T. (2003) Critical role for CXCR4 signaling in progenitor localization and T cell differentiation in the post-natal thymus. *J. Immunol.* **171**, 4521–4527.
29. Anderson, G., Owen, J. J., Moore, N. C., and Jenkinson, E. J. (1994) Thymic epithelial cells provide unique signals for positive selection of CD4+CD8+ thymocytes in vitro. *J. Exp. Med.* **179**, 2027–2031.
30. Ge, Q. and Chen, W. F. (2000) Effect of murine thymic epithelial cell line (MTEC1) on the functional expression of CD4(+)CD8(-) thymocyte subgroups. *Int. Immunol.* **12**, 1127–1133.
31. Moore, N. C., Anderson, G., Smith, C. A., Owen, J. J., and Jenkinson, E. J. (1993) Analysis of cytokine gene expression in subpopulations of freshly isolated thy-



- mocytes and thymic stromal cells using semiquantitative polymerase chain reaction. *Eur. J. Immunol.* **23**, 922–927.
32. Hare, K. J., Jenkinson, E. J., and Anderson, G. (2000) An essential role for the IL-7 receptor during intrathymic expansion of the positively selected neonatal T cell repertoire. *J. Immunol.* **165**, 2410–2414.
  33. Zamisch, M., Moore-Scott, B., Su, D. M., Lucas, P. J., Manley, N., and Richie, E. R. (2005) Ontogeny and regulation of IL-7-expressing thymic epithelial cells. *J. Immunol.* **174**, 60–67.
  34. von Freeden-Jeffry, U., Vieira, P., Lucian, L. A., McNeil, T., Burdach, S. E., and Murray, R. (1995) Lymphopenia in interleukin (IL)-7 gene-deleted mice identifies IL-7 as a nonredundant cytokine. *J. Exp. Med.* **181**, 1519–1526.
  35. Crompton, T., Outram, S. V., Buckland, J., and Owen, M. J. (1998) Distinct roles of the interleukin-7 receptor alpha chain in fetal and adult thymocyte development revealed by analysis of interleukin-7 receptor alpha-deficient mice. *Eur. J. Immunol.* **28**, 1859–1866.
  36. Zuniga-Pflucker, J. C., Di, J., and Lenardo, M. J. (1995) Requirement for TNF-alpha and IL-1 alpha in fetal thymocyte commitment and differentiation. *Science* **268**, 1906–1909.
  37. Savino, W., Mendes-da-Cruz, D. A., Silva, J. S., Dardenne, M., and Cotta-de-Almeida, V. (2002) Intrathymic T-cell migration: a combinatorial interplay of extracellular matrix and chemokines? *Trends Immunol.* **23**, 305–313.
  38. Misslitz, A., Pabst, O., Hintzen, G., Ohl, L., Kremmer, E., Petrie, H. T., and Forster, R. (2004) Thymic T cell development and progenitor localization depend on CCR7. *J. Exp. Med.* **200**, 481–491.
  39. Benz, C., Heinzl, K., and Bleul, C. C. (2004) Homing of immature thymocytes to the subcapsular microenvironment within the thymus is not an absolute requirement for T cell development. *Eur. J. Immunol.* **34**, 3652–3663.
  40. Cosgrove, D., Chan, S. H., Waltzinger, C., Benoist, C., and Mathis, D. (1992) The thymic compartment responsible for positive selection of CD4+ T cells. *Int. Immunol.* **4**, 707–710.
  41. Benoist, C. and Mathis, D. (1989) Positive selection of the T cell repertoire: where and when does it occur? *Cell* **58**, 1027–1033.
  42. Berg, L. J., Pullen, A. M., Fazekas de St. Groth, B., Mathis, D., Benoist, C., and Davis, M. M. (1989) Antigen/MHC-specific T cells are preferentially exported from the thymus in the presence of their MHC ligand. *Cell* **58**, 1035–1046.
  43. Wilson, A., MacDonald, H. R., and Radtke, F. (2001) Notch 1-deficient common lymphoid precursors adopt a B cell fate in the thymus. *J. Exp. Med.* **194**, 1003–1012.
  44. Radtke, F., Wilson, A., Stark, G., et al. (1999) Deficient T cell fate specification in mice with an induced inactivation of Notch1. *Immunity* **10**, 547–558.
  45. Harman, B. C., Jenkinson, E. J., and Anderson, G. (2003) Entry into the thymic microenvironment triggers Notch activation in the earliest migrant T cell progenitors. *J. Immunol.* **170**, 1299–1303.

46. Anderson, G., Pongracz, J., Parnell, S., and Jenkinson, E. J. (2001) Notch ligand-bearing thymic epithelial cells initiate and sustain Notch signaling in thymocytes independently of T cell receptor signaling. *Eur. J. Immunol.* **31**, 3349–3354.
47. Allman, D., Karnell, F. G., Punt, J. A., et al. (2001) Separation of Notch1 promoted lineage commitment and expansion/transformation in developing T cells. *J. Exp. Med.* **194**, 99–106.
48. Huang, E. Y., Gallegos, A. M., Richards, S. M., Lehar, S. M., and Bevan, M. J. (2003) Surface expression of Notch1 on thymocytes: correlation with the double-negative to double-positive transition. *J. Immunol.* **171**, 2296–2304.
49. Deftos, M. L., Huang, E., Ojala, E. W., Forbush, K. A., and Bevan, M. J. (2000) Notch1 signaling promotes the maturation of CD4 and CD8 SP thymocytes. *Immunity* **13**, 73–84.
50. Deftos, M. L., He, Y. W., Ojala, E. W., and Bevan, M. J. (1998) Correlating notch signaling with thymocyte maturation. *Immunity* **9**, 777–786.
51. Kyewski, B., Derbinski, J., Gotter, J., and Klein, L. (2002) Promiscuous gene expression and central T-cell tolerance: more than meets the eye. *Trends Immunol.* **23**, 364–371.
52. Gotter, J., Brors, B., Hergenbahn, M., and Kyewski, B. (2004) Medullary epithelial cells of the human thymus express a highly diverse selection of tissue-specific genes colocalized in chromosomal clusters. *J. Exp. Med.* **199**, 155–166.
53. Boehm, T., Scheu, S., Pfeffer, K., and Bleul, C. C. (2003) Thymic medullary epithelial cell differentiation, thymocyte emigration, and the control of autoimmunity require lympho-epithelial cross talk via LT $\beta$ R. *J. Exp. Med.* **198**, 757–769.
54. Anderson, M. S., Venanzi, E. S., Klein, L., et al. (2002) Projection of an immunological self shadow within the thymus by the aire protein. *Science* **298**, 1395–1401.
55. Chin, R. K., Lo, J. C., Kim, O., et al. (2003) Lymphotoxin pathway directs thymic Aire expression. *Nat. Immunol.* **4**, 1121–1127.
56. Gotter, J. and Kyewski, B. (2004) Regulating self-tolerance by deregulating gene expression. *Curr. Opin. Immunol.* **16**, 741–745.
57. Liston, A., Lesage, S., Wilson, J., Peltonen, L., and Goodnow, C. C. (2003) Aire regulates negative selection of organ-specific T cells. *Nat. Immunol.* **4**, 350–354.
58. Villasenor, J., Benoist, C., and Mathis, D. (2005) AIRE and APECED: molecular insights into an autoimmune disease. *Immunol. Rev.* **204**, 156–164.
59. Vogel, A., Liermann, H., Harms, A., Strassburg, C. P., Manns, M. P., and Obermayer-Straub, P. (2001) Autoimmune regulator AIRE: evidence for genetic differences between autoimmune hepatitis and hepatitis as part of the autoimmune polyglandular syndrome type 1. *Hepatology* **33**, 1047–1052.
60. Le Lievre, C. S. and Le Douarin, N. M. (1975) Mesenchymal derivatives of the neural crest: analysis of chimaeric quail and chick embryos. *J. Embryol. Exp. Morphol.* **34**, 125–154.
61. Jiang, X., Rowitch, D. H., Soriano, P., McMahon, A. P., and Sucov, H. M. (2000) Fate of the mammalian cardiac neural crest. *Development* **127**, 1607–1616.

62. Owen, J. J. and Ritter, M. A. (1969) Tissue interaction in the development of thymus lymphocytes. *J. Exp. Med.* **129**, 431–442.
63. Cordier, A. C. and Haumont, S. M. (1980) Development of thymus, parathyroids, and ultimobranchial bodies in NMRI and nude mice. *Am. J. Anat.* **157**, 227–263.
64. Jotereau, F., Heuze, F., Salomon-Vie, V., and Gascan, H. (1987) Cell kinetics in the fetal mouse thymus: precursor cell input, proliferation, and emigration. *J. Immunol.* **138**, 1026–1030.
65. Douagi, I., Andre, I., Ferraz, J. C., and Cumano, A. (2000) Characterization of T cell precursor activity in the murine fetal thymus: evidence for an input of T cell precursors between days 12 and 14 of gestation. *Eur. J. Immunol.* **30**, 2201–2210.
66. Bennett, A. R., Farley, A., Blair, N. F., Gordon, J., Sharp, L., and Blackburn, C. C. (2002) Identification and characterization of thymic epithelial progenitor cells. *Immunity* **16**, 803–814.
67. Klug, D. B., Carter, C., Gimenez-Conti, I. B., and Richie, E. R. (2002) Cutting edge: thymocyte-independent and thymocyte-dependent phases of epithelial patterning in the fetal thymus. *J. Immunol.* **169**, 2842–2845.
68. Jenkinson, W. E., Rossi, S. W., Jenkinson, E. J., and Anderson, G. (2005) Development of functional thymic epithelial cells occurs independently of lymphostromal interactions. *Mech. Dev.* **122**, 1294–1299.
69. Van Vliet, E., Melis, M., and Van Ewijk, W. (1984) Monoclonal antibodies to stromal cell types of the mouse thymus. *Eur. J. Immunol.* **14**, 524–529.
70. Cordier, A. C. and Heremans, J. F. (1975) Nude mouse embryo: ectodermal nature of the primordial thymic defect. *Scand. J. Immunol.* **4**, 193–196.
71. Le Douarin, N. M. and Jotereau, F. V. (1975) Tracing of cells of the avian thymus through embryonic life in interspecific chimeras. *J. Exp. Med.* **142**, 17–40.
72. Gordon, J., Wilson, V. A., Blair, N. F., et al. (2004) Functional evidence for a single endodermal origin for the thymic epithelium. *Nat. Immunol.* **5**, 546–553.
73. Blackburn, C. C. and Manley, N. R. (2004) Developing a new paradigm for thymus organogenesis. *Nat. Rev. Immunol.* **4**, 278–289.
74. Manley, N. R. and Blackburn, C. C. (2003) A developmental look at thymus organogenesis: where do the non-hematopoietic cells in the thymus come from? *Curr. Opin. Immunol.* **15**, 225–232.
75. Schluep, M., Willcox, N., Ritter, M. A., Newsom-Davis, J., Larche, M., and Brown, A. N. (1988) Myasthenia gravis thymus: clinical, histological and culture correlations. *J. Autoimmun.* **1**, 445–467.
76. Blackburn, C. C., Augustine, C. L., Li, R., et al. (1996) The nu gene acts cell-autonomously and is required for differentiation of thymic epithelial progenitors. *Proc. Natl. Acad. Sci. USA* **93**, 5742–5746.
77. Godfrey, D. I., Izon, D. J., Tucek, C. L., Wilson, T. J., and Boyd, R. L. (1990) The phenotypic heterogeneity of mouse thymic stromal cells. *Immunol. Today* **70**, 66–74.
78. Hollander, G. A., Wang, B., Nichogiannopoulou, A., et al. (1995) Developmental control point in the induction of thymic cortex regulated by a subpopulation of prothymocytes. *Nature* **373**, 350–353.

79. Gill, J., Malin, M., Hollander, G. A., and Boyd, R. (2002) Generation of a complete thymic microenvironment by MTS24(+) thymic epithelial cells. *Nat. Immunol.* **3**, 635–642.
80. Rodewald, H. R., Paul, S., Haller, C., Bluethmann, H., and Blum, C. (2001) Thymus medulla consisting of epithelial islets each derived from a single progenitor. *Nature* **414**, 763–768.
81. Klug, D. B., Crouch, E., Carter, C., Coghlan, L., Conti, C. J., and Richie, E. R. (2000) Transgenic expression of cyclin D1 in thymic epithelial precursors promotes epithelial and T cell development. *J. Immunol.* **164**, 1881–1888.
82. Norris, E. H. (1938) The morphogenesis and histogenesis of the thymus gland in man: in which the origin of the Hassall's corpuscle of the human thymus is discovered. *Contr. Embryol. Carnegie Instn.* **27**, 191–207.
83. Weller, G. L. (1933) Development of the thyroid, parathyroid and thymus glands in man. *Cont. Embryol.* **141**, 95–138.
84. Van Dyke, J. H. (1941) On the origin of accessory thymus tissue, thymus IV: the occurrence in man. *Anat. Rec.* **79**, 179–209.
85. Lampert, I. A. and Ritter, M. A. (1988) The origin of the diverse epithelial cells of the thymus: is there a common stem cell? In: *Thymus Update*, (Kendall, M. D. and Ritter, M. A., eds.), Harwood Academic, UK, pp. 5–25.
86. Lobach, D. F. and Haynes, B. F. (1986) Ontogeny of the human thymus during fetal development. *J. Clin. Immunol.* **7**, 81–97.
87. Auerbach, R. (1960) Morphogenetic interactions in the development of the mouse thymus gland. *Dev. Biol.* **2**, 271–284.
88. Bockman, D. E. and Kirby, M. L. (1984) Dependence of thymus development on derivatives of the neural crest. *Science* **223**, 498–500.
89. Revest, J. M., Suniara, R. K., Kerr, K., Owen, J. J., and Dickson, C. (2001) Development of the thymus requires signaling through the fibroblast growth factor receptor R2-IIIb. *J. Immunol.* **167**, 1954–1961.
90. Shinohara, T. and Honjo, T. (1997) Studies in vitro on the mechanism of the epithelial/mesenchymal interaction in the early fetal thymus. *Eur. J. Immunol.* **27**, 522–529.
91. Anderson, G. and Jenkinson, E. J. (2001) Lymphostromal interactions in thymic development and function. *Nat. Rev. Immunol.* **1**, 31–40.
92. Ritter, M. A. and Boyd, R. L. (1993) Development in the thymus: it takes two to tango. *Immunol. Today* **14**, 462–469.
93. Farr, A., Nelson, A., Hosier, S., and Kim, A. (1993) A novel cytokine-responsive cell surface glycoprotein defines a subset of medullary thymic epithelium in situ. *J. Immunol.* **150**, 1160–1171.
94. Ropke, C. and Elbroend, J. (1992) Human thymic epithelial cells in serum-free culture: nature and effects on thymocyte cell lines. *Dev. Immunol.* **2**, 111–121.
95. Galy, A. H. and Spits, H. (1992) CD40 is functionally expressed on human thymic epithelial cells. *J. Immunol.* **149**, 775–782.
96. Colic, M., Pejnovic, N., Kataranovski, M., Popovic, L., Gassic, S., and Dujic, A. (1992) Interferon gamma alters the phenotype of rat thymic epithelial cells in culture and increases interleukin-6 production. *Dev. Immunol.* **2**, 151–160.

97. Montgomery, R. A. and Dallman, M. J. (1991) Analysis of cytokine gene expression during fetal thymic ontogeny using the polymerase chain reaction. *J. Immunol.* **147**, 554–560.
98. Le, P. T., Lazorick, S., Whichard, L. P., Haynes, B. F., and Singer, K. H. (1991) Regulation of cytokine production in the human thymus: epidermal growth factor and transforming growth factor alpha regulate mRNA levels of interleukin 1 alpha (IL-1 alpha), IL-1 beta, and IL-6 in human thymic epithelial cells at a post-transcriptional level. *J. Exp. Med.* **174**, 1147–1157.
99. Galy, A. H. and Spits, H. (1991) IL-1, IL-4, and IFN-gamma differentially regulate cytokine production and cell surface molecule expression in cultured human thymic epithelial cells. *J. Immunol.* **147**, 3823–3830.
100. Dalloul, A. H., Arock, M., Fourcade, C., et al. (1991) Human thymic epithelial cells produce interleukin-3. *Blood* **77**, 69–74.
101. Colic, M., Pejnovic, N., Kataranovski, M., Stojanovic, N., Terzic, T., and Dujic, A. (1991) Rat thymic epithelial cells in culture constitutively secrete IL-1 and IL-6. *Int. Immunol.* **3**, 1165–1174.
102. Cohen-Kaminsky, S., Delattre, R. M., Devergne, O., et al. (1991) Synergistic induction of interleukin-6 production and gene expression in human thymic epithelial cells by LPS and cytokines. *Cell. Immunol.* **138**, 79–93.
103. Barcena, A., Sanchez, M. J., de la Pompa, J. L., Toribio, M. L., Kroemer, G., and Martinez, A. C. (1991) Involvement of the interleukin 4 pathway in the generation of functional gamma delta T cells from human pro-T cells. *Proc. Natl. Acad. Sci. USA* **88**, 7689–7693.
104. Le, P. T., Lazorick, S., Whichard, L. P., et al. (1990) Human thymic epithelial cells produce IL-6, granulocyte-monocyte-CSF, and leukemia inhibitory factor. *J. Immunol.* **145**, 3310–3315.
105. Erickson, M., Morkowski, S., Lehar, S., et al. (2002) Regulation of thymic epithelium by keratinocyte growth factor. *Blood* **100**, 3269–3278.
106. Jenkinson, W. E., Jenkinson, E. J., and Anderson, G. (2003) Differential requirement for mesenchyme in the proliferation and maturation of thymic epithelial progenitors. *J. Exp. Med.* **198**, 325–332.
107. Hu, T., Yamagishi, H., Maeda, J., McAnally, J., Yamagishi, C., and Srivastava, D. (2004) Tbx1 regulates fibroblast growth factors in the anterior heart field through a reinforcing autoregulatory loop involving forkhead transcription factors. *Development* **131**, 5491–5502.
108. Xu, H., Morishima, M., Wylie, J. N., et al. (2004) Tbx1 has a dual role in the morphogenesis of the cardiac outflow tract. *Development* **131**, 3217–3227.
109. Chapman, D. L., Garvey, N., Hancock, S., et al. (1996) Expression of the T-box family genes, Tbx1-Tbx5, during early mouse development. *Dev. Dyn.* **206**, 379–390.
110. Lindsay, E. A., Botta, A., Jurecic, V., et al. (1999) Congenital heart disease in mice deficient for the DiGeorge syndrome region. *Nature* **401**, 379–383.
111. Scambler, P. J. (2000) The 22q11 deletion syndromes. *Hum. Mol. Genet.* **9**, 2421–2426.

112. Taddei, I., Morishima, M., Huynh, T., and Lindsay, E. A. (2001) Genetic factors are major determinants of phenotypic variability in a mouse model of the DiGeorge/del22q11 syndromes. *Proc. Natl. Acad. Sci. USA* **98**, 11,428–11,431.
113. Paylor, R., McIlwain, K. L., McAninch, R., et al. (2001) Mice deleted for the DiGeorge/velocardiofacial syndrome region show abnormal sensorimotor gating and learning and memory impairments. *Hum. Mol. Genet.* **10**, 2645–2650.
114. Jerome, L. A. and Papaioannou, V. E. (2001) DiGeorge syndrome phenotype in mice mutant for the T-box gene, *Tbx1*. *Nat. Genet.* **27**, 286–291.
115. Lindsay, E. A., Vitelli, F., Su, H., et al. (2001) *Tbx1* haploinsufficiency in the DiGeorge syndrome region causes aortic arch defects in mice. *Nature* **410**, 97–101.
116. Merscher, S., Funke, B., Epstein, J. A., et al. (2001) *TBX1* is responsible for cardiovascular defects in velo-cardio-facial/DiGeorge syndrome. *Cell* **104**, 619–629.
117. Xu, H., Cerrato F., and Baldini, A. (2005) Timed mutation and cell-fate mapping reveal reiterated roles of *Tbx1* during embryogenesis, and a crucial function during segmentation of the pharyngeal system via regulation of endoderm expansion. *Development* **132**, 4387–4395.
118. Krumlauf, R. (1994) Hox genes in vertebrate development. *Cell* **78**, 191–201.
119. Manley, N. R. and Capecchi, M. R. (1998) Hox group 3 paralogs regulate the development and migration of the thymus, thyroid, and parathyroid glands. *Dev. Biol.* **195**, 1–15.
120. Manley, N. R. and Capecchi, M. R. (1995) The role of *Hoxa-3* in mouse thymus and thyroid development. *Development* **121**, 1989–2003.
121. Neubuser, A., Koseki, H., and Balling, R. (1995) Characterization and developmental expression of *Pax9*, a paired-box-containing gene related to *Pax1*. *Dev. Biol.* **170**, 701–716.
122. Wallin, J., Eibel, H., Neubuser, A., Wilting, J., Koseki, H., and Balling, R. (1996) *Pax1* is expressed during development of the thymus epithelium and is required for normal T-cell maturation. *Development* **122**, 23–30.
123. Su, D. M. and Manley, N. R. (2000) *Hoxa3* and *pax1* transcription factors regulate the ability of fetal thymic epithelial cells to promote thymocyte development. *J. Immunol.* **164**, 5753–5760.
124. Su, D., Ellis, S., Napier, A., Lee, K., and Manley, N. R. (2001) *Hoxa3* and *pax1* regulate epithelial cell death and proliferation during thymus and parathyroid organogenesis. *Dev. Biol.* **236**, 316–329.
125. Hetzer-Egger, C., Schorpp, M., Haas-Assenbaum, A., Balling, R., Peters, H., and Boehm, T. (2002) Thymopoiesis requires *Pax9* function in thymic epithelial cells. *Eur. J. Immunol.* **32**, 1175–1181.
126. Bonini, N. M., Leiserson, W. M., and Benzer, S. (1993) The eyes absent gene: genetic control of cell survival and differentiation in the developing *Drosophila* eye. *Cell* **72**, 379–395.
127. Xu, P. X., Zheng, W., Laclef, C., et al. (2002) *Eya1* is required for the morphogenesis of mammalian thymus, parathyroid and thyroid. *Development* **129**, 3033–3044.



128. Xu, P. X., Woo, I., Her, H., Beier, D. R., and Maas, R. L. (1997) Mouse Eya homologues of the *Drosophila* eyes absent gene require Pax6 for expression in lens and nasal placode. *Development* **124**, 219–231.
129. Oliver, G., Mailhos, A., Wehr, R., Copeland, N. G., Jenkins, N. A., and Gruss, P. (1995) Six3, a murine homologue of the sine oculis gene, demarcates the most anterior border of the developing neural plate and is expressed during eye development. *Development* **121**, 4045–4055.
130. Li, X., Oghi, K. A., Zhang, J., et al. (2003) Eya protein phosphatase activity regulates Six1-Dach-Eya transcriptional effects in mammalian organogenesis. *Nature* **426**, 247–254.
131. Pignoni, F., Hu, B., Zavitz, K. H., Xiao, J., Garrity, P. A., and Zipursky, S. L. (1997) The eye-specification proteins So and Eya form a complex and regulate multiple steps in *Drosophila* eye development. *Cell* **91**, 881–891.
132. Conway, S. J., Bundy, J., Chen, J., Dickman, E., Rogers, R., and Will, B. M. (2000) Decreased neural crest stem cell expansion is responsible for the conotruncal heart defects within the splotch (Sp(2H))/Pax3 mouse mutant. *Cardiovasc. Res.* **47**, 314–328.
133. Epstein, J. A., Li, J., Lang, D., et al. (2000) Migration of cardiac neural crest cells in Splotch embryos. *Development* **127**, 1869–1878.
134. Machado, A. F., Martin, L. J., and Collins, M. D. (2001) Pax3 and the splotch mutations: structure, function, and relationship to teratogenesis, including gene-chemical interactions. *Curr. Pharm. Des.* **7**, 751–785.
135. Boehm, T., Bleul, C. C., and Schorpp, M. (2003) Genetic dissection of thymus development in mouse and zebrafish. *Immunol. Rev.* **195**, 15–27.
136. Cordier, A. C. (1974) Ultrastructure of the thymus in “Nude” mice. *J. Ultrastruct. Res.* **47**, 26–40.
137. Gordon, J., Bennett, A. R., Blackburn, C. C., and Manley, N. R. (2001) Gcm2 and Foxn1 mark early parathyroid- and thymus-specific domains in the developing third pharyngeal pouch. *Mech. Dev.* **103**, 141–143.
138. Itoi, M., Kawamoto, H., Katsura, Y., and Amagai, T. (2001) Two distinct steps of immigration of hematopoietic progenitors into the early thymus anlage. *Int. Immunol.* **13**, 1203–1211.
139. Balciunaite, G., Keller, M. P., Balciunaite, E., et al. (2002) Wnt glycoproteins regulate the expression of FoxN1, the gene defective in nude mice. *Nat. Immunol.* **3**, 1102–1108.
140. Nehls, M., Kyewski, B., Messerle, M., et al. (1996) Two genetically separable steps in the differentiation of thymic epithelium. *Science* **272**, 886–889.
141. Flanagan, S. P. (1966) ‘Nude’, a new hairless gene with pleiotropic effects in the mouse. *Genet. Res.* **8**, 295–309.
142. Gunther, T., Chen, Z. F., Kim, J., et al. (2000) Genetic ablation of parathyroid glands reveals another source of parathyroid hormone. *Nature* **406**, 199–203.
143. Brissette, J. L., Li, J., Kamimura, J., Lee, D., and Dotto, G. P. (1996) The product of the mouse nude locus, Whn, regulates the balance between epithelial cell growth and differentiation. *Genes Dev.* **10**, 2212–2221.

144. Janes, S. M., Ofstad, T. A., Campbell, D. H., Watt, F. M., and Prowse, D. M. (2004) Transient activation of FOXP1 in keratinocytes induces a transcriptional programme that promotes terminal differentiation: contrasting roles of FOXP1 and Akt. *J. Cell Sci.* **117**, 4157–4168.
145. Bleul, C. C. and Boehm, T. (2001) Laser capture microdissection-based expression profiling identifies PD1-ligand as a target of the nude locus gene product. *Eur. J. Immunol.* **31**, 2497–2503.
146. Su, D. M., Navarre, S., Oh, W. J., Condie, B. G., and Manley, N. R. (2003) A domain of Foxp1 required for crosstalk-dependent thymic epithelial cell differentiation. *Nat. Immunol.* **4**, 1128–1135.
147. Nishimura, H., Agata, Y., Kawasaki, A., et al. (1996) Developmentally regulated expression of the PD-1 protein on the surface of double-negative (CD4-CD8-) thymocytes. *Int. Immunol.* **8**, 773–780.
148. Nishimura, H., Honjo, T., and Minato, N. (2000) Facilitation of beta selection and modification of positive selection in the thymus of PD-1-deficient mice. *J. Exp. Med.* **191**, 891–898.
149. Patel, S. R., Gordon, J., Mahbub, F., Blackburn, C. C., and Manley, N. (2006) Bmp4 and Noggin expression during early thymus and parathyroid organogenesis. *Gene Expr Patterns* **6**(8), 794–799.
150. Tsai, P. T., Lee, R. A., and Wu, H. (2003) BMP4 acts upstream of FGF in modulating thymic stroma and regulating thymopoiesis. *Blood* **102**, 3947–3953.
151. Bleul, C. C. and Boehm, T. (2005) BMP signaling is required for normal thymus development. *J. Immunol.* **175**, 5213–5221.
152. Abu-Issa, R., Smyth, G., Smoak, I., Yamamura, K., and Meyers, E. N. (2002) Fgf8 is required for pharyngeal arch and cardiovascular development in the mouse. *Development* **129**, 4613–4625.
153. Frank, D. U., Fotheringham, L. K., Brewer, J. A., et al. (2002) An Fgf8 mouse mutant phenocopies human 22q11 deletion syndrome. *Development* **129**, 4591–4603.
154. Conway, S. J., Henderson, D. J., and Copp, A. J. (1997) Pax3 is required for cardiac neural crest migration in the mouse: evidence from the splotch (Sp2H) mutant. *Development* **124**, 505–514.
155. Mitchell, P. J., Timmons, P. M., Hebert, J. M., Rigby, P. W., and Tjian, R. (1991) Transcription factor AP-2 is expressed in neural crest cell lineages during mouse embryogenesis. *Genes Dev.* **5**, 105–119.
156. Dencker, L., Annerwall, E., Busch, C., and Eriksson, U. (1990) Localization of specific retinoid-binding sites and expression of cellular retinoic-acid-binding protein (CRABP) in the early mouse embryo. *Development* **110**, 343–352.
157. Macatee, T. L., Hammond, B. P., Arenkiel, B. R., Francis, L., Frank, D. U., and Moon, A. M. (2003) Ablation of specific expression domains reveals discrete functions of ectoderm- and endoderm-derived FGF8 during cardiovascular and pharyngeal development. *Development* **130**, 6361–6374.
158. Suniara, R. K., Jenkinson, E. J., and Owen, J. J. (2000) An essential role for thymic mesenchyme in early T cell development. *J. Exp. Med.* **191**, 1051–1056.



159. Campbell, J. J., Pan, J., and Butcher, E. C. (1999) Cutting edge: developmental switches in chemokine responses during T cell maturation. *J. Immunol.* **163**, 2353–2357.
160. Wendling, O., Dennefeld, C., Chambon, P., and Mark, M. (2000) Retinoid signaling is essential for patterning the endoderm of the third and fourth pharyngeal arches. *Development* **127**, 1553–1562.
161. Ghyselinck, N. B., Dupe, V., Dierich, A., et al. (1997) Role of the retinoic acid receptor beta (RARbeta) during mouse development. *Int. J. Dev. Biol.* **41**, 425–447.
162. Kanariou, M., Huby, R., Ladyman, H., et al. (1989) Immunosuppression with cyclosporin A alters the thymic microenvironment. *Clin. Exp. Immunol.* **78**, 263–270.
163. Imami, N., Ladyman, H. M., Spanopoulou, E., and Ritter, M. A. (1992) A novel adhesion molecule in the murine thymic microenvironment: functional and biochemical analysis. *Dev. Immunol.* **2**, 161–173.
164. Rouse, R. V., Bolin, L. M., Bender, J. R., and Kyewski, B. A. (1988) Monoclonal antibodies reactive with subsets of mouse and human thymic epithelial cells. *J. Histochem. Cytochem.* **36**, 1511–1517.
165. Vicari, A., Abehsira-Amar, O., Papiernik, M., Boyd, R. L., and Tucek, C. L. (1994) MTS-32 monoclonal antibody defines CD4+8- thymocyte subsets that differ in their maturation level, lymphokine secretion, and selection patterns. *J. Immunol.* **152**, 2207–2213.
166. MacNeil, I., Kennedy, J., Godfrey, D. I., et al. (1993) Isolation of a cDNA encoding thymic shared antigen-1. A new member of the Ly6 family with a possible role in T cell development. *J. Immunol.* **151**, 6913–6923.
167. Randle, E. S., Waanders, G. A., Masciantonio, M., Godfrey, D.I., and Boyd, R. L. (1993) A lymphostromal molecule, thymic shared Ag-1, regulates early thymocyte development in fetal thymus organ culture. *J. Immunol.* **151**, 6027–6035.
168. Ivanov, V. and Ceredig, R. (1992) Transcription factors in mouse fetal thymus development. *Int. Immunol.* **4**, 729–737.

## Generation of a Tissue-Engineered Thymic Organoid

Fabrizio Vianello and Mark C. Poznansky

### Summary

The thymic microenvironment provides essential support for the generation of a functional and diverse population of human T cells. In particular, the three-dimensional (3D) thymic architecture contributes to critical cell–cell interactions. We report that thymic stroma, arrayed on a synthetic 3D matrix, supports the development of functional human T cells from hematopoietic precursor cells. Newly generated T cells contain T-cell receptor excision circles and are both fully mature and functional. The coculture of T-cell progenitors with thymic stroma can thus be used to generate *de novo* functional and diverse T-cell populations. This novel tissue engineered thymic system has biological applications for the study of T-lymphopoiesis and self-tolerance as well as potential therapeutic applications including the immune reconstitution of immunocompromised patients and the induction of tolerance in individuals receiving tissue or organ transplants.

**Key Words:** Tissue engineering; thymic organoid; Treg cells; thymic epithelial cells; tolerance.

### 1. Introduction

Tolerance describes a state in which the immune system fails to mount a response against a specific antigen in the absence of immunosuppression, while simultaneously maintaining responses to other antigens (1). Maintaining tolerance to self-antigens is an ongoing process, which depends upon central and peripheral components. Central tolerance refers to tolerance generated within the thymus, involving the deletion of potentially autoreactive T cells through a process known as negative selection. Both medullary thymic epithelial cells and thymic dendritic cells (DC) can mediate negative selection, although thymic DC probably play the dominant role (2). There is evidence that clinical tolerance may be achieved by manipulating the process of central

tolerance. In particular, donor-specific tolerance to solid organ allografts may be induced through central deletional mechanisms upon cotransplantation of allogeneic thymus tissue (3–5). Moreover, intrathymic injection of nonself molecules is effective in inducing tolerance to the same foreign antigens in non-immunosuppressed animals (6). Manipulation of the thymic stroma and thymocyte development in vitro may, therefore, allow the role of the thymus in transplantation tolerance to be more fully explored.

Although human hematopoietic stem cells, from any source, can develop into myeloid, erythroid, and pre-B cells in vitro as well as in vivo (7), T-cell development may be an exception because the T-cell lineage develops solely within a thymic microenvironment. More than 10 yr ago, it was demonstrated that human T cells develop in immunodeficient mice when human fetal thymus and fetal lymph nodes are implanted side-by-side under the kidney capsule with fetal liver cells (8). This model indicated that human hematopoietic stem cells possess the differentiation potential for T-cell lineages if an appropriate thymic microenvironment exists. The limitation for this technique, namely the relative lack of availability of human fetal thymus, was overcome when Fisher and colleagues demonstrated that CD4<sup>-</sup>CD8<sup>-</sup> “double-negative” human thymocytes could develop into mature CD4<sup>+</sup>CD8<sup>-</sup> or CD4<sup>-</sup>CD8<sup>+</sup> “single positive” (SP) T cells in a coculture system with murine fetal thymic lobes (9). During the process of T-cell maturation, the TCR-mediated positive and negative selection of T cells ensures the selection of a diverse TCR repertoire able to react with foreign peptides presented by autologous major histocompatibility complex (MHC) molecules, but tolerant to self-antigens.

Tissue engineering advances allow us to recapitulate the biology required for the formation and maintenance of complex tissues. The development of three-dimensional (3D) scaffolds, including CellFoam, has also facilitated this approach. CellFoam consists of a biocompatible, 3D, tantalum-coated porous biomaterial (10,11). The 3D of this material provides an opportunity to recreate an appropriate spatial arrangement of cells in a tissue. In particular, the thymic microenvironment is organized in a 3D structure, fundamental to keeping stromal cells in close proximity with T-cell precursors, thereby directing their maturation.

## 2. Case Study

### 2.1. Murine Thymic Stromal Cultures on 3D Matrices

3D matrices were created by culturing thymic fragments from 4- to 6-wk-old C57BL/6J mice on the surface of disks of CellFoam (Cytomatrix) (12a). The optimal-sized matrix for this system was found to measure 10 mm in diameter by 1 mm in depth, with an average pore density of 80 pores per inch (p.p.i.). Matrices were cultured in 24-well tissue culture plates, immersed in complete

medium based on Iscove's modified Dulbecco's medium, which was renewed every 4 d. Thymic fragments, cocultured in the presence of CellFoam, resulted in colonization with thymic stromal cells reaching 80% confluency, which were transferred to fresh culture plates before the addition of progenitor cells.

Isolation of progenitors was performed from human bone marrow using the phenotypic cell surface markers AC133 or CD34. AC133<sup>+</sup> cells were isolated from peripheral mononuclear cells using an AC133 Cell Isolation Kit (Miltenyi Biotec). To rule out contamination with CD2<sup>+</sup> T cells, CD34<sup>+</sup> cells were isolated using a CD34 Multisort Kit (Miltenyi Biotec) that allowed subsequent depletion of CD2<sup>+</sup> T cells, the efficiency of which was subsequently verified by flow cytometry.

AC133<sup>+</sup> or CD34<sup>+</sup> cells were added to the thymic stromal cultures to determine the optimal cell density. Using 10 × 1-mm matrices and input cell densities of 1 × 10<sup>4</sup> progenitor cells per well, approx 1.9 × 10<sup>4</sup> human CD45<sup>+</sup> leukocytes could be retrieved after 14 d in coculture. Of these, approx 80% were CD3<sup>+</sup>, representing the predominant cell population. Nonadherent cells, harvested after 14 d of culture, showed expression of CD2, CD4, and CD8. Expression of CD4 at day 14 is associated with upregulation of CD3. Discrete populations of CD4<sup>+</sup>CD8<sup>-</sup> and CD4<sup>+</sup>CD8<sup>+</sup> SP cells and their CD4<sup>+</sup>CD8<sup>+</sup> double-positive (DP) precursors were evident after 14 d, although the number of DP cells diminished significantly by day 21. TCRαβ was expressed by 80% and TCRγδ by 15% of CD3<sup>+</sup> SP cells. T cells generated using this coculture system express 13 of 24 TCR Vβ families. When tested for their functional properties, CD3<sup>+</sup>CD4<sup>+</sup>TCR<sup>+</sup> and CD3<sup>+</sup>CD8<sup>+</sup>TCR<sup>+</sup> cells removed from the cocultures after 14 d were shown to be capable of proliferating vigorously in the presence of interleukin-2 and phytohemagglutinin and of producing intracellular cytokines comparable to levels evident in control, fully mature peripheral blood T cells.

## **2.2. Extrathymic Epithelial Cells and DC Can Support T-Cell Development**

It has been shown that epithelial cells, stromal cells, DC, and lymphopoietic cytokines all contribute to the differentiation of bone marrow-derived hematopoietic precursors into mature, functional T cells (*12b*). Although epithelial and stromal cells of the thymus are the main players in the process of T-cell development, it is possible that similar human cell types derived from different anatomical locations, such as the skin, are also able to direct T-cell maturation. This may be particularly feasible when considering that the major difference between thymus and skin, other than their accessibility and availability, is the distinct 3D architecture, which can be recapitulated by our system.

Recently, keratinocytes and fibroblasts from normal adult human skin were found to be able to support the full development of T cells from hematopoietic precursors (13).

Following expansion of fibroblasts and keratinocytes from human skin, a 3D structure was created by coculturing skin cells onto artificial CellFoam matrices. Seeding of matrices with human hematopoietic precursors led to T-cell maturation progressing from CD4<sup>-</sup>CD8<sup>-</sup> double-negative to DP cells and subsequently to mature CD4<sup>+</sup> or CD8<sup>+</sup> SP cells. Thymocytes developing in the skin cell construct underwent positive selection, thereby determining their TCR repertoire. Furthermore, T cells failed to proliferate in response to self-MHC and other antigens, providing evidence that negative selection also occurred within the microenvironment afforded by the skin cell cultures. T cells produced in the skin construct proliferated in response to treatment with phytohemagglutinin and concanavalin A and they expressed robust levels of the early activation marker, CD69. Significant proliferation was also observed in mixed leukocyte reactions, in which newly generated T cells proliferated in response to allogeneic stimulator cells, further supporting their functional maturity. It is interesting to note that a series of mixed leukocyte reactions demonstrated that allogeneic DC were able to induce tolerance in developing T cells.

### 3. Applications

#### 3.1. Regeneration of the Peripheral T-Cell Repertoire

Generation of functional human T cells by means of tissue-engineered thymic organoids, has several potential clinical applications, including the possibility of replacing the T cell regenerating capacity of the thymus, lost as a result of infection, chemotherapy or age-dependent thymic involution (*see* Chapter 24). In particular, it provides an attractive strategy for the treatment of diseases such as HIV/AIDS, and complications arising from the use of chemotherapeutic agents and bone marrow transplantation (14). The application of thymic organoid-based technologies as techniques that mimic thymic generation of lymphocytes would have important advantages over general methods of T-cell expansion and, in particular, the generation of naïve T cells with a broad array of TCR repertoires. Our thymic organoid is of particular interest because it has the potential to generate not only normal autologous T cells but also allogeneic T cells that might be harnessed to mount a graft-vs-leukemia reaction in patients with relapsed disease (15).

Perhaps the most exciting potential application is, however, the possibility of manipulating the T-cell compartment with the aim of generating tolerance in the context of allogeneic transplantation or autoimmunity. Induction of specific

immunologic tolerance to donor antigens would avoid both chronic graft rejection and the side effects associated with immunosuppressive therapy (16).

### **3.2. Induction of Tolerance to Organ Allografts**

The role of the thymus in the establishment of systemic central tolerance is now universally accepted to involve the induction of anergy among potentially autoreactive T cells or their deletion upon exposure to the appropriate self-antigen, presented by thymic stromal cells (17–20). Similar intrathymic mechanisms may also be important in inducing donor-specific tolerance to alloantigens, indeed various studies have demonstrated that donor alloantigens injected directly into the thymus are able to induce donor-specific tolerance to the alloantigen *in vivo* or *in vitro* (21,22). Furthermore, there is convincing evidence that grafts of allogeneic thymic tissue have the capacity to induce tolerance to skin grafts sharing their MHC haplotype (23,24). Ectopic heart grafts of donor type may also be accepted (25). These findings show that naked thymic epithelium is able to attract allogeneic precursors, restore T-cell function and induce *in vivo* tolerance to tissue grafts of the same MHC haplotype. Interestingly, tolerance *in vivo* is not always correlated with *in vitro* tolerance, suggesting that complete clonal deletion is not required to induce physiological tolerance to tissue grafts.

Evidence also suggests that specific human T-cell tolerance can be induced toward xenogeneic tissues. In particular, it has been shown that porcine fetal thymic grafts can support the development of functional, normal human T cells, from hematopoietic precursors provided by human fetal liver cells (26). These human T cells showed specific immunological tolerance to porcine xenoantigens, whereas showing full responsiveness to allogeneic human stimulators and MHC-mismatched (i.e., nondonor) porcine antigens. These data establish the principle that human T-cell tolerance can be induced to a discordant xenogeneic donor.

### **3.3. Generation of Regulatory T Cells**

It has recently become evident that DC can be used for immune regulation, either for treatment of autoimmunity or for transplant rejection (27,28). The immune regulatory aspects of DC include the direct killing of T cells, induction of T-cell anergy or the generation of regulatory T cells (Treg). The tolerogenicity of DC could, therefore, be exploited by combining donor-derived thymic tissue with immature DC isolated from the recipient. These DC could be collected, expanded, and reintroduced into the transplant recipient, a strategy that is supported by the fact that antigen-pulsed thymic DC have been shown to re-enter the thymus of naïve recipients and induce tolerance to a nonself antigen (29).

Tolerogenic DC may also act by generating and inducing the migration of Treg cells. It has, for instance, been demonstrated that one mechanism by which the generation of Treg cells is markedly enhanced, relies on the migration of tolerogenic DC from the periphery to the thymus, where they positively select developing Treg cells. The therapeutic generation of Treg cells may, therefore, be pursued by coculturing autologous T cells with allogeneic thymic stromal cells, with the aim of generating and transferring to the recipient Treg cells capable of conferring dominant allograft tolerance (30).

Following the generation of tolerance by DC or Treg cells, it would be interesting to explore whether transplantation of a biocompatible thymic organoid composed of donor-derived thymic stroma may further consolidate tolerance to allografts. The existence of Treg cells inducing tolerance to allogeneic MHC could prevent rejection and loss of the allogeneic thymus graft. Overcoming thymic graft rejection may facilitate the induction of donor-specific tolerance through central deletional mechanisms.

#### 4. Conclusions

T cell-generating organoids may help to elucidate both the immune biology of T-cell maturation as well as influence T-cell specificity and reactivity to allogeneic transplants. Ultimately thymic organoids may be used therapeutically to regenerate T cells with defined antigen specificity in immune deficient or compromised individuals or, conversely, to induce tolerance to specific antigens in the context of organ transplantation or autoimmunity.

#### Acknowledgments

The authors were supported by Public Health Service grants RO1 AI49757, R21 AI049858.

#### References

1. Platt, J. L. and Lakkis, F. G. (2001) A scenic overlook on the road to clinical tolerance. *Trends Immunol.* **22**, 289–291.
2. Hogquist, K. A., Baldwin, T. A., and Jameson, S. C. (2005) Central tolerance: learning self-control in the thymus. *Nat. Rev. Immunol.* **5**, 772–782.
3. Haller, G. W., Esnaola, N., Yamada, K., et al. (1999) Thymic transplantation across an MHC class I barrier in swine. *J. Immunol.* **163**, 3785–3792.
4. Yamada, K., Shimizu, A., Ierino, F. L., et al. (1999) Thymic transplantation in miniature swine. I. Development and function of the “thymokidney.” *Transplantation* **68**, 1684–1692.
5. Kuschnaroff, L. M., Overbergh, L., Sefriouni, H., Sobis, H., Vandeputte, M., and Waer, M. (1999) Effect of staphylococcal enterotoxin B injection on the development of experimental autoimmune encephalomyelitis: influence of cytokine and inducible nitric oxide synthase production. *J. Neuroimmunol.* **99**, 157–168.

6. Naji, A. (1996) Induction of tolerance by intrathymic inoculation of alloantigen. *Curr. Opin. Immunol.* **8**, 704–709.
7. Freedman, A. R., Zhu, H., Levine, J. D., Kalams, S., and Scadden, D. T. (1996) Generation of human T lymphocytes from bone marrow CD34+ cells in vitro. *Nat. Med.* **2**, 46–51.
8. McCune, J. M., Namikawa, R., Kaneshima, H., Shultz, L. D., Lieberman, M., and Weissman, I. L. (1988) The SCID-hu mouse: murine model for the analysis of human hematolymphoid differentiation and function. *Science* **241**, 1632–1639.
9. Fisher, A. G., Larsson, L., Goff, L. K., Restall, D. E., Happerfield, L., and Merkenschlager, M. (1990) Human thymocyte development in mouse organ cultures. *Int. Immunol.* **2**, 571–578.
10. Black, J. (1994) Biological performance of tantalum. *Clin. Mater.* **16**, 167–173.
11. Bobyn, J. D., Stackpool, G. J., Hacking, S. A., Tanzer, M., and Krygier, J. J. (1999) Characteristics of bone ingrowth and interface mechanics of a new porous tantalum biomaterial. *J. Bone Joint Surg. Br.* **81**, 907–914.
- 12a. Poznansky, M., Evans, R. H., Foxall, R. B., et al. (2000) Efficient generation of human T cells from a tissue-engineered thymic organoid. *Nat. Biotechnol.* **18**, 729–734.
- 12b. Anderson, G. and Jenkinson, E. J. (2001) Lymphostromal interactions in thymic development and function. *Nat. Rev. Immunol.* **1**, 31–40.
13. Clark, R. A., Yamanaka, K. I., Bai, M., Dowgiert, R., and Kupper, T. S. (2005) Human skin cells support thymus-independent T cell development. *J. Clin. Invest.* **115**, 3239–3249.
14. Hiesse, C., Rieu, P., Kriaa, F., et al. (1997) Malignancy after renal transplantation: analysis of incidence and risk factors in 1700 patients followed during a 25-year period. *Transplant. Proc.* **29**, 831–833.
15. Garlie, N. K., LeFever, A. V., Siebenlist, R. E., Levine, B. L., June, C. H., and Lum, L. G. (1999) T cells coactivated with immobilized anti-CD3 and anti-CD28 as potential immunotherapy for cancer. *J. Immunother.* **22**, 336–345.
16. Port, F. K., Dykstra, D. M., Merion, R. M., and Wolfe, R. A. (2004) Organ donation and transplantation trends in the USA (2003). *Am. J. Transplant.* **4**, 7–12.
17. Kappler, J. W., Roehm, N., and Marrack, P. (1987) T cell tolerance by clonal elimination in the thymus. *Cell* **49**, 273–280.
18. Kappler, J. W., Staerz, U., White, J., and Marrack, P. C. (1988) Self-tolerance eliminates T cells specific for MIs-modified products of the major histocompatibility complex. *Nature* **332**, 35–40.
19. Sprent, J., Lo, D., Gao, E. K., and Ron, Y. (1988) T cell selection in the thymus. *Immunol. Rev.* **101**, 173–190.
20. Coutinho, A., Salaun, J., Corbel, C., Bandeira, A., and Le Douarin, N. (1993) The role of thymic epithelium in the establishment of transplantation tolerance. *Immunol. Rev.* **133**, 225–240.
21. Oluwole, S. F., Chowdhury, N. C., and Fawwaz, R. A. (1993) Induction of donor-specific unresponsiveness to rat cardiac allografts by pretreatment with intrathymic donor MHC class I antigens. *Transplantation* **55**, 1396–1402.



22. Posselt, A. M., Barker, C. F., Friedman, A. L., and Naji, A. (1992) Prevention of autoimmune diabetes in the BB rat by intrathymic islet transplantation at birth. *Science* **256**, 1321–1324.
23. Lee, L. A., Gritsch, H. A., Sergio, J. J., et al. (1994) Specific tolerance across a discordant xenogeneic transplantation barrier. *Proc. Natl. Acad. Sci. USA* **91**, 10,864–10,867.
24. Zhao, Y., Swenson, K., Sergio, J. J., Arn, J. S., Sachs, D. H., and Sykes, M. (1996) Skin graft tolerance across a discordant xenogeneic barrier. *Nat. Med.* **2**, 1211–1216.
25. Mezrich, J. D., Benjamin, L. C., Sachs, J. A., et al. (2005) Role of the thymus and kidney graft in the maintenance of tolerance to heart grafts in miniature swine. *Transplantation* **79**, 1663–1673.
26. Nikolic, B., Gardner J. P., Scadden, D. T., Arn, J. S., Sachs, D. H., and Sykes, M. (1999) Normal development in porcine thymus grafts and specific tolerance of human T cells to porcine donor MHC. *J. Immunol.* **162**, 3402–3407.
27. Ichim, T. E., Zhong, R., and Min, W. P. (2003) Prevention of allograft rejection by in vitro generated tolerogenic dendritic cells. *Transpl. Immunol.* **11**, 295–306.
28. Steinman, R. M., Hawiger, D., and Nussenzweig, M. C. (2003) Tolerogenic dendritic cells. *Annu. Rev. Immunol.* **21**, 685–711.
29. Khoury, S. J., Gallon, L., Chen, W., et al. (1995) Mechanisms of acquired thymic tolerance in experimental autoimmune encephalomyelitis: thymic dendritic-enriched cells induce specific peripheral T cell unresponsiveness in vivo. *J. Exp. Med.* **182**, 357–366.
30. Bushell, A., Jones, E., Gallimore, A., and Wood, K. (2005) The generation of CD25+ CD4+ regulatory T cells that prevent allograft rejection does not compromise immunity to a viral pathogen. *J. Immunol.* **174**, 3290–3297.

## Studying T-Cell Repertoire Selection Using Fetal Thymus Organ Culture

Philip G. Ashton-Rickardt

### Summary

T lymphocytes express receptors (T-cell receptor) that are not only specific for antigenic peptide but also molecules encoded by the major histocompatibility complex (MHC) that present peptide on the surface of cells (MHC-restricted antigen recognition). However, the vast majority of T cells are tolerant to their own MHC molecules and do not give rise to autoimmune disease. This MHC-restricted, but tolerant, repertoire of T cells is determined by selection triggered by the appropriate recognition of peptide/MHC on thymic stromal cell by immature thymocytes. We have developed a fetal thymus organ culture (FTOC) system based on transporter associated with antigen processing (TAP) 1-deficient mice to examine the role of peptide/MHC in triggering the differentiation of T cells restricted to class I MHC (positive selection). We also describe an FTOC system to study central T-cell tolerance, which occurs through clonal deletion in the thymus (negative selection).

**Key Words:** Thymus; positive selection; negative selection; TAP1; MHC; peptide; FTOC; flow-cytometer.

### 1. Introduction

Two types of cellular events that take place in the thymus shape the repertoire of antigen specificities of T lymphocytes. Positive selection ensures that T cells leaving the thymus recognize peptide presented by self-major histocompatibility complex (MHC) molecules (1,2). Negative selection eliminates those T cells that are potentially auto-reactive (3). The stable surface expression of class I MHC requires the binding of specific peptides that can be derived from antigen or self-proteins (4). Positive selection is triggered by the engagement of T-cell receptors (TCR) on thymocytes with self-MHC molecules on thymic epithelial cells and results in the rescue from apoptosis and differentiation into

either CD4<sup>+</sup>CD8<sup>-</sup> or CD4<sup>+</sup>CD8<sup>+</sup> mature T cells (5,6). Negative selection is triggered by the binding of TCRs with self-MHC molecules on bone-marrow derived thymic stromal cells and results in the induction of apoptosis of immature CD4<sup>+</sup>CD8<sup>+</sup> thymocytes.

To address the role of peptides in determining the repertoire of CD8<sup>+</sup> T cells we exploited TAP1 (for transporter associated with antigen processing 1) mutant mice (TAP1<sup>-</sup> mice) (7). In TAP1<sup>-</sup> mice, the loading of peptide into MHC class I molecules in the endoplasmic reticulum is blocked. Consequently, surface expression of MHC class I molecules is reduced and the selection of CD8<sup>+</sup> T cells is severely hampered. However, the “empty” unstable MHC class I molecules can be loaded and stabilized with peptide provided extracellularly in the presence of  $\beta$ 2-microglobulin (4,7,8). Experiments with cultured fetal thymi from TAP1<sup>-</sup> mice showed that peptide presented by MHC class I was specifically recognized by the TCRs of immature thymocytes during positive selection (8). The role of peptide in negative selection can also be studied in FTOC. Transgenic thymocytes that express the P14 TCR, which is specific for an epitope from lymphocytic choriomeningitis virus (LCMV) (9), undergo negative selection when cultured with antigen peptide (LCMV peptide) (10). Thus, FTOC from TAP1<sup>-</sup> mice allows one to examine how the recognition of peptide triggers positive selection, and P14 FTOC how the recognition of peptide triggers negative selection. Together, both FTOC systems can be used to investigate the role of positive and negative selection in determining the repertoire of antigen specificities displayed by CD8<sup>+</sup> T cells.

## 2. Materials

### 2.1. Fetal Thymus Organ Culture

1. Embryonic material is obtained from matings of mice within the inbred strains C57BL/6J (TAP1<sup>+</sup>) (H-2<sup>b</sup>) and *Tap1*<sup>tm1Atp</sup> (TAP1<sup>-</sup>) C57BL/6 (H-2<sup>b</sup>) (Jackson Laboratory, Bar Harbor ME). For P14 fetal thymus organ culture (FTOC), C57BL/6J (TAP1<sup>+</sup>) (H-2<sup>b</sup>) mice were mated with *LCMV P14* (P14<sup>+/+</sup>) transgenic mice (H-2<sup>b</sup>) (Taconic, Hudson, NY).
2. Dissection is carried out under  $\times 4$ – $7$  magnification with a Leica Stereo Zoom 7 microscope.
3. Roswell Park Memorial Institute (RPMI) 1640 medium (Invitrogen-Gibco, Carlsbad, CA) is supplemented with 1% Nutridoma Media Supplement (Roche Applied Science, Indianapolis, IN),  $5 \times 10^{-5}$  M 2-mercaptoethanol. Glutamine, nonessential amino acids, sodium pyruvate, penicillin, and streptomycin are added at 1X from 100X stocks (Invitrogen-Gibco). The medium is further supplemented with 30  $\mu$ g/mL human  $\beta$ 2-microglobulin (Sigma-Aldrich, St. Louis, MO) (see Note 1).
4. RPMI 1640 (Invitrogen-Gibco) supplemented 10% fetal calf serum (FCS) (Invitrogen-Gibco).

5. Nitrocellulose filters (0.2- $\mu\text{m}$  pore size) (Millipore, Billerica, MA) are placed on collagen sponges cut into 2- to 5-cm<sup>2</sup> pieces (Colla-Tec Inc, Plainsboro, NJ) saturated with medium and placed in 6  $\times$  1.5-cm tissue culture dishes (Falcon 3004, Becton, Dickinson and Company, Plymouth, UK).
6. Peptides are produced by solid-phase synthesis and purified by high-pressure liquid chromatography (Research Genetics, Huntsville, AL) (*see Note 2*). Amino acid sequences of class I MHC-specific synthetic peptides are as follows: influenza virus nucleoprotein peptide (amino acids 366–374) (IF peptide) ASNENMETM (H-2D<sup>b</sup>-specific), ovalbumin peptide (amino acids 257–264) (OVA peptide) SIINFEKL (H-2K<sup>b</sup>-specific), vesicular stomatitis virus nucleoprotein (amino acids 52–59) (VSV peptide) RGYVYQGL (H-2K<sup>b</sup>-specific), Sendai virus nucleoprotein (amino acids 324–332) (SV peptide) FAPGNYPAL, LCMV glycoprotein (amino acids 33–41) (LCMV peptide) KAVYNFATM, DB-S peptide SSSSNSSSM (*see Note 3*).

## 2.2. Flow-Cytometric Analysis

1. Staining buffer: PBS supplemented with 1% FCS (Invitrogen-Gibco) and 0.1% sodium azide (Sigma-Aldrich).
2. Digestion buffer for the disaggregation of thymic stroma: 2.5% trypsin and 384 U/mL collagenase type IV (both from Sigma-Aldrich) in PBS.
3. Thymocyte specific conjugated-monoclonal antibodies (BD-Pharmingen, San Diego, CA): anti-CD4 (allophycocyanin [APC]-labeled), anti-CD8 $\alpha$  (fluorescein isothiocyanate [FITC]-labeled), anti-CD3 $\epsilon$  (R phycoerythrin [PE]-labeled), anti-TCR V $\beta$ 7 (biotin labeled), anti-TCR V $\beta$ 5 (biotin labeled), anti-TCR V $\beta$ 11 (biotin labeled), anti-TCR V $\beta$ 9 (biotin labeled), anti-TCR V $\beta$ 8 (biotin labeled), and anti-TCR V $\beta$ 10 (biotin labeled), anti-TCR V $\alpha$ 2-PE.
4. Thymic stroma specific conjugated-monoclonal antibodies: anti-H-2A<sup>b</sup>-PE (BD-Pharmingen), anti-H-2K<sup>b</sup>-biotin (clone AF6.44,  $\alpha$ 2 domain-specific)-FITC (BD-Pharmingen) and anti-H-2D<sup>b</sup> (clone B22-249R1,  $\alpha$ 1 domain specific)-FITC (American Tissue Culture Collection).
5. For biotin-conjugated antibodies, either streptavidin (SA)-APC, SA-PE, or SA-Texas Red (BD-Pharmingen) are used to visualize cells.
6. Stained cells are analyzed on a dual laser FACStar<sup>plus</sup> (Becton, Dickinson and Company, Franklin Lakes, NJ) (*see Note 4*).

## 3. Methods

The culture of explanted mouse fetal thymi on solid supports is a powerful tool to study T-cell development in the thymus (11). Explanted d 14–16 mouse fetal thymi successfully support the differentiation of immature CD4<sup>+</sup> CD8<sup>+</sup> thymocytes and subsequent positive selection into CD8<sup>+</sup>CD4<sup>-</sup> and CD4<sup>+</sup>CD8<sup>-</sup> thymocytes. The major advantages of FTOC are the ease of manipulating thymocyte development by the addition of reagents to the supporting tissue culture medium, and the ability to obtain statistical significance by the simultaneous

culture of multiple thymic lobes. The addition of class I MHC binding peptides to cultured fetal thymi from TAP1<sup>-</sup> mice allows the rescue of class I expression on thymic stromal cells. This allows one to address the role of peptide in the positive selection of CD8<sup>+</sup> thymocytes. Using this system, one can examine the sequence and density requirements of an individual peptide for positive selection. In addition, one can determine the effect of peptide complexity on the repertoire of CD8<sup>+</sup> T cells selected by mixtures of peptides (8).

The role of peptide in positive selection using TAP1<sup>-</sup> FTOC is based on two simple measurements. First, the level of peptide/class I MHC is determined by rescue of surface expression of TAP1<sup>-</sup> thymic stroma after addition of exogenous peptide. Second, the consequence of the expression of specific peptide/MHC complexes on positive selection is measured by determining the number and diversity of TCRs expressed by the resulting CD8<sup>+</sup> CD4<sup>-</sup> thymocytes. Negative selection of P14 CD8<sup>+</sup> T cells by the nominal antigen LCMV peptide, leads to a drastic reduction in the percentage and absolute number of CD8<sup>+</sup> P14 cells and CD4<sup>+</sup> CD8<sup>+</sup> precursor thymocytes both *in vivo* (9) and *in vitro* (12). The deletion of these thymocyte populations is used to measure negative selection by peptide in P14 FTOC (10).

### 3.1. FTOC

1. Male and female mice maintained on an 8 h dark, 16 h light schedule are caged together overnight, and checked for vaginal plugs the next morning. The day of finding a vaginal plug is designated as day 0.
2. After d 14 and 16, mice are sacrificed by cervical dislocation and the uterus placed intact in a tissue culture hood. Under sterile conditions, fetuses are dissected from the uterus, freed of membrane, and immersed in RPMI-10% FCS. Fetuses are pinned to an aluminum foil-covered polystyrene board with 20-gauge needles through the mouth and out the back of the head. Fetuses are then sectioned across the diaphragm with a razor blade and the bottom half discarded. Under magnification ( $\times 2-7$ ), using fine watchmakers forceps, the liver, heart, lungs, esophagus, trachea are pulled out leaving the thymic lobes still attached to the body wall. Both thymic lobes are then removed intact by clasp attached connective tissue with fine watchmakers' forceps. Immersed in RPMI-10% FCS, residual connective tissue is removed with two 20-gauge needles and the thymic lobes separated.
3. In a tissue culture hood under sterile conditions, collagen sponges are placed in 5 mL of RPMI-1% Nutridoma medium in 1.5  $\times$  6-cm Petri dishes then nitrocellulose filters placed on top. Peptides (50–500  $\mu$ M) are dissolved directly into the medium before setting up the culture (*see Note 5*). About four to eight thymic lobes are placed on each filter and the top of the Petri dish replaced. Dishes are incubated at 37°C/5% CO<sub>2</sub> in a humidified incubator.
4. Every other day, old medium is removed and new medium containing fresh peptide is added to the dishes. After 10 d, thymi are analyzed for MHC class I expression and thymocyte subsets.

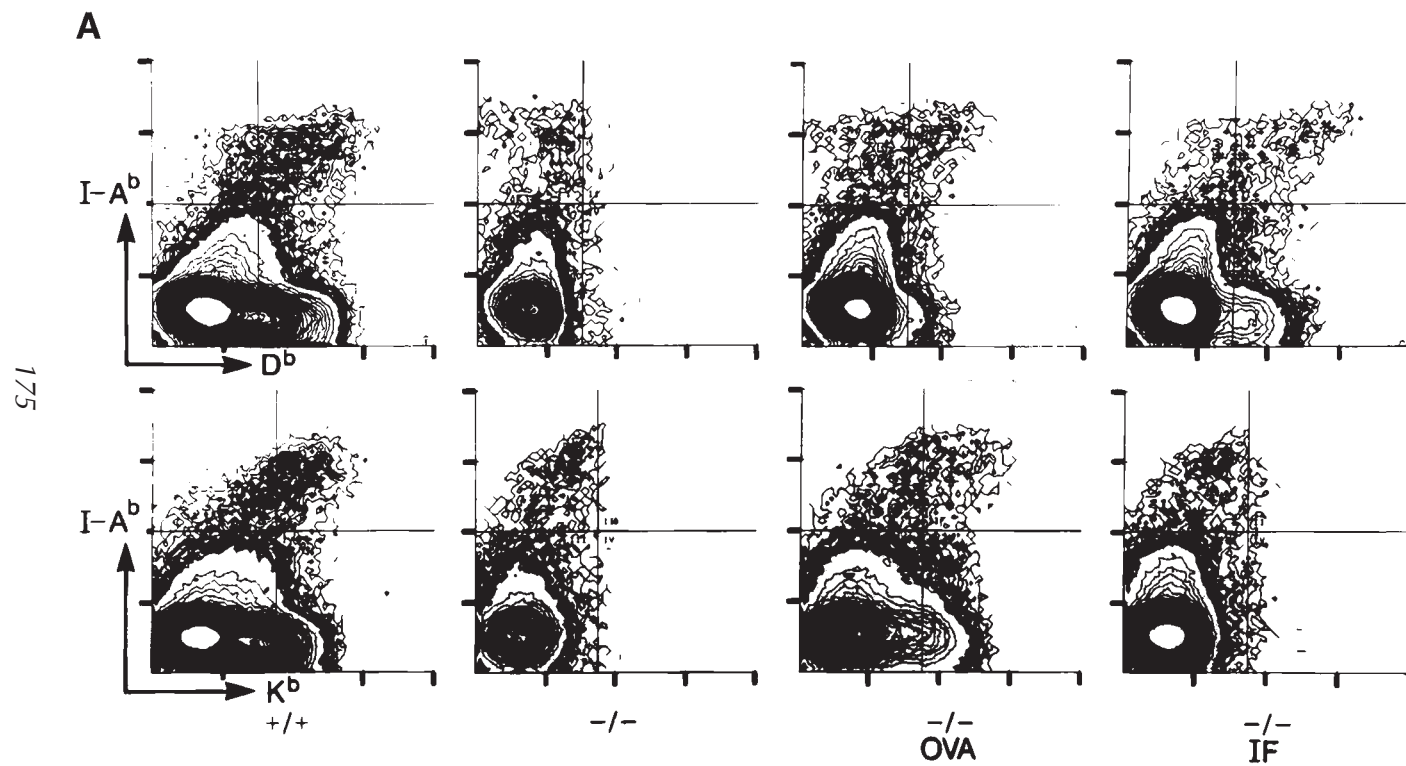
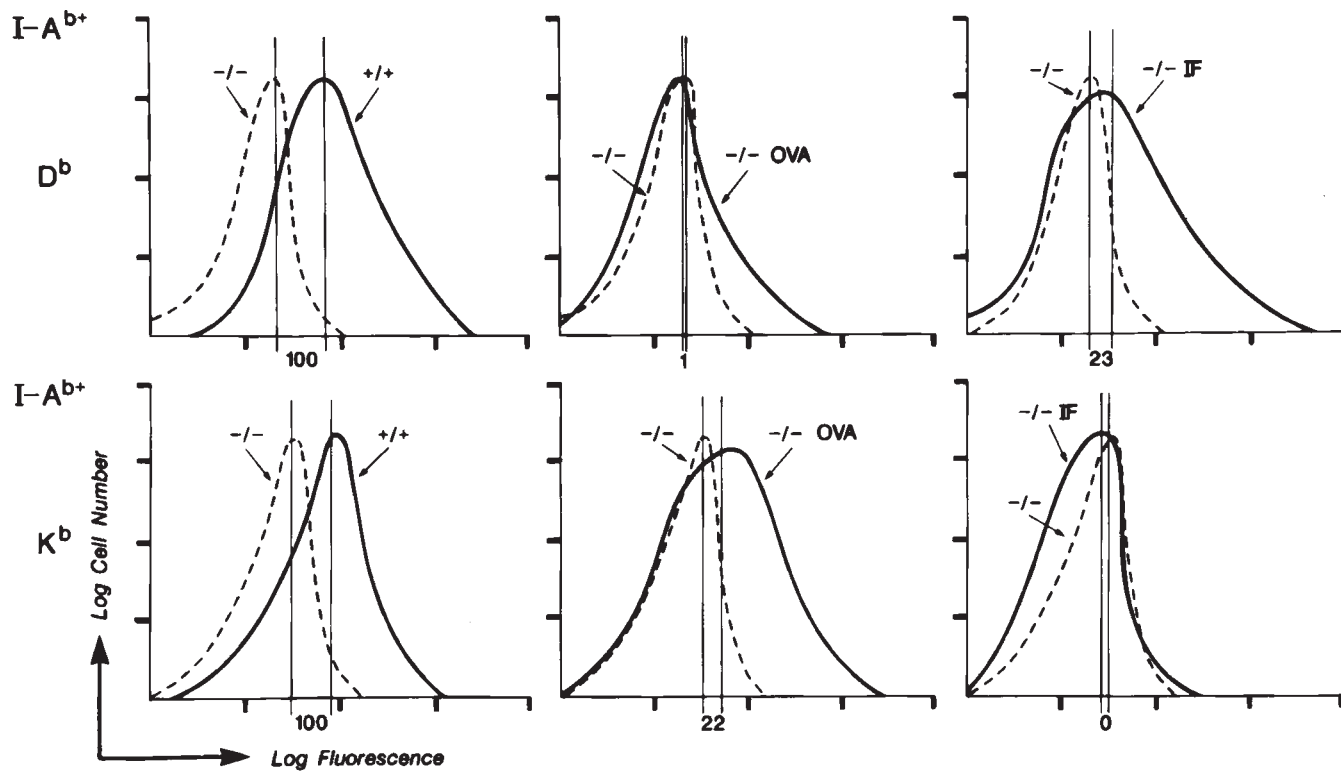


Fig. 1. (Continued)

**B**

### 3.2. Analyzing Expression of MHC Molecules on Thymic Stromal Cells

1. Thymic lobes (5–10) are washed three times in PBS then finely minced with scissors to about 1 mm.
2. Thymic material is incubated in digestion buffer (10 mL) in a 37°C water bath with vigorous agitation.
3. Digestion is stopped by addition of an equal volume of FCS. The cell suspension is separated from the remaining undigested particulate matter by gravity, then cells recovered by centrifugation at 200g at 4°C for 5 min. Cells are washed by resuspension in 4 mL staining buffer and washed twice in staining buffer recovered by centrifugation at 200g at 4°C for 5 min. The washing/centrifugation procedure is then performed once more. Repeating **step 2** further digests the undigested thymic material to generate more cell suspension, which is recovered as described above.
4. Thymic cell suspensions ( $2 \times 10^5$ ) are stained with anti-H-2A<sup>b</sup>-PE, anti-H-2D<sup>b</sup>-biotin and anti-H-2K<sup>b</sup>-FITC (5 µg/mL) in 0.2 mL in 12 × 75-mm tubes for 30 min at 4°C. Cells are washed with staining buffer (1 mL) then recovered by centrifugation at 200g at 4°C for 5 min, centrifuged then stained with SA-APC (2 µg/mL) at 4°C for 15 min. Cells are then washed/centrifuged resuspended in staining buffer (0.5 mL) then analyzed by flow cytometry.
5. Cells are analyzed by three-color flow-cytometry. Dead cells are excluded from the analysis by staining with propidium iodide (PI) and based on their forward and side light scattering properties (*see Note 6*). Thymic stromal cells are identified by their positive staining for H-2A<sup>b</sup>. The expression of class I MHC is determined from histograms for H-2D<sup>b</sup> and H-2K<sup>b</sup> staining, generated from H-2A<sup>b+</sup> cells (*see Fig. 1*).
6. The median intensity of staining for H-2D<sup>b</sup> and H-2K<sup>b</sup> on H-2A<sup>b+</sup> cells in TAP1<sup>-</sup> FTOC incubated with peptide is compared to TAP1<sup>-</sup> FTOC incubated alone. In all experiments, TAP1<sup>+</sup> C57BL/6J wild-type FTOC is analyzed in parallel. Rescue of class I MHC by peptide in TAP1<sup>-</sup> FTOC is expressed as a percentage of the TAP1<sup>+</sup> control (*see Fig. 1*).

---

Fig. 1. (*Opposite page*) Peptide stabilization of class I surface expression in transporter associated with antigen processing 1 (TAP1<sup>-</sup>) fetal thymus organ culture (FTOC). C57BL/6J (+/+) and TAP1<sup>-</sup> (-/-) thymic lobes were cultured for 10 d with the synthetic peptides OVA or IF (500 µM). (A) Thymic stromal cells ( $2 \times 10^5$ ) pooled from 10 protease-digested thymi and stained for H-2A<sup>b</sup>, H-2D<sup>b</sup>, and H-2K<sup>b</sup> surface expression and analyzed by flow-cytometry. (B) To quantitate the surface expression of class I molecules on the gated H-2A<sup>b+</sup> stromal cells, the log relative fluorescence intensity resulting from staining with labeled class I-specific monoclonal antibodies was plotted against the log relative cell number. The histograms for TAP1<sup>-</sup> (-/-) thymi cultured without peptide was compared with the histograms for TAP1<sup>-</sup> (-/-) thymi cultured with peptide or histograms for TAP1<sup>+</sup> (+/+) thymi. The differences between the levels of log mean fluorescence are shown and are expressed as a percentage of the TAP1<sup>+</sup> (+/+) value. (Reproduced from *ref. 8* with permission from Elsevier Science.)



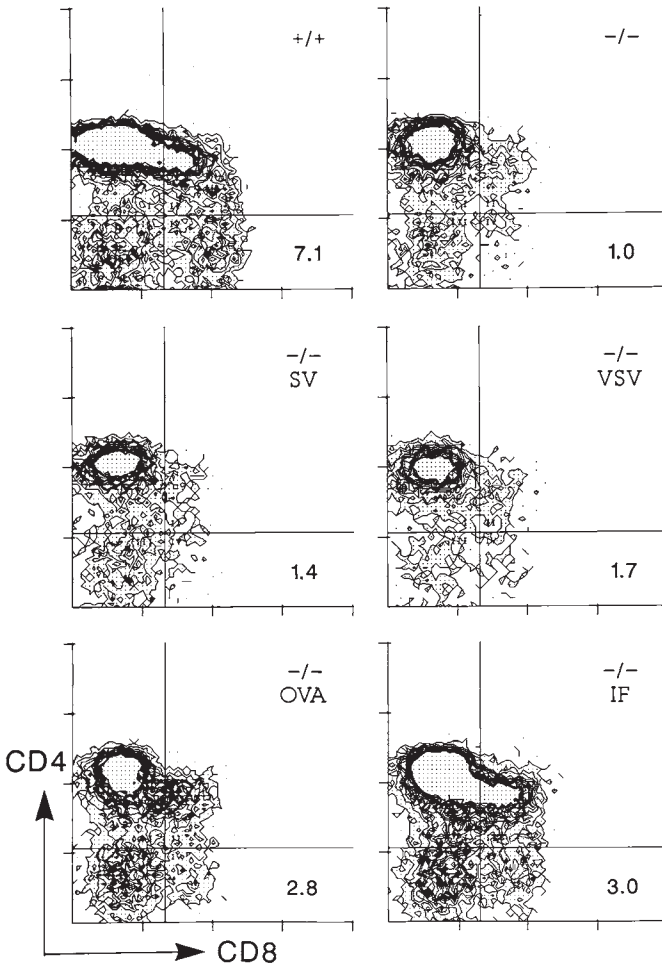


Fig. 2. Synthetic peptides induce the positive selection of CD8<sup>+</sup> cells in transporter associated with antigen processing 1 (TAP1<sup>-</sup>) fetal thymus organ culture (FTOC). C57BL/6J (+/+) and TAP1<sup>-</sup> (-/-) thymic lobes were cultured as described in Fig. 1, with peptide (500  $\mu$ M) where indicated. The peptides used were as follows SV, VSV, OVA, and IF. Thymocytes prepared from individual thymic lobes (about  $1 \times 10^5$ ) were stained for CD3, CD4, and CD8 surface makers and analyzed by flow cytometry. Cells ( $0.5-1 \times 10^5$ ) were gated for high expression of CD3 (typically 10–20% of thymocytes), and then displayed for log fluorescence intensity resulting from staining with CD4 and CD8. The percentages of the gated cells that were CD8<sup>+</sup> CD4<sup>-</sup> are indicated. (Reproduced from ref. 8 with permission from Elsevier Science.)

### 3.3. Analyzing Thymocyte Positive Selection by Flow-Cytometry

1. FTOC is performed as stated above, and after 10 d, lobes mechanically disaggregated in staining buffer.

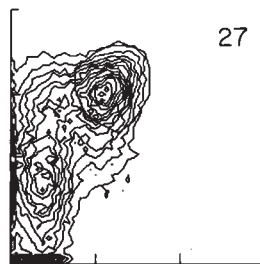
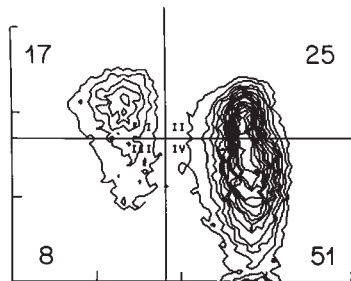
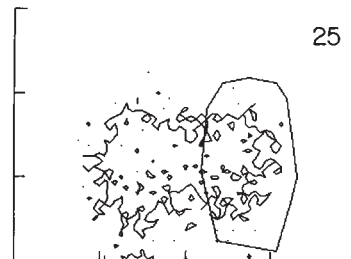
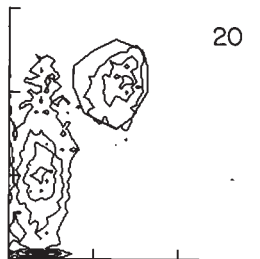
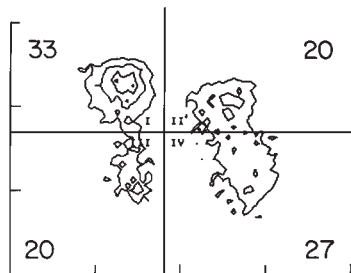
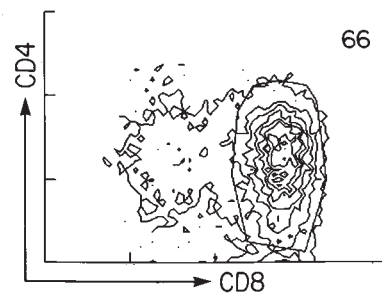
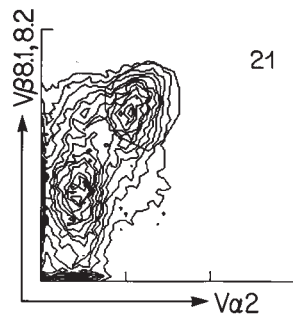
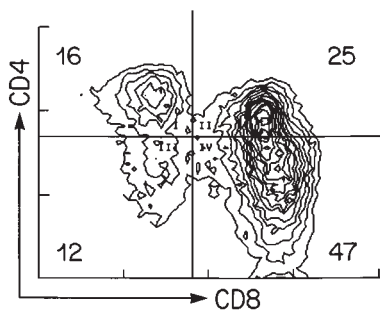
2. Thymocytes ( $1 \times 10^5$ ) are stained with anti-CD4-APC, anti-CD8-FITC, and anti-CD3 $\epsilon$ -PE (all 5  $\mu\text{g}/\text{mL}$ ) for 30 min in 0.2 mL in  $12 \times 75$ -mm tubes at  $4^\circ\text{C}$ . Cells are washed with staining buffer (1 mL) then recovered by centrifugation at 200g at  $4^\circ\text{C}$  for 5 min, twice, then resuspended in staining buffer (0.5 mL).
3. Cells are analyzed by three-color flow-cytometry and dead cells are excluded as in **Subheading 3.2**. Cells successfully positively selected by class I MHC are identified by the CD3 $\epsilon^{\text{hi}}$  CD4 $^-$  CD8 $^+$  phenotype (see **Fig. 2**).
4. The percentage of CD3 $\epsilon^{\text{high}}$  CD4 $^-$  CD8 $^+$  cells in TAP1 $^-$  FTOC incubated with peptide compared to TAP1 $^-$  FTOC incubated alone is determined. In all experiments TAP1 $^+$  C57BL/6J wild-type FTOC is analyzed in parallel to control for variations in CD3 $\epsilon^{\text{hi}}$  CD4 $^-$  CD8 $^+$  cell levels over multiple experiments (see **Fig. 2**). An increase in CD3 $\epsilon^{\text{hi}}$  CD4 $^-$  CD8 $^+$  cell levels in TAP1 mutant mice will indicate that at the given concentration and level of class I rescue, that peptide induces positive selection (see **Note 7**).

### 3.4. Analyzing the Repertoire of Positively Selected Thymocytes by Flow-Cytometry

1. FTOC is performed as stated above, and after 10 d, lobes mechanically disaggregated in staining buffer.
2. Thymocytes ( $1 \times 10^5$ ) are stained with anti-CD3 $\epsilon$ , anti-CD8-FITC, and anti-TCR V $\beta$ -biotin antibodies (all 5  $\mu\text{g}/\text{mL}$ ) for 30 min at in 0.2 mL in  $12 \times 75$ -mm tubes at  $4^\circ\text{C}$ . Cells are washed with staining buffer (1 mL) then recovered by centrifugation at 200g at  $4^\circ\text{C}$ . Cells are then stained with SA-PE (2  $\mu\text{g}/\text{mL}$ ) for 15 min in 0.2 mL in  $12 \times 75$ -mm tubes at  $4^\circ\text{C}$ , then washed/centrifuged twice and resuspended in staining buffer (0.5 mL).
3. Cells are analyzed by three-color flow-cytometry and dead cells are excluded as in **Subheading 3.2**.
4. Thymocytes are gated for CD3 $\epsilon^{\text{hi}}$  cells then the percentage V $\beta^+$  of CD8 $^+$  thymocytes determined (percentage V $\beta^+$  CD8 $^+$  of total CD8 $^+$  of CD3 $\epsilon^{\text{hi}}$ ). This is repeated for a range of TCR V $\beta$  elements (see **Subheading 2.2**).
5. The percent V $\beta^+$  CD8 $^+$  of total CD8 $^+$  of CD3 $\epsilon^{\text{hi}}$  thymocytes is determined for TAP1 $^-$  FTOC incubated with various single peptides or mixtures and compared with TAP1 $^+$  FTOC. If a peptide selects a diverse repertoire of CD8 $^+$  thymocytes one expects to see all of the V $\beta^+$  subpopulations tested represented. Variation in the proportion of a given V $\beta^+$  subpopulation from that of the level in TAP1 $^+$  FTOC indicates a skewing of the repertoire by a given peptide (see **Note 8**).

### 3.5. Analyzing Negative Selection in P14 FTOC

1. FTOC from the offspring of P14 $^{+/+}$   $\times$  wild-type C57BL/6J mice are cultured as in **Subheading 3.1**. for 9 d in the presence or absence of LCMV (3–300  $\mu\text{M}$ ) or an irrelevant peptide control (DB-S or IF at 300  $\mu\text{M}$ ) (see **Note 10**).
2. Thymic lobes are disaggregated (**Subheading 3.3**.) and the number of live thymocytes determined. Trypan blue (1%) is added to thymocyte suspensions (10  $\mu\text{L}$ ) and viable trypan blue excluding cells counted under a light microscope ( $\times 40$  magnification) (see **Note 9**).

*TAP-1<sup>+</sup>**TAP-1<sup>+</sup>*  
*LCMV*  
*(30 μM)**TAP-1<sup>+</sup>*  
*IF*  
*(300 μM)*

3. Thymocytes are stained with anti-CD8-FITC, anti-CD4-APC, anti-TCR V $\alpha$ 2-PE, and anti-TCR V $\beta$ 8.1, 8.2-biotin (-SA-Texas Red) antibodies then analyzed by four-color flow-cytometry (see **Subheading 3.3.** and **Note 11**).
4. Thymocytes are gated for high expression of V $\alpha$ 2 and V $\beta$ 8.1, 8.2 (P14 TCR) then analyzed for CD4 and CD8 expression (see **Fig. 3**). The overall percentage of CD8<sup>+</sup> P14 cells is determined by multiplying the percentage of V $\alpha$ 2<sup>+</sup> high, V $\beta$ 8.1, 8.2<sup>+</sup> high cells by the percentage of the gated CD4<sup>-</sup> CD8<sup>+</sup> cells. The percentage of CD4<sup>-</sup> CD8<sup>-</sup>, CD4<sup>+</sup> CD8<sup>+</sup>, and CD4<sup>+</sup> CD8<sup>-</sup> is determined from CD4 by CD8 plots without TCR gating (see **Fig. 3**) (see **Note 12**).
5. The absolute cell numbers of the CD8<sup>+</sup> P14, CD4<sup>-</sup>CD8<sup>-</sup>, CD4<sup>+</sup>CD8<sup>+</sup>, and CD4<sup>+</sup>CD8<sup>-</sup> populations are calculated by multiplying the total number of thymocytes by the relevant percentage.
6. Negative selection is indicated by a decrease in the absolute cell number of CD8<sup>+</sup> P14 and CD4<sup>+</sup>CD8<sup>+</sup> populations (see **Fig. 4** and **Note 13**).

#### 4. Notes

1. An exogenous source of  $\beta$ 2-microglobulin must be provided in the culture medium for the stabilization of peptide:MHC class I heavy chains on thymic stromal cells (8). If purified human  $\beta$ 2-microglobulin is unavailable, the bovine  $\beta$ 2-microglobulin present in RPMI 1640 –10% FCS is sufficient for the stabilization of MHC class I on TAP1<sup>-</sup> FTOC by synthetic peptides (10).
2. After solid phase synthesis, it is common for peptides to be contaminated with toxic organics and truncated peptides. High-pressure liquid chromatography purification ensures that only full-length peptides free from toxic contaminants are used in FTOC.
3. For the LCMV peptide, the C-terminal cysteine residue (C) is replaced by a methionine (M) to avoid solubility problems associated with the formation of aggregates after oxidation.

---

Fig. 3. (*Opposite page*) Negative selection of CD8<sup>+</sup> transgenic P14 cells by the nominal antigen peptide in transporter associated with antigen processing 1 (TAP1<sup>+</sup>) fetal thymus organ culture (FTOC). P14 TAP1<sup>+</sup> thymic lobes were cultured with or without lymphocytic choriomeningitis virus (LCMV) peptide (30  $\mu$ M) or the IF peptide (300  $\mu$ M) for 9 d. Cells ( $4 \times 10^4$ ) were stained with anti-CD8-FITC, anti-CD4-APC, anti-TCR V $\alpha$ 2-PE, and anti-TCR V $\beta$ 8.1, 8.2-biotin (-SA-Texas Red) antibodies then analyzed by flow-cytometry. The percentages of cells falling into quadrants resulting from the analysis of CD4 and CD8 staining are indicated. Stained cells were gated for high expression of V $\alpha$ 2 and V $\beta$ 8.1, 8.2 (P14) (percentage shown next to window) and then displayed for log fluorescence intensity resulting from staining for CD4 and CD8. The percentage of this gated population positive for CD8 and negative for CD4 is shown next to the window. The overall percentage of CD8<sup>+</sup> P14 cells was determined by multiplying the percentage of V $\alpha$ 2<sup>+</sup> high, V $\beta$ 8.1, 8.2<sup>+</sup> high cells by the percentage of the gated CD4<sup>-</sup> CD8<sup>+</sup> cells. (Reproduced from **ref. 10** with permission from Elsevier Science.)

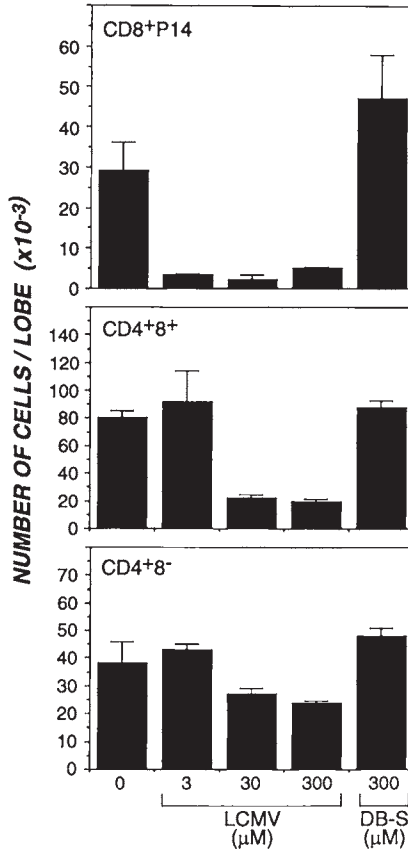


Fig. 4. Histograms showing the negative selection of P14 CD8<sup>+</sup> thymocytes in P14 fetal thymus organ culture (FTOC). P14 thymic lobes were cultured with lymphocytic choriomeningitis virus (LCMV) (3–300 μM) or an irrelevant peptide control DB-S (300 μM) for 9 d as described in Fig. 3 and the percentages of thymocyte subsets determined. The absolute number of a given cell type per lobe was determined by multiplying the percentage by the number of thymocytes per lobe and is the mean (±SEM) from six lobes. (Reproduced from ref. 10 with permission from Elsevier Science).

4. For the combination of fluorochromes used, most dual laser flow-cytometers will be appropriate. Commonly available instruments are the BD FACSCalibur (48-nm argon-ion laser, 635-nm red diode laser) and the BD FACSCanto (488-nm sapphire OPSL laser, 633-nm He Ne laser) (Becton, Dickinson and Company).
5. When added directly to culture medium, peptides with a high proportion of large hydrophobic residues may not go into solution immediately. Warming the resuspended peptide at 37°C for 30 min and shaking can remedy this. This is usually a problem only at peptide concentrations >100 μM.

6. It is common to have clumps of dead cells in suspensions of trypsinized FTOC that may cause blockages during flow-cytometry. Therefore, it is recommended to filter cell suspensions through a fine mesh, such as Spectramesh (Spectrum Laboratories, Rancho Dominguez, CA) cut into 2-cm squares, to remove clumps of dead cells. In addition, care should be taken to gate out dead cells during flow-cytometry. Dead cells are identified by staining positive with PI (1  $\mu\text{g}/\text{mL}$ ) added directly to staining buffer and on the basis of characteristically high light side-scatter and low light forward-scatter.
7. Not all peptides that stabilize class I MHC molecules on the surface of TAP1<sup>-</sup> thymic stromal cells will rescue the positive selection of CD4<sup>-</sup>CD8<sup>+</sup> thymocytes (8). This is because peptide presented by MHC class I molecules is specifically recognized by the TCRs of CD4<sup>+</sup>CD8<sup>+</sup> thymocytes during positive selection. Mixtures of MHC class I-binding peptides have been shown to be more effective than single peptides at inducing the selection of CD4<sup>-</sup>CD8<sup>+</sup> thymocytes in TAP1<sup>-</sup> FTOC (8). These can be generated synthetically or as preparations of self-peptides (8,13).
8. To improve the resolution of TCR repertoire analysis of positively selected CD4<sup>-</sup>CD8<sup>+</sup> thymocytes, one can employ molecular biology methods. These include spectrotyping, which determines the frequencies of thymocytes expressing individual V $\alpha$  and V $\beta$  gene segments, and the cloning and sequencing of clonally expressed rearranged TCR genes (14).
9. One can use the flow-cytometer to count the number of viable thymocytes. This may be useful if an experiment involves a large number of thymic lobes. Most flow-cytometers can be set to acquire cells for a set time (e.g., 1 min) and with knowledge of the flow-rate (10–100  $\mu\text{L}/\text{min}$ ) the number of cells in a suspension derived from a single thymic lobe can be determined.
10. The DB-S and IF peptides can bind H-2D<sup>b</sup> but have negligible affinity for the P14 TCR and so can not induce the negative selection of P14 CD8 thymocytes (10). Therefore these irrelevant peptides are useful controls for the effects of nonspecific toxicity of peptide on the recovery of thymocytes from P14 FTOC.
11. For multicolor analysis it is standard practice to first run single and multiply stained control cells to set the voltage and compensations for a given flow-cytometer. One should follow the detailed instructions of the manufacturer to calibrate the flow-cytometer before acquiring data from stained cells.
12. Because of variation in thymocyte numbers between lobes, at least four lobes should be analyzed for a given concentration of peptide.
13. To determine the onset of negative selection, it is vitally important to determine the absolute number as well as the percentages of thymocyte subsets. The deletion of CD4<sup>+</sup>CD8<sup>+</sup> or even CD4<sup>-</sup>CD8<sup>+</sup> may not always give a decrease in percentage but will always give a decrease in absolute cell number (10). Some also interpret an increase in the percentage of CD4<sup>-</sup>CD8<sup>-</sup> thymocytes as evidence of negative selection (10).

## Acknowledgments

The author would like to thank Professors Luc Van Kaer, Susumu Tonegawa, and Hidde Ploegh, for their help and support in developing TAP1<sup>-</sup> FTOC and Carol Browne for technical assistance.

## References

1. Zinkernagel, R. M. and Doherty, P. C. (1974) Restriction of *in vitro* T cell mediated cytotoxicity in lymphocytic choriomeningitis within a syngeneic or semi-allogeneic system. *Nature* **248**, 701–702.
2. Bevan, M. J. (1977) In a radiation chimera, host H-2 antigens determine immune responsiveness of donor cytotoxic cells. *Nature* **269**, 417–418.
3. Schwartz, R. (1989) Acquisition of immunological self-tolerance. *Cell* **57**, 1073–1081.
4. Townsend, A., Ohlen, C., Bastin, J., Ljunggren, H. -G., Foster, L., and Karre, K. (1989) Association of class I major histocompatibility heavy and light chains induced by viral peptides. *Nature* **340**, 443–448.
5. Lo, D. and Sprent, J. (1986) Identity of cells that imprint H-2 restricted T cell specificity in the thymus. *Nature* **319**, 672–675.
6. Teh, H. S., Kisielow, P., Scott, B., et al. (1988) Thymic major histocompatibility complex antigens and the alpha beta T-cell receptor determine the CD4/CD8 phenotype of T cells. *Nature* **335**, 229–233.
7. Van Kaer, L., Ashton-Rickardt, P. G., Ploegh, H. L., and Tonegawa, S. (1992) TAP1 mutant mice are deficient in antigen presentation, surface class I molecules, and CD4-8+ T cells. *Cell* **71**, 1205–1214.
8. Ashton-Rickardt, P. G., Van Kaer, L., Schumacher, T. N., Ploegh, H. L., and Tonegawa, S. (1993) Peptide contributes to the specificity of positive selection of CD8+ T cells in the thymus. *Cell* **73**, 1041–1049.
9. Pircher, H. -P., Burki, K., Lang, R., Hengartner, H., and Zinkernagel, R. M. (1989) Tolerance induction in double specific T cell receptor transgenic mice varies with antigen. *Nature* **342**, 559–561.
10. Ashton-Rickardt, P. G., Bandeira, A., Delaney, J. R., et al. (1994) Evidence for a differential avidity model of T cell selection in the thymus. *Cell* **76**, 651–663.
11. Jenkinson, E. J., Van Ewijk, W., and Owen, J. J. (1981) Major histocompatibility complex antigen expression on the epithelium of the developing thymus in normal and nude mice. *J. Exp. Med.* **153**, 280–292.
12. Pircher, H. -P., Brduscha, K., Steinhoff, U., et al. (1993) Tolerance induction by clonal deletion of CD4+8+ thymocytes *in vitro* does not require dedicated antigen-presenting cells. *Eur. J. Immunol.* **28**, 669–674.
13. Hu, Q., Bazemore Walker, C. R., Girao, C., et al. (1997) Specific recognition of thymic self-peptides induces the positive selection of cytotoxic T lymphocytes. *Immunity* **7**, 221–231.
14. Pacholczyk, R., Kraj, P., and Ignatowicz, L. (2001) An incremental increase in the complexity of peptides bound to class II MHC changes the diversity of positively selected alpha beta TCRs. *J. Immunol.* **166**, 2357–2363.

## Investigating Central Tolerance With Reaggregate Thymus Organ Cultures

Graham Anderson and Eric J. Jenkinson

### Summary

In the thymus, immature CD4<sup>+</sup>8<sup>+</sup> thymocytes expressing randomly rearranged T-cell receptor  $\alpha$ - and  $\beta$ -chain genes undergo positive and negative selection events based on their ability to recognize self-peptide/major histocompatibility complex (MHC) molecules expressed by thymic stromal cells. In vivo analysis of the role of thymic stromal cells during intrathymic selection is made difficult by the cellular complexity of the thymic microenvironment in the steady-state adult thymus, and by the lack of appropriate targeting strategies to manipulate gene expression in particular thymic stromal compartments. We have shown that the thymic microenvironment can be readily manipulated in vitro through the use of reaggregate thymus organ cultures, which allow the preparation of three-dimensional thymus lobes from defined stromal and lymphoid cells. Although other in vitro systems support some aspects of T-cell development, reaggregate thymus organ culture remains the only in vitro system able to support efficient MHC class I and II-mediated thymocyte selection events, and so can be used as an effective tool to study the cellular and molecular regulation of positive and negative selection in the thymus.

**Key Words:** Thymus organ culture; reaggregate thymus organ culture; repertoire selection; thymic stromal cells; thymic microenvironment; cell separation.

### 1. Introduction

To mount effective immune responses, the peripheral lymphocyte pool must contain functionally competent CD4<sup>+</sup> and CD8<sup>+</sup> T cells that are capable of responding to invading foreign pathogens, while remaining tolerant to self-antigens. Self/nonself discrimination in the T-cell lineage is imposed in the thymus, where the specificities of  $\alpha\beta$ T-cell receptor ( $\alpha\beta$ TCR) complexes expressed by immature CD4<sup>+</sup>CD8<sup>+</sup> precursors are screened for their ability to recognize self-peptide/major histocompatibility complexes (MHC). Although failure to recognize self-peptide/MHC results in death by neglect (*1*), thymocytes expressing  $\alpha\beta$ TCRs



that bind with low affinity/avidity are triggered to undergo a differentiation program termed positive selection, resulting in the generation of MHC class I restricted CD8<sup>+</sup> and MHC class II restricted CD4<sup>+</sup> T cells (2). In contrast, high affinity/avidity interactions between TCR and self-peptide/MHC results in negative selection, where potentially autoreactive T cells are eliminated from the developing TCR repertoire by the induction of apoptosis (3,4).

Interactions between developing thymocytes and thymic stromal cells play a critical role during intrathymic selection events. For example, experiments using T-cell receptor transgenic mice demonstrated that radio-resistant thymic stromal elements are important in the regulation of positive selection, while bone marrow-derived thymic stromal cells are effective mediators of negative selection (reviewed in ref. 5). Thus, functional compartmentalisation of the thymic stromal microenvironment plays a role in the regulation of positive and negative selection of thymocytes (6). However, unlike the range of cell-type and stage-specific constructs (e.g., p56<sup>lck</sup> transgene promoter, p56<sup>lck</sup> Cre-recombinase) that allow study of the consequences of manipulating gene expression in defined T-cell precursor populations in vivo (7,8), gaining a better understanding of the mechanisms regulating thymic selection is hampered by difficulties in manipulating, and assessing the function of, thymic stromal cells in vivo.

In recent years, the use of engineered stromal cell lines such as OP9DL1 have proved to be effective tools to study the role of Notch signaling in the development of early T-cell precursors (9). However, with regard to the study of T-cell repertoire selection, the absence of MHC class II expression by OP9DL1 currently prevents the use of this system for the study of CD4<sup>+</sup> T-cell positive selection. Moreover, although coculture of immature CD4<sup>+</sup>8<sup>-</sup> precursors with OP9DL1 has been shown to result in the generation of mature CD8<sup>+</sup> T cells, it is unclear whether this involves a typical positive selection program involving maturation from a CD4<sup>+</sup>8<sup>+</sup> precursor (10). To provide an accessible in vitro system with which to study T-cell selection events, we developed an experimental approach that allows us to monitor the responses of a single cohort of preselection CD4<sup>+</sup>8<sup>+</sup> thymocytes in the context of defined thymic stromal cells, in the absence of other stages and events normally occurring within the steady-state thymus (11). The experimental approaches described here detail the generation of cultures to study positive selection of immature CD4<sup>+</sup>8<sup>+</sup> thymocytes by thymic epithelial cells. Dendritic cell preparations can also be added to the cell mixtures prior to reaggregate formation, to enable the study of thymocyte negative selection (11,12). These approaches can be readily manipulated, for example by the addition of antigenic peptides, neutralizing antibodies, and, more recently, through the use of gene targeted thymic stromal cells (13), to provide the user with a system to investigate cellular and molecular aspects of MHC class I- and II-mediated thymic selection.

**Table 1**  
**Preparation of RPMI-1640 +10% FCS for Dissection and Cell Handling**

Medium and additives	Volume	Final concentration
RPMI-1640 + 20 mM HEPES, with L-glutamine, without bicarbonate	10 mL	–
200 mM L-Glutamine	100 $\mu$ L	2 mM
5000 IU/mL Penicillin and 5000 $\mu$ g/mL streptomycin	200 $\mu$ L	100 IU/mL, 100 $\mu$ g/mL
Heat-inactivated fetal calf serum	1 mL	10%

**Table 2**  
**Preparation of DMEM + 10% FCS for Organ Culture**

Medium and additives	Volume	Final concentration
Dulbecco's medium with 3.7 g/L bicarbonate, without glutamine	10 mL	–
100X Nonessential amino acids	100 $\mu$ L	1X
1 M HEPES	100 $\mu$ L	10 mM
$5 \times 10^{-3}$ M 2-Mercaptoethanol	100 $\mu$ L	$5 \times 10^{-5}$ M
200 mM L-Glutamine	200 $\mu$ L	4 mM
5000 IU/mL Penicillin and 5000 $\mu$ g/mL streptomycin	200 $\mu$ L	100 IU/mL, 100 $\mu$ g/mL
Heat-inactivated fetal calf serum	1 mL	10%

## 2. Materials

### 2.1. Cell Culture

1. Dulbecco's modified Eagle's medium (DMEM) supplemented as shown in [Table 1](#).
2. RPMI-1640 medium, supplemented as shown in [Table 2](#).
3. Additives stored at  $-20^{\circ}\text{C}$ : heat-inactivated fetal calf serum (FCS), 200 mM glutamine, 5000 IU/mL penicillin, and 5000  $\mu$ g/mL streptomycin. Additives stored at  $4^{\circ}\text{C}$ : 100X nonessential amino acids, 2-mercaptoethanol, 1 M HEPES.
4. 2-Deoxyguanosine (2-dGuo, Sigma) is added to organ culture medium to eliminate endogenous lymphoid and dendritic cells from fetal thymic lobes ([14](#)). Store stock solutions of 9 mM 2-dGuo at  $-20^{\circ}\text{C}$  prior to addition to culture medium to give a final concentration of 1.35 mM (*see Note 1*).

### 2.2. Microdissection and Handling of Fetal Thymus Lobes

1. Surgical scissors and no. 5 watchmakers' forceps (TAAB, Berkshire, UK).
2. Aspirator tube assembly for use with mouth capillary pipets (Sigma, cat. no. A5177-SEA).
3. Glass rods to make capillary pipets (soda-lime tubing with internal diameter of 4 mm, Fisher Scientific, Loughborough, UK, cat. no. FB1460).

### **2.3. *Thymus Organ Culture***

1. Timed pregnant mice, at 14–15 d of gestation, with day 0 as day of detection of vaginal plug.
2. Isopore membrane filters (Millipore, Watford, UK; cat. no. ATTP01300), 0.8- $\mu$ m pore size, 13 mm in diameter. Prior to use, boil once in large volume of double-distilled water (DDW), and place in bacteriological grade 90-mm diameter Petri dishes (Sterilin) in a laminar flow hood to dry.
3. Artwrap sponge (Medipost Ltd., Weymouth, Dorset, UK), cut into 1-cm<sup>2</sup> pieces. Prior to use, boil three times in large volumes of DDW, and place in bacteriological grade 90-mm diameter Petri dishes in a laminar flow hood to dry.
4. Plastic sandwich boxes with fitted lids (174-mm length, 60-mm depth, 45-mm height, Watkins and Doncaster, Cranbrook, Kent, UK; cat. no. E6052).
5. Sterile bacteriological grade 90-mm Petri dishes.
6. Tissue culture incubator set at 37°C with an input of 10% CO<sub>2</sub> in air, or a cylinder containing 10% CO<sub>2</sub> in air to gas culture boxes prior to transfer to a non-CO<sub>2</sub> tissue culture incubator.

### **2.4. *Fetal Thymic Disaggregation***

1. Phosphate buffered saline (PBS) without Ca<sup>2+</sup>/Mg<sup>2+</sup>.
2. Trypsin in Hank's balanced salt solution, stored at –20°C as a 2.5% stock. Prior to use, dilute in 0.02% EDTA in Ca<sup>2+</sup>/Mg<sup>2+</sup> free PBS to give a working concentration of 0.25%.

### **2.5. *Depletion of CD45<sup>+</sup> Macrophages From 2-dGuo Stromal Preparations***

1. Anti-rat IgG coated Dynabeads (Dynal, Wirral, UK; cat. no. 110.35).
2. Dynal Magnetic Particle Collector (MPC-E, Dynal, cat. no. 120.04).
3. Rat-anti mouse CD45 antibody (any pan-CD45 clone, e.g., M1/9).
4. 2-mL Round-bottomed cryogenic freezing vials.

### **2.6. *Preparation of CD4<sup>+</sup>8<sup>+</sup> Thymocytes From Neonatal Thymus***

1. Anti-rat IgG-coated Dynabeads (Dynal).
2. Magnetic particle collector (Dynal).
3. 2-mL Round-bottomed cryogenic freezing vials.
4. Rat-anti mouse CD8 $\alpha$  (e.g., clone 53-6.7, eBioscience).
5. Rat-anti mouse CD3 (e.g., clone KT3, Serotec).

## **3. Methods**

All procedures are performed in a laminar flow tissue culture hood, with surfaces swabbed with 70% ethanol prior to use. A stereo-dissection microscope with an objective lens magnification range of  $\times 0.8$  to  $\times 5$ , fitted with  $\times 10$  eyepieces is very useful for embryonic dissection and for the formation of reaggregate cultures.

We currently use several types of dissecting microscopes (e.g., Stemi SV11, Zeiss; SMZ645, Nikon) that work well for the procedures described here. For general cell handling and dissection of tissue, we use RPMI-1640 +10% FCS supplemented as shown in **Table 1**. All centrifugation steps are performed at 4°C for 10 min at 400g. For all organ and reaggregate cultures, we use DMEM containing 10% FCS, supplemented as in **Table 2**.

### 3.1. Preparation of 2-dGuo-Treated Alynphoid Thymus Organ Cultures

1. Pregnant mice are killed by cervical dislocation at day 14 or 15 of pregnancy. Following deflection of the skin to avoid contamination by fur, cut through the abdominal wall and remove the intact uterus, which is removed by making a “V”-shaped incision in the abdominal region, from the two lateral horns of the uterus to the bladder in the midline.
2. Remove the embryos from the uterus still in their amniotic sacs by cutting along the length of the uterine wall with surgical scissors (*see Note 2*).
3. Wash the embryos in a 90-mm Petri dish containing 10 mL PBS, and remove the amniotic sac and placenta of each embryo by carefully tearing it open using two pairs of watchmakers’ forceps. Transfer the embryos to a fresh Petri dish containing 10 mL of a 50:50 mixture of PBS:RPMI-1640 medium supplemented with 10% FCS.
4. Using a stereo-dissecting microscope, with the embryo submerged in medium, decapitate the embryo using watchmakers’ forceps and manoeuvre it onto its back (*see Note 3*). Open the anterior surface of the chest wall by placing the tips of a closed pair of forceps into the chest cavity, and then allow the forceps to open, to reveal the internal thoracic cavity. Remove the entire thoracic tree—heart, lungs, trachea, and thymuses—by grasping gently below the heart (seen as a red “apple-shaped” organ) and place into a dish containing 10 mL RPMI-1640 +10% FCS.
5. In a 14- to 15-d embryo, the thymic rudiments are situated in the midline above the heart, on either side of the trachea. Remove individual thymus lobes from the thoracic trees using watchmakers’ forceps, and remove excess connective tissue and any adherent blood before explanting in organ culture.
6. For 2-dGuo organ culture, place 600  $\mu$ L of 9 mM stock of thawed 2-dGuo into a 90-mm bacterial plastic Petri dish, and add 4 mL prewarmed DMEM medium supplemented as shown in **Table 1**. Ensure that all the surface of the Petri dish is covered with medium, and no bare areas of plastic remain.
7. Using forceps, place two sterile Artwrap sponges (precut to 1 cm<sup>2</sup>) into the dish. After 30 s to allow medium to pass into the sponge, turn the sponge over so that both sides are wet. This ensures that medium in the dish has access to the tissue. Again using forceps, place a 0.8- $\mu$ m filter onto the surface of each sponge.
8. Use the glass tubing described in **Subheading 2.2**. to make a fine glass capillary pipet (*see Notes 4 and 5*). Start by heating the glass tubing in a Bunsen flame until the glass is pliable. Once this stage is achieved, remove the glass from the flame and pull on both ends to stretch the heated glass, much in the same way as making

a Pasteur pipet from a glass rod. Aim to stretch the glass no more than 10 cm, and then let it cool. Once cool, pull on each end to snap the stretched area, which will produce two tapered glass pipets, where the thinned area of each is around 5 cm in length, and the diameter of the end of the pipet is around 0.5 mm.

9. Place the untapered end of the glass pipet into the tubing of the mouth capillary apparatus, and place a small disposable plastic pipet tip in the other end of the tubing, as a mouthpiece. Using careful mouth control, pick up individual thymus lobes and place on the surface of the 0.8- $\mu\text{m}$  filter in organ culture (*see Note 6*).
10. Once sufficient dishes are set up, place up to three dishes into a plastic sandwich box containing DDW and the lid of a 90-mm Petri dish as a support. The level of water should not be above the level of the platform. Seal the lid on the box with adhesive tape. The lid of the sandwich box has two 5-mm drilled holes in opposite corners, as air holes. Boxes can be gassed with a mixture of 10%  $\text{CO}_2$  in air directly from a gas cylinder where the air is filtered by placing a 0.2- $\mu\text{m}$  filter membrane in the tubing from the cylinder to the box. After 10 min, air holes are sealed with adhesive tape and the box is placed in a 37°C tissue culture incubator. Alternatively, boxes can be placed with unsealed air holes into 37°C tissue culture incubators with a source of 10%  $\text{CO}_2$  in air (*see Note 7*).

### **3.2. Disaggregation of 2-dGuo-Treated Thymus Lobes To Produce Thymus Stromal Preparations**

1. Harvest 2-dGuo treated thymus lobes after 5–7 d, by transferring the 0.8- $\mu\text{m}$  filters to a Petri dish containing RPMI-1640 +10% FCS, and then submerging them. Thymus lobes that do not float off immediately after submersion can be gently pushed off using the closed end of a pair of Watchmakers' forceps (*see Note 8*).
2. Once all lobes have been harvested, use a 1-mL blue tip on a pipet to transfer the lobes to a 1.5-mL Eppendorf tube.
3. Allow the lobes to settle to the bottom of the tube under unit gravity and remove the medium.
4. Wash the lobes by placing 1 mL  $\text{Ca}^{2+}/\text{Mg}^{2+}$  free PBS into the Eppendorf tube, and then let the lobes sink to the bottom again. Repeat this so the lobes get three 1-mL washes.
5. Remove the last PBS wash, and add 600  $\mu\text{L}$  of an ice cold 0.25% trypsin solution (made from a 1:10 dilution of freshly thawed 2.5% stock, using 0.02% EDTA in  $\text{Ca}^{2+}/\text{Mg}^{2+}$  free PBS as the diluent).
6. Place the Eppendorf tube in a 37°C incubator for 25 min.
7. Gently resuspend the lobes using a 1-mL blue tip on a pipet for 10 s, and then place back in the incubator for 20 min.
8. Use a 1-mL blue tip on a P1000 Pipetman Gilson pipet to complete the disaggregation of the thymus lobes to form a single cell suspension. This should take about 30 s to complete.
9. Add 400  $\mu\text{L}$  of ice cold RPMI-1640 +10% FCS to neutralize the trypsin, and pellet cells by centrifugation. Resuspend the pellet in 1 mL RPMI-1640 +10% FCS and count cells (*see Note 9*).

### **3.3. Depletion of Residual CD45<sup>+</sup> Macrophages With Antibody-Coated Magnetic Beads**

1. To prepare anti-CD45 coated Dynabeads, wash 100  $\mu$ L of anti-rat IgG Dynabeads three times in 1-mL volumes of RPMI-1640 +10% FCS (*see Note 10*).
2. Resuspend beads in 500- $\mu$ L volume of 5  $\mu$ g/mL pan anti-CD45 antibody, and leave at 4°C overnight to allow antibody to bind to the beads.
3. After overnight incubation, wash beads three times in 1-mL volumes of RPMI-1640 +10% FCS to remove excess antibody, and resuspend in 100  $\mu$ L RPMI-1640 +10% FCS.
4. Resuspend freshly disaggregated 2-dGuo-treated thymic stromal cells in 200  $\mu$ L RPMI-1640 +10% FCS and transfer to 2-mL round-bottomed freezing vial (*see Note 11*).
5. Add 50  $\mu$ L of the anti-CD45 coated anti-rat IgG beads and centrifuge. This centrifugation step facilitates bead–cell interactions, and results in effective rosette formation.
6. Resuspend cells by gentle pipetting and transfer to a 1.5-mL Eppendorf tube.
7. Place the tube on Dynal Magnetic Particle Collector and allow rosetted cells to accumulate on the magnet. Carefully remove the supernatant and discard the bead pellet.
8. Transfer unrosetted cells to a fresh freezing vial and repeat **steps 5–7**.
9. After final centrifugation with beads, resuspend the cells in 1 mL RPMI-1640 +10% FCS and count (*see Note 12*).

### **3.4. Preparation of CD4<sup>+</sup>8<sup>+</sup> Thymocytes From Newborn Thymus**

1. To prepare anti-CD3 coated Dynabeads, wash 300  $\mu$ L of anti-rat IgG Dynabeads three times in 1-mL volumes of RPMI-1640 +10% FCS.
2. Resuspend beads in a 1-mL volume of 10  $\mu$ g/mL pan anti-CD3 antibody, and leave at 4°C overnight to allow antibody to bind to the beads.
3. To prepare anti-CD8 coated Dynabeads, wash 100  $\mu$ L of anti-rat IgG Dynabeads three times in 1-mL volumes of RPMI-1640 +10% FCS.
4. Resuspend beads in a 500- $\mu$ L volume of 5  $\mu$ g/mL of anti-CD8 antibody, and leave at 4°C overnight to allow antibody to bind to the beads.
5. After overnight incubation, wash both types of beads three times in 1-mL volumes of RPMI-1640 +10% FCS to remove excess antibody, and resuspend in RPMI-1640 +10% FCS (100  $\mu$ L for anti-CD8 beads and 300  $\mu$ L for anti-CD3 beads).
6. Remove thymus lobes from 1–2 d old neonatal mice. First, decapitate the neonate, and use scissors to cut through the anterior aspect of the ribcage. Open the thorax and remove the thymus lobes, lying above the heart, with forceps. Clean off excess blood and transfer to fresh RPMI-1640 medium containing 10% FCS.
7. Tease apart the newborn thymus using Watchmakers' forceps and prepare a cell suspension of  $1.2 \times 10^7$  cells.
8. Centrifuge cells and resuspend in 200  $\mu$ L RPMI-1640 +10% FCS. Transfer to a freezing vial.
9. Add 100  $\mu$ L of anti-CD3 coated beads and centrifuge. Resuspend the pellet and spin again.

10. Remove and discard the rosetted cells on Dynal magnetic particle collector, as in **Subheading 3.3**.
11. Repeat **steps 9 and 10** until three rounds of depletion have been achieved, each using 100  $\mu\text{L}$  of beads.
12. Count the cells, and add an appropriate volume of anti-CD8 coated beads to give a final ratio of cells to beads of 1:3.
13. Centrifuge, resuspend the pellet, and centrifuge again.
14. Collect the rosetted cells by magnet and wash three times in 600  $\mu\text{L}$  of  $\text{Ca}^{2+}/\text{Mg}^{2+}$  free PBS.
15. Resuspend rosettes in 600  $\mu\text{L}$  0.25% trypsin/0.02% EDTA for 2 min at 37°C, pipetting after 1 min.
16. Make up the volume to 1 mL with medium, remove the beads and remaining rosettes by magnet.
17. Centrifuge, resuspend cells in fresh RPMI-1640 +10% FCS and count.

### **3.5. Formation of Reaggregate Thymus Organ Cultures**

1. In a 1.5-mL Eppendorf tube, mix preselection  $\text{CD4}^{+8+}$  thymocytes with freshly prepared CD45 depleted 2-dGuo-treated thymic stromal cells (*see Note 13*).
2. Pellet cells by centrifugation.
3. Using a 200- $\mu\text{L}$  tip on a P200 Pipetman Gilson pipet, carefully remove all the supernatant from the cell pellet (*see Note 14*).
4. Vortex the cell pellet for 10 s on a benchtop Whirlimixer, to form a cell slurry.
5. Using a mouth-controlled finely drawn glass pipet, draw the slurry into the pipet, keeping the suspension of cells at the tip of the pipet (*see Note 15*).
6. Under direct visual observation, deposit the cell slurry using mouth control, into the center of the surface of a 0.8- $\mu\text{m}$  filter, supported by an Artwrap sponge in a 90-mm Petri dish containing 4 mL DMEM +10% FCS (*see Note 16*).
7. Place the dish in a plastic sandwich box containing DDW and a Petri dish lid for support, and gas and seal as for 2-dGuo-treated thymus organ cultures.
8. Depending upon the analysis to be performed, reaggregate cultures can be harvested after 18 h. Typically, with an input population of  $\text{CD4}^{+8+}$  thymocytes, 4–5 d of culture results in the efficient generation of both  $\text{CD4}^{+8-}$  and  $\text{CD4}^{-8+}$  mature thymocyte subsets (*see Notes 17 and 18*).

## **4. Notes**

1. When making up the 9-mM stock of 2-dGuo, it is helpful to incubate the solution at 37°C for 1–2 h to help dissolve the 2-dGuo. Immediately after thawing, 2-dGuo can come out of solution and appears as a milky liquid. It is important to let the 2-dGuo stand for 1–2 h to redissolve prior to use.
2. To keep dissection instruments clean and sterile, these are plunged into 70% ethanol and allowed to air-dry prior to use. Scissors in particular can become coated with blood when opening the uterus. Placing blood-coated scissors back in ethanol tends to fix the blood to the scissors, so these are washed in DDW prior to transfer to ethanol.

3. After removing the head and placing the embryo on its back, we find that opening of the thorax and removal of the thoracic tree is easiest for right-handed people if the head-end of the embryo is toward the right, and for left-handed people toward the left. Also, complete submersion of the embryo allows for a clearer view as the medium helps in the dispersal of any blood.
4. For transfer of the thymus lobes to the organ culture filter, we use the mouth-controlled glass pipet method. It is also possible to place the lobes on the filter surface using Watchmakers' forceps. We favor the first approach as the latter can result in tearing of the thymus lobes, and may also result in the transfer of a volume of medium to the filter surface.
5. To make glass pipets for lobe transfer, we draw the glass rods in a Fishtail Bunsen burner. The fan-shaped flame of this type of Bunsen, as compared to the conical flame seen with a conventional Bunsen, allows for greater control of the amount of glass that is being heated, and so facilitates the preparation of finer pipets.
6. We recommend placing 5–6 thymus lobes on each 0.8- $\mu$ m filter, making a total of 10–12 thymus lobes per dish. This allows plenty of space for growth and ensures efficient elimination of endogenous lymphoid cells can occur with the amount of 2-dGuo used.
7. We favor the approach of individually gassing boxes via a cylinder and sealing them, as opposed to use of a CO<sub>2</sub> incubator. This method helps prevent fluctuations in CO<sub>2</sub> levels that can occur if the incubator is opened frequently, and also helps maintain the humidified atmosphere within each culture box.
8. When disaggregating 2-dGuo-treated lobes in trypsin, we recommend that a maximum of 50 lobes be digested per Eppendorf tube. More than this amount can result in incomplete disaggregation, and large cell clumps. Over-trypsinisation resulting in cell damage can also be a problem, this is often seen as strings of DNA rising up the Eppendorf tube from the cell pellet after centrifugation.
9. When resuspending the cell pellet after disaggregation, the pellet often comes away from the sides intact. Careful mechanical pipetting with a 1-mL blue-tip pipet for approx 30 s will resuspend the pellet.
10. For up to 100 2-dGuo treated thymus organ cultures, 100  $\mu$ L of anti-CD45-coated beads will be sufficient to efficiently deplete residual macrophages.
11. We use cryogenic freezing vials for immunomagnetic cell depletion with anti-CD45-coated Dynabeads. This is because the rounded bottom of the vial provides a large surface area for optimal interaction between cells and beads.
12. On average, we find that each day 15 embryonic thymus lobe cultured for 5 d in 2-dGuo will yield approx  $3 \times 10^4$  CD45-negative stromal cells. This figure can be used to determine the number of embryos and 2-dGuo lobes required for each particular experiment.
13. The number of cells used to prepare reaggregate cultures varies depending upon the number of cells available and the experiment to be performed. With regard to a lower limit, we find that reaggregation is reproducibly successful with a cell number of  $1 \times 10^5$ . For an upper cell limit, we would recommend  $1.5 \times 10^6$ . Any higher than this may result in too large a reaggregate culture forming which may,



owing to its size, suffer from central necrosis. With regard to ratios of thymocyte precursors to thymic stromal cells, for CD4<sup>+</sup>8<sup>+</sup> thymocytes we use a ratio of 1:1, typically with  $5 \times 10^5$  thymocytes and  $5 \times 10^5$  stromal cells. As many of the CD4<sup>+</sup>8<sup>+</sup> thymocytes fail to undergo selection to the single positive stages, such cultures typically yield around 20% of the input number of thymocytes.

14. A key step in the formation of reaggregate thymus organ cultures is the removal of all the visible supernatant from the cell pellet. Leaving too large a volume above the cell pellet results in the formation of a “thin” cell suspension that will spread over the surface of the organ culture filter and prevent proper reaggregation. We remove the supernatant in steps of 200- $\mu$ L volumes using a hand-controlled pipet with a 200- $\mu$ L tip on a P200 Pipetman Gilson pipet. Removing the supernatant with the tip held centrally, as opposed to the side of the tube, ensures that no fluid is caught between the tube and the tip. If too large a volume of liquid remains on the pellet, rather than trying to transfer the cells to the organ culture dish, we recommend resuspending the cell pellet in a 1-mL volume and recentrifuging, and repeating the supernatant removal. Typically, we may place a single reaggregate culture on each 0.8- $\mu$ m filter in organ culture.
15. When placing the cell slurry into the glass pipet, some of the slurry will be drawn in by capillary force, so it is important to only apply mouth pressure for the remaining suspension. Ensure that the suspension is held at the tip of the pipet, and not up into the body, as this can result in cell loss. Once drawn into the pipet, the cell slurry will be held in the pipet by capillary action.
16. We deposit the slurry onto the surface of the 0.8- $\mu$ m filter in organ culture using direct visual observation with a dissecting microscope. Choose a magnification where the entire filter can be seen, and gradually start to deposit the cells into the center of the filter by gently blowing. Residual fluid in the cell slurry should drain away from the cells through the pores in the filter. Ideally, cells should be placed on the filter surface on as small an area as possible, ideally a circle of 1–2 mm in diameter. If the slurry begins to spread out, the deposition of cells can be halted by placing the tip of the tongue over the end of the pipet tubing. This will allow fluid to drain through the pores before depositing the remaining cells. Reaggregate cultures form into intact structures within 18 h of culture. If the cells have been deposited over a large area of the filter, rather than formation of a single reaggregate lobe, quite often smaller “satellite” lobes can form.
17. With regard to timing of the harvesting of cultures, reaggregate cultures are intact structures within 18 h after explant, and so thymocytes are easily recovered from cultures at this time point. To analyze the appearance of CD4<sup>+</sup>8<sup>-</sup> and CD4<sup>-</sup>8<sup>+</sup> subsets, we usually harvest on days 4 or 5. Thymocytes are harvested from reaggregate cultures by removing lobes from organ culture filters into fresh RPMI-1640 +10% FCS, and gently teasing them apart with the closed ends of two pairs of watchmakers’ forceps. This can be done using a dissection microscope. Harvesting the cultures this way produces a single cell suspension of thymocytes and clumps of stromal cells can easily be removed.

18. These methods describe a system in which positive selection by thymic epithelial cells can be studied. These methods can also be readily modified to allow study of dendritic cell-mediated negative selection, by the introduction of defined numbers of purified dendritic cells to the cell suspension prior to reaggregation ([11,12,15](#)). Use of TCR-transgenic thymocytes, or MHC class I-deficient or MHC class II-deficient thymic stromal cells can also be used to allow separate investigation of CD8<sup>+</sup> and CD4<sup>+</sup> T-cell selection ([16](#)).

## Acknowledgments

This work was supported by an MRC program grant to E. J. Jenkinson, and G. Anderson.

## References

1. Surh, C. D. and Sprent, J. (1995) T-cell apoptosis detected in situ during positive and negative selection in the thymus. *Nature* **372**, 100–103.
2. Jameson, S. C., Hogquist, K. A., and Bevan, M. J. (1995) Positive selection of thymocytes. *Ann. Rev. Immunol.* **13**, 93–126.
3. Palmer, E. (2003) Negative selection: clearing out the bad apples from the T-cell repertoire. *Nat. Rev. Immunol.* **3**, 383–391.
4. Hogquist, K. A., Baldwin, T. A., and Jameson, S. C. (2005) Central tolerance: learning self-control in the thymus. *Nat. Rev. Immunol.* **5**, 772–782.
5. von Boehmer, H., Teh, H. S., and Kisielow, P. (1989) The thymus selects the useful, neglects the useless and destroys the harmful. *Immunol. Today* **10**, 57–61.
6. Anderson, G. and Jenkinson, E. J. (2001) Lymphostromal interactions in thymic development and function. *Nat. Rev. Immunol.* **1**, 31–40.
7. Levin, S. D., Anderson, S. J., Forbush, K. A., and Perlmutter, R. M. (1993) A dominant-negative transgene defines a role for p56lck in thymopoiesis. *EMBO J.* **12**, 1671–1680.
8. Wolfer, A., Wilson, A., Nemir, M., MacDonald, H. R., and Radtke, F. (2002) Inactivation of Notch1 impairs VDJbeta rearrangement and allows pre-TCR-independent survival of early alpha beta Lineage Thymocytes. *Immunity* **16**, 869–879.
9. Zuniga-Pflucker, J. C. (2004) T-cell development made simple. *Nat. Rev. Immunol.* **4**, 67–72.
10. Schmitt, T. M. and Zuniga-Pflucker, J. C. (2002) Induction of T cell development from hematopoietic progenitor cells by delta-like-1 in vitro. *Immunity* **17**, 749–756.
11. Jenkinson, E. J., Anderson, G., and Owen, J. J. T. (1992) Studies on T cell maturation on defined thymic stromal cell populations in vitro. *J. Exp. Med.* **176**, 845–853.
12. Anderson, G., Partington, K. M., and Jenkinson, E. J. (1998) Differential effects of peptide diversity and stromal cell type in positive and negative selection in the thymus. *J. Immunol.* **161**, 6599–6603.
13. Hare, K. J., Pongrac'z, J., Jenkinson, E. J., and Anderson, G. (2003) Modeling TCR signaling complex formation in positive selection. *J. Immunol.* **171**, 2825–2831.

14. Jenkinson, E. J., Franchi, L. L., Kingston, R., and Owen, J. J. T. (1982) Effect of deoxyguanosine on lymphopoiesis in the developing thymus rudiment in vitro: application in the production of chimeric thymus rudiments. *Eur. J. Immunol.* **12**, 583–587.
15. Volkmann, A., Zal, T., and Stockinger, B. (1997) Antigen-presenting cells in the thymus that can negatively select MHC class II-restricted T cells recognizing a circulating self-antigen. *J. Immunol.* **158**, 693–706.
16. Hare, K. J., Jenkinson, E. J., and Anderson, G. (1999) CD69 expression discriminates MHC-dependent and -independent stages of thymocyte positive selection. *J. Immunol.* **162**, 3978–3983.

## Estimating Thymic Function Through Quantification of T-Cell Receptor Excision Circles

Marie-Lise Dion, Rafick-Pierre Sékaly, and Rémi Cheynier

### Summary

Analysis of immune reconstitution is of major importance in clinical settings such as following bone marrow transplantation or during anti-retroviral treatment of HIV-infected patients. In these patients, thymic function is essential for the reconstitution of a diversified T-cell receptor (TCR) repertoire. During thymopoiesis, several genetic rearrangements lead to the generation of fully functional TCR. By-products of these processes, the T-cell receptor excision circles (TRECs), are present in cells exported from the thymus but do not replicate during mitosis; they can thus be used as molecular markers for recent thymic emigrants. We demonstrate how thymic function can be assessed in a quantitative and noninvasive fashion in humans by estimating intrathymic precursor T-cell proliferation through the quantification of distinct TREC molecules in peripheral blood cells.

**Key Words:** T-cell receptor excision circle; thymic production; real-time quantitative PCR; sj/ $\beta$ TREC ratio; thymus.

### 1. Introduction

Several methods reported in the literature have been used to estimate thymic function *in vivo*. In animal models, direct injection of fluorescent dye into the thymus (1) or introduction of bromodeoxyuridine into the drinking water (2) have been used to label the cells *in situ* so that they can be identified in the periphery. However, these methods are neither accurate nor applicable to humans. In humans, the sole noninvasive method reported to date is a measure of thymic mass through CT scan, which provides a semiquantitative estimate of thymic volume, its size being proportional to its ability to sustain thymopoiesis (3). Based on the known molecular events occurring in the differentiating cells in the thymus, a new methodology was developed: a test aimed at measuring the

frequency of recent thymic emigrants, as well as thymic output, through real time PCR quantification of DNA molecules generated during thymocyte differentiation (4,5). This test provides a novel quantitative and noninvasive assessment of thymic production.

### 1.1. Thymopoiesis

From the colonization of the thymus by CD34<sup>+</sup> precursor cells to the production of mature T cells, thymocytes migrate to specific regions of the thymus and interact with thymic epithelial cells (TEC) and thymic dendritic cells (DC). Signals received by thymocytes through contacts with TEC and DC lead to thymocyte differentiation, proliferation, survival, or death (6–8). During this maturation process, thymocytes undergo genomic, transcriptional, and phenotypic changes as they mature from the CD4<sup>-</sup>CD8<sup>-</sup> double negative (DN) phenotype to CD4<sup>+</sup>CD8<sup>+</sup> double positive thymocytes (DP) then to single positive CD4<sup>+</sup> or CD8<sup>+</sup> T cells (9,10). Throughout this process, thymocytes randomly generate and express a wide array of T-cell receptors (TCR). The TCR-bearing thymocytes are then subjected to negative selection, whereby auto reactive DP thymocytes are eliminated. This is followed by the positive selection of thymocytes endowed with optimal TCR-MHC binding, ultimately leading to the export of functional, but not self-reactive, naïve T cells (9,10).

### 1.2. Generation of TREC Molecules

As mentioned above, during the thymocyte maturation process, highly diverse TCR molecules are generated to ensure that all T cells leaving the thymus harbor a specific TCR endowed with a unique antigenic specificity. Such diversity is made possible through multiple chromosomal rearrangements both at the TCRB and TCRA loci. At the TCRB locus, two subsequent genetic rearrangements occur. The fusion of a D $\beta$  (diversity) segment with a J $\beta$  (junction) segment, followed by the junction of a V $\beta$  (variable) segment to the already rearranged D $\beta$ J $\beta$  segments leads to the generation of the third hypervariable domain (CDR3) of the TCRB chain (see Fig. 1). Similarly, at the TCRA locus, the junction of a V $\alpha$  segment to a J $\alpha$  segment defines the TCRA CDR3 region (see Fig. 2). During each of these rearrangement processes, the excised DNA sequence is circularized as stable episomal DNA, termed TCR rearrangement excision circles (TRECs). According to the number of V $\alpha$ , J $\alpha$ , V $\beta$ , D $\beta$ , and J $\beta$  segments present on the chromosomes, many different TRECs can be produced by the different rearrangements (several hundreds for VJ $\alpha$ TRECs, dozens for VD $\beta$ TRECs, and at least 13 for DJ $\beta$ TRECs). Moreover, before the rearrangement at the TCRA locus, a vast majority of precursor T cells will delete the TCRD locus, that is flanked by V $\alpha$  and J $\alpha$  segments. This TCRD locus excision is mainly realized through specific rearrangement of the  $\delta$ Rec and  $\Psi$ J $\alpha$

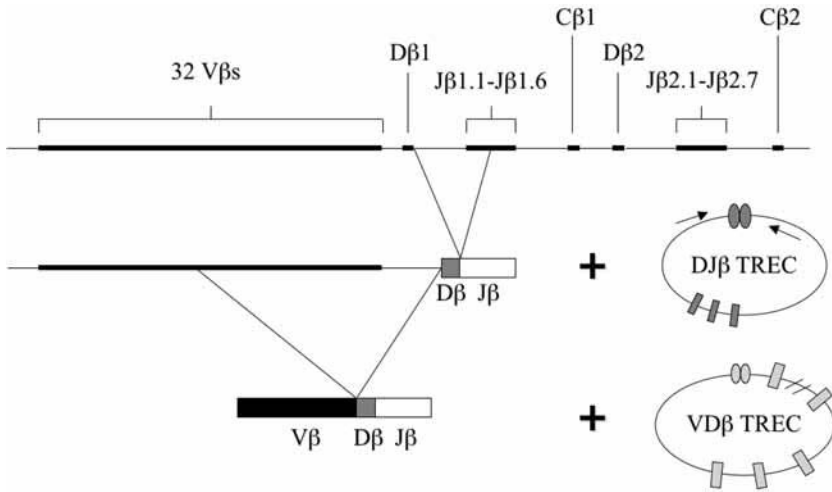


Fig. 1. Rearrangements at the human T-cell receptor (TCR)B locus. Rearrangement of the TCR germline DNA is a stochastic procedure by which noncontiguous variable (V), diversity (D) and joining (J) segments are fused to form complete and, more importantly, variable TCR sequences. The 685 kb human TCRB chain sequence is composed of 2 Dβ -Jβ clusters that are both accompanied by nearly identical constant Cβ sequences (Dβ -Jβ1.1-1.6- Cβ1 and Dβ2- Jβ2.1-2.7- Cβ2). Sixty-five Vβ segments (grouped into 32 families according to sequence homology) are found upstream of these clusters and enhance the multiplicity of possible combinations. The rearrangement of the TCRBD to TCRBJ segments occurs first and generates a by-product: a specific DJβTRECs that can be quantified by PCR. This is followed by the recombination of the V to DJ segments, which also generates a specific VDβTREC. These VDβTRECs can also be quantified, but they are not used in the evaluation of the sjβTREC ratio as with 65 different Vβ segments, the possibilities are much too numerous to cover all rearrangements.

deleting elements and leads to the generation of a specific TREC molecule that is present in a majority of cells (about 70%) exiting the thymus: the latter has justified the use of the sjTREC (signal joint TCR rearrangement excision circle) to quantify thymic output (4,5).

TRECs are stable episomal DNA molecules that persist in a cell until mitosis. As TRECs are not duplicated during cell division, only one of the daughter cells will inherit a TREC molecule. Accordingly, the TREC frequency in a given T cell population is inversely proportional to its proliferative history subsequent to TREC generation. Concerning the sjTREC molecule that is produced late during thymopoiesis, most of this proliferation occurs in the periphery and corresponds to homeostatic proliferation of mature naïve T cells. However, the DJβTRECs are also diluted during their intrathymic maturation as TCRB+

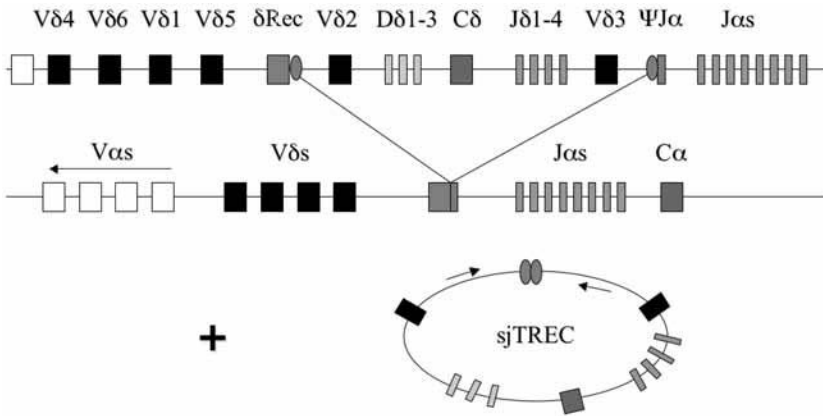


Fig. 2. Rearrangements at the human T-cell receptor (TCR)A locus. The TCRA chain sequence, devoid of D segments, is composed of approx 70 V $\alpha$  and 60 J $\alpha$  segments that, interestingly, border the TCRD locus. To successfully rearrange a TCRA chain and draw the V and J segments nearer, the small DP thymocytes must first excise the TCRD loci, committing the T cell to  $\alpha\beta$  T cell lineage. In most thymocytes (70%), the removal of the TCRD loci is governed by the rearrangement of two deleting elements of the  $\alpha$  locus,  $\delta$ Rec and  $\Psi$ J $\alpha$ . This generates the sjTREC, that can be quantified by PCR. V $\alpha$  and J $\alpha$  segments are then rearranged and a structurally in-frame product of the TCR $\alpha$  chain pairs with the TCR $\beta$  chain and form the complete TCR.

thymocytes undergo massive clonal expansion at late DN, intermediate single positive (ISP) and early DP differentiation stages (termed  $\beta$ -selection), before the excision of the TCRD locus and the generation of the sjTREC molecule.

### 1.3. The sjTREC Frequency as an Estimate of Thymic Function

As TRECs are stable molecules that are only diluted during cell proliferation, the sjTREC, a unique molecule generated in the majority of differentiating thymocytes, has been used for several years as a surrogate marker for thymic function. Several studies have demonstrated that in animal models, such as the chicken and mouse, as well as in healthy human subjects, the frequency of circulating sjTREC<sup>+</sup> cells correlates with thymic activity (4,11–17). In addition, as expected from the observations of age-related thymic atrophy, sjTREC frequency negatively correlates with age, illustrating its relevance to thymic activity (4,5). SjTREC levels also correlate with thymic size as estimated through CT scan (18). However, in certain clinical settings, such as HIV infection or following bone marrow transplantation, the relationship between the sjTREC frequency and thymic output seems to be lost. This is mainly due to the fact that, in lymphopenic hosts, the enhanced naïve T-cell proliferation aimed at restoring T-cell numbers, dilutes TREC molecules, reducing their

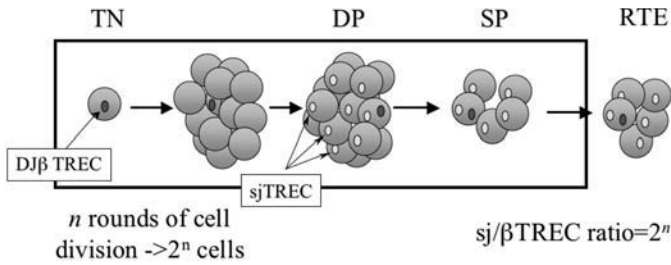


Fig 3. The generation of the sj/βTREC ratio. Following the rearrangements of the T-cell receptor (TCR)B chain and subsequent generation of DJβTRECs, proliferation occurs. As TRECs are episomal DNA molecules that do not replicate, this proliferation dilutes the DJβTRECs. In most (70%) of the resulting cells, the excision of the TCRD within the TCRA will produce a sjTREC. This will create a differential sjTREC/DJβTREC ratio, (simplified to sj/βTREC ratio) that will persist in peripheral blood cells, reflecting the intrathymic proliferative history of these cells.

frequency, regardless of thymic activity. This renders the relative contribution of both modifications of thymic output and peripheral proliferation difficult to estimate. Thus, the simple quantification of the sjTREC molecule cannot be used as a reliable and accurate marker for thymic function in such clinical settings.

#### 1.4. The sj/βTREC Ratio as a Direct Estimate of Thymopoiesis

As described above, intense proliferation occurs during thymocyte differentiation, between late triple negative (TN) and early DP differentiation stages. As DJβTRECs are generated before this proliferation, the frequency of DJβTRECs in DP cells is inversely proportional to the number of division cycles these cells have undergone during their differentiation (*see Fig. 3*). Moreover, because the sjTREC molecule is produced after this extensive proliferation stage, sjTRECs are not diluted by this intrathymic cell division. Accordingly, we have demonstrated that the extent of intrathymic precursor T-cell proliferation, that is proportional to thymic output, can be estimated through quantification of both the sjTREC and DJβTREC frequencies and calculation of the sj/βTREC ratio (sjTREC frequency/DJβTREC frequency) measured in peripheral blood mononuclear cells (5).

#### 1.5. Real-Time PCR Method: An Overview

Real-time PCR techniques are currently used in several fields of modern science. They allow an absolute quantification of a specific target DNA sequence in any DNA template. These methods are based on the measurement, in real time, of the progression of a specific PCR reaction. In such assays, probes



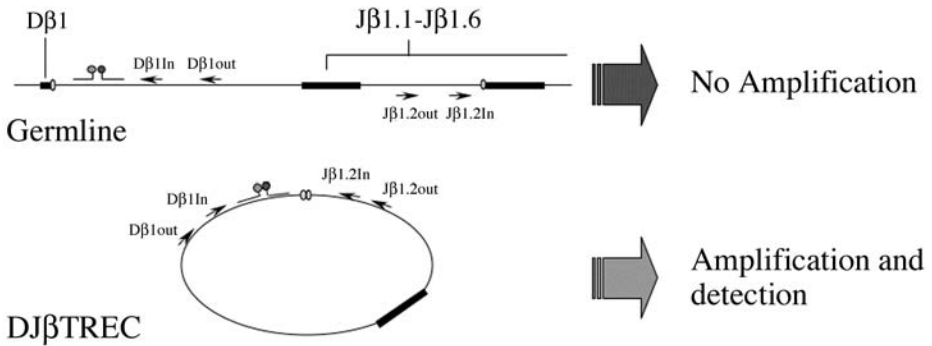


Fig. 4. Primer design for T-cell receptor excision circles (TREC) quantification. TRECs carry the same sequence as their corresponding germline segments. Thus, to discriminate TRECs from germline, PCR primers are oriented to amplify the joining region of the circular TREC. This prevents amplification of the germline TCR as the primers are directed outward from each other upon hybridization on chromosomal DNA. Upon the amplification of TRECs, specific probes bind to the sequence. The proximity of these probes activates the fluorescence resonance energy transfer, thus emission of the specific wavelength (640 and 705 nm) measured by the LightCycler.

(molecular beacons, Taqman probes, LightCycler probes, and so on) specific for the quantified target are added to a PCR reaction, and run in a real time PCR machine capable of detecting such signals. At the end of each amplification cycle, the intensity of the signal generated by the probe is proportional to the quantity of probes bound to the target sequence and thus directly reflects the amount of target sequence. During the log-linear phase of the PCR reaction, the amount of initial input target sequences is inversely proportional to the number of cycles necessary to reach a defined level of signal. This allows, by determination of this number of cycles, the estimation of the initial amount of target present in the sample.

### 1.6. Detecting TRECs: Primers and Probes

As TREC molecules carry the same sequences as the germline DNA that encodes the TCR V, D, and J segments, primers must be designed to solely amplify these sequences that are organized in a circular DNA molecule (TRECs). To do so, the primers are directed toward the junction, enabling a specific amplification of this region. On the other hand, on the germline DNA, the primers are directed outward from each other, preventing any amplification (*see Fig. 4*).

This technique requires the measurement of very small amounts of targets; DJβTREC molecules are scarce in adult peripheral blood cells due to high dilution in the thymus. For this reason, the protocol for their quantification is

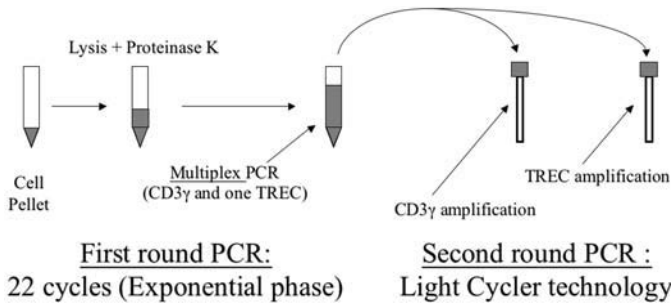


Fig. 5. Overview of sample process for T-cell receptor excision circles (TREC) quantification. First, cell pellets are lysed and subjected to proteinase K treatment, releasing their nuclear DNA, now free of histones. The samples then undergo a first round of 22 PCR amplification cycles using the “out” primers for both TREC and CD3 $\gamma$  gene in the same reaction. The now amplified products are diluted to minimize the concentration of first round PCR reagents that could interfere with the second round of PCR. The second round of PCR using the “in” primers is performed in a real-time PCR machine such as the Roche LightCycler. A separate amplification and quantification of the TREC and CD3 $\gamma$  reporter gene is performed for the same samples, enabling “TREC/cell” readout.

performed by nested PCR, i.e., two rounds of amplification, allowing the generation of a greater amount of product that will be detectable by real-time PCR (*see Fig. 5*). Two rounds of PCR entails two sets of primers: the first, “out” primers, are positioned furthest from the joining region, and the second, “in” primers, are positioned within the amplicon produced by “out” primers, nearer to the junction region. Having four instead of two specific primers, allows a greater amplification of the target, as well as a higher specificity of the PCR amplification.

## 2. Materials

### 2.1. PCR-Dedicated Laboratories

Even more importantly than for PCR reactions in general, contamination should be considered as “the enemy” of quantitative PCR. The unique way to avoid PCR contamination is to physically separate sample preparation and analysis of PCR amplified products. To do so, a fully equipped PCR room is necessary. In this room both sample preparation and the first step of PCR amplification should be performed. Moreover, this room should be kept plasmid- and amplicon-free (*see Note 1*). A second PCR room, separated from the molecular biology laboratory, should house the PCR machine and the real time PCR apparatus. In this room, the pre-PCR products will be diluted and the real time quantitative PCR performed. In the main molecular biology room, the plasmids will be kept and manipulated. They should never be handled in any of the PCR rooms.

## 2.2. Sample Preparation and Pre-PCR

The different compounds for both lysis and pre-PCR should be stored in the PCR room.

1. Lysis buffer: Tris-HCl (pH 8.0) 10 mM, Tween-20/NP40 (0.05% each), and proteinase K (100 µg/mL). Adjust concentrations with PCR-grade water. Lysis buffer should be prepared extemporaneously. A stock solution containing Tween-20 (0.5%) and NP40 (0.5%) should be prepared in advance as these compounds are highly viscous.
2. Pre-PCR: DNTP (10 mM each), Taq DNA polymerase and associated buffer, MgCl<sub>2</sub> (50 mM), PCR-grade water.
3. PCR primers (prepare stock solutions at 100 µM):

CD3-out5	5'-ACTGACATGGAACAGGGGAAG-3'
CD3-out3	5'-CCAGCTCTGAAGTAGGGAAACATAT-3'
CD3-in5	5'-GGCTATCATTCTTCTTCAAGGT-3'
CD3-in3	5'-CCTCTCTTCAGCCATTTAAGTA-3'
sj-out3	5'-ACTCACTTTTCCGAGGCTGA-3'
sj-out5	5'-CTCTCCTATCTCTGCTCTGAA-3'
sj-In3	5'-GTGCTGGCATCAGAGTGTGT-3'
sj-In5	5'-CCTCTGTCAACAAAGGTGAT-3'
Db1 VeryOut	5'-CCTGAGGCAGTCTTCTTATGT-3'
Db1-Out	5'-CTCATCTGGGCCTGTCCCTTGT-3'
Db1-in	5'-TGTGACCCAGGAGGAAAGAAG-3'
1.1 VeryOut	5'-TCTGAATGGGGCATCCTTTGA-3'
1.1 Out	5'-GAACCTAGGACCCTGTGGA-3'
1.1 In	5'-CCCTCTCTATGCCTTCAATGT-3'
1.2 VeryOut	5'-CTTTTTGTACCTGCCTGAGT-3'
1.2 Out	5'-ACAAGGCACCAGACTCACAGTT-3'
1.2 in	5'-CAGATCCGTCACAGGGAAAAGT-3'
1.3 VeryOut	5'-CTTTTTGTACCTGCCTGAGT-3'
1.3 Out	5'-AAGGGAACACAGAGTACTGGAA-3'
1.3 In	5'-TGTCCCTGTGAGGGAAGAGTT-3'
1.4 VeryOut	5'-TCCCTCACACAGAAAGGAGA-3'
1.4 Out	5'-GGATCACACGGGGCCTAATT-3'
1.4 In	5'-TGGACTTGGGGAGGCAGGA-3'
1.5 VeryOut	5'-CTCTCTGTCTTGGGTATGTA-3'
1.5 Out	5'-GAAACTGAGAACACAGCCAAGAA-3'
1.5 In	5'-CTCATAAAATGTGGGTCAGTGGA-3'
1.6 VeryOut	5'-GCTCATCCTCCCTCTTATGT-3'
1.6 Out	5'-ATCCTCCCTCTTATGTGCATGG-3'
1.6 In	5'-TGAATCCAGGCAGAGAAAGG-3'
Db2-VeryOut	5'-CCCTCAGGGTTTTATCAGTT-3'
Db2-out	5'-ATTCCTTGGAAAGCCGAGT-3'
Db2-in	5'-GGACCAGCCCCAGAGAA-3'

---

2.1 VeryOut	5'-GCAAGGTCTAGCCTGCAATAT-3'
2.1 Out	5'-CTCCTCTGCAAATTGGTGGT-3'
2.1 In	5'-CCAGCTAACTCGAGACAGGAA-3'
2.2 VeryOut	5'-TGCTCCTACAATGAGCAGTT-3'
2.2 Out	5'-CACCGTGCTAGGTAAGAA-3'
2.2 In	5'-GAACCCTGTTCTTAGGGGAGT-3'
2.3 VeryOut	5'-AGGCTGACCGTACTGGGTAA-3'
2.3 Out	5'-TACTGGGTAAGGAGGCGGTT-3'
2.3 In	5'-TGAGAGGGGCTGTGCTGAGA-3'
2.4 VeryOut	5'-CCCAGGCACCCGGCTGA-3'
2.4 Out	5'-GGCTGACAGTGCTCGGTAA-3'
2.4 In	5'-AAGCGGGGGCTCCCGCTGAA-3'
2.5 VeryOut	5'-TCTCGGGGCTGTGAGCCAAA-3'
2.5 Out	5'-GTGAGCCAAAAACATTCAGT-3'
2.5 In	5'-CGGCTCTCAGTGCTGGGTAA-3'
2.6 VeryOut	5'-GCTCGGGGCCGTGACCAAGA-3'
2.6 Out	5'-GACCAAGAGACCCAGTA-3'
2.6 In	5'-GTCTGGTTTTTTCGGGGAGT-3'
2.7 VeryOut	5'-CTCTGGGGCCAACGTCCTGA-3'
2.7 Out	5'-GACCGTGCTGGGTGAGTT-3'
2.7 In	5'-GGAGCTCGGGGAGCCTTA-3'

---

### 2.3. Real-Time PCR

1. The quantification of preamplified products described in this chapter is performed using LightCycler (Roche) technology. However, it can be adapted to any real time PCR system. To perform the quantification in the best conditions for this instrument, we routinely use the LightCycler DNA Master hybridization probes kit (Roche).
2. Prepare probes at a concentration of 4  $\mu$ M. However, as the fluorochrome conjugates are quite unstable, it is important to store them in small, highly concentrated aliquots. For example, the probes can be resuspended at 1 mM and distributed in 5- $\mu$ L aliquots for storage. These aliquots will be further diluted 250-fold (4  $\mu$ M) and distributed in 130- $\mu$ L aliquots (enough for 10 and 5 LightCycler carousels for probe 1 and probe 2, respectively).

LightCycler Probes:

---

CD3-P1	5'-GGCTGAAGGTTAGGGATACCAATATTCCTGTCTCfluo-3'
CD3-P2	5'-(red705)CTAGTGATGGGCTCTTCCCTTGAGCCCTTCp-3'
sj-P1	5'-AATAAGTTCAGCCCTCCATGTCACACTfluo-3'
sj-P2	5'-(red640)TGTTTTCCATCCTGGGGAGTGTTTCAp-3'
Db1-P1	5'-CTGGGAGTTGGGACCGCCAGAGAGGTfluo-3'
Db1-P2	5'-(Red640)TTTGTAAGGTTTCCCGTAGAGTTGAATCATT GTGp-3'
Db2-P1	5'-GATTCAGGTAGAGGAGGTGCTTTTACAAfluo-3'
Db2-P2	5'-(Red640)AAACCCTGATGCAGTAAGCATCCCCACCP-3'

---

### 3. Methods

#### 3.1. Preparation of Plasmids Necessary for Standard Curves

The basis of a precise quantification of TRECs is a DNA plasmid that contains both the amplified TREC sequence and the housekeeping gene sequence (in this case, a region of the *CD3 $\gamma$*  gene). This ensures a 1:1 ratio of both sequences that will be followed in the same standard curve throughout the experiment. Indeed, using the exact same serial dilution of this plasmid for the quantification of both targets will eliminate errors related to direct DNA quantification and permit an accurate assessment of the relative frequencies of TRECs and the number of cells (defined by the *CD3 $\gamma$*  quantification).

No specific protocol is required and any cloning method can be used; however all experiments must be carried out in the main molecular biology laboratory and the material to be used must not come in contact with the other designated rooms. As routine cloning protocols vary, we have included only a brief overview of the method used in our case.

1. Perform a PCR amplification of the genomic *CD3 $\gamma$*  region on purified human genomic DNA using *CD3 $\gamma$* -specific outer primers. For this particular PCR, a tail containing a restriction enzyme target site (*EcoRI*) was added to the 5'-end of both outer primers. At the 5'-end of the primers, it is important to add a random six base tail to help the enzyme recognize the restriction site.
2. Verify the efficacy of the PCR amplification by gel electrophoresis (2% agarose gel), the *CD3 $\gamma$* -out primers should generate a unique band of 381bp.
3. Excise the PCR product from the gel and purify the insert using PCR purification kit.
4. Digest the insert (*CD3 $\gamma$* ) and the plasmid (1  $\mu$ g of Bluescript) with *EcoRI* for 2 h at 37°C. Heat-inactivate the restriction enzyme. Combine the insert and the plasmid to a 5:1 ratio in the presence of T4 DNA ligase and ligase buffer. Incubate overnight at 15°C.
5. Transform competent *Escherichia coli* DH5 $\alpha$  bacteria with the ligation product. Plate on LB agar with ampicillin (100  $\mu$ g/mL). Grow overnight at 37°C.
6. Pick colonies and grow them overnight in 4 mL LB media with ampicillin (100  $\mu$ g/mL) at 37°C. Harvest the bacteria and isolate episomal DNA using a kit-based mini-prep technique. After purification, the presence of the inserts in the plasmids should be verified by PCR using specific *CD3 $\gamma$*  outer and inner primers. To avoid contamination, the PCR mix must be prepared in a different laboratory from where the inserts were cloned (for example in the PCR room), the plasmids should be added at the very end, in the molecular biology room. Also, it is imperative to add the appropriate negative controls: one by replacing the plasmids with water from the molecular biology lab, and the other by replacing the plasmids with water from the PCR room.
7. The identified *CD3 $\gamma$* -positive clone should be sequenced to ensure that it contains a nonmutated copy of the *CD3 $\gamma$*  chain. This construct (pCD3) will be the basis for the following cloning procedures.

8. From the pCD3, repeat the **steps 1–5** for each of the different TREC sequences using outer primers containing the *HindIII* restriction site. As TRECs are only present in some lymphoid cells (thymocytes, recent thymic emigrants, and a proportion of naïve T cells), it is necessary to perform these amplifications on DNA extracted either from peripheral mononuclear cells or from thymocytes (which are richer in TRECs) if available. To do so, a first amplification must be performed using primers located outside of the amplicon to be cloned (VeryOut primers). The second step of the amplification is then performed on the latter PCR product using the outer primers containing the *HindIII* restriction site and a 6 bp tail at their 5' extremity. The PCR product generated by this nested PCR amplification will then be cloned at the *HindIII* site of the pCD3 plasmid. This will create pCD3-TREC plasmids for each TREC (sjTREC, D $\beta$ 1-J $\beta$ 1.1 to D $\beta$ 1-J $\beta$ 1.6, and D $\beta$ 2-J $\beta$ 2.1 to D $\beta$ 2-D $\beta$ 2.7 TRECs).
9. After having cloned each of the TREC amplicons into the pCD3-plasmid, the pCD3-TREC plasmids must be sequenced to verify that the amplification/cloning procedure did not introduce any mutation.
10. Grow a positive clone for each pCD3-TREC and isolate the plasmids. Prepare a stock solution of  $10^{12}$  DNA molecules/ $\mu$ L and dilute for use at  $10^7$  molecules/ $\mu$ L. These plasmids will constitute the basic material for the standard curves in all subsequent experiments.

### 3.2. Sample Preparation

Samples can be peripheral blood mononuclear cells isolated from whole blood by gradient-density Ficoll-Hypaque or from peripheral lymphoid organs. They can consist of nonpurified total lymphocytes or enriched fractions of T-cell subsets obtained by cell sorting. After isolation or purification, lymphocytes should be washed in PBS, divided into aliquots of  $3 \times 10^6$  to  $5 \times 10^6$  cells and stored at  $-20^\circ\text{C}$  as a dry pellet for further use. If the cells were purified using FACS sorting following fixation, it is important to perform three washes in PBS to fully eliminate the fixative agent that could interfere with Taq polymerase efficiency (*see Note 2*).

### 3.3. Cell Lysis: In the PCR Room

1. Thaw the samples and resuspend the pellet in lysis buffer at  $10^7$  cells/mL. The detergents (Tween-20 and NP40) will dissolve cell and nuclear membranes and release the nuclear contents. Transfer the cell lysate into 500- $\mu$ L PCR tubes. For maximum recovery, it is important to ensure a complete dissolution of the cell pellet at this stage.
2. Incubate the tubes for 30 min at  $56^\circ\text{C}$  in the PCR machine. The proteinase K will digest all DNA-bound proteins, such as histones, and release the DNA molecules for amplification.
3. Incubate for 15 min at  $98^\circ\text{C}$  in the PCR machine. This step will inactivate the proteinase K, eliminating the interference it will have on further enzymatic activity, including the Taq polymerase activity, required in the following steps.
4. Store the cell lysates at  $4^\circ\text{C}$  until use. Limiting successive freezing and thawing is recommended as this could lead to nonspecific breaks in DNA molecules.

### 3.4. Pre-PCR Procedure: In the PCR Room

1. Transfer 10  $\mu\text{L}$  of cell lysate into individual PCR tubes.
2. Prepare the pre-PCR cocktail as follows, adding the Taq polymerase last: 10  $\mu\text{L}$  10X PCR buffer ( $\text{MgCl}_2$  free) (volume per tube), 7  $\mu\text{L}$   $\text{MgCl}_2$  (50 mM), 1  $\mu\text{L}$  Oligo TREC 3' (100  $\mu\text{M}$ ), 1  $\mu\text{L}$  Oligo TREC 5' (100  $\mu\text{M}$ ), 1  $\mu\text{L}$  Oligo CD3 $\gamma$  3' (100  $\mu\text{M}$ ), 1  $\mu\text{L}$  Oligo CD3 $\gamma$ 5' (100  $\mu\text{M}$ ), 1  $\mu\text{L}$  DNTPs (10 mM each), 67  $\mu\text{L}$  PCR grade  $\text{H}_2\text{O}$ , 1  $\mu\text{L}$  Taq polymerase (5 U/ $\mu\text{L}$ ).
3. Distribute 90  $\mu\text{L}$  of PCR cocktail into each PCR tube taking care not to transfer lysate material between tubes. Add 60  $\mu\text{L}$  of mineral oil if necessary. PCR controls are as follows: negative control: substitute DNA sample with 10  $\mu\text{L}$  of PCR grade  $\text{H}_2\text{O}$ . Positive control: 10  $\mu\text{L}$  of diluted plasmid ( $10^8$  copies). This tube will serve both as a positive control and to generate the standard curves.

Although all the sample tubes and the negative control should be filled and closed in the plasmid-free PCR room, the plasmid should be added to the positive control tube in the molecular biology laboratory, just before starting the PCR machine.

4. Place the tubes into a standard PCR machine and run the following amplification program. Initial denaturation: 10 min at 95°C, 22 amplification cycles (*see Note 3*), 95°C for 30 s, 60°C for 30 s, 72°C for 2 min, hold at 20°C.

The pre-PCR samples at this point can be stored at 4°C for up to 2 mo, before the next step.

### 3.5. Real-Time PCR Procedure

1. Sample preparation: in the second PCR room, perform a 10-fold dilution of all pre-PCR samples (except the one that contains the plasmid, which will be diluted in the molecular biology room). Vortex the tubes vigorously and transfer 20  $\mu\text{L}$  of pre-PCR sample to 180  $\mu\text{L}$  of PCR-grade deionized water. Diluting the samples is intended to reduce the concentration of PCR-related reagents from the pre-PCR that could interfere with the real-time PCR reaction. These same sample dilutions will be used for TREC and CD3 $\gamma$  quantification, thus, for optimal preservation, keep all dilutions on ice.
2. Standard curve preparation: in the molecular biology room, dilute the pre-PCR tube containing the amplified plasmid inserts. Perform this step in the same manner as for dilution of the samples (i.e., 20  $\mu\text{L}$  in 180  $\mu\text{L}$  of water). This will be the first point of the standard curve. From this preparation, serially dilute with increments of 1/10 (i.e., 20  $\mu\text{L}$  of the previous tube in 180  $\mu\text{L}$  of water and so on) to create a standard curve of eight points. Regular vortexing, precise pipetting and pipet-tip changes between dilutions are key at this step, as even a small error can strongly skew the results in quantitative real-time PCR. As described above, this same standard curve will be used for TREC and CD3 $\gamma$  quantification thus for optimal preservation, keep all standard curve dilutions on ice.
3. The LightCycler system is set up for the use of capillaries as PCR reaction tubes. This allows rapid temperature changes to occur optimizing the amplification process within the machine. A cooling block support for the capillaries is provided to

prevent changes in temperature during sample preparation. After cooling the support for a minimum of 4 h at 4°C, distribute LightCycler capillaries within the block.

Prepare the LightCycler cocktail, maintaining the reagents, as well as the mix, in the cooling block. Taq, as well as the amplification buffer, must again be added last to the solution. Per 32 capillaries: 60 µL MgCl<sub>2</sub> (25 mM), 70 µL H<sub>2</sub>O, 12.5 µL Oligo In5' (100 µM), 12.5 µL Oligo In3' (100 µM), 12.5 µL Probe 1 (4 µM), 25 µL Probe 2 (4 µM), LightCycler DNA Master 1, 50 µL for hybridization probes, Taq polymerase 7.5 µL.

1. Incubate the cocktail at 65°C for 5 min and distribute 7 µL of cocktail per capillary.
2. Vortex the diluted samples and negative control and add 7 µL of each to the individual capillaries. Cap the full capillaries (sample + mix).
3. Vortex and distribute the standard curve (7 µL) into eight capillaries. Cap the full capillaries (standard + mix).
4. Spin down (quick spin 1000 rpm) the filled capillaries in small table-top centrifuge suited for 1.5-mL tubes. Place the capillaries on the carousel into the LightCycler and start the run.
5. Set up of the LightCycler run. PCR protocol:
  - a. Initial denaturation: 95°C for 1 min.
  - b. Cycling (read the intensity of fluorescence at the end of the annealing step).
    - i. Denaturation 95°C for 1 s.
    - ii. Annealing 60°C for 10 s.
    - iii. Elongation 72°C for 15 s.
  - c. Melting curve.
    - i. Denaturation 95°C for 1 s.
    - ii. Annealing 40°C for 5 min.
    - iii. Denaturation with continuous reading of the fluorescence and slow temperature increase rate (0.2°C/s) up to 95°C.
  - d. Cooling down to 40°C.
6. The quantification procedure (**step 5**) is identical for both TREC and CD3γ quantification, using inner primers specific for each amplicon. The samples and standard curves prepared at **steps 1** and **2** are used for both quantifications.

### 3.6. Analysis of Results

1. Upon entering sample identification, mark and assign numerical values to the standard curve capillary positions. This will be the reference for the quantification of both CD3γ and TREC. As it is their ratio that will ultimately determine TREC frequencies, the exact numbers given to the standard curve is not of capital importance. Nevertheless, through experiments using a precise number of cells, allocating 10<sup>6</sup> copies to the most concentrated point (and 10-fold downward) has been shown to roughly represent the quantity of DNA found before preamplification. In other words, the amount of CD3γ amplicon from 10<sup>5</sup> cells following 22 cycles of preamplification will be detectable by the LightCycler after roughly the same number of cycles as the second standard curve point (10<sup>5</sup> copies).



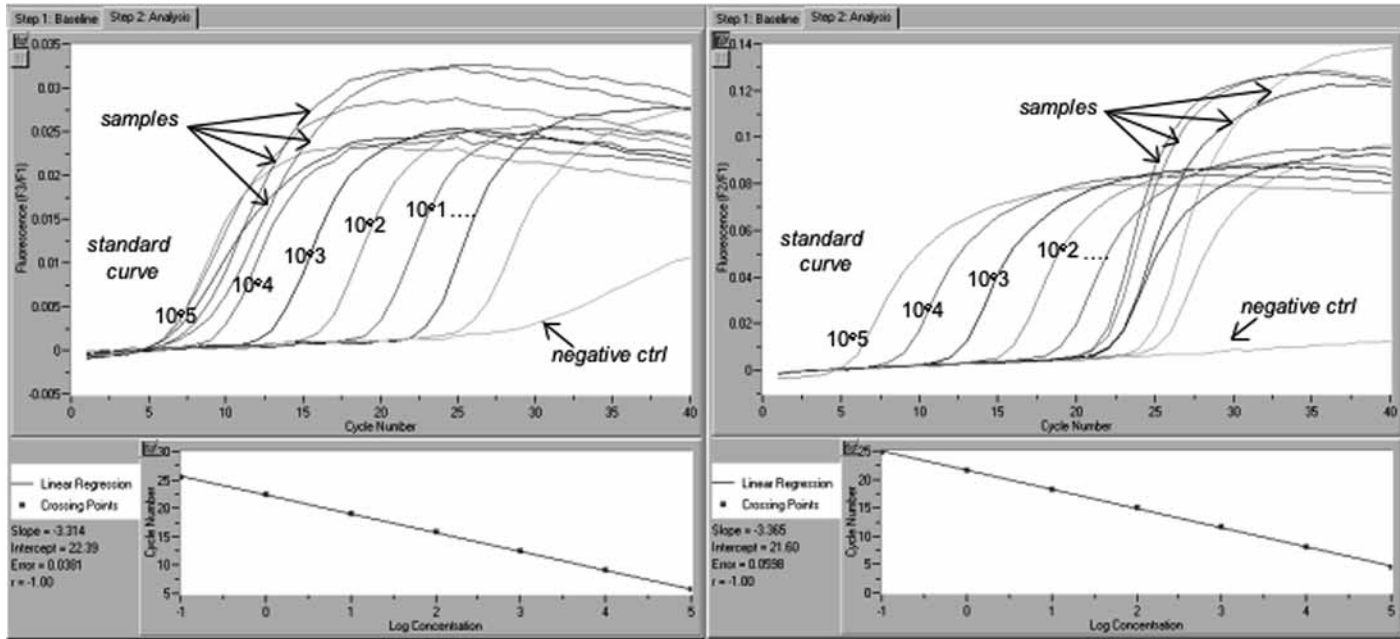
Real-time amplification of the CD3 $\gamma$ Real-time amplification of the D $\beta$ 1J $\beta$ 1.2TREC

Fig. 6. Example of real-time PCR readout. The second round of PCR amplification occurs in the presence of fluorescent hybridization probes that allow the quantification of the product after each round of amplification. These readouts are represented by the curves, each sample being followed throughout the 40 cycles of PCR. At this stage, the samples are concomitantly amplified alongside a standard curve composed of sequentially diluted plasmids that contain the amplified sequence. To monitor the dilution and amplification efficacy, the standard curve is plotted and must have a slope closest to 3.325 with minimal error (3.325 is a theoretical value expected for the amplification of 10-fold dilutions). Here is represented the separate amplification and quantification of the D $\beta$ 1-J $\beta$ 1 T-cell receptor excision circles (TREC) and the CD3 $\gamma$  reporter gene. To correct any possible variation in the real-time PCR reaction, both amplifications are compared to the same serial dilution of the standard curve, a plasmid that contains both TREC sequences and the reference gene CD3 $\gamma$  in a 1:1 ratio. A negative control is always present to ensure no plasmid contamination in sample tubes.

- Using the LightCycler analysis program, reference the number of cycles to detection for your samples to those of the standard curve, the latter having an ideal slope of 3.325 (as  $2^{3.325} = 10$ , the dilution factor between points) and minimal error (see Fig. 6). Although a margin of error is acceptable (between 3.2 and 3.4 for the slope), a standard curve that does not meet these criteria reflects either (1) a poor dilution of the amplified plasmids or (2) a suboptimal LightCycler amplification. The second alternative can be verified by comparing the amplification pitch of all samples and standard curve to previous LightCycler runs. If the amplification seems less efficient, verify the concentration, freshness and storage of the primers, buffer, and Taq. Replace if necessary. Rapid and effective manipulation is also important in a successful real-time PCR reaction.
- Each experimental sample is quantified for both a TREC and CD3 $\gamma$  (see Fig. 6). From these data, estimated with reference to the standard curve, the frequency of TREC molecule per  $10^5$  cells is given by (see Note 4):

$$\frac{2 \times 10^5 \times \text{TREC frequency}}{\text{CD3}\gamma \text{ frequency}}$$

- To calculate the sj/ $\beta$ TREC ratio of any given sample, sjTREC and DJ $\beta$ TREC (1.1–2.7) quantifications must be performed as described here from the same lysed sample. From these data, the sjTREC value must be divided by the sum of the DJ $\beta$ TREC values, from which the sj/ $\beta$ TREC ratio is obtained. Duplicate quantification of each TREC molecule is necessary to obtain an accurate estimate of the sj/ $\beta$ TREC ratio (see Note 4).

#### 4. Notes

- To keep the PCR room free of plasmids, it is crucial not to enter this room after being in the molecular biology room. Plasmid molecules are quite volatile and can easily be transported from one place to another through hair, clothes, or other objects. Because the molecular biology room is in most cases the main laboratory, it is important that all pre-PCR experiments be carried out before any other manipulation planned that day, minimizing the risk of plasmid contamination. The benches in the PCR rooms should be periodically decontaminated using 0.1 N HCl and fully rinsed with clean water.
- Contrary to the quantification of integrated sequences, the quantification of TRECs cannot be accurately performed on purified extracted DNA because the relative efficiency of extraction of high- and low-molecular-weight DNA is different, whatever purification method is used. Indeed, purified DNA is always enriched in low molecular weight DNA that includes the TREC molecules, as compared to high molecular weight DNA that includes the housekeeping gene.
- We fixed the number of cycles for the pre-PCR at 22 because, after this point, the amplification of the CD3 $\gamma$  chain for  $10^5$  cells reaches a plateau phase. After this point, the amplification of the TREC molecule amplicons continues thus, the relative frequency of both amplicons changes, leading to an overestimation of the TREC frequency. It is thus very important, to preserve the accuracy of the TREC

quantification, to both limit the pre-PCR amplification to a maximum of 22 cycles and limit the amount of input lysate to the equivalent of about  $10^5$  cells.

- Using this nested PCR quantification method, the sj/ $\beta$ TREC ratio can be estimated with a less than twofold variation.

## Acknowledgments

This work was supported by grants to R. P. Sékaly from the NIH, CIHR, FRSQ, and CANVAC.

## References

- Staton, T. L., Johnston, B., Butcher, E. C., and Campbell, D. J. (2004) Murine CD8<sup>+</sup> recent thymic emigrants are alphaE integrin-positive and CC chemokine ligand 25 responsive. *J. Immunol.* **172**, 7282–7288.
- Tough, D. F. and Sprent, J. (1994) Turnover of naïve- and memory-phenotype T cells. *J. Exp. Med.* **179**, 1127–1135.
- Taub, D. D. and Longo, D. L. (2005) Insights into thymic aging and regeneration. *Immunol. Rev.* **205**, 72–93.
- Douek, D. C., McFarland, R. D., Keiser, P. H., et al. (1998) Changes in thymic function with age and during the treatment of HIV infection. *Nature* **396**, 690–695.
- Dion, M. L., Poulin, J. F., Bordi, R., et al. (2004) HIV infection rapidly induces and maintains a substantial suppression of thymocyte proliferation. *Immunity* **21**, 757–768.
- Anderson, G., Moore, N. C., Owen, J. J., and Jenkinson, E. J. (1996) Cellular interactions in thymocyte development. *Annu. Rev. Immunol.* **14**, 73–99.
- Boyd, R. L., Tucek, C. L., Godfrey, D. I., et al. (1993) The thymic microenvironment. *Immunol. Today* **14**, 445–459.
- van Ewijk, W. (1991) T-cell differentiation is influenced by thymic microenvironments. *Annu. Rev. Immunol.* **9**, 591–615.
- Jameson, S. C., Hogquist, K. A., and Bevan, M. J. (1995) Positive selection of thymocytes. *Annu. Rev. Immunol.* **13**, 93–126.
- Starr, T. K., Jameson, S. C., and Hogquist, K. A. (2003) Positive and negative selection of T cells. *Annu. Rev. Immunol.* **21**, 139–176.
- Haynes, B. F., Markert, M. L., Sempowski, G. D., Patel, D. D., and Hale, L. P. (2000) The role of the thymus in immune reconstitution in aging, bone marrow transplantation and HIV-1 infection. *Annu. Rev. Immunol.* **18**, 529–560.
- De Rossi, A., Walker, A. S., Klein, N., De Forni, D., King, D., and Gibb, D. M. (2002) Increased thymic output after initiation of antiretroviral therapy in human immunodeficiency virus type I-infected children in the Paediatric European Network for Treatment of AIDS (PENTA) 5 Trial. *J. Infect. Dis.* **186**, 312–320.
- Delgado, J., Leal, M., Ruiz-Mateos, E., et al. (2002) Evidence of thymic function in heavily antiretroviral-treated human immunodeficiency virus type 1-infected adults with long term virologic treatment failure. *J. Infect. Dis.* **186**, 410–414.

14. Douek, D. C., Betts, M. R., Hill, B. J., et al. (2001) Evidence for increased T cell turnover and decreased thymic output in HIV infection. *J. Immunol.* **167**, 6663–6668.
15. Hatzakis, A., Touloumi, G., Karanicolos, R., et al. (2000) Effect of recent thymic emigrants on progression of HIV-1 disease. *Lancet* **355**, 599–604.
16. Kolte, L., Dreves, A. M., Ersboll, A. K., et al. (2002) Association between larger thymic size and higher thymic output in human immunodeficiency virus-infected patients receiving highly active antiretroviral therapy. *J. Infect. Dis.* **185**, 1578–1585.
17. Ometto, L., De Forni, D., Patiri, F., et al. (2002) Immune reconstitution in HIV-1 infected children nonantiretroviral therapy: role of thymic output and viral fitness. *AIDS* **16**, 839–849.
18. Harris, J. M., Hazenberg, M. D., Poulin, J. F., et al. (2005) Multiparameter evaluation of human thymic function: interpretations and caveats. *Clin. Immunol.* **115**, 138–146.



## Gene Expression Profiling of Dendritic Cells by Microarray

Maria Foti, Paola Ricciardi-Castagnoli, and Francesca Granucci

### Summary

The immune system of vertebrate animals has evolved to respond to different types of perturbations (invading pathogens, stress signals), limiting self-tissue damage. The decision to activate an immune response is made by antigen-presenting cells (APCs) that are quiescent until they encounter a foreign microorganism or inflammatory stimuli. Early activated APCs trigger innate immune responses that represent the first line of reaction against invading pathogens to limit the infections. At later times, activated APCs acquire the ability to prime antigen-specific immune responses that clear the infections and give rise to memory. During the immune response self-tissue damage is limited and tolerance to self is maintained through life. Among the cells that constitute the immune system, dendritic cells (DC) play a central role. They are extremely versatile APCs involved in the initiation of both innate and adaptive immunity and also in the differentiation of regulatory T cells required for the maintenance of self-tolerance. How DC can mediate these diverse and almost contradictory functions has recently been investigated. The plasticity of these cells allows them to undergo a complete genetic reprogramming in response to external microbial stimuli with the sequential acquisition of different regulatory functions in innate and adaptive immunity. The specific genetic reprogramming DC undergo upon activation can be easily investigated by using microarrays to perform global gene expression analysis in different conditions.

**Key Words:** Dendritic cells; innate immune response; microarray; global gene expression analysis.

### 1. Introduction

Resting immature dendritic cells (DC) are highly phagocytic and continuously internalize soluble and particulate antigens that are processed and presented, although inefficiently, to T cells. The interaction of immature DC with T cells induces an abortive T-cell activation with the induction of T-cell

energy (1) or the differentiation of regulatory T cells (2). In contrast, microbial stimuli that are recognized through a complex DC innate receptor repertoire induce DC maturation that is completed after 24 h (3,4). The extent and the type of innate and adaptive responses induced by DC are related to the type of signal they have received (4). Many different stimuli can induce myeloid DC activation both in mice and humans. These stimuli can be generically divided into stimuli that induce full DC maturation and stimuli that induce a semi-mature DC state. Full maturation stimuli are microbial stimuli and inflammatory products, such as prostaglandins (5). Among the microbial stimuli, some bind Toll-like receptors (TLRs) and other ones act in a TLR-independent manner. The stimulation of different TLRs at the DC surface results in the activation of different signaling pathways and the induction of diverse maturation processes that influence the outcome of adaptive immunity (4).

Ten TLRs have been identified so far and they recognize constitutive and conserved microbial structures absent in host mammalian cells called microbial-associated molecular patterns (6). In particular, TLR1, TLR2, and TLR6 interact with peptidoglycan, zymosan, and other microbial products (7,8), TLR3 binds double-stranded RNA (9), TLR4 lipopolysaccharide (10), TLR5 flagellin (11), TLR7 and TLR8 imidazoquinolines and single-stranded RNA (12–14), and TLR9 unmethylated CpG DNA (15). Microbial products that activate DC in a TLR-independent manner are represented by toxins, such as pertussis toxin (PT) and cholera toxin (CT) (16,17). Semimaturation stimuli described so far are two cytokines rarely, tumor necrosis factor (TNF) $\alpha$  and interleukin (IL)-4 (18–20). DC exposed to TNF $\alpha$ , do not become fully mature DC (18) but have the capacity to induce the differentiation of regulatory T cells (19) whereas IL-4-stimulated DC, though not able to prime naïve T cells, are able to trigger natural killer cell functions (20).

Comparative global gene expression analyses performed on immature DC and DC exposed to different stimuli are a valuable tool for the identification of genes responsible for the diverse DC functions.

## 2. Materials

### 2.1. Cell Culture and FACS Analysis

1. Iscove's modified Dulbecco's medium (Euroclone) supplemented with 2 mM L-glutamine, 100 U/mL penicillin, 100  $\mu$ g/mL streptomycin, 50  $\mu$ M 2-mercaptoethanol (all from Sigma), 10% heat-inactivated fetal bovine serum, and 10% supernatant granulocyte-macrophage colony-stimulating factor transduced B16 tumor cells (21).
2. Solution of ethylenediamine tetraacetic acid (EDTA) (10 mM) from Gibco/BRL.
3. Suspension culture plates from Corning.

4. Anti-CD11c, anti-CD40, anti-B7.1, anti B7.2, and anti-MHC class II monoclonal antibodies directly conjugated with fluorescein isothiocyanate or phycoerythrin (Pharmingen).
5. Phosphate buffered solution (PBS) for 1 L of 10X: 80 g NaCl, 2 g KCl, 2 g  $\text{KH}_2\text{PO}_4$ , 11.5 g  $\text{Na}_2\text{HPO}_4$ , bring to 1 L with ddH<sub>2</sub>O, pH 7.3. Filter-sterilize and store at room temperature.
6. FACS-fix solution: 1 g glucose, 100 mL PBS, 1 mL formaldehyde. Store at 4°C.

## 2.2. DC Stimulation

1. Use the stimulus adequate for your experiments. Example of stimuli are: lipopolysaccharide (Sigma, final concentration 10  $\mu\text{g}/\text{mL}$ ); zymosan (Sigma, used at 10  $\mu\text{g}/\text{mL}$ ); rTNF $\alpha$  (Genentech, final concentration 100 U/mL); rIL-1 $\beta$  (Genzyme, used at 10  $\mu\text{g}/\text{mL}$ ); CpG oligonucleotides (Primm, used at 1  $\mu\text{M}$ ); Pam3Cys (EMC microcollections GmbH, final concentration 10  $\mu\text{g}/\text{mL}$ ); endotoxin free (endotoxin concentration in the stock solution <0.0007 ng/mL according to the Limulus test) CT (List Biological Lab., 1  $\mu\text{g}/\text{mL}$  final concentration); prostaglandin E2 (Sigma, 1  $\mu\text{M}$  final concentration); Gram-positive and -negative nonpathogen bacteria (multiplicity of infection, MOI, of 10); Gram-positive and -negative pathogen bacteria (MOI of 5); *Leishmania mexicana* promastigote (MOI of 5); PT (Sigma, 1  $\mu\text{g}/\text{mL}$  final concentration). Before usage, purify PT on endotoxin removal columns (Detoxi-Gel, Pierce Biotechnology).

## 2.3. Sample Preparation and Hybridization

1. Total RNA isolation: DEPC-treated water (Ambion), TRIzol Reagent (Invitrogen), RNeasy RNA isolation Mini Kit (Qiagen). Quantification of RNA: 6000 Nano LabChip Kit (Agilent).
2. cDNA synthesis and in vitro transcription reaction: One-Cycle Target Labeling and Control Reagents (Affymetrix), GeneChip<sup>®</sup> Sample Cleanup Module, 30 eukaryotic reactions (Affymetrix).
3. Absolute ethanol (stored at -20°C for RNA precipitation; store ethanol at room temperature for use with the GeneChip Sample Cleanup Module). 80% ethanol (stored at -20°C for RNA precipitation; store ethanol at room temperature for use with the GeneChip Sample Cleanup Module).
4. 5X RNA fragmentation buffer (200 mM Tris-acetate, pH 8.1, 500 mM KOAc, 150 mM MgOAc).
5. 2X Hybridization buffer: prepare 12X MES Stock (1.22 M MES, 0.89 M [Na<sup>+</sup>]); for 1 L: 70.4 g MES-free acid monohydrate, 193.3 g MES sodium salt, 800 mL of molecular biology grade water. Mix and adjust volume to 1 L. The pH should be between 6.5 and 6.7. Filter through a 0.2- $\mu\text{m}$  filter.
6. 1X Hybridization buffer: 100 mM MES, 1 M (Na<sup>+</sup>), 20 mM EDTA, 0.01% Tween-20. For 50 mL, mix 8.3 mL of 12X MES stock, 17.7 mL of 5 M NaCl, 4.0 mL of 0.5 M EDTA, 0.1 mL of 10% Tween-20, 19.9 mL of water. Store at 2–8°C and shield from light.



7. Hybridization cocktail for single probe array: 50 pM Control oligonucleotide B2 (Affymetrix) (stored at  $-20^{\circ}\text{C}$ ), 0.1 mg/mL of herring sperm DNA (Promega, stored at  $-20^{\circ}\text{C}$ ), 0.5 mg/mL of acetylated BSA (Invitrogen, stored at  $4^{\circ}\text{C}$ ), 2X hybridization buffer (stored at  $4^{\circ}\text{C}$ ), 20X eukaryotic hybridization controls containing 1.5, 5, 25, and 100 pM, respectively of controls Bio B, C, D, and *Cre*, Affymetrix, stored at  $-20^{\circ}\text{C}$ . For a standard array format, prepare a final volume of 300  $\mu\text{L}$  by adding: 15  $\mu\text{g}$  of fragmented cRNA at 0.05  $\mu\text{g}/\mu\text{L}$ , 5  $\mu\text{L}$  of control oligonucleotide B2 (3 nM), 15  $\mu\text{L}$  of 20X eukaryotic hybridization controls, 3  $\mu\text{L}$  of herring sperm (10 mg/mL), 3  $\mu\text{L}$  of acetylated BSA (50 mg/mL), 150  $\mu\text{L}$  of 2X hybridization buffer, and water to a final volume of 300  $\mu\text{L}$ .
8. Staining buffer: R-phycoerythrin streptavidin (Molecular Probes), goat IgG, reagent grade (Sigma-Aldrich), anti-streptavidin antibody (goat) biotinylated (final 1X concentration: 100 mM MES, 1 M  $[\text{Na}^+]$ , 0.05% Tween-20).

### 3. Methods

#### 3.1. Generation of DC From Bone Marrow Cells

1. Remove femurs and tibias from 8- to 12-wk-old mice.
2. Remove bone marrow by cutting both ends of the bones with sterile scissors and flushing out the marrow using a 1-mL syringe filled with DC culture medium. The syringe should have a 23-gauge needle.
3. Resuspend the bone marrow from each mouse in 10 mL of medium.
4. Plate the cells in 10-mL suspension plates at a concentration of  $10^6$  cells/mL and add fresh medium every 2 d.
5. After 7–10 d of culture, analyze the cells for CD11c expression and use them in assays when more than 90% are CD11c<sup>+</sup>.
6. To collect the cells, remove the supernatant and put it in a 50-mL Falcon tube, add to the plate PBS containing 2 mM EDTA, pipet to collect the cells, add the recovered cells to the 50-mL tube containing the supernatant, centrifuge and resuspend the cells in a small volume of medium to count them.

#### 3.2. FACS Analysis

1. Resuspend  $10^5$  DC in 50  $\mu\text{L}$  of PBS with the antibodies at a concentration of 1  $\mu\text{g}/\text{mL}$ .
2. Incubate the cells in ice for 15 min.
3. Wash the cells once with 1 mL of PBS and resuspend them in 1 mL of FACS-fix.
4. Analyze the cells with a flow cytometer.

#### 3.3. DC Stimulation

1. Add the relevant stimulus to the cell culture at an appropriate concentration. When live microorganisms are used, remove them, by washing the cells with PBS, after 1.5-h incubation, otherwise leave the stimulus in contact with the DC. If bacteria are used, perform DC stimulation in medium without antibiotics, after 1.5 h, wash out the bacteria using PBS and add to the activated DC fresh medium containing gentamicin (50  $\mu\text{g}/\text{mL}$ , Sigma) and tetracyclin (30  $\mu\text{g}/\text{mL}$ , Sigma).

2. At different time points upon stimulation, remove the cells. Use a proportion of the cells for RNA extraction and analyze the remaining cells by FACS to evaluate the expression of B7.1, B7.2, CD40, and MHC class II.

### 3.4. RNA Extraction

1. Count the cells and calculate the volume of TRIzol to be used (maximum of  $5 \times 10^6$  cells per 1.5-mL tube).
2. Pellet the cells by centrifugation in a 1.5-mL Eppendorf, and remove the supernatant (PBS or culture medium). Resuspend the cell pellet by flicking the tube.
3. Add the appropriate volume of TRIzol. Pipet/mix the suspension until all cell debris dissolves and no lumps are apparent. Incubate the mixture at room temperature for 5 min to complete homogenization.
4. Follow the TRIzol protocol for the aqueous layer phase.
5. Spin the sample at 12,000g and at 4°C for 15 min. Carefully remove the upper aqueous phase and place into a fresh 1.5-mL tube.
6. Slowly add an equal volume of 70% ethanol to the aqueous phase and gently mix the tube by inversion. Once the ethanol has been mixed in, pipet the appropriate volume of the mixture into the RNA binding column.
7. Centrifuge the column using the appropriate conditions of the kit, e.g., 8000g for 15 s, and discard the flow-through.
8. If the aqueous phase and ethanol mixture was greater than the recommended loading volume for the particular column, load the column two or three times and repeat the spin, always discarding the flow-through, until all of the aqueous phase/ethanol mixture has passed through the column.
9. Continue with the specific protocol for column washing and RNA elution. Elute the RNA in non-DEPC treated RNase-free water. After this, maintain the RNA solution at 4°C by keeping the tube buried in ice. The total RNA used to make samples for Affymetrix chips has to be of the highest quality. This is the most important quality control factor in the experiment as it has the greatest effect on sample failure.
10. RNA quality and degradation can be assessed by electrophoretic analysis of the sample or by using the Agilent Bioanalyser. Degraded RNA samples will be evident in the ribosomal bands/peaks as either a smear in the gel, or a shoulder or shallow slope in the peaks on the chip. Ratio of 28s to 18s should ideally be 2. An indication of genomic DNA contamination can also be given with these two methods, the results of which may lead you to perform a DNase treatment on your samples, although we have never worried about it. For GeneChip analysis it is also imperative that the RNA extracted is of high-purity, displaying A260/280 values between 1.9 and 2.1.

### 3.5. cDNA Synthesis

1. First-strand cDNA synthesis: mix 1–5 µg total RNA and 1 µL T7-oligo(dT), add water to reach 12 µL.
2. Heat the mixture at 70°C in a PCR block for 10 min, spin briefly, keep at 42°C; add 2 µL of 10X first strand buffer, 1 µL of RNase inhibitor, 4 µL of dNTP mix, and 1 µL of reverse transcriptase.

3. Gently mix, incubate at 42°C for 2 h in a PCR block, spin briefly and place on ice.
4. For second strand synthesis, mix together 20 µL of cDNA first strand mix, 91 µL of RNase-free H<sub>2</sub>O, 30 µL of 5X second strand reaction buffer, 3 µL of dNTP mix, 1 µL of *E. coli* DNA ligase, 4 µL of *E. coli* DNA polymerase I, and 1 µL of RNase H.
5. Gently mix, spin briefly. Incubate at 16°C in a PCR block for 2 h. Add 2 µL of T4 DNA polymerase and incubate 5 min at 16°C. After incubation add 10 µL of 0.5 M EDTA. Store at -20°C or immediately proceed to cDNA purification using the Affymetrix cleanup module.
6. cDNA purification: add 600 µL of cDNA binding buffer to the double-stranded cDNA synthesis preparation. Mix by vortexing for 3 s.
7. Apply 500 µL of the sample to the cDNA cleanup spin column sitting in a 2-mL collection tube. Centrifuge for 1 min at 8000g. Discard the flow-through, reload the spin column with the remaining mixture and centrifuge as above. Discard the flow-through and the collection tube.
8. Apply 750 µL of cDNA wash buffer onto the spin column and centrifuge 1 min at 8000g. Discard the flow-through and spin for another 5 min at the maximum speed. Discard the flow-through and the collection tube.
9. Apply 14 µL of cDNA elution buffer to the center of the filter, keep it at room temperature for 1 min. Centrifuge for 1 min at maximum speed to elute.

### 3.6. Synthesis of Biotin-Labeled cRNA

1. IVT reaction: mix 12 µL of cDNA (if starting with 5–8 µg of total RNA), 4 µL of 10X IVT labeling buffer, 12 µL of labeling NTP mix, 4 µL of IVT labeling enzyme mix, 8 µL of water for a total volume of 40 µL.
2. Incubate at 37°C for 16 h. Store the labeled cRNA at -20°C, or -70°C if not purifying immediately.
3. cRNA purification: add 60 µL of RNase-free water to the IVT reaction and mix by vortexing for 3 s.
4. Add 350 µL of IVT cRNA binding buffer to the sample and mix by vortexing for 3 s.
5. Add 250 µL of 100% ethanol to each cRNA sample mix thoroughly and load onto the center of a cRNA cleanup column. Centrifuge for 15 s at 8000g. Discard the flow through and the collection tube.
6. Pipet 500 µL of IVT cRNA wash buffer onto the spin column and centrifuge for 15 s at 8000g. Discard the flow-through.
7. Pipet 500 µL of 80% (v/v) ethanol onto the spin column and centrifuge for 15 s at 8000g. Discard the flow-through and centrifuge for additional 5 min with open caps at maximum speed.
8. Apply 11 µL of RNase-free H<sub>2</sub>O to the center of the spin column membrane, keep it at room temperature for 2 min. Centrifuge 1 min at 25,000g. Repeat the elution with a second 10 µL of RNase-free H<sub>2</sub>O.
9. Quantification of cRNA concentration by UV absorbance: measure OD with spectrophotometer. Adjust the total yield with the following formula:

amount of RNA = RNAm – (starting total RNA) – (y)

RNAm = amount of cRNA measured after IVT ( $\mu\text{g}$ )

y = % (fraction) of sample used in IVT

10. Fragmentation. The final concentration of RNA must be  $>0.5 \mu\text{g}/\mu\text{L}$ . Add  $8 \mu\text{L}$  of 5X fragmentation buffer for every  $20 \mu\text{g}$  of cRNA, add RNase-free water to  $40 \mu\text{L}$  final volume. Heat at  $95^\circ\text{C}$  for 35 min. Save an aliquot for analysis on the bioanalyzer.

### 3.7. cRNA Hybridization

1. Prepare the hybridization mixture: add  $15 \mu\text{g}$  of cRNA,  $5 \mu\text{L}$  of control oligo B2,  $15 \mu\text{L}$  of 20X eukaryotic controls (heat to  $65^\circ\text{C}$  to dissolve),  $3 \mu\text{L}$  of herring sperm DNA ( $10 \text{ mg}/\text{mL}$ ),  $3 \mu\text{L}$  of BSA ( $50 \text{ mg}/\text{mL}$ ),  $150 \mu\text{L}$  of 2X hybridization buffer,  $30 \mu\text{L}$  of DMSO to a final volume of  $300 \mu\text{L}$ .
2. Heat at  $99^\circ\text{C}$  for 5 min. Switch to  $45^\circ\text{C}$  for 5 min. Spin at max rpm for 5 min.
3. Now, the hybridization mixture is ready to be added to the chip.
4. Take out the Affy chip from  $4^\circ\text{C}$  and keep it at room temperature for 10 min. Add 1X hybridization buffer to wet the chip. Put the chip in the hybridization oven, rotate at 60 rpm for 5 min. Remove the hybridization buffer from the chip.
5. Add  $250 \mu\text{L}$  of hybridization mixture to the chip. Place the chip to the rotisserie box in  $45^\circ\text{C}$ , rotate at 60 rpm. Hybridize for 16 h. Wash and stain.
6. Use the Affymetrix fluidics station and follow the manufacturer's instructions. Wash buffers: nonstringent buffer (A) 6X SSPE, 0.01% Tween-20. Stringent buffer (B), 100 mM MES buffer, 0.1 M, NaCl, 0.01% Tween-20. SAPE stain:  $600 \mu\text{L}$  MES stain buffer,  $48 \mu\text{L}$  acetylated BSA,  $12 \mu\text{L}$  streptavidin/phycoerythrin conjugate ( $1 \text{ mg}/\text{mL}$ ),  $540 \mu\text{L}$  water,  $1200 \mu\text{L}$  total. Mix and divide into two tubes (each  $600 \mu\text{L}$ ), one tube used as stain 1 and the other as stain 3. Antibody solution:  $300 \mu\text{L}$  of MES stain buffer,  $24 \mu\text{L}$  of acetylated BSA,  $6 \mu\text{L}$  of normal goat IgG,  $3.6 \mu\text{L}$  of biotinylated antibody,  $266.4 \mu\text{L}$  of water to achieve a total volume of  $600 \mu\text{L}$ . This will be used as stain 2. The chip is now ready for the scanning protocol.
7. Use the Affymetrix scanner and follow the instructions to scan the array.

### 3.8. Data Analysis

1. Quality control: the array image scan is processed with Affymetrix GCOS software. The GeneChip expression arrays contain control probe sets for both spiked and endogenous RNA transcripts (e.g., BioB, BioC, BioD, CreX, and species-specific actin and GAPDH). After performing the image processing and the absolute analysis of the array pattern with GCOS, six values are examined to assess the overall assay performance: background, noise, average signal, percent present, ratio of signal values for probe sets representing the 5'- and 3'-ends of actin and GAPDH transcripts, and total signal for probe sets for BioC, BioD, and CreX. Assays demonstrating poor or marginal performance are flagged.

2. Normalization: expression indices are calculated using the RMA algorithm and arrays are normalized using either the quantile or the Q spline methods (22).
3. Prefiltering: to reduce noisy data, two filtering steps are performed. The first filter is based on the Affymetrix calls and the second one is based on signal intensity. Remove all genes flagged as “absent” by the GCOS software and all the genes that present expression values less than the 95th percentile of the entire “absent” signals.
4. Sample similarities: cluster methods are used to visualize differences in expression between samples. These diagrams can be used in a diagnostic manner, because outliers and clusters of samples will be clearly visible.
5. Gene selection: one common selection method is to perform a pair wise comparison in GCOS and selected genes where the expression is changed between samples. We also use other selection methods, for example: group wise comparisons (t-test, SAM, PLGEM [23]) depending on the experimental design and on the replicates generated. We use different clustering methods, for example: PAM-clustering method to group genes with similar expression profiles over all conditions. We visualize members of a specific gene family or genes with specific function or protein localization.
6. Annotation: Affymetrix microarray features are supported by large amounts of annotation data available via Affymetrix NetAffx Analysis Center, an online resource for Affymetrix users. Information includes probe design, annotation method, public domain references, functional annotations, sequence information, and more. We perform functional annotation of differentially expressed genes also using the annotation files of the Bioconductor project (24). This annotation includes GeneOntology and KEGG.
7. Advanced analysis: if the microarray design contains sufficient number of experimental conditions, for example time series experiments, the datasets from multiple experimental conditions are compared using correspondence analysis. This multivariate analysis reveals relationships between genes and samples.

## Acknowledgments

This work was supported by fellowships and grants from the Italian Ministry of Education and Research (FIRB and COFIN projects), the European Commission 6th Framework Program (contracts DC VACC LSHB-CT-2003-503037 and DC THERA LSHB-CT-2004-512074), and Sekmed s.r.l.

## References

1. Hawiger, D., Inaba, K., Dorsett, Y., et al. (2001) Dendritic cells induce peripheral T cell unresponsiveness under steady state conditions in vivo. *J. Exp. Med.* **194**, 769–779.
2. Jonuleit, H., Schmitt, E., Schuler, G., Knop, J., and Enk, A. H. (2000) Induction of interleukin 10-producing, nonproliferating CD4(+) T cells with regulatory properties by repetitive stimulation with allogeneic immature human dendritic cells. *J. Exp. Med.* **192**, 1213–1222.

3. Granucci, F., Vizzardelli, C., Pavelka, N., et al. (2001) Inducible IL-2 production by dendritic cells revealed by global gene expression analysis. *Nat. Immunol.* **2**, 882–888.
4. Huang, Q., Liu, D., Majewski, P., et al. (2001) The plasticity of dendritic cell responses to pathogens and their components. *Science* **294**, 870–875.
5. Scandella, E., Men, Y., Gillessen, S., Forster, R., and Groettrup, M. (2002) Prostaglandin E2 is a key factor for CCR7 surface expression and migration of monocyte-derived dendritic cells. *Blood* **100**, 1354–1361.
6. Medzhitov, R. and Janeway, C. A., Jr. (2000) How does the immune system distinguish self from nonself? *Semin. Immunol.* **12**, 185–188.
7. Campos, M. A., Almeida, I. C., Takeuchi, O., et al. (2001) Activation of Toll-like receptor-2 by glycosylphosphatidylinositol anchors from a protozoan parasite. *J. Immunol.* **167**, 416–423.
8. Underhill, D. M., Ozinsky, A., Hajjar, A. M., et al. (1999) The Toll-like receptor 2 is recruited to macrophage phagosomes and discriminates between pathogens. *Nature* **401**, 811–815.
9. Alexopoulou, L., Holt, A. C., Medzhitov, R., and Flavell, R. A. (2001) Recognition of double-stranded RNA and activation of NF-kappaB by Toll-like receptor 3. *Nature* **413**, 732–738.
10. Poltorak, A., He, X., Smirnova, I., et al. (1998) Defective LPS signaling in C3H/HeJ and C57BL/10ScCr mice: mutations in Tlr4 gene. *Science* **282**, 2085–2088.
11. Hayashi, F., Smith, K. D., Ozinsky, A., et al. (2001) The innate immune response to bacterial flagellin is mediated by Toll-like receptor 5. *Nature* **410**, 1099–1103.
12. Akira, S. and Hemmi, H. (2003) Recognition of pathogen-associated molecular patterns by TLR family. *Immunol. Lett.* **85**, 85–95.
13. Hemmi, H., Kaisho, T., Takeuchi, O., et al. (2002) Small anti-viral compounds activate immune cells via the TLR7 MyD88-dependent signaling pathway. *Nat. Immunol.* **3**, 196–200.
14. Heil, F., Hemmi, H., Hochrein, H., et al. (2004) Species-specific recognition of single-stranded RNA via toll-like receptor 7 and 8. *Science* **303**, 1526–1529.
15. Krieg, A. M. (2002) CpG motifs in bacterial DNA and their immune effects. *Annu. Rev. Immunol.* **20**, 709–760.
16. Ausiello, C. M., Fedele, G., Urbani, F., Lande, R., Di Carlo, B., and Cassone, A. (2002) Native and genetically inactivated pertussis toxins induce human dendritic cell maturation and synergize with lipopolysaccharide in promoting T helper type 1 responses. *J. Infect. Dis.* **186**, 351–360.
17. Gagliardi, M. C., Sallusto, F., Marinaro, M., Langenkamp, A., Lanzavecchia, A., and De Magistris, M. T. (2000) Cholera toxin induces maturation of human dendritic cells and licenses them for Th2 priming. *Eur. J. Immunol.* **30**, 2394–2403.
18. Granucci, F., Vizzardelli, C., Virzi, E., Rescigno, M., and Ricciardi-Castagnoli, P. (2001) Transcriptional reprogramming of dendritic cells by differentiation stimuli. *Eur. J. Immunol.* **31**, 2539–2546.
19. Menges, M., Rossner, S., Voigtlander, C., et al. (2002) Repetitive injections of dendritic cells matured with tumor necrosis factor alpha induce antigen-specific protection of mice from autoimmunity. *J. Exp. Med.* **195**, 15–21.

20. Terme, M., Tomasello, E., Maruyama, K., et al. (2004) IL-4 confers NK stimulatory capacity to murine dendritic cells: a signaling pathway involving KARAP/DAP12-triggering receptor expressed on myeloid cell 2 molecules. *J. Immunol.* **172**, 5957–5966.
21. Dranoff, G., Jaffee, E., Lazenby, A., et al. (1993) Vaccination with irradiated tumor cells engineered to secrete murine granulocyte-macrophage colony-stimulating factor stimulates potent, specific, and long-lasting anti-tumor immunity. *Proc. Natl. Acad. Sci. USA* **90**, 3539–3543.
22. Workman, C., Jensen, L. J., Jarmer, H., et al. (2002) A new non-linear normalization method for reducing variability in DNA microarray experiments. *Genome Biol.* **3**, R48.
23. Pavelka, N., Pelizzola, M., Vizzardelli, C., et al. (2004) A power law global error model for the identification of differentially expressed genes in microarray data. *BMC Bioinformatics* **5**, 203.
24. Gentleman, R. C., Carey, V. J., Bates, D. M., et al. (2004) Bioconductor: open software development for computational biology and bioinformatics. *Genome Biol.* **5**, R80.

## SAGE Analysis of Cell Types Involved in Tolerance Induction

Kathleen F. Nolan, Stephen P. Cobbold, and Herman Waldmann

### Summary

Investigations into the mechanisms of immunological tolerance are currently hindered by a paucity of convenient markers, both for the identification and isolation of tolerant cell types and for monitoring the establishment of tolerance in *in vivo* models. Although high-affinity autoreactive T cells are deleted in the thymus during the establishment of central tolerance, escaping autoreactive cells require modulation in the periphery. Dendritic cells (DC) and regulatory T cells (Treg) are both implicated in the establishment and maintenance of peripheral tolerance, although specific interactions and mechanisms remain to be established. The serial analysis of gene expression (SAGE) approach to transcript profiling offers potential, not only for new insight into tolerogenic mechanisms, unbiased by current dogma, but also for the identification of novel molecular markers of tolerance. SAGE provides both quantitative and qualitative information on transcripts sampled on the basis of frequency of occurrence in the initial mRNA pool. This information is generated in the form of electronic databases that accumulate as a permanent resource and confer on SAGE the ability to readily compare across wide datasets. This offers particular potential when attempting to correlate gene expression with functional phenotype. By comparing variously generated functionally distinct/related immune populations, such as effector T cells and either natural, CD4<sup>+</sup>CD25<sup>+</sup>, or adaptive, Tr1, Tregs and/or immune and tolerance prone DC, it should be possible, using SAGE, to identify both individual genes and also signatures of genes associated with protolerogenic rather than immunogenic phenotypes.

**Key Words:** Serial analysis of gene expression; SAGE; transcript profiling; dendritic cells; regulatory T cells; immunological tolerance.

### 1. Introduction

Serial analysis of gene expression (SAGE) was originally developed based on three key principles: (1) that a short sequence tag of 9–10 bp is sufficient to uniquely identify a transcript, provided the tag is isolated from a defined position; (2) that efficient sequencing of these short tags can be achieved by



concatenation, provided there is a means to register the boundaries of each tag; and (3) that the number of times a tag is sampled reflects the relative frequency of the associated transcript in the starting mRNA pool (1). Modifications from the original procedure reflect fine-tuning to provide increased robustness and efficiency, and incorporation of an alternative restriction enzyme to generate longer more informative SAGE tags. A schematic representation of the SAGE procedure as it is currently performed in our hands is outlined in Fig. 1.

SAGE libraries must be generated from high quality mRNA isolated from well-defined cell populations. Double stranded cDNA is generated directly on the magnetic beads used for mRNA isolation and the resulting bead-linked cDNA digested using a frequent cutting restriction enzyme (most commonly *Nla* III, recognition site, CATG<sup>▼</sup>). This enzyme defines the position within the transcript from which the tag will be isolated and is referred to as the “anchor enzyme” (AE) (see Note 1). The most 3' restriction fragments are magnetically isolated, the sample divided in two, and unique adaptor linkers (1 and 2) ligated onto either half (see Note 2). The sample is recombined and digested using a type IIS restriction enzyme that recognizes a nonpalindromic sequence within each linker and cleaves downstream of this site to release a “linker+tag” unit. This enzyme defines the length of the SAGE tag and is referred to as the “tagging enzyme” (TE). The original TE, BsmF 1, generated “short” tags of approx 10 bp (+4 bp contributed by the AE site). The current enzyme *Mme* I cuts 7 bp further away to yield approx (17+4) bp “long” tags. These longer tags confer distinct benefits for tag-to-gene annotation in that they can be mapped directly to the genome, avoiding inconsistencies encountered from the use of incomplete cDNA/Unigene database entries (2,3). So long as the AE is retained in common, “long” and “short” SAGE libraries remain directly comparable over the common sequence (AE + proximal 10 bp). Following *Mme* I digestion the 3' cDNA ends that are still bound to the beads are removed magnetically and the linker+tag units purified from the supernatant by precipitation. For “long” SAGE these units are cohesively ligated to generate approx 130 bp PCR templates (see Notes 3 and 4). Amplification is performed using biotinylated primers 1 and 2 that bind within the linker sequences (see Fig. 2) and “ditags” are released from the amplified products using the AE. The ditags are gel-purified and any remaining traces of linker removed using streptavidin-coated magnetic beads to promote efficient concatenation (4). A limited concatenation reaction is performed, ideally generating the majority of concatemers within the size range 700 to 900 bp. Removal of small concatenation fragments, using a commercial PCR clean-up column prior to size selection on a polyacrylamide gel (PAG), improves the subsequent cloning of larger concatemers and consequently the efficiency of the downstream screening and sequencing process (5). High-throughput

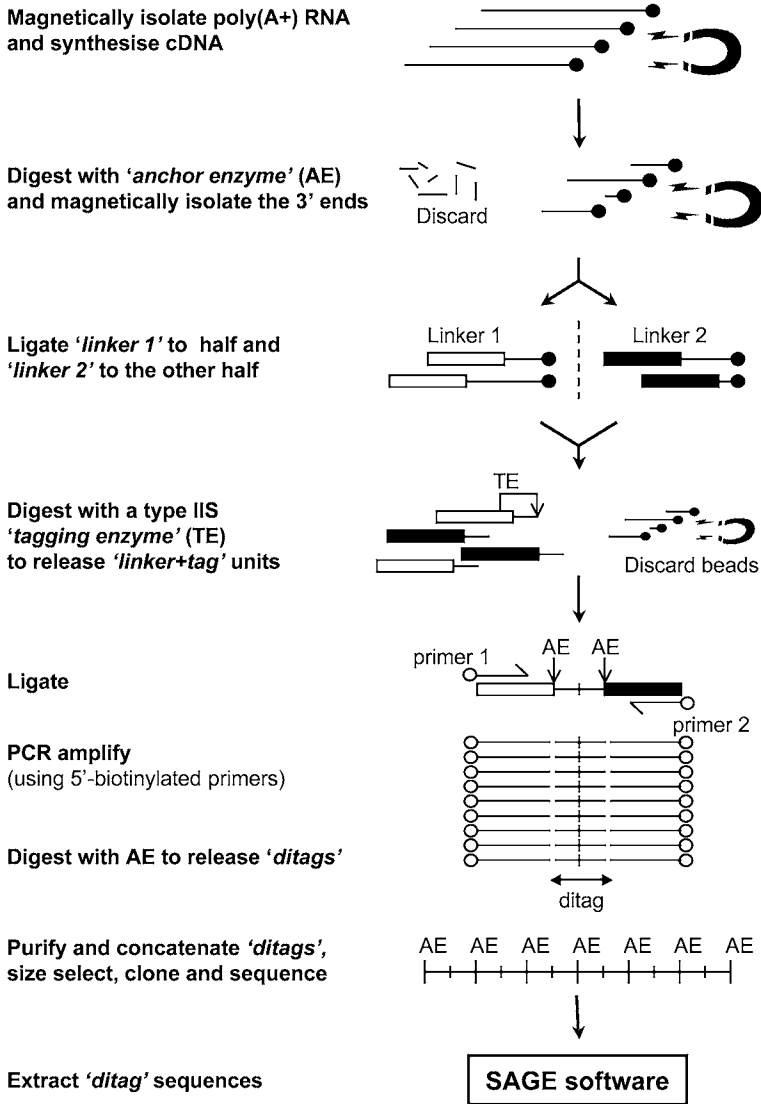


Fig. 1. Schematic outline describing the construction of a serial analysis of gene expression library (see text for details).

analysis of the cloned concatemers is achieved in 96-well format by PCR amplification, followed by direct, single-pass sequencing of polyethylene glycol (PEG) precipitated products. Sequence data are transferred directly to SAGE software that locates the punctuating AE sites in the concatemers and extracts the intervening “ditag” sequence information.

**Long SAGE linker 1:****Long SAGE Bi primer 1**

5'-[Bi]gtgctcgtgggatttgctggtgcagtaca-3'&gt;

5'- TTTGGATTTGCTGGTGCAGTACAACCTAGGCTTAATATCCG**CATG** -3'

3'- [C7mod]CCTAAACGACCACGTCATGTTGATCCGAATTATAGGCT -5'

**Long SAGE linker 2:****Long SAGE Bi primer 2**

5'-[Bi]gagctcgtgctgctcgaattcaagcttct-3'&gt;

5'- TTTCTGCTCGAATTCAAGCTTCTAACGATGTACGTC**CCGACATG** -3'

3'- [C7mod]GACGAGCTTAAGTTCGAAGATTGCTACATGCAGGCT -5'

\***Mme I**                    TCC (A/G) AC (N<sub>20</sub>)  
                               AGG (T/C) TG (N<sub>18</sub>)

Fig. 2. Long serial analysis of gene expression (SAGE) linkers 1 and 2. Each adapter linker includes a 3' *Nla* III compatible overhang (CATG, bolded) overlapping the recognition site of the type IIS restriction enzyme *Mme* I, (underlined, and detailed \*). *Mme* I cleaves downstream of the recognition site to generate 21-bp SAGE tags (including the *Nla* III recognition sequence). The 3'-end of the bottom strand in each linker is recessed and blocked to prevent inappropriate ligation by the addition of a C7-aminolink modification. The corresponding 5'-biotinylated PCR primers (1 and 2) are shown in lower case.

Any SAGE library database can be compared with any other library or combination of libraries generated from the same species, including those generated in different laboratories, provided the same AE has been used (6). As such, SAGE represents a particularly versatile tool for elucidating patterns of gene expression extending across a number of cell populations. A large resource of both human and murine libraries is available at the gene expression omnibus data repository at the national center for biotechnology information and can be downloaded *via* the internet for inclusion in such comparative analyses. In addition to potentially relevant libraries, phenotypically unrelated libraries can be included in analyses to remove "noise" generated by abundant "house-keeping" type genes.

For informative library comparisons the authenticity and homogeneity of the starting cell populations must be well established. We have generated a resource, currently comprising of the order of 50 murine SAGE libraries, derived from well-defined immunological cell populations, to investigate tolerogenic mechanisms. Libraries have been generated from immature and LPS-matured bone marrow derived DC (bmDC) populations and from bmDC counter-modulated for tolerance by exposure to agents such as IL-10 (+/- LPS),

TGF- $\beta$  and  $1\alpha,25$ -dihydroxyvitamin D<sub>3</sub> (6,7), and from embryonic stem (ES) cells and populations of DC differentiated from them, again with and without maturation in response to LPS (6,8–10). Libraries have also been generated from polarized effector (Th1 and Th2) and regulatory (“adaptive,” Tr1-like) T-cell clones and functionally distinct primary T-cell populations, including “natural” CD4<sup>+</sup>CD25<sup>+</sup> regulatory populations (6,11–13). Libraries generated from a B-cell population and a number of nonimmune related populations, such as a fibroblast line and organs such as the heart and brain have been included in the database for the purpose of subtracting broadly expressed genes (6). Both “long” and “short” SAGE libraries are represented in the resource, and new libraries are continually added as they become available.

## 2. Materials

### 2.1. Extraction of Total RNA

1. RNase-free disposable plasticware.
2. An appropriately scaled commercial RNA extraction kit.
3. Access to an Agilent Technologies 2100 bioanalyzer.

### 2.2. Binding of mRNA to Magnetic Beads and cDNA Synthesis

1. Oligo(dT)-coated magnetic beads, binding and wash buffers and reagents for both the first and second strand cDNA synthesis reactions (I-SAGE™ long kit, Invitrogen) (see Notes 5–7).
2. Siliconized 1.5-mL microcentrifuge tubes.
3. Magnetic 1.5-mL microfuge tube stand.

### 2.3. Cleavage of cDNA Using Anchor Enzyme Nla III

1. Nla III, 10X restriction buffer (see Note 8).
2. Wash buffers C and D (I-SAGE long kit, Invitrogen).
3. Magnetic 1.5-mL microfuge tube stand.

### 2.4. PCR to Assess the Efficiency of cDNA Synthesis and Verify the Nla III Digestion

1. PCR reagents: 10X PCR buffer, 50 mM MgCl<sub>2</sub>, 2 mM dNTPs, Taq polymerase, autoclaved Milli-Q water, 10  $\mu$ M HPRT PCR primers (see Note 9): 5'-GTTGGA TACAGGCCAGACTTTGTG-3' and 5'-GAGGGTAGGCTGGCCTATAG GCT-3'.
2. LoTE: 3 mM Tris-HCl, pH 7.5, 0.2 mM EDTA, pH 8.0, prepared by dilution from autoclaved stock solutions.
3. Ficoll-Orange-G loading dye (FOG): 20% (v/v) Ficoll-400 in LoTE, with sufficient orange-G dye to make it orange in appearance.
4. 1.5% (w/v) Agarose gel.
5. 1-kb DNA ladder.

### **2.5. Ligating Adaptor Linkers to Bound 3'-cDNA Ends**

1. Adaptor linkers (I-SAGE long kit, Invitrogen).
2. 10X Ligase buffer and T4 DNA ligase (I-SAGE long kit, Invitrogen).
3. Relevant wash buffers (I-SAGE long kit, Invitrogen).
4. Magnetic 1.5-mL microfuge tube stand.

### **2.6. Release of SAGE Tags Using Tagging Enzyme *Mme* I**

1. 32 mM *S*-adenosylamine (SAM) (I-SAGE long kit, Invitrogen).
2. 10X Restriction buffer and *Mme* I (I-SAGE long kit, Invitrogen).
3. Magnetic 1.5-mL microfuge tube stand.
4. Phenol/chloroform/isoamylalcohol (25:24:1).
5. 7.5 M NH<sub>4</sub>OAc (I-SAGE long kit, Invitrogen).
6. 20 mg/mL Mussel glycogen (I-SAGE long kit, Invitrogen).
7. LoTE (I-SAGE long kit, Invitrogen).
8. Ethanol.

### **2.7. Ligating the Tags to Form Ditags**

1. 10X Ligase buffer (I-SAGE long kit, Invitrogen).
2. 3 mM Tris-HCl, pH 7.5 (I-SAGE long kit, Invitrogen).
3. T4 DNA ligase (I-SAGE long kit, Invitrogen).

### **2.8. Optimizing Conditions for PCR Amplification of Ditags**

1. PCR reagents: a proofreading, thermostable polymerase, aliquots of 10X PCR buffer, 50 mM MgCl<sub>2</sub>, DMSO, sterile water, 100 mM dATP, dTTP, dCTP, and dGTP, 5' biotinylated long-SAGE PCR primers 1 and 2, as detailed in [Fig. 2](#), obtained HPSF- or HPLC-purified and stored as single use 500- $\mu$ M aliquots at -80°C (see [Notes 10](#) and [11](#)).
2. 96-Well PCR machine.
3. 96-Well PCR plates with adhesive sealing film.
4. 10% (w/v) PAG, prepared using a 10-well comb (see [Note 12](#)).
5. 25-bp DNA ladder.

### **2.9. Preparative PCR Amplification of Ditags**

1. PCR reagents (see [Subheading 2.8](#)).
2. A pipette capable of automatically dispensing 50- $\mu$ L aliquots.
3. 15-mL Polypropylene tubes.
4. 3 M NaOAc, pH 5.6 (autoclaved and aliquoted).
5. Ethanol.
6. 20 mg/mL Mussel glycogen (I-SAGE long kit, Invitrogen).
7. 10% (w/v) PAG, prepared using a 10-well comb (see [Note 12](#)).
8. 25-bp DNA ladder.

**2.10. Gel Purification of the Approx 130-bp Amplified Ditag Species**

1. Two 10% (w/v) PAGs, prepared using a preparative comb (*see Note 12*).
2. 25-bp DNA ladder.
3. Razor blade.
4. 21-Gauge syringe needle
5. LoTE (*see Subheading 2.4.*).
6. 10 M NH<sub>4</sub>OAc (filter-sterilized and aliquoted).
7. Microcentrifuge tube filter assemblies (consisting of a 0.22- $\mu$ m cellulose acetate filter basket in a 2-mL collection tube).
8. Phenol/chloroform/isoamylalcohol (25:24:1).
9. 20 mg/mL Mussel glycogen (I-SAGE long kit, Invitrogen).
10. Ethanol.
11. 10% (w/v) PAG, prepared using a 15-well comb (*see Note 12*).
12. 25-bp DNA ladder.
13.  $\lambda$  DNA as a quantification standard.
14. EtBr, diluted to 1  $\mu$ g/mL in LoTE.

**2.11. Isolation of Approx 40 bp Ditags**

1. *Nla* III (*see Note 8*).
2. 4% (w/v) Low melting point agarose gel.
3. 25-bp DNA ladder.
4. Phenol/chloroform/isoamylalcohol (25:24:1).
5. LoTE.
6. 10 M NH<sub>4</sub>OAc.
7. 20 mg/mL Mussel glycogen.
8. Ethanol.
9. 14% (w/v) PAG, prepared using a preparative comb (*see Note 12*).
10. 25-bp DNA ladder.
11. Razor blade.
12. 21-Gauge syringe needle.
13. Microcentrifuge tube filter assemblies.

**2.12. Removal of Residual Linkers**

1. Streptavidin-coated magnetic beads.
2. Magnetic 1.5-mL microfuge tube stand.
3. 1X Bind+wash (1XB+W) buffer: 10 mM Tris-HCl, pH 7.5, 1 mM EDTA, pH 8.0, 2 M NaCl, prepared by dilution of autoclaved stock solutions.
4. 10 M NH<sub>4</sub>OAc (I-SAGE long kit, Invitrogen).
5. 20 mg/mL Mussel glycogen (I-SAGE long kit, Invitrogen).
6. Ethanol.
7.  $\lambda$  DNA standard and EtBr, 1  $\mu$ g/mL (*see Subheading 2.10.*).

### **2.13. Concatenation of Dtags and Isolation of Size Selected Concatemers**

1. 10X Ligase buffer.
2. T4 DNA ligase.
3. QIA quick PCR clean up column, binding buffer (PB), wash buffer (PE), and elution buffer (EB) (Qiagen).
4. A 6% (w/v) PAG, prepared using a 10-well comb (*see Note 12*).
5. 1-kb DNA ladder.
6. Razor blade.
7. 21-Gauge syringe needle.
8. LoTE.
9. 10 M NH<sub>4</sub>OAc (*see Subheading 2.10.*).
10. 20 mg/mL Mussel glycogen (I-SAGE long kit, Invitrogen).
11. Ethanol.

### **2.14. Cloning of Size-Selected Concatemers (see Note 13)**

1. pZErO<sup>®</sup>-1 and *Sph* I (I-SAGE long kit, Invitrogen) (*see Note 14*).
2. LoTE.
3. Phenol/chloroform/isoamylalcohol (25:24:1).
4. 3 M NaOAc, pH 5.6 (*see Subheading 2.9.*).
5. 20 mg/mL Mussel glycogen (I-SAGE long kit, Invitrogen).
6. Ethanol.
7. 10X Ligase buffer (I-SAGE long kit, Invitrogen).
8. T4 DNA ligase (I-SAGE long kit, Invitrogen).
9. One Shot<sup>®</sup> TOP10 Electrocomp<sup>®</sup> *Escherichia coli* and SOC medium from the I-SAGE long kit (Invitrogen) (*see Note 15*).
10. Electroporation cuvetts (0.1 cm) and an electroporator.
11. Low salt LB agar plates containing zeocin:1% (w/v) tryptone, 0.5% (w/v) yeast extract, 0.5% (w/v) NaCl, if required adjust pH to 7.5 using NaOH and then add agar to 1.5% (w/v). Autoclave and store the low salt agar at room temperature. As required, melt the agar, equilibrate it to 50°C and add Zeocin to 50 µg/mL. Pour into 10-cm diameter Petri dishes (*see Note 16*).

### **2.15. PCR Screening of Transformants and Sequencing the Amplified Inserts**

1. 96-Well PCR plates with adhesive sealing film.
2. PCR reagents: 10X PCR buffer, 50 mM MgCl<sub>2</sub>, 2 mM dNTPs, *Taq* polymerase, sterile water, 10 µM M13 -40 and M13 rev PCR primers: 5'-GTTTTCGCCAGT CACGACGTTGTA-3' and 5'-GGAAACAGCTATGACCATG-3'.
3. Multichannel and electronic multidispensing pipettes.
4. 1% (w/v) Agarose slab gel.
5. 1-kb DNA ladder.
6. 96-Well agarose gel analysis system.

7. PEG/NaOAc solution: 66.5 g polyethylene glycol, Mr 8000, 1665  $\mu$ L 1 M MgCl<sub>2</sub>, 50 mL 3 M NaOAc, pH 5.6, add water to a final volume of 250 mL.
8. 70% (v/v) Ethanol wash.
9. DNA sequencing reagents.
10. 100% Cold ethanol ( $-20^{\circ}$ C).
11. Access to a 96-well capillary DNA sequencer.

### **2.16. Handling of Raw SAGE Data**

1. SAGE300 software (*see Note 17*).
2. SAGEScreen software (*see Note 18*).
3. Automated tag-to-gene annotation software (*see Note 19*).
4. iSAGEClus software (*see Note 20*).

## **3. Methods**

For SAGE to provide informative comparisons it is essential that the authenticity and homogeneity of the starting cell populations are well established. Selection of appropriate populations, including the isolation procedures (which, if prolonged or deleterious to the cells, can effect gene expression profiles) should represent a significant consideration prior to embarking on this protocol. Considering the relative advantages of “long” tags over “short” tags with respect to resolving sequence generated artifacts (*see Note 18*) and facilitating tag-to-gene annotations (2,3), we now exclusively use the long SAGE procedure and this is described here.

It is essential that cross-contamination of samples does not occur throughout the SAGE process. This is of particular concern with respect to PCR contamination. All work areas and pipettes should be thoroughly cleaned before embarking on a new library. Reagents should be prealiquoted in an area physically isolated from areas previously exposed to amplifiable SAGE products, with fresh aliquots used for each library. It is advisable that, until experience is acquired with the technique, only one library should be attempted at a time.

Competency in standard molecular biology techniques is required for the successful outcome of SAGE. Further background detail and guidance on the individual techniques used can be obtained by reference to a standard laboratory manual.

### **3.1. Extraction of Total RNA**

General precautions should be observed to avoid RNA degradation. Use either 10% (v/v) bleach, or one of numerous commercial reagents, to generate a nuclease-free work area. Wear gloves, changing them regularly and wherever possible use disposable RNase-free plastic ware.



The method of choice for preparing RNA for SAGE is not critical, although an RNase-free DNase digestion step should be included to remove any traces of genomic DNA and it is essential that high quality RNA is generated. The integrity of each RNA sample should be formally established immediately prior to the SAGE process, as even partial degradation can impact on the expression profile obtained (*see Note 21*). Typically libraries are generated using 2–10  $\mu\text{g}$  of high quality total RNA, with no requirement for the incorporation of preamplification procedures (*14–17*).

### 3.2. Binding of mRNA to Magnetic Beads and Synthesis of cDNA

In the original description of SAGE (*1*), poly A+ mRNA was isolated using oligo(dT)-coated magnetic beads, eluted and cDNA synthesis performed in solution, primed using a biotinylated oligo(dT) primer. Following *Nla* III digestion, a further magnetic isolation was required to purify the 3' cDNA restriction fragments. The efficiency of this process has now been improved by the introduction of an on-bead cDNA synthesis procedure (*see Notes 5 and 7*).

1. Magnetically isolate 60  $\mu\text{L}$  of oligo(dT)-coated magnetic beads (binding capacity 0.6  $\mu\text{g}$ ). Resuspend the beads using 250  $\mu\text{L}$  of binding buffer and transfer them directly to 5  $\mu\text{g}$  of total RNA, aliquoted into a 1.5-mL siliconized microfuge tube with the volume adjusted to 250  $\mu\text{L}$  using binding buffer (*see Notes 22 and 23*).
2. Rotate at room temperature over a period of 30 min.
3. Magnetically isolate the mRNA bound to the beads and remove the unbound, polyA- fraction, contained in the supernatant.
4. Wash the beads, twice using 500  $\mu\text{L}$  of wash buffer A, once using 500  $\mu\text{L}$  of wash buffer B and then equilibrate them in first strand synthesis buffer using four consecutive 50- $\mu\text{L}$  washes.
5. Perform first and second strand synthesis reactions sequentially on the beads (*see Note 5*).
6. Stop the second strand synthesis reaction (final volume 375  $\mu\text{L}$ ) by adding 22.5  $\mu\text{L}$  of 0.5 M EDTA and magnetically isolate the cDNA-coated beads.
7. Discard the supernatant and add 375  $\mu\text{L}$  of wash buffer C, prewarmed to 75°C. Mix well and heat the beads to 75°C for 10 min to completely inactivate any remaining *E. coli* DNA polymerase (*see Note 24*).
8. Wash the beads again using 375  $\mu\text{L}$  of wash buffer C and then four times using 375  $\mu\text{L}$  of buffer D. Retain 2.5  $\mu\text{L}$  of beads from the final wash for subsequent assessment of cDNA yield and *Nla* III digestion (*see Subheading 3.3*).
9. Resuspend the beads using 100  $\mu\text{L}$  of 1X *Nla* III restriction buffer and transfer them to a fresh siliconized microfuge tube, to further avoid any residual traces of *E. coli* DNA polymerase. Wash the old tube using a 100  $\mu\text{L}$  of 1X *Nla* III restriction buffer and combine this with the contents of the new tube.
10. Magnetically separate the beads and wash again using 100  $\mu\text{L}$  of 1X *Nla* III restriction buffer. At this point the beads can be stored overnight at 4°C.

### 3.3. Cleavage of cDNA Using Anchor Enzyme *Nla* III

1. Magnetically separate the cDNA-coated beads from **Subheading 3.2.** and resuspend them in a final volume of 100  $\mu\text{L}$ , composed of 1X *Nla* III restriction buffer containing 30 U of *Nla* III (see **Note 8**), and digest the cDNA for 1 h at 37°C, with intermittent agitation of the beads.
2. Remove the *Nla* III and any unbound restriction fragments by magnetic separation, washing twice using 375  $\mu\text{L}$  of wash buffer C, prewarmed to 37°C to avoid precipitation of the sodium dodecyl sulfate.
3. Wash the beads a further four times using 375  $\mu\text{L}$  of buffer D, retaining 2.5  $\mu\text{L}$  of sample from the final wash step to assess the extent of the *Nla* III digestion. At this stage, the sample can be stored overnight at 4°C, although it is good practice to avoid this in an attempt to maintain the integrity of the *Nla* III compatible single-stranded terminal overhangs.

### 3.4. PCR to Assess the Efficiency of cDNA Synthesis and Verify the *Nla* III Digestion

1. Prepare a five-fold dilution series (1/5–1/3125) of the retained aliquots of cDNA (see **Subheading 3.2.**) and *Nla* III-digested cDNA (see **Subheading 3.3.**).
2. Add 2.5  $\mu\text{L}$  of each serial dilution, or water as a negative control, to a 10- $\mu\text{L}$  PCR reaction consisting of 1X PCR buffer, 1.5 mM  $\text{MgCl}_2$ , 0.2 mM of each dNTP, 0.5  $\mu\text{M}$  of each primer, and 0.5 U of enzyme, and amplify for 30 cycles of 94°C for 20 s, 54°C for 30 s, and 72°C for 30 s, using a standard nonproofreading *Taq* polymerase (see **Note 9**).
3. Analyze the products on a 1.5% (w/v) agarose gel against a 1-kb ladder. We routinely observe amplification titering as far as the 1/625 and 1/3125 dilutions. If the *Nla* III digestion is complete, amplicons including a *Nla* III site should be unavailable for amplification. In general some amplification is still observed, but titers out toward the 1/25 to 1/125 dilution.

### 3.5. Ligating Adaptor Linkers to Bound 3' cDNA Ends

1. Magnetically separate the beads coated with 3' terminal cDNA *Nla* III restriction fragments and equilibrate them in 1X ligase buffer, using two 75- $\mu\text{L}$  washes. After the second wash resuspend the beads in 50  $\mu\text{L}$  of 1X ligase buffer and transfer 25  $\mu\text{L}$  to each of two fresh siliconized 1.5-mL microfuge tubes.
2. Wash each set of beads, using a further 25  $\mu\text{L}$  of 1X ligase buffer.
3. Resuspend each bead fraction in 7  $\mu\text{L}$  of LoTE by flicking the tube gently with a finger.
4. Add 1  $\mu\text{L}$  of 10X ligase buffer and 0.75  $\mu\text{L}$  of either adaptor 1 or 2 (40 ng/ $\mu\text{L}$ ) (see **Note 25**). Heat at 50°C for 2 min and then cool to room temperature over a 15 min period, allowing the adaptor linkers to anneal to the compatible cohesive ends of the bead-linked 3' cDNA restriction fragments.
5. Add 1.25  $\mu\text{L}$  (4 U/ $\mu\text{L}$ ) of T4 DNA ligase and ligate for 2 h at 16°C, with intermittent agitation.

6. Magnetically separate the beads and remove the supernatant, containing unbound linker.
7. In contrast to many protocols, to minimize subsequent washing steps, we combine the adaptor 1- and 2-linked beads at this point by resuspending and recombining them in a fresh 1.5-mL microfuge tube using four tube washes of 125  $\mu$ L of wash buffer D.
8. Further wash the combined beads using three 500- $\mu$ L washes of buffer D.

### 3.6. Release of SAGE Tags Using Tagging Enzyme *Mme* I

1. Prepare 10X SAM by adding 0.5  $\mu$ L of 32 mM SAM to 40  $\mu$ L of water, and prepare 1X *Mme* I restriction buffer/1X SAM by adding 0.5  $\mu$ L of 32 mM SAM to 400  $\mu$ L of 1X *Mme* I restriction buffer.
2. Magnetically separate the adaptor 1- and 2-linked beads. Discard the supernatant and wash twice using 200  $\mu$ L of 1X *Mme* I restriction buffer/1X SAM, carefully removing the final wash.
3. Resuspend the beads in 70  $\mu$ L of LoTE and add 10  $\mu$ L of 10X *Mme* I restriction buffer, 10  $\mu$ L of 10X SAM and 10  $\mu$ L of 2 U/ $\mu$ L of *Mme* I. Digest for 2.5 h at 37°C, with intermittent agitation of the beads.
4. Magnetically separate the beads and carefully transfer the supernatant, containing the released SAGE tags linked to either adaptor 1 or 2, to a fresh tube. Resuspend the beads in 100  $\mu$ L of LoTE, magnetically separate and combine the wash with the first supernatant containing the released tags.
5. Add 200  $\mu$ L phenol/chloroform/isoamylalcohol (25:24:1), vortex to mix and centrifuge at maximum speed in a microfuge for 3 min at room temperature.
6. Transfer the upper aqueous phase to a fresh 1.5-mL microfuge tube and add 133  $\mu$ L of 7.5 M  $\text{NH}_4\text{OAc}$ , 3  $\mu$ L of 20 mg/mL mussel glycogen and 1 mL of ethanol. Vortex to mix and pellet the linker+tag units by centrifugation at maximum speed in a microfuge for 30–60 min at 4°C. Carefully remove the supernatant and wash the pellet once using 500  $\mu$ L of 70% (v/v) ethanol. Remove any residual ethanol carefully and briefly air-dry before resuspending the pellet in 4  $\mu$ L of LoTE.

### 3.7. Ligating the Tags to Form Ditags (see Note 3)

1. Prepare a 2X-ditag reaction mix by adding 0.9  $\mu$ L of 10X ligase buffer to 1.5  $\mu$ L of 3 mM Tris-HCl, pH 7.5, 0.9  $\mu$ L of sterile water and 1.2  $\mu$ L of T4 DNA ligase (4 U/ $\mu$ L).
2. Add 4  $\mu$ L of the 2X-ditag reaction mix to the 4  $\mu$ L of adaptor-linked SAGE tags from **Subheading 3.6.** and ligate at 16°C overnight.
3. Dilute the reaction to a final volume of 14  $\mu$ L by adding 6  $\mu$ L of LoTE. The samples can now be stored at –20°C.

### 3.8. Optimizing Conditions for PCR Amplification of Ditags

Use small-scale PCR to determine the optimum amount of template and number of cycles for the preparative ditag amplification.

1. Use 0.5  $\mu$ L of sample to assemble a five-fold dilution series of the ligated ditags (1/5 to 1/3125).

2. Prepare a seven-fold “hot-start PCR premix” for use with a proof-reading thermostable polymerase: 35  $\mu\text{L}$  of 10X PCR buffer, 32.9  $\mu\text{L}$  of 50 mM  $\text{MgCl}_2$  (final concentration 4.7 mM), 5.25  $\mu\text{L}$  of each 100 mM dNTP, 21  $\mu\text{L}$  of DMSO, 0.7  $\mu\text{L}$  of each 500  $\mu\text{M}$  biotinylated long SAGE primer stock (see **Note 10** and **Fig. 2**), and 56.7  $\mu\text{L}$  of sterile water.
3. Aliquot 24  $\mu\text{L}$  of “hot-start PCR premix” to 6-wells of a 96-well PCR plate.
4. Add either 1  $\mu\text{L}$  of ligated template serial dilution or water as a negative control.
5. Prepare 175  $\mu\text{L}$  of 0.1 U/ $\mu\text{L}$  of “hot-start enzyme premix,” using a proofreading thermostable polymerase such as *Pfu*.
6. Heat the 96-well PCR plate to 94°C for 3 min and then, maintaining the plate at 94°C, add 25  $\mu\text{L}$  of enzyme premix to each reaction, taking care not to cross-contaminate the wells. PCR amplify for 30 cycles of 94°C for 20 s, 55°C for 30 s, and 72°C for 30 s.
7. Following amplification, combine 10  $\mu\text{L}$  from each well with 2  $\mu\text{L}$  of FOG and analyze on a 10% (w/v) PAG gel (10-well comb), against 25-bp DNA ladder (see **Note 12**). Electrophorese at 180 V until the orange-G dye reaches the bottom of the gel. A strong clear band of ditag amplification should be observed at approx 130 bp, with a less intense band at approx 100 bp, representing amplification from ligated adaptor–adaptor species with no ditag insert. The water blank should be negative and, if this is not the case, then the PCR should be repeated using fresh aliquots of all reagents (see **Note 26**). If the amount of product is not satisfactory, it may be necessary to further optimize the PCR using different cycle numbers. The appearance of higher molecular weight species indicates that either the cycle number or amount of template should be reduced. Using the protocol as described here, starting with 5  $\mu\text{g}$  of total RNA, the optimal conditions for large-scale ditag amplification are invariably found to correspond to a scale-up of 5 mL, with 30 cycles of amplification, performed using a template amount equivalent to 1  $\mu\text{L}$  of the 1/25 ditag dilution used in these small-scale reactions (see **Note 27**).

### 3.9. Preparative PCR Amplification of Ditags (see Note 28)

Use the conditions determined in **Subheading 3.7**. to provide sufficient quantities of ditags for concatenation and SAGE library construction.

1. For scale-up to 5 mL (50X 100- $\mu\text{L}$  PCR reactions), prepare hot start PCR mix as follows: 500  $\mu\text{L}$  of 10X PCR buffer, 470  $\mu\text{L}$  of 50 mM  $\text{MgCl}_2$ , 75  $\mu\text{L}$  of each 100 mM dNTP, 300  $\mu\text{L}$  of DMSO, 10  $\mu\text{L}$  of each 500  $\mu\text{M}$  biotinylated long SAGE primer, and 910  $\mu\text{L}$  of sterile water.
2. Transfer 50  $\mu\text{L}$  of the hot-start PCR premix to one well of a 96-well PCR plate to serve as the no-template negative control.
3. To the remainder of the premix, add 4  $\mu\text{L}$  of the ligated ditags (see **Subheading 3.7.**) (equivalent to the 1/25 dilution in **Subheading 3.8.**) and aliquot 50  $\mu\text{L}$  to each of 48 further wells of the PCR plate.
4. Prepare 2.5 mL of 0.1 U/ $\mu\text{L}$  of proofreading enzyme premix.
5. Heat the PCR plate to 94°C for 1–3 min and then, maintaining the plate at 94°C, add 50  $\mu\text{L}$  of the enzyme premix, first to the negative control well and then to the remaining ditag wells, using a multidispensing pipet.

6. PCR amplify for the required number of cycles (most commonly 30 cycles) of 94°C for 20 s, 55°C for 30 s, and 72°C for 30 s.
7. Following amplification, transfer the contents of the negative control well to a fresh microfuge tube and combine the contents of the remaining ditag wells (~5 mL) in a 15-mL centrifuge tube.
8. Remove 5  $\mu$ L each of the negative and the pooled positive PCR samples to 2  $\mu$ L of FOG and electrophorese on a 10% (w/v) PAG gel (10-well comb), at 180 V, against 25-bp ladder, until the orange-G dye reaches the bottom of the gel. It is essential that the no-template, negative control lane is blank. If it is not, then the scale-up reaction must be discarded and repeated using fresh aliquots of all reagents.
9. To precipitate the amplified ditags, add 3  $\mu$ L of 20 mg/mL glycogen, 400  $\mu$ L of 3 M NaOAc, pH 5.6 and 9 mL of cold (-20°C) ethanol to the 5 mL of pooled ditag amplifications. Mix by inversion and pellet the ditags by centrifugation at 14,500g for 30 min at 4°C. Carefully tip off the supernatant, wash the pellet using 70% (v/v) ethanol and air-dry the pellet. At this point the pellet itself can be stored at -20°C.

### **3.10. Gel Purification of the Approx 130 bp Amplified Ditag Species**

1. Remove the amplified ditag pellet from the freezer and briefly air-dry to remove any accumulated condensation.
2. Add 400  $\mu$ L of LoTE and soak the pellet on ice while preparing two 10% (w/v) preparative PAGs.
3. Add 50  $\mu$ L of FOG to the resuspended ditag pellet and distribute across the two PAGs. Electrophorese at 140 V until the xylene cynol (slow blue) dye from the 25-bp ladder is approx 2 cm from the bottom of the gel (approx 65 min).
4. Visualize the DNA using EtBr and excise the two gel slices containing the approx 130-bp amplified ditags.
5. Divide each slice into three equal fragments. Cut each of these fragments into several smaller pieces and transfer them to a 0.5-mL microfuge tube (i.e., a total of six tubes) pierced in the base using a 21-gauge needle. Place each pierced 0.5-mL tube into a 1.5-mL microfuge tube and macerate the gel fragments by forcing them through to the lower tube by centrifugation at maximum speed in a microfuge for 3 min. Check that all of the gel has passed to the lower tubes.
6. To the macerated gel, add 262.5  $\mu$ L of LoTE and 37.5  $\mu$ L of 10 M  $\text{NH}_4\text{OAc}$ . Mix gently by pulsing on a vortex and elute the ditags by incubating at 65°C for 15 min, with gentle intermittent mixing.
7. Carefully transfer each macerated elution mix to the upper basket of a microcentrifuge tube filter assembly, using a 1000- $\mu$ L pipet tip trimmed to remove 2–3 mm of the end. Tease any remaining elution mix to the filter assembly.
8. Centrifuge at maximum speed in a microfuge for 5 min, rotate the filter assembly 180° and centrifuge for a further 5 min. Remove and discard the filter baskets.
9. Add 300  $\mu$ L of phenol/chloroform/isoamylalcohol to each filtrate, vortex, and centrifuge at maximum speed in a microfuge for 3 min.

10. Transfer the upper aqueous phase (300  $\mu\text{L}$ ) to a fresh 1.5-mL microfuge tube and to each add 1  $\mu\text{L}$  of 20 mg/mL glycogen, 75  $\mu\text{L}$  of 10 M  $\text{NH}_4\text{OAc}$  and 1 mL of cold ethanol. Vortex to mix and pellet the ditags by centrifuging at maximum speed in a microfuge, for 30–60 min at 4°C. Alternatively, the ditags can be precipitated overnight at –20°C and centrifuged the following day.
11. Wash the pellets once using 70% (v/v) ethanol and briefly air-dry before resuspending and recombining the pellets in 102  $\mu\text{L}$  of LoTE.
12. Remove 1  $\mu\text{L}$  for analysis on a 10% (w/v) PAG (15-well comb), to confirm the size and homogeneity of the purified approx 103-bp ditags.
13. Remove a further 1  $\mu\text{L}$  to estimate the yield of ditags (see **Note 29**). Although values of 15–30  $\mu\text{g}$  are more ideal, 4  $\mu\text{g}$  of material is sufficient to proceed. If necessary, repeat the preparative amplification step to achieve sufficient material.

### 3.11. Isolation of Approx 40 bp Ditags

The approx 130 bp amplification products isolated in **Subheading 3.10** consist of adaptors 1 and 2 flanking two independent SAGE tags linked end-to-end as a “ditag.” The amplified, approx 40 bp, ditags are released by once again digesting with the anchor enzyme *Nla* III.

1. To the 100  $\mu\text{L}$  of gel-purified, approx 130-bp amplified ditag species (see **Subheading 3.10**), add 150 U of *Nla* III, in a reaction volume of 400  $\mu\text{L}$ , using the recommended restriction buffer.
2. After 1 h at 37°C, 5  $\mu\text{L}$  of the digest can be removed and analyzed against 25-bp ladder on a 4% (w/v) low melting temperature agarose gel to monitor the digestion (see **Note 30**).
3. After 90 min, extract the digest using phenol/chloroform/isoamylalcohol and divide the resulting aqueous layer (~400  $\mu\text{L}$ ) between two fresh 1.5-mL microfuge tubes.
4. To each tube add 2  $\mu\text{L}$  of 20 mg/mL glycogen, 67  $\mu\text{L}$  of 10 M  $\text{NH}_4\text{OAc}$ , and 733  $\mu\text{L}$  of cold (–20°C) ethanol. Mix well and pellet the digested products by centrifugation at maximum speed in a microfuge for 30 min at 4°C. Tip off the supernatants, remove any residual ethanol and air-dry the pellets.
5. Resuspend and recombine the pellets in 200  $\mu\text{L}$  of LoTE.
6. Add 20  $\mu\text{L}$  of FOG and distribute the sample over two 14% (w/v) preparative PAGs at 4°C (see **Note 31**). Electrophorese at 160 V until the bromophenol (fast) blue dye from the 25-bp ladder is leaving the bottom of the gel (~115 min).
7. The approx 40 bp ditags should be resolved from the approx 45- to 47-bp linker derived species. Carefully excise gel slices containing the approx 40-bp ditags. Divide each gel slice in half. Cut each half to several smaller pieces and macerate them using pierced 0.5-mL microfuge tubes (total of four tubes), as described in **Subheading 3.10**.
8. Add 262.5  $\mu\text{L}$  of LoTE and 37.5  $\mu\text{L}$  of 10 M  $\text{NH}_4\text{OAc}$  and elute for 20 min at 37°C (see **Note 31**). Isolate the eluants by centrifugation through microfuge filter assemblies, extract using phenol/chloroform/isoamylalcohol and ethanol precipitate, as described in **Subheading 3.10**.

### 3.12. Removal of Residual Linkers (see Note 32)

1. Resuspend the gel-purified ditag pellet from **Subheading 3.11.** in 50  $\mu\text{L}$  of 1XB+W buffer.
2. Remove 20  $\mu\text{L}$  of 10 mg/mL streptavidin-coated magnetic beads and wash twice using 100  $\mu\text{L}$  of 1XB+W buffer. Finally resuspend the beads in 50  $\mu\text{L}$  of 1XB+W buffer and transfer them to the tube containing the ditags.
3. Incubate at room temperature for 10 min with intermittent mixing to enable the residual linker species to bind to the beads.
4. Magnetically separate the beads and transfer the supernatant containing the ditags to a fresh 1.5-mL microfuge tube. Wash the beads twice using 100  $\mu\text{L}$  of 1XB+W buffer, combining the wash supernatants with the ditag supernatant.
5. Magnetically separate the combined supernatant (300  $\mu\text{L}$ ) for a further 10 min to remove any remaining beads and transfer the cleared supernatant to a further fresh 1.5-mL microfuge tube.
6. Precipitate the ditags by adding 3  $\mu\text{L}$  of 20 mg/mL glycogen, 100  $\mu\text{L}$  of 10 M  $\text{NH}_4\text{OAc}$ , and 1100  $\mu\text{L}$  of cold ( $-20^\circ\text{C}$ ) ethanol. Mix well and pellet at  $4^\circ\text{C}$  for 60 min at maximum speed in a microfuge. Alternatively, precipitate the ditags overnight at  $-20^\circ\text{C}$  and pellet them the following day.
7. Wash the pellet twice using 70% (v/v) ethanol, air-dry, and resuspend the ditags in 8.5  $\mu\text{L}$  of sterile water. Use 0.5  $\mu\text{L}$  to estimate the yield of ditags (see **Note 29**).

### 3.13. Concatenation of Ditags and Isolation of Size Selected Concatemer

Yields of several hundred nanograms of ditags are ideal for the concatenation steps described here. Slightly longer ligation times, together with combining the sample to one well for gel isolation, are suggested with lower yields.

1. Concatenate at  $16^\circ\text{C}$  in a 10- $\mu\text{L}$  reaction, containing the 8  $\mu\text{L}$  of ditags from **Subheading 3.12.**, 1  $\mu\text{L}$  of 10X ligase buffer and 1  $\mu\text{L}$  of T4 DNA ligase (3 U/ $\mu\text{L}$ ).
2. After 15 min, remove 5  $\mu\text{L}$  of ligation mixture and stop the reaction by heating at  $65^\circ\text{C}$  for 15 min.
3. Return the remainder of the ligation reaction to  $16^\circ\text{C}$  for a further 15 min before stopping it by likewise heating at  $65^\circ\text{C}$  for 15 min.
4. Combine the two concatemer reactions in a single tube, washing out the empty tube using 50  $\mu\text{L}$  of binding buffer from a Qiagen QIA quick PCR clean up kit (see **Note 33**).
5. Load the entire concatemer volume onto a QIAquick spin column in a 2-mL collection tube. Centrifuge at full speed in a microfuge for 30 s.
6. Discard the flow-through and wash twice using 750  $\mu\text{L}$  of Qiagen wash buffer PE, centrifuging for 30 s between each wash and discarding each flow-through.
7. Following the final wash, centrifuge for a further 1 min to remove any residual ethanol.
8. Transfer the spin column to a fresh 1.5-mL microfuge tube and add 40  $\mu\text{L}$  of Qiagen elution buffer EB. Stand at room temperature for 2 min prior to centrifuging at full speed for 1 min to collect the eluted concatemers.

9. Add 10  $\mu\text{L}$  of FOG to the concatemers and load across 2 wells of a 6% (w/v) PAG (10-well comb). In separate wells, load 25 and 50 ng of 1-kb ladder. Electrophorese at 150 V until the slow blue (xylene cynol) of the 1-kb ladder is leaving the bottom of the gel (~75 min).
10. Using a razor blade, carefully, but quickly (to minimize ultraviolet exposure), excise gel slices containing concatemer size fractions (450–600 bp, 600–900 bp, 900 bp-several kb).
11. Transfer each fraction to a 0.5-mL microfuge tube pierced in the base using a 21-gauge needle, macerate, as described in **Subheading 3.10.**, and elute at 65°C for 15 min in 300  $\mu\text{L}$  of LoTE.
12. Following recovery of the eluants using microfuge filter assemblies (*see Subheading 3.10.*), precipitate the concatemers by adding 2  $\mu\text{L}$  of 20 mg/mL glycogen, 100  $\mu\text{L}$  of 10 M  $\text{NH}_4\text{OAc}$ , and 933  $\mu\text{L}$  of cold (–20°C) ethanol. Mix well and pellet by centrifugation at maximum speed in a microfuge at 4°C for 60 min. Alternatively, precipitate overnight at –20°C and centrifuge the following day.
13. Wash the pellets twice using 70% (v/v) ethanol, air-dry, and resuspend each of the size selected concatemer fractions in 8.0  $\mu\text{L}$  of LoTE.

### 3.14. Cloning of Size-Selected Concatemers

Prior to cloning, it is essential to generate an efficient preparation of linearized cloning vector. Once established, the linear vector can be stored as single use aliquots at –80°C. Invitrogen's pZErO<sup>®</sup>-1 vector facilitates direct selection of inserts via disruption of a lethal gene, *ccdB* (*see Note 14*). Care is taken throughout the vector preparation and cloning processes to maintain the integrity of this gene in the absence of a cloned insert (*see Note 34*).

1. Digest 1  $\mu\text{g}$  of pZErO-1 in a 25- $\mu\text{L}$  reaction at 37°C for 30 min using 10 U of *Sph* I. Stop the reaction by heating at 65°C for 10 min and then snap-cool on ice. Add 175  $\mu\text{L}$  of LoTE and extract using phenol/chloroform/isoamylalcohol. Transfer the upper aqueous phase to a fresh 1.5-mL microfuge tube and precipitate by adding 0.5  $\mu\text{L}$  of 20 mg/mL glycogen, 20  $\mu\text{L}$  of 3 M sodium acetate, pH 5.6, and 500  $\mu\text{L}$  of ethanol. Mix well and centrifuge at full speed for 30 min in a microfuge at 4°C. Wash the pellet using 70% (v/v) ethanol, briefly air-dry, and resuspend in 60  $\mu\text{L}$  of LoTE.
2. To establish the ligation efficiency of the vector, ligate 2  $\mu\text{L}$  of linearized vector, using 8 U of T4 DNA ligase, in a reaction volume of 10  $\mu\text{L}$ , with and without inclusion of 4  $\mu\text{L}$  of 20 ng/ $\mu\text{L}$  test insert (*see Note 35*). Incubate the test ligations for 3–4 h at 16°C. Increase the volume of the reactions to 200  $\mu\text{L}$  using LoTE, extract with phenol/chloroform/isoamylalcohol, ethanol precipitate, and resuspend the final pellets each in 12  $\mu\text{L}$  of LoTE. Add 2  $\mu\text{L}$  of each ligation mix to a 50  $\mu\text{L}$  aliquot of One Shot<sup>®</sup> TOP10 Electrocomp<sup>™</sup> *E. coli* (Invitrogen) (*see Note 15*) and transfer to 0.1-cm electroporation cuvetts on ice for 10 min. Electroporate at 1.7 KV and recover for 1 h shaking at 37°C in 250  $\mu\text{L}$  prewarmed SOC medium.



Add a further 750  $\mu\text{L}$  SOC medium and plate 33  $\mu\text{L}$  onto low salt LB agar plates containing 50  $\mu\text{g}/\text{mL}$  Zeocin (*see Note 16*). Incubate the plates inverted at 37°C overnight. No colonies should grow on the “no insert” plate, whereas 500–5000 colonies should be observed on the “insert” plate.

3. Store the linearized vector as 2.25- $\mu\text{L}$  aliquots at  $-80^{\circ}\text{C}$ .
4. Initially assess concatemer cloning using the medium sized concatemer fraction. Ligate 4  $\mu\text{L}$  of the concatemers to 1  $\mu\text{L}$  of linearized pZErO-1 in a 10- $\mu\text{L}$  reaction containing 8 U of T4 DNA ligase for 3–4 h at 16°C. Increase the volume of the ligations to 200  $\mu\text{L}$  using LoTE, extract using phenol/chloroform/isoamylalcohol and ethanol precipitate, resuspending the final pellet in 12  $\mu\text{L}$  of LoTE. Use 2  $\mu\text{L}$  of the ligation to transform 50  $\mu\text{L}$  of TOP10 Electrocomp *E. coli* as described above. Initially, plate 33  $\mu\text{L}$  to each of three low salt LB agar plates containing 50  $\mu\text{g}/\text{mL}$  Zeocin.
5. Based on the number of colonies and size of inserts obtained from this preliminary cloning (*see Subheading 3.15.*), either plate sufficient colonies to achieve the required library size or else investigate the possibility of using the other concatemer size fractions. Ideally, insert sizes should be such that they can be efficiently sequenced in a single sequence run. Smaller concatemers tend to clone most readily, but reduce the efficiency of the sequencing process. Larger concatemers ensure that the sequence reagents are used efficiently, but tend to clone less well. The medium fraction often presents a compromise of robust cloning and good-sized (~700 bp) inserts.

### **3.15. PCR Screening of Transformants and Sequencing the Amplified Inserts**

To assess concatemer cloning, as described in **Subheading 3.14.**, colony screening is performed as 30- $\mu\text{L}$  reactions in a 96-well format with 10  $\mu\text{L}$  of the amplified inserts analyzed on a 1% (v/v) agarose slab gel. Once efficient cloning has been established, subsequent screens are performed as 20- $\mu\text{L}$  reactions, with 3  $\mu\text{L}$  analyzed on a 96-well agarose gel running system (*see Note 36*). PEG precipitation is used to desalt the remaining amplified inserts and purify them away from any PCR primers to facilitate direct sequencing.

1. Prepare appropriately sized PCR premixes for colony screening: 1.5 mM  $\text{MgCl}_2$ , 0.2 mM each dNTP, 0.5  $\mu\text{M}$  each primer (M13-40 and M13rev), in 1X PCR buffer, containing 0.0125 U/ $\mu\text{L}$  of *Taq* polymerase.
2. Pick colonies to dry wells of a 96-well PCR plate, leaving the toothpick in the well as a guide. Discard the toothpicks and, using a multidispensing pipet, aliquot PCR premix to each well. Pulse spin the sealed PCR plate and amplify by heat denaturing at 94°C for 5 min, followed by 30 cycles of 94°C for 20 s, 50°C for 30 s, and 72°C for 30 s.
3. Following removal of an appropriate aliquot for gel analysis add a volume of PEG/NaOAc equivalent to twice the original PCR volume using a 12-channel pipette, with mixing. Incubate at room temperature for 10 min.

4. Pellet the precipitated PCR products by centrifuging in a bench-top centrifuge at 2200g for 30 min (*see Note 37*).
5. Invert the plate onto a bed of absorbent paper towels and pulse the centrifuge to 40–50g to remove the PEG supernatant. Replace the towels and repeat.
6. Using a 12-channel multipipette add 100  $\mu\text{L}$  of ethanol and centrifuge for 5 min at 2200g. Tip off the ethanol wash and repeat. Following the second wash, remove any residual ethanol using an inverted pulse spin, as described for removing the PEG supernatant.
7. Briefly air-dry the plate and add 8  $\mu\text{L}$  of water to each well.
8. Prepare an appropriately scaled sequencing premix (*see Note 38*). For a single 96-well plate, add 50  $\mu\text{L}$  of 10  $\mu\text{M}$  M13 –40 primer and 360  $\mu\text{L}$  of ET terminator mix to 190  $\mu\text{L}$  of sterile water and aliquot 6  $\mu\text{L}$  to each well using an electronic multidispensing pipette.
9. Using a 12-channel pipette, mix to ensure the amplified insert pellet is resuspended, and transfer 3  $\mu\text{L}$  of each well to the corresponding well of the sequencing plate. Perform 30 cycles of sequencing as 95°C for 20 s, 50°C for 15 s, and 60°C for 1 min.
10. Prepare 5.5 mL of cold ethanol containing 1.1 mL of sterile water and 200  $\mu\text{L}$  of 7.5 M  $\text{NH}_4\text{OAc}$  and transfer 68  $\mu\text{L}$  to each completed sequencing reaction, with mixing, using a 12-channel pipette. Precipitate at room temperature for 10 min and pellet the products by centrifugation in a bench top centrifuge at 2200g for 30 min.
11. Tip off the supernatant and add 100  $\mu\text{L}$  of 70% ethanol wash to each well. Centrifuge for a further 5 min, tip off the wash and remove any residual ethanol by performing a brief inverted pulse spin, as previously described.
12. Air-dry the pellets and add 10  $\mu\text{L}$  of ET loading buffer. Heat denature at 99°C for 2 min and transfer to ice prior to analysis on a MegaBace 1000 96-well capillary sequencer. Reflecting a compromise between cost, labor, the number of new tags required to provide additional statistically relevant information and the number of libraries to be generated, our target tag accumulation has been approx 30,000 per library (6).

### 3.16. Handling of RAW SAGE Data

1. Obtain sequence data as uniquely named fasta files (*see Note 39*) and enter it directly to SAGE300 software (*see Note 17*). This software locates the punctuating *Nla* III anchor enzyme sites in the concatemers and extracts the intervening “ditag” sequence information. Specify a tag length of 17 with a maximum ditag length of 36 to account for any “wobble” that may be exhibited in the distance that *Mme* I cleaves from its recognition site (18,19). Repeated ditags are registered in the software, but only entered into the library database once (*see Notes 4 and 40*).
2. Use SAGEScreen software to correct for the effects of nonrandom sequencing errors (*see Note 18*).
3. To avoid artifacts generated as a result of inconsistencies in public cDNA databases, we recommend the use of an automated hierarchical process for assigning tag-to-gene annotations (*see Note 19*).

4. Finally, import the corrected, annotated tag database into iSAGEClus software (see **Note 20**). This software removes specified artifact tags, for example those potentially arising from linkers or primers, and facilitates statistical pairwise and global library comparisons. Pairwise scatter plots with associated automated annotation links readily identify genes differentially expressed between two populations, such as tolerogenic and immunogenic DC. Global cluster analyses provide a measure of the similarity/relatedness of different cell populations with respect to their gene expression patterns, and can identify clusters of genes associated with related populations. Alternatively, “seed” tags exhibiting idealized hypothetical expression profiles that mirror a particular phenotype, e.g., tolerogenic or immunogenic cells, can be introduced and tags with the closest matching profiles identified. Combinations of these methods can be used to highlight groups of tolerance associated candidate genes, or “signatures.” To facilitate rapid simultaneous analysis of these signature genes in various different samples, including biological replicates of the populations used for the SAGE, kinetic time-course or induction studies and to investigate the representation of candidate genes in samples from in vivo models, genes can be selectively assembled on custom oligonucleotide microarrays. Custom SAGE libraries can be generated to reveal molecular mechanisms by which specific genes affect regulation.

Unlike hybridization-based technologies, SAGE has no requirement for prerequisite sequence information (apart from the presence of a *Nla* III site) and has the potential to reveal novel transcripts (7). Depending on the relative positioning, SAGE tags can also distinguish alternatively spliced transcripts. More recent advances in SAGE technology have opened up the potential to generate comprehensive data on both extremes of transcripts, to provide information on transcription start sites and the alternative use of promoters as well as polyadenylation sites, a task that has so far thwarted automated genome annotation procedures and represents a further level for investigation of immune control (19–21).

#### 4. Notes

1. Theoretically, 4-bp restriction sites occur on average every 256 bp ( $4^4$ ), such that an AE will cleave at least once in every transcript (1). Although this assumption is flawed, the informative transcript loss is considered to be small, <1% (22).
2. Two distinct SAGE adaptor linker sequences are required as use of a single sequence results in an inhibitory “snap-back” effect during subsequent PCR amplification.
3. In short SAGE, the tag length is maximized by klenow fill-in of the 3′-recessed ends generated by cleavage with *Bsmf* I, prior to ligation to form ditags. *Mme* I generates a 2 bp 3′ protruding overhang, which would require removal to achieve blunt ends. To maximize the information content of “long” SAGE tags, the 2-bp overhang is not polished, but rather the linker-tags are directly dimerized as a “sticky-end” ligation.

4. Generation of ditags prior to PCR amplification provides an important safeguard against PCR-generated data distortions, as well as inadvertent multiple analysis of the same data (**1**).
5. Although SAGE libraries can be generated using individually sourced reagents, commercial kits for both “short” and “long” SAGE library construction are now available from Invitrogen. The kits are user-friendly and certainly facilitate the use of SAGE technology by less specialized laboratories, particularly if commercial outsourcing is then also employed for the large-scale sequencing component. In our experience, the efficiency of Invitrogen’s on-bead cDNA synthesis step and the reliability of the Zero Background™ Cloning system promote the use of lower amounts of starting material and confer increased efficiency on the downstream sequencing process. Use of the kits and most of their components is recommended, as is attention to Invitrogen’s excellently written protocols. A number of procedural modifications, deriving from substantial experience with the technique prior to the introduction of the kits, are retained in the protocol as described here, including adaptations to facilitate the use of “mini-gel” systems.
6. Aliquot all reagents, including the components of the I-SAGE kit, in an area physically isolated from areas in which amplifiable SAGE products are generated and handled.
7. I-SAGE kit components can be used at half the manufacturer’s recommended reaction volumes.
8. Although *Nla* III is included in the I-SAGE kits (Invitrogen), the half-life at  $-20^{\circ}\text{C}$  is short (2–3 mo) and it may be necessary to purchase fresh enzyme. Incomplete cDNA digestion will lead to the isolation of artifact tags, located adjacent to *Nla* III sites other than the most 3′ site in an individual transcript. *Nla* III is stored as single use aliquots at  $-80^{\circ}\text{C}$ , with long-term storage (>2 mo) avoided.
9. The HPRT PCR primers described here amplify a 352-bp region of murine HPRT that spans two exon boundaries and includes an *Nla* III site. We use these primers both to access the original yield of cDNA and also to verify the extent of the *Nla* III digestion. Primer pairs are provided in the I-SAGE kits (Invitrogen) that amplify a region of GAPDH that includes an *Nla* III site, and a region of the EF gene that does not include an *Nla* III site and so can be used to also estimate the yield of digested cDNA.
10. Biotinylated PCR primers are used in preference to the primers provided in the I-SAGE kits (Invitrogen) to facilitate subsequent removal of trace linker species from gel-purified ditag preparations prior to concatenation (**4**). Even small amounts of linker-derived species in these preparations have been repeatedly found to interfere with the concatenation process, resulting in short, unclonable products.
11. Biotinylation of each fresh batch of PCR primer is verified by incubating 200 ng of primer with 1  $\mu\text{L}$  of 1 mg/mL streptavidin at room temperature for 15–20 min. The primer/streptavidin complexes generated are observed by mobility shift on a 20% PAG (*see* **Note 12**).

12. This protocol has been optimized using the Bio-Rad Mini-protean gel system with 0.75-mm spacers. For a single PAG, prepare 4.85 mL of 40% (w/v) acrylamide-bis, (19:1) and water at the appropriate ratio. Add 100  $\mu$ L of 50X TAE: 2 M Tris-HCl, 50 mM EDTA, pH adjusted to 8.5 using glacial acetic acid, and 50  $\mu$ L of freshly prepared 10% (w/v) ammonium persulfate. Following addition of 4.3  $\mu$ L of TEMED, pour the gel immediately and insert an appropriate well-forming spacer. Following electrophoresis using 1X TAE buffer, briefly stain the gels by rocking gently for approx 5 min in 1X TAE containing EtBr (approx 0.25  $\mu$ g/mL) and visualize the DNA using ultraviolet irradiation.
13. Efficient cloning is vital for the successful generation of SAGE libraries. In our hands, Invitrogen's Zero Background Cloning system has proved particularly efficient. This system is provided with the I-SAGE kits, but can also be purchased independently if required.
14. pZErO-1 contains a lethal *lacZ $\alpha$ -ccdB* gene fusion. Insertion of a DNA fragment disrupts expression of this gene, permitting growth. A Zeocin resistance gene is also present for selection in *E. coli*.
15. *E. coli* TOP10 is the recommended host strain for pZErO-1 as it allows constitutive expression of the *lacZ-ccdB* fusion protein without the need for IPTG induction. Strains containing the complete Tn5 transposon should not be used as they are already Zeocin resistant. Strains containing the F plasmid (either F+ or F') encode a potent inhibitor of *ccdB* and should also not be used.
16. Zeocin is inactivated by high salt and acidity or alkalinity and is light sensitive. Plates should be stored at 4°C protected from the light. It is good practice to use plates within a few days of pouring to further ensure zero background colonies.
17. The I-SAGE kits (Invitrogen) include access to proprietary computer software owned by John's Hopkins University, Baltimore, MD. A detailed, user-friendly protocol for its download and use are included. Alternatively, the SAGE300 software can be obtained directly from Prof K. W. Kinzler, John's Hopkins Oncology Center, <http://www.sagenet.org>.
18. Data entered into the SAGE software is single-pass and unedited. Low sequence quality either obscures the serial pattern of AE punctuation, or leads to the introduction of ambiguous bases, both of which cause the sequence to be discarded and not entered into the final dataset. Tags generated as a result of random sequence errors fail to accumulate statistical counts and are ignored. Nonrandom sequence errors arising from highly abundant tags are a source of artifact tags and limit the effective depth to which transcriptomes can practically be probed (6). A numerical manipulation, excluding tags matching 9 out of 10 bases of any other tag occurring at a >10-fold frequency, has been used to account for these errors in "short" SAGE, whereas for "long" SAGE the longer tag length has facilitated development of SAGEScreen software that incorporates a cluster algorithm for this purpose (23).
19. Inconsistencies, such as partial entries, in cDNA databases interfere with simple, automated tag-to-gene annotation processes. However automated annotations can

be achieved using database software such as Microsoft Access and a hierarchical process, such as that described by Cobbold et al. (6), based on Unigene full mapping files and a search algorithm giving priority to a list of hand-annotated entries. In this case, for each hand-annotated entry the existence of a plausible poly-adenylation sequence has been confirmed, as has the tag location immediately downstream of the most 3' AE site. The next annotation priority is given to cDNAs with a polyadenylation signal in the correct orientation, then EST clusters with a probable polyadenylation signal, cDNAs with no polyadenylation signal and finally other matching ESTs.

20. [Http://users.path.ox.ac.uk/~scobbold/tig/software/softlist.html](http://users.path.ox.ac.uk/~scobbold/tig/software/softlist.html) (6).
21. Agarose gel analysis is insufficient to critically assess partial RNA degradation. Rather, RNA should be analyzed on an Agilent Technologies 2100 Bioanalyser. Agilent have now introduced a measured term, the RNA integrity number, ranging from 0 = highly degraded to 10 = highly intact for scoring samples that is based on the entire electropherogram rather than just the ratio of the 28s and 18s rRNAs.
22. During magnetic separations, use siliconized microfuge tubes to reduce bead losses. Perform bead separations on a magnetic stand for 1–2 min. Carefully remove the supernatant from the opposite side of the tube using a pipette, without disturbing the beads, and replace it with the required volume of the appropriate solution. Remove the microfuge tube from the magnetic stand and mix the beads by mild vortexing or flicking of the tubes in preference to pipetting as this can lead to loss of beads. Recover droplets of beads from the caps of the microfuge tubes by a low speed centrifuge pulse prior to magnetic separation. Take care to prevent drying out or clumping of the beads, both of which will reduce product yields.
23. Assuming that polyA+ mRNA represents approx 1–5% of total RNA, it is estimated that the oligo(dT)-coated magnetic beads are being added in  $\geq 2.4$ -fold excess, and that this is sufficient to ensure efficient isolation of mRNA.
24. Residual *E. coli* DNA polymerase will interfere with subsequent reactions by digesting single-stranded overhangs required for cohesive ligations.
25. The amount of adaptor linker added has been optimized for efficient ligation. Excessive linker drives self-ligation, with subsequent amplification of an artificial, approx 100 bp PCR product that can be detrimental to the final yield of amplified ditags.
26. Most SAGE protocols include an additional “no ligase” control reaction when ligating tags to form ditags. Amplification from this “no ligase” control, but not the water blank, is considered indicative of contamination of the SAGE template itself. It is our experience that amplification consistently occurs in the “no ligase” control, possibly by a mechanism involving template switching. Considering this, the relevance of this control has become unclear and misleading and we no longer include it. It is possible that the absence of product reported in the original protocols could be related to the high cycle numbers used in combination with the exonuclease activity of the proof-reading polymerase, although the current

Invitrogen protocol no longer uses high cycle numbers for the negative controls and maintains that they still observe no amplification at this step.

27. To determine the yield of ditags, and so the extent of the scale-up reaction required, the Invitrogen SAGE kits recommend a comparison with amplification achieved from a control template. Although this can provide a level of confidence for the inexperienced user, because of the general consistency observed using the indicated amounts, we do not find this reference to be necessary and so avoid the introduction of a potential source of amplifiable contamination by omitting this step.
28. PCR contamination at the preparative amplification stage is expensive, both in reagents and in terms of template. Use fresh aliquots of all reagents and aerosol-resistant filtered pipette tips, and perform steps prior to the addition of template in an area physically isolated from areas in which template or amplified products are handled.
29. Add 2  $\mu\text{L}$  of a 1  $\mu\text{g}/\text{mL}$  EtBr solution to an equal volume of appropriately diluted sample on saran wrap on an ultraviolet box. Estimate sample yield by comparison of relative fluorescence generated from a serial dilution of the sample (1/5–1/125), with that of a five-fold dilution series of a known quantity of  $\lambda$  DNA standard (50–1.56  $\text{ng}/\mu\text{L}$ ). Analysis using a nanodrop spectrophotometer offers a simpler more quantitative approach if available.
30. The *Nla* III digestion should be approaching completion after 1 h at 37°C. If this is not the case then it is our experience that it will not be improved by the addition of further enzyme or prolonged incubation. *Nla* III resistant 130-bp ditag species can result from exonuclease activity at the time of linker adaptor ligation, causing blunt ligations and destruction of the *Nla* III sites.
31. Short SAGE ditags released by *Nla* III digestion are sufficiently short (26 bp) that it is necessary to take precautions against thermal denaturation and the loss of AT-rich ditags. The increased length of the long SAGE ditags makes this less of a concern, but we have continued to electrophorese them at 4°C and also to subsequently elute them from the gel at 37°C, rather than 65°C, as is used for elution of the 130-bp species.
32. Although the majority of linker-derived species will have been removed by gel purification (*see Subheading 3.11.*), residual linker species do remain in the ditag preparation, particularly when using the mini-gel system. Care must be taken to remove these remaining linker species as they will bind to and block the ends of growing concatemers, limiting their length and preventing cloning. By using biotinylated primers to amplify the approx 130 bp species, the linker-derived contaminants are biotinylated and can be removed magnetically using streptavidin-coated magnetic beads (4).
33. Incorporating a commercial PCR clean-up column prior to size-selection on a PAG appears to remove small concatenation fragments and to improve the mobility of the concatemers within the PAG, both of which promote more efficient cloning of larger concatemers, improving the efficiency and cost effectiveness of the downstream screening and sequencing processes (5).
34. Linearization of pZErO-1 is limited to 30 min to avoid any nuclease activity that may, on religation in the absence of an insert, disrupt expression of the lethal

*lacZ $\alpha$ -ccdB* gene. Likewise the period of incubation for vector-concatemer ligation is also limited to 3–4 h. Freeze-thawing, which could also affect the integrity of the linearized vector ends, is also avoided by storage as single use aliquots at  $-80^{\circ}\text{C}$ . The linearized vector is heat-denatured and flash-cooled on ice prior to storage to avoid any tendency for the linear vector to recircularize.

35. The ligation efficiency of each linear vector preparation is tested using an approx 750 bp (i.e., approximately equivalent to the size of an idealized concatemer), gel-purified, *Sph* I fragment, diluted to approx 20 ng/ $\mu\text{L}$  (an estimate of an average concatemer concentration). *Sph* I digestion of the Clontech vector pIRES2-EGFP yields a suitable 763-bp fragment, with quantitation determined using the nano-drop spectrophotometer.
36. In a 96-well plate, add 3  $\mu\text{L}$  of PCR reaction to 7  $\mu\text{L}$  of standard glycerol dyes, diluted 1 in 30 using water. Load the samples to a 1.2% preformed agarose gel using a 12-channel pipette. Using Pharmacia's Ready-To-Run apparatus electrophoresis for 5 min at 90 V is sufficient to observe the amplified inserts. It is not possible to accurately determine the insert size. This process is used once a robust insert size has been established and is used to highlight problems at the PCR level prior to the costly sequencing step.
37. To prevent physical distortion of the 96-well PCR plates during the centrifugation steps, the plates are supported in plastic racks.
38. The cycle sequencing protocol described here has been optimized using DYEnamic ET dye terminator sequencing reagents (Amersham Biosciences) for analysis on a MegaBace 1000 capillary electrophoresis machine (Amersham Biosciences).
39. For entry into the SAGE300 software (see **Note 17**) sequence data must be in simple text format, arranged in uniquely named files. Fasta format satisfies the requirements for simple text and a simple computer script is used to automatically prefix individual well names with a specified plate number.
40. The probability of any two tags being coupled in the same ditag on more than one occasion is assumed to be very low, and accumulation of repeated ditag sequences is used as an indicator that the library has been skewed. In fact, repeated ditags do occur composed of the most abundant tags, and lack of inclusion of these ditags can mean that expression of the most highly expressed genes is to some degree under estimated.

## References

1. Velculescu, V. E., Zhang, L., Vogelstein, B., and Kinzler, K. W. (1995) Serial analysis of gene expression. *Science* **270**, 484–487.
2. Lu, J., Lal, A., Merriman, B., Nelson, S., and Riggins, G. (2004) A comparison of gene expression profiles produced by SAGE, long SAGE, and oligonucleotide chips. *Genomics* **84**, 631–636.
3. Saha, S., Sparks, A. B., Rago, C., et al. (2002) Using the transcriptome to annotate the genome. *Nat. Biotechnol.* **20**, 508–512.
4. Powell, J. (1998) Enhanced concatemer cloning—a modification to the SAGE (serial analysis of gene expression) technique. *Nucleic Acids Res.* **26**, 3445–3446.



5. Du, Z., Scott, A. D., and May, G. D. (2003) Amplification of high-quantity serial analysis of gene expression ditags and improvement of concatemer cloning efficiency. *Biotechniques* **35**, 66–72.
6. Cobbold, S. P., Nolan, K. F., Graca, L., et al. (2003) Regulatory T cells and dendritic cells in transplantation tolerance: molecular markers and mechanisms. *Immunol. Rev.* **196**, 109–124.
7. Nolan, K. F., Strong, V., Soler, D., et al. (2004) IL-10-conditioned dendritic cells, decommissioned for recruitment of adaptive immunity, elicit innate inflammatory gene products in response to danger signals. *J. Immunol.* **172**, 2201–2209.
8. Fairchild, P. J., Nolan, K. F., and Waldmann, H. (2003) Probing dendritic cell function by guiding the differentiation of embryonic stem cells. *Methods Enzymol.* **365**, 169–186.
9. Fairchild, P. J., Brook, F. A., Gardner, R. L., et al. (2000) Directed differentiation of dendritic cells from mouse embryonic stem cells. *Curr. Biol.* **10**, 1515–1518.
10. Fairchild, P. J., Cartland, S., Nolan, K. F., and Waldmann, H. (2004) Embryonic stem cells and the challenge of transplantation tolerance. *Trends Immunol.* **25**, 465–470.
11. Zelenika, D., Adams, E., Humm, S., Lin, C. Y., Waldmann, H., and Cobbold, S. P. (2001) The role of CD4+ T-cell subsets in determining transplantation rejection or tolerance. *Immunol. Rev.* **182**, 164–179.
12. Zelenika, D., Adams, E., Humm, S., et al. (2002) Regulatory T cells overexpress a subset of Th2 gene transcripts. *J. Immunol.* **168**, 1069–1079.
13. Graca, L., Thompson, S., Lin, C. Y., Adams, E., Cobbold, S. P., and Waldmann, H. (2002) Both CD4(+)/CD25(+) and CD4(+)/CD25(-) regulatory cells mediate dominant transplantation tolerance. *J. Immunol.* **168**, 5558–5565.
14. Heidenblut, A. M., Luttes, J., Buchholz, M., et al. (2004) aRNA-longSAGE: a new approach to generate SAGE libraries from microdissected cells. *Nucleic Acids Res.* **32**, e131.
15. Neilson, L., Andalibi, A., Kang, D., et al. (2000) Molecular phenotype of the human oocyte by PCR-SAGE. *Genomics* **63**, 13–24.
16. Peters, D. G., Kassam, A. B., Yonas, H., O'Hare, E. H., Ferrell, R. E., and Brufsky, A. M. (1999) Comprehensive transcript analysis in small quantities of mRNA by SAGE-lite. *Nucleic Acids Res.* **27**, e39.
17. Vilain, C., Libert, F., Venet, D., Costagliola, S., and Vassart, G. (2003) Small amplified RNA-SAGE: an alternative approach to study transcriptome from limiting amount of mRNA. *Nucleic Acids Res.* **31**, e24.
18. Dunn, J. J., McCorkle, S. R., Praissman, L. A., et al. (2002) Genomic signature tags (GSTs): a system for profiling genomic DNA. *Genome Res* **12**, 1756–1765.
19. Wei, C. L., Ng, P., Chiu, K. P., et al. (2004) 5' Long serial analysis of gene expression (LongSAGE) and 3' LongSAGE for transcriptome characterization and genome annotation. *Proc. Natl. Acad. Sci. USA* **101**, 11,701–11,706.
20. Hashimoto, S., Suzuki, Y., Kasai, Y., et al. (2004) 5'-end SAGE for the analysis of transcriptional start sites. *Nat. Biotechnol.* **22**, 1146–1149.

21. Ng, P., Wei, C. L., Sung, W. K., et al. (2005) Gene identification signature (GIS) analysis for transcriptome characterization and genome annotation. *Nat. Methods* **2**, 105–111.
22. Boon, K., Osorio, E. C., Greenhut, S. F., et al. (2002) An anatomy of normal and malignant gene expression. *Proc. Natl. Acad. Sci. USA* **99**, 11,287–11,292.
23. Akmaev, V. R. and Wang, C. J. (2004) Correction of sequence-based artifacts in serial analysis of gene expression. *Bioinformatics* **20**, 1254–1263.



## Analyzing the Physicodynamics of Immune Cells in a Three-Dimensional Collagen Matrix

Peter Reichardt, Frank Gunzer, and Matthias Gunzer

### Summary

The movement of immune cells is an indispensable prerequisite for their function. All essential steps of cellular immunity rely on the ability of cells to migrate and to interact with each other. Although observation of these phenomena *in vivo* would be the most physiological approach, intravital imaging is technically very demanding and not optimally suited for routine or high-throughput analysis. Any good *in vitro* experimental system should reflect the inherent three-dimensionality of cell migration and interaction in living tissues. Data generated over the last decade show that important cellular parameters like cell velocity, cell shape, and the physicodynamics of cell—cell interactions closely resemble values observed *in vivo* when measured in a three-dimensional (3D) collagen matrix assay, featuring a hydrated network of fibers consisting of type I collagen, the major component of the extracellular matrix. In this chapter, we describe in detail the experimental use of the 3D collagen matrix system. We delineate the preparation of immune cells exemplified by bone marrow-derived dendritic cells and antigen specific T-helper cells of the mouse, the build-up and use of the 3D collagen matrix chamber, the procedures of real time fluorescence microscopic analysis of cell migration and cell—cell interaction, as well as data analysis supported by a self-developed software for computer-assisted cell tracking.

**Key Words:** Immune system; cell motility; 3D collagen matrix; T lymphocytes; dendritic cells; cell tracking; physicodynamics; fluorescence microscopy

### 1. Introduction

The movement of immune cells is an indispensable prerequisite for their function. All essential steps of cellular immunity rely on the ability of cells to migrate and to interact with each other. Hematopoietic precursors migrate out of the bone marrow to enter the thymus or peripheral lymphatic organs. Within the thymus effective motility is necessary for thymocytes, the precursors of T cells,

for successful interaction with thymic stromal cells and dendritic cells upon positive or negative selection processes (1,2). Once out of the thymus, T cells are passively transported within the blood stream to enter lymph nodes (3) where profound lymphocyte motility has also been observed during antigen specific interaction with local antigen-presenting cells (4–7). In addition, many cells, and, in particular, immune cells, need to transiently interact with each other to exchange specific signals (8).

Although observation of these phenomena *in vivo* would be the most physiological approach, intravital imaging is technically very demanding and not optimally suited for routine or high-throughput analysis of cell migration (9). Thus, the development of suitable *in vitro* models for the analysis of cell migration and cell–cell interaction is needed. One paramount feature of the *in vivo* milieu is its inherent and ubiquitous three-dimensionality (10). Therefore, any good experimental system should reflect the three dimensional nature of living tissues. It has been shown that cell motility and cell–cell interactions can fundamentally change when observation switches from 2D (i.e., liquid-covered surfaces) to three-dimensional (3D) environments (11).

Our system, the 3D collagen matrix, features a hydrated network of fibers consisting of type I collagen, the major component of the extracellular matrix. Data generated over a period of more than 10 yr, conclusively show that important cellular parameters like cell velocity, cell shape, as well as the physico-dynamics of cell–cell interaction measured in the 3D collagen matrix assay, closely resemble values observed *in vivo* (4,8,11–13). The similarity of cell behavior in 3D collagen and *in vivo* has meanwhile been corroborated by results from other laboratories (14).

The following chapter describes the experimental use of the 3D collagen matrix system for the analysis of cell migration and cell–cell interaction. We delineate the preparation of immune cells, exemplified by bone marrow–derived dendritic cells (BMDC), and antigen specific T helper cells of the mouse, the build-up and use of the 3D collagen matrix chamber, the procedures of real time fluorescence microscopy analysis as well as data analysis using a self-developed software for computer assisted cell tracking.

## 2. Materials

### 2.1. Mice

1. Balb/c mice.
2. DO11.10 mice, transgenic for a T-cell receptor (TCR) specific for OVA323-339/H-2A<sup>d</sup> (15).

## 2.2. Media

### 1. DC medium:

Substance	Source	Catalog number	Stock	Add	Final concentration
NEAA	Gibco	11140-035	100X	5 mL	1X
FCS	PAA	A15-649		25 mL	5%
L-Glutamine	Gibco	25030-24	200 mM	5 mL	2 mM
Beta-mercapto-ethanol	Gibco	31350-010	50 mM	500 $\mu$ L	50 $\mu$ M
Gentamycin	Gibco	15750-037	50 mg/mL	500 $\mu$ L	50 $\mu$ g/mL
IL-4 supernatant <sup>a</sup>				33.3 mL	6.5 Vol%
GM-CSF supernatant <sup>a</sup>				25 mL	5 Vol%

<sup>a</sup>In our experiments, murine granulocyte-macrophage colony-stimulating factor (GM-CSF) and IL-4 were kindly provided by Thomas Blankenstein, MDC Berlin. The concentration/activity was 700 U/mL (GM-CSF), and 150 U/mL (IL-4), respectively. NEAA, non essential amino acids.

Dissolve in 500 mL of RPMI 1640 (Gibco, cat. no. 31870-025).

### 2. Complete medium (CM):

Substance	Source	Catalog number	Stock	Add	Final concentration
NEAA	Gibco	11140-035	100X	5 mL	1X
FCS	PAA	A15-649	1X	50 mL	10%
L-Glutamine	Gibco	25030-24	200 mM	5 mL	2 mM
Beta-mercaptoethanol	Gibco	31350-010	50 mM	500 $\mu$ L	50 $\mu$ M
Gentamycin	Gibco	15750-037	50 mg/mL	500 $\mu$ L	50 $\mu$ g/mL
HEPES	Gibco	15630-056	1 M	5 mL	10 mM
Sodium pyruvate	Gibco	11360-039	100 mM	5 mL	1 mM
Penicillin/streptomycin	Gibco	15240-122	10,000 U/mL	5 mL	100 U/mL

Dissolve in 500 mL of RPMI 1640.

3. Erythrocyte lysis buffer: dissolve the following in 500 mL of deionized H<sub>2</sub>O: 4.15 g of NH<sub>4</sub>Cl, 0.5 g of KHCO<sub>3</sub>, 1.85 mg of NaEDTA. Filter-sterilize using a 0.2- $\mu$ m filter and store at 4°C.

## 2.3. Other Materials

1. 100-mm Diameter Petri dish (100  $\times$  20 mm, Corning, Corning, NY).
2. Six-well plate (Nuclon surface; Nunc, Roskilde, Danmark; cat. no. 140675).
3. Nylon sieve (100  $\mu$ m, BD Biosciences, Falcon, cat. no. 352360).
4. 15- and 50-mL Tubes.
5. 1.5- and 2-mL Eppendorf tubes.

## 2.4. Reagents

1. CD4<sup>+</sup> T cell separation kit (Miltenyi, Bergisch-Gladbach, Germany; cat. no. 130-090-860).
2. Lipopolysaccharide (from *E. coli* strain 0111:B4, Sigma) kept at  $-20^{\circ}\text{C}$  as 20- $\mu\text{g}/\text{mL}$  aliquots.
3. TCR clonotypic monoclonal antibody (MAb) (clone KJ1-26) (Caltag, Burlingame, CA; cat. no. MM7504).
4. Ovalbumin peptide (OVA323-339: ISQAVHAAHAEINEAGR) (Peptide Synthesis Core Facility, GBF Braunschweig, Germany), stored at  $-20^{\circ}\text{C}$  in aliquots of 1 mg/mL in PBS.
5. 5,6-carboxyfluorescein diacetate, succinimidyl ester (CFSE): 5 mM stocks in DMSO, stored at  $-20^{\circ}\text{C}$  (Molecular Probes, Leiden, The Netherlands).
6. CMTMR (Cell Tracker Orange, CTO): 5 mM stocks in DMSO, stored at  $-20^{\circ}\text{C}$  (Molecular Probes).

## 2.5. Collagen Chamber Build-Up

1. Microscopic slide 76  $\times$  26 mm (Menzel, Braunschweig).
2. Cover slip 24  $\times$  24  $\times$  0.17 mm (Menzel, Braunschweig).
3. Vaseline (petroleum jelly, ENZBORN, Eimermacher, Wels, Austria).
4. Paraffin wax (Fluka, cat no. 76244).
5. Vitrogen 100, Bovine Collagen Type I (Nutacon, Leimuiden, NL, stored at  $4^{\circ}\text{C}$ ).
6. MEM: 10X MEM Eagle (Mod) with Earle's salts, containing phenol red (MP Biomedicals, cat. no. 141 0049) stored at  $4^{\circ}\text{C}$ .
7. Sodium bicarbonate, 7.5% (Gibco BRL, cat. no. 25080-060, stored at  $4^{\circ}\text{C}$ ).
8. Paint brush (width 6 mm), e.g., Pelikan type 24, size 4 (Pelikan, Hannover, Germany).

## 2.6. Real-Time Imaging System

*Real-time imaging system Cell<sup>^</sup>R (Olympus Biosystems, Planegg, Germany)* consisting of the following components:

1. Microscope Olympus BX-61 (upright optics).
2. UPlanAPO lens (20X/340, NA 0.75, WD 0.6 mm) optimized for throughput at 340 nm.
3. UplanAPO lens (40X, NA 0.85, WD 0.51 mm).
4. LUMPlanFI/IR lens (60X, NA 0.9, water immersion, WD 2 mm).
5. Multiposition motorized microscopic stage (Maerzhaeuser, Wetzlar, Germany).
6. USB controller, shutter controller, PC.
7. MT20 high-speed light source with excitation filter wheel and Xenon burner 150 W.
8. Excitation-Emission-Filter set: (Chroma Technology Corp San Jose, CA) set no. 62010 (DAPI/FITC/Cy3). Specific values are: Exciter S405/25, Exciter S490/15, Exciter S560/20, Emitter 19293, Beam splitter 102109.
9. Cell<sup>^</sup>R software 2.0.

### 3. Methods

As a representative experiment, we describe the procedures for monitoring the interaction of mouse BMDC, loaded with a peptide (OVA323-339) and stained in red (CTO), with DO11.10 CD4<sup>+</sup> T cells, stained in green (CFSE), expressing a transgenic TCR specific for this OVA peptide presented by H-2A<sup>d</sup>. The procedures of cell preparation, staining, and imaging have all been previously described by us in **ref. 4**.

#### 3.1. DC and T Cell Preparation

##### 3.1.1. Generation of Mature BMDC

BMDC are generated in 8-d cultures as previously described (**16**).

1. Sacrifice mice by cervical dislocation.
2. Remove femur and tibia surgically and free from adhering fat and muscle tissue.
3. Open bones carefully by removing the proximal and distal ends with small scissors.
4. Flush each marrow cavity into an empty Petri dish with approx 5 mL of PBS/1% FCS using a 27-gauge needle.
5. Transform the resulting solution to a single cell suspension by performing several strokes up and down a 1-mL blue Eppendorf pipet tip and transfer the solution into a 50-mL tube.
6. Centrifuge the cells at 250g for 5 min, discard the supernatant and resuspend the pellet carefully in erythrocyte lysis buffer (3 mL per mouse).
7. Incubate for 3 min at room temperature, with slight manual shaking.
8. Fill up the tube to a volume of 20 mL with cold PBS.
9. Filter through a 100- $\mu$ m nylon sieve into a fresh 50-mL tube.
10. Centrifuge the cells (250g for 5 min) and resuspend the pellet in DC medium containing GM-CSF and IL-4 (10 mL of medium per mouse).
11. Plate the solution in a Petri dish and allow to rest there for 2 h at 37°C/7% CO<sub>2</sub>.
12. Remove adherent cells by gently swirling the medium several times in the plate before collecting only the supernatant into a 50-mL tube (do not flush the plate, as this will dislodge any adherent cells).
13. Pellet the cells (250g for 5 min) and resuspend in fresh DC medium.
14. Count and adjust the cells to  $6 \times 10^5$ /mL in DC medium.
15. Culture the cells in six-well plates (5 mL/well) at 37°C/7% CO<sub>2</sub>.
16. On d 3, replace two-thirds of the medium with fresh medium for optimal nutritional supply.
17. On d 6, collect the total medium from all wells and pool in a 50-mL tube to remove adherent cells.
18. Pellet the cells (250g for 5 min) and resuspend in fresh DC medium.
19. Count and adjust the cells to  $6 \times 10^5$ /mL in DC medium.
20. Transfer the cells into a fresh six-well plate (5 mL/well).
21. Add 20 ng/mL of lipopolysaccharide for the final 48 h to activate the DC (this step is optional, and should be performed only if activated DC are required).



22. Load the cells with peptide antigen (e.g., 10  $\mu\text{g}/\text{mL}$  of OVA323-339) by adding the peptide for the last 2 h of the culture (at day 8).
23. Collect the nonadherent cells on day 8 (as described in **step 17**).
24. After washing, the cells are ready for use (*see* **step 10** and **Note 1**).

### 3.1.2. Purification of CD4<sup>+</sup> T Cells

Naive CD4<sup>+</sup> T cells from the spleens of DO11.10 TCR transgenic mice are enriched to a purity of >95% (75–85% transgenic TCR as tested with the clonotypic MAb KJ1-26) by negative isolation using a magnetic bead separation system, such as the MACS system (Miltenyi, Bergisch Gladbach, Germany) including MAb specific for CD8 $\alpha$  (Ly-2), CD45R (B220), CD49b (DX5), CD11b (Mac-1), and Ter-119 (*see* **Note 2**). When using a commercial separation system such as MACS, we follow the manufacturer's recommendations exactly step-by-step, as outlined in the product description accompanying the product and available online.

### 3.1.3. Staining of DC and T Cells

DC and T cells are labeled with different fluorescent dyes. Typically, DC are labeled with CMTMR (Cell Tracker Orange, CTO) and T cells with CFSE.

1. In a 2-mL Eppendorf tube, resuspend up to  $1 \times 10^7$  DC in 1 mL of PBS.
2. Add CTO to yield a final concentration of 0.5  $\mu\text{M}$ .
3. Keep the solution in the tube with lid open at 37°C/7% CO<sub>2</sub> for 30 min.
4. Top up the tube with PBS/1% FCS and centrifuge the cells (250g for 5 min).
5. Resuspend the pellet in 1 mL of CM and incubate for another 30 min in the incubator.
6. Wash twice (as described above) with CM (*see* **Note 3**).
7. Stain the T cells as described in **steps 1–6** using 0.5  $\mu\text{M}$  CFSE in PBS for 10 min at room temperature.
8. Wash the cells twice with CM before introducing either cell type into a collagen chamber for microscopic analysis (*see* **Note 4**).

## 3.2. The 3D Collagen Matrix, Chamber Build-up, and Cell Loading

### 3.2.1. Preparing the Paraffin Mix

1. In a heat stable beaker, mix one part of petroleum jelly (Vaseline) with eight parts of paraffin.
2. Heat to 60°C. This will result in a clear solution that can be used for chamber building using a paint-brush.
3. The solution can be repeatedly reheated and used many times.

### 3.2.2. Building the Collagen Gel Chamber

The microscope slide is painted with heated paraffin mix to create a U-shaped wall structure (*see* **Fig. 1**).

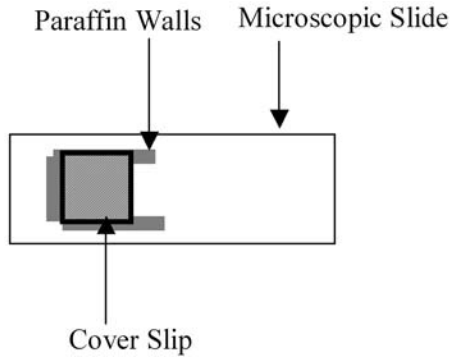


Fig. 1. Construction of a collagen chamber.

1. Using a small paint-brush (width 6 mm), add the paraffin mix (*see Subheading 3.2.1.*) in three layers to give a U-shaped support of approx 300- $\mu\text{m}$  height with one open end (*see Note 5*).
2. Place a cover slip on top of the U-structure and fix by one additional paraffin mix layer along three sides of the cover slip.
3. The fourth side remains open as the chamber will be filled from this direction.

### 3.2.3. Preparing the Collagen Mix

This protocol yields an amount of collagen stock sufficient to produce a 100  $\mu\text{L}$  gel that will fill one standard chamber.

1. In a 1.5-mL Eppendorf tube pipet 5  $\mu\text{L}$  of sodium bicarbonate.
2. Add 10  $\mu\text{L}$  of 10X MEM. The solution should turn pink.
3. Add 75  $\mu\text{L}$  of collagen (*see Note 6*).
4. Mix well, taking care to avoid generating air bubbles.

These volumes can be multiplied by any factor to yield more of the collagen mix.

### 3.2.4. Mixing Cells and Collagen

1. Resuspend the cells in CM at an appropriate concentration. For monitoring T cell—DC interactions, for example, prepare  $1.5 \times 10^6$  T cells in 50  $\mu\text{L}$  and  $1.5 \times 10^5$  DC in 50  $\mu\text{L}$  in two separate 1.5-mL Eppendorf tubes.
2. In a fresh 1.5-mL Eppendorf tube, mix 16.7  $\mu\text{L}$  of the T cell suspension with 16.7  $\mu\text{L}$  of DC.
3. Add 66.6  $\mu\text{L}$  of collagen mixture.
4. Mix well, taking care to avoid generating air bubbles.
5. Fill the collagen chamber with this mixture to about half its volume (*see Fig. 2*), which, depending on the size of the chamber, should require 100  $\mu\text{L}$  or less.
6. Let the collagen gel polymerize for 30–60 min in a 37°C/7%  $\text{CO}_2$  incubator.
7. The polymerization process is complete when the gel is entirely hazy (*see Note 7*).

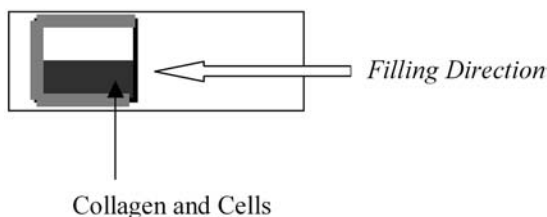


Fig. 2. Filling a collagen chamber.

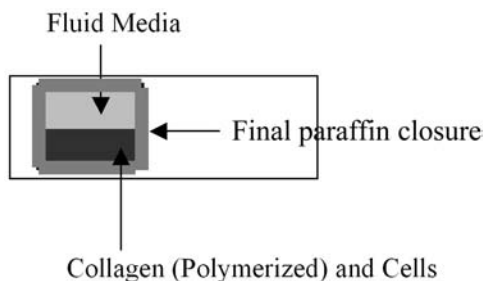


Fig. 3. A sealed collagen chamber ready for imaging.

### 3.2.5. Sealing the Chamber

1. Add CM to fill the chamber completely.
2. Add a layer (or two if necessary) of hot paraffin mix to the remaining side of the cover slip, thereby sealing the chamber (*see Fig. 3*).

## 3.3. Real Time Imaging of 3D Cell Migration and Cell—Cell Interaction

### 3.3.1. Hardware for Imaging

DC—T cell interactions within 3D collagen gels are analyzed as described (8). For more specific considerations on imaging hardware *see Note 8*. Cell migration and fluorescence are monitored simultaneously by time-lapse fluorescence microscopy (12), using an upright microscope and, usually, a  $\times 20$  lens coupled to a real-time imaging system. For high-resolution imaging we use  $\times 40$  and  $\times 60$  lenses. Owing to the set up of the system, when using multiple positions high NA oil immersion is not possible but water immersion works well.

### 3.3.2. Preparation of the Microscope and Loading of the Samples

1. For stability of focus, make sure that the entire microscope system is prewarmed to  $37^\circ\text{C}$  before the start of the experiments (*see Note 9*).
2. Manually focus on areas of interest in the probe.
3. Move along the  $z$ -axis to find the upper end (top) and the lower end (bottom) of the collagen gel.

4. Move to a  $z$ -position safely between these two extremes. This makes sure that observed cells are truly within the 3D collagen matrix.
5. Another proof of correct location in the gel is that, upon focusing, a few sharply focused cells will become evident, as well as a greater number of cells at different focal planes. Although out of focus, these cells may also be used for tracking, as long as their fluorescent color can be recognized.

### 3.3.3. Performing an Imaging Experiment

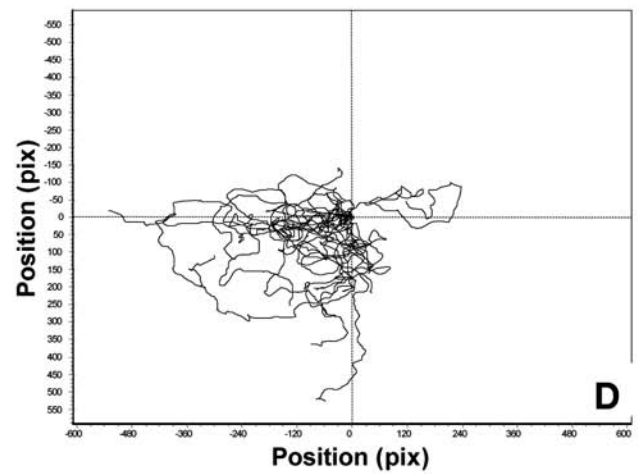
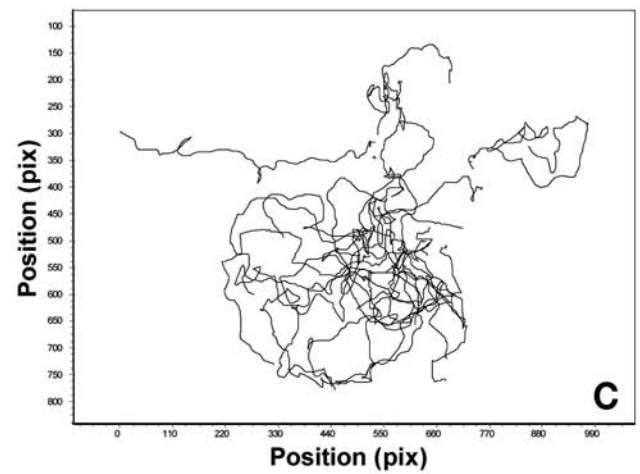
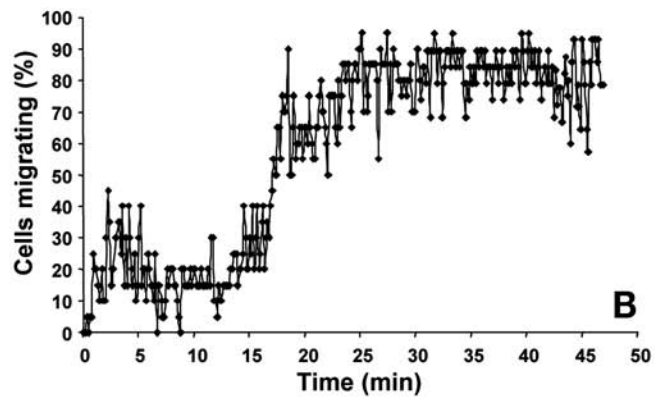
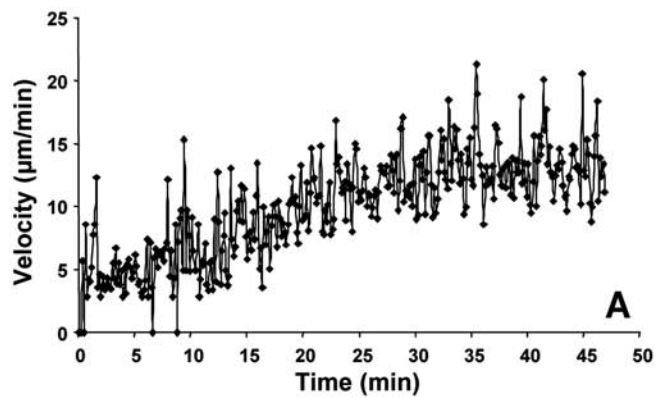
We describe the procedures for using the Cell<sup>^</sup>R system which allows the creation of an experiment plan at the beginning of the experiment which is then automatically exercised by the system. A typical experiment plan consists of three parts:

1. Defining image types and exposure: for instance, one might wish to have a bright-field image for overall cell structures first, immediately followed by a fluorescence image of CFSE, followed by one showing the CTO signal. Thus, in our example, the system would generate three separate images (Brightfield, CFSE, CTO), which can then be combined for multicolor images. Exposure time and light intensity will have to be determined for each color individually at the beginning of the experiment. It is important to always use the lowest possible amount of light to exclude photo damage and photo bleaching, especially during long-term imaging.
2. Defining positions: optimal positions for imaging are those, where a sufficient number of cells is visible both in the brightfield as well as all fluorescent channels. By loading a (potentially unlimited) number of such positions in a software based position table, the system is programmed to subsequently perform the sequence of images defined in **step 1** at every position.
3. Defining frequency and total number of images: for watching DC—T cell interactions, intervals of 30–60 s are preferable and sufficient. In our hands, experiments of up to 12–48 h are possible, without obvious changes in DC or T cell viability and behavior.

### 3.4. Data Analysis: Choosing Suitable Parameters for Cell Tracking

We have focused on the following parameters, which have proven to be especially useful for analyzing cell behavior:

1. Velocity: this parameter describes the speed of locomotion (usually in micrometer per minute) of one cell, or of a cell population, when calculated for numerous cells (see **Fig. 4A**). Essentially, velocity does not include periods of resting (i.e., with locomotion of zero), which frequently occur during cell migration.
2. Speed: this is a similar parameter to velocity but includes resting periods. This differentiation can be of importance when situations occur leading to stopping and reorientation, e.g., during interaction with neighboring cells.
3. Activity: the proportion of time periods during which locomotion occurs relative to the total number of time periods observed. This parameter can very nicely depict the kinetics of cell recruitment (see **Fig. 4B**).



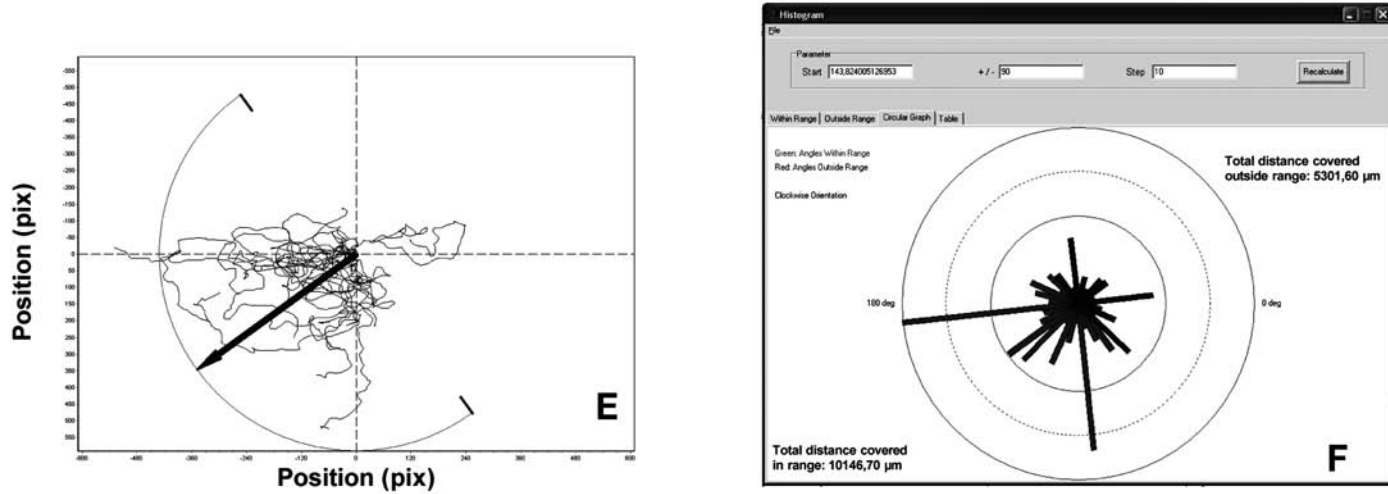


Fig. 4. Computer assisted tracking of cell migration in three-dimensional (3D) collagen matrices. Human peripheral blood neutrophils were incorporated into a 3D collagen matrix. After polymerization of the gel a solution containing 10 nM fMLP was added to the gels from the lower left side immediately before start of imaging (*see ref. 18* for experimental details). Shown are paths of 20 neutrophils individually tracked for 47 min using software developed by the authors. Paths, as they developed within the field of observation (C). The same paths have been drawn to begin in a common spot at the center of the picture. Note the tendency of the cells to move into the lower left corner (D). An expected main migration vector (large arrow) and an angular distribution (circular arc with bars at both ends) can be arbitrarily chosen by the investigator based on the experimental results (E). Circular graph showing the angular distribution of path lengths, thereby differentiating in color the paths inside and outside the area of interest defined before (F). Velocity of the population of 20 tracked neutrophils over time. Note the gradual increase followed by a plateau reached after 35 min (A). Percentage of cells migrating (activity) of the neutrophils. Note the sharp increase of the motile population (recruitment) occurring between 15 and 25 min corresponding to the sensing of a chemokinetic agent (fMLP) by the cells (B).

4. Orientation of migration: the distribution of the cell migration angles in a given field of observation. This is useful for detecting directional migration. When computing this parameter, it is important that cell tracking is able not only to count the steps in a particular direction, but to measure the total distance migrated in the relevant direction. This gives a more accurate evaluation of directional migration (see Fig. 4C–F).
5. Cell—cell interaction: typical determinators are frequency, duration, and (cell-type) specificity of interactions, as well as the cells' biophysical appearance (changes in cell shape, cell polarization, cells pushing or being pulled, and so on [4,5]).

With the exception of the very complex cell—cell interaction analysis (parameter 5), which has to be performed entirely “by hand,” we have developed the software “cell tracker,” that allows the computer assisted generation of data for the listed parameters. The software is described below. It may be obtained from the authors, upon request.

### **3.5. “Cell Tracker”: Software for Computer-Assisted Cell Tracking**

#### *3.5.1. General Considerations*

The automatic tracking of moving objects by software is an intensively investigated topic of research but still remains difficult to achieve. The problem is less the identification of an object in an image, as the reidentification of the same object in a subsequent image, which is the essential step in tracking an object in motion. This is further confounded when the shape of the object changes (such as in flexible cells), when the motion is not continuous enough (i.e., jumps occur between two positions), or when the object collides with another object. Under these circumstances, reidentification becomes very difficult.

Unfortunately, these problems are typical when using microscopy for the investigation of cells in 3D environments, as described in this chapter. The cells move in three dimensions and, thus, their size and sharpness constantly varies in the two-dimensional image captured by the microscope. In addition, the motion can undergo abrupt changes due to interactions with matrix fibers and cells frequently collide with each other either in the form of a real collision or just in the two-dimensional projection of their 3D position. Consequently, to the best of our knowledge no automated tracking system for widefield observations of microscopic particles in 3D environments has so far been developed.

#### *3.5.2. Description of the Software*

##### 3.5.2.1. PRINCIPLE OF TRACKING

The application allows the relatively easy computer-assisted manual tracking of individual cells in computer-displayed image sequences.

1. After a video sequence is started, tracking is performed by the user moving the mouse pointer along with any cell under investigation (over the center of gravity of the cell).
2. The application records the mouse position in fixed time intervals.
3. From these raw data, the software automatically generates essential migration parameters, allows for a simple statistical analysis of the data and generates publishable figures.
4. Raw data files, as well as resulting figures, can be exported to typical secondary applications (*see Fig. 4*).

#### 3.5.2.2. MARKING AND TRACKING OF CELLS

1. Load an AVI file showing the motion of the cells. AVI files are easily exported from modern live-cell imaging systems.
2. In the first frame of the movie (with the investigator not knowing the future behavior of the cells and thus not being biased in marking very motile cells) place numbers on the cells to be investigated by clicking on them with the left button of the mouse.
3. Specify measurement-specific parameters (time per frame, number of frames to be shown, number of frames between two mouse position recordings).
4. Double-click on a number on a cell. This starts the replay of the AVI and the recording of the mouse positions.
5. Track the cell while the movie is played (*see Subheading 3.5.2.1*).
6. The tracking stops automatically at the end of the AVI, after which the mouse positions are saved.
7. Stop tracking at any time by clicking on the right mouse button. Track data obtained so far for this cell may be saved or discarded. This can, for instance, be necessary when a migrating cell leaves the field of observation or becomes un-detectable due to movements in the *z*-axis.
8. The tracks can be displayed to obtain an overview of the quality of the tracking and to avoid double tracking of the same cell, a frequent error in crowded gels.

During tracking, the mouse only should be moved, when the cell really “locomotes.” Frequently, cells can be observed shaking but remaining fixed to the spot (i.e., running on the spot). To reduce tracking noise, it is advisable not to follow these “pseudo-locomotions” by producing little movements with the computer mouse.

#### 3.5.2.3. DATA GENERATION

1. Along with the raw data (i.e., frame number and mouse position), angle and distance information for each step of the motion are automatically calculated.
2. Additionally, a table is created that shows the whole distance covered by the cell during the tracking. It is possible to perform a distance calibration so that the program saves the distance values using length units and not pixels.
3. All data are saved as text files suitable for export to spreadsheet applications like MS EXCEL. Here, secondary analysis can be performed to calculate and plot parameters such as the velocity and activity of individual cells or cell populations over time (*see Fig. 4A,B*).



4. Furthermore, the software allows the representation of the data in two diagram types:
  - a. A diagram with the tracks depicted as they were recorded (see Fig. 4C).
  - b. A diagram with all the tracks starting in the center of the screen (see Fig. 4D). This type is helpful in detecting a common direction of motion.
5. In addition, the original tracks can be shown in front of a background picture, such as the first frame of the AVI, so that the paths of the corresponding cells are visible (not shown).
6. For statistical analysis, the application can generate histograms showing the pattern of cell motion directions (i.e., direction angles weighted with the distance covered in the corresponding direction). This can be done separately for angles inside and outside a range of interest defined by the investigator (see Fig. 4E).
7. The resulting histograms are either displayed as single diagrams (not shown), or grouped in a normalized circular bar graph which gives a better representation of the migration patterns (see Fig. 4F).
8. All the diagram types can be copied for use in other applications.

#### 4. Notes

1. The peptide concentration can vary greatly depending on the type of antigen presenting cell used, the nature of the antigen, and possibly also the experimental readout. For OVA323-339, DC require 0.1–1  $\mu\text{g}/\text{mL}$  of peptide to induce maximal T-cell proliferation, whereas resting B cells need 100  $\mu\text{g}/\text{mL}$  for maximum responses (4). In contrast, amounts as little as 10  $\text{ng}/\text{mL}$  can be optimal for DC-presentation of a peptide like SIINFEKL, the cognate antigen for the TCR transgenic line, OT-I. Although mature DC can reach high levels of peptide density on their surface after only 2 h of loading with peptide, a period of 24 h may be beneficial when loading less efficient antigen presenting cells, such as naïve B cells.
2. Although a self-developed method of negative T-cell separation (17) yields excellent results combined with high cost-efficiency, we have recently achieved equally good results coupled to greater ease of handling using the commercially available magnetic bead systems of Miltenyi (MACS) and Dynal (DYNABEADS) all of which yield purities of 95%  $\text{CD4}^+$  cells when separating DO11.10 T cells.
3. The rather lengthy staining and washing procedure described, together with a rather low concentration of CTO, has proven to help assure maximum de-esterification of the dye inside cells and efficient wash-out of the esterified proportion. This protocol helps to maintain low background fluorescence in the surroundings during microscopic observation over extended periods of time, where residual uncoupled dye can leak from the cells.
4. Other combinations of fluorescent dyes may also prove useful. We have obtained good results with a great variety of fluorescent dyes from Molecular Probes, among them the blue DNA probe DAPI (4',6-diamidino-2-phenylindole), Cell Tracker Blue CMAC (7-amino-4-chloromethylcoumarin), or, as an alternative to CTO, SNARF-1-AM (seminaphthorhodafluor-1-acetoxymethylester), which has similar fluorescence spectra to CTO, but can additionally be used as an intracellular

pH indicator. For ratiometric calcium imaging, the use of Fura-2 AM has given good results in our hands (*see Note 8*).

5. To reproducibly create chambers of equal size, you will need some experimenting with your particular petroleum jelly mix. Note that, depending on the microscopic system, chambers that are too high may be inconvenient, especially if you decide to observe (as a control) cell interactions in fluid media instead of collagen gel. The gathering of the cells at the bottom of the chamber, together with the small working distance of your lens, can ultimately make proper microscopic observation impossible.
6. When mixing the components, make sure no air bubbles are generated. The solution should turn from deep pink to a very clear pink color (salmon). If the solution remains deep pink, the bicarbonate may have expired and needs to be changed.
7. For filling the tracking chamber and subsequent polymerization of collagen, it is essential to keep the chamber standing upright on its edge rather than lying flat. Ideally put it into a slide holder. This positioning prevents the cells from sinking to the bottom of the chamber during polymerization.
8. In principle, cells can be imaged with any live cell microscope. However, it is very desirable to include detection of brightfield channels for cell morphology as well as several fluorescence channels. This detection needs to occur at almost the same time. Furthermore, given possible changes in cell physiology, it is necessary to analyze experimental and control conditions in one experiment. Ideally, this can be achieved by imaging internal controls within the same field of observation (e.g., in a different color). Alternatively, multiple independent microscope systems can be used. A more elegant solution is the use of an automated microscope stage. Based on these considerations, we use an imaging system (Cell<sup>^</sup>R with MT20, Olympus Biosystems) featuring a real-time excitation shuttering, a fast rotating eight-position excitation filter wheel, and a motorized multiposition stage. The system is coupled to an upright microscope with dichroic emission filter cube and a CCD camera linked to a PC, and allows for almost simultaneous measurement of fluorescence signals emitted in response to light of different wave lengths as well as capturing of a brightfield image. As it is essential to limit the light input from the burner to the lowest value that still permits detection of the signal when analyzing fluorescently labeled cells, the system allows dimming of the light intensity to as low as 1% as well as shuttering the light path in real time (i.e., in 1 ms, if necessary). The fast switching between excitation filters is especially useful for the ratiometric determination of calcium dyes such as Fura-2 AM, when instantaneous switching of excitation between 340 and 380 nm is needed. Using the multi position motorized stage, we can include in one experiment up to six different collagen chambers with a theoretically indefinite number of positions. Both microscope and stage are covered by a self-constructed Perspex-lined box serving as a thermo box for maintaining a constant temperature. A wire-based temperature gage, connected to a heating element and a fan, is positioned at slide level to ensure a constant temperature of 37°C in the probes.

9. Allow sufficient time to prewarm the microscope system to 37°C. This prevents fluctuations in the focal plane of the microscopic slide, which otherwise invariably occur during the first hour of observation upon warming up of the microscope-stage hardware. This is of lesser importance in 3D experimental systems such as collagen matrix where cells move up and down over time anyway but can be a pit-fall in setting with fluid media or when imaging is focused on adherent cells. If the system is used regularly, it might be useful to keep it permanently warmed.

## References

1. Bousso, P., Bhakta, N. R., Lewis, R. S., and Robey, E. (2002) Dynamics of thymocyte-stromal cell interactions visualized by two-photon microscopy. *Science* **296**, 1876–1880.
2. Bhakta, N. R., Oh, D. Y., and Lewis, R. S. (2005) Calcium oscillations regulate thymocyte motility during positive selection in the three-dimensional thymic environment. *Nat. Immunol.* **6**, 143–151.
3. Reichardt, P. and Gunzer, M. (2006) The biophysics of T lymphocyte activation in vitro and in vivo. *Results Probl. Cell Differ.* **9**, 199–218.
4. Gunzer, M., Weishaupt, C., Hillmer, A., et al. (2004) A spectrum of biophysical interaction modes between T cells and different antigen presenting cells during priming in 3D collagen and in vivo. *Blood* **104**, 2801–2809.
5. Okada, T., Miller, M. J., Parker, I., et al. (2005) Antigen-engaged B cells undergo chemotaxis toward the T zone and form motile conjugates with helper T cells. *PLoS Biol.* **3**, e150.
6. Miller, M. J., Wei, S. H., Parker, I., and Cahalan, M. D. (2002) Two-photon imaging of lymphocyte motility and antigen response in intact lymph node. *Science* **296**, 1869–1873.
7. Mempel, T. R., Henrickson, S. E., and von Andrian, U. H. (2004) T-cell priming by dendritic cells in lymph nodes occurs in three distinct phases. *Nature* **427**, 154–159.
8. Gunzer, M., Schäfer, A., Borgmann, S., et al. (2000) Antigen presentation in extracellular matrix: interactions of T cells with dendritic cells are dynamic, short lived, and sequential. *Immunity* **13**, 323–332.
9. Halin, C., Rodrigo, M. J., Sumen, C., and von Andrian, U. H. (2005) In vivo imaging of lymphocyte trafficking. *Annu. Rev. Cell Dev. Biol.* **21**, 581–603.
10. Friedl, P. and Brocker, E. B. (2000) The biology of cell locomotion within three-dimensional extracellular matrix. *Cell. Mol. Life Sci.* **57**, 41–64.
11. Gunzer, M., Friedl, P., Niggemann, B., Bröcker, E. -B., Kämpgen, E., and Zänker, K. S. (2000) Migration of dendritic cells within 3D collagen lattices is dependent on tissue origin, state of maturation, and matrix structure and is maintained by proinflammatory cytokines. *J. Leukoc. Biol.* **67**, 622–629.
12. Gunzer, M., Kämpgen, E., Bröcker, E. -B., Zänker, K. S., and Friedl, P. (1997) Migration of dendritic cells in 3D-collagen lattices: visualisation of dynamic interactions with the substratum and the distribution of surface structures via a novel confocal reflection imaging technique. *Adv. Exp. Med. Biol.* **417**, 97–103.

13. Friedl, P., Noble, P. B., and Zänker, K. S. (1993) Lymphocyte migration in three-dimensional collagen gels. Comparison of three quantitative methods for analysing cell trajectories. *J. Immunol. Meth.* **165**, 157–165.
14. Huang, N. N., Han, S. B., Hwang, I. Y., and Kehrl, J. H. (2005) B cells productively engage soluble antigen-pulsed dendritic cells: visualization of live-cell dynamics of B cell-dendritic cell interactions. *J. Immunol.* **175**, 7125–7134.
15. Murphy, K. M., Heimberger, A. B., and Loh, D. Y. (1990) Induction by antigen of intrathymic apoptosis of CD4<sup>+</sup>CD8<sup>+</sup>TCR<sup>lo</sup> thymocytes in vivo. *Science* **250**, 1720–1723.
16. Labeur, M. S., Roters, B., Pers, B., et al. (1999) Generation of tumor immunity by bone marrow-derived dendritic cells correlates with dendritic cell maturation stage. *J. Immunol.* **162**, 168–175.
17. Gunzer, M., Weishaupt, C., Planelles, L., and Grabbe, S. (2001) 2-step negative enrichment of CD4<sup>+</sup> and CD8<sup>+</sup> T cells from murine spleen via nylon wool adherence and an optimized antibody cocktail. *J. Immunol. Methods* **258**, 55–63.
18. Entschladen, F., Gunzer, M., Scheuffele, C. M., Niggemann, B., and Zänker, K. S. (2000) T lymphocytes and neutrophil granulocytes differ in regulatory signaling and migratory dynamics with regard to spontaneous locomotion and chemotaxis. *Cell. Immunol.* **199**, 104–114.



## Etiology of Autoimmune Disease

### *How T Cells Escape Self-Tolerance*

**Eli Sercarz and Claudia Raja-Gabaglia**

#### Summary

Despite central and peripheral regulatory mechanisms designed to prevent self-reactivity, autoimmune disease is a common condition. This article explores several ways in which both high and low affinity T cells can avoid negative selection. The concept of intramolecular sequestration indicates that there will be a hierarchy of presentation of different antigenic determinants derived from a protein antigen, such that some determinants will be efficiently presented whereas others will be poorly presented or not presented at all. Generally, only well-presented determinants will induce tolerance among T cells with sufficient affinity/avidity. Escape from this negative regulation can occur via effects of the antigen processing and presentation system denying determinants access to the peptide-binding grooves of major histocompatibility complex molecules. Another escape mechanism involves avoidance of the regulatory circuitry.

**Key Words:** Intramolecular sequestration; antigen processing and presentation; T-cell repertoire; immune regulation; immunodominance; thymic antigen expression; crypticity; immune hierarchies.

#### 1. Introduction

It is evident to all students of immune tolerance that each individual has a repertoire of T and B cells capable of responding to self-antigens. Furthermore, the nature of the balance established in the immune system is such that all individuals of all species manage to cope with this possibly self-destructive potential, except in the unfortunate case of pathogenic autoimmunity. The peripheral T-cell repertoire generally responds to most foreign antigens whereas failing to respond to self-antigens. The mechanisms underlying this largely successful avoidance of immune damage will be the subject of this chapter.

Autoimmunity is now considered to be the result of two coupled singularities in the usually balanced immune system: the existence of a lymphocytic repertoire capable of strong reactivity against self antigens, and a defective regulatory circuit preventing adequate control. This most recently developed contemporary view of autoimmunity indicates the flaws: flaws in the regulatory arm of the repertoire are just as important as the quality of the effector arm of the self-reactive repertoire.

Immune tolerance, establishing a homeostatic set point in a stable system, is usually attributed to (1) the negative selection of high affinity T-cell clones during lymphocyte development, (2) the induction of anergy in self-reactive clones, (3) the existence of a regulatory apparatus that prevents the reactivity of putatively aggressive clones, and (4) a more vague state of ignorance or sequestration of the self antigen(s) away from the immune system. This fourth possibility should be considered a state of ignorance rather than tolerance and can be challenged on the basis of the definition of immune tolerance. Tolerance is induced by the *positive* action of antigen or peptide-major histocompatibility complex (MHC) complexes on the sensitive cell, or on the regulatory cell, directly or indirectly causing an effect on a target self-reactive cell. Tolerance can be tested by challenge with an immunogenic form of the antigen, which, in such a tolerant animal, yields no response. "Ignorance" is simply a state of naïvete, because, if antigen is provided in a form accessible to the lymphocytic cell, an immune response will occur: thus, "acquired immune tolerance" as originally defined (i.e., a state of nonresponsiveness induced by prior exposure to the antigen in question [1]) never had been induced, despite the fact that the individual appeared to be "tolerant" to the provision of the native antigen. Presumably, in the ignorant individual, the entire antigen could be characterized as "sequestered."

## 2. Immunodominance

### 2.1. Intramolecular Sequestration

We believe that it is crucial to the understanding of tolerance to consider the concept of "intramolecular sequestration." The fundamental idea is that only the well-presented determinants of an antigen, embedded in the groove of MHC class I or II molecules, which are usually the dominant determinants, are available in a sufficient concentration to induce an immune response, or to negatively select the susceptible repertoire. The poorly or nonpresented determinants, accordingly, can be considered to be sequestered within the molecule (2). Therefore, within each antigenic molecule there is a hierarchy of determinant expression and, in the case of T-cell activation, the openness of the molecule and its ability to be processed to make available the full potential set of determinants, will lead to a clear

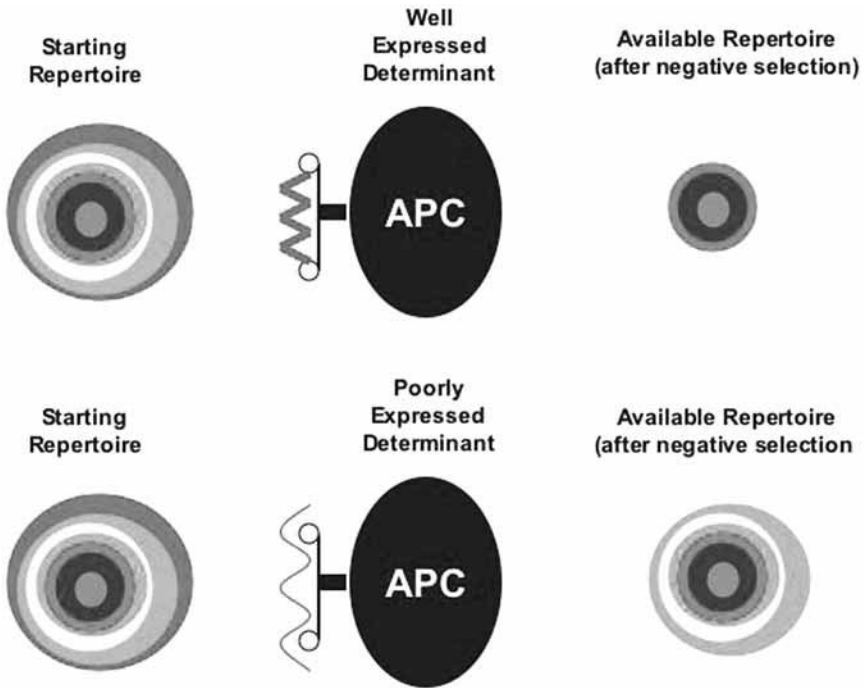


Fig. 1. The top row shows the effect on the repertoire of negative selection imposed by a well-presented antigenic determinant. Affinities of components of the T-cell repertoire are represented by concentric rings with the highest affinity/avidity T cells in the outermost ring. With such a determinant, much of the repertoire is negatively selected, except for the very poorly binding components, represented at the center of the rings. With a poorly presented antigenic determinant, only the highest affinity/avidity T cells are negatively selected. In the absence of binding of a particular determinant, the full complementary repertoire should be released to the periphery.

rank-order of epitopes in the induction of responsiveness or tolerance. This component of tolerance induction relates to the determinant density, whereas the second component, which contributes to the establishment of the repertoire, is the hierarchy of T-cell receptor (TCR) affinities (*see Fig. 1*). **Figure 1** shows that the residual, available repertoire is a product of both determinant density and TCR affinity. Even in the case of poorly presented determinants, the outermost layer, representing the T cells with the highest affinity receptors, will be rendered tolerant in the thymus. However, under conditions where there is absolutely no detectable determinant within the groove of the MHC class II molecule, we expect that the *complete* repertoire directed against this determinant will enter the periphery, following abortive negative selection.



## **2.2. Processing and Presentation of Determinants From a Native Protein**

Direct proof that there is a vast difference in the number of different determinants on an antigen that eventually are displayed by MHC class II molecules has been provided by Unanue and colleagues (3). Four determinant families were examined from hen egg white lysozyme (HEL): 18–33, 31–47, 48–62, and 115–129, and a 250-fold difference in affinity was measured between the highest and lowest binding family. Early evidence, using this same HEL antigen system, demonstrated that, when used to induce tolerance, only T cells directed against dominant determinants were rendered tolerant whereas the residual repertoire still contained T cells directed against subdominant and cryptic determinants (4). A parallel study in another mouse strain (the BALB/c H-2<sup>d</sup> mouse) revealed a similar result (5), showing that there was a direct relationship between the serum level of HEL and the degree of tolerance obtained.

Clearly, one broad contribution to the residual repertoire available in the periphery after negative selection, arises from those T cells directed against the partially and the largely sequestered determinants. However, in addition there are those T cells with low affinity receptors, which easily manage to avoid perdition, despite being directed against well-presented determinants. The final and possibly most dangerous group of self-directed T cells are, therefore, those displaying high affinity for peptide–MHC complexes, which manage to avoid annihilation owing to complete sequestration of their specific antigenic moiety from the MHC groove; this last group will be discussed in the context of the pathogenic response to myelin basic protein (MBP) (*see Subheading 3.1.*).

## **2.3. The T-Cell Repertoire as a Factor in Immunodominance**

The foregoing discussion has concerned the display of antigen as a guiding force in determining the balance between dominance and crypticity. Of equivalent importance is the T-cell repertoire, because an efficient T cell with a high affinity for peptide–MHC complexes may render a poor MHC-binding peptide dominant. For example, in the case of MBP, the amino-terminal nonamer, Ac-ASQKRPSQR, binds very weakly to the MHC, but is, nevertheless, the dominant determinant in the B10.PL mouse.

A feature that needs to be discussed is the frequency of particular T cells within the T-cell repertoire. A T cell that is at a very low frequency in the repertoire will not make a significant imprint on the immune response. An interesting case in the well-studied HEL model, is HEL85-96, an H-2E<sup>k</sup>-restricted determinant that is cryptic, despite binding strongly to the MHC. Nevertheless, HEL-primed mice do not respond to peptide 85-96 *in vitro*. In a TCR transgenic

mouse, in which the transgene product recognizes this determinant, the frequency of specific precursor cells is at least 10–20 times greater, resulting in a conversion of this cryptic determinant to a dominant one (6). We can conclude that the dominance/crypticity continuum is dependent on both the quality of antigen processing and presentation, as well as the frequency and affinity of the T-cell population specific for that determinant.

### 3. The Antigenic Perspective

#### 3.1. Preventing Access to the MHC in Experimental Autoimmune Encephalomyelitis

An illustrative example of the interplay of these forces can be seen in the response of the B10.PL (H-2<sup>u</sup>) mouse to MBP. Immunization of this mouse with MBP leads to a response directed to the amino-terminal Ac1-9 determinant, whereas other potential determinants derived from MBP (e.g., 7–16 and 121–140 [7]) remain cryptic, despite binding much better to H-2A<sup>u</sup>. The response that emerges is propelled by a single driver clone of relatively high affinity, a BV8S2/BJ2S7 clone, which we have called “DAGGGY” because of its CDR3 amino acid sequence. This clone clearly is the agent that promotes the Ac1-9 antigenic determinant to dominance. The determinant MBP7-16 binds avidly to H-2A<sup>u</sup>, and thereby leads to the negative selection of most medium and high affinity T cells directed against the epitope. Accordingly, this determinant becomes cryptic despite its avid binding to MHC, owing to the nature of the residual peripheral repertoire, now comprised of low-affinity T-cell remnants.

The form of MBP expressed in the fetal B10.PL mouse is called Golli-MBP (Golli = genes of the oligodendrocyte lineage), because there are three upstream 5' exons, amino acids 1–134, which are contiguous to the exons of the adult form of MBP (8). The last four amino acid residues of the embryonic Golli (Golli-MBP131-134) are LDVM and because of the methionine residue at position 4, the hybrid determinant, LDVMASQKR, is an excellent binder to H-2A<sup>u</sup>. Position 4 in 1-9 (ASQKRPSQR) is a lysine, which leads to a 10,000 times lower affinity of binding to H-2A<sup>u</sup> than the nonamer in which the K4 is replaced by M or Y. Therefore, LDVMASQKR competes favorably with ASQKRPSQR for the H-2A<sup>u</sup> groove and always wins (9). Likewise 7-16 (SQRSKYLATA) is an excellent competitor because the tyrosine in this determinant again makes it an efficient binder. The result of having flanking contiguous determinants of much greater affinity for MHC class II is that 1-9 is probably completely excluded from the H-2A<sup>u</sup>-binding groove. To test the notion that 1-9 would be an excellent determinant in the absence of these two competitors, we produced four peptides containing these three overlapping determinants, or variants

**Table 1**  
**The Amino-Terminal Nonamer of MBP is a Strong Antigen,**  
**If Flanking Determinants Are Removed**

Tri-determinant peptides	Response of MBP (1-9)-specific T cell hybridoma
LDVMASQKRPSQRSKYLATA	0
SDVGASQKRPSQRSKYLATA	0
LDVMASQKRPSQRSKDEATA	0
SDVGASQKRPSQRSKDEATA	+

thereof, and tested the altered peptides for their ability to activate 1-9-specific hybridomas (*see Table 1*). Only when both the N-terminal flanking determinant and the C-terminal flanking determinant were deprived of their ability to bind competitively to the H-2A<sup>u</sup> molecule, by substitution with nonbinding residues, was the activity of the central 1-9 determinant revealed. Evidently, 1-9 is not such a poor immunogen in the absence of competition. In this example, the driver T cell, DAGGGY, escapes tolerance induction owing to the stifling competition by the flanking determinants. A confirmation of our findings, using an entirely different approach, came from the work of Goverman and colleagues (*10*). They discovered that the most abundant epitopes obtainable by elution of peptides bound to H-2A<sup>u</sup> were 1-17 and 1-18. Within these peptides were a high affinity register, shown to be 5-16, and the low affinity 1-9 register. The former complex with H-2A<sup>u</sup> dissociated very slowly, whereas the complex of MBP1-18 with H-2A<sup>u</sup> dissociated with biphasic kinetics. If the tyrosine residue at position 12 was mutated, abrogating binding of the 5-16 register, single-phase rapid dissociation resulted. The experiments with the overlapping N-terminal Golli determinant (*9*) better explain the fact that the DAGGGY clone is able to escape thymic negative selection; without that additional N-terminal competitor for attachment to the MHC class II molecule, Ac1-9 is able to bind, albeit poorly, and to induce a pathogenic immune response.

Such high affinity T cells as DAGGGY may escape annihilation rather readily and then provide the individual with a potentially dangerous self-directed repertoire, only manageable if a regulatory circuit is available to control its proclivities. To again refer to *Fig. 1*, it is unknown for each of the concentric rings representing areas of diminishing T-cell affinity, how much a determinant would have to be exposed to successfully obliterate the high affinity members of the repertoire. But one can easily see how important it is to have a fully functional regulatory system in place to serve as a last ditch defense in the avoidance of autoimmunity, caused by such subversive T cells.

### **3.2. InterDeterminant Competition**

Another situation in which there are three contiguous determinants and where processing enzymes play an important part in repertoire choice, appears in the way the SJL mouse responds to MBP89-101 (**11**). In this case, the cores of the three determinants are 89-94, 92-98, and 95-101, and the central determinant (92-98) is dominant. However, when the enzyme asparagine endopeptidase cleaves MBP at asparagine 94 (**12**), the dominant determinant is obliterated and the two flanking determinants gain a degree of freedom from the constraints of molecular rigidity. The cryptic determinant, whose core is MBP89-94, thus indirectly achieves dominance within the context of the whole molecule.

### **3.3. Influence of the Affinity of the Peptide Ligand for MHC**

Another study in the MBP system emphasizes the importance of affinity/avidity of the peptide ligand for the MHC in influencing consequent T-cell repertoire selection and disease susceptibility (**13**). H-2<sup>u</sup> mice were immunized with MBP Ac1-9 peptide or its analogs, which display higher MHC-binding capabilities. Immunization with the Ac1-9 wild type peptide, which has the weakest binding affinity, expanded high affinity T cells that induce encephalomyelitis, whereas immunization with high affinity analogs prevented disease development by elimination of the high avidity T-cell repertoire by apoptosis.

#### *3.3.1. Revealing Cryptic Determinants and Conversion to Dominance*

Under certain conditions, a possibly pathogenic determinant might not be immunogenic because it is sequestered and not readily presented. An alteration in the molecule creating a site for endopeptidic attack can then expose this determinant. In the HEL model system, the determinant 23-32 is cryptic in the BALB/c H-2<sup>d</sup> strain. Because amino acid 33 is a lysine, Schneider et al. (**14**) were able to take advantage of the fact that certain proprotein convertase enzymes recognize and cleave dibasic sites, removing them from the molecule and creating a peptide strand break (**15**). Thus, F34K and F34R (HEL with residue phenylalanine 34 replaced by lysine or arginine, creating two parallel dibasic sites) were prepared by site-directed mutagenesis and, when used to immunize BALB/c mice, were found to induce a dominant response to 23-32.

#### *3.3.2. A Self-Antigen System*

This approach was reexamined in a self-antigen system, to find out whether the crypticity of certain determinants of mouse lysozyme M (ML-M) could be attributed to the nonavailability of a proteolytic site (**16**). Accordingly, dibasic

motifs were created as targets for intracellular proteases in the regions adjoining three cryptic determinants—46-61, 66-79, or 105-119 for different mouse haplotypes. The mutated lysozyme proteins, in contrast to unmutated ML-M, were rendered immunogenic in mice, and these anti-self T-cell responses were associated with the generation of autoantibodies against self-lysozyme. Thus, in the heightened inflammatory states often seen at the onset of autoimmunity, the activation of proteolytic enzymes may allow pathogenic determinants to become exposed and to engender new attacks by T-cell clones escaping from ignorance.

### **3.4. Shaping of the T-Cell Repertoire to a Self Antigen**

Work by Moudgil's group on ML-M provides an excellent example of the shaping of the T-cell repertoire for self antigens. In a recent publication (17), ML-M knockout (ML-M<sup>-/-</sup>) LysM(cre) mice on the C3H background were used to compare the hierarchy profile of T-cell responses with the wild type C3H strain. As expected, the ML-M<sup>-/-</sup> mice develop robust responses upon immunization with ML-M. The dominant and codominant responses localize within the 95-125 region of ML-M. The wild type mice do not respond upon ML-M immunization, nor do ML-M<sup>-/-</sup> mice that have been tolerized neonatally by immunization with the dominant ML105-119 peptide in incomplete Freund's adjuvant, clearly demonstrating the role of dominant peptides in tolerization of the available T-cell repertoire. As expected, the cryptic ML-M determinants, capable of binding to H-2A<sup>k</sup> or H-2E<sup>k</sup> (peptides 1-15, 50-64, and 99-113) evoke potent immune responses from both ML<sup>-/-</sup> and wild type mice upon peptide immunization. Furthermore, macrophages from nonimmunized wild type animals, presumably displaying ML-M, are capable of eliciting T cell responses from ML-M immunized knockout mice. ML-M is typically produced by cells of the myeloid lineage, reaching serum concentrations of 1–2 µg/mL, and the dominant 105-119 peptide is naturally processed and displayed by wild type mouse macrophages. These studies address questions related to the differential hierarchy of tolerance induction among the determinants on a self-protein.

### **3.5. Regulation of Thymic Antigen Expression**

The question of how thymic negative selection takes place for the multitude of tissue-restricted antigens has been largely elucidated during recent years. Previously, it was assumed that very few, if any such antigens gained access to the thymus, which was supposedly reserved for ubiquitous and blood-borne self-antigens. In reality, a surprisingly large number of genes, 5–10% of all mouse genes (about 2000–3000) are expressed in highly specialized medullary thymic epithelial cells. These genes code for such antigens as MBP, insulin, but also others representing all parenchymal tissues. It appears likely that this assemblage, the result of "promiscuous gene expression" (18), fits the needs for

repertoire shaping, and a variety of devices conspire to optimize the levels of such antigens, raising them to the point at which thymic negative selection can readily occur. A transcriptional regulator known as *AIRE* (for “autoimmune regulator”) controls the expansion of a subset of the promiscuously expressed genes, especially those restricted to terminally differentiated cells (19).

In the absence of *AIRE*, owing to mutation, many autoimmune manifestations appear such as lymphocytic infiltration into multiple organs. In addition, there are many self-antigens whose expression is controlled by other transcriptional regulators. Lines of investigation into thymic promiscuous gene expression are still in their early days. Interestingly, another set of genes that is upregulated in medullary thymic epithelial cells is related to antigen processing and presentation, including MHC class II, H-2M, and a variety of cathepsins (20).

### **3.6. Antigen Processing and Determinant Choice**

The interactions of the processing system that influence determinant choice are slowly becoming revealed. Competitions arise among the processing endopeptidases for making the first cut in a tight protein antigen, and varying amounts of different proteolytic enzymes in the central and peripheral lymphoid organs eventuate in currently unpredictable pathways of processing that should dramatically affect the composition of the eventual T-cell repertoire. Possible differences between thymic and peripheral antigen processing may emerge to complicate repertoire shaping. For example, enzymatic destruction of a dominant determinant in the thymic environment may lead to the escape of an otherwise leading candidate for imprinting negative selection, whereas in the periphery, conditions favoring such an enzyme may not exist, permitting peripheral negative selection of the escapee clone.

## **4. The Repertoire and Regulatory Perspective**

### **4.1. Avoiding Immunoregulation**

To reiterate a point made at the outset of this chapter, one route to escape from negative selection involves the avoidance of regulatory influences at any of several points. One of these is in the thymus, where the *AIRE* gene regulates the transcription of many autoantigens (*see Subheading 3.6.*). In the periphery, there are many sites at which regulation can fail and any one of these may abrogate control of otherwise forbidden clones. Three other examples will follow, one describing how failure to process a regulatory determinant leads to arthritis, another showing how the lack of control over determinant spreading can lead to an autoimmune disease state, and a third describing effects arising from the frequency of regulatory components. In a mouse strain such as the nonobese diabetic mouse, where there appear to be several general failures in overall regulation (for example, in the appropriate timing and extent of apoptosis [21,22]),

there is an overall susceptibility, traceable to 20 different genetic loci, which leads to a variety of autoimmune conditions in different organs (23). In this case, the closely related nonobese resistant strain, with several non-MHC gene differences, overrides one or a few of these regulatory failures and re-establishes a state of disease resistance.

#### **4.2. Indolent Processing Leads to a Delay in Regulation**

Moudgil's work on the rat model of adjuvant arthritis has revealed how indolent processing can affect the response to regulatory cryptic determinants in heat shock protein 65 (hsp65). The Lewis rat strain is susceptible to adjuvant arthritis, primarily because it does not process hsp65 rapidly enough to permit the regulatory determinants at the C-terminal end of the molecule to be presented to the regulatory T-cell (Treg) population. The closely related Wistar Kyoto strain of rat does process and present these determinants rapidly and is resistant to the disease (24). Provision of the regulatory peptides to the Lewis strain prevents adjuvant arthritis. Rat hsp65 (Rhsp65) is a self-protein, but Lewis rats exhibit strong proliferative responses and IFN $\gamma$  secretion upon immunization with Rhsp65 in incomplete Freund's adjuvant. Furthermore, the dominant determinants localized at the carboxy-terminus of Rhsp65 also contribute to downregulation of adjuvant arthritis induced by heat-killed mycobacterial antigens, as demonstrated by disease attenuation through the transfer of carboxy-terminal reactive T cells in naïve animals before disease induction (25). Interestingly, priming with mycobacterial hsp65 does not generate responses to its own carboxy-terminal determinants but elicits responses to the dominant carboxy-terminal peptides of self Rhsp65. These cross-reactive responses induced by cryptic mycobacterial determinants accordingly play an important immunomodulatory role in adjuvant arthritis. Viewed from the perspective of the Lewis rat, its disease-causing T cells are allowed to escape peripheral suppressive regulation, owing to a putative lesion in its antigen processing machinery.

#### **4.3. Determinant Spreading and Driver Clones (26)**

Initial experiments on determinant spreading (27) described the induction of a response to a dominant determinant within the immunogen followed by an initiation of responses to other, previously subdominant or cryptic determinants. This broadening of the response, if not regulated, could lead to devastating autoimmune consequences (28). Sometimes, as in the response to Ac1-9 in the B10.PL mouse, a driver clone is the first T cell to be engaged, and, because it is necessary for the driver to continually maintain the conditions for propagating the response, its inhibition halts spreading. Any generic lesion in the regulatory mechanisms that would usually shut down the driver clone might, therefore, permit engagement of a whole panoply of recruitable clones.



#### 4.4. The Frequency of Regulatory Clones

The frequency of regulatory clones can be an important factor in allowing the escape of target pathogenic clones. In experimental autoimmune encephalomyelitis in mice of the H-2<sup>u</sup> haplotype (B10.PL and PL/J strains), PL/J mice display a delay of several days in the time of disease onset, a less severe intensity of disease, as well as more rapid remission. Recently, we have found that the frequency of the BV14 CD4<sup>+</sup> Treg cell found in both strains is approx 6- to 10-fold higher in the PL/J, by two different frequency assays (limiting dilution and ELISA-spot) (Madakamutil et al., manuscript submitted).

#### 4.5. Cancer Immunotherapy Via the Residual Repertoire

The available postthymic residual repertoire specific for self antigens, is, in part, comprised of clones that evaded negative selection, either because of their low affinity for antigen, or because their complementary self-determinant failed to gain access to the MHC to permit tolerance induction. This repertoire may serve as a convenient source of cells for generating an anticancer response, based on the contention that most tumor-associated antigens are actually highly expressed normal self-antigens. Most often, these clones will be directed against subdominant or cryptic determinants, and therefore attempts have been made to alter their target determinants to convert them into more effective immunogens, able to induce proinflammatory Th1 responses (29). Other approaches include the enhancement of costimulatory effects (30,31) and the neutralization of inhibitory elements such as CTLA-4 (32). It is evident that the interests of the autoimmunologist and the tumor immunologist merge in seeking ways to provide immunotherapy against this set of chronic diseases. The fortuitous escape by certain clones from destruction, provides tools for the clever cancer immunotherapist providing she succeeds in evading the clutches of the regulators.

#### Acknowledgments

The authors would like to thank Lindsey Harvey and Drs. Todd Braciak and Yang Dai for their contributions to this manuscript. Work in the authors' laboratories was supported by the NIH, the National Multiple Sclerosis Society, the Multiple Sclerosis National Research Institute, the Juvenile Diabetes Research Foundation and the Diabetes National Research Group.

#### References

1. Billingham, R. E., Brent, L., and Medawar, P. B. (1953) Activity acquired tolerance of foreign cells. *Nature* **172**, 603–606.
2. Sercarz, E. E., Lehmann, P. V., Ametani, A., Benichou, G., Miller, A., and Moudgil, K. (1993) Dominance and crypticity of T cell antigenic determinants. *Annu. Rev. Immunol.* **11**, 729–766.



3. Velazquez, C., DiPaolo, R., and Unanue, E. R. (2001) Quantitation of lysozyme peptides bound to class II MHC molecules indicates very large differences in levels of presentation. *J. Immunol.* **166**, 5488–5494.
4. Gammon, G. and Sercarz, E. (1989) How some T cells escape tolerance induction. *Nature* **342**, 183–185.
5. Cibotti, R., Kanellopoulos, J. M., Cabaniols, J. P., et al. (1992) Tolerance to a self-protein involves its immunodominant but does not involve its subdominant determinants. *Proc. Natl. Acad. Sci. USA* **89**, 416–420.
6. Thatcher, T. H., O'Brien, D. P., Altuwajiri, S., and Barth, R. K. (2000) Increasing the frequency of T-cell precursors specific for a cryptic epitope of hen-egg lysozyme converts it to an immunodominant epitope. *Immunol.* **99**, 235–242.
7. Bhardwaj, V., Kumar, V., Geysen, H. M., and Sercarz, E. E. (1993) Degenerate recognition of a dissimilar antigenic peptide by myelin basic protein-reactive T cells. Implications for thymic education and autoimmunity. *J. Immunol.* **151**, 5000–5010.
8. Pribyl, T. M., Campagnoni, C. W., Kampf, K., et al. (1993) The human myelin basic protein gene is included within a 179-kilobase transcription unit: expression in the immune and central nervous systems. *Proc. Natl. Acad. Sci. USA* **90**, 10,695–10,699.
9. Maverakis, E., Beech, J., Stevens, D. B., et al. (2003) Autoreactive T cells can be protected from tolerance induction through competition by flanking determinants for access to class II MHC. *Proc. Natl. Acad. Sci. USA* **100**, 5342–5347.
10. Seamons, A., Sutton, J., Bai, D., et al. (2003) Competition between two MHC binding registers in a single peptide processed from myelin basic protein influences tolerance and susceptibility to autoimmunity. *J. Exp. Med.* **197**, 1391–1397.
11. Anderton, S. M., Viner, N. J., Matharu, P., Lowrey, P. A., and Wraith, D. C. (2002) Influence of a dominant cryptic epitope on autoimmune T cell tolerance. *Nat. Immunol.* **3**, 175–181.
12. Watts, C., Matthews, S. P., Mazzeo, D., Manoury, B., and Moss, C. X. (2005) Asparaginyl endopeptidase: case history of a class II MHC compartment protease. *Immunol. Rev.* **207**, 218–228.
13. Anderton, S. M., Radu, C. G., Lowrey, P. A., Ward, E. S., and Wraith, D. C. (2001) Negative selection during the peripheral immune response to antigen. *J. Exp. Med.* **193**, 1–11.
14. Schneider, S. C., Ohmen, J., Fosdick, L., et al. (2000) Cutting edge: introduction of an endopeptidase cleavage motif into a determinant flanking region of hen egg lysozyme results in enhanced T cell determinant display. *J. Immunol.* **165**, 20–23.
15. Seidah, N. G. and Chretien, M. (1999) Proprotein and prohormone convertases: a family of subtilases generating diverse bioactive polypeptides. *Brain Res.* **848**, 45–62.
16. Zhu, H., Liu, K., Cerny, J., Imoto, T., and Moudgil, K. D. (2005) Insertion of the dibasic motif in the flanking region of a cryptic self-determinant leads to activation of the epitope-specific T cells. *J. Immunol.* **175**, 2252–2260.

17. Sinha, P., Chi, H. H., Kim, H. R., et al. (2004) Mouse lysozyme-M knockout mice reveal how the self-determinant hierarchy shapes the T cell repertoire against this circulating self antigen in wild-type mice. *J. Immunol.* **173**, 1763–1771.
18. Kyewski, B. and Derbinski, J. (2004) Self-representation in the thymus: an extended view. *Nat. Rev. Immunol.* **4**, 688–698.
19. Su, M. A. and Anderson, M. S. (2004) Aire: an update. *Curr. Opin. Immunol.* **16**, 746–752.
20. Derbinski, J., Gabler, J., Brors, B., et al. (2005) Promiscuous gene expression in thymic epithelial cells is regulated at multiple levels. *J. Exp. Med.* **202**, 33–45.
21. Quinn, A., Melo, M., Ethell, D., and Sercarz, E. E. (2001) Relative resistance to nasally induced tolerance in non-obese diabetic mice but not other I-A(g7)-expressing mouse strains. *Int. Immunol.* **13**, 1321–1333.
22. Kishimoto, H. and Sprent, J. (2001) A defect in central tolerance in NOD mice. *Nat. Immunol.* **2**, 1025–1031.
23. Maier, L. M. and Wicker, L. S. (2005) Genetic susceptibility to type 1 diabetes. *Curr. Opin. Immunol.* **17**, 601–608.
24. Stevens, D. B., Gold, D. P., Sercarz, E. E., and Moudgil, K. D. (2002) The Wistar Kyoto (RT1(l)) rat is resistant to myelin basic protein-induced experimental autoimmune encephalomyelitis: comparison with the susceptible Lewis (RT1(l)) strain with regard to the MBP-directed CD4+ T cell repertoire and its regulation. *J. Neuroimmunol.* **126**, 25–36.
25. Durai, M., Kim, H. R., and Moudgil, K. D. (2004) The regulatory C-terminal determinants within mycobacterial heat shock protein 65 are cryptic and cross-reactive with the dominant self homologs: implications for the pathogenesis of autoimmune arthritis. *J. Immunol.* **173**, 181–188.
26. Sercarz, E. E. (2000) Driver clones and determinant spreading. *J. Autoimmun.* **14**, 275–277.
27. Lehmann, P. V., Forsthuber, T., Miller, A., and Sercarz, E. E. (1992) Spreading of T-cell autoimmunity to cryptic determinants of an autoantigen. *Nature* **358**, 155–157.
28. Vanderlugt, C. L. and Miller, S. D. (2002) Epitope spreading in immune-mediated diseases: implications for immunotherapy. *Nat. Rev. Immunol.* **2**, 85–95.
29. Parkhurst, M. R., Salgaller, M. L., Southwood, S., et al. (1996) Improved induction of melanoma-reactive CTL with peptides from the melanoma antigen gp100 modified at HLA-A\*0201-binding residues. *J. Immunol.* **157**, 2539–2548.
30. Curtsinger, J. M., Johnson, C. M., and Mescher, M. F. (2003) CD8 T cell clonal expansion and development of effector function require prolonged exposure to antigen, costimulation, and signal 3 cytokine. *J. Immunol.* **171**, 5165–5171.
31. Wang, E., Panelli, M. C., and Marincola, F. M. (2005) Understanding the response to immunotherapy in humans. *Springer Semin. Immunopathol.* **27**, 105–117.
32. Egen, J. G., Kuhns, M. S., and Allison, J. P. (2002) CTLA-4: new insights into its biological function and use in tumor immunotherapy. *Nat. Immunol.* **3**, 611–618.



## Animal Models of Spontaneous Autoimmune Disease

### *Type 1 Diabetes in the Nonobese Diabetic Mouse*

Nadia Giarratana, Giuseppe Penna, and Luciano Adorini

#### Summary

The nonobese diabetic (NOD) mouse represents probably the best spontaneous model for a human autoimmune disease. It has provided not only essential information on type 1 diabetes (T1D) pathogenesis, but also valuable insights into mechanisms of immunoregulation and tolerance. Importantly, it allows testing of immunointervention strategies potentially applicable to man. The fact that T1D incidence in the NOD mouse is sensitive to environmental conditions, and responds, sometimes dramatically, to immunomanipulation, does not represent a limit of the model, but is likely to render it even more similar to its human counterpart. In both cases, macrophages, dendritic cells, CD4<sup>+</sup>, CD8<sup>+</sup>, and B cells are present in the diseased islets. T1D is a polygenic disease, but, both in human and in NOD mouse T1D, the primary susceptibility gene is located within the MHC. On the other hand, T1D incidence is significantly higher in NOD females, although insulinitis is similar in both sexes, whereas in humans, T1D occurs with about equal frequency in males and females. In addition, NOD mice have a more widespread autoimmune disorder, which is not the case in the majority of human T1D cases. Despite these differences, the NOD mouse remains the most representative model of human T1D, with similarities also in the putative target autoantigens, including glutamic acid decarboxylase IA-2, and insulin.

**Key Words:** Autoimmunity; type 1 diabetes; NOD mouse; tolerance; immunoregulation.

#### 1. Introduction

Autoimmunity is a complex process that results from the summation of multiple defective tolerance mechanisms. The nonobese diabetic (NOD) mouse strain is an excellent model of autoimmune disease, so it is an important tool for dissecting tolerance mechanisms and studying tolerance induction (1,2). In addition to autoimmune insulin-dependent diabetes mellitus, type 1 diabetes (T1D), NOD mice may develop autoimmune thyroiditis, sialoadenitis, hemolytic anemia, oophoritis, gastritis, and prostatitis (3). NOD mice exhibit

a number of immune defects that may contribute to their expression of autoimmunity. These include defective macrophage maturation and function (4), low levels of natural killer (NK) cell activity (5,6), defects in NKT cells (7,8), deficiencies in the regulatory CD4<sup>+</sup>CD25<sup>+</sup> T-cell population (9,10), and the absence of C5a and hemolytic complement (11).

The NOD mouse is, however, mostly studied for its propensity to spontaneously develop T1D that closely resembles the human disease (1,2). T1D is a result of the destruction of the insulin-producing pancreatic islet  $\beta$  cells and it is associated with infiltration of the islets by macrophages, dendritic cells, T and B cells, and with cellular and humoral immunity against islet antigens. In this review, we will examine the basic features of the NOD mouse model, and highlight its contribution to studies of immunological tolerance.

## 2. The NOD Mouse Model

### 2.1. Strain Origin and Characteristics

The NOD mouse was derived from the Jcl:ICR strain by Makino and colleagues in the late 1970s (12) and since then many NOD colonies have been established worldwide (13). NOD mice can be obtained from different suppliers, including The Jackson Laboratory, ME, Taconic Farms, NY, and Charles River, Calco, Italy.

Although NOD mouse colonies can differ widely in age of onset and incidence of T1D (13), in general mononuclear cell infiltration of the pancreatic islets (insulinitis) is detected at 4–6 wk of age in both sexes. The islet mononuclear infiltrate composition is complex. The majority of cells are CD4<sup>+</sup> T cells, but CD8<sup>+</sup> T cells, NK cells, B cells, dendritic cells, and macrophages can also be identified in the lesion (3,12) (Fig. 1). The islet inflammation leads to onset of spontaneous overt T1D between 12 and 16 wk of age, more frequently in females (70–90%) than in males (10–40%). The finding that the reduced incidence in male mice occurs in spite of similar levels of early insulinitis suggests that the autoimmune process in the pancreas of NOD mice includes two checkpoints: checkpoint 1, or insulinitis, which is completely penetrant and checkpoint 2, or overt diabetes, which is not completely penetrant (14).

The exacerbated development of T1D, or the protection from the disease, observed in treated, knock-out, transgenic, cell-transferred NOD mice offers useful tools to identify the molecules involved in immunological tolerance.

### 2.2. Diagnosis of T1D in NOD Mice

T1D is defined by hyperglycemia. A mouse is diagnosed diabetic when blood glucose values are greater than 200 mg/dL for two consecutive measurements. Blood glucose is conveniently monitored by applying a drop of blood, usually from the tail vein, to a glucose test strip and it is read with a small portable spectrometer.

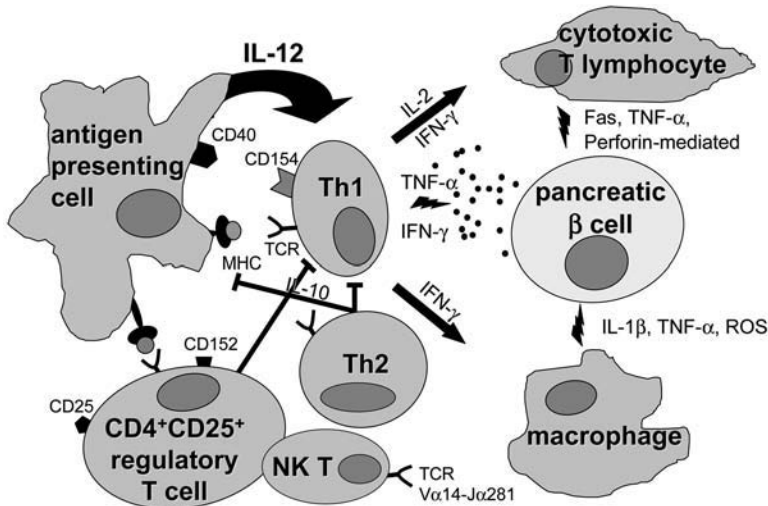


Fig. 1. Schematic view of pathogenic and protective cells in the pathogenesis of autoimmune diabetes. Antigen-presenting cells (APCs), dendritic cells (DCs) and macrophages (Mφ), driven to the islets by IP-10 and other chemokines produced by pancreatic β cells, can secrete, upon activation by different stimuli of bacterial or viral origin, cytokines with opposing effects. If IL-12 predominates, Th1 cells are preferentially induced. Th1 cells themselves are potent inducers of IL-12 production by DCs via engagement of CD40 by its ligand CD154. Th1 cells produce high amounts of IFN-γ that amplifies the IL-12-induced Th1-cell development. IFN-γ also activates Mφ to exert cytotoxic activity and to secrete cytokines potentially toxic for pancreatic β cells such as IL-1β or TNF-α, as well as reactive oxygen species. In addition, IFN-γ and IL-2 stimulate CD8+ cytotoxic T cells (CTL), which secrete TNF-α as well as additional IFN-γ and can kill β cells via Fas, TNF, or perforin-mediated mechanisms. These different effector mechanisms can lead to destruction of β cells and release of β-cell antigens such as (pro)insulin, GAD and IA-2, which can be presented by pancreatic APCs to antigen-specific T cells. Regulatory CD4+CD25+ T cells, expressing CD152, can inhibit the pathogenic activity of Th1 cells via direct cell–cell contact. An inhibitory role could also be played by Th2 cells, secreting IL-10 that inhibits IL-12 production by DCs and activation of Th1 cells, and by natural killer T (NKT) cells. All these three suppressor T-cell subsets are defective in the NOD mouse.

Insulinitis is detected histologically by inspection of islets in pancreas sections. Usually pancreata are fixed in Bouin’s solution and sections stained with hematoxylin and eosin. In histological examination of the NOD pancreas, an insulinitis score can be assigned to each islet as follows: 0, no infiltrate; 1, peri-islet infiltrate at the vascular pole only; 2, peri-islet infiltrate encompassing most of the islet section; 3, intra-islet infiltrate occupying <50% of the islet; 4, intra-islet

infiltrate occupying >50% of the islet. This scoring system is somewhat arbitrary, but it is useful for comparative purposes. Ideally, at least 10 sections from each pancreas should be inspected, each at least 100  $\mu\text{m}$  apart, and over 25 islets should be scored to determine a mean or median value.

The islet infiltrating cells can be analyzed by immunohistochemistry or by *in situ* mRNA hybridization techniques, for example to define specific surface markers or cytokine producing cells. For immunohistochemistry, pancreata can be snap-frozen in OCT (Tissue-Tek), and 5- $\mu\text{m}$  thick cryostat sections fixed and incubated with unconjugated or biotinylated primary antibodies. After washing, sections are stained with secondary antibodies conjugated to horseradish peroxidase, which can be visualized using diaminobenzidine or 3 amino-9 ethyl-carbazole (Sigma Chemical Co., St. Louis, MO) as chromogen and hematoxylin as counterstain.

### 3. Spontaneous and Induced T1D in NOD Mice

#### 3.1. Spontaneous T1D

Age of onset and incidence of spontaneous T1D depend on multiple factors. Among them most important are the genetic drift among colonies and the environmental conditions (13,15). Under SPF conditions T1D onset occurs earlier and the incidence of disease is higher. Viral infections have been associated with increased or decreased T1D incidence (16), and coxsackie virus immunization with delayed T1D development (17), highlighting the complex interaction between infections and autoimmune diseases (18). In addition, stress (including frequent bleeding) and diet can modify T1D incidence, and elevated environmental temperature reduces it (19). For longitudinal comparative studies, e.g., of therapeutic regimens, NOD mice must be maintained under standardized conditions of housing, diet and handling. Frequent handling early in life reduces the incidence of T1D. To avoid interference with T1D incidence, blood sampling for glucose monitoring should be reduced to a minimum before 14 wk of age.

#### 3.2. Chemically Induced T1D

Toxic agents with selectivity for pancreatic  $\beta$  cells, like streptozotocin (STZ) (20) and alloxan (21) can induce T1D. A single, high dose of STZ (70–250 mg/kg body weight) given ip causes complete destruction of pancreatic  $\beta$  cells in most species within 24 h by a direct toxic effect not involving immunological mechanisms. Conversely, repeated ip administration of low dose STZ (e.g., five daily injections of 25 mg/kg in male, 35 mg/kg in female mice) induces insulinitis followed by progressive  $\beta$  cell destruction leading, after 2–3 wk, to T1D (22). STZ is labile in solution. It should be stored dry and dissolved in citrate-phosphate

buffer, pH 4.5, just before injection. Being potentially mutagenic and carcinogenic, it must be handled with care.

T1D can be induced by low dose STZ in any mouse strain, but, in general, males are more sensitive than females. The feeding state of mice influences their susceptibility to STZ; fasting promotes and feeding impairs the action of STZ. NOD mice are susceptible to lower doses of STZ as compared to other mouse strains, and T1D in NOD mice is accelerated by multiple low dose STZ treatment (23). Although T1D induced by low dose STZ appears to be of autoimmune origin, it can also be induced in NOD scid/scid mice lacking functional lymphocytes (24).

### 3.3. Cyclophosphamide-Accelerated T1D

T1D in NOD mice can be accelerated by cyclophosphamide (CY), an alkylating agent used as a cytotoxic and immunosuppressive drug (25). Two ip injections of 200 mg/kg 14 d apart, or a single injection of 350 mg/kg, induce T1D within 2–3 wk in a high percentage (>75%) of 10-wk-old female mice. CY is supplied as a powder, which should be dissolved in sterile water immediately before injection. Following CY treatment, the islet infiltrate initially disappears; after 3–4 d the islets are reinfilitrated with activated macrophages, followed by CD4<sup>+</sup> T cells and after 8–10 d by relatively greater numbers of CD8<sup>+</sup> T-cells concomitant with the onset of  $\beta$  cell destruction (26). The mechanism of action of CY treatment appears to involve selective elimination of regulatory cells (27).

### 3.4. Cell Transfer

T1D can be transferred to irradiated (750 rad) nondiabetic NOD mice or to NOD-scid/scid mice (28) by spleen cells or purified T cells from diabetic mice. Usually,  $1-2 \times 10^7$  spleen cells from recently diabetic mice are injected iv into the tail vein of male or female NOD recipients, irradiated on the morning of the experiment (29). The majority of recipients should become diabetic within 4 wk after transfer.

NOD disease is primarily dependent on CD4<sup>+</sup> and CD8<sup>+</sup> T cells (1,29,30): evidence for this includes the fact that both CD4<sup>+</sup> and CD8<sup>+</sup> T cells are required to transfer disease (30), the ability of individual T-cell clones (both class I and II restricted) derived from NOD islet to passively transfer disease (31,32), and the fact that T-cell modulating therapies inhibit disease incidence (33–37). Whereas diabetes can be transferred from affected animals by passive transfer of splenocytes, it cannot be transferred by autoantibodies from new onset diabetic donors, although B cells are also clearly important for the development of disease (38).



**Table 1**  
**Development of Insulinitis and Autoimmune Diabetes in Transgenic NOD Mice**

Transgene	Insulinitis	Hyperglycemia	References
<i>MHC molecules</i>			
Aβ <sup>k</sup> ;Aβ <sup>g7</sup> (D57)	→	→	69,129
Aβ <sup>d</sup>	→	↓	130
Aα <sup>k</sup> Aβ <sup>k</sup> ; Aβ <sup>k</sup> (S57); Aβ <sup>g7</sup> (P56)	↓	↓	67,70,131
Eα <sup>k</sup> ; Eα <sup>d</sup>	no	no	68,71
Eα::Sma; Eα <sup>k</sup> :ΔY	↓	→	71
Eα:ΔX	→	→	71
HLA-DRα	→	→	132
HLA-DQ6;HLA-DQ8	↓	↓	133,134
L <sup>d</sup>	↓	↓	135
<i>Cytokines</i>			
IL-2	↑	↑	136
IL-4	variable	variable	86,87
IL-6	↑	↓	137
IL-10	↑	↑	138,139
IL12p40 homodimer	↓	↓	84
TNF-α	variable	variable	43,44
TGF-β1	↓	↓	140
<i>Autoantigens</i>			
Proinsulin	no	↓	78
Residue 16 mutated proinsulin	no	no	141
Hsp60	↓	↓	142
GAD	→	→	143
<i>T-cell receptor</i>			
BDC2.5 (CD4 <sup>+</sup> )	↑	↑	144
8.3 (CD8 <sup>+</sup> )	↑	↑	145
GAD 65	no	no	146
<i>Costimulatory molecules</i>			
CD152 (CTLA-4)	↑	↑	46
CD80	↑	↑	45
<i>B-cell receptor</i>			
VH125		↑	47
VH281		no	47
<i>Molecules involved in β-cell destruction</i>			
DCR3	↓	no	50
FasL		↑	48

Besides experiments of cell transfer, where the role in tolerance induction of different cell subpopulations can be explored, during the past 15 yr, investigators have used a wide variety of protocols to study T1D in NOD mice, including transgenic and knock-out NOD strains.

**Table 2**  
**Development of Insulinitis and Autoimmune Diabetes**  
**in Gene-Targeted NOD Mice**

Gene targeted	Insulinitis	Hyperglycemia	References
<i>MHC molecules</i>			
$\beta$ 2 microglobulin	no	no	<a href="#">51,52</a>
CIITA	↓	no	<a href="#">53</a>
<i>Cytokines</i>			
IFN- $\gamma$	→	→	<a href="#">147</a>
IL-4	→	→	<a href="#">59</a>
IL-10	→	→	<a href="#">58</a>
IFN- $\gamma$ R	→	→	<a href="#">148</a>
IL-12p40	→	→	<a href="#">56</a>
TNFR1	→	↓	<a href="#">149</a>
<i>Autoantigens</i>			
Proinsulin 2	↑	↑	<a href="#">150</a>
GAD	↓	↓	<a href="#">80</a>
<i>Costimulatory molecules</i>			
CD80/CD86	↑	↑	<a href="#">9</a>
CD28	↑	↑	<a href="#">46</a>
CD152 (CTLA-4)	↑	↑	<a href="#">151</a>
CD154	no	no	<a href="#">61</a>
CD54		no	<a href="#">62</a>
<i>B cells</i>			
B cells	no	no	<a href="#">152</a>
<i>Molecules involved in <math>\beta</math>-cell destruction</i>			
Perforin	→	no	<a href="#">153</a>
Fas		↓	<a href="#">49</a>

↑ increased, ↓ decreased, → unchanged.

IL, interleukin; TNF, tumor necrosis factor; TGF, transforming growth factor; Hsp, heat-shock protein; GAD, glutamic acid decarboxylase; IFN, interferon; TNFR1, TNF receptor 1.

#### 4. T1D in Transgenic and Knock-Out NOD Mice

A wealth of information on the pathogenesis of autoimmune diabetes and on the causes that lead NOD mice to the breakdown of immunological tolerance has been accumulated by expressing different transgenes in the NOD mouse (**Table 1**), especially in pancreatic  $\beta$  cells under the control of the rat insulin gene promoter, and by selective gene targeting (**Table 2**). T1D occurs in most transgenic mice but in some cases it is not because of an immune reaction, as demonstrated by the absence of insulinitis. Transgenes can be introduced into NOD mice by direct microinjection of NOD embryos, and NOD embryonic stem cells have been developed, which permit the analysis of gene-targeted NOD mice without the need for back-crossing.

### 4.1. Transgenic Models in the NOD Mouse

Given the pivotal role of MHC alleles in the pathogenesis of autoimmune diabetes, effects of expressing transgenic MHC molecules in NOD mice have been extensively analyzed. The class I MHC genes of the NOD comprise  $K^d$  and  $D^b$  alleles. The expressed class II molecule,  $A\alpha^d:A\beta^{g7}$  ( $I-A^{g7}$ ), is unusual and  $I-E$  molecules are not expressed on the cell surface owing to a deletion in the  $E\alpha$  promoter. Both the absence of  $I-E$  and homozygous expression of  $I-A^{g7}$  genes are necessary for diabetes development (39). Indeed, the introduction of other MHC molecules into the NOD genetic background usually causes complete or partial protection from insulinitis and autoimmune diabetes (Table 1).

Several cytokines have been selectively expressed in the pancreatic  $\beta$  cells of the NOD mouse. Transgenic expression of interleukin (IL)-2 and IL-10 in  $\beta$  cells accelerates the development of autoimmune diabetes. The effect of transgenic IL-10, possibly because of B cell-induced activation of T-cells specific for cryptic determinants of self antigens, was surprising, given the capacity of IL-10 to inhibit disease development when administered to adult NOD mice (40). Although the mechanisms by which rat insulin gene promoter-IL-10 accelerates diabetes development are not yet well understood, ICAM-1 has been shown to play an important role (41). Conversely, viral IL-10, which shares anti-inflammatory but not immunostimulatory properties with cellular IL-10, induces leukocyte migration but inhibits the activation of Th1 cells and T1D development when expressed in  $\beta$  cells, probably by suppressing the production of IL-12 by dendritic cells and macrophages (42). Recruitment and activation of dendritic cells and macrophages to present self-antigens to autoreactive T cells has also been invoked to explain diabetes acceleration induced by transgenic tumor necrosis factor (TNF)- $\alpha$  expression from birth (43), whereas TNF- $\alpha$  expression or treatment in adult NOD mice results in inhibition of autoreactive T cells and disease prevention (44). Conversely, as expected, transgenic expression in  $\beta$  cells of the anti-inflammatory cytokines IL-4, IL-12p40 homodimer (a natural antagonist of IL-12), and TGF- $\beta$  inhibits T1D development (Table 1).

NOD mice expressing transgenic T-cell receptor (TCR) from diabetogenic CD4<sup>+</sup> (BDC2.5) or CD8<sup>+</sup> (8.3) T-cell clones specific for undefined islet antigens have accelerated diabetes, which is fulminant when these TCRs are the only ones expressed in crosses between BDC2.5 transgenic and C $\alpha$ - or RAG-2-deficient mice (14).

Expression of the costimulatory molecule CD80 in pancreatic  $\beta$  cells accelerates autoimmune diabetes, by increasing antigen presentation to CD8<sup>+</sup> cells (45). Also CD152 (CTLA-4)-transgenic mice that express soluble circulating CTLA-4Ig, a molecule that binds with high affinity to CD80/CD86 molecules

and blocks costimulation, develop accelerated autoimmune diabetes (46). Glutamic acid decarboxylase (GAD)-specific T cells from these mice are skewed to the Th1 phenotype, probably reflecting the lack of a costimulation-dependent regulatory T-cell population (9).

NOD genetically deficient in B lymphocytes are resistant to T1D (38) (Table 2): B cells could affect susceptibility to T1D through their APC function. To determine the role of Ag-specific B cells in the disease, V(H) genes with different potential for insulin binding have been introduced into the NOD background as H chain transgenes. VH125 H chain combines with endogenous L chains to produce a repertoire in which 1–3% of mature B cells are insulin specific, and these mice develop accelerated T1D. In contrast, NOD mice harboring a similar transgene, VH281, with limited insulin-binding develop insulinitis but are protected from T1D, suggesting that antigen-specific components in the B-cell repertoire may alter the disease course (47).

Several mechanisms have been proposed as responsible for islet  $\beta$  cell destruction; one of them is Fas/Fas-ligand triggering. Fas ligand (FasL) is a type 2 membrane protein belonging to the TNF family, whereas Fas is a death receptor: ligation of Fas receptors by FasL results in apoptosis of the Fas-expressing cell. Both Fas and FasL have been demonstrated to be expressed by  $\beta$  cells in response to cytokine stimulation. Transgenic NOD mice with  $\beta$  cells expressing a FasL transgene develop an accelerated form of diabetes (48), whereas NOD mice with  $\beta$  cell-specific expression of a dominant-negative point mutation in a death domain of Fas show a delay in T1D development (49) (Table 2). Thus, blocking the Fas-FasL pathway may be useful in the prevention or treatment of T1D. Transgenic over-expression of decoy receptor 3 (DCR3), that halts Fas ligand-induced cell deaths in  $\beta$  cells, protects mice from autoimmune diabetes in a dose-dependent manner and significantly reduces the severity of insulinitis (50).

#### 4.2. Gene-Targeted NOD Mice

Several gene-targeted mice on the NOD background have been generated (Table 2). NOD mice deficient in the expression of class I (51,52) or class II (53) MHC molecules fail to develop T1D, and reconstitution of MHC class I expression on  $\beta$  cells demonstrates that CD8<sup>+</sup> T cells are not only essential for  $\beta$  cell killing, but also for disease initiation (54).

Targeting cytokine genes and their receptors has, however, provided some unexpected results. Although T1D in the NOD mouse is mediated by Th1 cells (55), deletion of IL-12p40 (56), or the interferon (IFN)- $\gamma$  (57) genes does not affect diabetes development. These results demonstrate that the genetic program for autoimmune diabetes induction is redundant and disease can develop

in the absence of Th1-inducing cytokines that have been shown to contribute to disease when neutralized in unmanipulated NOD mice (40). Similarly, deletion of IL-10 (58) or IL-4 (59), prototypical anti-inflammatory cytokines, has no impact on diabetes development. However, transgenic expression of IL-4 in  $\beta$  cells can activate self-reactive BDC2.5 T cells and trigger T1D by increasing presentation of GAD epitopes by macrophages and dendritic cells (60).

Costimulation of naïve T cells plays an important role in preventing auto-reactive responses. T1D is exacerbated in both CD80/CD86-deficient and CD28-deficient NOD mice, sharing a profound decrease in immunoregulatory CD4<sup>+</sup> CD25<sup>+</sup> T cells that control T1D in prediabetic NOD mice (9,46). These results suggest that the CD28-CD80/CD86 costimulatory pathway is essential for the development and homeostasis of regulatory T cells that control autoimmune diabetes. On the other hand, CD154-deficient mice do not develop insulinitis or T1D, suggesting that the CD154/CD40 pathway may play a direct role in effector T-cell activation (61). Among the molecules involved both in the delivery of costimulatory signals and in leukocyte trafficking into inflammatory sites, CD54 appears to be critical and to have a nonredundant role, as shown by the finding that NOD mice with a disrupted CD54 gene are completely protected from T1D (62).

## 5. Immunological Tolerance: Lessons From NOD Mice

The detailed mechanisms leading to T1D in NOD mice are still largely unknown. Given the evidence for T-cell involvement in T1D pathogenesis, a large number of studies has examined whether defects in central or peripheral tolerance may account for disease induction and development, and we will highlight studies using the NOD mouse as a tool to study central and peripheral mechanisms of tolerance.

Several studies suggest that defects in thymic deletion process may contribute to T1D susceptibility. For example, a defect in the expression of *Aire*, the gene that controls the ectopic expression of many self-proteins (including insulin) in the thymus and regulates the negative selection of self-reactive thymocytes specific for *Aire*-driven transcripts (63), has been recently described in the NOD strain (64). Nevertheless, the fact that autoreactive T cells specific for islet antigens exist in normal healthy subjects (65,66) indicates that thymic deletion is not complete. Thus, other peripheral mechanisms, which occur after lymphocyte maturation and migration into peripheral tissue and lymphoid organs, must keep the autoreactive cells in check.

### 5.1. Predisposing and Protective MHC Alleles

In the NOD mouse, disease-associated MHC genes, and in particular I-A<sup>g7</sup> (67), are necessary but not sufficient for diabetes development (39). The

mechanism of action of protective alleles has been extensively studied in the NOD mouse. NOD-E $\alpha$  transgenic mice, which express E $\alpha$ :E $\beta$ <sup>g7</sup> together with I-A<sup>g7</sup>, fail to develop autoimmune diabetes either spontaneously or after treatment with cyclophosphamide, an agent that accelerates diabetes in wild-type NOD mice (68–71).

The mechanisms underlying this protective effect are still unclear. I-E molecules, either directly or in association with endogenous superantigens, can lead to clonal deletion of specific V $\beta$ -bearing pathogenic T cells. However, little I-E-mediated negative selection of V $\beta$  families occurs on the NOD background (71). Diabetogenic T cells are present in E $\alpha$  transgenic NOD mice and can be revealed by IL-12 administration followed by T-cell transfer into NOD-SCID recipients (72). Protection mediated by I-E molecules could not be ascribed to deletion or anergy of T cells expressing specific V $\beta$  chains (71). Nevertheless, deletion of I-A<sup>g7</sup>-restricted pathogenic autoreactive T cells by transgenic class II molecules has been proposed to occur in the thymic medulla, independently of endogenous superantigens, via presentation of a non-autoantigenic peptide to TCR-transgenic diabetogenic thymocytes (73). Therefore, clonal deletion as a mechanism of protection has not been ruled out. Peripheral mechanisms involving interference of I-E molecules with the presentation of diabetogenic peptides by I-A<sup>g7</sup> have also been proposed (39). In fact, mechanisms accounting for I-E-mediated protection could involve both thymic and peripheral events, including the positive selection of I-E-restricted regulatory T cells that could deviate or down regulate Th1-mediated  $\beta$ -cell destruction.

### 5.2. The Antigenic Specificity of Autoreactive T Cells

Both central and peripheral tolerance mechanisms could be defective in the NOD mouse. The association of class II molecules with autoimmune diabetes reflects their capacity to present peptides to autoreactive CD4<sup>+</sup> cells that could lead, under different conditions, to their deletion in the thymus and activation in the periphery. It has been suggested that NOD I-A<sup>g7</sup> (74) is unstable and binds peptides poorly, making them defective in mediating thymic negative selection of autoreactive T cells (75). However, binding studies (76) and structural analysis of I-A<sup>g7</sup> (77) do not support this hypothesis.

Several self-antigens have been associated with autoimmune diabetes, but three appear to be most relevant, both in NOD and in human T1D: (pro)insulin, GAD, and the tyrosine phosphatase-like islet antigen IA-2. Accumulating evidence favours a role for proinsulin as a key autoantigen in diabetes. The proinsulin/insulin molecules have a sequence that is a primary target of the autoimmunity: NOD mice knock-out for insulin 1 and insulin 2 genes and expressing a mutated proinsulin transgene (in which residue 16 on the  $\beta$  chain was changed to alanine) do not develop insulin autoantibodies, insulinitis or

autoimmune diabetes. NOD mice expressing transgenic proinsulin under a MHC class II promoter show complete prevention of autoimmune diabetes, probably as a result of efficient expression of this autoantigen in the thymus allowing negative selection of proinsulin-specific T cells (78); NOD proinsulin 2<sup>-/-</sup> mice develop accelerated insulinitis and diabetes: proinsulin 2 thymic expression is essential because it leads to silencing of T cells specific for an epitope shared by proinsulin 1 and proinsulin 2. Using tetrameric H-2K<sup>d</sup>-peptide complexes, about 85% of T cells infiltrating the islets of 4-wk-old NOD mice were found to recognize the insulin  $\beta$  chain residues 15-23 (79), consistent with other evidence that insulin-specific CD8<sup>+</sup> cells provoke the initial insulinitic attack (54).

In the NOD mouse, GAD-specific IFN- $\gamma$ -producing T cells have been found at the onset of insulinitis. Prevention of GAD expression exclusively in islet  $\beta$  cells by a transgenic GAD65 antisense DNA sequence prevented autoimmune diabetes (80) whereas NOD mice expressing a transgenic TCR specific for a peptide epitope of GAD65 are paradoxically protected from diabetes. These T cells may play a protective role in diabetes pathogenesis by regulating pathogenic T-cell responses (81).

The identification of T-cell responses against the intracytoplasmic portion of IA-2 in the unprimed NOD mouse and the acceleration of disease by IA-2 administration (82) demonstrates that IA-2 is also a relevant autoantigen in the NOD mouse, further strengthening the similarities between the human and NOD mouse disease. Interestingly, IFN- $\gamma$  production in response to IA-2 and autoimmune diabetes acceleration could be induced by administering IL-12 to 12-d-old NOD mice, indicating the early involvement of IL-12 in disease pathogenesis (82).

### **5.3. Pathogenic and Protective T Cells**

#### *5.3.1. Th1 and Th2 Cells*

The available evidence indicates a pathogenic role for Th1 cells in autoimmune diabetes (83); and a critical role in the disease has also been documented for IL-12, the most important cytokine driving Th1 cell development (55,84). Nevertheless, wild-type and IL-12-deficient NOD mice develop similar insulinitis and T1D (56). Because Th1 and Th2 responses reciprocally regulate each other through their respective cytokines, Th2 cells could have a role in protecting against the development of autoimmune diabetes, although a deviation to the Th2 pathway could be an effect, rather than the cause of resistance to disease (85).

Consistent with a protective role of Th2 cells, NOD mice that express IL-4 in their pancreatic  $\beta$  cells are protected from insulinitis and autoimmune diabetes

(86) by antigen-specific Th2 cells that block the action of diabetogenic T cells in the pancreas. However, limitation of T-cell diversity by back-crossing to BDC2.5 transgenic mice leads to accelerated disease (87), possibly because IL-4 can increase islet cell presentation by macrophages and dendritic cells (60). Conversely, neither NOD nor BDC2.5 transgenic mice show modification of diabetes development when rendered IL-4-deficient (59), indicating that IL-4 plays no role in controlling disease severity. In contrast to their benign role in normal NOD mice, Th2 cells have been shown to induce acute pancreatitis and autoimmune diabetes in NOD.SCID recipients, via production of IL-10 but not IL-4 (88), suggesting that lymphocyte-deficient recipients lack T cells able to regulate Th2 responses in wild-type mice.

In the Th1/Th2 balance the NKT cells seem to play an important role: they have regulatory properties and can protect from Th1 diseases by inducing a Th2 shift. NKT cells are restricted to the non-MHC CD1d molecule and express TCRs that use an invariant V $\alpha$ 14-J $\alpha$ 1 chain and a limited number of TCR $\beta$  chains. When stimulated by CD1d-expressing APCs, these cells can produce an array of cytokines early in the immune response, including IFN- $\gamma$  and IL-4, that could polarize T cells toward a Th2 phenotype.

NK T cells are quantitatively and qualitatively defective in the NOD mouse (89), and protection from T1D has been observed in NOD mice restored with high numbers of NK T cells (90–93). In addition, treatment with  $\alpha$ -GalCer, an agent that activates NK T cells, has also been shown to inhibit T1D development in NOD mice (7,94,95). Finally, germ-line deletion of CD1d, the restriction molecule of NK T cells, in the NOD background leads to exacerbation of T1D (8,96).

### 5.3.2. CD4<sup>+</sup>CD25<sup>+</sup> Regulatory T Cells

A subset of CD4<sup>+</sup> T cells, characterized by constitutive expression of CD25, (CD4<sup>+</sup>CD25<sup>+</sup> cells), has been convincingly shown to possess immunosuppressive activity (97). They are not the only type of regulatory T cells observed in the NOD mouse (98), but are the best characterized. CD8<sup>+</sup>  $\gamma$  $\delta$  regulatory cells induced by mucosally delivered insulin have been shown to block disease transfer and prevent autoimmune diabetes (99).

CD4<sup>+</sup>CD25<sup>+</sup> cells prevent the activation and proliferation of potentially autoreactive T cells that have escaped thymic deletion (100). They fail to proliferate and secrete cytokines in response to polyclonal or antigen-specific stimulation, and are not only anergic, but also inhibit the activation of responsive T cells (101). Although CD25, CD152, and glucocorticoid-induced tumor necrosis factor receptor family-related gene are markers of CD4<sup>+</sup>CD25<sup>+</sup> cells, they are also expressed by activated T cells (101). A more faithful marker



distinguishing CD4<sup>+</sup>CD25<sup>+</sup> cells from recently activated CD4<sup>+</sup>T cells is Foxp3, a transcription factor that is required for CD4<sup>+</sup>CD25<sup>+</sup> cell development and is sufficient for their suppressive function (102–104). Foxp3<sup>+</sup> CD4<sup>+</sup>CD25<sup>+</sup> cells play an important role in preventing the induction of several autoimmune diseases, such as the autoimmune syndrome induced by day-3 thymectomy in genetically susceptible mice (100), inflammatory bowel disease (105), T1D in thymectomized rats (106), and in NOD mice (9,107). CD4<sup>+</sup>CD25<sup>+</sup> cells are reduced in NOD compared to other mouse strains and this reduction could be a factor in their susceptibility to T1D (9,10). Mice with a defect in Foxp3, required for the generation and activity of regulatory T cells, exhibit massive lymphoproliferation and severe inflammatory infiltration of multiple organs, in particular the lungs, liver, and skin (103). This phenotype is influenced by an additional defect in central tolerance induction, generated by either crossing in a null mutation of the *Aire* gene or substituting the NOD genetic background. The double-deficient mice undergo fulminant autoimmunity in very early life, and display a gravely shortened lifespan compared to single-deficient littermates (108).

Transfer of CD4<sup>+</sup>CD25<sup>+</sup> T cells can prevent autoimmune diabetes in thymectomized rats (106) and inhibits T1D induced in immunodeficient NOD mice by diabetogenic T cells (9,10,109), indicating the potential of a cell-based therapy in controlling, and possibly reversing, disease progression. Although these data have established a preclinical proof of concept for this approach, the heterogeneity within the CD4<sup>+</sup>CD25<sup>+</sup> T-cell population and the low precursor frequency of cells specific for islet autoantigens makes it quite inefficient, usually requiring a relatively high ratio of suppressor to T effector cells to effectively inhibit T1D development.

To overcome these limitations, two different strategies for in vitro expansion of antigen-specific CD4<sup>+</sup>CD25<sup>+</sup> T cells have been pursued in the NOD model. The first approach utilizes a combination of anti-CD3, anti-CD28, and IL-2 to expand in vitro purified CD4<sup>+</sup>CD25<sup>+</sup> T cells from BDC2.5 TCR transgenic mice (110). The expanded CD4<sup>+</sup>CD25<sup>+</sup> T cells are very efficient suppressor cells, and they can not only prevent T1D transfer, but also stably reverse it after disease onset in the majority of recipients, a key point for the clinical applicability of this approach. Alternatively, IL-2 and TGF- $\beta$  can also be used to generate large numbers of CD4<sup>+</sup>CD25<sup>+</sup> T cells ex vivo from naïve T cells (111). Interestingly, adoptively transferred CD4<sup>+</sup>CD25<sup>+</sup> T cells induced ex vivo by IL-2/TGF- $\beta$  could generate new CD4<sup>+</sup>CD25<sup>+</sup> T cells in vivo, thus sustaining long-term suppressive effects (112).

The second approach utilizes DCs from NOD mice to directly expand CD4<sup>+</sup>CD25<sup>+</sup> T cells from BDC2.5 TCR transgenic mice (113,114). In this case, CD4<sup>+</sup>CD25<sup>+</sup> T cells expanded by DCs pulsed with an autoantigenic peptide

mimotope could suppress T1D development very efficiently, and very low numbers of CD4<sup>+</sup>CD25<sup>+</sup> T cells, as low as  $5 \times 10^3$ /recipient, were sufficient to inhibit disease in about 50% of the recipients (114). Reversal of overt T1D has not yet been demonstrated in this model, although DC-expanded CD4<sup>+</sup>CD25<sup>+</sup> T cells could still block diabetes development when transferred 15 d after diabetogenic cells (114).

Costimulatory molecules have been implicated in the development and homeostasis of regulatory T cells because both CD80/CD86-deficient and CD28-deficient NOD mice show increased incidence and earlier onset of autoimmune diabetes, associated with a profound decrease of the CD4<sup>+</sup>CD25<sup>+</sup> regulatory T cells (9). In terms of effector function, it appears that naturally occurring regulatory T cells in the NOD system can dispense with IL-10 and -4 to mediate their suppressive activity, whereas their reactivity seems to be dependent on TGF- $\beta$  (98,115): a transient pulse of this cytokine in the islets was able to induce their expansion. This expansion correlated with the ability to suppress T1D (116), and is consistent with the observation that TGF- $\beta$  can induce Foxp3 expression (117).

#### 5.4. Role of Chemokines

Chemokines, acting as chemoattractant cytokines for the recruitment and activation of leukocytes, are the central mediators of cell trafficking and have been implicated in the development of NOD and human T1D (118). Chemokine genes are present within the diabetes susceptibility locus *Idd4* in the NOD mouse (119), one of the loci associated with T1D development. Several chemokines are produced by NOD pancreatic  $\beta$  cells, including CCL2 (120,121), CCL5, CXCL10 (121), and low levels of CCL3 (122), suggesting a direct role of  $\beta$  cells in leukocyte recruitment into the pancreatic islets. The constitutive and inducible production by islet cells of CXCL10, a ligand for CXCR3 expressed by Th1 cells (123), is most prominent. CXCL10 has previously been shown to be produced by the NOD  $\beta$ -cell line NIT-1 stimulated with inflammatory cytokines (121), and the higher constitutive levels observed in the NOD background, compared with diabetes-resistant strains (122), further supports its important role in the pathogenesis of T1D.

We have shown that mouse and human islet cells, including insulin-producing  $\beta$  cells, express all of the TLRs and their triggering markedly increases the secretion of proinflammatory chemokines (122). These findings suggest that, among the initial events in T1D development, triggering of islet TLRs by microbial products could upregulate the secretion of chemokines able to attract Th1 cells, macrophages, and dendritic cells. Because these cell types are involved in the pathogenesis of T1D, the TLR-mediated upregulation of proinflammatory chemokine production by islet cells could represent an important

**Table 3**  
**Pathways for Terminating Immune Responses That are Defective in the NOD Mouse**

---

Upregulated expression of anti-apoptotic proteins such as Bcl-2, leading to defective elimination of lymphocytes
Decreased activation-induced cell death via Fas-FasL or TNF- $\alpha$ -TNFR1 interactions
Impaired production of IL-4
Impaired induction of T-cell anergy by autoantigen recognition in the absence of costimulation
Decreased number of CD4 <sup>+</sup> CD25 <sup>+</sup> regulatory T cells

---

element in the early steps of T1D development leading to leukocyte infiltration into the pancreatic islets and to the loss of immunological tolerance.

CXCR3-deficient NOD mice display a substantially delayed T1D development, highlighting the role of CXCL10 in the disease process (121). We have shown that vitamin D receptor agonists can inhibit islet chemokine production, including CXCL10, in vitro and in vivo in the NOD mouse, and the NOD model allowed us to determine that downregulation of chemokine production by islet cells was associated with reduced T-cell recruitment to the pancreas and inhibition of T1D development (122).

### **5.5. Faulty Termination of Immune Responses in the Pathogenesis of T1D**

In the pathogenesis of autoimmune diseases, emphasis is usually placed on inductive steps and on the breaking of mechanisms that control tolerance to self antigens. Although these are certainly important, emerging evidence suggests that a key feature of T1D, and possibly of other autoimmune diseases, is the failure of mechanisms that normally terminate immune responses.

The main pathways for the termination of immune responses appear to be defective in the NOD mouse (Table 3). Intriguingly, the autoimmune diabetes susceptibility locus *idd3* has been mapped to a 0.35-cM interval containing the IL-2 gene (124). The NOD IL-2 gene appears to be an allelic variant resulting in a serine-to-proline substitution at position 6 of the mature IL-2 protein, which is, nevertheless, functional (124). IL-2 or IL-2 receptor-deficient mice develop severe autoimmune diseases, probably due to the non-redundant function of IL-2 in tolerance to self via two major pathways: homeostasis of CD4<sup>+</sup>CD25<sup>+</sup> regulatory T cells (125), and priming for apoptosis of proliferating T cells (126).

*Idd5* has been mapped to the CTLA-4-CD28 region and shown to control resistance to apoptosis of NOD peripheral T cells (127). Another autoimmune

diabetes-associated locus maps to the region containing the anti-apoptotic gene Bcl-2; Idd7 maps to the region containing the TGF $\beta$ 1 locus that controls progression of insulinitis to overt disease (128) and could also be implicated in faulty termination of immune responses in the NOD mouse.

## References

1. Bach, J. -F. (1994) Insulin-dependent diabetes mellitus as an autoimmune disease. *Endocrine Rev.* **15**, 516–542.
2. Adorini, L., Gregori, S., and Harrison, L. C. (2002) Understanding autoimmune diabetes: insights from mouse models. *Trends Mol. Med.* **8**, 31–38.
3. Kikutani, H. and Makino, S. (1992) The murine autoimmune diabetes model: NOD and related strains. *Adv. Immunol.* **51**, 285–322.
4. Serreze, D. V., Gaedeke, J. W., and Leiter, E. H. (1993) Hematopoietic stem-cell defects underlying abnormal macrophage development and maturation in NOD/Lt mice: defective regulation of cytokine receptors and protein kinase C. *Proc. Natl. Acad. Sci. USA* **90**, 9625–9629.
5. Kataoka, S., Satoh, J., Fujiya, H., et al. (1983) Immunologic aspects of the nonobese diabetic (NOD) mouse. Abnormalities of cellular immunity. *Diabetes* **32**, 247–253.
6. Ogasawara, K., Hamerman, J. A., Hsin, H., et al. (2003) Impairment of NK cell function by NKG2D modulation in NOD mice. *Immunity* **18**, 41–51.
7. Naumov, Y. N., Bahjat, K. S., Gausling, R., et al. (2001) Activation of CD1 d-restricted T cells protects NOD mice from developing diabetes by regulating dendritic cell subsets. *Proc. Natl. Acad. Sci. USA* **98**, 13,838–13,843.
8. Wang, B., Geng, Y. B., and Wang, C. R. (2001) CD1-restricted NK T cells protect nonobese diabetic mice from developing diabetes. *J. Exp. Med.* **194**, 313–320.
9. Salomon, B., Lenschow, D. J., Rhee, L., et al. (2000) B7/CD28 costimulation is essential for the homeostasis of the CD4+CD25+ immunoregulatory T cells that control autoimmune diabetes. *Immunity* **12**, 431–440.
10. Gregori, S., Giarratana, N., Smiroldo, S., and Adorini, L. (2003) Dynamics of pathogenic and suppressor T cells in autoimmune diabetes development. *J. Immunol.* **171**, 4040–4047.
11. Baxter, A. G. and Cooke, A. (1993) Complement lytic activity has no role in the pathogenesis of autoimmune diabetes in NOD mice. *Diabetes* **42**, 1574–1578.
12. Makino, S., Kunitomo, K., Muraoka, Y., Mizushima, Y., Katagiri, K., and Tochino, Y. (1980) Breeding of a non-obese, diabetic strain of mice. *Exp. Animal* **29**, 1–13.
13. Pozzilli, P., Signore, A., Williams, A. J., and Beales, P. E. (1993) NOD mouse colonies around the world: recent facts and figures. *Immunol. Today* **14**, 193–196.
14. Andre, I., Gonzalez, A., Wang, B., Katz, J., Benoist, C., and Mathis, D. (1996) Checkpoints in the progression of autoimmune disease: lessons from diabetes models. *Proc. Natl. Acad. Sci. USA* **93**, 2260–2263.

15. Yoon, J. W. (1990) The role of viruses and environmental factors in the induction of diabetes. *Curr. Top. Microbiol. Immunol.* **164**, 95–123.
16. Yoon, J. W. (1992) Induction and prevention of type 1 diabetes mellitus by viruses. *Diabete Metab.* **18**, 378–386.
17. Davydova, B., Harkonen, T., Kaialainen, S., Hovi, T., Vaarala, O., and Roivainen, M. (2003) Coxsackievirus immunization delays onset of diabetes in non-obese diabetic mice. *J. Med. Virol.* **69**, 510–520.
18. Bach, J. F. (2005) Infections and autoimmune diseases. *J. Autoimmun.* **25**, 74–80.
19. Williams, A. J., Krug, J., Lampeter, E. F., et al. (1990) Raised temperature reduces the incidence of diabetes in the NOD mouse. *Diabetologia* **33**, 635–637.
20. Like, A. A. and Rossini, A. A. (1976) Streptozotocin-induced pancreatic insulinitis: new model of diabetes mellitus. *Science* **193**, 415–417.
21. Malaisse, W. J. (1982) Alloxan toxicity to the pancreatic B cell. A new hypothesis. *Biochem. Pharmacol.* **31**, 3527–3534.
22. Kolb, H. and Kroencke, K. -D. (1993) IDDM. Lessons from the low-dose streptozocin model in mice. *Diabetes Rev.* **1**, 116–126.
23. Cossel, L., Schneider, E., Kuttler, B., et al. (1985) Low dose streptozotocin induced diabetes in mice. Metabolic, light microscopical, histochemical, immunofluorescence microscopical, electron microscopical and morphometrical findings. *Exp. Clin. Endocrinol.* **85**, 7–26.
24. Gerling, I. C., Friedman, H., Greiner, D. L., Shultz, L. D., and Leiter, E. H. (1994) Multiple low-dose streptozocin-induced diabetes in NOD-*scid/scid* mice in the absence of functional lymphocytes. *Diabetes* **43**, 433–440.
25. Harada, M. and Makino, S. (1984) Promotion of spontaneous diabetes in non-obese diabetes-prone mice by cyclophosphamide. *Diabetologia* **27**, 604–606.
26. Kay, T. W., Campbell, I. L., and Harrison, L. C. (1991) Characterization of pancreatic T lymphocytes associated with beta cell destruction in the non-obese diabetic (NOD) mouse. *J. Autoimmun.* **4**, 263–276.
27. Yasunami, R. and Bach, J. -F. (1988) Anti-suppressor effect of cyclophosphamide on the development of spontaneous diabetes in NOD mice. *Eur. J. Immunol.* **18**, 481–484.
28. Christianson, S. W., Shultz, L. D., and Leiter, E. H. (1993) Adoptive transfer of diabetes into immunodeficient NOD-*scid/scid* mice. Relative contributions of CD4<sup>+</sup> and CD8<sup>+</sup> T-cells from diabetic versus prediabetic NOD.NON-*Thy-1<sup>a</sup>* donors. *Diabetes* **42**, 44–55.
29. Wicker, L. S., Miller, B. J., and Mullen, Y. (1986) Transfer of autoimmune diabetes mellitus with splenocytes from nonobese diabetic (NOD) mice. *Diabetes* **35**, 855–860.
30. Bendelac, A., Carnaud, C., Boitard, C., and Bach, J. -F. (1987) Syngeneic transfer of autoimmune diabetes from diabetic NOD mice to healthy neonates. Requirement for both L3T4<sup>+</sup> and Lyt-2<sup>+</sup> T cells. *J. Exp. Med.* **166**, 823–832.
31. Wong, F. S., Visintin, I., Wen, L., Flavell, R. A., and Janeway, C. A., Jr. (1996) CD8 T cell clones from young nonobese diabetic (NOD) islets can transfer rapid onset of diabetes in NOD mice in the absence of CD4 cells. *J. Exp. Med.* **183**, 67–76.

32. Haskins, K. and Wegmann, D. (1996) Diabetogenic T-cell clones. *Diabetes* **45**, 1299–1305.
33. Chatenoud, L., Thervet, E., Primo, J., and Bach, J. F. (1994) Anti-CD3 antibody induces long-term remission of overt autoimmunity in nonobese diabetic mice. *Proc. Natl. Acad. Sci. USA* **91**, 123–127.
34. Wang, B., Gonzales, A., Benoist, C., and Mathis, D. (1996) The role of CD8<sup>+</sup> cells in the initiation of insulin-dependent diabetes mellitus. *Eur. J. Immunol.* **26**, 1762–1769.
35. Shizuru, J. A., Taylor-Edwards, C., Banks, B. A., Gregory, A. K., and Fathman, C. G. (1988) Immunotherapy of the nonobese diabetic mouse: treatment with an antibody to T-helper lymphocytes. *Science* **240**, 659–662.
36. Kurasawa, K., Sakamoto, A., Maeda, T., et al. (1993) Short-term administration of anti-L3T4 MoAb prevents diabetes in NOD mice. *Clin. Exp. Immunol.* **91**, 376–380.
37. Mori, Y., Suko, M., Okudaira, H., et al. (1986) Preventive effects of cyclosporin on diabetes in NOD mice. *Diabetologia* **29**, 244–247.
38. Serreze, D. V., Fleming, S. A., Chapman, H. D., Richard, S. D., Leiter, E. H., and Tisch, R. M. (1998) B lymphocytes are critical antigen-presenting cells for the initiation of T cell-mediated autoimmune diabetes in nonobese diabetic mice. *J. Immunol.* **161**, 3912–3918.
39. Wicker, L., Todd, J., and Peterson, L. (1995) Genetic control of autoimmune diabetes in the NOD mouse. *Annu. Rev. Immunol.* **13**, 179–200.
40. Falcone, M. and Sarvetnick, N. (1999) Cytokines that regulate autoimmune responses. *Curr. Opin. Immunol.* **11**, 670–676.
41. Balasa, B., A. La Cava, K. Van Gunst, L., et al. (2000) A mechanism for IL-10-mediated diabetes in the nonobese diabetic (NOD) mouse: ICAM-1 deficiency blocks accelerated diabetes. *J. Immunol.* **165**, 7330.
42. Kawamoto, S., Nitta, Y., Tashiro, F., et al. (2001) Suppression of T(h)1 cell activation and prevention of autoimmune diabetes in NOD mice by local expression of viral IL-10. *Int. Immunol.* **13**, 685–694.
43. Green, E. A., Eynon, E. E., and Flavell, R. A. (1998) Local expression of TNF $\alpha$  in neonatal NOD mice promotes diabetes by enhancing presentation of islet antigens. *Immunity* **9**, 733–743.
44. Grewal, I. S., Grewal, K. D., Wong, F. S., Picarella, D. E., Janeway C. A., Jr., and Flavell, R. A. (1996) Local expression of transgene encoded TNF  $\alpha$  in islets prevents autoimmune diabetes in nonobese diabetic (NOD) mice by preventing the development of auto-reactive islet-specific T cells. *J. Exp. Med.* **184**, 1963–1974.
45. Wong, S., Guerder, S., Visintin, I., et al. (1995) Expression of the co-stimulator molecule B7-1 in pancreatic beta-cells accelerates diabetes in the NOD mouse. *Diabetes* **44**, 326–329.
46. Lenschow, D. J., Herold, K. C., Rhee, L., et al. (1996) CD28/B7 regulation of TH1 and TH2 subsets in the development of autoimmune diabetes. *Immunity* **5**, 285–293.
47. Hulbert, C., Riseili, B., Rojas, M., and Thomas, J. (2001) B cell specificity contributes to the outcome of diabetes in nonobese diabetic mice. *J. Immunol.* **167**, 5535–5538.

48. Petrovsky, N., Silva, D., Socha, L., Slattery, R., and Charlton, B. (2002) The role of Fas ligand in beta cell destruction in autoimmune diabetes of NOD mice. *Ann. NY Acad. Sci.* **958**, 204–208.
49. Savinov, A., Tcherepanov, A., Green, E., Flavell, R., and Chervonsky, A. (2003) Contribution of Fas to diabetes development. *Proc. Natl. Acad. Sci. USA* **100**, 628–632.
50. Sung, H., Juang, J., Lin, Y., et al. (2004) Transgenic expression of decoy receptor 3 protects islets from spontaneous and chemical-induced autoimmune destruction in nonobese diabetic mice. *J. Exp. Med.* **199**, 1143–1151.
51. Katz, J., Benoist, C., and Mathis, D. (1993) Major histocompatibility complex class I molecules are required for the development of insulinitis in non-obese diabetic mice. *Eur. J. Immunol.* **23**, 3358–3360.
52. Wicker, L. S., Leiter, E. H., Todd, J. A., et al. (1994) Beta 2-microglobulin-deficient NOD mice do not develop insulinitis or diabetes. *Diabetes* **43**, 500–504.
53. Mora, C., Wong, F. S., Chang, C. H., and Flavell, R. A. (1999) Pancreatic infiltration but not diabetes occurs in the relative absence of MHC class II-restricted CD4 T cells: studies using NOD/CIITA-deficient mice. *J. Immunol.* **162**, 4576–4588.
54. Kay, T. W. H., Parker, J. L., Stephens, L. A., Thomas, H. E., and Allison, J. (1996) RIP- $b_2$ -microglobulin transgene expression restores insulinitis, but not diabetes, in  $b_2$ -microglobulin<sup>null</sup> nonobese diabetic mice. *J. Immunol.* **157**, 3688–3693.
55. Trembleau, S., Germann, T., Gately, M. K., and Adorini, L. (1995) The role of IL-12 in the induction of organ-specific autoimmune diseases. *Immunol. Today* **16**, 383–386.
56. Trembleau, S., Penna, G., Gregori, S., et al. (1999) Pancreas-infiltrating Th1 cells and diabetes develop in IL-12-deficient nonobese diabetic mice. *J. Immunol.* **163**, 2960–2968.
57. Trembleau, S., Penna, G., Gregori, S., Giarratana, N., and Adorini, L. (2003) IL-12 administration accelerates autoimmune diabetes in both wild-type and IFN-gamma-deficient nonobese diabetic mice, revealing pathogenic and protective effects of IL-12-induced IFN-gamma. *J. Immunol.* **170**, 5491–5501.
58. Balasa, B., Van Gunst, K., Jung, N., Katz, J. D., and Sarvetnick, N. (2000) IL-10 deficiency does not inhibit insulinitis and accelerates cyclophosphamide-induced diabetes in the nonobese diabetic mouse. *Cell. Immunol.* **202**, 97–102.
59. Wang, B., Gonzalez, A., Hoglund, P., Katz, J. D., Benoist, C., and Mathis, D. (1998) Interleukin-4 deficiency does not exacerbate disease in NOD mice. *Diabetes* **47**, 1207–1211.
60. Falcone, M., Yeung, B., Tucker, L., Rodriguez, E., Krahl, T., and Sarvetnick, N. (2001) IL-4 triggers autoimmune diabetes by increasing self-antigen presentation within the pancreatic Islets. *Clin. Immunol.* **98**, 190–199.
61. Green, E. A., Wong, F. S., Eshima, K., Mora, C., and Flavell, R. A. (2000) Neonatal tumor necrosis factor alpha promotes diabetes in nonobese diabetic mice by CD154-independent antigen presentation to CD8(+) T cells. *J. Exp. Med.* **191**, 225–238.

62. Martin, S., van den Engel, N. K., Vinke, A., Heidenthal, E., Schulte, B., and Kolb, H. (2001) Dominant role of intercellular adhesion molecule-1 in the pathogenesis of autoimmune diabetes in non-obese diabetic mice. *J. Autoimmun.* **17**, 109.
63. Anderson, M. S., Venanzi, E. S., Chen, Z., Berzins, S. P., Benoist, C., and Mathis, D. (2005) The cellular mechanism of Aire control of T cell tolerance. *Immunity* **23**, 227–239.
64. Villasenor, J., Benoist, C., and Mathis, D. (2005) AIRE and APECED: molecular insights into an autoimmune disease. *Immunol. Rev.* **204**, 156–164.
65. Lohmann, T., Leslie, R. D., and Londei, M. (1996) T cell clones to epitopes of glutamic acid decarboxylase 65 raised from normal subjects and patients with insulin-dependent diabetes. *J. Autoimmun.* **9**, 385–389.
66. Semana, G., Gausling, R., Jackson, R. A., and Hafler, D. A. (1999) T cell autoreactivity to proinsulin epitopes in diabetic patients and healthy subjects. *J. Autoimmun.* **12**, 259–267.
67. Miyazaki, T., Uno, M., Uehira, M., et al. (1990) Direct evidence for the contribution of the unique I-ANOD to the development of insulinitis in non-obese diabetic mice. *Nature* **345**, 722–724.
68. Nishimoto, H., Kikutani, H., Yamamura, K. I., and Kishimoto, T. (1987) Prevention of autoimmune insulinitis by expression of I-E molecules in NOD mice. *Nature* **328**, 432–434.
69. Uehira, M., Onu, M., Miyazaki, J., Nishimoto, H., Kishimoto, T., and Yamamura, K. (1989) Development of autoimmune insulinitis is prevented in E alpha d but not in A beta k NOD transgenic mice. *Int. Immunol.* **1**, 209–213.
70. Lund, T., O'Reilly, L., Hutchings, P., et al. (1990) Prevention of insulin-dependent diabetes in non-obese diabetic mice by transgenes encoding modified I-A b-chain or normal I-E a-chain. *Nature* **345**, 727–729.
71. Boehme, J., Schuhbaur, B., Kanagawa, O., Benoist, C., and Mathis, D. (1990) MHC-linked protection from diabetes dissociated from clonal deletion of T cells. *Science* **249**, 293–295.
72. Trembleau, S., Gregori, S., Penna, G., Gorny, I., and Adorini, L. (2001) IL-12 administration reveals diabetogenic T cells in genetically resistant I-Ealpha-transgenic nonobese diabetic mice: resistance to autoimmune diabetes is associated with binding of Ealpha-derived peptides to the I-A(g7) molecule. *J. Immunol.* **167**, 4104–4114.
73. Schmidt, D., Amrani, A., Verdaguer, J., Bou, S., and Santamaria, P. (1999) Autoantigen-independent deletion of diabetogenic CD4+ thymocytes by protective MHC class II molecules. *J. Immunol.* **162**, 4627–4636.
74. Carrasco-Marin, E., Shimizu, J., Kanagawa, O., and Unanue, E. (1996) The class II MHC I-Ag7 molecules from non-obese diabetic mice are poor peptide binders. *J. Immunol.* **156**, 450–458.
75. Ridgway, W. M. and Fathman, C. G. (1999) MHC structure and autoimmune T cell repertoire development. *Curr. Opin. Immunol.* **11**, 638–642.



76. Harrison, L. C., Honeyman, M. C., Trembleau, S., et al. (1997) A peptide-binding motif for I-Ag7, the class II MHC molecule of NOD and Biozzi AB/H mice. *J. Exp. Med.* **185**, 1013–1021.
77. Corper, A. L., Stratmann, T., Apostolopoulos, V., et al. (2000) A structural framework for deciphering the link between I-Ag7 and autoimmune diabetes. *Science* **288**, 505–511.
78. French, M. B., Allison, J., Cram, D. S., et al. (1997) Transgenic expression of mouse proinsulin II prevents diabetes in nonobese diabetic mice. *Diabetes* **46**, 34–39.
79. Wong, F. S., Karttunen, J., Dumont, C., et al. (1999) Identification of an MHC class I-restricted autoantigen in type 1 diabetes by screening an organ-specific cDNA library. *Nat. Med.* **5**, 1026–1031.
80. Yoon, J. W., Yoon, C. S., Lim, H. W., et al. (1999) Control of autoimmune diabetes in NOD mice by GAD expression or suppression in beta cells. *Science* **284**, 1183–1187.
81. Ranheim, E. A., Tarbell, K., Krogsgaard, M., et al. (2004) Selection of aberrant class II restricted CD8+ T cells in NOD mice expressing a glutamic acid decarboxylase (GAD)65-specific T cell receptor transgene. *Autoimmunity* **37**, 555–567.
82. Trembleau, S., Penna, G., Gregori, S., Magistrelli, G., Isacchi, A., and Adorini, L. (2000) Early Th1 response in unprimed nonobese diabetic mice to the tyrosine phosphatase-like insulinoma-associated protein 2, an autoantigen in type 1 diabetes. *J. Immunol.* **165**, 6748–6755.
83. Trembleau, S., Penna, G., Bosi, E., Mortara, A., Gately, M. K., and Adorini, L. (1995) IL-12 administration induces Th1 cells and accelerates autoimmune diabetes in NOD mice. *J. Exp. Med.* **181**, 817–821.
84. Nitta, Y., Kawamoto, S., Tashiro, F., et al. (2001) IL-12 plays a pathologic role at the inflammatory loci in the development of diabetes in NOD mice. *J. Autoimmun.* **16**, 97–104.
85. Serreze, D. V., Chapman, H. D., Post, C. M., Johnson, E. A., Suarez-Pinzon, W. L., and Rabinovitch, A. (2001) Th1 to Th2 cytokine shifts in nonobese diabetic mice: sometimes an outcome, rather than the cause, of diabetes resistance elicited by immunostimulation. *J. Immunol.* **166**, 1352–1359.
86. Mueller, R., Krahl, T., and Sarvetnick, N. (1996) Pancreatic expression of interleukin-4 abrogates insulinitis and autoimmune diabetes in nonobese diabetic (NOD) mice. *J. Exp. Med.* **184**, 1093–1099.
87. Mueller, R., Bradley, L. M., Krahl, T., and Sarvetnick, N. (1997) Mechanism underlying counterregulation of autoimmune diabetes by IL-4. *Immunity* **7**, 411–418.
88. Pakala, S. V., Kurrer, M. O., and Katz, J. D. (1997) T helper 2 (Th2) T cells induce acute pancreatitis and diabetes in immune-compromised nonobese diabetic (NOD) mice. *J. Exp. Med.* **186**, 299–306.
89. Godfrey, D. I., Hammond, K. J., Poulton, L. D., Smyth, M. J., and Baxter, A. G. (2000) NKT cells: facts, functions and fallacies. *Immunol. Today* **21**, 573–583.
90. Hammond, K. J., Pellicci, D. G., Poulton, L. D., et al. (2001) CD1d-restricted NKT cells: an interstrain comparison. *J. Immunol.* **167**, 1164–1173.

91. Baxter, A. G., Kinder, S. J., Hammond, K. J., Scollay, R., and Godfrey, D. I. (1997) Association between alphabetaTCR+CD4-CD8- T-cell deficiency and IDDM in NOD/Lt mice. *Diabetes* **46**, 572–582.
92. Hammond, K. J., Poulton, L. D., Palmisano, L. J., Silveira, P. A., Godfrey, D. I., and Baxter, A. G. (1998) alpha/beta-T cell receptor (TCR)+CD4-CD8- (NKT) thymocytes prevent insulin-dependent diabetes mellitus in nonobese diabetic (NOD)/Lt mice by the influence of interleukin (IL)-4 and/or IL-10. *J. Exp. Med.* **187**, 1047–1056.
93. Lehuen, A., Lantz, O., Beaudoin, L., et al. (1998) Overexpression of natural killer T cells protects Valpha14- Jalpha281 transgenic nonobese diabetic mice against diabetes. *J. Exp. Med.* **188**, 1831–1839.
94. Sharif, S., Arreaza, G. A., Zucker, P., et al. (2001) Activation of natural killer T cells by alpha-galactosylceramide treatment prevents the onset and recurrence of autoimmune Type 1 diabetes. *Nat. Med.* **7**, 1057–1062.
95. Hong, S., Wilson, M. T., Serizawa, I., et al. (2001) The natural killer T-cell ligand alpha-galactosylceramide prevents autoimmune diabetes in non-obese diabetic mice. *Nat. Med.* **7**, 1052–1056.
96. Shi, F. D., Flodstrom, M., Balasa, B., et al. (2001) Germ line deletion of the CD1 locus exacerbates diabetes in the NOD mouse. *Proc. Natl. Acad. Sci. USA* **98**, 6777–6782.
97. Shevach, E. M. (2000) Regulatory T cells in autoimmunity. *Annu. Rev. Immunol.* **18**, 423–449.
98. Lepault, F. and Gagnerault, M. C. (2000) Characterization of peripheral regulatory CD4+ T cells that prevent diabetes onset in nonobese diabetic mice. *J. Immunol.* **164**, 240–247.
99. Hanninen, A. and Harrison, L. C. (2000) Gamma delta T cells as mediators of mucosal tolerance: the autoimmune diabetes model. *Immunol. Rev.* **173**, 109–119.
100. Sakaguchi, S. (2000) Regulatory T cells: key controllers of immunologic self-tolerance. *Cell* **101**, 455–458.
101. Shevach, E. M. (2002) CD4+ CD25+ suppressor T cells: more questions than answers. *Nat. Rev. Immunol.* **2**, 389.
102. Hori, S., Nomura, T., and Sakaguchi, S. (2003) Control of regulatory T cell development by the transcription factor Foxp3. *Science* **299**, 1057–1061.
103. Fontenot, J. D., Gavin, M. A., and Rudensky, A. Y. (2003) Foxp3 programs the development and function of CD4+ CD25+ regulatory T cells. *Nat. Immunol.* **4**, 330–336.
104. Khattri, R., Cox, T., Yasayko, S. A., and Ramsdell, F. (2003) An essential role for Scurfin in CD4+CD25+ T regulatory cells. *Nat. Immunol.* **4**, 337–342.
105. Read, S., Malmstrom, V., and Powrie, F. (2000) Cytotoxic T lymphocyte-associated antigen 4 plays an essential role in the function of CD25(+)/CD4(+) regulatory cells that control intestinal inflammation. *J. Exp. Med.* **192**, 295–302.
106. Stephens, L. A. and Mason, D. (2000) CD25 is a marker for CD4+ thymocytes that prevent autoimmune diabetes in rats, but peripheral T cells with this function are found in both CD25+ and CD25- subpopulations. *J. Immunol.* **165**, 3105–3110.

107. Wu, A. J., Hua, H., Munson, S. H., and McDevitt, H. O. (2002) Tumor necrosis factor- $\alpha$  regulation of CD4+CD25+ T cell levels in NOD mice. *Proc. Natl. Acad. Sci. USA* **99**, 12,287–12,292.
108. Chen, Z., Benoist, C., and Mathis, D. (2005) How defects in central tolerance impinge on a deficiency in regulatory T cells. *Proc. Natl. Acad. Sci. USA* **102**, 14,735–14,740.
109. Szanya, V., Ermann, J., Taylor, C., Holness, C., and Fathman, C. G. (2002) The subpopulation of CD4+CD25+ splenocytes that delays adoptive transfer of diabetes expresses L-selectin and high levels of CCR7. *J. Immunol.* **169**, 2461–2465.
110. Tang, Q., Henriksen, K. J., Bi, M., et al. (2004) In vitro-expanded antigen-specific regulatory T cells suppress autoimmune diabetes. *J. Exp. Med.* **199**, 1455–1465.
111. Horwitz, D. A., Zheng, S. G., Gray, J. D., Wang, J. H., Ohtsuka, K., and Yamagiwa, S. (2004) Regulatory T cells generated ex vivo as an approach for the therapy of autoimmune disease. *Semin. Immunol.* **16**, 135–143.
112. Zheng, S. G., Wang, J. H., Gray, J. D., Soucier, H., and Horwitz, D. A. (2004) Natural and induced CD4+CD25+ cells educate CD4+CD25- cells to develop suppressive activity: the role of IL-2, TGF- $\beta$ , and IL-10. *J. Immunol.* **172**, 5213–5221.
113. Yamazaki, S., Iyoda, T., Tarbell, K., et al. (2003) Direct expansion of functional CD25+ CD4+ regulatory T cells by antigen-processing dendritic cells. *J. Exp. Med.* **198**, 235–247.
114. Tarbell, K. V., Yamazaki, S., Olson, K., Toy, P., and Steinman, R. M. (2004) CD25+ CD4+ T cells, expanded with dendritic cells presenting a single autoantigenic peptide, suppress autoimmune diabetes. *J. Exp. Med.* **199**, 1467–1477.
115. Belghith, M., Bluestone, J. A., Barriot, S., Megret, J., Bach, J. F., and Chatenoud, L. (2003) TGF- $\beta$ -dependent mechanisms mediate restoration of self-tolerance induced by antibodies to CD3 in overt autoimmune diabetes. *Nat. Med.* **9**, 1202–1208.
116. Peng, Y., Laouar, Y., Li, M. O., Green, E. A., and Flavell, R. A. (2004) TGF- $\beta$  regulates in vivo expansion of Foxp3-expressing CD4+CD25+ regulatory T cells responsible for protection against diabetes. *Proc. Natl. Acad. Sci. USA* **101**, 4572–4577.
117. Fantini, M. C., Becker, C., Monteleone, G., Pallone, F., Galle, P. R., and Neurath, M. F. (2004) Cutting edge: TGF- $\beta$  induces a regulatory phenotype in CD4+CD25- T cells through Foxp3 induction and down-regulation of Smad7. *J. Immunol.* **172**, 5149–5153.
118. Atkinson, M. A. and Wilson, S. B. (2002) Fatal attraction: chemokines and type 1 diabetes. *J. Clin. Invest.* **110**, 1611–1613.
119. Grattan, M., Mi, Q. S., Meagher, C., and Delovitch, T. L. (2002) Congenic mapping of the diabetogenic locus Idd4 to a 5.2-cM region of chromosome 11 in NOD mice: identification of two potential candidate subloci. *Diabetes* **51**, 215–223.

120. Chen, M. C., Schuit, F., and Eizirik, D. L. (1999) Identification of IL-1 $\beta$ -induced messenger RNAs in rat pancreatic beta cells by differential display of messenger RNA. *Diabetologia* **42**, 1199–1203.
121. Frigerio, S., Junt, T., Lu, B., et al. (2002) Beta cells are responsible for CXCR3-mediated T-cell infiltration in insulinitis. *Nat. Med.* **8**, 1414–1420.
122. Giarratana, N., Penna, G., Amuchastegui, S., Mariani, R., Daniel, K. C., and Adorini, L. (2004) A vitamin D analog down-regulates proinflammatory chemokine production by pancreatic islets inhibiting T cell recruitment and type 1 diabetes development. *J. Immunol.* **173**, 2280–2287.
123. Rossi, D. and Zlotnik, A. (2000) The biology of chemokines and their receptors. *Annu. Rev. Immunol.* **18**, 217–242.
124. Denny, P., Lord, C. J., Hill, N. J., et al. (1997) Mapping of the IDDM locus Idd3 to a 0.35-cM interval containing the interleukin-2 gene. *Diabetes* **46**, 695–700.
125. Knoechel, B., Lohr, J., Kahn, E., Bluestone, J. A., and Abbas, A. K. (2005) Sequential development of interleukin 2-dependent effector and regulatory T cells in response to endogenous systemic antigen. *J. Exp. Med.* **202**, 1375–1386.
126. Refaeli, Y., Van Parijs, L., and Abbas, A. K. (1999) Genetic models of abnormal apoptosis in lymphocytes. *Immunol. Rev.* **169**, 273–282.
127. Colucci, F., Bergman, M. -L., Penha-Goncalves, C., Cilio, C. M., and Holmberg, D. (1997) Apoptosis resistance of NOD peripheral lymphocytes linked to the *idd5* diabetes susceptibility region. *Proc. Natl. Acad. Sci. USA* **94**, 8670–8674.
128. Gonzalez, A., Katz, J. D., Mattei, M. G., Kikutani, H., Benoist, C., and Mathis, D. (1997) Genetic control of diabetes progression. *Immunity* **7**, 873–883.
129. Quartey-Papafio, R., Lund, T., Chandler, P., et al. (1995) Aspartate at position 57 of nonobese diabetic I-Ag7 b-chain diminishes the spontaneous incidence of insulin-dependent diabetes mellitus. *J. Immunol.* **154**, 5567–5575.
130. Singer, S., Tisch, R., Yang, X. D., and McDevitt, H. O. (1993) An Abd transgene prevents diabetes in nonobese diabetic mice by inducing regulatory T cells. *Proc. Natl. Acad. Sci. USA* **90**, 9566–9570.
131. Slattery, R. M., Kjer-Nielsen, L., Allison, J., Charlton, B., Mandel, T. E., and Miller, J. F. (1990) Prevention of diabetes in non-obese diabetic I-Ak transgenic mice. *Nature* **345**, 724–726.
132. Lawrance, S. K., Karlsson, L., Price, J., et al. (1989) Transgenic HLA-DRa faithfully reconstitutes I-E-controlled immune functions and induces cross-tolerance to Ea in Ea<sup>o</sup> mutant mice. *Cell* **58**, 583–594.
133. Liu, J., Purdy, L. E., Rabinovitch, S., Jevnikar, A. M., and Elliott, J. F. (1999) Major DQ8-restricted T-cell epitopes for human GAD65 mapped using human CD4, DQA1\*0301, DQB1\*0302 transgenic IA(null) NOD mice. *Diabetes* **48**, 469–477.
134. Fukui, Y., Nishimura, Y., Iwanga, T., et al. (1989) Glycosuria and insulinitis in NOD mice expressing the HLA-DQw6 molecule. *J. Immunogenet.* **16**, 445–453.
135. Miyazaki, T., Matsuda, Y., Toyonaga, T., Miyazaki, J., Yazaki, Y., and Yamamura, K. (1992) Prevention of autoimmune insulinitis in nonobese diabetic mice by

- expression of major histocompatibility complex class I Ld molecules. *Proc. Natl. Acad. Sci. USA* **89**, 9519–9523.
136. Allison, J., McClive, P., Oxbrow, L., Baxter, A., Morahan, G., and Miller, J. F. A. P. (1994) Genetic requirements for acceleration of diabetes in non-obese diabetic mice expressing interleukin-2 in islet beta-cells. *Eur. J. Immunol.* **24**, 2535–2541.
  137. DiCosmo, B. F., Picarella, D., and Flavell, R. A. (1994) Local production of human IL-6 promotes insulinitis but retards the onset of insulin-dependent diabetes mellitus in non-obese diabetic mice. *Int. Immunol.* **6**, 1829–1837.
  138. Wogensen, L., Lee, M. -S., and Sarvetnick, N. (1994) Production of interleukin 10 by islet cells accelerates immune-mediated destruction of beta cells in nonobese diabetic mice. *J. Exp. Med.* **179**, 1379–1384.
  139. Moritani, M., Yoshimoto, K., Tashiro, F., et al. (1994) Transgenic expression of IL-10 in pancreatic islet A cells accelerates autoimmune insulinitis and diabetes in non-obese diabetic mice. *Int. Immunol.* **6**, 1927–1936.
  140. King, C., Davies, J., Mueller, R., et al. (1998) TGF-beta1 alters APC preference, polarizing islet antigen responses toward a Th2 phenotype. *Immunity* **8**, 601–613.
  141. Nakayama, M., Abiru, N., Moriyama, H., et al. (2005) Prime role for an insulin epitope in the development of type 1 diabetes in NOD mice. *Nature* **435**, 220–223.
  142. Birk, O. S., Douek, D. C., Elias, D., et al. (1996) A role of Hsp60 in autoimmune diabetes: analysis in a transgenic model. *Proc. Natl. Acad. Sci. USA* **93**, 1032–1037.
  143. Geng, L., Solimena, M., Flavell, R. A., Sherwin, R. S., and Hayday, A. C. (1998) Widespread expression of an autoantigen-GAD65 transgene does not tolerize non-obese diabetic mice and can exacerbate disease. *Proc. Natl. Acad. Sci. USA* **95**, 10,055–10,060.
  144. Katz, J. D., Wang, B., Haskins, K., Benoist, C., and Mathis, D. (1993) Following a diabetogenic T cell from genesis through pathogenesis. *Cell* **74**, 1089–1100.
  145. Verdager, J., Yoon, J. W., Anderson, B., et al. (1996) Acceleration of spontaneous diabetes in TCR-beta-transgenic nonobese diabetic mice by beta-cell cytotoxic CD8+ T cells expressing identical endogenous TCR-alpha chains. *J. Immunol.* **157**, 4726–4735.
  146. Kim, S. K., Tarbell, K. V., Sanna, M., et al. (2004) Prevention of type I diabetes transfer by glutamic acid decarboxylase 65 peptide 206-220-specific T cells. *Proc. Natl. Acad. Sci. USA* **101**, 14,204–14,209.
  147. Hultgren, B., Huang, X., Dybdal, N., and Stewart, T. A. (1996) Genetic absence of gamma-interferon delays but does not prevent diabetes in NOD mice. *Diabetes* **45**, 812–817.
  148. Kanagawa, O., Xu, G., Tevaarwerk, A., and Vaupel, B. A. (2000) Protection of nonobese diabetic mice from diabetes by gene(s) closely linked to IFN-gamma receptor loci. *J. Immunol.* **164**, 3919–3923.
  149. Kagi, D., Ho, A., Odermatt, B., Zakarian, A., Ohashi, P. S., and Mak, T. W. (1999) TNF receptor 1-dependent beta cell toxicity as an effector pathway in autoimmune diabetes. *J. Immunol.* **162**, 4598–4605.

150. Thebault-Baumont, K., Dubois-Laforgue, D., Krief, P., et al. (2003) Acceleration of type 1 diabetes mellitus in proinsulin 2-deficient NOD mice. *J. Clin. Invest.* **111**, 851–857.
151. Luhder, F., Chambers, C., Allison, J. P., Benoist, C., and Mathis, D. (2000) Pinpointing when T cell costimulatory receptor CTLA-4 must be engaged to dampen diabetogenic T cells. *Proc. Natl. Acad. Sci. USA* **97**, 12,204–12,209.
152. Serreze, D. V., Chapman, H. D., Varnum, D. S., et al. (1996) B lymphocytes are essential for the initiation of T cell-mediated autoimmune diabetes: analysis of a new “speed congenic” stock of NOD.Ig mu null mice. *J. Exp. Med.* **184**, 2049–2053.
153. Kagi, D., Odermatt, B., Ohashi, P. S., Zinkernagel, R. M., and Hengartner, H. (1996) Development of insulinitis without diabetes in transgenic mice lacking perforin-dependent cytotoxicity. *J. Exp. Med.* **183**, 2143–2152.



## Antigen-Based Therapy and Immune-Regulation in Experimental Autoimmune Encephalomyelitis

Mandy J. McGeachy, Richard O'Connor, Leigh A. Stephens, and Stephen M. Anderton

### Summary

Experimental autoimmune encephalomyelitis is a long-established mouse model of multiple sclerosis. The requirements for autoreactive T-cell activation in this disease have been characterized extensively and novel strategies for immune-intervention are being developed continually. Notably, identification of immunodominant T-cell epitopes allows the induction of T-cell tolerance with synthetic peptides. Several transgenic mouse lines that express transgenic T-cell receptors recognizing myelin autoantigenic epitopes have been developed. These allow adoptive transfer studies to analyse the activation of naïve autoreactive T cells *in vivo* during the induction of tolerance vs immunity. More recently, our attention has focused on immune mechanisms underlying the natural recovery from disease. Sampling of the lymphoid cell infiltrate within the central nervous system has identified the accumulation of regulatory T cells in the target organ during this period of resolution.

**Key Words:** T cells; autoimmunity; multiple sclerosis; tolerance; immunotherapy; regulation.

### 1. Introduction

Experimental autoimmune encephalomyelitis (EAE) is a commonly used immune-mediated disease characterized by inflammation and demyelination of the central nervous system (CNS) and, as such, serves as an animal model of multiple sclerosis (*1*). EAE can be induced in several species of laboratory animal (here, we shall focus on mouse models) by active immunization with autoantigens derived from CNS myelin, emulsified in complete Freund's adjuvant. The disease is essentially driven by the activation of autoreactive CD4<sup>+</sup> T lymphocytes, although pathology in the CNS is largely effected by activated macrophages. In some models there are clear pathogenic roles for



autoantibodies that target the myelin sheath (2) and for complement (3). The central role for CD4<sup>+</sup> cells is highlighted by the ability to passively transfer disease using recently activated cells (either established T-cell lines or clones, or derived from lymph nodes of previously immunized mice) (1). Because the antigenic epitopes recognized by the pathogenic T cells have been gradually defined, the disease can often now be induced fully using synthetic peptides of around 10 amino acids in length. Over the past 12 yr transgenic mice expressing T-cell receptors (TCR) that recognize defined myelin epitopes have been developed (4–7). The level of spontaneous disease in these transgenic mice varies, but they provide an invaluable source of unmanipulated naïve T cells for activation studies in vitro and in vivo.

EAE is amenable to many forms of therapeutic intervention. Particularly, because the antigenic epitopes have been defined, we can use the administration of peptide antigens to modify T-cell activation and provide protection against EAE (8). Here, we shall describe one such approach—the systemic administration of soluble peptides to establish T-cell tolerance (9). The exact nature of the tolerance produced can vary between models and laboratories and there is some debate over which might be most useful in treating human disease. We describe methods to elucidate the form of tolerance using in vitro analysis of T-cell numbers and function. We also describe the isolation of CNS infiltrating lymphoid cells, which is important for the study of both pathogenic and potentially immune-regulating populations in the target organ.

Combinations of these various protocols allow flexibility in dissecting immune-reactivity in EAE. For example, soluble peptides can be used to induce tolerance (**Subheading 3.7.**) before EAE induction (**Subheading 3.1.**). Subsequent in vitro analysis of antigen-induced T-cell proliferation (**Subheading 3.2.**) and cytokine production (**Subheading 3.4.**) can confirm unresponsiveness and may indicate deviation to an immunoregulatory phenotype (e.g., production of interleukin [IL-10] or transforming growth factor- $\beta$ ). Furthermore, it is possible to define which cells are proliferating (**Subheading 3.3.**). Transfer of congenic (e.g., CD45-disparate) TCR transgenic T cells (**Subheading 3.6.**) allows flow cytometric analysis (**Subheadings 3.9.** and **3.10.**) of myelin-reactive T-cell expansion under conditions of immunity or tolerance, and analysis of function by intracellular staining for cytokine production and expression of the “Treg-specific” transcription factor, Foxp3 (**Subheading 3.11.**). Isolation of infiltrating lymphoid populations from the CNS (**Subheading 3.8.**) allows analysis of T-cell phenotype within the target organ at different stages of disease, as well as their analysis using in vitro recall assays.

**Table 1**  
**Examples of Encephalitogenic Peptides From MBP, PLP, and MOG**

Strain (MHC-restriction) <sup>a</sup>	Peptide	Peptide sequence
SJL (I-A <sup>s</sup> )	PLP (139-151)	HCLGKWLGHDPDKF
	PLP (178-191)	NTWTTCQSIAPFSK
	MBP (89-101)	VHFFKNIVTPRTP
PL/J, B10.PL (I-A <sup>u</sup> )	MBP (Ac1-9)	Ac-ASQKRPSQR
C57BL/6 (I-A <sup>b</sup> , D <sup>b</sup> ) <sup>b</sup>	MOG (35-55)	MEVGWYRSPFSVVHLRNGK
NOD (I-A <sup>g7</sup> )	MOG (35-55)	MEVGWYRSPFSVVHLRNGK
Biozzi/ABH (I-A <sup>g7</sup> )	PLP (56-70)	DYEYLINVIHAFQYV
	MOG (8-22)	PGYPIRALVGDEQED
	MOG (35-55)	MEVGWYRSPFSVVHLRNGK
	MBP (12-26)	YLATASTMDHARHGF
DBA/1 (I-A <sup>q</sup> ) <sup>c</sup>	MOG (79-96)	GKVALRIONVRFSDHGGY

<sup>a</sup>All of these peptides induce major histocompatibility complex class II-restricted CD4<sup>+</sup> T-cell responses.

<sup>b</sup>MOG<sub>35-55</sub> is known induce an H-2A<sup>b</sup>-restricted CD4<sup>+</sup> response and an H-2D<sup>b</sup>-restricted CD8<sup>+</sup> response in C57BL/6 mice.

<sup>c</sup>MOG<sub>79-96</sub> induces both CD4<sup>+</sup> and CD8<sup>+</sup> responses in DBA/1 mice.

## 2. Materials

### 2.1. Active Induction of EAE by Immunization

1. Mice: EAE can be induced in various strains of mice (*see Table 1*). In general, mice can be maintained in conventional housing. Because infection can influence disease incidence/severity, it may be preferable to use a specific-pathogen free facility. Ideally mice should be 6–8 wk old at immunization, but we have used mice up to 16 wk old and obtained approx 100% incidence. In SJL/J mice, incidence is higher in females than males. In other strains this is not the case, but the use of females obviates problems caused by males fighting between and within litters.
2. Antigens: whole myelin preparations can be produced by isolation of spinal cords (*see Subheading 3.8.*) followed by homogenization and freeze-drying. More commonly synthetic peptide antigens are used (*see Table 1*). These may be prepared by standard Fmoc chemistry either in-house or from commercial suppliers. Complete Freund's adjuvant (CFA) is used for immunizations. This can be sourced as ready-made CFA containing 1mg/mL heat-killed mycobacteria (e.g., Sigma, Poole, UK). Suppliers also offer incomplete Freund's adjuvant (IFA, without mycobacteria) and heat-killed mycobacteria individually. This allows in-house production of CFA with varying concentrations of mycobacteria. *Mycobacterium tuberculosis* strain H37RA (Sigma) is the preparation of choice.
3. Pertussis toxin (PT) can also be obtained from several suppliers (e.g., the Health Protection Agency, UK, or List Biologicals, USA). Lyophilized PT is dissolved in

50% ddH<sub>2</sub>O/50% glycerol (v/v) at a concentration of 200 µg/mL. Store in 100-µL aliquots at -20°C.

4. Sonicator (e.g., Soniprep 150, with an exponential microprobe, MSE, Beckenham, UK).
5. Bijou tubes.
6. Disposable plastic 1- and 2.5-mL syringes, 25-gauge needles and 18-gauge blunt drawing-up needles (all from BD Plastipak, Oxford, UK).

## **2.2. In Vitro Analysis of Antigen-Induced T-Cell Proliferation by <sup>3</sup>H-Thymidine Incorporation**

1. Tissue culture medium: X-VIVO-15™ serum-free medium (BioWhittaker, Maidenhead, UK) supplemented with 2 mM L-glutamine and 5 × 10<sup>-5</sup> M 2-mercaptoethanol (both from Gibco, Invitrogen, Paisley, UK).
2. Wash medium: RPMI 1640 medium containing 25 mM HEPES buffer, supplemented with 2 mM L-glutamine, 100 U/mL penicillin, and 100 µg/mL streptomycin and 5 × 10<sup>-5</sup> M 2-mercaptoethanol (all from Gibco).
3. Filcotex nylon gauze (Sefar, Bury, UK), cut into approx 3-cm<sup>2</sup> pieces, autoclaved and kept sterile.
4. Red cell lysis buffer (Sigma, Poole, UK).
5. Peptides, as described in **Subheading 2.1**.
6. 96-Well flat-bottom microtiter plates and 15-mL falcon tubes (Corning Costar, Corning, NY), 90 mm diameter Petri-dishes (Scientific Lab Supplies, Nottingham, UK).
7. Tritiated thymidine (<sup>3</sup>H-TdR) (Amersham Biosciences, Amersham, UK) diluted in wash medium to give a specific activity of 0.5 µCi per 25 µL.
8. Glass fiber filter mats and MeltiLex scintillator sheets (both from Wallace, Turku, Finland).
9. Cell harvester (e.g., Harvester 96 Mk III, Tomtec, Hamden, UK) and a liquid scintillation counter (e.g., 1450 Microbeta Trilux, Wallac).

## **2.3. In Vitro Analysis of Antigen-Induced T-Cell Proliferation by CFSE-Dilution**

1. Carboxy-fluorescein diacetate succinimidyl ester (CFSE, Molecular Probes, Invitrogen, Paisley, UK) diluted to 50 µM in dimethyl sulfoxide (DMSO). Store in aliquots in the dark at -20°C.
2. Appropriate T cell-specific monoclonal antibodies (MAb), fluorescently labeled with fluorochromes other than FITC.
3. Wash medium (*see Subheading 2.2.*), supplemented with 5% heat-inactivated (56°C, 30 min) fetal calf serum (HI-FCS, Sigma).
4. FACS buffer: PBS, 2% HI-FCS, 0.05% (w/v) sodium azide.

## **2.4. In Vitro Analysis of Antigen-Induced Cytokine Production by ELISA**

1. Materials and reagents as described in **Subheading 2.2.**, items 1–6.
2. Maxisorb ELISA plates (Nalge Nunc, Hereford, UK).

3. Anti-cytokine capture MAb, biotinylated detection MAb and recombinant cytokine standards (all from BD Pharmingen, Oxford, UK).
4. Extravidin-horseradish peroxidase (Sigma).
5. Wash buffers: PBS; PBS, 0.1% Tween-20 (Sigma); PBS, 1% bovine serum albumin (BSA, Sigma).
6. Bicarbonate buffer: 15 mM Na<sub>2</sub>CO<sub>3</sub>, 35 mM NaHCO<sub>3</sub>, pH 9.6.
7. Phosphate-citrate buffer: 50 mM Na<sub>2</sub>HPO<sub>4</sub>, 25 mM anhydrous citric acid, pH 5.0.
8. Tetramethyl benzidine (TMB), diluted to 10 mg/mL in DMSO and stored in aliquots at -20°C.
9. Peroxidase substrate: 100 µL TMB, 9.9 mL phosphate-citrate buffer, 3 µL H<sub>2</sub>O<sub>2</sub> (Sigma).
10. 2 M H<sub>2</sub>SO<sub>4</sub>.
11. ELISA plate reader.

### 2.5. Passive Induction of EAE by Transfer of Activated T Cells

1. Dulbecco's PBS (Gibco), CFA (Sigma), peptide antigen (*see Subheading 2.1.*). 1- and 2.5-mL syringes and 25-gauge needles.
2. Wash medium: RPMI 1640 medium, supplemented as described in **Subheading 2.2., item 1.**
3. Tissue culture medium: wash medium supplemented with 10% HI-FCS.
4. Recombinant IL-2, -12, and -18 (all from R&D systems, Abingdon, UK).
5. 24- or 6-Well tissue culture plates (Corning Costar).

### 2.6. Transfer of TCR Transgenic T Cells

1. Cold buffer: RPMI 1640, or PBS containing 2% HI-FCS (*see Note 1*).
2. Depleting MAb cocktail: MAb to cell surface markers not expressed on the cell type of interest are mixed in buffer, each at a final concentration of 10 µg/mL. For mouse CD4<sup>+</sup> T-cell enrichment, MAb to CD8, B220, Mac-1 and MHC class II result in CD4<sup>+</sup> T-cell purity of 70–95%, depending on the mouse strain and source of cells (*see Note 2*).
3. Dynabeads: sheep anti-rat IgG M450 magnetic beads (Dynal Biotech, Wirral, UK).
4. Magnet for cell separation (e.g., MPC-1, Dynal Biotech).

### 2.7. Systemic Administration of Soluble Peptide Antigens

1. Synthetic peptides are obtained as in **Subheading 2.1.**
2. Endotoxin-free PBS (Gibco) is used as diluent.

### 2.8. Isolation of CNS-Infiltrating Lymphoid Populations

1. Wash medium (*see Subheading 2.2., item 2*).
2. Bovine collagenase (Worthington Biochemicals) diluted to 8 mg/mL in wash buffer. Store at -20°C.
3. Deoxyribonuclease (Sigma) diluted to 10 mg/mL in wash buffer. Store at -20°C.
4. Percoll (Gibco) solutions are freshly prepared at 30 and 70% (v/v) in wash buffer.

## **2.9. Phenotypic Analysis of T Cells in Lymphoid Populations by Flow Cytometry**

1. FACS buffer: PBS, 2% HI-FCS +/- 0.05% (w/v) sodium azide (*see Note 3*).
2. FACS tubes (BD Plastipak).
3. Fluorescently labeled MAb.
4. Flow cytometer.

## **2.10. Intracellular Staining for Cytokines and the Foxp3 Transcription Factor**

1. Phorbol myristate acetate (PMA) and ionomycin (both Sigma) prepared individually at 1 mg/mL in ethanol and stored at  $-20^{\circ}\text{C}$ . Make 100X stocks (5  $\mu\text{g}/\text{mL}$  for PMA, 100  $\mu\text{g}/\text{mL}$  for ionomycin) in wash buffer (*see Subheading 2.2.*) and store at  $-20^{\circ}\text{C}$ . The final working concentrations are 50 ng/mL PMA and 1  $\mu\text{g}/\text{mL}$  ionomycin, made freshly from these 100X stocks.
2. Golgistop (BD Pharmingen).
3. 2% Paraformaldehyde prepared by the following protocol: add 2 g of paraformaldehyde to 50 mL ddH<sub>2</sub>O and heat to  $60^{\circ}\text{C}$  for 15 min. Add a few drops of 1 M NaOH to clear the solution. Add 10 mL 10X PBS and 30 mL ddH<sub>2</sub>O. Adjust the pH to 7.4 and make up to final volume 100 mL. Store in the dark at  $4^{\circ}\text{C}$ . Dilute 1:1 with PBS or FACS buffer for fixing cells.
4. Permash buffer: 0.1% Saponin (Sigma) in FACS buffer. Store at  $4^{\circ}\text{C}$  for up to 1 wk (*see Note 4*).

## **3. Methods**

### **3.1. Active Induction of EAE by Immunization**

The precise immunization protocols used to induce EAE vary between laboratories and between models. Here, we describe the protocol we have recently used successfully to induce EAE with the MOG<sub>35-55</sub> peptide in C57Bl/6 mice and the MBP<sub>Ac1-9</sub> peptide in B10.PL mice. Group sizes of five or six are usually sufficient to reach statistical significance.

1. Peptide is diluted to a concentration of 2 mg/mL in PBS. CFA (1 mg mycobacteria/mL) is added (taking care to fully resuspend the heat-killed mycobacteria first) to produce a 1:1 mixture. A total volume of between 1 and 4 mL can be prepared in a single bijou tube. Greater volumes are best divided equally in two or more bijou (*see Note 5*). The mixture is vortexed and sonicated (set amplitude at 10  $\mu$ ) with three or four 5-s pulses moving the sonicator probe throughout the mixture. A good emulsion allows the bijou to be inverted without the mixture running down the side of the tube. Over-heating the mixture must be avoided. Therefore, having the sonicator within a cold-room is helpful. Otherwise the bijou should be plunged into ice for at least 10 s between sonicating bursts.
2. The emulsion is drawn into plastic 1-mL syringes using blunt 18-gauge drawing-up needles. Air is removed by vigorous tapping of the syringe, with the needle end

- upward. Care must be taken at this stage to prevent the emulsion splashing during tapping. Eye protection and gloves must be worn. A final volume of 500–600  $\mu\text{L}$  per syringe is best. The drawing-up needle is replaced with a 25-gauge needle.
3. Mice are immunized by injection of 50  $\mu\text{L}$  of emulsion subcutaneously into each hind leg. This gives an immunization dose of 100  $\mu\text{g}$  peptide and 50  $\mu\text{g}$  mycobacteria per mouse. Again, eye protection must be worn at this stage.
  4. PT (200 ng diluted in 500  $\mu\text{L}$  PBS) is given intraperitoneally (ip) on the same day and 2 d later.
  5. Clinical signs of EAE are assessed daily using the following scoring index: 0, no signs; 1, flaccid tail; 2, impaired righting reflex and/or impaired gate; 3, partial hind leg paralysis; 4, total hind leg paralysis; 5, hind and fore leg paralysis; 6, moribund or dead. Any cage with one or two mice of score 2 or more should be supplemented with hydrated food on the floor of the cage in a Petri dish. Any mouse with a score of 5 for two consecutive days should be culled. Typically disease develops after 7–10 d. Mice have usually recovered by around 30 d. In some strains, continued monitoring may identify relapses. Disease profiles are routinely displayed as mean EAE score for each group on each day. Differences between groups are determined using Fisher's exact test for disease incidence and the Mann-Whitney U test for total disease burden.
  6. EAE can be reinduced by immunization as described above, but using IFA instead of CFA (a second dose of CFA can cause severe granuloma formation and ulceration) and injecting into two sites on the flanks.

### **3.2. In Vitro Analysis of Antigen-Induced T-Cell Proliferation by $^3\text{H}$ -TdR Incorporation**

1. Mice are sacrificed and the draining lymph nodes removed (the inguinal and para-aortic nodes drain the site of immunization for EAE induction) into bijoux tubes containing 2 mL of wash medium. The spleen can also be sampled.
2. In a class 2 biological safety cabinet, samples are placed between two pieces of nylon gauze in a Petri dish and are disrupted using two pairs of small angled forceps. Wash buffer (5 mL) is added and any cell clumps are further disrupted by pipetting up and down with a Gilson P1000. The cell suspension is transferred to a 15-mL falcon tube and washed by centrifugation (400g for 5 min at room temperature). The supernatant is discarded prior to resuspension of the cell pellet. At this point spleen samples should be depleted of erythrocytes by incubating the pellet at room temperature with 2 mL of red cell lysis buffer for 2 min with gentle agitation by hand. Lysis is stopped by adding 10 mL of wash buffer. Cells are centrifuged as listed above and washed a further twice in wash buffer.
3. After the final wash, cells are resuspended in tissue culture medium, counted (using trypan blue exclusion to assess viability) and adjusted to  $6 \times 10^6/\text{mL}$  (for lymph node samples), or  $8 \times 10^6/\text{mL}$  (for spleen samples).
4. Serial dilutions of peptide antigen are prepared in tissue culture medium, at concentrations that are twice the desired final doses for the assay. One hundred microliters of each dose is added to a 96-well plate in triplicate. One hundred microliters

of cell sample is then added to each well. This gives the desired final peptide concentration (i.e., a twofold dilution of the original serial dilutions) and  $6 \times 10^5$  lymph node cells or  $8 \times 10^5$  spleen cells per well.

5. Cultures are incubated at 37°C in 5% CO<sub>2</sub> and 95% humidity. After 48 h, 25 µL (0.5 µCi) <sup>3</sup>H-TdR is added before culture for a further 18–24 h. Cultures are then harvested onto filter mats and thymidine incorporation is determined using a liquid scintillation β-counter.

### **3.3. In Vitro Analysis of Antigen-Induced T-Cell Proliferation by CFSE-Dilution**

This protocol provides a means to determine division of cells expressing a particular marker of interest (e.g., CD4 vs CD8, or a congenic CD45 or CD90 marker) using flow cytometry. Cells are loaded with CFSE *ex vivo*. As they divide, the dye is distributed equally into the two daughter cells, which therefore have half the fluorescence intensity. Both the number of cells entering mitosis and the number of divisions (up to nine) can be assessed.

1. Lymph node and/or spleen cells are prepared as described in **Subheading 3.2., steps 1 and 2**. Cells are resuspended at  $0.1\text{--}1 \times 10^7/\text{mL}$  in wash medium containing 5% HI-FCS.
2. CFSE is added at a final concentration of 5 µM and the cells are mixed quickly and thoroughly, then incubated for 5–10 min at room temperature. Cells are washed three times (400g, 5 min) with cold wash medium (*see Note 6*).
3. After the final wash, the pellet is resuspended in tissue culture medium, counted and adjusted to  $6 \times 10^6/\text{mL}$  (lymph node samples), or  $8 \times 10^6$  (spleen samples). Cells are cultured with an appropriate dose of peptide, or medium alone, for 48–72 h as described in **Subheading 3.2., step 4**.
4. Cells are resuspended, washed twice in FACS buffer, and incubated for 20–30 min on ice with the appropriate dilution of MAb directed against the chosen marker. If possible, this MAb should be conjugated with a fluorophore other than phycoerythrin (e.g., allophycocyanin). This avoids problems with fluorescence compensation as CFSE staining can be very bright and leaks into the FL2 channel. Alternatively, a two-step staining protocol can be used by incubation with a biotinylated MAb, followed by allophycocyanin-conjugated streptavidin. Cells are washed twice with FACS buffer and resuspended in PBS prior to analysis on a flow cytometer.
5. The cell population of interest is gated and CFSE staining of samples from culture with and without peptide is compared. The use of FlowJo™ software (TreeStar Inc., CA) allows accurate analysis of cell divisions.

### **3.4. In Vitro Analysis of Antigen-Induced Cytokine Production by ELISA**

1. Lymph node and/or spleen cultures are set up with peptide as described in **Subheading 3.2., steps 1–4**.
2. After 24 h, ELISA plates are coated with the relevant anticytokine capture MAb diluted as per the manufacturer's instructions in bicarbonate buffer (50 µL per well)

**Table 2**  
**Final Concentrations of Reagents Used in Cytokine ELISA**

Cytokine	Capture antibody	Detection antibody	Top concentration of recombinant cytokine for standard curve
IL-2, IL-4	2 $\mu\text{g/mL}$	0.5 $\mu\text{g/mL}$	5 ng/mL
IL-10, IFN $\gamma$	2 $\mu\text{g/mL}$	0.5 $\mu\text{g/mL}$	100 ng/mL
TNF $\alpha$	8 $\mu\text{g/mL}$	0.5 $\mu\text{g/mL}$	100 ng/mL

All reagents are from BD Pharmingen.

(see **Table 2**) allowing enough wells for samples from each culture well and 24 extra wells (these represent 4 blank wells and a 10-point, twofold serial dilution of the cytokine standard, in duplicate). Plates are incubated overnight at 4°C.

3. ELISA plates are washed twice with PBS/0.1% Tween-20, blocked for 1 h at 37°C with PBS/1% BSA, and then washed twice with PBS/0.1% and twice with PBS.
4. A standard curve is set up with twofold serial dilutions of the cytokine standard in PBS/1% BSA (100  $\mu\text{L}$  per well) (see **Table 2**). One hundred microliters of culture supernatant is transferred from each of the culture wells to the corresponding well on the ELISA plate and incubated for 2 h at room temperature.
5. Supernatants are discarded and the ELISA plates are washed four times with PBS/0.1% Tween-20. The appropriate biotinylated detection MAb is added at 100  $\mu\text{L}$  per well of in PBS/1% BSA (see **Table 2**) and incubated at room temperature for 1 h.
6. Plates are washed six times with PBS/0.1% Tween-20. Extravidin-HRP (100  $\mu\text{L}$  per well) is added in PBS/1% BSA and incubated at room temperature for 30 min.
7. Plates are washed six times with PBS/0.1% Tween-20 and 100  $\mu\text{L}$  of substrate is then added per well. As color develops the reaction is stopped with 100  $\mu\text{L}$  of 2 M  $\text{H}_2\text{SO}_4$ . Plates are read immediately at 450 nm.

### 3.5. Passive Induction of EAE by Transfer of Activated T Cells

1. Donor mice are immunized as described in **Subheading 3.1., steps 1–3** (without PT).
2. Seven to ten days later, draining (inguinal and para-aortic) lymph nodes are removed and single cell suspensions prepared as described in **Subheading 3.2., steps 1 and 2**. Cells are resuspended at  $1 \times 10^7/\text{mL}$  in tissue culture medium.
3. Tissue culture medium containing 20  $\mu\text{g/mL}$  of the immunizing peptide, together with IL-12 and IL-18 (both at 50 ng/mL) and IL-2 (20 U/mL) is mixed 1:1 with the cell suspension (to achieve final culture conditions of  $5 \times 10^6$  cells/mL, 10  $\mu\text{g/mL}$  peptide, 25 ng/mL IL-12, 25 ng/mL IL-18, and 10 U/mL IL-2).
4. Cells are cultured in 24-well (2 mL/well) or 6-well (5 mL/well) plates at 37°C, 5%  $\text{CO}_2$ .



5. After 48 h, each well is split and supplemented with an equal volume of fresh tissue culture medium containing 40 U/mL IL-2 (to achieve a final concentration of 20 U/mL IL-2).
6. After 72 h of total culture time, cells are harvested by repeated flushing of the wells with sterile Pasteur pipets and centrifuged (400g for 5 min at 4°C).
7. Cells are resuspended in serum free PBS and the number of viable cells determined by trypan blue exclusion, noting the number of blasting cells.
8. Cells are washed and resuspended in serum free PBS at a density of  $5 \times 10^6$  blasts per 200  $\mu$ L.
9. Two hundred microliters of the donor cell suspension is injected intravenously (i.v.) via the lateral tail vein to each host mouse. On the same day as cell transfer, each host mouse is also given 200 ng of PT (in 500  $\mu$ L of sterile PBS) by i.p. injection.

### 3.6. Transfer of TCR Transgenic T Cells

There are several methods for the purification of naïve T cells from TCR transgenic mice for transfer into recipient mice. The method of choice will be a compromise between the required yield and the purity of the cell population of interest, as well as whether time or cost is the more important consideration. Here, we describe the method for negative selection of CD4<sup>+</sup> T cells using Dynabeads which, in our hands, is relatively cost-effective and provides good yields.

1. Single cell suspensions are prepared from pooled spleen and lymph nodes of TCR transgenic mice as described in **Subheading 3.2., steps 1 and 2** (we routinely take cervical, axillary, brachial, inguinal, mesenteric, and iliac nodes).
2. Cells are resuspended in the depleting MAb cocktail of choice at a concentration of  $2 \times 10^8$  cells/mL and incubated for 20–30 min on ice. Cells are washed twice and resuspended at  $10^8$  cells/mL in buffer.
3. An equal number of sheep anti-rat Dynabeads are washed twice (by placing a tube containing the beads on a magnet and aspirating the supernatant) and then resuspended at  $10^8$  beads/mL (*see Note 7*).
4. Cells and beads are then mixed together in a round-bottomed tube and rotated on a wheel at 4°C for 20–30 min.
5. Unbound cells are recovered by aspirating the supernatant after 2 min on the magnet. For better purity, cells are placed on the magnet a second time and unbound cells again recovered.
6. The purity of cells can be checked by staining a small aliquot of cells for flow cytometric analysis using MAb to CD4 and to rat IgG. If MAb-labeled cells remain, a second round of depletion with more beads can be performed.
7. Enriched CD4<sup>+</sup> T cells are counted, spun down, and resuspended in serum-free PBS at the required concentration for i.v. injection into the tail vein of mice (200  $\mu$ L per mouse following brief exposure of mice to an infrared heat lamp).

### 3.7. Systemic Administration of Soluble Peptide Antigens

Antigen-specific T-cell tolerance can be induced by giving peptides containing immunodominant myelin epitopes in soluble form (in PBS) (*see Note 8*). This can be achieved reliably using the i.v., i.p., or intranasal routes. Giving peptides orally can induce tolerance but does not provide a reliable route for all peptides. We routinely use the i.p and i.v. routes.

1. i.p. route: peptide is given in 500  $\mu$ L PBS using a 2.5-mL syringe and a 25-gauge needle, either as a single dose of 100–500  $\mu$ g 7 d before immunization, or as three doses of 100–200  $\mu$ g, given 8, 6, and 4 d before immunization.
2. i.v. route: peptide (20–500  $\mu$ g per mouse) is injected into a tail vein in a volume of 200  $\mu$ L of PBS using a 1-mL syringe and a 27-gauge needle. Mice are warmed briefly (~2 min) using a heating lamp before injection. Pressure with a tissue is applied for several seconds after injection to limit blood loss.

### 3.8. Isolation of CNS-Infiltrating Lymphoid Populations

1. Mice are sacrificed by CO<sub>2</sub> asphyxiation. Immediately after death the lower vena cava is cut and the mice are perfused with 10–20 mL of PBS injected by 20-mL syringe and 25-gauge needle through the left ventricle of the heart. Completeness of perfusion is assessed by the color of the liver (which turns pale) and also the clearness of the injected PBS.
2. Spinal cords are removed by intrathecal hydrostatic pressure: after making incisions through the spinal column at the neck and lumbosacral area, cold PBS is injected with a 20-mL syringe and 19-gauge needle into the caudal vertebral column. Brains are removed by dissection. Single cords/brains are placed into a bijoux containing 1 mL wash buffer (*see Note 9*).
3. Cords and brains are cut into small pieces with scissors in the bijoux. Five hundred microliters of collagenase stock and 100  $\mu$ L of DNase stock is then added to each bijoux and the tissue is incubated in a 37°C water bath for 30 min.
4. After digestion, mechanical disaggregation is used to obtain a single cell suspension (by mashing through nylon gauze or by pipetting as described in **Subheading 3.2.**).
5. Cells are centrifuged (500g for 5 min) then resuspended in 4–5 mL 30% percoll solution in a 15-mL Falcon tube. This is overlaid with 2 mL of 70% percoll solution and the gradients are centrifuged at 850g for 20 min without braking.
6. The gradient interface is harvested and cells washed thoroughly in wash buffer before further analysis. The first wash should be performed at 680g for 10 min, subsequent washes are at 400g for 5 min.

### 3.9. Phenotypic Analysis of T Cells in Lymphoid Populations by Flow Cytometry

With modern flow cytometers it is generally possible to stain cells with between three and six different fluorescently labeled antibodies at the same

time. Congenic markers with allelic differences between stains, such as CD45.1/2 and CD90.1/2, are useful in distinguishing donor cells from host cells after transfer of defined cell populations to CD45/CD90-disparate recipients.

1. Single cell suspensions are obtained, as described in **Subheading 3.2**. The required number of cells is added to FACS tubes and spun at 400g for 5 min at 4°C. The supernatant is aspirated and the cells resuspended by gently flicking the tubes (*see Note 10*).
2. Fifty microliters of appropriately diluted fluorescent MAb, or isotype control antibodies are added in cold FACS buffer and incubated on ice for approx 20 min (*see Note 11*).
3. The cells are washed twice by addition of approx 2 mL FACS buffer and centrifugation.
4. The cells are resuspended in 200–400 µL FACS buffer and kept on ice until analysis on the flow cytometer (*see Notes 12–14*).

### **3.10. Indirect Staining of Cell Surface Molecules**

1. Cells are stained first with unconjugated (or biotinylated) MAb and washed.
2. The cells are then incubated with a fluorescently labeled detection MAb (or streptavidin).
3. Cells need to be blocked for 20 min on ice with 2% serum of the species in which the primary MAb was raised to ensure all binding sites of the detection MAb are blocked, before addition of the rest of the fluorescently labeled MAb.

### **3.11. Intracellular Staining for Cytokines and the Foxp3 Transcription Factor**

1. Single cell suspensions are prepared in tissue culture medium and added to 24-well plates at  $2\text{--}5 \times 10^6$  cells per well in 900 µL.
2. To each well, 100 µL of culture medium containing 500 ng/mL of PMA, 10 µg/mL of ionomycin, and 10 µL/mL of golgistop is added. The cells are stimulated for 4 h at 37°C.
3. The cells are harvested and first stained for extracellular surface markers as described in **Subheading 3.9**. (as most epitopes recognized by MAb to lymphocyte cell surface molecules are destroyed during subsequent fixation).
4. The cells are then fixed by adding 1% paraformaldehyde at 4°C for 20 min, or can be left overnight at 4°C, in the dark.
5. The cells are permeabilized by washing (400g for 5 min at 4°C) in permwash and incubated for 5 min in permwash, while preparing the MAb (*see Note 15*).
6. After spinning down, the cells are resuspended in 50 µL of MAb cocktail (for example anti-IFNγ-FITC and anti-IL-10-phycoerythrin), each at 2 µg/mL in permwash buffer, and incubated at 4°C in the dark for 30–40 min (*see Note 16*).
7. Cells are washed once in 2 mL permwash and then resuspended in PBS for FACS analysis.

#### 4. Notes

1. It helps to include HEPES in the buffer to maintain the pH. If cell clumping is a problem, it can help to add EDTA, and if cell survival is an issue, the addition of extra glucose can be helpful.
2. Addition of extra MAb whose target antigen is not expressed on the cell type of interest, e.g., NK1.1, can result in even greater cell purity.
3. It is important to ensure that cells and buffers are kept cold to avoid capping/internalization of MAb, and that fluorescent labels are protected from light as much as possible to avoid degradation of the fluorescent signal.
4. An alternative to making paraformaldehyde and permwash is to purchase the Cytotfix/Cytoperm kit from BD Pharmingen.
5. When making an emulsion with Freund's adjuvants, it is important to remember that the volume reduces considerably and there is also loss within the tube. Allow for a total loss of 50% (i.e., if 100  $\mu$ L for each of five mice is required, start with an antigen/adjuvant mix that totals at least 1 mL before sonication).
6. It is important to mix the CFSE quickly after adding to ensure uniform labeling of cells.
7. The optimum bead:cell ratio needs to be determined empirically. If more than one round of depletion with beads is performed then less beads are generally needed overall.
8. It is important that the peptides are entirely soluble for the induction of tolerance. The use of insoluble peptides can (1) lead to productive immune responses, or (2) create problems with vascular blockage if given by the i.v. route.
9. Attempting to combine several cords in one tube can result in lower yields—one to two cords and one brain per tube is optimal.
10. We routinely stain  $0.5\text{--}1 \times 10^6$  cells. More cells can be stained if the cells of interest are a minority population, and less cells if there are insufficient cells in the sample. If the number of cells per tube varies from the standard, it may be necessary to add either an increased volume or concentration of MAb to ensure it is saturating.
11. The appropriate concentration of MAb should be determined empirically by careful titration using a fixed volume and number of cells. As a guide, for the standard protocol previously listed, saturating doses of antibody are usually reached with antibody concentrations between 0.5 and 5  $\mu$ g/mL.
12. If nonspecific binding of MAb via Fc receptors is a problem in the cell type of interest, Fc receptors can be blocked by preincubation of cells before staining with either an antibody to Fc receptors (e.g., 2G4.2), or 1–2% normal mouse serum (or alternatively the same concentration of serum from the species in which the MAb is made).
13. Staining for flow cytometric analysis can be performed in 96-well plates if there are many samples. In this case, cells are washed more times in a smaller volume (e.g., three washes in 200  $\mu$ L). It can be helpful to leave spaces between wells to avoid cross-contamination of cells.

14. Dead cells can be excluded in unfixed samples by the addition of PI (FL2/3) or DAPI (if an ultraviolet laser is available) immediately before acquisition, if desired.
15. Cells can be fixed and permeabilized by resuspension in 250  $\mu$ L of a commercially available Fix/Perm buffer (e.g., BD Pharmingen, eBiosciences) to resuspended cell pellets followed by incubation for 20 min, or overnight in the fridge.
16. Cells can be preincubated with 2% serum from the species in which the MAb is made to block nonspecific binding.

## Acknowledgments

Work in the authors' lab is supported by the Medical Research Council (UK), the Wellcome Trust and the Multiple Sclerosis Society (UK). S.M.A. is an MRC Senior Research Fellow.

## References

1. Martin, R. and McFarland, H. F. (1995) Immunological aspects of experimental allergic encephalomyelitis and multiple sclerosis. *Crit. Rev. Clin. Lab. Sci.* **32**, 121–182.
2. Litztenburger, T., Fassler, R., Bauer, J., et al. (1998) B lymphocytes producing demyelinating autoantibodies: development and function in gene-targeted transgenic mice. *J. Exp. Med.* **188**, 169–180.
3. Calida, D. M., Constantinescu, C., Purev, E., et al. (2001) Cutting edge: C3, a key component of complement activation, is not required for the development of myelin oligodendrocyte glycoprotein peptide-induced experimental autoimmune encephalomyelitis in mice. *J. Immunol.* **166**, 723–726.
4. Goverman, J., Woods, A., Larson, L., Weiner, L. P., Hood, L., and Zaller, D. M. (1993) Transgenic mice that express a myelin basic protein-specific T cell receptor develop spontaneous autoimmunity. *Cell* **72**, 551–560.
5. Lafaille, J. J., Nagashima, K., Katsuki, M., and Tonegawa, S. (1994) High incidence of spontaneous autoimmune encephalomyelitis in immunodeficient anti-myelin basic protein T cell receptor transgenic mice. *Cell* **78**, 399–408.
6. Liu, G. Y., Fairchild, P. J., Smith, R. M., Prowle, J. R., Kioussis, D., and Wraith, D. C. (1995) Low avidity recognition of self-antigen by T cells permits escape from central tolerance. *Immunity* **3**, 407–415.
7. Waldner, H., Whitters, M. J., Sobel, R. A., Collins, M., and Kuchroo, V. K. (2000) Fulminant spontaneous autoimmunity of the central nervous system in mice transgenic for the myelin proteolipid protein-specific T cell receptor. *Proc. Natl. Acad. Sci. USA* **97**, 3412–3417.
8. Anderton, S., Anderton, S., Burkhart, C., Metzler, B., and Wraith, D. (1999) Mechanisms of central and peripheral T-cell tolerance: lessons from experimental models of multiple sclerosis. *Immunol. Rev.* **169**, 123–137.
9. Anderton, S. M. (2001) Peptide-based immunotherapy of autoimmunity: a path of puzzles, paradoxes and possibilities. *Immunol.* **104**, 367–376.

## Induction and Regulation of Inflammatory Bowel Disease in Immunodeficient Mice by Distinct CD4<sup>+</sup> T-Cell Subsets

Kevin J. Maloy

### Summary

Although the etiology of human inflammatory bowel disease (IBD) has not yet been completely defined, the current prevailing hypothesis is that it is caused by aberrant immune responses, or loss of tolerance, toward components of the intestinal bacterial microflora. During the past decade, several animal models of IBD have been developed that reproduce many features of the human disease. This article will outline one of the best characterized murine IBD models, the “T-cell transfer model” where colitis rapidly develops following adoptive transfer of naïve CD4<sup>+</sup>CD45RB<sup>high</sup> T cells into immunodeficient *scid* or RAG<sup>-/-</sup> mice. This model has also been instrumental in characterizing the potent suppressive activities of CD4<sup>+</sup>CD25<sup>+</sup> regulatory T cells that prevent the development of IBD when cotransferred with the naïve CD4<sup>+</sup> T cells. The T cell transfer model of IBD is reproducible and easily manipulated and therefore provides an excellent system for the study of immunopathology and immune regulation in the intestine.

**Key Words:** Colitis; inflammatory bowel disease; regulatory T cells; mucosal immunology; cell sorting.

### 1. Introduction

Human inflammatory bowel diseases (IBD), encompassing Crohn’s disease (CD) and ulcerative colitis (UC), are chronic debilitating conditions of poorly defined etiology for which there is no current cure (1). Over the past 10 yr our understanding of the immunopathogenesis of IBD has been greatly advanced by the development of a number of animal models that exhibit many of the features of human IBD. The critical role of the immune system in maintaining intestinal homeostasis was illustrated by the spontaneous development of severe colitis in transgenic mice harboring immune defects that affected T cell function, such as TCR $\alpha$ <sup>-/-</sup>, IL-10<sup>-/-</sup>, or IL-2<sup>-/-</sup> mice (reviewed in refs. 2 and 3).

From: *Methods in Molecular Biology*, vol. 380: *Immunological Tolerance: Methods and Protocols*  
Edited by: P. J. Fairchild © Humana Press Inc., Totowa, NJ

Although useful, these spontaneous IBD models had several limitations, firstly that both the incidence and kinetics of disease were variable, often taking 3–4 mo to develop, and second, colitis was highly dependent on the bacterial microflora, often disappearing when the animals were housed under specific-pathogen-free (SPF) conditions (2,3).

The T-cell transfer model of IBD was pioneered by Powrie and colleagues, who observed that reconstitution of immune deficient C.B-17 *scid* mice with naïve CD4<sup>+</sup>CD45RB<sup>high</sup> T cells isolated from normal BALB/c mice led to the development of colitis (4). This intestinal inflammation exhibited many of the same histopathological characteristics as human IBD, including extensive leukocyte infiltration, pronounced epithelial hyperplasia, depletion of mucin-secreting goblet cells, and ulceration. Disease is driven by the differentiation and expansion of pathogenic CD4<sup>+</sup> T cells that appear to react toward components of the normal intestinal commensal flora (5,6). The T-cell transfer model of IBD has several advantages over the spontaneous models, including rapid onset, high reproducibility under SPF-conditions, well-defined kinetics and the ability to follow disease development by analyzing several parameters of gross pathology. Furthermore, as an induced model of IBD, it is readily amenable to experimental manipulation. One key finding using this model was that the reciprocal population of CD4<sup>+</sup>CD45RB<sup>low</sup> T cells from normal mice did not elicit colitis following adoptive transfer into immune deficient mice and, in fact, even suppressed the development of disease in immune deficient mice that also received pathogenic CD4<sup>+</sup>CD45RB<sup>high</sup> T cells (4). Further experiments demonstrated that this suppressive activity was present mainly within the CD4<sup>+</sup>CD25<sup>+</sup> T cell population, which, together with parallel studies by other investigators, indicated that CD25<sup>+</sup> regulatory T cells (Treg) play a crucial role in the maintenance of self-tolerance and regulation of harmful inflammatory responses (7–10).

The basis of this model is the purification of distinct subsets of CD4<sup>+</sup> T cells from normal mice that either induce IBD (CD4<sup>+</sup>CD45RB<sup>high</sup> T cells) or prevent disease (CD25<sup>+</sup> Treg cells) after adoptive transfer into immune deficient recipient mice. As outlined in Fig. 1, the model can be broken down into several steps as follows: enrichment of CD4<sup>+</sup> T cells by negative selection; labeling with fluorescent antibodies and isolation of distinct subsets by FACS sorting; induction or prevention of IBD by adoptive transfer of purified CD4<sup>+</sup> T cell subsets into immune deficient hosts; monitoring and analysis of IBD.

## 2. Materials

### 2.1. Mice

SPF wild type mice are used as CD4<sup>+</sup> T cell donors and syngeneic, immune deficient mice used as recipients. Although this model was originally described using BALB/c donors and C.B-17 *scid* recipients, it also works well on most other genetic backgrounds including the C57Bl/6 strain (see Note 1).

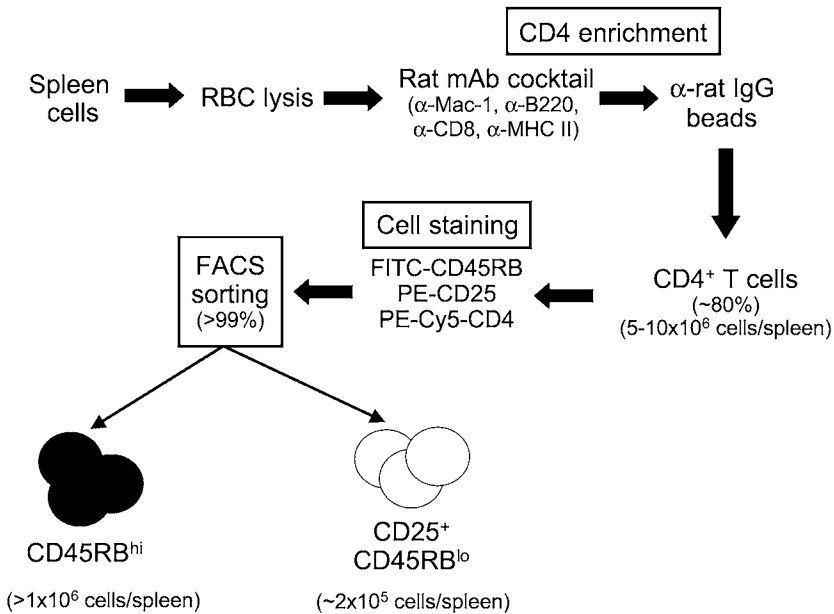


Fig. 1. Overview of CD4<sup>+</sup> T-cell subset isolation procedure. Estimated yields at each step are also indicated.

Maintenance of donor and recipient mice under SPF-conditions is extremely important, as pathogenic organisms or changes in commensal flora can significantly alter the results obtained (*see Notes 2 and 3*).

## 2.2. Reagents and Solutions

Unless otherwise stated, all solutions should be sterilized by filtration and can be kept for up to 2 mo at 4°C.

1. FACS buffer (FB): HBSS, 0.1% BSA, 2 mM EDTA.
2. 100-mm Disposable Petri dishes.
3. 5-mL Disposable syringes.
4. 50-mL Polypropylene conical tubes.
5. Erythrocyte lysis (ACK) buffer: 0.15 M NH<sub>4</sub>Cl, 10 mM KHCO<sub>3</sub>, 0.1 mM Na<sub>2</sub>EDTA, pH to 7.2 with 1 M HCl.
6. Cell strainers: 100-μm nylon (BD Biosciences).
7. 14-mL Polystyrene round-bottom tubes.
8. Trypan blue solution: 0.2% (w/v) Trypan blue in PBS.
9. CD4 enrichment antibody mix, containing all of the following at a final concentration of 10 μg/mL in FB (*see Note 4*):
  - a. Rat anti-mouse B220 (RA3-6B2).
  - b. Rat anti-mouse CD8 (YTS 169).
  - c. Rat anti-mouse CD11b (Mac-1, M1/70).
  - d. Rat anti-mouse MHC II (TIB120).



10. Goat anti-rat IgG magnetic beads (Dynabeads, Dynal Biotech) and appropriate magnet (MPC-1, Dynal Biotech).
11. Fluorescent antibodies—all from BD Biosciences Pharmingen: FITC-conjugated anti-mouse CD45RB (clone 16A), PE-conjugated anti-mouse CD25 (clone 7D4), PE-Cy5-conjugated anti-mouse CD4 (clone H129.19) (*see Note 5*).
12. 5-mL Polystyrene round-bottom tubes (for FACS).
13. Heat-inactivated fetal calf serum (FCS).
14. 1-mL Disposable syringes.
15. Electronic balance for weighing mice.
16. Dissecting instruments: scissors, forceps, and scalpel.
17. Formal saline: PBS containing 3.6% (v/v) formaldehyde. No need to filter.

### 3. Methods

#### 3.1. Prepare Single Cell Suspension

1. Remove spleens from normal mice into FACS buffer (FB). The number required will depend on the desired number of purified CD4<sup>+</sup> T cells. Ten spleens should yield around  $1 \times 10^7$  CD4<sup>+</sup>CD45RB<sup>high</sup> T cells and at least  $1 \times 10^6$  CD4<sup>+</sup>CD25<sup>+</sup> Treg cells.
2. Grind batches of five spleens in 10 mL FB in plastic Petri dish, by passing through 100- $\mu$ m nylon cell strainer using plunger from disposable 5-mL syringe. Rinse strainer with an additional 10 mL FB and pipet repeatedly in Petri dish to obtain a single cell suspension.

#### 3.2. Erythrocyte Lysis

1. Pellet cells in 50-mL tubes, by centrifugation at 400g for 5 min.
2. Discard supernatant and disperse residual cell pellet on a vortex mixer.
3. Add 500  $\mu$ L per spleen of ACK buffer and resuspend cells thoroughly. Incubate for 3 min at room temperature.
4. Make volume up to 40 mL with FB and filter suspension through 100- $\mu$ m cell strainer into fresh 50-mL tube to remove clumps and debris. Pellet cells by centrifugation as above.
5. Discard supernatant and resuspend cell pellets in 20 mL FB. Pellets from up to 10 spleens can be pooled. Take an aliquot of the cell suspension and count viable cells using a hemocytometer and trypan blue. Pellet the cells by centrifugation as described above.

#### 3.3. CD4 Enrichment

1. Discard supernatant and resuspend cells to  $2 \times 10^8$  cells/mL in the CD4 enrichment antibody mix as described above (*see Note 4*) i.e., 50  $\mu$ L antibody mix per  $10^7$  cells. Incubate at 4°C for 30 min.
2. Thoroughly resuspend the goat anti-rat IgG magnetic beads in the stock bottle and remove the amount required to give a ratio of magnetic beads to total cells of 1:1. Add the beads to a 15-mL polypropylene tube containing 7 mL FB.

3. Wash beads by applying magnet to tube for 30 s and then aspirating buffer. Remove beads from magnet and repeat washing process using fresh FB. Resuspend beads at  $1 \times 10^8$ /mL in FB and keep on ice.
4. Add 20 mL FB to antibody-stained cells from **step 8** and pellet by centrifugation as before. Resuspend at  $1 \times 10^8$ /mL in FB.
5. Combine the cells and magnetic beads in a 15-mL polypropylene tube and incubate at 4°C for 30 min on a rotary mixer.
6. Separate labeled cells bound to the magnetic beads by applying magnet to tube for 30 s and remove CD4 enriched cell suspension into a fresh 15-mL centrifuge tube. Repeat magnetic separation to ensure removal of all beads.
7. Count viable CD4<sup>+</sup> T cells, as described above, and remove aliquots as staining controls for cell sorting (*see Note 6*). Pellet the cells by centrifugation.

### 3.4. Sorting CD4<sup>+</sup> T-Cell Subpopulations

1. Resuspend CD4<sup>+</sup> T cells in a 15-mL polystyrene tube at  $10^8$  cells/mL in FB containing 10 µg/mL FITC-conjugated anti-mouse CD45RB, 2 µg/mL PE-conjugated anti-mouse CD25 and 2 µg/mL PE-Cy5-conjugated anti-mouse CD4 (*see Notes 5 and 6*). Incubate for 30 min at 4°C in the dark.
2. Add 10 mL FB and pellet cells by centrifugation. Resuspend pellet in 10 mL fresh FB and pass through a cell strainer to remove any clumps—this is important to ensure that the cell sorter does not become blocked during sorting. Pellet again by centrifugation and resuspend cells at  $2\text{--}5 \times 10^7$ /mL in FB for sorting. Cells should be kept on ice and protected from light prior to sorting.
3. Set up the cell sorter by running control samples to determine correct compensations for sorting (*see Notes 6 and 7*).
4. Apply labeled CD4<sup>+</sup> T cells to the sorter and set up appropriate sorting gates. A series of gates are set to define the desired populations. A forward and side scatter gate is used to identify viable lymphocytes and a second gate is used to select the CD4<sup>+</sup> T cells (approx 80–90% of viable cells should be CD4<sup>+</sup>). Within this CD4<sup>+</sup> T cell fraction, sorting gates are defined to isolate CD25<sup>-</sup>CD45RB<sup>high</sup> (approx 30–40% of CD4<sup>+</sup> T cells) and CD25<sup>+</sup>CD45RB<sup>low</sup> (approx 5% of CD4<sup>+</sup> T cells) subpopulations, as illustrated in **Fig. 2**. Sorted cells are collected into 5-mL FACS tubes containing a cushion of 100 µL heat-inactivated FCS and kept on ice.
5. Pellet sorted cells by centrifugation, resuspend in FB and count viable cells by trypan blue exclusion.
6. Remove aliquots ( $2 \times 10^5$  cells) from each fraction and reanalyze on flow cytometer to verify purity of sorted subpopulations, which should be >99%.

### 3.5. Induction and Monitoring of IBD

1. Pellet the purified CD4<sup>+</sup> T cell subsets and resuspend CD4<sup>+</sup>CD45RB<sup>high</sup> T cells at  $4 \times 10^6$ /mL and the CD4<sup>+</sup>CD25<sup>+</sup> Treg cells at  $1 \times 10^6$ /mL in HBSS/BSA. For induction of colitis remove  $4 \times 10^5$  CD4<sup>+</sup>CD45RB<sup>high</sup> T cells (100 µL) per recipient, dilute with an equal volume of HBSS/BSA and inject 200 µL intraperitoneally into immune deficient recipients. For protection from disease, mix  $4 \times 10^5$

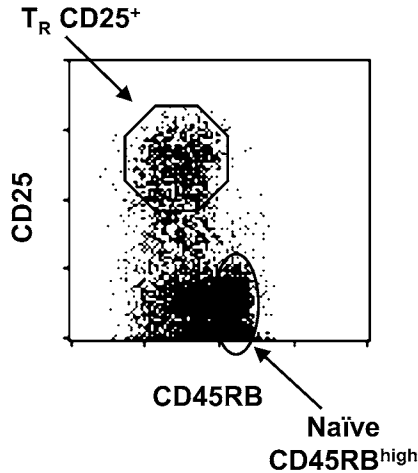


Fig. 2. Typical sorting gates applied to isolate naïve CD4<sup>+</sup>CD45RB<sup>high</sup> T cells and regulatory CD4<sup>+</sup> CD25<sup>+</sup> Treg cells. Plot shows staining profile of CD25 and CD45RB expression on gated live CD4<sup>+</sup> T cells.

CD4<sup>+</sup>CD45RB<sup>high</sup> T cells (100  $\mu$ L) together with  $1 \times 10^5$  CD4<sup>+</sup>CD25<sup>+</sup> T cells (100  $\mu$ L) per recipient and inject 200  $\mu$ L of the cell mixture as above.

2. Mark each recipient individually by ear punching or other identification method. Weigh each mouse at the time of T cell transfer and at weekly intervals thereafter.
3. Development of IBD is accompanied by progressive weight loss, hunching, and loose stools/diarrhea and such symptoms should be monitored weekly in the first instance, but daily when they exhibit disease symptoms (*see Note 8*). Cull mice when they develop chronic diarrhea or have lost 10–20% of their initial body weight, usually around 6–8 wk after T-cell transfer (*see Note 8*).
4. Open abdomen, cut colon immediately below the cecum and just above the anus and remove into ice-cold PBS. Lay colon lengthwise on a piece of paper towel moistened with PBS and trim away any adherent mesentery and fatty tissue using fine dissecting scissors and forceps.
5. Using a scalpel, cut 5- to 7-mm pieces from proximal (ascending), mid (transverse), and distal (descending) colon (*see Note 9*) and gently remove any luminal contents using forceps. Place tissue samples into a plastic universal tube containing 10 mL formal saline and allow to fix for at least 48 h. Tubes should be coded and labeled and samples can be maintained in formal saline for up to 1 mo.
6. Submit samples to a histology lab for histological processing and staining. Samples should be paraffin-embedded and 4- to 5- $\mu$ m transverse sections cut, mounted onto slides and stained with hematoxylin and eosin (H&E), with two to three stained sections prepared per sample.
7. Histological samples should be assessed by light microscopy and intestinal inflammation graded semiquantitatively on a scale from 0 (normal) to 4 (severe

**Table 1**  
**Histological Grading of Colitis**

Score	Typical features of lesions
0	Normal colonic crypt architecture, few leukocytes present and plentiful goblet cells.
1	Mild inflammation. Slight epithelial hyperplasia and increased numbers of leukocytes in the mucosa.
2	Moderate colitis. Pronounced epithelial hyperplasia (two- to threefold increase in crypt length), significant leukocyte infiltration of the mucosa and decreased number of goblet cells.
3	Severe colitis. Marked epithelial hyperplasia (>fivefold increase in crypt length) with extensive leukocyte infiltration of the mucosa, sub-mucosa and tunica muscularis. Significant depletion (<50%) of goblet cells, occasional ulceration, or crypt abscesses.
4	Very severe colitis. Marked epithelial hyperplasia (>fivefold increase in crypt length) with extensive, dense trans-mural leukocyte infiltration from the submucosa through to the serosa. Severe depletion (>50%) of goblet cells, many crypt abscesses and marked ulceration.

Adapted from ref. [11](#).

colitis), according to the characteristics described in [Table 1 \(11\)](#). Someone who is familiar with normal and diseased colonic architecture should evaluate slides in a blinded fashion.

- Data may be presented as mean score (0–4) from the most affected region (usually mid-colon), or as cumulative scores from each colon section (0–12). Nonparametric statistical analysis (e.g., Mann Whitney U-test) should be applied to test for significant differences between groups.

#### 4. Notes

- The model has been shown to work well using transfer of naïve CD4<sup>+</sup> T cells from C57Bl/6 into C57Bl/6.*Rag*<sup>-/-</sup>, from BALB/c into BALB/c.*Rag*<sup>-/-</sup> and from NOD into NOD.*scid* mice. However, the precise incidence and kinetics of disease may vary depending on the strain background. Not all strains are suitable, for example 129SvEv.*Rag*<sup>-/-</sup> mice develop only mild inflammation after transfer of 129SvEv naïve CD4<sup>+</sup> T cells ([12](#)).
- SPF-status is crucial as the presence of pathogens in either the donor or recipient mice can have drastic effects. Typical signs of pathogens are when immune deficient recipients develop wasting disease very rapidly (within 2 wk) after T-cell transfer, or if significant sudden mortality occurs in recipient groups. In such cases the chief suspects are *Pneumocystis carinii* or viral infection. Another common problem is the presence of intestinal *Helicobacter* spp, which are endemic in many animal facilities and can greatly exacerbate intestinal inflammation. To avoid such problems it is crucial that all mouse colonies are subjected to regular pathogen

screening and, in the case of immune deficient mice, use of sentinel animals is essential. To further minimize the risk of infection, we house all mice in an individually ventilated cage system, using Thoren racks that provide a source of HEPA-filtered air to individual cages.

3. Although the precise organisms and antigens involved are not yet known, the intestinal commensal flora plays a crucial role in pathogenesis, by providing stimuli for the differentiation of the effector T cells that drive colitis. This microflora is probably the most important factor that determines the characteristics of disease within a given animal facility and any changes in the commensal flora can consequently alter the incidence and kinetics of disease. For this reason great care should be taken regarding the treatment of mice with antibiotics or other agents that may alter the enteric flora, such as chlorine tablets used to sterilize water supplies. Such agents should be either avoided altogether, or used in doses that have been empirically titrated and shown not to affect disease incidence.
4. Tissue culture supernatants, ascites, or purified immunoglobulin can be used as a source of antibodies. CD4 enrichment antibody mix can be prepared in advance and 1-mL aliquots stored at  $-20^{\circ}\text{C}$  until use. Commercial suppliers also produce kits that contain antibody mixtures and magnetic beads used for isolation of CD4<sup>+</sup> T cells, e.g., CD4 Negative Isolation Kit (DynaL Biotech).
5. Successful purification requires good staining of desired cell populations and it is especially important to have good separation between the CD45RB<sup>high</sup> and CD45RB<sup>low</sup> fractions. We use fluorescently labeled antibodies from a commercial source (BD Biosciences Pharmingen) and if antibodies are produced in-house it is necessary to titrate them beforehand to determine optimal concentrations for use. When isolating CD4<sup>+</sup> CD25<sup>+</sup> Treg cells, it is essential that the anti-mouse CD25 monoclonal antibody clone 7D4 is used and not the widely available clone PC61, because clone PC61 mediates the depletion of CD25<sup>+</sup> Treg cells in vivo.
6. Accurate definition of cell populations requires precise calibration and compensation of the flow cytometer, using control samples. Immediately after CD4 enrichment, aliquots of approx  $5 \times 10^5$  cells should be removed for this purpose. Controls should include an unstained cell sample as well as samples stained with each fluorescent antibody individually.
7. High-speed cell sorting normally requires a highly trained operator, whose competence plays a crucial role in the successful isolation of pure cell subpopulations. It is, therefore, essential to discuss your goals as well as the characteristics and specifications of the cell sorter with the operator prior to commencing this type of experiment. We use a Dako Mo-Flo cytometer that sorts around 15,000–20,000 cells/s with a running pressure of about 40–60 psi.
8. Symptoms of wasting disease and diarrhea usually appear about 4 wk after T cell transfer, progressing to severe colitis at around weeks 6–8, but this may vary depending on the strain of mice used and the environmental conditions under which they are maintained. Monitoring body weight is an excellent method of tracking disease, but once severe colitis is present there may be rapid weight loss

and death in a matter of days. Therefore, mice exhibiting signs of disease should be monitored on a daily basis and sacrificed before they have lost more than 20% of their initial body weight.

9. As disease incidence and severity are not always uniform, it is important to evaluate samples from each section of colon. Proximal colon samples are taken around 1–2 cm from the start of the colon. Mid-colon samples, which usually provide the most reliable indicators of histological disease score, are taken from the centre point. Distal colon samples are taken around 1–2 cm from the end of the colon.

## Acknowledgments

The author is supported by a Wellcome Trust Career Development Fellowship.

## References

1. Podolsky, D. K. (2002) Inflammatory bowel disease. *N. Engl. J. Med.* **347**, 417–429.
2. Strober, W., Fuss, I. J., and Blumberg, R. S. (2002) The immunology of mucosal models of inflammation. *Annu. Rev. Immunol.* **20**, 495–549.
3. Elson, C. O., Cong, Y., McCracken, V. J., Dimmitt, R. A., Lorenz, R. G., and Weaver, C. T. (2005) Experimental models of inflammatory bowel disease reveal innate, adaptive, and regulatory mechanisms of host dialogue with the microbiota. *Immunol. Rev.* **206**, 260–276.
4. Powrie, F., Leach, M. W., Mauze, S., Caddle, L. B., and Coffman, R. L. (1993) Phenotypically distinct subsets of CD4+ T cells induce or protect from chronic intestinal inflammation in C. B-17 scid mice. *Int. Immunol.* **5**, 1461–1471.
5. Powrie, F., Leach, M. W., Mauze, S., Menon, S., Caddle, L. B., and Coffman, R. L. (1994) Inhibition of Th1 responses prevents inflammatory bowel disease in scid mice reconstituted with CD45RBhi CD4+ T cells. *Immunity* **1**, 553–562.
6. Powrie, F. (1995) T cells in inflammatory bowel disease: protective and pathogenic roles. *Immunity* **3**, 171–174.
7. Maloy, K. J. and Powrie, F. (2001) Regulatory T cells in the control of immune pathology. *Nat. Immunol.* **2**, 816–822.
8. Sakaguchi, S. (2004) Naturally arising CD4+ regulatory t cells for immunologic self-tolerance and negative control of immune responses. *Annu. Rev. Immunol.* **22**, 531–562.
9. Shevach, E. M. (2002) CD4+ CD25+ suppressor T cells: more questions than answers. *Nat. Rev. Immunol.* **2**, 389–400.
10. Coombes, J. L., Robinson, N. J., Maloy, K. J., Uhlig, H. H., and Powrie, F. (2005) Regulatory T cells and intestinal homeostasis. *Immunol. Rev.* **204**, 184–194.
11. Leach, M. W., Bean, A. G., Mauze, S., Coffman, R. L., and Powrie, F. (1996) Inflammatory bowel disease in C.B-17 scid mice reconstituted with the CD45RBhigh subset of CD4+ T cells. *Am. J. Pathol.* **148**, 1503–1515.
12. Maloy, K. J., Salaun, L., Cahill, R., Dougan, G., Saunders, N. J., and Powrie, F. (2003) CD4+CD25+ T(R) cells suppress innate immune pathology through cytokine-dependent mechanisms. *J. Exp. Med.* **197**, 111–119.



## In Vivo Models for the Study of Transplantation Tolerance

Hannah Stewart, Rommel Ravanan, and Richard Smith

### Summary

Experimental models of transplantation remain essential tools for the study of immunological tolerance. The immunological mechanisms resulting in acute allograft rejection may differ depending on the tissue transplanted and the antigenic mismatch between donor and recipient. Murine skin grafting is a model frequently used to study transplantation tolerance because it is readily learned and is not time consuming. Second grafts can be performed easily to confirm the induction of tolerance and its antigenic specificity. However, these grafts are strongly immunogenic and secondarily revascularized and may not, therefore, reproduce the conditions operating in clinical transplantation of primarily revascularized organs, such as the kidney and heart. Experimental rodent models of revascularized solid organ transplantation have been established, but given the technical skills required to perform them, are beyond the scope of this chapter. However, cellular transplants, including the use of islets, are of interest as they are being developed clinically and can be reproduced experimentally. Here, we describe the technique of renal subcapsular transplantation of pancreatic islets of Langerhans.

**Key Words:** Allograft; skin transplantation; heart transplantation; islet transplantation.

### 1. Introduction

Historically, animal models of allotransplantation have been central to the study of immunological tolerance. Furthermore, the prevention of acute cellular allograft rejection remains essential for clinical transplantation, with the induction of tolerance remaining the “Holy Grail.” The full repertoire of immunological effector mechanisms may be recruited during the rejection of allografts: humoral responses, delayed type hypersensitivity responses, CD4<sup>+</sup> helper cell-dependent cytotoxic T-lymphocyte responses, CD4<sup>+</sup> helper cell-independent cytotoxic T-lymphocyte responses, and cytotoxic CD4<sup>+</sup> T cell responses. Major histocompatibility complex (MHC) class II-restricted CD4<sup>+</sup> T



cells involved in these responses may recognise antigen via the “classical” indirect recognition of processed graft antigens or direct recognition of cell surface antigen expressed by cells of the graft itself. In addition, innate immune mechanisms may significantly damage the graft, particularly during the first 48 h posttransplantation. Great care must be taken when interpreting results obtained using models of allograft rejection, as the dominant immunological mechanisms recruited may differ significantly depending on the transplant model used and the degree of antigenic disparity between donor and recipient (1,2). Differences in the susceptibility of specific tissues to killing by different effector mechanisms may be important (3) and there may be significant differences between strains and species (4).

In this chapter, three models of allotransplantation will be discussed representing three important types of allograft. Most clinical transplants involve the use of solid organs, which are primarily revascularized (e.g., kidney, liver, heart, or lung). Rodent vascularized heart transplantation represents a model for studying the rejection of such grafts. Experimental rodent heart transplantation may, in principle, be performed using three techniques. Heart tissue may be transplanted into a skin pocket, such as the ear, without vascular anastomosis. Such models are equivalent to other secondarily revascularized tissue grafts, e.g., skin. Two types of vascularized heart graft model have also been described. We have used the heterotopic transplant model, previously described by Chen (5) in which the heart is transplanted into the neck. The donor aorta is anastomosed to the recipient carotid artery and the donor pulmonary artery to the recipient jugular vein. This results in perfusion of the transplanted cardiac tissue via the coronary circulation ensuring tissue viability. Although in this model the heart continues to beat, the recipient is not dependent on the pumping action of the heart for survival; consequently, this model does not assess the mechanical function of the heart. The transplanted heart can be palpated easily in the neck, the day of rejection being taken as the first day when the heartbeat can no longer be palpated. One refinement of this technique, is to monitor electrical activity of the heart by ECG recording. An alternative vascularized model is transplantation of the heart into the abdomen. The disadvantage of this model is that it does not easily allow monitoring of the graft by palpation. Both of these vascularized heart transplant models require significant microsurgical skills and not all individuals will be able to acquire the techniques successfully. It is essential that the techniques are learned from an experienced operator which can be expected to take up to 3 mo. These techniques are, therefore, not discussed further here.

Although allogeneic skin transplantation is not a routine clinical procedure, it has been used to assess immunoreactivity between potential live donor transplant recipients (6). Experimental skin transplants are readily performed, the majority

of the experimental transplantation literature having made use of this model. Skin transplants represent secondarily vascularized tissue transplants, the lack of primary revascularization being akin to the situation encountered with cellular transplants. Finally, there is a growing interest in clinical cellular transplantation (e.g., pancreatic islet transplantation for type 1 diabetes or neuronal transplants for Parkinson's disease). Transplantation of isolated islets under the kidney capsule of mice or rats is a useful model for the study of secondarily revascularized cellular allograft rejection and the induction of immunological tolerance. To draw conclusions of clinical relevance, however, it is essential that the principles elucidated in these models are confirmed in large animal models, as significant differences may be evident. This is perhaps of most relevance in islet transplantation where intraportal embolization of islets is the preferred clinical technique. This approach is possible in rodents but most easily reproduced in porcine or primate models.

Classical protocols for the demonstration of tolerance require prolonged graft survival in the absence of ongoing immunosuppression (typically survival beyond 100 d posttransplantation is considered sufficient). It should then be demonstrated that, in tolerant animals, a second allograft, from the same strain as the original graft, is not rejected. Ideally, antigenic specificity of tolerance and immunocompetence of the recipient should then be confirmed by demonstrating rejection of a third party graft. For islet transplantation, surgical removal of the graft by nephrectomy provides definitive proof that restoration of normal glucose homeostasis is due to the function of the graft, rather than recovery of endogenous pancreatic function.

## **2. Materials**

### **2.1. General**

1. Mice: mice can be maintained in conventional housing. Because infection can influence tolerance induction, it may be preferable to use a specific-pathogen free facility. Ideally animals should be 6–8 wk old at the time of transplantation. Mice up to 12 wk old may be used. The strains selected will depend on the degree of antigenic mismatch required. Definitive information concerning the MHC genotype of available mouse strains can be found on the Jackson website ([www.jax.org](http://www.jax.org)). For study of immunological mechanisms resulting in rejection of islet transplants (as opposed to the autoimmune disease process) it is not necessary to use spontaneously diabetic mice (i.e., NOD mice). Diabetes can be induced by injection of streptozotocin (STZ), allowing monitoring of graft function by the measurement of blood sugar levels. NOD mice may reproduce some unique features of the “diabetic” genetic background. If it is considered desirable to use this strain, development of autoimmune diabetes may confound interpretation of results of experiments designed to investigate immunological mechanisms operating in transplant rejection. At 6–8 wk of age NOD mice will not yet have developed

spontaneous autoimmune diabetes. Use of STZ to induce diabetes in such animals will permit the study of immunological mechanisms of rejection in the optimal background strain without the confounding effects of autoimmune disease. Ultimately, studies can be extended to spontaneously diabetic animals to study the effect of tolerogenic regimens on both the acute rejection and autoimmune disease processes. For islet transplantation animals should weigh 20–30 g, if diabetes is to be induced using STZ (*vide infra*).

2. Anesthetic: fluanisone (Hypnorm, Janssen, UK) and midazolam (Hypnovel, Roche) made up by dilution of fluanisone (40 mg/mL), midazolam (20 mg/mL), and sterile water in a 1:1:2 ratio, giving final concentrations of 10 and 5 mg/mL, respectively.
3. Surgical instruments: the basic surgical kit should contain a scalpel handle (no. 3 or 7 Swann-Morton, Sheffield, UK), scalpel blades (Swann-Morton, no. 6, 11, or 15), two pairs of small scissors (e.g., 11 cm straight iris scissors [[www.medisave.co.uk](http://www.medisave.co.uk)]), two pairs of small toothed fine dissecting forceps (e.g., Gillies 152 mm [[www.surgicalholdings.co.uk](http://www.surgicalholdings.co.uk)]), five small bulldog clamps (e.g., Debakey 20-mm bulldog clamps [[www.surgicalholdings.co.uk](http://www.surgicalholdings.co.uk)]), and wound clips ([www.royem.co.uk](http://www.royem.co.uk)). All instruments should be autoclaved before use.

## 2.2. Skin Transplantation

1. Paraffin gauze (e.g., Jelonet™ Smith and Nephew, Hull, UK) cut into 1- to 1.5-cm squares.
2. Gauze swab (e.g., Multi-gauze [[www.frontiermultigate.co.uk](http://www.frontiermultigate.co.uk)]) cut into 1.5–2 × 5-cm strips.
3. Plaster of Paris bandage ([www.medisave.co.uk](http://www.medisave.co.uk)) cut into 1.5–2 × 10-cm strips.
4. Phosphate buffered saline (Gibco, Invitrogen, Paisley, UK).
5. 6-cm Diameter Petri dish (BD).

## 2.3. Islet Transplantation

### 2.3.1. Murine Islet Isolation

1. Collagenase P (Roche Diagnostics, UK) at 1 mg/mL.
2. Hanks balanced salt solution (HBSS) supplemented with 0.01 M HEPES (Gibco).
3. Fetal calf serum (Sigma, UK).
4. UW solution (Biowhittaker, UK).
5. RPMI-1640 (Gibco).
6. Citrate buffer: 0.1 M sodium citrate, 0.1 M citric acid, pH 4.5.
7. 1-mm Sieve (e.g., Endecotts sieves [[www.ukge.co.uk](http://www.ukge.co.uk)]).
8. Polysucrose 400 Ficoll (Sigma, UK). A 25% stock solution is made by adding 50 g of Ficoll to 150 mL of HBSS, 0.01 M HEPES and stirring overnight. The volume is then adjusted to 200 mL by addition of HBSS, 0.01 M HEPES. The different percentage Ficoll solutions required for the gradient are then prepared as documented in [Table 1](#).
9. Binocular dissecting microscope ([www.gxoptical.com](http://www.gxoptical.com)).

**Table 1**  
**Gradient Layers of Ficoll<sup>a</sup>**

Ficoll concentration	Stock Ficoll	1X HBSS, 10 mM HEPES
23%	46 mL	4 mL
20%	40 mL	10 mL
11%	22 mL	28 mL

<sup>a</sup>The Ficoll solutions for each layer should be made up as documented in the table.

### 2.3.2. Induction of Diabetes

1. STZ (Sigma).
2. Blood glucose monitor and blood monitoring strips (e.g., Roche AccuCheck, Roche, UK).

### 2.3.3. Transplantation

1. Candle wax or bottle top sealing wax (Sigma).
2. Gilson pipet and P200 tips.
3. Binocular dissecting microscope (vide supra).
4. Blunted watchmakers' forceps (e.g., Samco [www.lig-supplies.co.uk](http://www.lig-supplies.co.uk)).

## 3. Methods

### 3.1. Skin Transplantation

Billingham and Medawar (7) first described the technique most commonly used for skin transplantation.

1. Sacrifice an appropriate donor mouse by a schedule 1 method.
2. Make a circular incision, through the full thickness of the skin, at the base of the tail and a second longitudinal incision from the base towards the end of the tail.
3. Peel the skin edges apart using toothed forceps and place the excised skin into a 6-cm diameter Petri dish filled with phosphate buffered saline (PBS).
4. Cut the excised tail skin into pieces approx  $0.5 \times 0.5$  cm. Each tail should provide enough skin for approx 10 grafts.
5. Anesthetize the recipient and swab the thorax with 70% alcohol.
6. Prepare the graft bed by excising a circle of skin approx 0.75-cm diameter in the area between the shoulder and costal margin.
7. Place the graft on the graft bed and hold in place by covering with a single piece of paraffin gauze, large enough to cover the graft site (approx  $1-1.5 \times 1-1.5$  cm).
8. Wrap a strip of gauze swab (approx  $1.5-2 \times 6$  cm) around the thorax, covering the graft site.
9. Soak a strip of plaster of Paris bandage in water and wrap completely around the thorax, over the gauze swab.
10. Bring the ends of the plaster of Paris strip together over the back of the animal, trim to leave a 3- to 5-mm "join" standing proud of the animal and clip together

using two wound clips. The bandage should be applied sufficiently tightly to ensure that it cannot be removed but great care must be taken to ensure that it is not so tight that, as it hardens, it prevents thoracic wall movement, resulting in asphyxiation.

11. After 7 d, remove the bandage and score the grafts daily until rejection. Ideally this should be performed blinded by the same observer. A typical graft scoring scheme is as follows: lush hair growth (++); graft intact with no evidence of necrosis (+); graft showing some necrosis ( $\pm$ ); and >90% necrosis (-). The day of rejection is recorded as the first day when necrosis of >90% is observed.

## **3.2. Islet Transplantation**

### *3.2.1. Murine Islet Isolation*

Islet isolation techniques differ between laboratories but all rely on collagenase digestion of the pancreas to generate a cell suspension containing exocrine tissue and intact islets of Langerhans (1% of total tissue). Over-digestion results in fragmentation of islets because of disruption of the islet capsule: the function of such islets will be compromised. Under-digestion results in exocrine tissue remaining attached to the islets (referred to as “embedded islets”). We routinely isolate islets using a modification of the method described by Gotoh et al. (8).

1. Prepare a 1-mg/mL solution of Collagenase P (Roche Diagnostics) in 1X HBSS, 0.01 M HEPES and leave on ice until required.
2. Sacrifice the donor using a schedule 1 method.
3. Open the abdominal cavity using a midline incision from the xiphisternum to the symphysis pubis.
4. Expose and pin back the liver.
5. Locate the pancreatic duct running from the porta hepatis to the duodenum and clamp as close to the duodenum as possible with a bulldog clamp.
6. Aspirate the collagenase solution into a 5-mL syringe and attach a 27-gauge needle, bent at a 90° angle.
7. Cannulate the pancreatic duct and slowly inject 2–3 mL of collagenase solution into the pancreas. It may be necessary to place a bulldog clamp on the shaft of the needle to ensure no reflux of collagenase. When the pancreas is fully distended, release the clamp and dissect the pancreas free.
8. Collect up to three pancreases in a 50-mL tube and add sufficient collagenase P to just cover them completely.
9. Incubate at 37°C for 6–12 min. The time is dependent on the batch of collagenase and has to be optimized for each new batch. The aim is to maximize the number of islets obtained that are free of exocrine tissue, without resulting in fragmented islets due to over-digestion.
10. After digestion, top up to 35 mL with HBSS, 0.01 M HEPES supplemented with FCS to a final concentration of 5% (wash solution) and shake by hand for 15 s to break up the tissue.

11. Pellet the islets by centrifugation at 800g for 1 min and aspirate the supernatant to a volume of 7.5 mL.
12. Wash again by addition of a further 35 mL of wash solution, shake, and centrifuge for 1 min at 800g.
13. Aspirate the supernatant to approx 7.5 mL and resuspend the pellet in 20 mL of wash solution.
14. Pour the cell suspension through a 1-mm sieve into a fresh 50-mL tube to remove any undigested tissue or fat.
15. Add 15 mL of wash solution to the digestion tubes and swirl gently to ensure that all tissue is recovered and pour through the filter.
16. Rinse the filter with a final 15 mL of wash solution.
17. Centrifuge the cell suspension at 800g for 1 min.
18. Discard the supernatant, resuspend the cell pellet in 10 mL of UW solution (Biowhittaker), and leave on ice for 30 min.
19. Centrifuge at 800g for 1 min and carefully pour off the supernatant.
20. Prepare Ficoll solutions (*see Table 1*) and leave to equilibrate to room temperature for 30 min.
21. Resuspend the digested pancreas pellet from **step 19** in 15 mL of 25% Ficoll.
22. Add the next Ficoll layers very slowly by pipetting down the side of the tube: 10 mL of 23% Ficoll; 10 mL of 20% Ficoll; 5 mL of 11% Ficoll.
23. Centrifuge the gradients at 1800g for 10 min with no brake at room temperature.
24. Collect each layer and its interface separately into 50-mL tubes.
25. Top up each tube with wash solution and centrifuge for 2 min at 900g with the brake applied.
26. For each tube, aspirate the supernatant to approx 7.5 mL and wash by addition of 35 mL of wash solution. Pellet by centrifugation for 1 min at 800g and aspirate the supernatant as close to the islet pellet as possible.
27. Resuspend the pellet in 3 mL of RPMI supplemented with 5% FCS and place the islet fractions separately into 60-mm diameter Petri dishes. Top up with RPMI 5% FCS.
28. View under a dissecting microscope using a  $\times 10$  objective and aspirate the islets using a P200 Gilson pipet (*see Fig. 1*).
29. Place the aspirated islets into a clean Petri dish containing RPMI 5% FCS. It may be necessary to repeat this process to achieve high degrees of purity, as some exocrine tissue is inevitably aspirated along with the islets during the initial picking.

### 3.2.2. Transplantation

1. Count the required number of islets into a 1.5-mL tube and centrifuge for 3 min at 800g.
2. Remove the supernatant and resuspend the pellet of islets in 200  $\mu$ L of PBS. Draw up the islets into a P200 pipet tip and plug the tip by dipping it into molten wax to a depth of 2–3 mm.
3. Place the tip in a 15-mL tube and centrifuge for 3 min at 800g to pellet the islets on top of the wax.

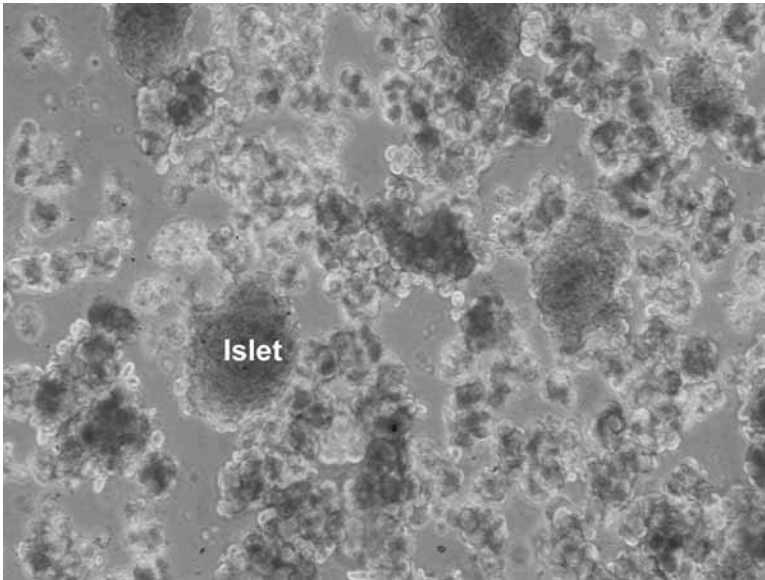


Fig. 1. Bright field view of digested pancreatic tissue.

4. Carefully pipet off the supernatant and, under a dissecting microscope, cut off the wax tip with a scalpel blade, leaving the islets ready for transplantation.
5. Anesthetize the recipient mouse and make a 5- to 7-mm incision in the abdominal wall on the left side, parallel to, and 5 mm below the line of the rib cage.
6. "Buttonhole" the kidney through the incision. Keep the kidney moist at all times by resting on gauze soaked in PBS and frequently syringing PBS over the surface.
7. Under a dissecting microscope, puncture the capsule of the kidney at one pole using blunted watchmakers' forceps.
8. Insert the pipet tip containing the islets under the capsule and advance it, in the subcapsular space, to the opposite pole of the kidney. Great care must be taken not to tear the kidney capsule.
9. Pipet the islets out into the subcapsular space and remove the pipet tip.
10. Return the kidney to the body cavity and staple the skin with wound clips.
11. Animals should be placed in a cage on a heating pad and observed until fully recovered from anaesthesia.

### 3.2.3. Induction of Diabetes

1. Select mice weighing between 20 and 30 g and starve overnight, allowing continued access to water.
2. The following day, inject intraperitoneally (i.p.) 100–160 mg of 4% (w/v) STZ (Sigma) dissolved in 0.1 M citrate buffer, pH 4.5.

3. Monitor blood glucose levels using a single drop of blood from a tail vein bleed and a blood glucose monitor (e.g., AccuCheck II, Roche). Mice may be considered diabetic and suitable for transplantation when their blood glucose measures greater than 20 mmol/L.
4. Transplant diabetic mice 3 d after STZ injection.
5. Measure urine glucose levels daily using urinalysis sticks (Roche). We measure blood glucose levels routinely twice weekly and if glycosuria is detected on urinalysis. An islet graft is considered to have failed or to have been rejected if the blood glucose levels measure more than 15 mmol/L on two consecutive readings.

#### 4. Notes

1. Grafts that fail in the first 24 h are considered technical failures. Technical competence should be confirmed by performing syngeneic grafts before proceeding to experimental work. Greater than 90% survival of syngeneic grafts for >100 d should be achieved.
2. The gauze strip both keeps the graft and paraffin gauze in place and prevents the plaster of Paris cast sticking to the hair of the thorax, thereby facilitating its removal.
3. *In situ* perfusion of the pancreas is not essential but greatly increases islet yield.
4. Multiple pancreases will be required to obtain sufficient islets for most experiments. Pancreases may be stored in a 50-mL tube on ice. We routinely retrieve no more than three pancreases at any one time, aiming to complete all surgery within 1 h, to prevent over-digestion of the first pancreas. All isolation steps have been optimized for this number of pancreases.
5. Equilibration of Ficoll solutions to room temperature is essential.
6. It is important to ensure that islets are exposed to Ficoll for the minimum time possible as prolonged Ficoll exposure reduces their viability.
7. STZ must be made up fresh and used immediately. The dose of STZ required varies depending upon the strain of mouse and on the batch of STZ used, the correct dose for each batch being determined by initial titration experiments. In our experiments, the STZ dose range used for C57Bl/6 is between 100 and 120 mg of STZ per kilogram of body weight and for NOD mice is between 150 and 160 mg/kg of body weight.
8. Islet transplants are not carried out until 3 d post-STZ injection to ensure no STZ remains in the animal which might damage the transplant.
9. Watchmakers' forceps are blunted by carefully "flattening" the tip by rubbing on fine emery cloth. If observed under a dissecting microscope, a clear square end to the forceps should be produced with no barbs.
10. Intraperitoneal injection of 100–120  $\mu$ L of fluanisone and midazolam, made up as described above, is sufficient to anesthetize most mouse strains adequately for islet transplantation.
11. Following STZ injection, mice do not need to be maintained on insulin if transplanted within 3 d. Animals that become diabetic but are not transplanted should be culled.



## Acknowledgments

Rommel Ravanan was the recipient of an unrestricted educational grant from Amgen UK Ltd. Work in the authors' laboratory is supported by the MRC, Bristol Branch of Diabetes UK, Fujisawa UK Ltd., and Wyeth UK.

## References

1. Youssef, A. R., Otley, C., Mathieson, P. W., and Smith, R. M. (2004) Role of CD4<sup>+</sup> and CD8<sup>+</sup> T cells in murine skin and heart allograft rejection across different antigenic disparities. *Transpl. Immunol.* **13**, 297–304.
2. Youssef, A. R., Otley, C., Mathieson, P. W., and Smith, R. M. (2002) Effector mechanisms in murine allograft rejection: comparison of skin and heart grafts in fully allogeneic and minor histocompatibility antigen-mismatched strain combinations. *Transpl. Int.* **15**, 302–309.
3. Jones, N. D., Turvey, S. E., Van Maurik, A., et al. (2001) Differential susceptibility of heart, skin, and islet allografts to T cell-mediated rejection. *J. Immunol.* **166**, 2824–2830.
4. Eizirik, D. L., Pipeleers, D. G., Ling, Z., Welsh, N., Hellerstrom, C., and Andersson, A. (1994) Major species differences between humans and rodents in the susceptibility to pancreatic beta-cell injury. *Proc. Natl. Acad. Sci. USA* **91**, 9253–9256.
5. Chen, Z. (1991) A technique of cervical heterotopic heart transplantation in mice. *Transplantation* **52**, 1099–1101.
6. Ravanan, R., Dudley, C. R., Smith, R. M., Burton, C. J., Lear, P. A., and Unsworth, D. J. (2005) Use of skin grafting to demonstrate tolerance prior to kidney transplantation without immunosuppression in the recipient of a previous bone marrow transplant. *Transplantation* **79**, 375–376.
7. Billingham, R. E. and Medawar, P. B. (1951) The technique of free skin grafting in mammals. *J. Exp. Biol.* **28**, 385–402.
8. Gotoh, M., Maki, T., Satomi, S., Porter, J., and Monaco, A. P. (1986) Immunological characteristics of purified pancreatic islet grafts. *Transplantation* **42**, 387–390.

## Ectopic Transplantation of Tissues Under the Kidney Capsule

Nathan J. Robertson, Paul J. Fairchild, and Herman Waldmann

### Summary

The subcapsular region of the kidney has frequently served as the site of choice for transplantation studies owing to a number of compelling reasons. High levels of vascularization provide a ready blood supply, whereas the subcapsular region itself can accommodate tissues of a range of size and sources. Historically, transplantation to this site has proven important for studies of both central and peripheral tolerance. Here, the transplantation technique and its major variations are described for broad application.

**Key Words:** Kidney capsule; transplantation; immunogenicity; thymus; islet.

### 1. Introduction

The kidney is one of the most vascular organs of the body and its surrounding capsule has long been used as the transplantation site for a range of adult and embryonic tissues. Proximity to an efficient supply of blood ensures that the components necessary for healing and graft viability are readily available. Furthermore, the capsule can physically accommodate the transplantation of a range of different types of tissue and may expand to allow considerable growth.

Ectopic transplantation to the subcapsular region of the kidney has commonly been employed to study the differentiation, development, and function of a variety of tissues. This has led to significant advances toward our understanding of both central and peripheral tolerance. Reconstitution of alymphoid fetal thymi with bone marrow-derived progenitors following transplantation under the kidney capsule has, for instance, been used to study the mechanisms of positive and negative selection. Typically, thymus lobes from 14-d embryos are depleted of lymphoid cells by culture in 2'-deoxyguanosine (2-dGuo)

before transplantation under the kidney capsule of athymic nude mice. Twenty-one days after transplantation, histology may be employed to demonstrate the presence of both cortical and medullary regions of the thymus which have become efficiently recolonized with hematopoietic cells from the host's own pool of bone marrow-derived progenitors (see Fig. 1A). The appearance of mature CD4<sup>+</sup>CD8<sup>-</sup> T cells in a similar proportion to day 21 neonatal thymus indicates that the transplanted thymus lobes are competent to sustain both positive and negative selection (see Fig. 1B,C). A similar model has been used for the identification of the thymic epithelium as determining the major histocompatibility complex-restriction specificity of emerging T cells and thymic dendritic cells as being essential to the induction of central tolerance (1).

Unlike skin grafts, which can be readily monitored through visual appearance, systems involving transplantation to the kidney capsule require different methods of observation. Models have typically involved the generation of a loss of function in the recipient, such that the donor tissue may be tested for its ability to rescue the normal phenotype. A prime example is the induction of diabetes to test the function of transplanted islets or the recovery of immune competence in congenitally athymic mice by grafting with fetal thymus rudiments. Although the survival and function of pancreatic islets may be assessed through blood glucose levels or the presence of c-peptide, a byproduct of insulin posttranslational processing (2), the function of transplanted thymus tissue may be observed through the flow cytometric analysis of blood samples to indicate the output of T cells. Monitoring tolerance or immunity to tissues with no easily measurable function is achieved by histological analysis of tissue structure and cellular infiltration at a selected time point (3). More recently, magnetic resonance imaging, positron emission tomography, and fluorescent imaging systems have emerged as potential tools to investigate the survival and structure of transplanted tissue *in situ* in a noninvasive manner (4,5). Although the method of posttransplantation observation needs to be carefully considered, the kidney capsule boasts facilities for both flexible accommodation and efficient healing and growth, while being fully compatible with protocols for the study of tolerance and immunity.

## 2. Materials

1. Phosphate buffered saline (PBS) (Biowhittaker, cat. no. BE17-515Q).
2. 70% Ethanol, prepared using sterile distilled water and absolute ethanol (BDH/VWR International, cat. no. 10107).
3. 15-mL Corning centrifuge tubes (Appleton Woods Ltd., cat. no. BC029).
4. 1.5-mL Microcentrifuge tube (Treff AG).
5. 25-Gauge 0.5 × 16-mm sterile needles (Terumo, cat. no. NN-2516R).
6. 2-mL Sterile syringe (Terumo).

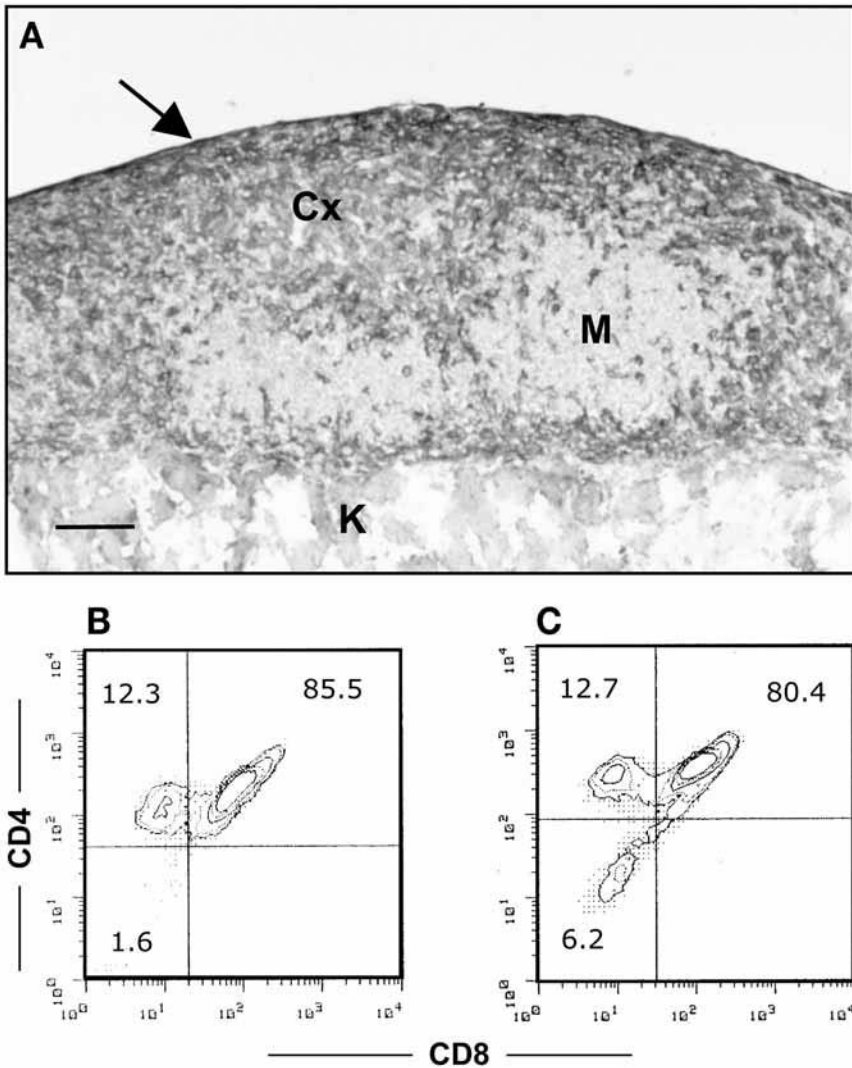


Fig. 1. Reconstitution of fetal thymus rudiments following transplantation under the kidney capsule. Thymus lobes from 14 d C3H/He embryos were depleted of lymphoid cells by culturing in 2-dGuo before being grafted under the kidney capsule of recipient BALB/c nude mice. (A) Frozen section stained using monoclonal antibodies specific for cortical thymic epithelium enabling the cortex (Cx) and medulla (M) of the thymus to be distinguished between the kidney capsule (arrow) and the kidney proper (K). Bar = 100  $\mu$ m. (B,C) Thymocytes were isolated from transplanted thymi and analyzed for the expression of CD4 and CD8 by flow cytometry (B) and compared with thymocytes derived from 21 d neonatal mice (C). Numbers represent the percentage of cells within the relevant quadrant.

7. Autoclaved, household cotton buds (Boots the Chemists Ltd.).
8. Micro-Fine insulin needles (BD Medical, cat. no. 324892).
9. Anesthetic: 1 mL of Ketaset (Fort Dodge Animal Health Ltd., cat. no. NADA 045-290) and 0.5 mL of 2% Rompun (Bayer Plc., cat. no. 00387512) diluted in 8.5 mL of PBS.
10. Analgesic: 1 mL of Vetergesic (Reckitt Benckiser Healthcare, cat. no. 138316) diluted in 9 mL of PBS.
11. Cozee Cumfort 2 heat electronic pad.
12. Autoclaved instruments including standard forceps, curved watchmaker's forceps, and scissors (10 cm in length).
13. Blunt-ended dressing forceps (10 cm in length) (Allgaier Instruments GmbH, cat. no. 08-420-100).
14. Scalpel fitted with sterile no. 23 scalpel blades (Swan-Morton, cat. no. 0303).
15. Electric shaver.
16. Vicryl-coated suture fitted with a 16-mm needle (Ethicon, cat no. W9442).

### 3. Methods

Please note that all measurements and doses described here are intended for murine models and that local ethical committee approval should be acquired before employing these protocols. All procedures should be carried out in a laminar flow tissue culture hood, and surfaces swabbed with 70% ethanol before use to ensure sterility.

#### 3.1. Aggregation of Donor Material Using a Blood Clot

Some tissues are ready for transplantation directly after washing with PBS. Transplantation of smaller tissues such as pancreatic islets or cell suspensions, however, may be facilitated by aggregation using a blood clot (6).

1. Sacrifice and swab the blood donor with 70% ethanol (*see Note 1*).
2. Insert a 25-gauge needle (attached to a 2-mL syringe) at the base of the sternum, aiming for the left side, and pointing downward at an angle of 20°. Blood should be drawn slowly to provide a yield of up to 1 mL in the case of mice aged between 6 and 8 wk and in excess of 1 mL for older mice.
3. Wash the cells to be transplanted at least twice by centrifugation at 400g and resuspend in PBS. A slower speed may be used for islets or other small tissues (*see Note 2*).
4. After the final wash, resuspend the cells or tissue at high density in PBS. For each recipient, transfer approx 50  $\mu$ L of the suspension onto a flat sterile surface, such as the inside of a lid removed from a 1.5-mL microcentrifuge tube.
5. Mix with approx 10  $\mu$ L of blood and leave for 5 min or until the blood has clotted.

#### 3.2. Transplantation of Tissue Under the Kidney Capsule

1. The material to be transplanted should be washed thoroughly with PBS. Cells should be centrifuged at 400g and resuspended in PBS after each wash. In the case

of whole tissues, allow them to settle to the bottom of a 15-mL centrifuge tube under unit gravity and replace the PBS (*see Note 2*).

2. Administer anaesthetic intraperitoneally to recipient mice (*see Note 3*). Approximately 200  $\mu\text{L}$  is required for 6-wk-old CBA/Ca mice, but this will vary according to strain and older mice may require a larger dose, proportional to their weight.
3. Shave the surgical site on one side, extending from the lower abdomen to just beyond the rib cage, taking care to contain any loose fur. If possible, the left side should be chosen because the spleen provides a useful anatomical marker for the location of the kidney.
4. Check that the anesthetic has taken effect (allowing at least 5 min) by testing for a reflex response.
5. Once anesthetized, administer 100  $\mu\text{L}$  of analgesic subcutaneously in the scruff of the neck.
6. Place on a heated mat, swabbed with 70% ethanol, to assist with thermoregulation.
7. Sterilize the skin by swabbing with 70% ethanol, taking care to limit the surface area covered, so as not to cool the animal unnecessarily.
8. The spleen lies posteriorly from the rib cage, and may be visible through the shaved skin. The kidney lies immediately adjacent to the spleen on the posterior side. Using forceps, lift the skin above the kidney and make a 1- to 2-cm incision perpendicular to the spine using scissors (*see Note 4*).
9. The kidney may be visible through the body wall adjacent to the spleen (*see Note 5*). Lifting the body wall using forceps, make an incision just smaller than the kidney (5–8 mm), and in the same orientation as its axis directly above it (*see Note 6*).
10. Use sterile cotton buds to press the body wall either side of the incision and massage the kidney so that it rests exposed on the body wall (*see Note 7*).
11. Wait several seconds to allow any moisture on the surface of the kidney to dry.
12. Use blunt-ended forceps to hold and lift the kidney capsule while using the curved watchmaker's forceps to puncture the capsule and create a tunnel between the parenchyma of the kidney and the capsule (*see Note 8*).
13. Holding the tunnel open with the blunt forceps insert the tissue in a manner appropriate for its size (*see Note 9*).
14. If necessary, use curved watchmaker's forceps to massage the tissue away from the opening in the capsule.
15. Rehydrate the organ with PBS, taking care not to dislodge the transplanted material.
16. Ease the kidney back into the body cavity by lifting the body wall over the kidney. Be careful that the body wall does not press against the kidney and dislodge the tissue.
17. Close the incision with one or two interrupted stitches in the body wall using absorbable suture.
18. Finally, close the incision in the skin using interrupted sutures, before returning the animal to a heated cage for recovery (*see Note 10*).

#### 4. Notes

1. The donor strain should be chosen with care because leukocytes in the donor blood could affect the outcome of transplantation studies. Using a strain deficient in the

recombinase activating gene (*RAG1*) will minimize the presence of lymphocytes that could initiate immunity toward host tissues, while a syngeneic donor strain should not provoke any immune response at all.

2. In the case of cultured tissues or cells, it is important to remove proteins from fetal calf serum used in the culture media that could affect their growth *in vivo* or contain foreign antigens.
3. For more efficient throughput, subsequent mice may be anesthetized before the final step of the procedure is carried out on the previous animal.
4. If the spleen is not visible, the center of the surgical site is roughly located at the center of an imaginary line that runs from the top of the base of the ear, to a spot 5 mm above the base of the tail.
5. In female and older male mice, the kidney is obscured by a large fat pad (associated with the ovary in females). This obscures the kidney from sight through the body wall and may confound exposure of the kidney. In this case, the spleen may be used as a marker for the incision in the body wall. Relative to the spleen, the kidney is located posteriorly and toward the spine.
6. Unlike the skin, the body wall is very taut and will not rise far enough to make the incision easily in one action. First, make a tiny incision into which one blade of the scissors can be inserted to complete the incision. If the incision is too large, the kidney will slip back into the body cavity and will not remain exposed. If this occurs, there are several options available to proceed. First, a “stay” suture that passes through any fat associated with the kidney can be used to hold the kidney in position. Second, a suture stitch can be used to partially close the incision. Third, the same action used to lift the kidney capsule may be used to hold the kidney in position.
7. Before exposure of the kidney in female mice, forceps may be used to deflect the fat pad to expose both the associated ovary and underlying kidney.
8. Although it is easier to lift the kidney capsule with blunt forceps once the moisture on the surface has dried, creation of the tunnel under the kidney capsule is facilitated by using curved watchmaker’s forceps, moistened with PBS.
9. Larger pieces of tissue, or material aggregated using a blood clot, can be placed under the kidney capsule using a scalpel blade or curved watchmaker’s forceps. Cells and smaller tissues, such as pancreatic islets, are injected using a syringe and needle or a drawn-out glass pipet. Intermediate sized material may be inserted using a Gilson pipet (or similar instrument), after trimming the length of the pipet tip using a scalpel blade, such that the tip end is a suitable diameter for the tissue.
10. Male mice on the C57Bl background can be more aggressive than other strains such as CBA, and this may result in the removal of sutures, antagonism of the site of surgery and prevention of wound healing. If females or alternative strains cannot be used, it may be necessary to house the mice individually or use plaster casts for protection.

## References

1. Lo, D. and Sprent, J. (1986) Identity of cell that imprint H-2-restricted T-cell specificity in the thymus. *Nature* **319**, 672–675.
2. Warnock, G. L., Ellis, D. K., Cattral, M., Untch, D., Kneteman, N. M., and Rajotte, R. V. (1989) Viable purified islets of Langerhans from collagenase-perfused human pancreas. *Diabetes* **38**(Suppl 1), 136–139.
3. Tze, W. J., Tai, J., and Cheung, S. (1990) Human islet xenograft survival in rats. A functional and immunohistological study. *Transplantation* **49**, 502–505.
4. Paty, B. W., Bonner-Weir, S., Laughlin, M. R., McEwan, A. J., and Shapiro, A. M. (2004) Toward development of imaging modalities for islets after transplantation: insights from the National Institutes of Health Workshop on Beta Cell Imaging. *Transplantation* **77**, 1133–1137.
5. Gao, X., Cui, Y., Levenson, R. M., Chung, L. W., and Nie, S. (2004) In vivo cancer targeting and imaging with semiconductor quantum dots. *Nat. Biotechnol.* **22**, 969–976.
6. Gray, D. W., McShane, P., and Morris, P. J. (1986) The effect of hyperglycemia on isolated rodent islets transplanted to the kidney capsule site. *Transplantation* **41**, 699–703.





## Intravital Two-Photon Imaging of T-Cell Priming and Tolerance in the Lymph Node

Susanna Celli and Philippe Bousso

### Summary

Two-photon microscopy makes it possible to image in real-time fluorescently labeled cells located in deep tissue environments. We describe a procedure to visualize the behavior of lymph node T cells during either priming or tolerance, in live, anesthetized mice. Intravital imaging of T lymphocytes is a powerful tool to study the cellular orchestration of adaptive immune responses in physiological settings. This method should provide new insights into the regulation of lymphocyte migration and cell–cell interactions in various immunological contexts.

**Key Words:** T-cell activation; tolerance; lymph node; intravital imaging; two-photon microscopy.

### 1. Introduction

Lymph nodes (LN) represent a specialized microenvironment for the activation of T lymphocytes (**1**). Depending on the immunological context, T-cell stimulation in LNs can result in either an effective T-cell response with the generation of effector and memory T cells or in an abortive response and the establishment of a state of tolerance (**2,3**). Parameters influencing this choice continue to be the subject of intense research. Notably, most studies have relied on the analysis of T-cell differentiation at single time points. Although these studies have provided an essential foundation for understanding of T-cell tolerance induction, little is known of the most dynamic aspects of T-cell activation in vivo.

Recent advances in imaging technology provide us with the opportunity to visualize T-cell activation-related events in real time, at the single cell level and in physiological settings. In particular, two-photon laser scanning microscopy is the technique of choice to track the behavior of T cells located up to 100–300  $\mu\text{m}$

below the LN surface (4–8). Initial studies have been performed using explanted lymph nodes maintained under physiological conditions of temperature and oxygen (9–11). Two-photon imaging of lymphocyte behavior in LN can also be performed in surgically exposed inguinal or popliteal LNs of live, anesthetized mice (12,13). Although more tedious, intravital imaging offers several advantages over imaging of explanted organs, including preservation of vascular and lymphatic flow, neural innervations, oxygen metabolism, and possibly soluble gradients. This approach also has some caveats such as possible biases introduced by the anesthesia and/or the surgical procedure. Intravital imaging of the LN also carries intrinsic technical challenges such as the avoidance of movements of the sample caused by breathing and maintenance of a physiological temperature close to the exposed LN. Here, we describe a procedure for intravital two-photon imaging of the popliteal LN. Some parts of this procedure were adapted from previous studies.

## 2. Materials

1. Two-photon laser scanning microscopy system including an upright microscope (see Note 1), a Ti:sapphire laser tuned to 800 nm, a  $\times 20$  or  $\times 40$  dipping objective with long working distance (for example, Olympus  $\times 20$  0.95 NA, Zeiss Achroplan  $\times 40$  0.8 NA).
2. Homemade heating platform (see Fig. 1A) consisting of a heating element glued onto a rectangular-shaped piece of duralumin ( $180 \times 140 \times 3$  mm) using thermal adhesive. The heating element is set up to heat the platform at  $37^\circ\text{C}$ . The platform should be designed to fit onto the microscope stage.
3. Sample heating setup: peristaltic pump, in-line solution heater (SH-27B Warner Instruments), heater controller (TC-344B Warner Instruments), semi-flexible vinyl temperature probe, Tygon tubes, and tube connectors.
4. Ring-shaped (I.D. 18 mm) metallic tube (inox, O.D. 3 mm, I.D. 2 mm), cover slip ( $22 \times 22 \times 0.13$  mm).
5. Dissecting microscope (Leica MZ 12/5) and fiber optics for incident illumination with cold light source (Leica CLS 150X).
6. Anesthesia: ketamine and medetomidine HCl (Dormitor), stored at  $4^\circ\text{C}$ .
7. Small animal clipper (Harvard apparatus).
8. Microsurgical instruments: Mayo scissors and Adson forceps for the skin, two microdissecting forceps (Dumont n°5), one pair of microdissecting scissors, microvascular clamp (micro glover curved), needle holder (Halsey standard), 6/0 and 8/0 silk (Ethicon), ophthalmic cautery fine type, polythene catheter O.D. 0.80 I.D. 0.4 mm (Portex, England).
9. 5- (and-6)-carboxyfluorescein diacetate, succinimidyl ester (CFSE), stock solution 10 mM in DMSO (stored at  $-20^\circ\text{C}$ ).
10. Phosphate buffered saline (PBS).
11. Fetal calf serum (heat-treated to inactivate complement).
12. 0.9% Sodium chloride solution for injection (Baxter).

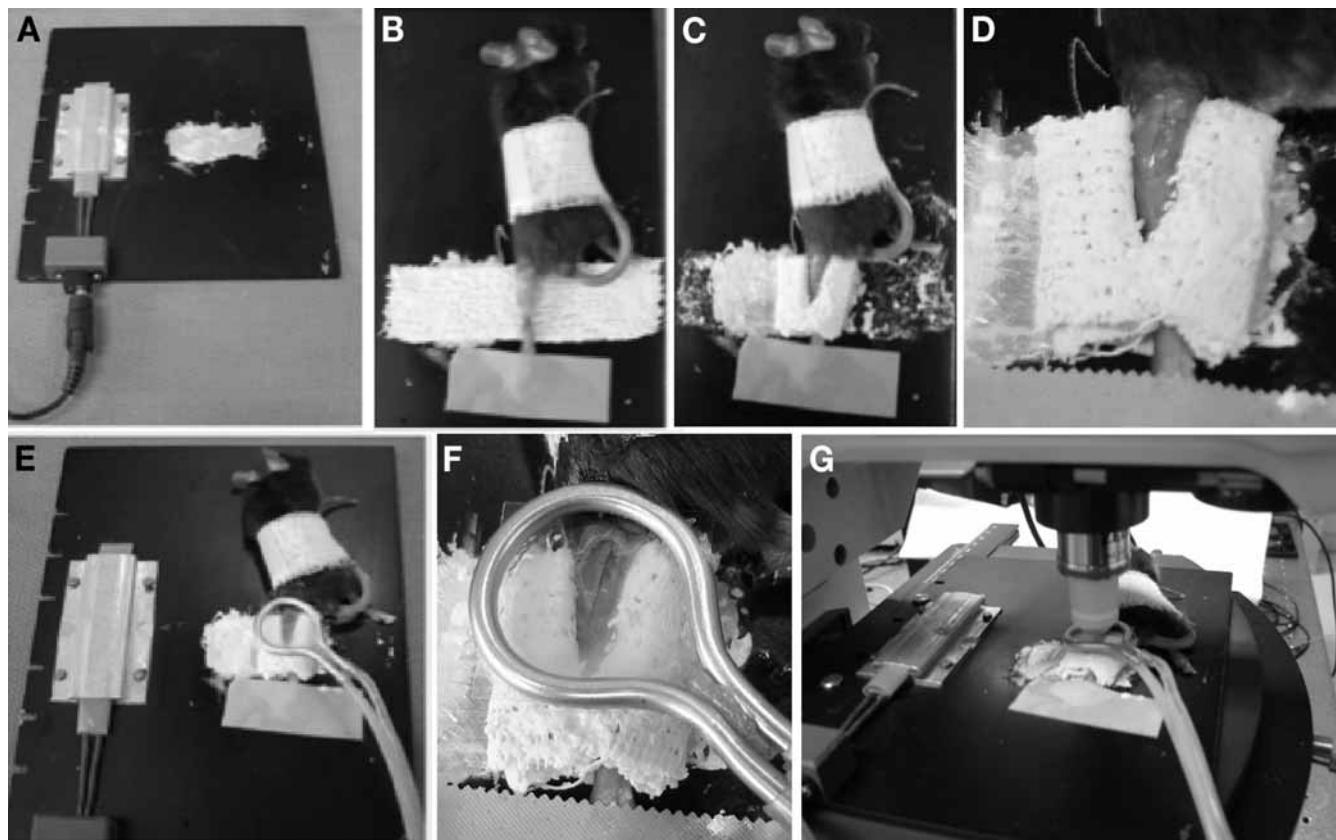


Fig. 1. Surgical exposure of the popliteal lymph nodes (LN) for intravital imaging. These pictures illustrate some of the important steps during the preparation of the popliteal LN for intravital imaging. (A) Custom-designed heating platform. (B–D) Preparation of the plaster cast to immobilize the lower hind leg. (E,F) A ring-shaped, metallic tube, glued to a cover slip is placed on the top of the popliteal LN. (G) After completing exposure of the LN, the heated platform is placed on the microscope stage.

13. Betadine solution (Asta Medica).
14. Heparin sodium.
15. Plaster bandages.
16. Surgical tape.
17. Cyanoacrylate glue.
18. Acetic silicone sealant.
19. Prewarmed distilled water (37°C).
20. Disposable sheets of cellulose fiber (Harvard apparatus).

### 3. Methods

We describe a procedure to visualize in real-time the behavior of fluorescently labeled T cells in the LN of live, anesthetized mice. These protocols can be adapted for the study of priming or tolerance induction under various conditions that will not be detailed here.

#### 3.1. Labeling and Adoptive Transfer of T Cells

1. Isolate the desired population of T cells (for example from the LN of mice, expressing a transgenic T-cell receptor) using magnetic sorting or a fluorescence activated cell sorter.
2. Resuspend  $1 \times 10^7$  T cells at  $2 \times 10^6$  cells/mL in PBS with 5  $\mu$ M CFSE. Incubate the cell suspension for 15 min at 37°C. Add 1 vol of fetal calf serum to stop the reaction. Wash twice and resuspend the cells in PBS.
3. Inject the cells intravenously (iv) into the recipient mice. One day later, immunize the animal using the desired protocol to induce priming or tolerance. Proceed with intravital imaging between 2 and 48 h later.

#### 3.2. Anesthesia

Inject the mouse intraperitoneally (ip) with ketamine (24 mg/kg) and intramuscularly (im) with medetomidine HCl (170  $\mu$ g/kg). Check the level of anesthesia by pinching the tail and by checking body and whisker movements. To maintain a deep level of anesthesia during the procedure (that may last several hours), it is recommended to administer a reduced dose of anesthetic each hour.

#### 3.3. Jugular Vein Cannulation (Optional)

Preparation of vascular access enables the injection of cells, dyes, or drugs during image acquisition (*see Note 2*). We choose to cannulate the external jugular vein that is distant from the site of the popliteal LN.

1. Shave the hair of the neck using a small animal clipper. Place the mouse on its back on the surgical board with its head toward the operator. Maintain the mouse head in extension by gently pulling its anterior teeth with a thin rubber band.
2. Clean the neck area with Betadine solution and perform a lateral skin incision along the neck.

3. Expose the external jugular vein by gently dissociating it from the surrounding tissues. Burn and cut all the collateral veins.
4. Place a vascular clamp on the jugular vein at the level of the clavicle to prevent air entry during the insertion of the cannula. Tie the other extremity of the jugular with 8/0 silk.
5. Perform a small incision on the superior wall of the jugular vein and insert the cannula filled with heparin solution.
6. Tie the cannula with 8/0 silk. The vascular clamp is removed and the blood flow through the cannula is checked. A drop of glue is used to fix the cannula to the surrounding tissues. The skin is closed by silk suture 6/0, once the glue is completely solidified. The cannula is washed regularly with heparin solution.

### 3.4. Preparation of the Popliteal LN

For all the following steps, the mouse should be transferred to the heated platform (*see Fig 1A*). The use of this stage simplifies the management of the mouse during the preparation of the sample and contributes to the overall stability of the intravital setup.

1. Shave the hair of the left lower hind leg using a small animal clipper.
2. Tape the tail of the mouse to the right side of the body using surgical tape. The left lower hind leg is gently pulled out and kept in extension using surgical tape as shown in *Fig. 1B*.
3. Perform a skin incision on the area of the popliteal space and remove a small circular piece of skin.
4. Carefully expose the popliteal LN by removing some of the fat covering the popliteal cavity (*see Note 3*).
5. Once exposed, cover the LN with a small piece of moist gauze. Immobilization of the leg is then achieved by preparing a plaster cast.
6. Cut two rectangular pieces of plaster bandage ( $80 \times 25$  mm), quickly immerse them in water and drain off the excess water. Place the plaster bandages one on the top of the other with the left leg lying in the middle (*see Fig. 1B*). Plaster bandages are folded twice to create a block of plaster on each side of the leg (*see Fig. 1C*). The height of the plaster blocks should match that of the LN surface (*see Note 4*). The two plaster bandages are connected at the ankle level to complete immobilization of the leg (*see Fig. 1D*).
7. Allow the plaster cast to dry (*see Note 5*). The shape of the plaster cast is designed (1) to prevent movements of the leg and movements as a result of breathing by fixing the leg to the heated platform and (2) to create a flat surface around the LN to attach a cover slip (*see below*).

### 3.5. Maintenance of the Exposed LN at Physiological Temperature

Keeping the LN at a physiological temperature is a critical part of the procedure because lymphocyte motility and behavior are highly temperature dependent (9). Several factors contribute to a temperature drop close to the sample,

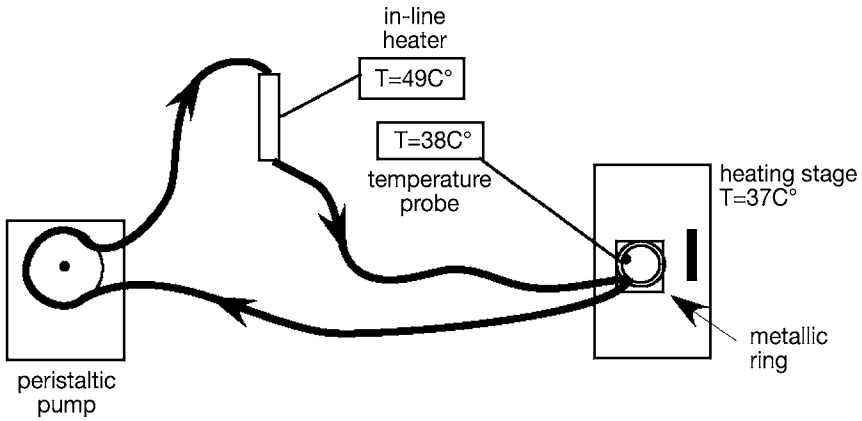


Fig. 2. Schematic representation of the water circuit used to maintain the temperature of lymph nodes (LN) within the physiological ranges. A peristaltic pump is used to circulate water in an in-line heater and then inside a ring-shaped metallic tube glued to a cover slip and placed on top of the LN. The ring and the cover slip create a small chamber filled with water to immerse a dipping objective. Water within the chamber is maintained at 38°C with the help of the warm water circulating in the metallic tube.

including anesthesia, surgical exposure of the LN and thermal transfer between the sample and the objective. Although the role of the heated platform is to help maintain the body temperature of the mouse within the physiological range, it is also essential to correct the temperature locally, close to the sample. An approach similar to that previously described by Mempel et al. is used with minor modifications (14).

1. Place and glue a cover slip onto the plaster cast. Only a film of saline solution should remain between the LN and the cover slip. A metallic ring-shaped tube should have been previously fixed on the top of the cover slip using silicone sealant (see Fig. 1F).
2. Place the heated platform with the intravital setup onto the stage of the microscope. Sheets of cellulose fibers can be used as a blanket to cover parts of the animal body that are not directly under the objective.
3. Connect the extremities of the metallic tube with Tygon tubes. Use a peristaltic pump so that distilled water heated with an in-line heater (set to 49°C) is able to circulate into the tube. A schematic representation of this set up is depicted in Fig. 2.
4. Add distilled water (prewarmed to 37°C) in the center of the metallic ring. The ring placed on the cover slip creates a “reservoir” that will enable the immersion of a dipping objective.
5. Monitor the temperature of the water in the ring with the help of the temperature probe. The heated liquid circulating inside the metallic tube should maintain the

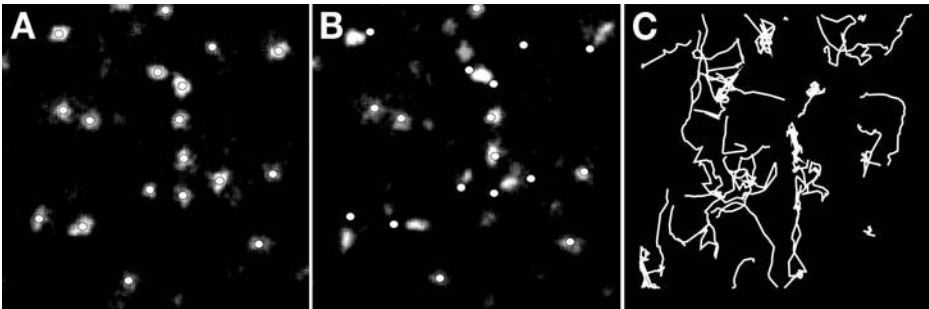


Fig. 3. In vivo imaging of T-cell behavior in the popliteal lymph nodes. Purified T cells were labeled with 5- (and-6)-carboxyfluorescein diacetate succinimidyl ester and injected i.v. At 24 h, the popliteal LN was prepared for intravital imaging. (A,B) Example of two images acquired 1 min 20 s apart. White dots mark T-cell positions at the first time point. (C) Example of T-cell trajectories analyzed from a time-lapse movie.

temperature of the water in the ring at 38°C. If necessary, adjust the temperature of the in-line heater accordingly.

### 3.6. Two-Photon Laser Scanning Microscopy

1. Tune the Ti:sapphire laser to 800 nm.
2. Set up the microscope configuration and filter (505–550 nm band pass) for the detection of CFSE.
3. Check that the dipping objective is properly immersed in the water contained within the metallic ring (*see Fig. 1G*). Add more warmed water if needed.
4. Using mercury lamp illumination, look through the eyepiece and focus onto the surface of the LN.
5. Start scanning using the Ti:sapphire laser (*see Note 6*). Adjust the gain and offset of the detectors. Typically, fluorescently labeled T cells can be detected in some areas of the LN starting 100  $\mu\text{m}$  below the tissue surface. While scanning, move long the  $x$ -,  $y$ -, and  $z$ -axes to locate an area containing a sufficiently high density of T cells.
6. Once an appropriate location is found, acquire Z-stacks of optical sections (typically 10 sections spaced by 4  $\mu\text{m}$ ) every 30 s for a total duration of 30–60 min (*see Note 7*).
7. Control the level of anesthesia before starting a new image acquisition. If necessary, proceed to an additional injection of anesthetics.
8. Process and analyze the data using 3D tracking software such as Imaris or Volocity (*see Note 8*). Quicktime movies can be generated following a maximum intensity projection of each Z-stack using the publicly available software ImageJ and OsiriX. Representative images and T-cell trajectories are shown in **Fig. 3**.



#### 4. Notes

1. It is recommended that nondescanned detectors (rather than internal photomultipliers) are used for optimal signal collection.
2. Intravenous injection of 2 mg tetramethylrhodamine-dextran (10 kDa) can be used to visualize blood vessels.
3. The popliteal LN is always located below the junction of the popliteal vein and one of its left branches.
4. During the preparation of the plaster cast, adjust the height of the plaster blocks to that of the LN by gently applying a microscope slide over the plaster blocks and mouse leg while the solidification process takes place.
5. This process is rather quick (5 min) on the heated stage.
6. Care should be taken to minimize the laser power used for excitation as excessive power can cause phototoxicity resulting in cell movement arrest (15).
7. In a nonimmunized animal, most T cells located in the paracortical area of the LN should be highly motile (with mean velocities of approx 10  $\mu\text{m}/\text{min}$ ). If this is not the case, check (1) that the temperature close to the sample is approx 37°C, (2) that immobility is not the result of phototoxicity, and (3) that the cover slip is not applying too much pressure to the LN.
8. Two-dimensional cell tracking can also be performed using the publicly available Mtrack2 plugin of ImageJ (<http://rsb.info.nih.gov/ij/plugins/index.html>).

#### References

1. von Andrian, U. H. and Mempel, T. R. (2003) Homing and cellular traffic in lymph nodes. *Nat. Rev. Immunol.* **3**, 867–878.
2. Kearney, E. R., Pape, K. A., Loh, D. Y., and Jenkins, M. K. (1994) Visualization of peptide specific T cell immunity and peripheral tolerance induction *in vivo*. *Immunity* **1**, 327–339.
3. Steinman, R. M., Hawiger, D., and Nussenzweig, M. C. (2003) Tolerogenic dendritic cells. *Annu. Rev. Immunol.* **21**, 685–711.
4. Denk, W., Strickler, J. H., and Webb, W. W. (1990) Two photon laser scanning fluorescence microscopy. *Science* **248**, 73–76.
5. Cahalan, M. D., Parker, I., Wei, S. H., and Miller, M. J. (2002) Two photon tissue imaging: seeing the immune system in a fresh light. *Nat. Rev. Immunol.* **2**, 872–880.
6. Bousso, P. and Robey, E. A. (2004) Dynamic behavior of T cells and thymocytes in lymphoid organs as revealed by two-photon microscopy. *Immunity* **21**, 349–355.
7. Huang, A. Y., Qi, H., and Germain, R. N. (2004) Illuminating the landscape of *in vivo* immunity: insights from dynamic *in situ* imaging of secondary lymphoid tissues. *Immunity* **21**, 331–339.
8. Dustin, M. L. (2004) Stop and go traffic to tune T cell responses. *Immunity* **21**, 305–314.

9. Miller, M. J., Wei, S. H., Parker, I., and Cahalan, M. D. (2002) Two-photon imaging of lymphocyte motility and antigen response in intact lymph node. *Science* **296**, 1869–1873.
10. Bousso, P. and Robey, E. (2003) Dynamics of CD8+ T cell priming by dendritic cells in intact lymph nodes. *Nat. Immunol.* **4**, 579–585.
11. Hugues, S., Fetler, L., Bonifaz, L., Helft, J., Amblard, F., and Amigorena, S. (2004) Distinct T cell dynamics in lymph nodes during the induction of tolerance and immunity. *Nat. Immunol.* **5**, 1235–1242.
12. Miller, M. J., Wei, S. H., Cahalan, M. D., and Parker, I. (2003) Autonomous T cell trafficking examined in vivo with intravital two-photon microscopy. *Proc. Natl. Acad. Sci. USA* **100**, 2604–2609.
13. Mempel, T. R., Henrickson, S. E., and Von Andrian, U. H. (2004) T-cell priming by dendritic cells in lymph nodes occurs in three distinct phases. *Nature* **427**, 154–159.
14. Mempel, T. R., Scimone, M. L., Mora, J. R., and von Andrian, U. H. (2004) in vivo imaging of leukocyte trafficking in blood vessels and tissues. *Curr. Opin. Immunol.* **16**, 406–417.
15. Shakhar, G., Lindquist, R. L., Skokos, D., et al. (2005) Stable T cell-dendritic cell interactions precede the development of both tolerance and immunity in vivo. *Nat. Immunol.* **6**, 707–714.



## Tracing Tolerance and Immunity In Vivo by CFSE-Labeling of Administered Cells

Elizabeth Ingulli

### Summary

Tracking antigen-specific cytotoxic T lymphocyte (CTL) function in vivo can be difficult due to the need to monitor the presence and subsequent destruction of antigen-bearing target cells. In this report, we describe a simple method using the fluorescent dye 5- (and 6-) carboxyfluorescein diacetate succinimidyl ester (CFSE) to evaluate CD8<sup>+</sup> T-cell effector function in vivo by flow cytometry. In this assay, peptide-pulsed and control target cells are labeled to different levels with CFSE and coadministered to animals that have been previously immunized or tolerized to the cognate antigen. Because naïve antigen-specific CD8<sup>+</sup> T cells cannot acquire effector function within the time frame of this assay, adoptively transferred nonimmunized animals are used as negative controls for in vivo CTL function. Target cells are syngeneic splenocytes pulsed with peptide antigen and control cells are unpulsed syngeneic splenocytes. The loss of antigen-specific target cells is indicative of cytotoxicity and immunity, whereas the lack of killing in the setting of antigen recognition is suggestive of tolerance.

**Key Words:** CTL; cytotoxicity; lymphocytes; CD8 T cells; peptide; antigen; splenocytes; CFSE; flow cytometry; TCR transgenic mice.

### 1. Introduction

The ability to eliminate viruses, tumors or solid organ transplants is dependent on the development of effective cytotoxic T lymphocytes (CTL). An effective CD8<sup>+</sup> T-cell immune response is the result of T-cell activation, proliferation, clonal expansion, differentiation, and development of effector function. Studies of T-cell receptors (TCR) transgenic T cells have revealed that clonal expansion can occur even when the outcome of the immune response is clonal deletion or unresponsiveness (*1,2*). In fact, a number of recent studies have shown that development of CTL activity can be uncoupled from proliferation and clonal expansion (*3–5*). Development of full CTL

activity is dependent upon naïve T cells receiving signals such as IL-12 in addition to peptide/major histocompatibility complex and B7 (6,7). Thus, *in vivo* cytotoxic function cannot be determined based solely on standard measurements of cell activation and cell division.

Measuring specific killing *in vivo* requires the ability to track a specific target population. The intravital fluorescent dye, carboxyfluorescein diacetate succinimidyl ester (CFSE), has been used for tracking cells *in vivo*. CFSE passively diffuses into cells where it is enzymatically cleaved and becomes highly fluorescent. Conjugation with intracellular proteins ensures retention of the dye within cells without leakage. Identification of adoptively transferred lymphocytes labeled with CFSE has been reported at least 2–3 mo after injection (8). The dye has been used extensively for studying lymphocyte migration (9) and cell division (10) and does not interfere with cytotoxic function (8). We (7) and others (6,11–14) have applied this versatile and easy to use dye to determine peptide-specific CD8<sup>+</sup> T-cell killing *in vivo*. The efficacy of the immunizing or tolerizing regimen is tested by coinjecting target and control splenocytes and monitoring the specific lysis of the peptide-bearing targets. The immunizing or tolerizing regimen and the timing of the target cell injection can vary depending on the system used and the question investigated. To ensure that effector cells are present and to determine their phenotype, the process of tracking these cells *in vivo* is also described in this chapter. Effector mice are prepared by adoptively transferring peptide-specific TCR transgenic CD8<sup>+</sup> T cells into syngeneic C57Bl/6 recipients. The adoptively transferred mice are immunized with antigen to generate effector CD8 T cells or left unimmunized (naïve) to serve as negative controls.

## 2. Materials

### 2.1. Preparation of Recipients for Target Cell Injection

1. C57Bl/6 mice.
2. OT-I.PL RAG<sup>-/-</sup> TCR transgenic mice.
3. EHAA complete medium: Click's medium (EHAA) (Biosource, Camarillo, CA) supplemented with 10% heat-inactivated (57°C for 20 min) fetal bovine serum (FBS, Atlas Biologicals, Fort Collins, CO), penicillin/streptomycin (final concentration of 100 I.U./mL), L-glutamine (final concentration of 2 mM), gentamicin (final concentration of 20 µg/mL), and 2-ME (final concentration of 50 µM, prepare a stock solution of 0.1 M diluted with PBS, filter-sterilize, and store at 4°C, do not inhale fumes) (*see Note 1*).
4. 60 × 15-mm Tissue culture dishes (BD Falcon, Bedford, MA).
5. 3-cc Syringes (Kendall, Mansfield, MA).
6. 50-mL Polypropylene conical tubes (BD Falcon).
7. 5-mL Polystyrene round-bottom tubes (BD Falcon).

8. Nylon filters (Sefar America, Depew, NY) (*see Note 2*).
9. Trypan blue solution (0.4%) (Sigma, St. Louis, MO) (toxic, wear gloves, prepare a stock solution that is 0.16% diluted with PBS, and stored in 4-mL aliquots at room temperature for use). Dilute 1:1 with PBS/cells for counting.
10. Hemocytometer.
11. Sorter buffer: HBSS (Gibco/BRL, Gaithersburg, MD) supplemented with 2% heat-inactivated FBS and 0.1% sodium azide (very toxic, wear gloves and mask, 5% stock solution made in ddH<sub>2</sub>O, dissolve solution thoroughly, and filter-sterilize, store at room temperature).
12. Phycoerythrin (PE)-labeled anti-CD8 $\alpha$  (eBioscience, San Diego, CA).
13. Fluorescein isothiocyanate (FITC)-labeled anti-V $\alpha$ 2 (BD PharMingen, San Diego, CA).
14. 1-cc Tuberculin syringes (Sherwood Medical, St. Louis, MO).

## 2.2. Single Cell Suspension of Target Splenocytes

1. C57Bl/6 mouse spleen.
2. 60  $\times$  15-mm Tissue culture dishes.
3. 3-cc Syringes.
4. 50-mL Polypropylene conical tubes.
5. Nylon filters.
6. EHAA complete medium.
7. ACK lysing buffer (Biosource).
8. PBS (Cellgro, Herndon, VA).

## 2.3. Peptide Labeling of Target Splenocytes

1. EHAA complete media.
2. OVA<sub>257-264</sub> synthetic peptide (SIINFEKL; Research Genetics) dissolved in PBS at 200-mM stock and stored at  $-80^{\circ}\text{C}$  in small aliquots for addition to cell suspensions as required.
3. Trypan blue.
4. Hemocytometer.
5. HBSS.

## 2.4. CFSE Cell Labeling and Intravenous Injection of Target Splenocytes

1. CFSE (Molecular Probes) dissolved at 5 mM in dimethyl sulfoxide (DMSO) and stored in small aliquots at  $-20^{\circ}\text{C}$  before being added to cell suspensions as required. Stock CFSE<sup>low</sup> solution is prepared fresh by diluting the 5 mM stock 1:10 in DMSO and is discarded after each use (*see Note 3*).
2. Trypan blue.
3. Hemocytometer.
4. HBSS.
5. EHAA complete medium.
6. 1-cc Tuberculin syringes.

### **2.5. Preparation of Splenocytes for Analysis**

1. EHAA complete medium.
2. 60 × 15-mm Tissue culture dishes.
3. 3-cc Syringes.
4. Sorter buffer (*see Subheading 2.1.*).
5. 50-mL Conical tubes.
6. Nylon filters.
7. 5-mL Round-bottom tubes.

### **2.6. Flow Cytometry to Determine Percent-Specific Cell Lysis**

1. Sorter buffer.
2. 5-mL Round-bottom tubes.

### **2.7. Antibody Staining and Flow Cytometry to Determine Percentage of Peptide-Specific CD8 T Cells**

1. Sorter buffer.
2. 5-mL Round-bottom tubes.
3. Allophycocyanin-labeled anti-CD8 $\alpha$  (eBioscience).
4. Peridinin chlorophyll protein-labeled anti-CD90.1 (BD PharMingen).

## **3. Methods**

### **3.1. Preparation of Recipients for Target Cell Injection**

1. The procedure should be performed under tissue culture conditions.
2. Pipet 1 mL of EHAA complete medium into a 60 × 15-mm tissue culture dish on ice.
3. Harvest OT-I.PL RAG<sup>-/-</sup> mouse lymph nodes (inguinal, brachial, axillary, cervical, mesenteric, and paraaortic) and place them in the tissue culture dish containing added medium on ice (*see Note 4*).
4. Mechanically disrupt/crush the lymph nodes with the flat portion of a 3-mL syringe plunger until only small fragments remain.
5. Wash the top portion of the syringe with 3 mL EHAA complete medium and add it to the tissue culture dish.
6. Pipet the cells up and down to break up any clumps.
7. Transfer the cells through a nylon filter into a 50-mL conical tube.
8. Rinse the tissue culture dish with 5 mL EHAA complete medium.
9. Pipet up and down and add to the filter.
10. Repeat rinses three to four times.
11. Centrifuge the cells at 400g for 5–10 min at 4°C.
12. Remove the supernatant and resuspend the pellet in 10 mL of EHAA complete medium.
13. Count the live mononuclear cells by trypan blue exclusion using a hemocytometer.
14. Remove 50  $\mu$ L of the single cell suspension and place in a 5-mL round-bottom tube for flow cytometry staining. Store the remaining cells on ice.

15. To the 50  $\mu\text{L}$  sample, add 150  $\mu\text{L}$  of sorter buffer with 0.5  $\mu\text{L}$  of PE-labeled anti-CD8 $\alpha$  and 0.5  $\mu\text{L}$  of FITC-labeled V $\alpha$ 2.
  - a. Incubate the cells on ice for 20 min.
  - b. Add 3 mL of sorter buffer.
  - c. Centrifuge the cells at 400g for 5–10 min at 4°C.
  - d. Remove the supernatant and resuspend the pellet in sorter buffer.
  - e. Wash the cells again with sorter buffer.
  - f. Add 0.5 mL of sorter buffer and proceed to flow cytometry.
  - g. Determine the percentage of CD8<sup>+</sup> V $\alpha$ 2<sup>+</sup> OT-I cells in the live lymphocyte gate. Representative flow cytometry dot plots are shown in [Fig. 1A](#).
  - h. Calculate the absolute number of CD8<sup>+</sup>V $\alpha$ 2<sup>+</sup> OT-I cells present by multiplying the total number of live mononuclear cells with the percentage of CD8<sup>+</sup>V $\alpha$ 2<sup>+</sup> OT-I cells.
16. Inject  $1 \times 10^6$  CD8<sup>+</sup>V $\alpha$ 2<sup>+</sup> OT-I cells in a volume of 0.3 mL per recipient (*see Note 5*).
17. The following day, immunize the mice, leaving one set of unimmunized (naïve) mice as control recipients.

### 3.2. Single Cell Suspension of Target Splenocytes

1. The procedure should be performed under sterile tissue culture conditions.
2. Pipet 1 mL of EHAA complete medium into a 60  $\times$  15-mm tissue culture dish on ice.
3. Harvest a C57Bl/6 mouse spleen and place it in the tissue culture dish containing medium on ice.
4. Mechanically disrupt/crush the spleen with the flat portion of a 3-cc syringe plunger until no fragments remain.
5. Wash the top portion of the syringe with 3 mL EHAA complete medium, adding it to the tissue culture dish.
6. Pipet the cells up and down to break up any clumps.
7. Transfer the cells through a nylon filter into a 50-mL conical tube.
8. Rinse the tissue culture dish with 5 mL of EHAA complete medium.
9. Pipet up and down and add to the filter.
10. Repeat rinses three to four times.
11. Centrifuge the cells at 400g for 5–10 min at 4°C.
12. Remove the supernatant and resuspend the pellet in 1–2 mL of ACK lysis buffer to lyse the red blood cells.
13. Mix/vortex the cells.
14. Let the cell suspension stand at room temperature for 1–3 min with gentle agitation until red blood cells have been lysed.
15. Fill the tube with cold PBS.
16. Centrifuge the cells at 400g for 5–10 min at 4°C.
17. Remove the supernatant and resuspend the cell pellet in PBS.
18. Wash the cells with PBS two more times.
19. Resuspend the cells in EHAA complete medium.
20. Refilter the cells if clumps are present.
21. Proceed to peptide labeling.



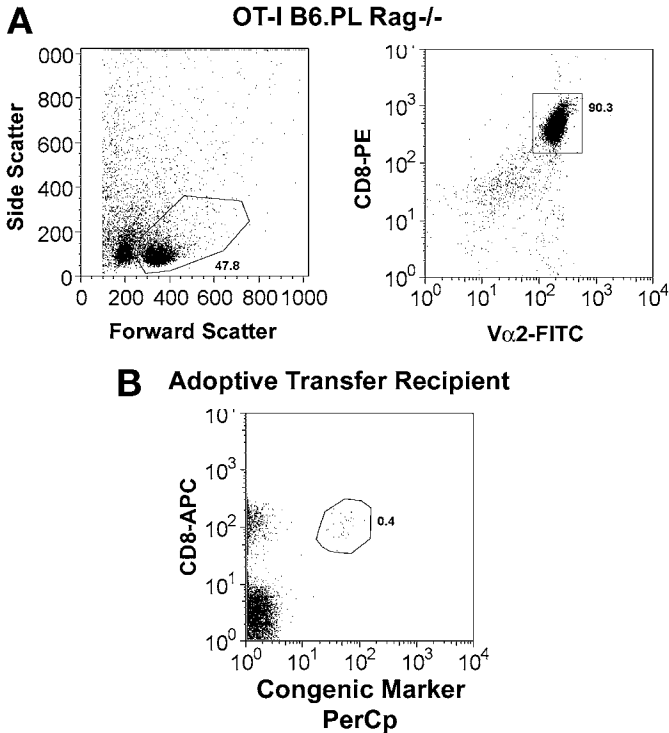


Fig. 1. Adoptive transfer of T-cell receptor (TCR) transgenic CD8<sup>+</sup> T cells. **(A)** Flow cytometry dot plots identifying OT-I cells from a single cell suspension of lymph node cells from an OT-I TCR transgenic Rag<sup>-/-</sup> mouse. The OT-I cells are CD8<sup>+</sup> and V $\alpha$ 2<sup>+</sup>. The numbers indicate the percentage of cells within the indicated gate. Ninety percent of the live mononuclear cells are the TCR transgenic T cells. **(B)** Flow cytometry dot plot identifying the percentage of OT-I cells within a single cell suspension of splenocytes from a naïve (nonimmunized) adoptively transferred mouse. The cells are separated from the endogenous C57Bl/6 CD8<sup>+</sup> T cells based on their cell surface expression of a congenic marker.

### 3.3. Peptide Labeling of Target Splenocytes

1. Count the mononuclear cells by trypan blue exclusion using a hemocytometer.
2. Resuspend the cells at  $5 \times 10^6$ /mL of EHAA complete medium.
3. Divide the cells equally into two tubes. Label one tube “peptide-pulsed” target cells and the other tube “unpulsed” target cells.
4. To the antigen-pulsed target cells, add OVA<sub>257–264</sub> peptide at 1  $\mu$ L/mL from a 200- $\mu$ M stock (*see Note 6*).
5. Add an equivalent amount of PBS (or a control peptide) to the unpulsed target cells.
6. Incubate the cells in a 37°C water bath for 1 h.
7. Wash the cells with EHAA complete medium.

8. Centrifuge the cells at 400g for 5–10 min at 4°C.
9. Resuspend the cell pellet in HBSS.
10. Wash the cells with HBSS two more times to assure removal of any unbound peptide.
11. Proceed to CFSE labeling.

### 3.4. CFSE Cell Labeling and Intravenous Injection of Target Splenocytes

1. Count *all* live cells (including residual red blood cells) by trypan blue exclusion using a hemocytometer.
2. Resuspend the cells in HBSS at  $50 \times 10^6$ /mL.
3. Thaw an aliquot of 5 mM stock CFSE solution.
4. Make a fresh CFSE<sup>low</sup> stock solution by diluting 5 mM stock 1:10 in DMSO (a final concentration of 0.5 mM).
5. Incubate the unpulsed target splenocytes with the higher concentration of CFSE (CFSE<sup>high</sup>): add 1  $\mu$ L of the 5 mM stock CFSE for each milliliter of peptide-pulsed target splenocytes (yielding a final concentration of 5  $\mu$ M). Pipet the cells up and down to ensure homogenous mixing (*see Note 7*).
6. Incubate the peptide-pulsed splenocytes with the lower concentration of CFSE (CFSE<sup>low</sup>): add 1  $\mu$ L of 0.5 mM stock CFSE for each milliliter of control-pulsed cells (final concentration of 0.5  $\mu$ M). Pipet the cells up and down to ensure homogenous mixing.
7. Incubate the cells in a water bath at 37°C for 10 min. Gently and periodically agitate the cells.
8. Add 5–10X the volume of prewarmed EHAA complete medium to the dye-labeled cells to stop the reaction (*see Note 8*).
9. Centrifuge the cells at 400g for 5–10 min at 4°C.
10. Remove the supernatant and resuspend the pellet in cold EHAA complete medium.
11. Wash the cells two more times with cold EHAA complete medium.
12. Recount the mononuclear cells by trypan blue exclusion using a hemocytometer.
13. Wash the cells with HBSS.
14. Resuspend each cell population in HBSS at a concentration of  $67 \times 10^6$  mononuclear cells per milliliter.
15. Combine an equal volume (~equal numbers) of peptide-pulsed CFSE<sup>low</sup> cells with control-pulsed CFSE<sup>high</sup> cells.
16. Inject intravenously 300  $\mu$ L of the combined cell populations into the tail vein of each recipient prepared in **Subheading 3.1**. Each recipient should receive approx  $10 \times 10^6$  peptide-pulsed target splenocytes combined with approx  $10 \times 10^6$  unpulsed splenocytes (*see Note 9*).
17. Wait for 4 h then proceed to the analysis.

### 3.5. Preparation of Splenocytes for Analysis

1. Pipet 1 mL of EHAA complete medium into a 60  $\times$  15-mm tissue culture dish. Place the tissue culture dish on ice. One tissue culture dish is required for each spleen harvested.

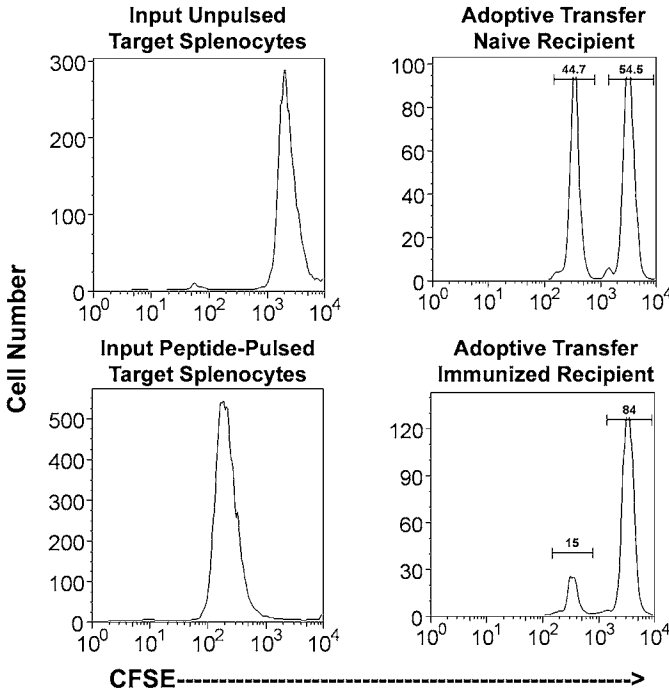
2. Harvest spleens from recipient mice injected with CFSE-labeled target cells 4 h earlier and place each spleen into a separate tissue culture dish containing the added medium on ice.
3. Mechanically disrupt/crush the spleen with the flat portion of a 3-cc syringe plunger until no fragments remain.
4. Wash the top portion of the syringe with 3 mL of sorter buffer, adding it to the tissue culture dish.
5. Pipet the cells up and down to break up any clumps.
6. Transfer the cells through a nylon filter into a 50-mL conical tube.
7. Rinse the tissue culture dish with 5 mL of sorter buffer.
8. Pipet up and down and add to the filter.
9. Repeat rinses three to four times.
10. Centrifuge the cells at 400g for 5–10 min at 4°C.
11. Remove the supernatant and resuspend the pellet in 10 mL of sorter buffer.
12. Remove 0.5 mL of spleen cell suspension and place in a 5-mL round-bottom tube for flow cytometric analysis to determine the percent-specific cell lysis.
13. Proceed to flow cytometry.

### **3.6. Flow Cytometry to Determine Percent-Specific Cell Lysis**

1. Flow cytometry is performed to determine the percentage of cells having low and high content of CFSE. The two target populations are distinguished based on the differences in their CFSE intensity. CFSE can be analyzed using a flow cytometer equipped with 488 nm excitation and emission filters, appropriate for fluorescein.
2. Set the flow cytometry gates using naïve recipient mice (i.e., not challenged with antigen) that have been injected with the two target populations. Representative flow cytometry histograms are shown in [Fig. 2](#).
3. Draw a gate identifying CFSE<sup>low</sup> cells.
4. Draw a gate identifying CFSE<sup>high</sup> cells.
5. Collect 5000–10,000 total CFSE positive cells.
6. Determine the percentage of CFSE<sup>high</sup> and CFSE<sup>low</sup> cells.
7. Calculate the ratio of unpulsed to pulsed target cells in the naïve (unimmunized) mice. This will define the 0% lysis level.
8. The percent-specific lysis is determined by loss of the antigen-pulsed CFSE<sup>low</sup> population compared with the unpulsed CFSE<sup>high</sup> control population using the formula:  $[1 - (\text{ratio in naive mouse} / \text{ratio in experimental mouse})] \times 100$ .

### **3.7. Antibody Staining and Flow Cytometry to Determine the Percentage of Antigen-Specific CD8<sup>+</sup> T Cells**

1. Remove 0.2 mL of spleen cell suspension and place in a 5-mL round-bottom tube for flow cytometric analysis to determine the percentage of antigen-specific CD8<sup>+</sup> T cells present.
2. Determine the number of live mononuclear cells in the single spleen cell suspension by trypan blue exclusion using a hemocytometer.



**Calculation**

Ratio in Naive Mouse = 54.5%/44.7% = 1.2

Ratio in Immunized Mouse = 84%/15% = 5.6

**Percent-Specific Lysis** =  $[1 - (1.2/5.6)] \times 100 = [1 - 0.21] \times 100 = 79\%$

Fig. 2. Determining cytotoxic T lymphocyte (CTL) killing in vivo. The left upper panel is a representative histogram plot depicting the carboxyfluorescein diacetate succinimidyl ester (CFSE) intensity of the CFSE<sup>high</sup>-labeled unpulsed target splenocytes before injection. The left lower panel is a representative histogram plot depicting the CFSE intensity of the CFSE<sup>low</sup>-labeled peptide-pulsed target splenocytes before injection. The right upper panel is a representative histogram plot depicting the CFSE intensity of the total CFSE positive population. Markers are used to distinguish the CFSE<sup>high</sup> and CFSE<sup>low</sup> populations. The numbers above the markers indicate the percentage of the total CFSE positive population. The calculation determines the percent-specific lysis from the formula described in **Subheading 3.6**.

3. Add 1  $\mu$ L of allophycocyanin-labeled anti-CD8 and 1  $\mu$ L of peridinin chlorophyll protein-labeled anti-CD90.1 to each sample and incubate the cells on ice for 20 min. Protect cells from the light.
4. Add 3 mL of sorter buffer.

5. Centrifuge the cells at 400g for 5–10 min at 4°C.
6. Remove the supernatant and resuspend the pellet in sorter buffer.
7. Wash the cells once more with sorter buffer.
8. Resuspend the pellet in 0.5 mL of sorter buffer.
9. Proceed to flow cytometry.
10. Flow cytometry is performed to determine the numbers of peptide-specific cells present in the spleen suspension.
11. The peptide-specific CD8<sup>+</sup> T-cell population is identified based on its expression of CD8 and the congenic marker CD90.1.
12. Set the flow cytometry gates using control mice administered with antigen-specific CD8<sup>+</sup> T cells but not immunized. This will determine the baseline level of antigen-specific T cells.
13. Collect at least 50,000–100,000 live lymphocytes.
14. Determine the percentage of CD8<sup>+</sup>CD90.1<sup>+</sup> cells. A representative flow cytometry dot plot is shown in **Fig. 1B**.
15. Calculate the absolute number of antigen-specific cells by multiplying the percentage of cells by the number of live mononuclear cells determined (*see Note 10*).

#### 4. Notes

1. All solutions should be prepared using sterile conditions and lipopolysaccharide-free reagents. Media should be filter-sterilized.
2. Nylon filters should be cut into 2 × 2 in. squares and autoclaved.
3. Lyophilized CFSE powder should be warmed and dissolved in high quality DMSO to create a 5-mM stock solution. CFSE is best stored at –20°C, desiccated and protected from light. To avoid repeated freezing and thawing, store the stock solution in small aliquots. Add to cell suspensions as required.
4. The protocol is written for the adoptive transfer of ovalbumin peptide-specific TCR transgenic CD8<sup>+</sup> T cells as the effector population but could be adopted for other TCR transgenic CD8<sup>+</sup> T cells. Identification and tracking of these cells *in vivo* is by the cell surface expression of a congenic marker, CD90.1. Other congenic markers such as, CD45.1 could also be used. In addition, tracing an endogenous population of CD8<sup>+</sup> T cells using major histocompatibility complex class I peptide tetramers could be applied.
5. Air bubbles must be removed from the syringe. Mice can be warmed under a heat lamp for 1–3 min. Wipe the tail with ethyl alcohol swabs before injections.
6. This protocol was written for use of a specific ovalbumin peptide but can be adapted for other peptide target systems. The peptide used to pulse the splenocytes can be replaced with the peptide of choice. The concentration to add to the splenocytes would need to be optimized. Sufficient washing of cells after labeling should be performed to ensure removal of any unbound peptide.
7. Dye-labeling may vary. To ensure uniform staining, be sure that cells are in a single cell suspension without clumps, debris, or cell aggregates. Pipet the cells gently after CFSE is added to the suspension. We have found that optimal separation

between the two target populations is achieved using a 10-fold difference in dye concentrations. We have labeled the peptide-pulsed target population with the higher and the lower concentration of CFSE with similar results.

8. Prewarmed EHAA complete medium decreases cell death/loss from the dye-labeling process.
9. One recipient of the combined target splenocytes should be a naïve (nonimmunized) recipient and used as a control to determine the 0% lysis level.
10. The naïve recipient should be used as a control for the baseline number of transferred OT-I cells. The phenotype of the effector OT-I cells could be obtained using more than four-color flow cytometry to further phenotype the cells. Avoid using fluorescent dyes that are identified in the FL-2 channel because of difficulty, at times, compensating for the CFSE labeling.

## Acknowledgments

The author would like to thank Dr. Traci Zell for her critical review of the manuscript and to Dawn Taylor for technical assistance. The work was supported by the American Heart Association, the American Society of Nephrology and the American Transplant Society.

## References

1. Itano, A. A., McSorley, S. J., Reinhardt, R. L., et al. (2003) Distinct dendritic cell populations sequentially present antigen to CD4 T cells and stimulate different aspects of cell-mediated immunity. *Immunity* **19**, 47–57.
2. Kearney, E. R., Pape, K. A., Loh, D. Y., and Jenkins, M. K. (1994) Visualization of peptide-specific T cell immunity and peripheral tolerance induction *in vivo*. *Immunity* **1**, 327–339.
3. Curtsinger, J. M., Johnson, C. M., and Mescher, M. F. (2003) CD8 T cell clonal expansion and development of effector function require prolonged exposure to antigen, costimulation, and signal 3 cytokine. *J. Immunol.* **171**, 5165–5171.
4. Grabie, N., Delfs, M. W., Westrich, J. R., et al. (2003) IL-12 is required for differentiation of pathogenic CD8+ T cell effectors that cause myocarditis. *J. Clin. Invest.* **111**, 671–680.
5. Hernandez, J., Aung, S., Marquardt, K., and Sherman, L. A. (2002) Uncoupling of proliferative potential and gain of effector function by CD8(+) T cells responding to self-antigens. *J. Exp. Med.* **196**, 323–333.
6. Curtsinger, J. M., Lins, D. C., and Mescher, M. F. (2003) Signal 3 determines tolerance versus full activation of naïve CD8 T cells: dissociating proliferation and development of effector function. *J. Exp. Med.* **197**, 1141–1151.
7. Filatenkov, A. A., Jacovetty, E. L., Fischer, U. B., Curtsinger, J. M., Mescher, M. F., and Ingulli, E. (2005) CD4 T cell-dependent conditioning of dendritic cells to produce IL-12 results in CD8-mediated graft rejection and avoidance of tolerance. *J. Immunol.* **174**, 6909–6917.

8. Oehen, S., Brduscha-Riem, K., Oxenius, A., and Odermatt, B. (1997) A simple method for evaluating the rejection of grafted spleen cells by flow cytometry and tracing adoptively transferred cells by light microscopy. *J. Immunol. Methods* **207**, 33–42.
9. Weston, S. A. and Parish, C. R. (1990) New fluorescent dyes for lymphocyte migration studies. Analysis by flow cytometry and fluorescence microscopy. *J. Immunol. Methods* **133**, 87–97.
10. Lyons, A. B. and Parish, C. R. (1994) Determination of lymphocyte division by flow cytometry. *J. Immunol. Methods* **171**, 131–137.
11. Aichele, P., Brduscha-Riem, K., Oehen, S., et al. (1997) Peptide antigen treatment of naive and virus-immune mice: antigen-specific tolerance versus immunopathology. *Immunity* **6**, 519–529.
12. Coles, R. M., Mueller, S. N., Heath, W. R., Carbone, F. R., and Brooks, A. G. (2002) Progression of armed CTL from draining lymph node to spleen shortly after localized infection with herpes simplex virus 1. *J. Immunol.* **168**, 834–838.
13. Mueller, S. N., Jones, C. M., Smith, C. M., Heath, W. R., and Carbone, F. R. (2002) Rapid cytotoxic T lymphocyte activation occurs in the draining lymph nodes after cutaneous herpes simplex virus infection as a result of early antigen presentation and not the presence of virus. *J. Exp. Med.* **195**, 651–656.
14. Oehen, S. and Brduscha-Riem, K. (1998) Differentiation of naive CTL to effector and memory CTL: correlation of effector function with phenotype and cell division. *J. Immunol.* **161**, 5338–5346.

## Thymic Involution

### *Implications for Self-Tolerance*

Frances T. Hakim and Ronald E. Gress

#### Summary

The thymus contributes to the regulation of tolerance and the prevention of autoimmunity at many levels. First, auto-reactive CD4<sup>+</sup> and CD8<sup>+</sup> T cells are clonally deleted during negative selection in the thymus, establishing central tolerance. The unique expression of the AIRE (autoimmune regulator) gene in medullary thymic epithelial cells results in expression of a broad array of tissue-specific antigens. Thymocytes bearing T-cell receptors that bind to these tissue-specific antigens are clonally deleted. This process removes self-reactive T cells from the repertoire before T cells are exported to the periphery. Second, CD4<sup>+</sup>CD25<sup>bright</sup> regulatory T cells (Treg) develop in parallel with CD4<sup>+</sup> and CD8<sup>+</sup> effector T cells in the thymus (1,2). Unlike T effector cells, Treg fail to be deleted by exposure to tissue antigens during thymic maturation (3). After export to the periphery, Treg cells play a critical role in the prevention of autoimmunity, suppression of inflammatory responses, and the modulation of T-cell homeostasis (4,5). Finally, productive thymopoiesis, in and of itself, may be a factor deterring autoimmunity. The thymus continuously generates stable, resting populations of naïve T cells that maintain the numbers and the diversity of the T-cell repertoire. Under conditions of lymphopenia prolonged by inadequate thymopoiesis, compensatory peripheral expansion of T cells occurs to maintain stable T-cell levels. Under circumstances in which the repertoire is limited, homeostatic proliferation may increase the opportunity for T-cells reactive with self antigens to expand, leading to autoimmune disorders (6). In all of these respects, the thymus maintains immunologic tolerance to self. Given the importance of the thymus in control of autoimmunity, the gradual age-dependent decline in thymic cytoarchitecture and thymopoietic productivity may, therefore, contribute to the development of auto-reactivity and loss of self-tolerance.

**Key Words:** Thymopoiesis; regulatory T cells; involution; immune reconstitution.

### 1. Age-Dependent Thymic Involution

The thymus attains its greatest size and cellularity in the late fetal and early neonatal period. By computerized tomography, the thymic profile is largest in

From: *Methods in Molecular Biology*, vol. 380: *Immunological Tolerance: Methods and Protocols*  
Edited by: P. J. Fairchild © Humana Press Inc., Totowa, NJ



young children, but declines markedly with age (7). The radiodense parenchyma dwindles and is gradually replaced with diffuse strands in middle-aged adults; frequently, in older individuals no thymic profile is observable (8,9). Histologically, the thymus undergoes progressive involutional changes with age (10–12). Cortical thymic epithelial cell (TEC) markers gradually decline and the lympho–epithelial complexes characteristic of thymic nurse cells decrease. Thymocyte depletion begins in the subcapsular area and then progresses throughout the cortex (11). Perivascular spaces containing connective tissue expand, and thymic medullary and cortical tissues are reduced to small islands, surrounded by adipose and fibrous tissue (10,12).

Despite the quantitative reductions in cortical and medullary tissue, thymopoiesis at some level continues throughout life (10). The processes of positive and negative selection appear to remain qualitatively intact (13). The thymus continues to generate new T cells into the adult years and even into old age (14–16). Thymic productivity has been assessed by the frequency of T cells in the peripheral blood that bear naïve phenotypic markers such as CD45RA and CCR7 or CD62L, or by the frequency of T-cell receptor rearrangement excision circles (TREC). The latter are stable nonreplicating episomal DNA circles generated during thymocyte development, which are retained in T cells, even after export to the periphery (see Chapter 12). Phenotypically, naïve or TREC-bearing cells are found in the peripheral blood, even in the elderly. Yet the frequency of naïve cells steadily declines with age (14–16), as does the main engine of thymic productivity, the intrathymic expansion of developing T cells (17).

A major consequence of the decline in production of naïve cells with age is a decrease in the overall T-cell receptor (TCR) repertoire. Although, naïve T cells express a broad range of TCR, even in the elderly (15,18), the overall TCR repertoire is skewed and marked by oligoclonal expansions. Over time, the expansion of activated T cells in response to antigenic stimulation occupies increased fractions of the repertoire (19–21). Long-lived naïve T cells of diverse repertoire proliferate only at a low rate (22,23), whereas memory T-cells proliferate more rapidly, driven by ongoing cytokine-dependent homeostatic mechanisms (24–26). These mechanisms maintain T-cell numbers at stable levels through the life span of the individual, but, in the face of declining thymic output, gradually reduce repertoire diversity.

Less is known of age or involution-dependent changes in thymic production of regulatory T cells (Treg) relative to CD4<sup>+</sup> or CD8<sup>+</sup> effector T cells. CD4<sup>+</sup>CD25<sup>bright</sup> Treg cells with immunosuppressive function have been found in pediatric thymuses and in cord blood in man (1,2). Although CD4<sup>+</sup>CD25<sup>bright</sup> Treg cells bearing naïve markers (CD45RA<sup>+</sup>CCR7<sup>+</sup>) have been found in adults, those with central or effector memory phenotype are more common (27,28).

Like effector T cells, Treg cells can expand in the periphery after activation; TREC frequencies even in Treg with naïve phenotypes are low, consistent with peripheral expansion (29). Furthermore, activated CD4<sup>+</sup>CD25<sup>-</sup> cells can be converted into CD4<sup>+</sup>CD25<sup>bright</sup> Treg, although the *in vivo* functional role of Treg cells generated by such a conversion has not been determined (30). The numbers of Treg cells in the periphery have been found to actually increase with age, although it is unclear whether these are directly thymically generated or arise by expansion or conversion of effector T cells in the periphery (31). Furthermore, the functional activity of such Treg cells in older donors has been questioned (32).

## 2. Factors Contributing to Thymic Involution

Factors that contribute to thymic involution can be broadly subdivided into those that result from age-dependent systemic changes outside the thymus, those dependent on the thymic epithelial cells that support thymopoiesis, and those intrinsic to thymocyte progenitors and the thymocytes themselves. First, changes in thymopoiesis may result from systemic hormonal changes that occur over the life span of the individual. Growth hormone (GH) levels peak in man in the early twenties and decline with age. This pituitary hormone mediates its functions through production of insulin-like growth factor (IGF)-1, which is primarily produced in the liver but also made by the bone marrow and thymic stroma. The age-dependent decline in GH/IGF-1 has been linked to reduced hematopoiesis and increased deposition of adipose tissue in the bone marrow and thymus (33). HIV+ adults and children have demonstrated a consistent increase in thymic mass and naïve T-cell levels when GH was added to antiretroviral therapy (34,35). Whereas lymphopoiesis may decline due to the age-dependent decrease in GH/IGF-1, the rise in gonadal steroids after puberty—estrogens, progesterone, and androgens—may contribute to the same effect. Ovariectomy produces an increase in the size and cellularity of the thymic cortex and medulla that can be reversed by 17 $\beta$ -estradiol or progesterone (36). Surgical castration results in thymic enlargement and increased T-cell populations, even in the thymuses of old rats, whereas androgen treatment induces involutional changes (37,38). Pharmacologic androgen blockade in man can similarly enhance thymopoiesis, increasing naïve T-cell and TREC levels (39). These data suggest that systemic changes in pituitary and gonadal hormones play a major role in modulating thymic involution.

Second, age-dependent changes in the thymic microenvironment may result in thymic involution. The associated histological changes involve parallel losses in both thymocytes and the nonlymphoid stromal supportive cells. Transplants of young marrow into irradiated aged mice result in repopulation of the thymus with a normal thymocyte subset distribution, but do not reverse the reduced thymocyte

numbers and histological abnormalities found in the thymuses of aged hosts (13). One proposed mechanism for this age-dependent decline in thymopoiesis is reduced production by TEC of the cytokine Interleukin-7 (IL-7). IL-7 is necessary for thymocyte maturation, as evidenced by severely reduced T-cell maturation in both IL-7<sup>-/-</sup> and IL-7R $\alpha$ <sup>-/-</sup> mice (40). IL-7 therapy in vivo and in vitro reduces the apoptotic loss of thymocytes during the transition between subsets of double negative (DN; CD4<sup>-</sup>8<sup>-</sup>) thymocytes in aged mice: the DN1 to DN2 transition (41,42). Levels of IL-7 mRNA in murine thymic stroma do not change for the first 7 mo of life, but then decline 15-fold over the next year (42,43). In contrast, other mRNA associated with the cortical TEC, such as Connexin 43 and keratin-8, decline in the first 3 mo, and then stabilize after 7 mo (42). These differences suggest that the decline in IL-7 is not merely a drop in the relative proportion of cortical TEC in the thymus, but a specific change in the regulation of IL-7 expression (42). Running counter to the argument for a central role for TEC-derived IL-7 is, however, evidence that long-term enhancement of intrathymic IL-7 production does not prevent age-dependent involution or the decline in either double positive thymocytes (DP; CD4<sup>+</sup>8<sup>+</sup>) or single positive cells (SP; CD4<sup>+</sup>8<sup>-</sup> or CD4<sup>+</sup>8<sup>+</sup>) (41). Furthermore, in man, thymic IL-7 mRNA levels are maintained with aging, but intrathymic production of inflammatory cytokines such as leukemia inhibitory factor, oncostatin-M, and IL-6 increases (44). When these cytokines were administered to mice, the cortical DP thymocytes declined and the thymus atrophied (44). Hence, TEC-generated factors, other than IL-7, may play a role in thymic involution.

Finally, T lineage-committed progenitors and thymocytes may be less common or less functional in aged marrow than in young marrow owing to intrinsic programming rather than TEC-derived or systemic factors. In clinical trials, umbilical cord stem cells resulted in higher TREC frequencies than adult bone marrow stem cells, even in young adult recipients (45). In murine competitive repopulation experiments performed on irradiated hosts or in fetal thymic organ cultures, marrow from young mice was consistently more productive than that from old donors in generating thymocytes (46,47). These studies suggest that the frequency of stem cells capable of T lineage commitment may decrease with age. Intrinsic thymocyte programs of gene expression may be altered with age. Ortman has observed a marked decline in the expression of E2A in thymocytes in aging mice and an increase in LMO2, a negative regulator of E2A activities (43). The E2A-encoded transcription factors, E12 and E47, are critical to T-cell maturation, regulating the expression of RAG genes and pre-T $\alpha$  and promoting TCR gene rearrangement. Furthermore, the frequency of functional DN thymocytes may decline with age. The absolute numbers of DN1 cells in the thymuses of young and aged mice are quite comparable in number,

but Min has shown that the DN1 of aged mice have a 40-fold lower frequency of true early thymocyte progenitors (ETP) based on phenotypic criteria (Lin<sup>-</sup>CD4<sup>-</sup>CD8<sup>-</sup>CD44<sup>+</sup>CD25<sup>-</sup>CD117<sup>+</sup>CD127<sup>-</sup>) (48). Furthermore these ETP are functionally less productive in fetal thymic organ cultures and more susceptible to apoptosis (48). This evidence suggests that there is an age-dependent accumulation of dysfunctional progenitors in the thymus.

A deficit in the proportion of functional DN thymocytes present at the earliest step of thymopoiesis could have cascading effects on thymocyte numbers and thymic structure. Adoptive transfer experiments have shown that the number of progenitor binding sites in the thymus is limited and can be saturated (49), and that functional and dysfunctional DN thymocytes can compete for these limited numbers of sites (50). Overall, thymic productivity is determined by the proportion of functional thymocytes present (51). If the dysfunctional T progenitors identified by Min in aged thymuses occupy binding sites for DN cells but do not mature, then there would be less “space” for normal progenitors. An accumulation of dysfunctional ETP in aged thymuses could, therefore, limit stromal sites available for thymopoiesis. Indeed, because the level of expansion of thymic stroma reflects the proportion of functional thymocytes (50), a reduction in functional ETP could result in a loss in TEC and thymic size.

### 3. Capacity for Renewal of Thymopoiesis

Despite the emphasis on the inevitable age-dependent decline of the thymus, the thymus is remarkably capable of renewal of thymopoiesis after severe peripheral cyto-reduction in some adults (9,52). In a cohort of middle-aged to elderly patients undergoing autologous hematopoietic stem cell transplantation for treatment of breast cancer, we were able to examine the frequency, time course, and consequences of thymic recovery without the presence of confounding factors such as hematologic malignancy, immunosuppressive drugs, or graft-vs-host disease (9).

We assessed thymic structural change during the posttransplant period by evaluating serial thoracic CT scans using a four-point thymic size index (8,9,53). The thymic profile was extremely reduced in size by the end of transplant conditioning (thymic index [TI] = 0) and, in most patients, thymic size remained minimal after transplantation (*see* Figs. 1 and 2). In one-third of the patients, however, thymic size gradually increased, attaining a maximum TI at or more than 2, the size of the typical thymus in middle-aged adults (8,9). Furthermore 7 of 32 patients achieved a TI of at least 3, a significantly larger thymic profile with moderate cellularity (*see* Fig. 1D–F). This change in size and radiodensity is particularly remarkable given that only two of these patients had a TI of three prior to the start of therapy. Thus, the development

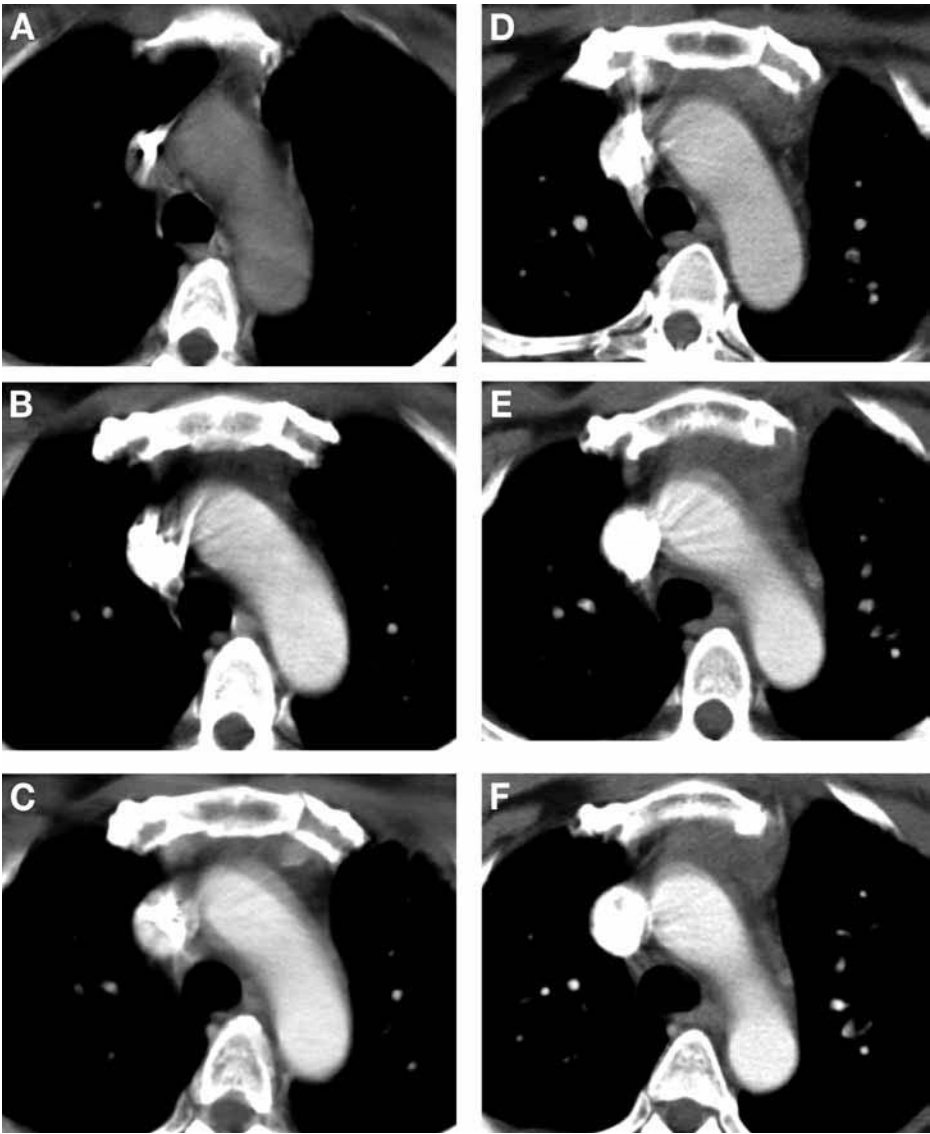


Fig. 1. Time course of thymic recovery following autologous hematopoietic stem cell transplant by serial CT. The patient was 43 yr old at the time of transplantation. The thymus was reduced to a small remnant between the aorta and the sternum at the end of the pretransplant conditioning regimen (thymic index = TI = 1) (A), and was little changed in 6 wk (TI = 1) (B). By 6 mo posttransplant, the expanded thymus had radiodense areas (TI = 2) (C). At 12, 18, and 24 mo posttransplant (D,E,F), the thymus remained large and cellular (TI = 3).

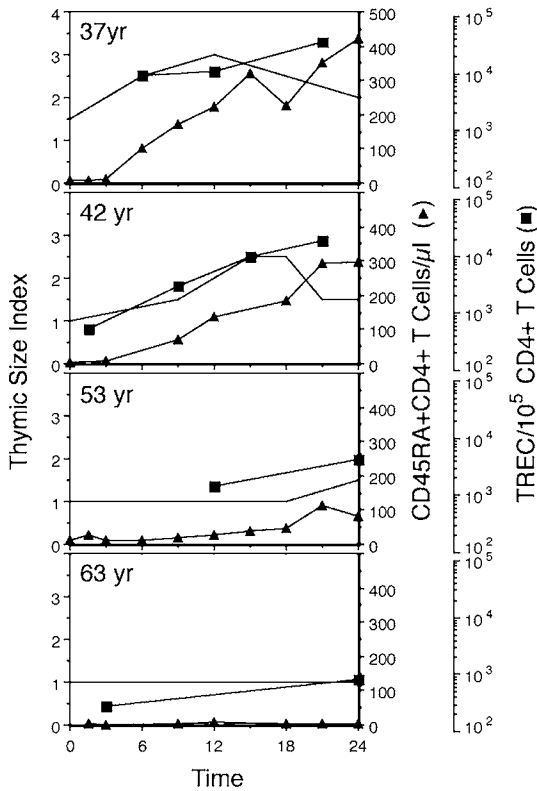


Fig. 2. Time course of the posttransplant recovery of thymic size (solid line), CD45RA<sup>+</sup>CD62L<sup>+</sup> CD4<sup>+</sup> T cells (cells/ $\mu$ L; triangles) and TREC-bearing CD4<sup>+</sup> T cells (TREC/ $10^5$  CD4<sup>+</sup> cells; squares) in the peripheral blood of four typical patients. The 37-yr-old patient demonstrates marked increase in thymic size by 6 mo, peaking at 12 mo. The frequency of TREC-bearing cells is elevated in the CD4<sup>+</sup> T-cell population by 6 mo and the absolute number of naive CD4<sup>+</sup> cells steadily increases during the first 24 mo. The 42-yr-old patient demonstrates a similar renewal of thymopoiesis, but over a more protracted time course, and a lower recovery of naive cells. At 53 and 63 yr, typical patients demonstrate little thymic recovery or return of naive cells.

of a radiodense thymic profile posttransplant in these patients represented not merely a return to the pretreatment condition, but an increase over their previous status.

Two points are worth noting. The first is that the maximum thymic size attained correlated strongly with age. Whereas four out of five of the patients aged 30–39 showed a significant thymic enlargement, the incidence of thymic recovery dropped to only 6 of 13 patients among those aged 40–49, and only

2 of 14 over 50 yr of age demonstrated any thymic enlargement from the treatment nadir (9). Second, the development of thymic enlargement proceeded very slowly, requiring 6–12 mo in younger patients to reach maximal size and as long as 24 mo in older patients showing thymic recovery (see Figs. 1 and 2).

The changes in thymic profiles represented a renewal of thymopoiesis. The recovery of radiodense thymic mass correlated strongly with the recovery of newly matured CD4<sup>+</sup> T cells in the peripheral blood. Because more than 95% of naïve CD4<sup>+</sup> T cells are lost during transplant regimens, the reappearance and increase of phenotypically naïve T cells posttransplant can provide an estimate of recovery of newly matured cells and hence an assessment of thymic function (7,54,55). Following APBSCT, levels of naïve (CD45RA<sup>+</sup>CD62L<sup>+</sup>) CD4<sup>+</sup> T cells remained low, returning to normal levels of naïve cells only in the second year, even in patients with the best recovery (see Fig. 2) (9). Consistent with the pattern of thymic enlargement, the production of naïve cells at the end of 2 yr was strongly age dependent, even within this middle-aged cohort of patients. Patients with evident thymic enlargement recovered naïve CD4<sup>+</sup> T cells in the periphery more rapidly and attained the highest levels of phenotypically naïve CD4<sup>+</sup> T cells. We further corroborated the emergence of newly matured T cells from the thymus (recent thymic emigrants [RTE]) by quantitative PCR of TREC in peripheral blood CD3<sup>+</sup>CD4<sup>+</sup> T cells. Using this method, we confirmed that the incidence of patients with a marked recovery of phenotypically naïve or TREC-bearing CD4<sup>+</sup> cells, the total level of these cells achieved over 2 yr, and even the overall time course of naïve T-cell recovery were all age dependent (see Fig. 2). Finally, we examined the TCR repertoire diversity of the newly matured naïve populations posttransplant, determining that a broadly diverse repertoire was generated within naïve CD45RA<sup>+</sup> CD4<sup>+</sup> T cells within a few months. Hence, the thymic role of generating TCR repertoire diversity was maintained in the restored thymus posttransplant.

Renewal of thymopoiesis was further demonstrated to significantly affect overall CD4<sup>+</sup> T-cell recovery. Independent of any early peripheral expansions of residual CD4<sup>+</sup> T cells, the long term recovery of quantitatively normal levels of CD4<sup>+</sup> T cells was strongly based upon renewed thymopoiesis. Individuals with evidence of renewed thymopoiesis were capable of quantitatively restoring normal levels of CD4<sup>+</sup> cells; those lacking effective thymopoiesis remained deficient in CD4<sup>+</sup> populations for as long as 5 yr. Second, renewed thymopoiesis restored the balance of resting effector memory and central memory CD4<sup>+</sup> cells. This effect on memory populations is consistent with an ongoing process of utilization of cells out of the naïve pool, which then restores resting memory pools. Expanding the naïve pool through renewed thymopoiesis would therefore contribute to rebalancing memory populations. The same dependence upon thymopoiesis underlies the recovery of TCR V $\beta$  repertoire diversity in the





severe cyto reduction (and this may be a key factor), the thymus is capable of being recolonized with ETP, expanding and generating significant numbers of naïve T cells. Not only in children, but in most adults under 45 yr of age, the thymus can restore naïve T-cell populations to normal levels, including a broad repertoire of TCR, within 1–2 yr (9,56). The capacity to regenerate Treg populations in adults by thymopoiesis rather than peripheral conversion or expansion has not been adequately studied. Nevertheless, conditions of lymphopenia can contribute to Treg recovery (57). Certainly the recovery of naïve cells with a broad repertoire would run counter to lymphopenia-induced homeostatic expansion and skewing of the repertoire toward autoreactivity (6). The second implication is that age is a critical determinant in deciding whether to use thymic-dependent or thymic-independent strategies for establishing tolerance. In older individuals, strategies that induce tolerance in existing peripheral T-cell populations may be preferable. As described in the following chapters, these strategies may provide alternative routes when thymic-based mechanisms to induce tolerance have failed.

## References

1. Wing, K., Ekmark, A., Karlsson, H., Rudin, A., and Suri-Payer, E. (2002) Characterization of human CD25+ CD4+ T cells in thymus, cord and adult blood. *Immunol.* **106**, 190–199.
2. Wing, K., Larsson, P., Sandstrom, K., Lundin, S. B., Suri-Payer, E., and Rudin, A. (2005) CD4+ CD25+ FOXP3+ regulatory T cells from human thymus and cord blood suppress antigen-specific T cell responses. *Immunol.* **115**, 516–525.
3. Anderson, M. S., Venanzi, E. S., Chen, Z., Berzins, S. P., Benoist, C., and Mathis, D. (2005) The cellular mechanism of Aire control of T cell tolerance. *Immunity* **23**, 227–239.
4. Sakaguchi, S. (2005) Naturally arising Foxp3-expressing CD25(+)CD4(+) regulatory T cells in immunological tolerance to self and non-self. *Nat. Immunol.* **6**, 345–352.
5. Shen, S., Ding, Y., Tadokoro, C. E., et al. (2005) Control of homeostatic proliferation by regulatory T cells. *J. Clin. Invest.* **115**, 3517–3526.
6. King, C., Ilic, A., Koelsch, K., and Sarvetnick, N. (2004) Homeostatic expansion of T cells during immune insufficiency generates autoimmunity. *Cell* **117**, 265–277.
7. Mackall, C. L., Fleisher, T. A., Brown, M. R., et al. (1995) Age, thymopoiesis, and CD4+ T-lymphocyte regeneration after intensive chemotherapy. *N. Engl. J. Med.* **332**, 143–149.
8. McCune, J. M., Loftus, R., Schmidt, D. K., et al. (1998) High prevalence of thymic tissue in adults with human immunodeficiency virus-1 infection. *J. Clin. Invest.* **101**, 2301–2308.
9. Hakim, F. T., Memon, S. A., Cepeda, R., et al. (2005) Age-dependent incidence, time course, and consequences of thymic renewal in adults. *J. Clin. Invest.* **115**, 930–939.

10. Haynes, B. F., Markert, M. L., Sempowski, G. D., Patel, D. D., and Hale, L. P. (2000) The role of the thymus in immune reconstitution in aging, bone marrow transplantation, and HIV-1 infection. *Annu. Rev. Immunol.* **18**, 529–560.
11. Brelinska, R. (2003) Thymic epithelial cells in age-dependent involution. *Microscopy Res. Technique* **62**, 488–500.
12. Shiraishi, J., Utsuyama, M., Seki, S., et al. (2003) Essential microenvironment for thymopoiesis is preserved in human adult and aged thymus. *Clin. Dev. Immunol.* **10**, 53–59.
13. Mackall, C. L., Punt, J. A., Morgan, P., Farr, A. G., and Gress, R. E. (1998) Thymic function in young/old chimeras: substantial thymic T cell regenerative capacity despite irreversible age-associated thymic involution. *Eur. J. Immunol.* **28**, 1886–1893.
14. Douek, D. C. and Koup, R. A. (2000) Evidence for thymic function in the elderly. *Vaccine* **18**, 1638–1641.
15. Jamieson, B. D., Douek, D. C., Killian, S., et al. (1999) Generation of functional thymocytes in the human adult. *Immunity* **10**, 569–575.
16. Douek, D. C., McFarland, R. D., Keiser, P. H., et al. (1998) Changes in thymic function with age and during the treatment of HIV infection. *Nature* **396**, 690–695.
17. Dion, M. L., Poulin, J. F., Bordi, R., et al. (2004) HIV infection rapidly induces and maintains a substantial suppression of thymocyte proliferation. *Immunity* **21**, 757–768.
18. Schwab, R., Szabo, P., Manavalan, J. S., et al. (1997) Expanded CD4+ and CD8+ T cell clones in elderly humans. *J. Immunol.* **158**, 4493–4499.
19. Ouyang, Q., Wagner, W. M., Walter, S., et al. (2003) An age-related increase in the number of CD8+ T cells carrying receptors for an immunodominant Epstein-Barr virus (EBV) epitope is counteracted by a decreased frequency of their antigen-specific responsiveness. *Mech. Ageing Dev.* **124**, 477–485.
20. Ouyang, Q., Wagner, W. M., Wikby, A., et al. (2003) Large numbers of dysfunctional CD8+ T lymphocytes bearing receptors for a single dominant CMV epitope in the very old. *J. Clin. Immunol.* **23**, 247–257.
21. Mackall, C. L., Bare, C. V., Granger, L. A., Sharrow, S. O., Titus, J. A., and Gress, R. E. (1996) Thymic-independent T cell regeneration occurs via antigen-driven expansion of peripheral T cells resulting in a repertoire that is limited in diversity and prone to skewing. *J. Immunol.* **156**, 4609–4616.
22. Goldrath, A. W., Bogatzki, L. Y., and Bevan, M. J. (2000) Naïve T cells transiently acquire a memory-like phenotype during homeostasis-driven proliferation. *J. Exp. Med.* **192**, 557–564.
23. Tough, D. F. and Sprent, J. (1994) Turnover of naïve- and memory-phenotype T cells. *J. Exp. Med.* **179**, 1127–1135.
24. Geginat, J., Lanzavecchia, A., and Sallusto, F. (2003) Proliferation and differentiation potential of human CD8+ memory T-cell subsets in response to antigen or homeostatic cytokines. *Blood* **101**, 4260–4266.
25. Geginat, J., Sallusto, F., and Lanzavecchia, A. (2001) Cytokine-driven proliferation and differentiation of human naïve, central memory, and effector memory CD4(+) T cells. *J. Exp. Med.* **194**, 1711–1719.

26. Fry, T. J. and Mackall, C. L. (2005) The many faces of IL-7: from lymphopoiesis to peripheral T cell maintenance. *J. Immunol.* **174**, 6571–6576.
27. Beyer, M., Kochanek, M., Giese, T., et al. (2006) In vivo peripheral expansion of naïve CD4+CD25high FOXP3+ regulatory T cells in patients with multiple myeloma. *Blood* **107**, 3940–3949.
28. Seddiki, N., Santner-Nanan, B., Tangye, S. G., et al. (2006) Persistence of naïve CD45RA+ regulatory T cells in adult life. *Blood* **107**, 2830–2838.
29. Beyer, M., Kochanek, M., Darabi, K., et al. (2005) Reduced frequencies and suppressive function of CD4+CD25hi regulatory T cells in patients with chronic lymphocytic leukemia after therapy with fludarabine. *Blood* **106**, 2018–2025.
30. Walker, M. R., Kasprovicz, D. J., Gersuk, V. H., et al. (2003) Induction of FoxP3 and acquisition of T regulatory activity by stimulated human CD4+CD25- T cells. *J. Clin. Invest.* **112**, 1437–1443.
31. Gregg, R., Smith, C. M., Clark, F. J., et al. (2005) The number of human peripheral blood CD4+ CD25high regulatory T cells increases with age. *Clin. Exp. Immunol.* **140**, 540–546.
32. Tsaknaris, L., Spencer, L., Culbertson, N., et al. (2003) Functional assay for human CD4+CD25+ Treg cells reveals an age-dependent loss of suppressive activity. *J. Neurosci. Res.* **74**, 296–308.
33. French, R. A., Broussard, S. R., Meier, W. A., et al. (2002) Age-associated loss of bone marrow hematopoietic cells is reversed by GH and accompanies thymic reconstitution. *Endocrinol.* **143**, 690–699.
34. Viganò, A., Saresella, M., Trabattoni, D., et al. (2004) Growth hormone in T-lymphocyte thymic and postthymic development: a study in HIV-infected children. *J. Pediatr.* **145**, 542–548.
35. Napolitano, L. A., Lo, J. C., Gotway, M. B., et al. (2002) Increased thymic mass and circulating naïve CD4 T cells in HIV-1-infected adults treated with growth hormone. *Aids* **16**, 1103–1111.
36. Leposavic, G., Obradovic, S., Kosec, D., Pejčić-Karapetrovic, B., and Vidic-Dankovic, B. (2001) In vivo modulation of the distribution of thymocyte subsets by female sex steroid hormones. *Int. Immunopharmacol.* **1**, 1–12.
37. Greenstein, B. D., Fitzpatrick, F. T., Adcock, I. M., Kendall, M. D., and Wheeler, M. J. (1986) Reappearance of the thymus in old rats after orchidectomy: inhibition of regeneration by testosterone. *J. Endocrinol.* **110**, 417–422.
38. Windmill, K. F. and Lee, V. W. (1998) Effects of castration on the lymphocytes of the thymus, spleen and lymph nodes. *Tissue Cell* **30**, 104–111.
39. Sutherland, J. S., Goldberg, G. L., Hammett, M. V., et al. (2005) Activation of thymic regeneration in mice and humans following androgen blockade. *J. Immunol.* **175**, 2741–2753.
40. Peschon, J. J., Morrissey, P. J., Grabstein, K. H., et al. (1994) Early lymphocyte expansion is severely impaired in interleukin 7 receptor-deficient mice. *J. Exp. Med.* **180**, 1955–1960.

41. Phillips, J. A., Brondstetter, T. I., English, C. A., Lee, H. E., Virts, E. L., and Thoman, M. L. (2004) IL-7 gene therapy in aging restores early thymopoiesis without reversing involution. *J. Immunol.* **173**, 4867–4874.
42. Andrew, D. and Aspinall, R. (2002) Age-associated thymic atrophy is linked to a decline in IL-7 production. *Exp. Gerontol.* **37**, 455–463.
43. Ortman, C. L., Dittmar, K. A., Witte, P. L., and Le, P. T. (2002) Molecular characterization of the mouse involuted thymus: aberrations in expression of transcription regulators in thymocyte and epithelial compartments. *Int. Immunol.* **14**, 813–822.
44. Sempowski, G. D., Hale, L. P., Sundy, J. S., et al. (2000) Leukemia inhibitory factor, oncostatin M, IL-6, and stem cell factor mRNA expression in human thymus increases with age and is associated with thymic atrophy. *J. Immunol.* **164**, 2180–2187.
45. Talvensarri, K., Clave, E., Douay, C., et al. (2002) A broad T-cell repertoire diversity and an efficient thymic function indicate a favorable long-term immune reconstitution after cord blood stem cell transplantation. *Blood* **99**, 1458–1464.
46. Sharp, A., Kukulansky, T., and Globerson, A. (1990) In vitro analysis of age-related changes in the developmental potential of bone-marrow thymocyte progenitors. *Eur. J. Immunol.* **20**, 2541–2546.
47. Hirokawa, K., Kubo, S., Utsuyama, M., Kurashima, C., and Sado, T. (1986) Age-related change in the potential of bone marrow cells to repopulate the thymus and splenic T cells in mice. *Cell. Immunol.* **100**, 443–451.
48. Min, H., Montecino-Rodriguez, E., and Dorshkind, K. (2004) Reduction in the developmental potential of intrathymic T cell progenitors with age. *J. Immunol.* **173**, 245–250.
49. Foss, D. L., Donskoy, E., and Goldschneider, I. (2001) The importation of hematogenous precursors by the thymus is a gated phenomenon in normal adult mice. *J. Exp. Med.* **193**, 365–374.
50. Prockop, S. E. and Petrie, H. T. (2004) Regulation of thymus size by competition for stromal niches among early T cell progenitors. *J. Immunol.* **173**, 1604–1611.
51. Almeida, A. R., Borghans, J. A., and Freitas, A. A. (2001) T cell homeostasis: thymus regeneration and peripheral T cell restoration in mice with a reduced fraction of competent precursors. *J. Exp. Med.* **194**, 591–599.
52. Douek, D. C., Vescio, R. A., Betts, M. R., et al. (2000) Assessment of thymic output in adults after haematopoietic stem-cell transplantation and prediction of T-cell reconstitution. *Lancet* **355**, 1875–1881.
53. Kolte, L., Strandberg, C., Dreves, A. M., et al. (2002) Thymic involvement in immune recovery during antiretroviral treatment of HIV infection in adults; comparison of CT and sonographic findings. *Scand. J. Infect. Dis.* **34**, 668–672.
54. Dumont-Girard, F., Roux, E., van Lier, R. A., et al. (1998) Reconstitution of the T-cell compartment after bone marrow transplantation: restoration of the repertoire by thymic emigrants. *Blood* **92**, 4464–4471.

55. Hakim, F. T., Cepeda, R., Kaimei, S., et al. (1997) Constraints on CD4 recovery postchemotherapy in adults: thymic insufficiency and apoptotic decline of expanded peripheral CD4 cells. *Blood* **90**, 3789–3798.
56. Muraro, P. A., Douek, D. C., Packer, A., et al. (2005) Thymic output generates a new and diverse TCR repertoire after autologous stem cell transplantation in multiple sclerosis patients. *J. Exp. Med.* **201**, 805–816.
57. Zhang, H., Chua, K. S., Guimond, M., et al. (2005) Lymphopenia and interleukin-2 therapy alter homeostasis of CD4+CD25+ regulatory T cells. *Nat. Med.* **11**, 1238–1243.

## Inducing Mixed Chimerism and Transplantation Tolerance Through Allogeneic Bone Marrow Transplantation With Costimulation Blockade

Ines Pree and Thomas Wekerle

### Summary

Induction of mixed chimerism (i.e., coexistence of donor and recipient hematopoietic cells) through transplantation of allogeneic donor bone marrow under appropriate host conditioning, is one of the most reliable strategies to induce transplantation tolerance. Robust tolerance is evident in mixed chimeras as they permanently accept donor skin grafts while promptly rejecting third party grafts. Although historically, myeloablative and T-cell depleting regimens have been described, milder protocols involving costimulation blockade have recently been developed. The prototypical murine protocol described in this chapter, involves the use of CTLA4Ig and a monoclonal antibody-specific for CD154 (CD40L) for costimulation blockade, 3 Gy of nonmyeloablative total body irradiation and a conventional number of  $20 \times 10^6$  fully allogeneic bone marrow cells. Flow cytometry is used to determine levels of multilineage hematopoietic chimerism and deletion of donor-reactive CD4<sup>+</sup> T cells. Tolerance is assessed in vivo by grafting of donor and third party skin.

**Key Words:** Tolerance; transplantation; mixed chimerism; bone marrow transplantation; costimulation blockade; experimental.

### 1. Introduction

Mixed chimerism reliably induces permanent tolerance in numerous rodent and large animal models. Once donor stem cells have engrafted, they coexist and develop together with those of recipient origin giving rise to all hematopoietic cell types. Consequently, not only self-reactive but also donor-reactive thymocytes are intrathymically eliminated through negative selection, leading to a robust state of tolerance.

To surmount physiological and immunological barriers for successful bone marrow cell (BMC) engraftment, various myeloablative or nonmyeloablative

conditioning protocols have been developed involving the global elimination of recipient T cells (1–4). Myeloablative irradiation leads to complete destruction of the hematopoietic repertoire of the host, which is then reconstituted by donor BMC. Apart from the toxicity of this approach, full chimerism is associated with some degree of immunoincompetence and is, therefore, clinically undesirable. Mixed chimerism can be achieved by nonmyeloablative doses of total body irradiation (TBI) combined with administration of T-cell depleting monoclonal antibody (MAb) to overcome preexisting allo-reactive T cells in the periphery plus a more restricted irradiation to the thymic region preventing intrathymic alloreactivity (2). Alternatively, thymus irradiation can be eliminated by repeated administration of T-cell depleting MAb (5). The least toxic approach developed so far for inducing mixed chimerism experimentally is, however, based on the use of costimulation blockers as part of BMT protocols (6–8).

Costimulation blockade allowed the establishment of allogeneic mixed chimerism for the first time without global elimination of the recipient T-cell repertoire. Although noncytoreductive protocols have been published as well (without any irradiation) (9–10), they require clinically impractical doses of donor hematopoietic cells. Thus, for reasons of clinical relevance, a prototypical nonmyeloablative, fully allogeneic (Balb/c to C57Bl/6) costimulation blockade-based (anti-CD154 MAb and CTLA4Ig) protocol and its mechanisms will be the focus of this chapter (6,11).

Maintenance of tolerance in mixed chimeras relies predominantly, if not exclusively, on negative selection of alloreactive cells in the thymus (12). During the induction phase immediately post-BMT, two barriers need to be surmounted. A nonimmunological engraftment barrier is evident by the failure of moderate doses of even syngeneic BMC to engraft, unless the recipient is irradiated (or treated with cytotoxic drugs). The mechanisms by which irradiation promotes engraftment are not completely understood but may involve creating physical space for donor stem cells. Second, an immunological barrier needs to be overcome, which otherwise leads to the rejection of the transplanted donor BMC. In most of the recent mixed chimerism models this is achieved by the use of costimulation blockers. Costimulation blockade, consisting of an anti-CD154 MAb (given on the day of BMT) and the fusion protein CTLA4Ig (given 2 d post-BMT) inhibits CD40-CD40L and CD28-CD80/86 interactions between T-cells and (allo-) antigen presenting cells (13). Costimulation blockade in combination with BMT leads to progressive extrathymic deletion of mature donor-reactive T cells (6,14–16). In addition to deletion, regulatory mechanisms play an important role in the induction of tolerance (17,18).

Here, we outline a nonmyeloablative murine BMT protocol for chimerism induction (3 Gy TBI on d -1, a conventional dose of fully mismatched BMC

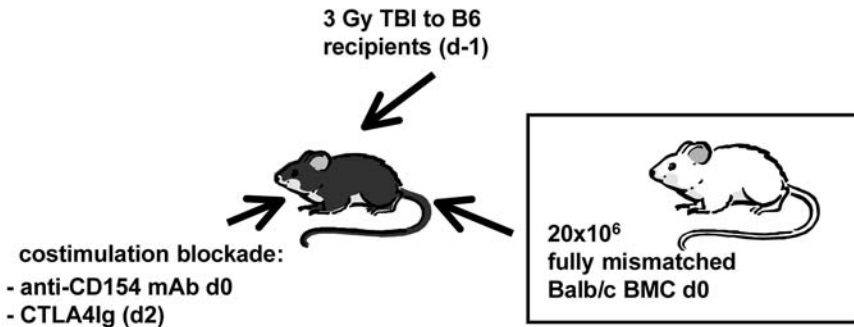


Fig. 1. Induction of chimerism via costimulation blockade and BMT. B6 recipients receive 3 Gy of total body irradiation 1 d before BMT. On the day of transplantation,  $20 \times 10^6$  fully mismatched BMC are injected into Balb/c recipients. Costimulation blockade consists of an anti-CD154 monoclonal antibody (given on the day of BMT) and the fusion protein CTLA4Ig (administered 2 d post-BMT).

plus a single dose injection of anti-CD154 on day 0 and administration of CTLA4Ig on d 2) (*see Fig. 1*), explain FCM analysis of multilineage chimerism and deletion of donor-reactive T cells and describe skin grafting as in vivo tolerance test. With this protocol, high levels of mixed chimerism (20–90%) in all tested lineages is induced and maintained for the length of follow-up, and donor skin is accepted permanently in the majority of chimeras, whereas third party skin is rejected promptly.

## 2. Materials

### 2.1. Animals

1. Female C57Bl/6 (B6: H-2<sup>b</sup>) are used as recipients, Balb/c (H-2<sup>d</sup>) donor mice and C3H (H-2<sup>k</sup>) as third party donors. All mice are housed under specific pathogen-free conditions. Recipient mice are used between 6 and 10 wk of age (*see Notes 1 and 2*).
2. Irradiator for TBI of recipients (*see Note 3*).
3. Numbered ear tags and special tagging device.
4. Scales for weighing mice.

### 2.2. BMT and Costimulation Blockade

1. B6 as recipients and Balb/c as bone marrow donors. One donor mouse provides, on average, approx  $30\text{--}50 \times 10^6$  BMC. Each recipient will be injected with approx  $20 \times 10^6$  BMC (*see Note 4*).
2. Freshly prepared bone marrow medium: 500 mL medium 199, 5 mL of stock 1 M HEPES buffer, 5 mL DNase (1 mg/mL), 40  $\mu$ L of gentamicin (50 mg/mL). Pass the supplemented medium through a sterile filter and keep it on ice (*see Note 5*).



3. In vivo MAb stocks should be stored at  $-80^{\circ}\text{C}$ . Before use, MAb are freshly diluted in PBS and kept at  $4^{\circ}\text{C}$ : 1 mg/mL hamster anti-mouse CD154 (clone MR1) and 0.5 mg/mL human CTLA4Ig (*see Note 6*). Costimulation blockade MAb can be purchased from commercial suppliers.
4. 70- $\mu\text{m}$  Mesh (Miltenyi-Biotec, Bergisch Gladbach, Germany).
5. 10-mL Syringes and 1- to 3-mL syringes
6. 21-, 25-, and 30-Gauge needles.
7. Sterile scissors and forceps.
8. ACK buffer for lysis of red blood cells.
9. Trypan blue for viability staining of cells under the light microscope.
10. Mouse restrainer.

### 2.3. Flow Cytometry

1. This method requires a flow cytometer and appropriate software for data analysis. Fluorochrome-conjugated MAb are light-sensitive and should be stored in the dark at  $4^{\circ}\text{C}$ . Flow cytometry (FCM) MAb are all titrated to select a dilution providing optimal staining for the amount of cells to be stained.
2. FCM medium: 1 L Hank's buffered salt solution (HBSS), 210  $\mu\text{L}$  of 1 N NaOH, 1 g of sodium azide, 1 g of BSA. This medium can be stored for several months at  $4^{\circ}\text{C}$ .
3. Cold Aqua bidest for hypotonic water lysis of erythrocytes.
4. 10X HBSS to stop lysis and rescue leukocytes.
5. MAb for measurement of chimerism: FITC-labeled anti-CD4, anti-CD8, anti-B220, and anti-MAC1 (*see Note 7*) and biotinylated anti-H-2D<sup>d</sup> (clone 34-2-12) together with appropriate isotype controls. Biotinylated MAb may be visualized with avidin-phycoerythrin for detection of donor cells.
6. MAb for measurement of superantigen-reactive T cells as markers for the deletion of donor-reactive CD4<sup>+</sup> T cells: FITC-labeled anti-V $\beta$ 5, anti-V $\beta$ 11 and anti-V $\beta$ 8 MAb s, and PE conjugated anti-CD4 MAB; isotype controls (*see Note 8*).
7. Propidium iodide (PI) stock solution at 1 mg/mL diluted 1:10 for staining dead cells (both stock and working solutions should be stored at  $4^{\circ}\text{C}$  and protected from light). PI is toxic, as it intercalates into nucleic acid molecules and can cause DNA damage; protective gloves should, therefore, be worn.

### 2.4. Skin Grafting

1. Balb/c donor mice and C3H mice as third party skin donors.
2. Autoclaved surgical instruments: needle holder, suture material (preferably 4-0), scissors, forceps, and scalpel.
3. Anesthesia: 0.4 mL of ketamine (100 mg/mL), 0.1 mL of 23.32 mg/mL xylazin, and 4.5 mL PBS or NaCl solution.
4. Razor.
5. Adhesive band-aids.

### 3. Methods

Host conditioning for successful BMC engraftment begins 1 d prior to BMT when mice receive a nonmyeloablative dose of TBI (3 Gy, day -1). Subsequently, mice are transplanted with a conventional dose of approx  $20 \times 10^6$  BMC (day 0) and are injected with 1 mg of MR1 MAb to block CD154 (day 0). Two days post-BMT mice receive 0.5 mg of the fusion protein CTLA4Ig. Two-color FCM is employed to distinguish donor and recipient cells of particular lineages among blood leukocytes. The first FCM analysis of chimerism is usually performed 2 wk post-BMT. Chimerism is followed thereafter every 4–6 wk; for at least 6 mo. Persistence of multilineage chimerism over such prolonged periods suggests that true hematopoietic stem cells of donor origin have engrafted (19).

Deletion of donor reactive cells is analyzed by following the percentage of CD4<sup>+</sup> cells expressing certain V $\beta$ -subunits of the T-cell receptor (TCR) (using two-color flow cytometry with FITC-conjugated antibodies against V $\beta$ 8.1/2 (control), V $\beta$ 11, V $\beta$ 5.1/2, and PE-conjugated MAb specific for CD4). The donor strain (Balb/c) expresses the major histocompatibility complex (MHC) class II molecule H-2 I-E, which is required to present superantigens derived from endogenous retroviruses encoded in the B6/Balb/c background genomes (20–22). Developing thymocytes whose TCR contain V $\beta$ 11 or V $\beta$ 5.1/2, and which therefore bind to these superantigens, are deleted in I-e<sup>+</sup> mice, but not in B6 mice because they do not express I-E. Once chimerism has been established, donor antigen presenting cells are present in the thymus mediating negative selection of donor-reactive thymocytes. Thus, newly developing, alloreactive T cells are continuously intrathymically deleted as long as chimerism persists. Furthermore, preexisting mature donor-reactive cells are deleted extrathymically immediately after BMT with costimulation blockade, being progressively eliminated from the periphery.

The specific acceptance of donor skin is commonly considered to be the most stringent test for tolerance. Thus, mice are tested for tolerance by grafting donor (Balb/c) skin and third party (C3H) tail skin. Systemic tolerance should allow skin graft acceptance at any time post-BMT, from the day of BMT to several months thereafter (9,23). Tolerance testing is essential because chimerism does not always lead to skin graft acceptance. Rejection despite chimerism implies incomplete tolerance, possibly a result of the failure to achieve tolerance toward skin specific antigens.

#### 3.1. TBI and Preparations for BMT

1. One day before BMT, B6 recipient mice are irradiated with a nonmyeloablative dose of 3 Gy TBI (see Note 9).

2. Afterward, mice should be randomly separated into cages according to experimental groups.
3. Each mouse receives an ear-tag with a number for individual follow up.

### 3.2. BMT and Costimulation Blockade

1. On the day of BMT, sacrifice Balb/c donor mice and put them in a container filled with alcohol. You can expect about  $30\text{--}50 \times 10^6$  BMC per donor mouse (each recipient will receive approx  $20 \times 10^6$  BMC). Work under sterile conditions in a laminar flow hood throughout the cell harvest and the transplantation procedure. Bone marrow medium should be freshly prepared.
2. Femurs, tibias, humeri, and pelvic bones are isolated from the donor mice. Take care to remove muscles from bones, and to harvest the full-length bones in their entirety. Bones are collected in a 50-mL tube filled with bone marrow medium.
3. Bone marrow is flushed out into a sterile Petri dish with a needle attached to a 10-mL syringe filled with cold medium. Use 25-gauge needles for the femurs and humerus and 30-gauge for the tibia and pelvic bones.
4. To create a single cell suspension, the 10-mL syringe barrel attached to a 21-gauge needle is filled and emptied repeatedly. Then cell suspension is filtered through a 70- $\mu\text{m}$  mesh (Miltenyi-Biotec, Bergisch Gladbach, Germany) and collected in 50-mL Falcon tubes. Rinse the Petri dish with medium to collect any remaining cells.
5. Centrifuge the Falcon tubes (850g for 5 min at 4°C) and decant the supernatant. Resuspend the pellets and pool the cells in an appropriate volume of bone marrow medium before final dilution (mice are later injected with  $20 \times 10^6$  BMC in a volume of 1 mL medium).
6. Resuspend the cells well before counting live cells under a light microscope using a counting chamber. Lyse the erythrocytes with ACK buffer for 2 min. The same volume of trypan blue is added to stop lysis and to stain dead cells. Then cells can be diluted to the required concentration for  $20 \times 10^6$  BMC for 1 mL injection per mouse (*see Note 10*).
7. Recipient mice (B6) are gently warmed under a heating lamp, which facilitates intravenous (i.v.) injection. Place the mice in a restrainer and carefully inject BMC ( $20 \times 10^6$  per mouse in 1 mL medium) into one of the lateral tail veins using a 2-mL syringe attached to a 30-gauge needle (*see Note 11*).
8. Costimulation blockade involves injection of 1 mg of hamster anti-mouse-CD154 MAb intraperitoneally (i.p.) on day 0, in a volume of 1 mL on the same day as BMT (*see Note 12*).
9. Two days post-BMT, mice are injected with the human CTLA4Ig fusion protein (0.5 mg injected i.p. in a volume of 1 mL).

### 3.3. Detection of Chimerism and Deletion by Flow Cytometry

1. For bleeding, gently warm mice until they start to become slightly agitated. Also take naïve Balb/c and B6 mice as controls for proper staining (*see Note 13*).
2. Place the mouse in a restrainer, gently cut a lateral tail vein using a scalpel blade and collect approx 250–500  $\mu\text{L}$  of blood in a tube containing a few drops of

heparin to avoid coagulation. Sample preparation for FCM can be performed under nonsterile working conditions (see **Note 14**).

3. Erythrocytes are lysed by hypotonic shock by adding 9 mL of Aqua bidest. for approx 20 s and rescuing the more resilient leukocytes by the addition of 1 mL 10X HBSS. This lysis procedure can be repeated to achieve more complete lysis of erythrocytes.
4. After centrifugation (850g for 5 min at 4°C), the supernatant is decanted, 200  $\mu$ L of medium are added and cells are divided according to the number of tubes/stains per mouse: five tubes are required for the detection of chimerism among CD4, CD8, B220, or MAC1 positive cells (plus isotype control); and cells are split into four tubes per mouse in the case of deletion analysis to provide staining for anti-V $\beta$ 8, anti-V $\beta$ 11, or anti-V $\beta$ 5 plus isotype control. Be sure to also have single positive samples for compensation of overlapping spectra while calibrating the cytometer before acquisition.
5. Cells are first incubated with FITC-conjugated MAb for 30 min at 4°C in the dark (lineage markers for chimerism analysis; V $\beta$  specific MAb for the analysis of deletion). Simultaneously, cells are incubated with biotinylated anti-H2D<sup>d</sup> (clone 34-2-12) MAb for chimerism analysis, or with anti-CD4-PE conjugated MAb for FCM analysis of deletion.
6. Staining is halted by adding 2 mL medium followed by 5 min centrifugation. Decant supernatant.
7. In case of chimerism analysis, incubate the cells with avidin-PE for 10 min. Avidin-PE binds to biotinylated 34-2-12. Stop staining reaction with 2 mL of medium and centrifuge again.
8. After centrifugation, resuspend the cells in a volume of approx 200  $\mu$ L.
9. Dead cells can be excluded by staining with PI: add 10  $\mu$ L of a 0.1 mg/mL solution immediately before sample acquisition (see **Note 15**).
10. For analysis, dot plots and histograms are gated on PI-negative leukocytes.
11. When analyzing chimerism (see **Fig. 2**), the percentage of donor cells is calculated by subtracting control staining from quadrants containing donor and host cells expressing a particular lineage marker, and by dividing the net percentage of donor cells by the total net percentage of donor plus host cells of that lineage. For the detection of deletion, gate on CD4<sup>+</sup> cells and analyze percentages of cells expressing a certain V $\beta$  subunit.

### 3.4. Skin Grafting

1. Skin donors are sacrificed and placed in ethanol for a few minutes. All instruments used should be autoclaved and all manipulations should be carefully carried out under sterile working conditions.
2. Prepare the grafts by removing the tails and storing them in a Petri dish with sterile PBS on ice. Grasp the tail with forceps and cut the skin in a straight line from the tip of the tail to its end, using a surgical blade. The skin can be peeled off in its entirety afterward. Skin is kept in cold PBS and cut into five to six square pieces per tail, approx 1 cm<sup>2</sup> in size.

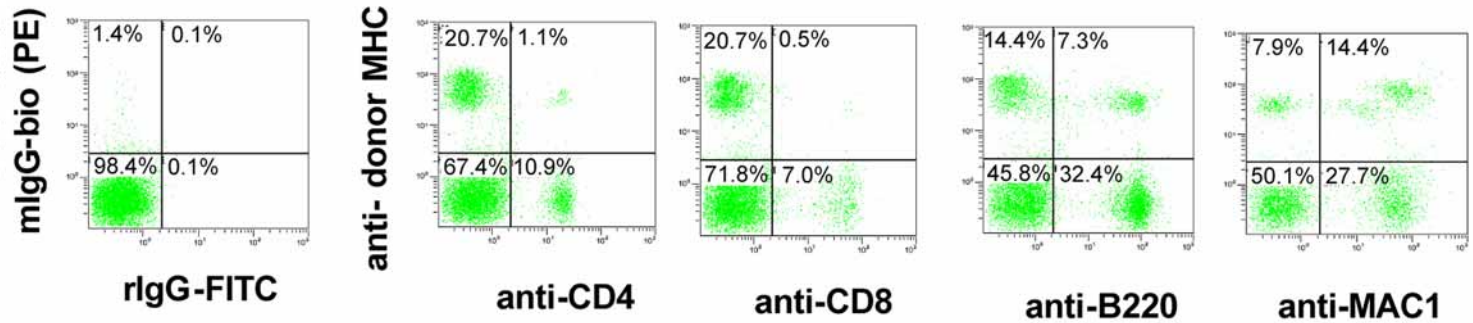


Fig. 2. Multilineage chimerism in a representative BMT recipient. FCM analysis of peripheral white blood cells 5 wk post-BMT reveals high levels of donor cells. CD4<sup>+</sup> T cells (anti-CD4), CD8<sup>+</sup> T cells (anti-CD8), B cells (anti-B220), and myeloid cells (anti-MAC1) were stained with fluorescein isothiocyanate-conjugated monoclonal antibody (MAB); donor-major histocompatibility complex class I was detected by a biotinylated anti-H-2D<sup>d</sup> MAB and visualized with phycoerythrin streptavidin allowing two-color plot analysis of recipient and donor cells.

3. Using 1-mL syringes attached to a 30-gauge needle, administer anesthesia i.p. to the recipients, consisting of 0.25 mL of xylazine/ketamine solution per mouse (*see Note 16*). Shave the flank of each recipient and disinfect the shaved area with ethanol.
4. On the dorsal thoracic wall of the recipient, prepare two graft beds approximately matching the size of the grafts, by pulling the skin up with forceps and cutting underneath using scissors, thereby removing only the upper skin and leaving the subcutaneous tissue intact. Bleeding should be avoided as hematomas can inhibit healing of the grafts.
5. Donor specific Balb/c and fully mismatched C3H (H-2<sup>k</sup>; third party) skin is placed on opposite sides of the flank and secured with sutures.
6. Finally, secure grafts with an adhesive band-aid applied tightly, but without inhibiting respiration.
7. Band-aids are carefully removed 1 wk after transplantation and grafts are monitored by visual and tactile inspections daily thereafter. Grafts are considered to be rejected when less than 10% of the tissue remains viable. Usually, third party skin and Balb/c skin of nonchimeric mice are rejected within 20 d. Although most chimeras accept donor skin permanently, some chimeric mice reject donor skin in a chronic fashion weeks or months after transplantation (*see Note 17*).

#### 4. Notes

1. Female mice are preferred because they are less aggressive and easier to handle, thus facilitating the technical success of skin grafting, for instance. Recipients of a particular experiment should be age-matched. Although there is no strict age limit, younger recipients are preferred. Donor mice of different ages can be used because BMC are pooled; the amount of BMC that can be harvested per mouse increases somewhat with age. Various strain combinations can be used. The transplantation model described here (Balb/c to B6) is a fully allogeneic one, involving MHC mismatches as well as mismatches at minor histocompatibility loci. Such a fully mismatched strain combination is closer to the clinical situation than MHC-congenic combinations involving MHC mismatches only (e.g., B10.A to B6). B6 have been reported to be relatively costimulation blockade resistant (24), thus providing a stringent, clinically relevant model.
2. All parts of the *in vivo* experiments (BMT, skin grafting, and so on) should be performed under strictly sterile working conditions. Subclinical infections can potentially influence the outcome, for example by interfering with tolerance induction. Specific pathogen free conditions foster reproducibility of the protocols and safeguard against infection with pathogens that would require the culling of the entire mouse colony.
3. TBI can be obviated in a noncytoreductive protocol in which an approx 10-fold higher dose of BMC is administered (9).
4. A conventional dose of  $15 \times 10^6$  BMC transplanted into a 25 g recipient corresponds to  $6 \times 10^8$  BMC/kg, which is similar to doses used in the clinical setting. The number of BMC injected may be varied somewhat from experiment to

- experiment (in a range of about  $15$  to  $25 \times 10^6$ ), but to allow comparability between groups, it is critical to inject each mouse with the exact same dose within a particular experiment.
5. DNase digests DNA present in the suspension owing to some damaged cells, thereby inhibiting clot formation. Although helpful, DNase is dispensable.
  6. Store MAb for use *in vivo* in small aliquots because they decline in quality if repeatedly thawed and refrozen. *In vivo* MAb must be free from endotoxin.
  7. Alternative surface markers for hematopoietic cell lineages can be used, e.g., anti-CD19 or anti-mouse IgM as B cell markers, or anti-Gr-1 as a myeloid marker.
  8. Alternatively, instead of detecting deletion of superantigen reactive T cells, deletion can also be demonstrated by following truly alloreactive T cells in TCR-transgenic mouse models (16,25).
  9. Do not change timing of TBI. TBI on the day of BMT is inefficient (26).
  10. The number of BMC injected is critical. Carefully count the cells before dilution and resuspend well before administering to recipients. Within a particular experiment, all mice should receive the same number of BMC.
  11. Avoid air bubbles in the syringe because mice die when injected *i.v.* with air. Take care that exactly 1 mL is injected *i.v.*
  12. Various dosing regimens have been described in the literature for MR1 and CTLA4Ig (7,27–29). Delayed administration of CTLA4Ig might be beneficial, possibly by allowing a signal through CTLA4 in the first 2 d (30,31).
  13. Be sure not to warm up mice too long because they may die if exposed for too long to the heating lamp. Stop the procedure once they begin jumping around.
  14. It is also possible to store blood samples at  $4^{\circ}\text{C}$  on a shaker overnight and perform the FCM the following day.
  15. Be aware that PI is toxic to the cells and must only be added immediately before sample acquisition.
  16. Dose anesthesia carefully because mice easily die if overdosed.
  17. In our Balb/c to B6 protocol, tolerance can be improved by short-term treatment with rapamycin, mycophenolate mofetil, and steroids, which also allows reduction of TBI to 1 Gy (11).

## Acknowledgments

We thank Nina Pilat for critical reading of the manuscript.

## References

1. Main, J. M. and Prehn, R. T. (1955) Successful skin homografts after the administration of high dosage X radiation and homologous bone marrow. *J. Natl. Cancer Inst.* **15**, 1023–1028.
2. Sharabi, Y. and Sachs, D. H. (1989) Mixed chimerism and permanent specific transplantation tolerance induced by a non-lethal preparative regimen. *J. Exp. Med.* **169**, 493–502.

3. Ildstad, S. T. and Sachs, D. H. (1984) Reconstitution with syngeneic plus allogeneic or xenogeneic bone marrow leads to specific acceptance of allografts or xenografts. *Nature* **307**, 168–170.
4. Wekerle, T. and Sykes, M. (2001) Mixed chimerism and transplantation tolerance. *Annu. Rev. Med.* **52**, 353–370.
5. Tomita, Y., Sachs, D. H., Khan, A., and Sykes, M. (1996) Additional mAb injections can replace thymic irradiation to allow induction of mixed chimerism and tolerance in mice receiving bone marrow transplantation after conditioning with anti-T cell mAbs and 3 Gy whole body irradiation. *Transplantation* **61**, 469–477.
6. Wekerle, T., Sayegh, M. H., Hill, J., et al. (1998) Extrathymic T cell deletion and allogeneic stem cell engraftment induced with costimulatory blockade is followed by central T cell tolerance. *J. Exp. Med.* **187**, 2037–2044.
7. Adams, A. B., Durham, M. M., Kean, L., et al. (2001) Costimulation blockade, busulfan, and bone marrow promote titratable macrochimerism, induce transplantation tolerance, and correct genetic hemoglobinopathies with minimal myelosuppression. *J. Immunol.* **167**, 1103–1111.
8. Taylor, P. A., Lees, C. J., Waldmann, H., Noelle, R. J., and Blazar, B. R. (2001) Requirements for the promotion of allogeneic engraftment by anti-CD154 (anti-CD40L) monoclonal antibody under nonmyeloablative conditions. *Blood* **98**, 467–474.
9. Wekerle, T., Kurtz, J., Ito, H., et al. (2000) Allogeneic bone marrow transplantation with co-stimulatory blockade induces macrochimerism and tolerance without cytoreductive host treatment. *Nat. Med.* **6**, 464–469.
10. Durham, M. M., Bingaman, A. W., Adams, A. B., et al. (2000) Administration of anti-CD40 ligand and donor bone marrow leads to hematopoietic chimerism and donor-specific tolerance without cytoreductive conditioning. *J. Immunol.* **165**, 1–4.
11. Blaha, P., Bigenzahn, S., Koporc, Z., et al. (2003) The influence of immunosuppressive drugs on tolerance induction through bone marrow transplantation with costimulation blockade. *Blood* **101**, 2886–2893.
12. Wekerle, T., Blaha, P., Koporc, Z., Bigenzahn, S., Pusch, M., and Muehlbacher, F. (2003) Mechanisms of tolerance induction through the transplantation of donor hematopoietic stem cells: central versus peripheral. *Transplantation* **75**, 21S–25S.
13. Wekerle, T., Kurtz, J., Bigenzahn, S., Takeuchi, Y., and Sykes, M. (2002) Mechanisms of transplant tolerance induction using costimulatory blockade. *Curr. Opin. Immunol.* **14**, 592–600.
14. Wekerle, T., Kurtz, J., Sayegh, M. H., et al. (2001) Peripheral deletion after bone marrow transplantation with costimulatory blockade has features of both activation-induced cell death and passive cell death. *J. Immunol.* **166**, 2311–2316.
15. Kurtz, J., Shaffer, J., Lie, A., Anosova, N., Benichou, G., and Sykes, M. (2004) Mechanisms of early peripheral CD4 T-cell tolerance induction by anti-CD154 monoclonal antibody and allogeneic bone marrow transplantation: evidence for anergy and deletion but not regulatory cells. *Blood* **103**, 4336–4343.



16. Fehr, T., Takeuchi, Y., Kurtz, J., Wekerle, T., and Sykes, M. (2005) Early regulation of CD8 T cell alloreactivity by CD4<sup>+</sup>CD25<sup>-</sup> T cells in recipients of anti-CD154 antibody and allogeneic BMT is followed by rapid peripheral deletion of donor-reactive CD8<sup>+</sup> T cells, precluding a role for sustained regulation. *Eur. J. Immunol.* **35**, 2679–2690.
17. Bigenzahn, S., Blaha, P., Koporc, Z., et al. (2005) The role of non-deletional tolerance mechanisms in a murine model of mixed chimerism with costimulation blockade. *Am. J. Transplant.* **5**, 1237–1247.
18. Kurtz, J., Wekerle, T., and Sykes, M. (2004) Tolerance in mixed chimerism: a role for regulatory cells? *Trends Immunol.* **25**, 518–523.
19. Down, J. D. and Ploemacher, R. E. (1993) Transient and permanent engraftment potential of murine hematopoietic stem cell subsets: differential effects of host conditioning with gamma radiation and cytotoxic drugs. *Exp. Hematol.* **21**, 913–921.
20. Acha-Orbea, H. and Palmer, E. (1991) MIs: a retrovirus exploits the immune system. *Immunol. Today* **12**, 356–361.
21. Tomonari, K. and Fairchild, S. (1991) The genetic basis of negative selection of Tcrb-V11+ T cells. *Immunogenetics* **33**, 157–162.
22. Dyson, P. J., Knight, A. M., Fairchild, S., Simpson, E., and Tomonari, K. (1991) Genes encoding ligands for deletion of Vβ11 T cells cosegregate with mammary tumour virus genomes. *Nature* **349**, 531–532.
23. Kurtz, J., Ito, H., Wekerle, T., Shaffer, J., and Sykes, M. (2001) Mechanisms involved in the establishment of tolerance through costimulatory blockade and BMT: lack of requirement for CD40L-mediated signaling for tolerance or deletion of donor-reactive CD4<sup>+</sup> cells. *Am. J. Transplant.* **1**, 339–349.
24. Williams, M. A., Trambley, J., Ha, J., et al. (2000) Genetic characterization of strain differences in the ability to mediate CD40/CD28-independent rejection of skin allografts. *J. Immunol.* **165**, 6849–6857.
25. Kurtz, J., Shaffer, J., Lie, A., Anosova, N., Benichou, G., and Sykes, M. (2004) Mechanisms of early peripheral CD4 T cell tolerance induction by anti-CD154 monoclonal antibody and allogeneic bone marrow transplantation: evidence for anergy and deletion, but not regulatory cells. *Blood* **103**, 4336–4343.
26. Takeuchi, Y., Ito, H., Kurtz, J., Wekerle, T., Ho, L., and Sykes, M. (2004) Earlier low-dose TBI or DST overcomes CD8<sup>+</sup> T-cell-mediated alloresistance to allogeneic marrow in recipients of anti-CD40L. *Am. J. Transplant.* **4**, 31–40.
27. Quesenberry, P. J., Zhong, S., Wang, H., and Stewart, M. (2001) Allogeneic chimerism with low-dose irradiation, antigen presensitization, and costimulator blockade in H-2 mismatched mice. *Blood* **97**, 557–564.
28. Ito, H., Kurtz, J., Shaffer, J., and Sykes, M. (2001) CD4 T cell-mediated alloresistance to fully MHC-mismatched allogeneic bone marrow engraftment is dependent on CD40-CD40 ligand interactions, and lasting T cell tolerance is induced by bone marrow transplantation with initial blockade of this pathway. *J. Immunol.* **166**, 2970–2981.

29. Guo, Z., Wang, J., Dong, Y., et al. (2003) Long-term survival of intestinal allografts induced by costimulation blockade, busulfan and donor bone marrow infusion. *Am. J. Transplant.* **3**, 1091–1098.
30. Perez, V. L., Van Parijs, L., Biuckians, A., Zheng, X. X., Strom, T. B., and Abbas, A. K. (1997) Induction of peripheral T cell tolerance in vivo requires CTLA-4 engagement. *Immunity* **6**, 411–417.
31. Lin, H., Bolling, S. F., Linsley, P. S., et al. (1993) Long-term acceptance of major histocompatibility complex mismatched cardiac allografts induced by CTLA4Ig plus donor-specific transfusion. *J. Exp. Med.* **178**, 1801–1806.



## Induction of Dominant Tolerance Using Monoclonal Antibodies

Ana Água-Doce and Luis Graça

### Summary

Monoclonal antibodies (MAb) have been shown to be effective in inducing immune tolerance in transplantation and autoimmunity. Several different MAb have tolerogenic properties and their effect has been studied in a range of experimental animal models and, in some cases, in clinical trials. The tolerant state seems to be maintained by CD4<sup>+</sup> regulatory T cells (Treg), induced in the periphery, capable of suppressing other T cells specific for the same antigens or antigens presented by the same antigen presenting cells. Furthermore, following the initial induction of Treg cells under MAb treatment, Treg cells themselves can maintain the tolerant state in a dominant way in the absence of the therapeutic MAb or other immunosuppressive agents, and are able to recruit other T cells into the regulatory pool—a process named infectious tolerance.

**Key Words:** Immune tolerance; monoclonal antibody; regulatory T cells; autoimmune diseases; transplantation; animal models; immunotherapy.

### 1. Introduction

Ever since the description of classical transplantation tolerance by Medawar and colleagues (1), the attainment of clinical transplantation tolerance has been considered the “Holy Grail” of immunology. Two decades have passed since the initial demonstration that long-term transplantation tolerance can be induced following a brief treatment with monoclonal antibodies (MAb) (2–4) and that tolerogenic CD4 MAb can be used to treat experimental allergic encephalomyelitis (EAE) (5). However, the mechanisms by which tolerance is induced and maintained are not yet fully understood. In recent years it has become clear that antibody-induced transplantation tolerance leads to both deletion of some alloreactive clones and regulatory T cells (Treg) cell expansion (6,7).

In the first examples of peripheral tolerance induced with MAb, depleting anti-CD4 MAb were used to induce tolerance in mice to foreign immunoglobulins

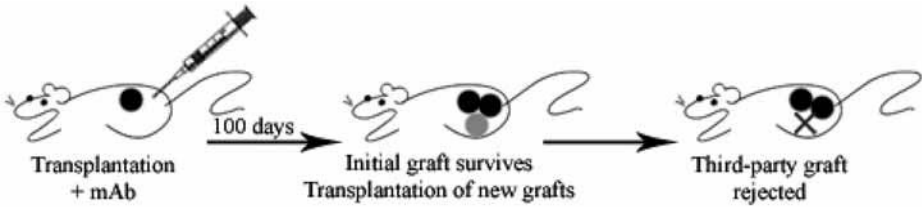


Fig. 1. Induction of transplantation tolerance with monoclonal antibody (MAB). Mice transplanted under the cover of tolerogenic MAb accept skin grafts indefinitely. To demonstrate that mice are indeed tolerant, one can simultaneously transplant a new graft of the tolerated type and a graft from an unrelated third-party donor, showing that tolerant mice remain fully competent to reject the latter.

(2,3). It was soon demonstrated that depletion of CD4<sup>+</sup> T cells was not required for tolerance induction, as similar results were obtained using F(ab')<sub>2</sub> fragments (8,9), nondepleting isotypes (10) or nondepleting doses of synergistic pairs of anti-CD4 MAb (11). A brief treatment with anti-CD4 MAb was also shown to lead to long-term acceptance of skin grafts differing in multiple minor antigens (10), even in presensitized recipients (12). The same results were also demonstrated for heart grafts across major histocompatibility complex (MHC) barriers (13,14) or concordant xenografts (13). The treated animals accepted the transplanted tissues indefinitely without the need for immunosuppression, and remained fully competent to reject unrelated (third-party) grafts. Clearly the antibody treatment had rendered them tolerant to antigens belonging to the transplanted tissue (see Fig. 1).

Following these studies, it became clear that MAb, other than anti-CD4, could be used to impose peripheral transplantation tolerance (see Table 1). Tolerance induced with MAb, such as CD4 or CD154 (CD40-Ligand), is dependent on Treg cells—both CD4<sup>+</sup>CD25<sup>+</sup> and CD4<sup>+</sup>CD25<sup>-</sup> (15). These Treg cells can be demonstrated both within lymphoid tissue and infiltrating the tolerated transplant (16). The dominant tolerance state, maintained by the Treg cells, allows the immune system to resist the adoptive transfer of nontolerant lymphocytes without tolerance break down (10,17). In addition, adoptively transferred nontolerant lymphocytes are rendered tolerant and regulatory when allowed to coexist with the initial cohort of Treg cells—a process usually referred to as *infectious tolerance* (18–20). The dominant tolerance state can be extended through *linked suppression* to additional antigens, if those new antigens are provided genetically linked with the tolerated ones within a new transplant (19,21–23).

In addition to tolerogenic antibodies, several experimental procedures may be used to facilitate tolerance induction (see Subheading 3.1.). Such is the case

**Table 1**  
**Therapeutic MAb Used to Induce Transplantation Tolerance**

Antibody	Transplantation	Reference
CD2	Delayed rejection of islet allografts and xenografts	<i>113</i>
CD3	Tolerance to heart allografts	<i>114</i>
CD3+ CD2	Long-term acceptance to heart grafts	<i>41</i>
CD4	Tolerance to antigens	<i>10,29</i>
CD4+CD8	Tolerance to minor mismatched skin, MHC-mismatched, and xenogeneic heart grafts	<i>10,19</i>
CD4+CD8+CD154	Tolerance to MHC-mismatched skin	<i>23</i>
CTLA4-Ig	Xenogeneic pancreatic islets	<i>43</i>
CD45RB	Long-term survival of MHC mismatched islets and kidney transplants	<i>42,115</i>
CD45RB + CD154	Long-term survival of MHC mismatched skin	<i>52</i>
CD134L (OX40L)	Long-term survival of minor mismatched heart allografts	<i>116</i>
CD134L+ CTLA4-Ig	Long-term acceptance of MHC-mismatched heart grafts	<i>108</i>
CD154	MHC-mismatched pancreatic islets	<i>44</i>
CD154+CD8dep	Tolerance to minor mismatched skin	<i>20,22</i>
CD154+CTLA4-Ig	Long-term acceptance MHC-mismatched skin	<i>45,60</i>
LFA-1	Tolerance to soluble antigen	<i>9</i>
LFA-1+ICAM-1	Long-term acceptance MHC-mismatched heart grafts	<i>46</i>
IL-2 + IL-15 Ig	Long-term acceptance of MHC-mismatched islets in diabetic NOD mice	<i>35</i>

with the administration of donor bone marrow (BM), or donor blood (donor-specific transfusion [DST]). The elimination of cell populations that may create an obstacle to graft survival with weak tolerogenic antibodies is also commonly used. Such is the case for CD154 tolerogenic antibodies, able to induce dominant tolerance within the CD4<sup>+</sup> T cells, but when used alone cannot prevent skin graft rejection mediated by CD8<sup>+</sup> T cells (*22,24*). As a consequence, CD8 depletion is often used when the tolerogenic properties of CD154 MAb are studied.

Tolerogenic MAb have been also used to reprogram the immune system in animal models of autoimmune diseases (*25*). However, it has been more difficult to confirm that the tolerant state, so induced, is dominant and mediated by Treg cells than in the context of transplantation, as experiments with third-party antigens are harder to conduct. Nevertheless, the characterization of the phenotype

of the dominant Treg population in maintaining self-tolerance as being CD4<sup>+</sup>CD25<sup>+</sup>Foxp3<sup>+</sup> has permitted the confirmation that tolerogenic MAb, such as the ones directed toward CD3, can prevent autoimmunity by eliciting Treg cells that maintain the tolerant state in a dominant manner (26). As a consequence, it appears that MAb, known to be able to induce dominant transplantation tolerance, may also restore dominant self-tolerance in autoimmunity.

## 2. Materials

### 2.1. Induction of Transplantation Tolerance With MAb

1. Animals: most animal studies have been performed in mice, although rats and nonhuman primates have been tolerized to foreign antigens and transplants with MAb. Transplant rejection or tolerance does not depend exclusively on the degree of mismatch between host and donor. Different strains of mice exhibit distinct behavior concerning the capacity to reject or become tolerant to transplants (27,28), which may be further modulated upon exposure to infectious microorganisms (see Note 1). In general, the hierarchy of strains, from the easiest to tolerize to the most difficult, is as follows: C3H, CBA/Ca, DBA/2, BALB/c, and C57Bl/6. Apparently, these properties are not primarily due to the MHC molecules present in each strain. For instance, B10.BR mice, expressing identical MHC molecules to CBA/CA mice, are as difficult to tolerize as C57Bl/6 with whom they share only minor antigens (27). The genetic basis of strain variability is still unknown.

Several studies have used T-cell receptor (TCR) transgenic animals, where all T cells share the same TCR. Even in these mice, it has been possible to use MAb, such as nondepleting CD4 or CD154, to induce a state of dominant tolerance where the *de novo* peripheral generation of Treg cells can be demonstrated (29). It should be noted that prior to tolerization, these TCR-transgenic animals have no demonstrable CD4<sup>+</sup>CD25<sup>+</sup>Foxp3<sup>+</sup> Treg cells.

2. Transplanted tissue: the capacity to accept a transplant also depends on the graft itself. In general, the greater the genetic disparity between donor and recipient, the more difficult it becomes to prevent rejection. The donor strain itself may also contribute to different outcomes in terms of tolerance. For example, BALB/c grafts are harder to tolerize than C57Bl/6 grafts in CBA/Ca recipients (23,30). In addition, different organs have been shown to have distinct requirements for succumbing to tolerance induction (31,32). Vascularized grafts are, in general, more easily accepted than nonvascularized grafts, such as skin. Acceptance of the liver is relatively easy to achieve, with many different liver allografts being spontaneously accepted by permissive strains without any treatment (33). Kidney allografts are also occasionally spontaneously accepted in rodents, although not as consistently as liver (32). In contrast, pancreatic islets and heart allografts are usually rejected in the absence of therapeutic intervention. It should be noted that in diabetic animals, such as nonobese diabetic (NOD) mice, it is more difficult to induce tolerance to islet allografts presumably because a primed autoimmune response must be overcome in addition

to the allogeneic barrier (34,35). The rejection of small intestine seems to be more vigorous than the above mentioned organs (32,36). However, skin grafts are even more difficult to tolerize as some treatments, capable of preventing rejection of heart allografts, are ineffective in inducing long-term survival of skin allografts (37–40). It is known that both CD4<sup>+</sup> and CD8<sup>+</sup> T cells can contribute to skin graft rejection, with each population capable of rejecting grafts independently (29).

3. Antibodies: several antibodies and fusion proteins have been shown to be effective at inducing dominant transplantation tolerance, either on their own or in combination (see Table 1). It is interesting to note that virtually all MAb able to induce peripheral tolerance, target molecules involved in the formation of the immune synapse: the coreceptor molecules CD3, CD4, and CD8 (10,41); CD45RB (42); the costimulatory molecules CD154 and CD28 (43–45); and the adhesion molecules leukocyte function-associated antigen 1 and intercellular adhesion molecule-1 (9,46). It is thus possible that tolerance induction requires T-cell activation under suboptimal conditions, i.e., in the presence of reagents that interfere with efficient T-cell activation, although this does not extend to conventional immunosuppressive agents (see Note 2) (47).

## 2.2. Induction of Tolerance With MAb in Autoimmunity

1. Animals: the use of MAb to restore the state of dominant regulation has been tested in several animal models of autoimmune and immune-inflammatory disease. Some of the most common examples are listed in Table 2. Such animal models can be divided into three broad categories: (1) animals developing the disease spontaneously, (2) animals where the disease is induced experimentally, and (3) TCR-transgenic animals where most or all the T cells are specific for a self-antigen. It should be noted that some animals, initially described as developing an autoimmune disease spontaneously, were later found to develop the disease following an environmental challenge. This is the case for SKG mice, carrying a mutation of the *ZAP-70* gene, that develop chronic autoimmune arthritis with features closely resembling rheumatoid arthritis (RA) (48). In spite of initial reports suggesting that autoimmune arthritis was spontaneous, it was recently shown that the disease is triggered by Dectin-1 agonists such as zymosan (49). It is also important to note that the immune systems of most animals used in animal models of autoimmune disease behave as lymphopenic (see Note 3) (50). Some of the most common animal models of autoimmune pathology are as follows:

Autoimmune diabetes: NOD mice spontaneously develop insulin-dependent diabetes and are a model of type I diabetes mellitus. Disease in these animals, as in humans, appears to be of autoimmune aetiology that is heavily influenced by both genetics and environment (51,52). The similarity between diabetes in the NOD mice and humans is extensive, including the influence of sex on the incidence of disease: whereas about 80% of female mice at 6 mo of age are diabetic, only 20% of males develop the disease (53). BB rats also develop autoimmune diabetes spontaneously but, as in humans, the disease incidence is similar in both sexes and not affected by gonadectomy or androgen administration (54). The immune system of these rats is



**Table 2**  
**Animal Models of Autoimmune Diseases**

	Associated human disease	Reference
<i>Mouse models</i>		
Spontaneous		
NOD	Type 1 diabetes	52
NZB × NZW	SLE	69
MRL/lpr	SLE	117
K/B × N	RA	59,60
T/R <sup>-</sup> (TCR transgenic to MBP)	MS	65
Induced		
DBA/1 + Type II collagen in IFA	RA	56–58
SKG + Dectin-1 agonists	RA	48,49
BALB/c + Spinal cord homogenate in CFA	MS	64
SJL + PLP in CFA	MS	61
SLJ + Thyroglobulin in CFA	Autoimmune thyroiditis	118
<i>Rat models</i>		
Spontaneous		
BB/wor	Type 1 diabetes	119
Komeda diabetes-prone (KDP)	Type 1 diabetes	120
Lewis (LEW.1AR1/Ztm)	Type 1 diabetes	121
Induced		
Lewis + retinal pigment epithelium-specific 65-kDa protein peptides	Autoimmune uveitis	122
Lewis + MBP in CFA	MS	123
Wistar + MBP in CFA	MS	32
Wistar + testis homogenates	Autoimmune orchitis	124

CFA, complete Freund's adjuvant; IBD, inflammatory bowel disease; IFA, incomplete Freund's adjuvant; MBP, myelin basic protein; MS, multiple sclerosis; RA, rheumatoid arthritis; SLE, systemic lupus erythematosus.

severely lymphopenic. Another rat model of diabetes is the LEW.1WR1 rat (*RT1<sup>u/u/a</sup>*) where the disease occurs spontaneously with a cumulative frequency of approx 2% at a median age of 59 d. Both sexes are affected, and islets of acutely diabetic rats are devoid of  $\beta$  cells whereas  $\alpha$  and  $\delta$  cell populations are spared (55).

RA: the most commonly used animal models of autoimmune arthritis are mice and rats in which the disease is induced with type II collagen and incomplete Freund's adjuvant (56–58). In these cases, the disease usually affects larger joints of the limbs and is self-limited. K/B×N mice spontaneously develop a progressive joint-specific autoimmune disease between 3 and 5 wk of age. Pathology of disease

in K/B×N mice is similar to human RA, with pannus formation, synovial hyperplasia, increased synovial fluid volume, and chaotic remodelling of cartilage and bone in the distal joints in the later stages (59,60). SKG mice, harboring T cells more resistant to TCR stimulation, also develop chronic autoimmune arthritis. Although disease in K/B×N mice is mediated by antibodies and can be adoptively transferred to healthy recipients by transferring the serum, in SKG mice arthritogenic T cells are sufficient to cause the disease as their adoptive transfer into lymphocyte-deficient hosts triggers autoimmune arthritis (48).

Multiple sclerosis: EAE is characterized by T cell-mediated destruction of the myelin sheath in the central nervous system. Myelin basic protein, myelin/oligodendrocyte glycoprotein, and proteolipid apoproteins when administered with adjuvant to mice or rats can induce autoreactive T cells that cause the disease (61–63). The same outcome has been reported following the administration of syngeneic mouse spinal cord homogenate in complete Freund's adjuvant (64). TCR transgenic mice in the RAG<sup>-/-</sup> background, in which all T cells express a TCR directed to a myelin protein, spontaneously develop EAE with 100% incidence at 8 mo (65,66). Interestingly, the disease is abrogated by the presence of additional CD4<sup>+</sup> T cells from wild-type syngeneic mice (67,68).

Systemic lupus erythematosus (SLE): MRL/lpr mice spontaneously develop a disease similar to SLE, because of defective apoptosis of activated B cells as the mice are deficient in Fas/FasL (69). Other mouse strains, such as the NZB × NZW and the BXSB, also develop a SLE-like syndrome that appears to be influenced by multiple genes (69).

2. Antibodies: several MAb have been tested for the treatment of autoimmune diseases. In many cases such MAb do not aim to restore tolerance but rather to control the inflammatory process (such as the anti-tumor necrosis factor  $\alpha$  or the anti-interleukin-1 MAb) (70), or induce immunosuppression by elimination of pathogenic lymphocyte populations (such as T-cell depletion with CAMPATH or B-cell depletion with anti-CD20) (71,72). However, tolerogenic MAb have also been reported to have a beneficial effect on the prevention or treatment of autoimmune pathology, although in many cases the true re-establishment of dominant self-tolerance based on T-cell regulation remains to be confirmed (see Table 3).

CD3: therapy with nonmitogenic CD3 MAb has been shown to prevent and revert type 1 diabetes in NOD mice and in virus-induced autoimmune diabetes (73–75). Different from most other tolerogenic MAb, anti-CD3 seems to be more effective if used after the onset of disease, apparently because activated T cells are the main targets of this treatment (74). In autoimmune arthritis the use of this antibody was not shown to be as effective as in type 1 diabetes, but in both systems, treatment causes a reduction in serum interferon- $\gamma$  and an increase in interleukin-4, interpreted as deviation to a Th2 response (76). Anti-CD3 MAb were also shown to lead to an increase in Treg cells able to suppress diabetogenic T cells and maintain a state of dominant tolerance (26,77).

CD4: following initial reports showing a beneficial effect of anti-CD4 on the treatment of EAE in rats (5), it has been shown that nondepleting CD4 MAb can

**Table 3**  
**Targets of Therapeutic MAb in Experimental Autoimmune Diseases**

MAb	Animal/disease	Outcome	Reference
CD2	Lewis rats (EAM)	Prevents onset	<i>125</i>
	Lewis rats (EAE)	Prevents onset	<i>126</i>
	BB/wor rats (type 1 diabetes)	Prevents onset	<i>119</i>
CD3	NOD mouse (Type 1 diabetes)	Ameliorates established disease	<i>26,73–75</i>
	DBA/1 mouse (CIA)	Delayed onset, reduced severity	<i>76</i>
CD4	NOD mouse (Type 1 diabetes)	Prevents onset	<i>78–81</i>
	NZB/NZW mouse (murine SLE)	Ameliorates established disease	<i>127</i>
	DBA/1 (CIA)	Prevents onset and ameliorates established disease	<i>86–87</i>
CD30L	NOD mouse (type 1 diabetes)	Prevents onset	<i>128</i>
OX40L	SJL mouse (EAE)	Ameliorates established disease	<i>61</i>
	C.B-17 SCID (IBD)	Ameliorates established disease	<i>138</i>
CTLA4-Ig	BALB/c mouse (EAE)	Ameliorates established disease	<i>64</i>
	NZB/NZW mouse (SLE)	Prevents onset	<i>129–132</i>
CD154	BXSB mouse (SLE)	Delayed onset, reduced severity	<i>133</i>
	Marmoset monkey (EAE)	Prevents onset	<i>134</i>
	B6/A (C57BL/6×A/J) (AOD)	Prevents onset	<i>98</i>
	B10.BR mouse (EAU)	Ameliorates established disease	<i>135</i>
	SJL mouse (EAT)	Less severity	<i>118</i>
	NZB/NZW mouse (SLE)	Prevents onset	<i>136–139</i>
CD40	Marmoset monkey (EAE)	Prevents onset	<i>140</i>
CD137	DBA/1 (CIA)	Prevents onset	<i>141</i>
	NZB/NZW mouse (SLE)	Ameliorates established disease	<i>142</i>
	C.B-17 SCID (IBD)	Ameliorates established disease	<i>143,144</i>
	C57BL/6 (EAE)	Ameliorates established disease	<i>63</i>

(Continued)

**Table 3 (Continued)**

MAB	Animal/disease	Outcome	Reference
LFA-1	NOD mouse (Type 1 diabetes)	Prevents onset	<a href="#">145</a>

EAE, experimental allergic encephalomyelitis; EAM, experimental autoimmune myelitis; AOD, autoimmune ovary disease; CIA, collagen-induced arthritis; EAU, experimental autoimmune uveoretinitis; IBD, inflammatory bowel disease; MS, multiple sclerosis; SLE, systemic lupus erythematosus.

prevent the onset of diabetes in NOD mice, as well as preventing pancreatic islet damage in recently established disease, with the animals tolerating islet transplants from prediabetic syngeneic donors or even islet allografts ([78–82](#)). The same MAb have also been shown to prevent the onset of experimental autoimmune arthritis as well as to ameliorate overt arthritis ([83–85](#)).

Several other MAb, such as the ones targeting CD154, CTLA4-Ig, and CD134L, have been shown effective in preventing or treating several experimental autoimmune diseases (*see* [Table 3](#)).

### 3. Methods

#### 3.1. Induction of Dominant Transplantation Tolerance With MAb

##### 3.1.1. Induction of Dominant Tolerance With Nondepleting MAb

Several protocols have been used to induce transplantation tolerance with nondepleting MAb in the absence of further treatment. In general, the animals are treated with the antibodies, administered intravenously (i.v.) or intraperitoneally (i.p.), at the time or shortly in advance of transplantation. The dose of MAb varies between protocols but usually neutralizing doses of the MAb (in excess of 75 mg/kg; or 1.5 mg per 20 g mouse) are required. An example protocol is shown, capable of inducing dominant tolerance to MHC mismatched skin allografts in euthymic mice ([23](#)):

1. Sex-matched mice at 8 wk of age are transplanted with donor skin grafts (*see* Chapter 20). This tolerogenic protocol is known to be efficient in either euthymic or thymectomized animals (*see* [Note 4](#)). To facilitate tolerance induction, depletion of T-cell subsets may be achieved by treating the recipient animals with appropriate depleting MAb (for example the anti-CD8 MAb YTS169 and YTS156) 5 d prior to transplantation ([29](#)). In this case, it is convenient to use adult thymectomized mice to block T-cell production. However, euthymic CBA/CA mice can be tolerized to C57Bl/10 skin without any treatment except the tolerogenic MAb ([23](#)).

2. The three different therapeutic MAb—nondepleting CD4 (YTS177), CD8 (YTS105), and CD154 (MR1)—are mixed together in PBS, at a final concentration of 3.33 mg/mL. Care should be taken to keep the MAb preparation sterile and pyrogen-free. On the day of transplantation, usually after the animals recover from the anaesthetic, a dose of 0.3 mL of the MAb cocktail is injected i.p. in each transplanted animal (i.e., each animal receives 1 mg of each of the three MAbs).
3. The MAb treatment is repeated in the same way twice, 2 and 4 d following the initial injection.
4. Graft rejection should be monitored daily by visual inspection of the transplanted skin.
5. Confirmation of tolerance can be performed as described in **Subheading 3.2**.

### 3.1.2. Induction of Dominant Tolerance With MAb and DST

For more than two decades, it has been observed that the infusion of whole blood from donors into recipients can prolong allograft survival in humans and mice (64,86). More recently, it has been shown that the prolonged survival of allografts induced by DST is synergistically enhanced by the coadministration of anti-CD154 MAb (44), CTLA4-Ig (87) or nondepleting anti-CD4 MAb (88). Furthermore, tolerance achieved in this way is dominant and dependent of Treg cells (89). In some experiments, whole blood can be replaced by splenic mononuclear cells from the donor (44). The following protocol for inducing tolerance using DST is adapted from ref. 89:

1. Adult CBA/Ca mice (8 wk of age) receive 200 µg of the anti-CD4 MAb (YTS177) i.v. on d -28 and -27.
2. On day -27, mice are transfused with 250 µL of C57Bl/10 whole blood i.v.
3. Mice, rendered tolerant with the previously listed treatment, can be transplanted with donor skin on d 0.

### 3.1.3. Induction of Dominant Tolerance With MAb and Donor BM

Donor BM has been used to induce transplantation tolerance ever since the pioneering work of Medawar et al. (1). However, the use of large doses of donor BM usually leads to tolerance by purging the repertoire of alloreactive T-cell clones and not to dominant tolerance (23,90–92). MAb, in particular anti-CD154, have been used in this setting to facilitate BM engraftment (23,93–95). Nevertheless, a quantitative study, using mice mismatched for minor antigens, has shown that although doses of donor BM equal or in excess of  $2 \times 10^6$  cells induce macrochimerism and tolerance by deletion, a dose of  $4 \times 10^5$  cells or less can be used to induce dominant tolerance without mixed chimerism, when given under the cover of tolerogenic CD4 and CD8 MAb (90). The following protocol is based on these observations:

1. T-cell depleted BM can be prepared by treating donor mice with depleting MAb targeting CD4 and CD8 (such as YTS3.1 and YTS191 targeting CD4; and YTS156

and YTS169 targeting CD8) 3–5 d prior to collection of the BM (29). Bone marrow cells can be recovered by flushing the femoral and tibial bones using RPMI 1640, supplemented with 10% fetal bovine serum, 50 µg/mL penicillin/streptomycin, 0.01 M HEPES buffer, and  $5 \times 10^{-5}$  M 2-mercaptoethanol.

2. After washing the BM cells in fresh medium, they are re-suspended in PBS at  $5 \times 10^5$  cells/mL, and 200 µL of the single cell suspension is injected i.v. in the lateral tail vein of recipient mice (each mouse will thus receive  $1 \times 10^5$  T-cell depleted, donor BM cells).
3. On the day of BM transplantation a dose of 0.5 mg of anti-CD4 (YTS177), and 0.25 mg of each of the anti-CD8 MAb YTS156 and YTS169 is administered i.p. to the recipient mice.
4. The MAb treatment is repeated twice, 2 and 4 d following the initial injection.
5. Donor skin can be grafted 6 wk following BM transplantation to assess the tolerant state.
6. Dominant tolerance can be confirmed using *linked suppression* as a readout, following transplantation of (DONOR  $\times$  THIRD-PARTY) $F_1$  skin grafts (*see below*).

### 3.2. Confirmation of the Dominant Tolerance State

#### 3.2.1. Tolerance vs Immunosuppression

Long-term allograft survival following MAb treatment does not prove dominant tolerance has been successfully induced. To demonstrate tolerance, it is necessary to confirm that the immune system is fully competent to mount a response against antigens other than the tolerated ones. Usually, a simultaneous transplant of tolerated-type and unrelated third-party grafts is used, to confirm that tolerant animals remain able to reject specifically the third-party transplant (*see Fig. 1*).

#### 3.2.2. The Antigen Specificity of the Tolerant State

The putative antigen-specificity of the tolerant state is frequently demonstrated simply by grafting a third-party and a tolerated type transplant, and observing that only third-party grafts are rejected. However, given the possible differences in the “rejectability” of the different types of grafts (*see Subheading 2.1.*), such results should be approached with caution (6). Ideally, these studies should be performed in criss-cross experiments: mice should be tolerized, in independent experiments, to transplants of different types. Then both groups should be tested for capacity to reject the appropriate third-party grafts (*see Fig. 2*).

Alternatively *linked suppression* can be used as an exquisite and straightforward assay for both specificity and the dominant nature of tolerance (*see below*).

#### 3.2.3. Dominant Tolerance

A direct way to assess the dominant tolerance status of an animal is through the infusion of T cells with the capacity to reject the graft. In such a challenge,

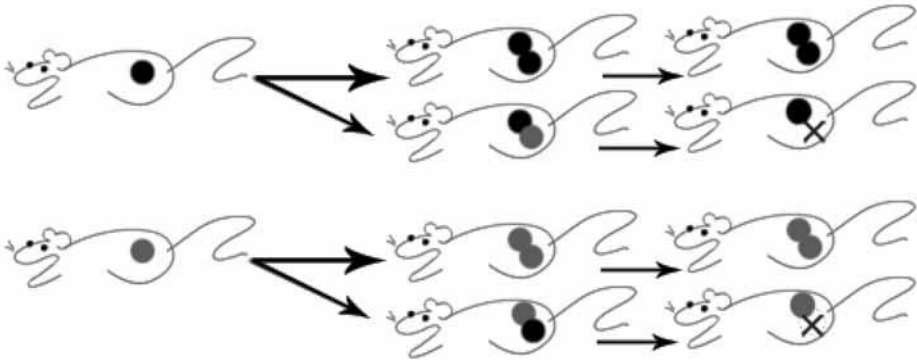


Fig. 2. Criss-cross experiment to demonstrate antigen-specific tolerance. To account for possible strain variations in tissue “rejectability,” tolerance can be assessed in mice tolerized to two different strains. The antigen-specificity of the tolerant state will determine that animals from both groups reject grafts from the third-party strain. The same sort of experiment can be used to test the antigen specificity of putative regulatory T cell populations following their adoptive transfer into lymphocyte-deficient animals.

T cells obtained from the spleens of naïve animals can be used (10,17). If the transfused cells are allowed to coexist with the tolerant ones for 6 wk, it becomes possible to demonstrate that they themselves have been rendered tolerant by ablating the initial population of T cells with depleting MAb directed to a specific marker (18,20). This recruitment of T cells toward a regulatory function is generally known as *infectious tolerance*.

Instead of using T cells from naïve wild-type animals, it is possible to transfuse TCR-transgenic T-cells specific for the tolerized alloantigens (63). This experimental setting allows the study of dominant tolerance effects on the cells being subjected to active regulation (63).

An alternative strategy to demonstrate dominant tolerance is to deplete putative populations of Treg cells, such as  $CD4^+$  or  $CD25^+$  T cells, unleashing aggressive cells to mediate rejection. It should be noted, however, that tolerizing treatments are often associated with a partial deletion of the alloreactive clones (60,96). In addition, besides the major populations of Treg cells (identified as  $CD4^+CD25^+$  and  $CD4^+CD25^-$ ) other minor populations of Treg cells may persist. This seems to be the case for  $CD8^+$  or double negative ( $CD4^-CD8^-$ ) Treg cells (32,97) in the light of which, it is not surprising that, in some cases, ablation of the major Treg cell populations—such as the  $CD4^+$  or the  $CD25^+$  cells—does not lead to the rejection of tolerized allografts.

Linked suppression has been used as an efficient assay for confirmation of both antigen-specificity of tolerized animals and for the dominant state of tolerance

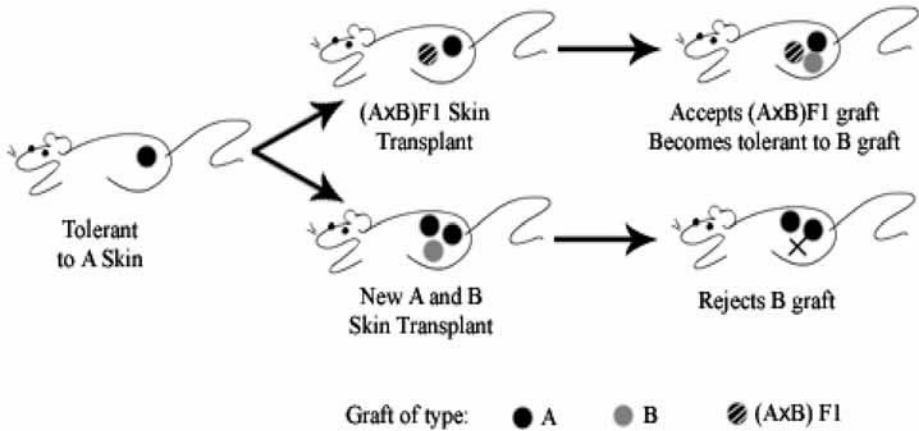


Fig. 3. Linked suppression. Animals tolerized to skin grafts of type A accept skin grafts from (Ax B)<sub>1</sub> donors, where third-party B-antigens are endogenous to cells that also express the tolerated A-antigens (top row). However, B-type grafts are readily rejected, even if a concomitant tolerated A-type graft is given (bottom row). Furthermore, the animals that accept the (Ax B)<sub>1</sub> grafts with the “linked” antigens become tolerant of grafts of the third-party B-type.

(23,91). These experiments are based on the observation that, once dominant tolerance has been established to a set of antigens present in an allograft, new transplants with cells simultaneously expressing tolerated antigens and third-party antigens are not rejected (*see Fig. 3*) (21). These data have been interpreted as evidence that Treg cells specific for the tolerated antigens actively suppress the aggressive cells directed to the “linked” third-party antigens. With time, those aggressive clones will themselves become tolerized, because animals start to accept transplants with the third-party antigens in the absence of the tolerated ones. It should be noted that third-party grafts, where the tolerated set of antigens is absent, are readily rejected in control animals. Linked suppression has been demonstrated in situations where tolerance is induced with coreceptor blockade, costimulation blockade or a combination of the two (21–23).

### 3.3. Tolerance Induction in Autoimmunity With MAb

MAb have been used either to prevent the onset of experimental autoimmune diseases, or to treat overt autoimmunity (*see Note 5*). For the prevention of autoimmunity, animals are often treated from the neonatal period (98). In some experiments, anti-CD3 MAb have been shown to be successful in treating overt diabetes in NOD mice, restoring a state of dominant tolerance mediated by Treg cells (73,74):



1. NOD females, at 10 wk of age, are screened, twice a week, until the glycemia scores are  $>4$  g/L for at least two consecutive measurements.
2. A group of mice receives i.v. treatment with nonmitogenic anti-CD3 MAb whereas another group receives an isotype control. The dosage is either 5  $\mu\text{g}/\text{d}$  (low dose) on five consecutive days (25  $\mu\text{g}$  in total) or 20  $\mu\text{g}/\text{d}$  (high dose) on five consecutive days (100  $\mu\text{g}$  in total).
3. Remission from sickness (i.e., disappearance of glycosuria and a return to normal glycemia) may be achieved 2–4 wk after treatment in 64–80% of the mice.
4. T cell (TCR/CD3<sup>+</sup>) depletion may be shown to be transient—approx 50% in mice treated with the low MAb dose and approx 75% of animal treated with high doses, recover basal CD3 levels in 25 and 35 d, respectively.

To confirm the induction of dominant tolerance, 20–40  $\times 10^6$  spleen cells may be transferred from protected mice into nontreated, sublethally irradiated (750 rad), syngeneic male recipients. This procedure renders the recipients diabetic, in a similar way to the recipients of splenocytes from overtly diabetic donors, proving that diabetogenic T cells persist in tolerant mice under the control of Treg cells (73).

### 3.4. Conclusions

Although MAb have been successful in inducing dominant tolerance in animal models of transplantation and autoimmune diseases, it will be important to investigate whether similar strategies can be adopted, in the context of allergy, to induce tolerance to allergens. Such experimental systems have been useful in understanding the biology of Treg cells and the suppressive mechanisms maintaining dominant tolerance. But besides such important contributions toward the basic understanding of the immune system and its regulation, there is a potential for clinical application of tolerogenic MAb. Recent observations have shown that MAb equivalent to the ones used in murine studies can be successfully used to induce tolerance in primates (29,104,111). Furthermore, a recent clinical trial has shown a beneficial effect of tolerogenic CD3 MAb in autoimmune diabetes (112). There are, therefore, reasons for optimism concerning the clinical use of tolerogenic antibodies in human immune pathology.

### 4. Notes

1. Active viral infection, with lymphocytic choriomeningitis virus, at the time of tolerance induction with costimulation blockade and DST can prevent the effectiveness of the treatment leading to graft rejection (80,99,100). However, this effect seems to be virus-specific, with some viral infections (murine cytomegalovirus and vaccinia virus) not leading to graft rejection (99). A persistent viral infection with lymphocytic choriomeningitis virus clone 13 can also prevent the establishment of

transplantation tolerance with a costimulation blockade-based regimen, and the antibody treatment can prevent an effective antiviral immune response (100). Furthermore, the persistence of memory T cells elicited by prior exposure to infectious agents has been reported as a barrier to the induction of transplantation tolerance, even in the absence of concomitant infection (101). This phenomenon is generally known as *heterologous immunity*. An explanation for these findings may be the cross-reactivity between viral and transplantation antigens (99,102). However, these obstacles do not seem to be complete. With coreceptor blockade, instead of costimulation blockade, it has been possible to induce tolerance to allografts in mice or rats previously primed to donor antigens (12,14). In addition, infection of tolerized mice (with anti-CD4<sup>+</sup> DST) with murine influenza PR8, at d 7 following heart transplantation, did not lead to impaired antiviral responses or to graft rejection (103).

2. It has been reported that successful induction of dominant tolerance following coreceptor blockade leads to expansion of Treg cells (20), and elimination of alloreactive cells through activation-induced cell death (60,96). Some conventional immunosuppressive drugs, such as corticosteroids and calcineurin inhibitors like cyclosporine-A and tacrolimus, by preventing T-cell activation and activation-induced cell death can abrogate the induction of dominant tolerance (60,96,104,105). The use of donor BM to induce tolerance by deletion of alloreactive clones does not seem to be affected by those drugs (106). Other immunosuppressive drugs, such as rapamycin or mycophenolate mofetil, do not seem to prevent tolerance induction and may be useful in addition to the tolerogenic MAb (60,105). The impact of the novel immunosuppressant FTY720, which induces a reversible sequestration of T cells in secondary lymphoid organs, in tolerance induction has not been established (107). Given that Treg cells can be found in tolerated allografts (16), it will be important to assess whether the impact on T-cell migration may prevent the onset of dominant tolerance.
3. Lymphopenia is a common feature in animal models of autoimmunity, appearing to be associated with the break down of tolerance (50). In transplantation experiments it was shown that T-cell depletion in advance of treatment with costimulation blockade + DST constituted a barrier for tolerance induction (108). Apparently, this effect is because of the acquisition of functional memory T cells (109). It remains to be established whether tolerizing regimens, successful in inducing tolerance in presensitized recipients (12,14), will remain effective when used with lymphopenic animals.
4. It is usually assumed that newly formed T cells exported from the thymus create an obstacle for dominant tolerance maintenance. In some stringent experimental systems, the use of thymectomized animals can facilitate maintenance of the tolerant state (52). Dominant tolerance, however, has been induced in either euthymic or thymectomized animals in many experimental systems, including stringent MHC-mismatched skin transplantation (23). The presence of the thymus is required for the induction of tolerance based on mixed-chimerism, where thymic deletion of alloreactive clones occurs (110).

## References

1. Billingham, R. E., Brent, L., and Medawar, P. B. (1953) Activity acquired tolerance of foreign cells. *Nature* **172**, 603–606.
2. Benjamin, R. J. and Waldmann, H. (1986) Induction of tolerance by monoclonal antibody therapy. *Nature* **320**, 449–451.
3. Gutstein, N. L., Seaman, W. E., Scott, J. H., and Wofsy, D. (1986) Induction of immune tolerance by administration of monoclonal antibody to L3T4. *J. Immunol.* **137**, 1127–1132.
4. Graca, L., Le Moine, A., Cobbold, S. P., and Waldmann, H. (2003) Antibody-induced transplantation tolerance: the role of dominant regulation. *Immunol. Res.* **28**, 181–191.
5. Brostoff, S. W. and Mason, D. W. (1984) Experimental allergic encephalomyelitis: successful treatment in vivo with a monoclonal antibody that recognizes T helper cells. *J. Immunol.* **133**, 1938–1942.
6. Graca, L., Le Moine, A., Cobbold, S. P., and Waldmann, H. (2003) Dominant transplantation tolerance. Opinion. *Curr. Opin. Immunol.* **15**, 499–506.
7. Zheng, X. X., Sanchez-Fueyo, A., Domenig, C., and Strom, T. B. (2003) The balance of deletion and regulation in allograft tolerance. *Immunol. Rev.* **196**, 75–84.
8. Carteron, N. L., Wofsy, D., and Seaman, W. E. (1988) Induction of immune tolerance during administration of monoclonal antibody to L3T4 does not depend on depletion of L3T4+ cells. *J. Immunol.* **140**, 713–716.
9. Benjamin, R. J., Qin, S. X., Wise, M. P., Cobbold, S. P., and Waldmann, H. (1988) Mechanisms of monoclonal antibody-facilitated tolerance induction: a possible role for the CD4 (L3T4) and CD11a (LFA-1) molecules in self-non-self discrimination. *Eur. J. Immunol.* **18**, 1079–1088.
10. Qin, S. X., Wise, M., Cobbold, S. P., et al. (1990) Induction of tolerance in peripheral T cells with monoclonal antibodies. *Eur. J. Immunol.* **20**, 2737–2745.
11. Qin, S., Cobbold, S., Tighe, H., Benjamin, R., and Waldmann, H. (1987) CD4 monoclonal antibody pairs for immunosuppression and tolerance induction. *Eur. J. Immunol.* **17**, 1159–1165.
12. Marshall, S. E., Cobbold, S. P., Davies, J. D., Martin, G. M., Phillips, J. M., and Waldmann, H. (1996) Tolerance and suppression in a primed immune system. *Transplantation* **62**, 1614–1621.
13. Chen, Z., Cobbold, S., Metcalfe, S., and Waldmann, H. (1992) Tolerance in the mouse to major histocompatibility complex-mismatched heart allografts, and to rat heart xenografts, using monoclonal antibodies to CD4 and CD8. *Eur. J. Immunol.* **22**, 805–810.
14. Onodera, K., Lehmann, M., Akalin, E., Volk, H. D., Sayegh, M. H., and Kupiec-Weglinski, J. W. (1996) Induction of “infectious” tolerance to MHC-incompatible cardiac allografts in CD4 monoclonal antibody-treated sensitized rat recipients. *J. Immunol.* **157**, 1944–1950.

15. Graca, L., Thompson, S., Lin, C. Y., Adams, E., Cobbold, S. P., and Waldmann, H. (2002) Both CD4(+)/CD25(+) and CD4(+)/CD25(-) regulatory cells mediate dominant transplantation tolerance. *J. Immunol.* **168**, 5558–5565.
16. Graca, L., Cobbold, S. P., and Waldmann, H. (2002) Identification of regulatory T cells in tolerated allografts. *J. Exp. Med.* **195**, 1641–1646.
17. Scully, R., Qin, S., Cobbold, S., and Waldmann, H. (1994) Mechanisms in CD4 antibody-mediated transplantation tolerance: kinetics of induction, antigen dependency and role of regulatory T cells. *Eur. J. Immunol.* **24**, 2383–2392.
18. Qin, S., Cobbold, S. P., Pope, H., et al. (1993) “Infectious” transplantation tolerance. *Science* **259**, 974–977.
19. Chen, Z. K., Cobbold, S. P., Waldmann, H., and Metcalfe, S. (1996) Amplification of natural regulatory immune mechanisms for transplantation tolerance. *Transplantation* **62**, 1200–1206.
20. Graca, L., Honey, K., Adams, E., Cobbold, S. P., and Waldmann, H. (2000) Cutting edge: anti-CD154 therapeutic antibodies induce infectious transplantation tolerance. *J. Immunol.* **165**, 4783–4786.
21. Davies, J. D., Leong, L. Y., Mellor, A., Cobbold, S. P., and Waldmann, H. (1996) T cell suppression in transplantation tolerance through linked recognition. *J. Immunol.* **156**, 3602–3607.
22. Honey, K., Cobbold, S. P., and Waldmann, H. (1999) CD40 ligand blockade induces CD4+ T cell tolerance and linked suppression. *J. Immunol.* **163**, 4805–4810.
23. Graca, L., Le Moine, A., Lin, C. Y., Fairchild, P. J., Cobbold, S. P., and Waldmann, H. (2004) Donor-specific transplantation tolerance: the paradoxical behavior of CD4+CD25+ T cells. *Proc. Natl. Acad. Sci. USA* **101**, 10,122–10,126.
24. Trambley, J., Bingaman, A. W., Lin, A., et al. (1999) Asialo GM1(+) CD8(+) T cells play a critical role in costimulation blockade-resistant allograft rejection. *J. Clin. Invest.* **104**, 1715–1722.
25. Chatenoud, L. (2005) Monoclonal antibody-based strategies in autoimmunity and transplantation. *Methods Mol. Med.* **109**, 297–328.
26. Chatenoud, L. (2003) CD3-specific antibody-induced active tolerance: from bench to bedside. *Nat. Rev. Immunol.* **3**, 123–132.
27. Davies, J. D., Cobbold, S. P., and Waldmann, H. (1997) Strain variation in susceptibility to monoclonal antibody-induced transplantation tolerance. *Transplantation* **63**, 1570–1573.
28. Williams, M. A., Trambley, J., Ha, J., et al. (2000) Genetic characterization of strain differences in the ability to mediate CD40/CD28-independent rejection of skin allografts. *J. Immunol.* **165**, 6849–6857.
29. Winsor-Hines, D., Merrill, C., O’Mahony, M., et al. (2004) Induction of immunological tolerance/hyporesponsiveness in baboons with a nondepleting CD4 antibody. *J. Immunol.* **173**, 4715–4723.
30. van Maurik, A., Wood, K. J., and Jones, N. D. (2002) Impact of both donor and recipient strains on cardiac allograft survival after blockade of the CD40-CD154 costimulatory pathway. *Transplantation* **74**, 740–743.

31. Jones, N. D., Turvey, S. E., Van Maurik, A., et al. (2001) Differential susceptibility of heart, skin, and islet allografts to T cell-mediated rejection. *J. Immunol.* **166**, 2824–2830.
32. Guo, L., Li, Y. H., Lin, H. Y., et al. (2004) Evaluation of a rat model of experimental autoimmune encephalomyelitis with human MBP as antigen. *Cell Mol. Immunol.* **1**, 387–391.
33. Qian, S., Demetris, A. J., Murase, N., Rao, A. S., Fung, J. J., and Starzl, T. E. (1994) Murine liver allograft transplantation: tolerance and donor cell chimerism. *Hepatology*. **19**, 916–924.
34. Markees, T. G., Serreze, D. V., Phillips, N. E., et al. (1999) NOD mice have a generalized defect in their response to transplantation tolerance induction. *Diabetes* **48**, 967–974.
35. Zheng, X. X., Sanchez-Fueyo, A., Sho, M., Domenig, C., Sayegh, M. H., and Strom, T. B. (2003) Favorably tipping the balance between cytopathic and regulatory T cells to create transplantation tolerance. *Immunity* **19**, 503–514.
36. Newell, K. A., He, G., Guo, Z., et al. (1999) Cutting edge: blockade of the CD28/B7 costimulatory pathway inhibits intestinal allograft rejection mediated by CD4+ but not CD8+ T cells. *J. Immunol.* **163**, 2358–2362.
37. Pearson, T. C., Darby, C. R., Bushell, A. R., West, L. J., Morris, P. J., and Wood, K. J. (1993) The assessment of transplantation tolerance induced by anti-CD4 monoclonal antibody in the murine model. *Transplantation* **55**, 361–367.
38. Pearson, T. C., Alexander, D. Z., Winn, K. J., Linsley, P. S., Lowry, R. P., and Larsen, C. P. (1994) Transplantation tolerance induced by CTLA4-Ig. *Transplantation* **57**, 1701–1706.
39. Cavazzana-Calvo, M., Sarnacki, S., Haddad, E., et al. (1995) Prevention of bone marrow and cardiac graft rejection in an H-2 haplotype disparate mouse combination by an anti-LFA-1 antibody. *Transplantation* **59**, 1576–1582.
40. Isobe, M., Suzuki, J., Yamazaki, S., and Sekiguchi, M. (1996) Acceptance of primary skin graft after treatment with anti-intercellular adhesion molecule-1 and anti-leukocyte function-associated antigen-1 monoclonal antibodies in mice. *Transplantation* **62**, 411–413.
41. Chavin, K. D., Qin, L., Lin, J., Yagita, H. and Bromberg, J. S. (1993) Combined anti-CD2 and anti-CD3 receptor monoclonal antibodies induce donor-specific tolerance in a cardiac transplant model. *J. Immunol.* **151**, 7249–7259.
42. Basadonna, G. P., Auersvald, L., Khuong, C. Q., et al. (1998) Antibody-mediated targeting of CD45 isoforms: a novel immunotherapeutic strategy. *Proc. Natl. Acad. Sci. USA* **95**, 3821–3826.
43. Lenschow, D. J., Zeng, Y., Thistlethwaite, J. R., et al. (1992) Long-term survival of xenogeneic pancreatic islet grafts induced by CTLA4Ig. *Science* **257**, 789–792.
44. Parker, D. C., Greiner, D. L., Phillips, N. E., et al. (1995) Survival of mouse pancreatic islet allografts in recipients treated with allogeneic small lymphocytes and antibody to CD40 ligand. *Proc. Natl. Acad. Sci. USA* **92**, 9560–9564.
45. Larsen, C. P., Elwood, E. T., Alexander, D. Z., et al. (1996) Long-term acceptance of skin and cardiac allografts after blocking CD40 and CD28 pathways. *Nature* **381**, 434–438.

46. Isobe, M., Yagita, H., Okumura, K., and Ihara, A. (1992) Specific acceptance of cardiac allograft after treatment with antibodies to ICAM-1 and LFA-1. *Science* **255**, 1125–1127.
47. Graca, L., Chen, T. C., Le Moine, A., Cobbold, S. P., Howie, D., and Waldmann, H. (2005) Dominant tolerance: activation thresholds for peripheral generation of regulatory T cells. *Trends Immunol.* **26**, 130–135.
48. Sakaguchi, N., Takahashi, T., Hata, H., et al. (2003) Altered thymic T-cell selection due to a mutation of the ZAP-70 gene causes autoimmune arthritis in mice. *Nature* **426**, 454–460.
49. Yoshitomi, H., Sakaguchi, N., Kobayashi, K., et al. (2005) A role for fungal {beta}-glucans and their receptor Dectin-1 in the induction of autoimmune arthritis in genetically susceptible mice. *J. Exp. Med.* **201**, 949–960.
50. Marleau, A. M. and Sarvetnick, N. (2005) T cell homeostasis in tolerance and immunity. *J. Leukoc. Biol.* **78**, 575–584.
51. Rossini, A. A., Handler, E. S., Greiner, D. L., and Mordes, J. P. (1991) Insulin dependent diabetes mellitus hypothesis of autoimmunity. *Autoimmunity* **8**, 221–235.
52. Shoda, L. K., Young, D. L., Ramanujan, S., et al. (2005) A comprehensive review of interventions in the NOD mouse and implications for translation. *Immunity* **23**, 115–126.
53. Fitzpatrick, F., Lepault, F., Homo-Delarche, F., Bach, J. F., and Dardenne, M. (1991) Influence of castration, alone or combined with thymectomy, on the development of diabetes in the nonobese diabetic mouse. *Endocrinol.* **129**, 1382–1390.
54. Like, A. A., Rossini, A. A., Guberski, D. L., Appel, M. C., and Williams, R. M. (1979) Spontaneous diabetes mellitus: reversal and prevention in the BB/W rat with antiserum to rat lymphocytes. *Science* **206**, 1421–1423.
55. Mordes, J. P., Guberski, D. L., Leif, J. H., et al. (2005) LEW.1WR1 rats develop autoimmune diabetes spontaneously and in response to environmental perturbation. *Diabetes* **54**, 2727–2733.
56. Holmdahl, R., Rubin, K., Klareskog, L., Larsson, E., and Wigzell, H. (1986) Characterization of the antibody response in mice with type II collagen-induced arthritis, using monoclonal anti-type II collagen antibodies. *Arthritis Rheum.* **29**, 400–410.
57. Wooley, P. H., Luthra, H. S., Stuart, J. M., and David, C. S. (1981) Type II collagen-induced arthritis in mice. I. Major histocompatibility complex (I region) linkage and antibody correlates. *J. Exp. Med.* **154**, 688–700.
58. Trentham, D. E., Townes, A. S., and Kang, A. H. (1977) Autoimmunity to type II collagen an experimental model of arthritis. *J. Exp. Med.* **146**, 857–868.
59. Kouskoff, V., Korganow, A. S., Duchatelle, V., Degott, C., Benoist, C., and Mathis, D. (1996) Organ-specific disease provoked by systemic autoimmunity. *Cell* **87**, 811–822.
60. Korganow, A. S., Ji, H., Mangialaio, S., et al. (1999) From systemic T cell self-reactivity to organ-specific autoimmune disease via immunoglobulins. *Immunity* **10**, 451–461.
61. Nohara, C., Akiba, H., Nakajima, A., et al. (2001) Amelioration of experimental autoimmune encephalomyelitis with anti-OX40 ligand monoclonal antibody: a

- critical role for OX40 ligand in migration, but not development, of pathogenic T cells. *J. Immunol.* **166**, 2108–2115.
62. von Budingen, H. C., Tanuma, N., Villoslada, P., Ouallet, J. C., Hauser, S. L., and Genain, C. P. (2001) Immune responses against the myelin/oligodendrocyte glycoprotein in experimental autoimmune demyelination. *J. Clin. Immunol.* **21**, 155–170.
  63. Sun, Y., Lin, X., Chen, H. M., Wu, Q., Subudhi, S. K., Chen, L., and Fu, Y. X. (2002) Administration of agonistic anti-4-1BB monoclonal antibody leads to the amelioration of experimental autoimmune encephalomyelitis. *J. Immunol.* **168**, 1457–1465.
  64. Croxford, J. L., O'Neill, J. K., Ali, R. R., et al. (1998) Local gene therapy with CTLA4-immunoglobulin fusion protein in experimental allergic encephalomyelitis. *Eur. J. Immunol.* **28**, 3904–3916.
  65. Lafaille, J. J., Nagashima, K., Katsuki, M., and Tonegawa, S. (1994) High incidence of spontaneous autoimmune encephalomyelitis in immunodeficient anti-myelin basic protein T cell receptor transgenic mice. *Cell* **78**, 399–408.
  66. Lafaille, J. J., Keere, F. V., Hsu, A. L., et al. (1997) Myelin basic protein-specific T helper 2 (Th2) cells cause experimental autoimmune encephalomyelitis in immunodeficient hosts rather than protect them from the disease. *J. Exp. Med.* **186**, 307–312.
  67. Olivares-Villagomez, D., Wang, Y., and Lafaille, J. J. (1998) Regulatory CD4(+) T cells expressing endogenous T cell receptor chains protect myelin basic protein-specific transgenic mice from spontaneous autoimmune encephalomyelitis. *J. Exp. Med.* **188**, 1883–1894.
  68. Hori, S., Haury, M., Coutinho, A., and Demengeot, J. (2002) Specificity requirements for selection and effector functions of CD25+4+ regulatory T cells in anti-myelin basic protein T cell receptor transgenic mice. *Proc. Natl. Acad. Sci. USA* **99**, 8213–8218.
  69. Andrews, B. S., Eisenberg, R. A., Theofilopoulos, A. N., et al. (1978) Spontaneous murine lupus-like syndromes. Clinical and immunopathological manifestations in several strains. *J. Exp. Med.* **148**, 1198–1215.
  70. Feldmann, M. and Maini, R. N. (2001) Anti-TNF alpha therapy of rheumatoid arthritis: what have we learned? *Annu. Rev. Immunol.* **19**, 163–196.
  71. Coles, A. J., Wing, M., Smith, S., et al. (1999) Pulsed monoclonal antibody treatment and autoimmune thyroid disease in multiple sclerosis. *Lancet* **354**, 1691–1695.
  72. Edwards, J. C., Szczepanski, L., Szechinski, J., et al. (2004) Efficacy of B-cell-targeted therapy with rituximab in patients with rheumatoid arthritis. *N. Engl. J. Med.* **350**, 2572–2581.
  73. Chatenoud, L., Thervet, E., Primo, J., and Bach, J. F. (1994) Anti-CD3 antibody induces long-term remission of overt autoimmunity in nonobese diabetic mice. *Proc. Natl. Acad. Sci. USA* **91**, 123–127.
  74. Chatenoud, L., Primo, J., and Bach, J. F. (1997) CD3 antibody-induced dominant self tolerance in overtly diabetic NOD mice. *J. Immunol.* **158**, 2947–2954.
  75. von Herrath, M. G., Coon, B., Wolfe, T., and Chatenoud, L. (2002) Nonmitogenic CD3 antibody reverses virally induced (rat insulin promoter-lymphocytic

- choriomeningitis virus) autoimmune diabetes without impeding viral clearance. *J. Immunol.* **168**, 933–941.
76. Hughes, C., Wolos, J. A., Giannini, E. H., and Hirsch, R. (1994) Induction of T helper cell hyporesponsiveness in an experimental model of autoimmunity by using nonmitogenic anti-CD3 monoclonal antibody. *J. Immunol.* **153**, 3319–3325.
77. Smith, J. A., Tso, J. Y., Clark, M. R., Cole, M. S., and Bluestone, J. A. (1997) Nonmitogenic anti-CD3 monoclonal antibodies deliver a partial T cell receptor signal and induce clonal anergy. *J. Exp. Med.* **185**, 1413–1422.
78. Hahn, H. J., Kuttler, B., Laube, F., and Emmrich, F. (1993) Anti-CD4 therapy in recent-onset IDDM. *Diabetes Metab. Rev.* **9**, 323–328.
79. Phillips, J. M., Harach, S. Z., Parish, N. M., Fehervari, Z., Haskins, K., and Cooke, A. (2000) Nondepleting anti-CD4 has an immediate action on diabetogenic effector cells, halting their destruction of pancreatic beta cells. *J. Immunol.* **165**, 1949–1955.
80. Guo, Z., Wu, T., Kirchhof, N., et al. (2001) Immunotherapy with nondepleting anti-CD4 monoclonal antibodies but not CD28 antagonists protects islet graft in spontaneously diabetic nod mice from autoimmune destruction and allogeneic and xenogeneic graft rejection. *Transplantation* **71**, 1656–1665.
81. Makhlof, L., Grey, S. T., Dong, V., et al. (2004) Depleting anti-CD4 monoclonal antibody cures new-onset diabetes, prevents recurrent autoimmune diabetes, and delays allograft rejection in nonobese diabetic mice. *Transplantation* **77**, 990–997.
82. Mottram, P. L., Murray-Segal, L. J., Han, W., Maguire, J., Stein-Oakley, A., and Mandel, T. E. (1998) Long-term survival of segmental pancreas isografts in NOD/Lt mice treated with anti-CD4 and anti-CD8 monoclonal antibodies. *Diabetes* **47**, 1399–1405.
83. Williams, R. O., Whyte, A., and Waldmann, H. (1989) Resistance to collagen-induced arthritis in DBA/1 mice by intraperitoneal administration of soluble type II collagen involves both CD4+ and CD8+ T lymphocytes. *Autoimmunity* **4**, 237–245.
84. Williams, R. O., Mason, L. J., Feldmann, M., and Maini, R. N. (1994) Synergy between anti-CD4 and anti-tumor necrosis factor in the amelioration of established collagen-induced arthritis. *Proc. Natl. Acad. Sci. USA* **91**, 2762–2766.
85. Mauri, C., Chu, C. Q., Woodrow, D., Mori, L., and Londei, M. (1997) Treatment of a newly established transgenic model of chronic arthritis with nondepleting anti-CD4 monoclonal antibody. *J. Immunol.* **159**, 5032–5041.
86. Maini, R. N., Elliott, M. J., Brennan, F. M., et al. (1995) Monoclonal anti-TNF alpha antibody as a probe of pathogenesis and therapy of rheumatoid disease. *Immunol. Rev.* **144**, 195–223.
87. Lin, H., Bolling, S. F., Linsley, P. S., et al. (1993) Long-term acceptance of major histocompatibility complex mismatched cardiac allografts induced by CTLA4Ig plus donor-specific transfusion. *J. Exp. Med.* **178**, 1801–1806.
88. Bushell, A., Morris, P. J., and Wood, K. J. (1994) Induction of operational tolerance by random blood transfusion combined with anti-CD4 antibody therapy. A protocol with significant clinical potential. *Transplantation* **58**, 133–139.



89. Choy, E. H., Adjaye, J., Forrest, L., Kingsley, G. H., and Panayi, G. S. (1993) Chimaeric anti-CD4 monoclonal antibody cross-linked by monocyte Fc gamma receptor mediates apoptosis of human CD4 lymphocytes. *Eur. J. Immunol.* **23**, 2676–2681.
90. Bemelman, F., Honey, K., Adams, E., Cobbold, S., and Waldmann, H. (1998) Bone marrow transplantation induces either clonal deletion or infectious tolerance depending on the dose. *J. Immunol.* **160**, 2645–2648.
91. Kurtz, J., Shaffer, J., Lie, A., Anosova, N., Benichou, G., and Sykes, M. (2004) Mechanisms of early peripheral CD4 T-cell tolerance induction by anti-CD154 monoclonal antibody and allogeneic bone marrow transplantation: evidence for anergy and deletion but not regulatory cells. *Blood* **103**, 4336–4343.
92. Markees, T. G., Pearson, T., Cuthbert, A., et al. (2004) Evaluation of donor-specific transfusion sources: unique failure of bone marrow cells to induce prolonged skin allograft survival with anti-CD154 monoclonal antibody. *Transplantation* **78**, 1601–1608.
93. Wekerle, T., Kurtz, J., Ito, H., et al. (2000) Allogeneic bone marrow transplantation with co-stimulatory blockade induces macrochimerism and tolerance without cytoreductive host treatment. *Nat. Med.* **6**, 464–469.
94. Durham, M. M., Bingaman, A. W., Adams, A. B., et al. (2000) Cutting edge: administration of anti-CD40 ligand and donor bone marrow leads to hemopoietic chimerism and donor-specific tolerance without cytoreductive conditioning. *J. Immunol.* **165**, 1–4.
95. Seung, E., Mordes, J. P., Rossini, A. A., and Greiner, D. L. (2003) Hematopoietic chimerism and central tolerance created by peripheral-tolerance induction without myeloablative conditioning. *J. Clin. Invest.* **112**, 795–808.
96. Wells, A. D., Li, X. C., Li, Y., et al. (1999) Requirement for T-cell apoptosis in the induction of peripheral transplantation tolerance. *Nat. Med.* **5**, 1303–1307.
97. Ciubotariu, R., Colovai, A. I., Pennesi, G., et al. (1998) Specific suppression of human CD4+ Th cell responses to pig MHC antigens by CD8+CD28– regulatory T cells. *J. Immunol.* **161**, 5193–5202.
98. Sharp, C., Thompson, C., Samy, E. T., Noelle, R., and Tung, K. S. (2003) CD40 ligand in pathogenesis of autoimmune ovarian disease of day 3-thymectomized mice: implication for CD40 ligand antibody therapy. *J. Immunol.* **170**, 1667–1674.
99. Welsh, R. M., Markees, T. G., Woda, B. A., et al. (2000) Virus-induced abrogation of transplantation tolerance induced by donor-specific transfusion and anti-CD154 antibody. *J. Virol.* **74**, 2210–2218.
100. Williams, M. A., Onami, T. M., Adams, A. B., et al. (2002) Cutting edge: persistent viral infection prevents tolerance induction and escapes immune control following CD28/CD40 blockade-based regimen. *J. Immunol.* **169**, 5387–5391.
101. Adams, A. B., Williams, M. A., Jones, T. R., et al. (2003) Heterologous immunity provides a potent barrier to transplantation tolerance. *J. Clin. Invest.* **111**, 1887–1895.
102. Adams, A. B., Pearson, T. C., and Larsen, C. P. (2003) Heterologous immunity: an overlooked barrier to tolerance. *Immunol. Rev.* **196**, 147–160.

103. Bushell, A., Jones, E., Gallimore, A., and Wood, K. (2005) The generation of CD25+ CD4+ regulatory T cells that prevent allograft rejection does not compromise immunity to a viral pathogen. *J. Immunol.* **174**, 3290–3297.
104. Kirk, A. D., Burkly, L. C., Batty, D. S., et al. (1999) Treatment with humanized monoclonal antibody against CD154 prevents acute renal allograft rejection in nonhuman primates. *Nat. Med.* **5**, 686–693.
105. Smiley, S. T., Csizmadia, V., Gao, W., Turka, L. A., and Hancock, W. W. (2000) Differential effects of cyclosporine A, methylprednisolone, mycophenolate, and rapamycin on CD154 induction and requirement for NFkappaB: implications for tolerance induction. *Transplantation* **70**, 415–419.
106. Adams, A. B., Shirasugi, N., Jones, T. R., et al. (2003) Conventional immunosuppression is compatible with costimulation blockade-based, mixed chimerism tolerance induction. *Am. J. Transplant.* **3**, 895–901.
107. Brinkmann, V. and Lynch, K. R. (2002) FTY720: targeting G-protein-coupled receptors for sphingosine 1-phosphate in transplantation and autoimmunity. *Curr. Opin. Immunol.* **14**, 569–575.
108. Wu, Z., Bensinger, S. J., Zhang, J., Chen, C., et al. (2004) Homeostatic proliferation is a barrier to transplantation tolerance. *Nat. Med.* **10**, 87–92.
109. Goldrath, A. W., Bogatzki, L. Y., and Bevan, M. J. (2000) Naive T cells transiently acquire a memory-like phenotype during homeostasis-driven proliferation. *J. Exp. Med.* **192**, 557–564.
110. Wekerle, T. and Sykes, M. (2001) Mixed chimerism and transplantation tolerance. *Annu. Rev. Med.* **52**, 353–370.
111. Kenyon, N. S., Chatzipetrou, M., Masetti, M., et al. (1999) Long-term survival and function of intrahepatic islet allografts in rhesus monkeys treated with humanized anti-CD154. *Proc. Natl. Acad. Sci. USA* **96**, 8132–8137.
112. Keymeulen, B., Vandemeulebroucke, E., Ziegler, A. G., et al. (2005) Insulin needs after CD3-antibody therapy in new-onset type 1 diabetes. *N. Engl. J. Med.* **352**, 2598–2608.
113. Chavin, K. D., Lau, H. T., and Bromberg, J. S. (1992) Prolongation of allograft and xenograft survival in mice by anti-CD2 monoclonal antibodies. *Transplantation* **54**, 286–291.
114. Nicolls, M. R., Aversa, G. G., Pearce, N. W., et al. (1993) Induction of long-term specific tolerance to allografts in rats by therapy with an anti-CD3-like monoclonal antibody. *Transplantation* **55**, 459–468.
115. Lazarovits, A. I., Poppema, S., Zhang, Z., et al. (1996) Prevention and reversal of renal allograft rejection by antibody against CD45RB. *Nature* **380**, 717–720.
116. Curry, A. J., Chikwe, J., Smith, X. G., et al. (2004) OX40 (CD134) blockade inhibits the co-stimulatory cascade and promotes heart allograft survival. *Transplantation* **78**, 807–814.
117. Furukawa, F. and Yoshimasu, T. (2005) Animal models of spontaneous and drug-induced cutaneous lupus erythematosus. *Autoimmun. Rev.* **4**, 345–350.
118. Carayanniotis, G., Masters, S. R., and Noelle, R. J. (1997) Suppression of murine thyroiditis via blockade of the CD40-CD40L interaction. *Immunol.* **90**, 421–426.

119. Barlow, A. K. and Like, A. A. (1992) Anti-CD2 monoclonal antibodies prevent spontaneous and adoptive transfer of diabetes in the BB/Wor rat. *Am. J. Pathol.* **141**, 1043–1051.
120. Yokoi, N., Komeda, K., Wang, H. Y., et al. (2002) Cblb is a major susceptibility gene for rat type 1 diabetes mellitus. *Nat. Genet.* **31**, 391–394.
121. Lenzen, S., Tiedge, M., Elsner, M., et al. (2001) The LEW.1AR1/Ztm-iddm rat: a new model of spontaneous insulin-dependent diabetes mellitus. *Diabetologia* **44**, 1189–1196.
122. Nakamura, H., Yamaki, K., Kondo, I., and Sakuragi, S. (2005) Experimental autoimmune uveitis induced by immunization with retinal pigment epithelium-specific 65-kDa protein peptides. *Curr. Eye Res.* **30**, 673–680.
123. Stanislaus, R., Gilg, A. G., Singh, A. K., and Singh, I. (2005) N-acetyl-L-cysteine ameliorates the inflammatory disease process in experimental autoimmune encephalomyelitis in Lewis rats. *J. Autoimmune Dis.* **2**, 4.
124. Fijak, M., Iosub, R., Schneider, E., et al. (2005) Identification of immunodominant autoantigens in rat autoimmune orchitis. *J. Pathol.* **207**, 127–138.
125. Inomata, T., Watanabe, T., Haga, M., et al. (2000) Anti-CD2 monoclonal antibodies prevent the induction of experimental autoimmune myocarditis. *Jpn Heart J.* **41**, 507–517.
126. Jung, S., Toyka, K., and Hartung, H. P. (1995) Suppression of experimental autoimmune encephalomyelitis in Lewis rats by antibodies against CD2. *Eur. J. Immunol.* **25**, 1391–1398.
127. Adachi, Y., Inaba, M., Sugihara, A., et al. (1998) Effects of administration of monoclonal antibodies (anti-CD4 or anti-CD8) on the development of autoimmune diseases in (NZW x BXSB)F1 mice. *Immunobiol.* **198**, 451–464.
128. Chakrabarty, S., Nagata, M., Yasuda, H., et al. (2003) Critical roles of CD30/CD30L interactions in murine autoimmune diabetes. *Clin. Exp. Immunol.* **133**, 318–325.
129. Finck, B. K., Linsley, P. S., and Wofsy, D. (1994) Treatment of murine lupus with CTLA4Ig. *Science* **265**, 1225–1227.
130. Mihara, M., Tan, I., Chuzhin, Y., et al. (2000) CTLA4Ig inhibits T cell-dependent B-cell maturation in murine systemic lupus erythematosus. *J. Clin. Invest.* **106**, 91–101.
131. Daikh, D. I. and Wofsy, D. (2001) Cutting edge: reversal of murine lupus nephritis with CTLA4Ig and cyclophosphamide. *J. Immunol.* **166**, 2913–2916.
132. Wang, X., Huang, W., Mihara, M., Sinha, J., and Davidson, A. (2002) Mechanism of action of combined short-term CTLA4Ig and anti-CD40 ligand in murine systemic lupus erythematosus. *J. Immunol.* **168**, 2046–2053.
133. Chu, E. B., Hobbs, M. V., Wilson, C. B., Romball, C. G., Linsley, P. S., and Weigle, W. O. (1996) Intervention of CD4+ cell subset shifts and autoimmunity in the BXSB mouse by murine CTLA4Ig. *J. Immunol.* **156**, 1262–1268.
134. Boon, L., Brok, H. P., Bauer, J., et al. (2001) Prevention of experimental autoimmune encephalomyelitis in the common marmoset (*Callithrix jacchus*) using a chimeric antagonist monoclonal antibody against human CD40 is associated with altered B cell responses. *J. Immunol.* **167**, 2942–2949.

135. Namba, K., Ogasawara, K., Kitaichi, N., et al. (2000) Amelioration of experimental autoimmune uveoretinitis by pretreatment with a pathogenic peptide in liposome and anti-CD40 ligand monoclonal antibody. *J. Immunol.* **165**, 2962–2969.
136. Early, G. S., Zhao, W., and Burns, C. M. (1996) Anti-CD40 ligand antibody treatment prevents the development of lupus-like nephritis in a subset of New Zealand black x New Zealand white mice. Response correlates with the absence of an anti-antibody response. *J. Immunol.* **157**, 3159–3164.
137. Zandman-Goddard, G. and Shoenfeld, Y. (2000) Novel approaches to therapy for systemic lupus erythematosus. *Eur. J. Intern. Med.* **11**, 130–134.
138. Kalled, S. L., Cutler, A. H., and Burkly, L. C. (2001) Apoptosis and altered dendritic cell homeostasis in lupus nephritis are limited by anti-CD154 treatment. *J. Immunol.* **167**, 1740–1747.
139. Quezada, S. A., Eckert, M., Adeyi, O. A., Schned, A. R., Noelle, R. J., and Burns, C. M. (2003) Distinct mechanisms of action of anti-CD154 in early versus late treatment of murine lupus nephritis. *Arthritis Rheum.* **48**, 2541–2554.
140. 't Hart, B. A., Blezer, E. L., Brok, H. P., et al. (2005) Treatment with chimeric anti-human CD40 antibody suppresses MRI-detectable inflammation and enlargement of pre-existing brain lesions in common marmosets affected by MOG-induced EAE. *J. Neuroimmunol.* **163**, 31–39.
141. Foell, J. L., Diez-Mendiondo, B. I., Diez, O. H., et al. (2004) Engagement of the CD137 (4-1BB) costimulatory molecule inhibits and reverses the autoimmune process in collagen-induced arthritis and establishes lasting disease resistance. *Immunol.* **113**, 89–98.
142. Foell, J., Strahotin, S., O'Neil, S. P., et al. (2003) CD137 costimulatory T cell receptor engagement reverses acute disease in lupus-prone NZB x NZW F1 mice. *J. Clin. Invest.* **111**, 1505–1518.
143. Malmstrom, V., Shipton, D., Singh, B., et al. (2001) CD134L expression on dendritic cells in the mesenteric lymph nodes drives colitis in T cell-restored SCID mice. *J. Immunol.* **166**, 6972–6981.
144. Lee, J., Lee, E. N., Kim, E. Y., et al. (2005) Administration of agonistic anti-4-1BB monoclonal antibody leads to the amelioration of inflammatory bowel disease. *Immunol. Lett.* **101**, 210–216.
145. Moriyama, H., Yokono, K., Amano, K., et al. (1996) Induction of tolerance in murine autoimmune diabetes by transient blockade of leukocyte function-associated antigen-1/intercellular adhesion molecule-1 pathway. *J. Immunol.* **157**, 3737–3743.



## Induction of Tolerance by Adoptive Transfer of Treg Cells

Kanji Nagahama, Eiji Nishimura, and Shimon Sakaguchi

### Summary

Naturally arising CD4<sup>+</sup>CD25<sup>+</sup> regulatory T (Treg) cells can be exploited to establish immunologic tolerance to allogeneic transplants. In vivo exposure of CD4<sup>+</sup>CD25<sup>+</sup> T cells from normal naïve mice to alloantigen in a T cell-deficient environment elicits spontaneous expansion of alloantigen-specific CD4<sup>+</sup>CD25<sup>+</sup> natural Treg cells, which are able to suppress allograft rejection mediated by subsequently transferred naïve T cells, leading to long-term graft tolerance. Similar antigen-specific expansion of natural Treg cells can also be achieved in vitro by stimulating CD4<sup>+</sup>CD25<sup>+</sup> T cells from normal animals with alloantigen in the presence of high doses of interleukin-2. The expanded CD4<sup>+</sup>CD25<sup>+</sup> Treg cells are even capable of suppressing secondary mixed leukocyte reaction in vitro and, by in vivo transfer, establishing antigen-specific long-term graft tolerance. Thus, in vivo or in vitro, direct or indirect ways of alloantigen-specific expansion of naturally arising CD4<sup>+</sup>CD25<sup>+</sup> Treg cells can establish antigen-specific dominant tolerance to allogeneic transplants.

**Key Words:** CD4<sup>+</sup>CD25<sup>+</sup> regulatory T cells; allograft tolerance induction; organ transplantation.

### 1. Introduction

It is hoped that immunologic tolerance to certain nonself antigens, such as alloantigens in organ transplants, can be established as stably as natural tolerance to self-constituents. There is accumulating evidence that naturally arising CD4<sup>+</sup>CD25<sup>+</sup> regulatory T (Treg) cells play a crucial role in the maintenance of immunologic self-tolerance and negative control of immune responses (1–3). For example, depletion of CD4<sup>+</sup>CD25<sup>+</sup> Treg cells leads to spontaneous development of various autoimmune diseases in normal animals and provokes effective tumor immunity in otherwise nonresponding animals (4–8). The depletion also enhances immune responses to nonself antigens including allogeneic transplantation antigens (4).

Natural CD4<sup>+</sup>CD25<sup>+</sup> Treg cells are at least in part produced by the normal thymus as a functionally mature T-cell subpopulation (9). They are functionally unique in that they proliferate poorly in response to in vitro antigenic stimulation unless interleukin (IL)-2 is provided and, upon in vitro stimulation with specific antigens, they potently suppress the activation/proliferation of other T cells in an antigen-nonspecific manner, seemingly through cell–cell interaction on antigen-presenting cells (APC) (9–12). Phenotypically, they constitutively express CTLA-4, certain members of Toll-like receptors, CD103 ( $\alpha_E$  integrin) and GITR (glucocorticoid-induced TNF receptor family-related gene) at high levels (13–19). They specifically express the transcription factor *Foxp3*, which appears to act as a master control gene for their development and function (20–22). Furthermore, recent studies utilizing CD4<sup>+</sup>CD25<sup>+</sup> Treg cells from T-cell receptor transgenic mice have shown that antigen-specific Treg cells can expand in vivo upon antigen stimulation along with potent adjuvant or mature dendritic cells (23–25). Natural CD4<sup>+</sup>CD25<sup>+</sup> Treg cells also show homeostatic proliferation in a T cell-deficient environment (26,27), and a fraction of them are proliferating in normal animals presumably by recognizing self-antigens (28,29). These findings collectively indicate that naturally arising CD4<sup>+</sup>CD25<sup>+</sup> Treg cells are a developmentally, phenotypically, and functionally distinct subpopulation of T cells (1).

We have previously shown that alloantigen-specific Treg cells present in the naturally arising CD4<sup>+</sup>CD25<sup>+</sup> Treg cell population can be expanded in vivo by sensitizing them to alloantigens, in contrast to their in vitro hypoproliferation upon allogeneic stimulation (30). Notably, permanent graft tolerance can be achieved when this in vivo antigen-specific expansion of natural Treg cells is allowed to the extent that they become sufficient in number and suppressive activity to control the expansion/activation of alloreactive effector T cells. Alloantigen-specific CD4<sup>+</sup>CD25<sup>+</sup> Treg cells can also be expanded in vitro in the presence of high dose IL-2 and exploited for inducing antigen-specific graft tolerance in vivo by transferring them to animals with allografts (31,32). In addition, recent reports have shown that natural CD4<sup>+</sup>CD25<sup>+</sup> Treg cells are also instrumental in the prevention of graft-vs-host disease after allogeneic bone marrow transplantation (33,34).

Based on these findings, we discuss in this chapter how donor-specific graft tolerance can be achieved by in vivo or in vitro expansion of antigen-specific CD4<sup>+</sup>CD25<sup>+</sup> natural Treg cells.

## 2. Materials

### 2.1. Mice

1. Six- to 8-wk-old female BALB/c, C57Bl/6 (B6), and C3H/He may be purchased from suppliers such as SLC Japan (Osaka, Japan).
2. BALB/c athymic nude mice may be obtained from Clea Japan (Tokyo, Japan).

## 2.2. Skin Transplantation and Cell Transfer

1. Full thickness tail skin is removed from euthanized donors, placed on sterile filter paper moistened with PBS, and kept at 4°C until use usually within 30 min. The dorsal surfaces of anesthetized recipient mice are washed with 70% ethanol. A graft bed is prepared with fine scissors by removing an area of epidermis and dermis down to the level of the muscle fascia. Skin grafts (0.5 cm<sup>2</sup>) are placed into the prepared bed without suturing and then covered with Vaseline-impregnated gauze and an adhesive plastic bandage. After 7 d, the bandage is removed.
2. Cell suspensions in 0.4 mL of RPMI 1640 medium (Gibco BRL, Gaithersburg, MD) are administered intravenously through a tail vein.
3. Skin graft survival is assessed four times a week by visual and tactile examination. Rejection is defined as the first day on which the entire epidermal surface of the graft becomes necrotic. Statistical analysis of graft survival is made by the log-rank method.

## 2.3. Monoclonal Antibodies and Reagents

1. Fluorescein isothiocyanate-, phycoerythrin-, CyChrome-labeled, or biotinylated monoclonal antibodies (MAb) to CD25 (clone 7D4) and CD4 (clones RM4-5 and H129.19) (PharMingen, San Diego, CA).
2. PE- or CyChrome-conjugated streptavidin, as the secondary reagent (PharMingen).
3. Affinity-purified goat anti-rat IgG (specific for the whole IgG molecule) (ICN Pharmaceuticals, Aurora, OH).
4. Normal rat IgG (Sigma, St. Louis, MO).
5. Murine recombinant IL (rIL)-2 ( $3.89 \times 10^6$  U/mg) (Shionogi Co., Osaka, Japan).

## 2.4. Fractionation of T-Cell Suspensions

1. Lymphocyte suspensions are prepared from spleens and inguinal, axillary, brachial, and mesenteric lymph nodes of 6- to 8-wk-old female BALB/c mice. Erythrocytes are lysed with ACK buffer (8.29 g of NH<sub>4</sub>Cl, 1 g of KHCO<sub>3</sub>, 37.2 mg of Na<sub>2</sub>EDTA, 800 mL of H<sub>2</sub>O, adjusted to pH to 7.2–7.4 with 1 N HCl, and topped up to 1 L with H<sub>2</sub>O).
2. B cells and adherent cells are depleted by treating with anti-CD24 (clone J11d) MAb (4°C, 30 min.) and incubating on plastic dishes precoated with goat anti-rat IgG at 4°C for 30 min (nontreated 100-mm dishes: IWAKI, 1020-100) (*see Note 1*).
3. For further depletion, the nonadherent cells (at  $5 \times 10^6$  cells/mL) are incubated with nontoxic rabbit serum (Cedarlane Laboratories, Ontario, Canada), as a complement source, diluted 1:10 as a final concentration, for 30 min at 37°C with occasional shaking.
4. To remove CD4<sup>+</sup>CD25<sup>+</sup> cells from splenic and lymph node cells, cell suspensions are incubated at  $5 \times 10^6$  cells/mL for 30 min at 4°C with the culture supernatant of hybridoma cells secreting anti-CD25 MAb (clone 7D4). They are then washed once and incubated with nontoxic rabbit serum diluted 1:10 as the final concentration, and incubated for 30 min at 37°C with occasional shaking. This procedure is repeated twice.



## 2.5. CD4<sup>+</sup>CD25<sup>+</sup> Treg and CD4<sup>+</sup>CD25<sup>-</sup> T Cells

1. For enrichment of CD4<sup>+</sup>CD25<sup>+</sup> T cells, spleen and lymph node cells are first incubated with anti-CD8 (clone 3.155) and anti-CD24 (clone J11d) MAb for 30 min at 4°C, then incubated at 4°C for 30 min on plastic dishes precoated with goat anti-rat IgG.
2. Nonadherent cells (>85% of which are usually CD4<sup>+</sup>) are stained with biotin-anti-CD25 MAb, followed by PE-streptavidin and fluorescein isothiocyanate-anti-CD4 MAb at 4°C for 30 min.
3. CD4<sup>+</sup>CD25<sup>+</sup> or CD4<sup>+</sup>CD25<sup>-</sup> T cells are purified by MoFlo cytometer (Dako-Cytomation, Carpinteria, CA) (the purity of the CD4<sup>+</sup>CD25<sup>+</sup> or CD4<sup>+</sup>CD25<sup>-</sup> population is usually >98% and ~99%, respectively). Alternatively, CD4<sup>+</sup>CD25<sup>+</sup> cells are enriched by the MACS system (magnetic cell sorting; Miltenyi Biotech).
4. The enriched CD4<sup>+</sup> T cells are stained with biotin-anti-CD25 MAb, PE-streptavidin, and then incubated with anti-PE microbeads according to the manufacturer's instructions.
5. Cells are positively selected on an LS separation column. The CD4<sup>+</sup>CD25<sup>+</sup> population is further enriched from the positive fraction by passing a second time over an LS column (*see Note 2*).
6. The cells in the negative fraction are incubated with anti-CD4 microbeads and the CD4<sup>+</sup>CD25<sup>-</sup> population is positively selected on an LS column (*see Note 2*). Purity of the CD4<sup>+</sup>CD25<sup>+</sup> and CD4<sup>+</sup>CD25<sup>-</sup> populations is usually >93% and approx 99%, respectively.

## 2.6. Mixed Leukocyte Reaction

1. BALB/c whole, CD4<sup>+</sup> or CD4<sup>+</sup>CD25<sup>-</sup> T cells ( $5 \times 10^4$ /well) together with various numbers of CD4<sup>+</sup>CD25<sup>+</sup> Treg cells ( $0-5 \times 10^4$ /well) are cultured with RBC-lysed and X-irradiated (20 Gy) B6 or C3H splenocytes ( $1 \times 10^5$ /well) as stimulators for 6 d in 96-well round-bottom plates (Corning Costar, Cambridge, MA) in Dulbecco's modified Eagles medium containing 10% fetal calf serum (PAA Laboratories, Newport Beach, CA), penicillin (100 U/mL), streptomycin (100 µg/mL), and 50 µM 2-ME.
2. Cultures are pulsed with [<sup>3</sup>H]thymidine ([<sup>3</sup>H]TdR) (37 kBq/well) (Du Pont/NEN) for the final 16 h.
3. To assess the secondary mixed leukocyte reaction (MLR), BALB/c CD4<sup>+</sup>CD25<sup>-</sup> T cells ( $5 \times 10^4$ /well) are precultured with irradiated B6 splenocytes for 7 d, washed, and then cultured with X-irradiated fresh B6 splenocytes for 5 d in the presence or absence of CD4<sup>+</sup>CD25<sup>+</sup> Treg cells.

## 3. Methods

### 3.1. Induction of Allograft Tolerance by Naturally Occurring CD4<sup>+</sup>CD25<sup>+</sup> Treg Cells

1. B6 tail skin is grafted on BALB/c nude mice, which are then reconstituted with CD25<sup>+</sup>-depleted cells from BALB/c mice. They reject B6 skin grafts significantly faster than those reconstituted with nondepleted cell suspensions (*see Fig. 1*). This indicates that CD4<sup>+</sup>CD25<sup>+</sup> Treg cells in normal naïve mice have the potential to downregulate immune response to alloantigens in vivo.

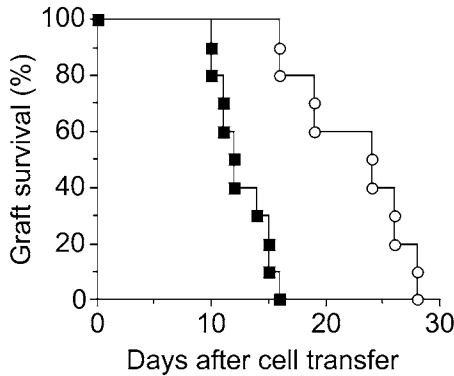


Fig. 1. Control of allograft rejection by natural CD4<sup>+</sup>CD25<sup>+</sup> regulatory T cells. BALB/c nude mice with B6 skin grafts were inoculated with  $5 \times 10^7$  CD25<sup>-</sup>-depleted cells (black squares,  $n = 10$ ) or nondepleted cells (white circles,  $n = 10$ ). Percentage survival of the grafts (ordinate) on days after cell transfer (abscissa) is shown as the total of 3 independent experiments (MST = 12 and 24 d, respectively,  $n = 10$  each,  $p < 0.0001$ ).

2. Cotransfer of CD4<sup>+</sup>CD25<sup>+</sup> Treg cells and naïve T cells into BALB/c nude mice with B6 skin grafts significantly prolongs graft survival compared with the transfer of naïve T cells alone (see Fig. 2).
3. Transfer of CD4<sup>+</sup>CD25<sup>+</sup> Treg cells 7 d prior to naïve T-cell transfer can prolong graft survival further than cotransfer of CD4<sup>+</sup>CD25<sup>+</sup> Treg and naïve T cells. This can be attributed to antigen-specific expansion of CD4<sup>+</sup>CD25<sup>+</sup> Treg cells during this 7 d period, which suppress allogeneic immune responses more effectively when naïve T cells are transferred (see Fig. 2). Notably, permanent graft tolerance is attained in more than 70% of the recipients when a threefold excess of CD4<sup>+</sup>CD25<sup>+</sup> Treg cells to naïve T cells are transferred 7 d prior to naïve T cells (see Fig. 2).

### 3.2. In Vitro Stimulation of CD4<sup>+</sup>CD25<sup>+</sup> Treg Cells

1. Naturally occurring CD4<sup>+</sup>CD25<sup>+</sup> Treg cells exhibit poor proliferative responses in primary allogeneic MLR in vitro, and suppress alloreactive proliferation of both CD4<sup>+</sup> T cells and CD8<sup>+</sup> T cells. However, with addition of rIL-2, the donor-specific cohort of fresh BALB/c CD4<sup>+</sup>CD25<sup>+</sup> Treg cells can expand in MLR with donor-type APC (see Fig. 3).
2. BALB/c CD4<sup>+</sup>CD25<sup>+</sup> Treg cells ( $2.5 \times 10^4$ /well) are cocultured with X-irradiated (15 Gy) B6 or C3H splenocytes ( $1 \times 10^5$ /well) for 7 d in the presence of 100 U/mL of rIL-2.
3. Cells are washed and added to the MLR or administered to skin-grafted nude mice.
4. These prestimulated Treg cells potently suppress a secondary MLR, whereas the same number of freshly prepared CD4<sup>+</sup>CD25<sup>+</sup> T cells fail to do so (see Fig. 4A).
5. The suppressive activity of the 4-wk-stimulated CD4<sup>+</sup>CD25<sup>+</sup> T cells is much higher than the activity of their 1-wk-stimulated counterparts (see Fig. 4A).

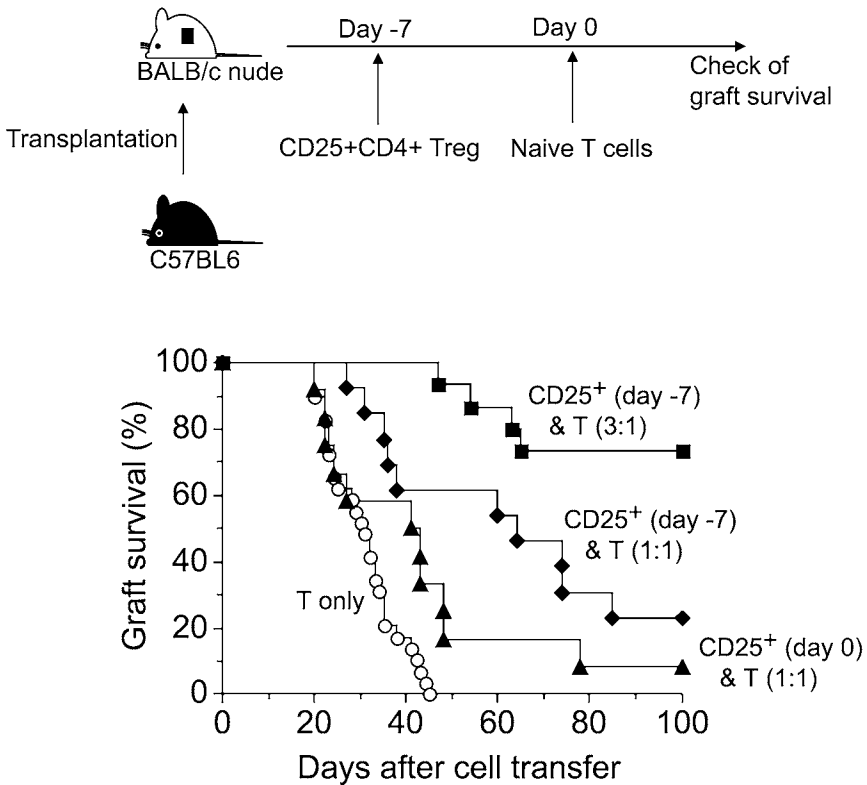


Fig. 2. Induction of allograft tolerance by natural CD4<sup>+</sup>CD25<sup>+</sup> regulatory T cells (Treg) cells. BALB/c nude mice with B6 skin grafts were reconstituted with naïve T cells ( $2 \times 10^5$ ) from normal BALB/c mice on day 0. Some mice were transferred with CD4<sup>+</sup>CD25<sup>+</sup> Treg cells ( $2 \times 10^5$ ) on day 0. Others were transferred with CD4<sup>+</sup>CD25<sup>+</sup> Treg cells ( $2 \times 10^5$  or  $6 \times 10^5$ ) 7 d prior (d -7) to transfer of naïve T cells. Control mice received naïve T cells only. The result shown is the total of 21 independent experiments. Although the cotransfer of CD4<sup>+</sup>CD25<sup>+</sup> Treg cells and naïve T cells significantly prolonged graft survival compared with transfer of naïve T cells alone (MST: 42 vs 31 d,  $n = 12$  and 29, respectively;  $p = 0.002$ ), inoculation of CD4<sup>+</sup>CD25<sup>+</sup> Treg cells 7 d prior to naïve T-cell transfer prolonged graft survival further (MST: 64 d,  $n = 13$ ,  $p = 0.0002$ ) with 23% of the mice showing long-term (>100 d) graft acceptance. Furthermore, when a threefold excess of CD4<sup>+</sup>CD25<sup>+</sup> Treg cells to naïve T cells was transferred 7 d apart, 73% of the recipients showed long-term acceptance of the grafts (MST: >100 d,  $n = 15$ ,  $p < 0.00001$ ).

6. Titration of the number of Treg cells required for a particular degree of suppression reveals that B6-prestimulated BALB/c CD4<sup>+</sup>CD25<sup>+</sup> T cells are more (nearly eightfold) potent than C3H-prestimulated BALB/c CD4<sup>+</sup>CD25<sup>+</sup> T cells in suppressing the response of BALB/c CD4<sup>+</sup>CD25<sup>+</sup> T cells to B6-stimulation;

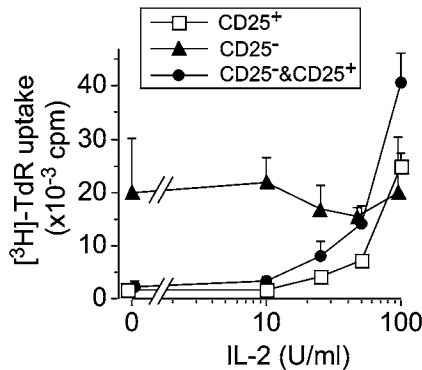


Fig. 3. In vitro expansion of alloantigen-specific CD4<sup>+</sup>CD25<sup>+</sup> regulatory T cells (Treg) cells. BALB/c CD4<sup>+</sup>CD25<sup>-</sup> T cells, CD4<sup>+</sup>CD25<sup>+</sup> Treg cells, or the two populations mixed at the ratio of 1:1, were stimulated with B6 splenocytes in the presence of various concentrations of IL-2.

the C3H-prestimulated CD4<sup>+</sup>CD25<sup>+</sup> T cells show a comparable suppressive activity to that of freshly prepared BALB/c CD4<sup>+</sup>CD25<sup>+</sup> T cells (*see Fig. 4B*).

7. Likewise, C3H-prestimulated BALB/c CD4<sup>+</sup>CD25<sup>+</sup> T cells more potently suppressed the response of BALB/c CD4<sup>+</sup>CD25<sup>-</sup> T cells to C3H stimulation than B6-prestimulated or freshly prepared BALB/c CD4<sup>+</sup>CD25<sup>+</sup> T cells (*see Fig. 4B*).
8. Thus, in vitro stimulation of CD4<sup>+</sup>CD25<sup>+</sup> Treg cells with allogeneic cells and in the presence of IL-2 can enhance their suppressive activity in an alloantigen-specific fashion as demonstrated by in vitro secondary MLR.

### 3.3. Antigen-Specific Suppression of Graft Rejection by Ex Vivo Stimulated CD4<sup>+</sup>CD25<sup>+</sup> Treg Cells

1. Donor-specific tolerance of skin grafts can be induced by the ex vivo prestimulated CD4<sup>+</sup>CD25<sup>+</sup> Treg cells described above. BALB/c CD4<sup>+</sup>CD25<sup>+</sup> Treg cells stimulated in vitro with B6 APCs plus 100 U/mL IL-2 for 1 wk are transferred to BALB/c nude mice carrying B6 skin grafts. The transfer significantly prolongs graft survival in a cell dose-dependent fashion (*see Fig. 5A*).
2. This prolongation is antigen-specific because B6-prestimulated CD4<sup>+</sup>CD25<sup>+</sup> T cells significantly prolong the survival of B6 grafts at 1:1 ratio of Treg cells and naïve T cells; the survival is significantly longer compared with the transfer of C3H-prestimulated CD4<sup>+</sup>CD25<sup>+</sup> T cells. Similarly, C3H-prestimulated CD4<sup>+</sup>CD25<sup>+</sup> T cells prolong the survival of C3H grafts significantly longer than B6-prestimulated CD4<sup>+</sup>CD25<sup>+</sup> T cells (*see Fig. 5B* and **Note 3**).
3. Thus, in vitro stimulation of CD4<sup>+</sup>CD25<sup>+</sup> Treg cells with allogeneic cells and in the presence of IL-2 can enhance their suppressive activity in an alloantigen-specific fashion as demonstrated by both in vivo and in vitro analysis.

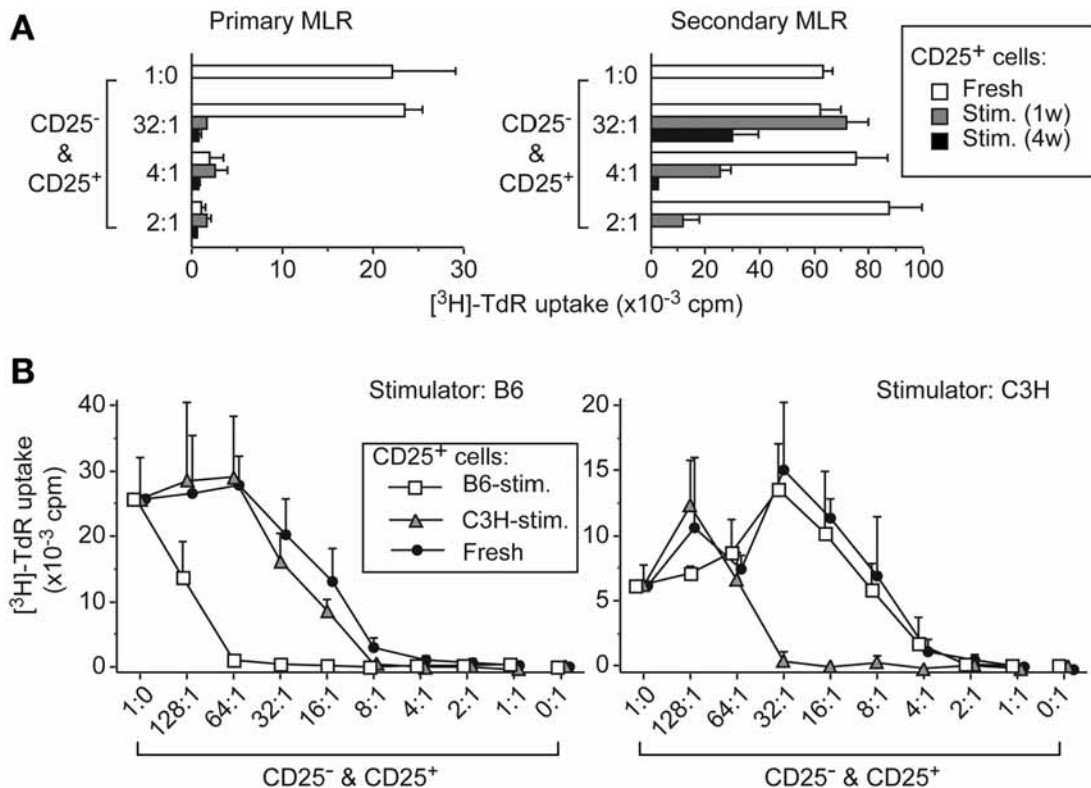


Fig. 4. In vitro expansion of alloantigen-specific CD4<sup>+</sup>CD25<sup>+</sup> regulatory T cells (Treg) cells and enhancement of their antigen-specific suppression. (A) BALB/c CD4<sup>+</sup>CD25<sup>+</sup> T cells freshly prepared, or prestimulated with B6 splenocytes plus interleukin (IL)-2 for 1 or 4 wk, were mixed with BALB/c CD4<sup>+</sup>CD25<sup>-</sup> T cells either freshly prepared (left) or prestimulated with B6 splenocytes for 7 d (right). The cell mixtures were stimulated with X-irradiated B6 splenocytes. (B) BALB/c CD4<sup>+</sup>CD25<sup>+</sup> T cells either freshly prepared, or prestimulated with B6 or C3H spleen cells plus IL-2 for 7 d, were mixed with freshly prepared BALB/c CD4<sup>+</sup>CD25<sup>-</sup> T cells at various ratios and stimulated with either X-irradiated B6 (left) or C3H (right) splenocytes.

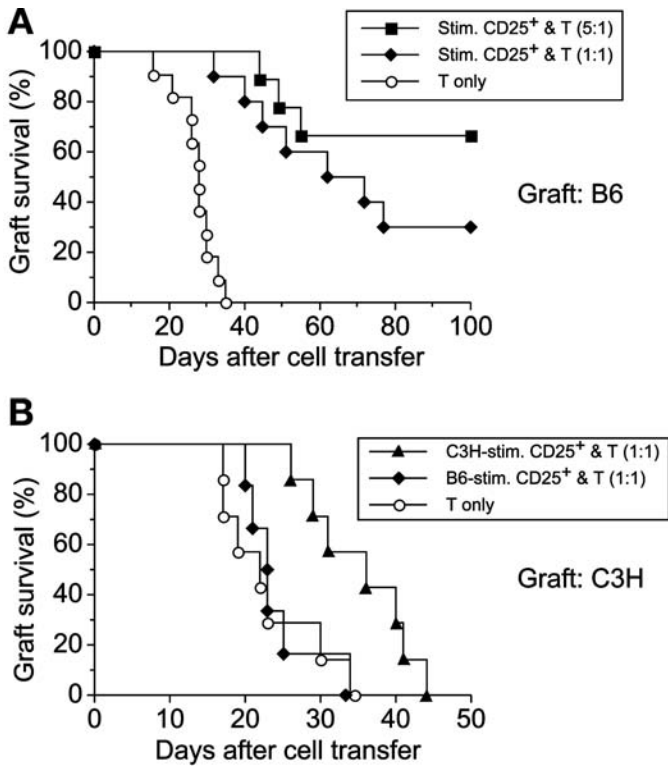


Fig. 5. Antigen-specific suppression of graft rejection by ex vivo antigen-stimulated CD4<sup>+</sup>CD25<sup>+</sup> regulatory T cells (Treg) cells. (A) BALB/c nude mice engrafted with B6 skin grafts received  $2 \times 10^5$  B6 or C3H-prestimulated BALB/c CD4<sup>+</sup>CD25<sup>+</sup> T cells,  $1 \times 10^6$  B6-prestimulated BALB/c CD4<sup>+</sup>CD25<sup>+</sup> T cells, or PBS alone as control. Seven days later, all mice received  $2 \times 10^5$  naïve BALB/c whole T cells. The transfer significantly prolonged graft survival in a cell dose-dependent fashion (MST = 67 d at 1:1 ratio of prestimulated CD4<sup>+</sup>CD25<sup>+</sup> T cells vs freshly prepared naïve T cells,  $n = 10$ , and MST >100 d at 5:1 ratio,  $n = 9$ ;  $p = 0.00004$  and  $0.00003$  vs control, respectively). B6-prestimulated CD4<sup>+</sup>CD25<sup>+</sup> T cells significantly prolonged the survival of B6 grafts at 1:1 ratio of Treg and naïve T cells and the survival was significantly longer compared with the transfer of C3H-prestimulated CD4<sup>+</sup>CD25<sup>+</sup> Treg cells (MST = 62 vs 40 d,  $p = 0.03$ ). (B) BALB/c nude mice engrafted with C3H skin grafts received  $2 \times 10^5$  B6 or C3H-prestimulated BALB/c CD4<sup>+</sup>CD25<sup>+</sup> T cells, or PBS alone as control. Seven days later, all mice received  $2 \times 10^5$  naïve BALB/c whole T cells. C3H-prestimulated CD4<sup>+</sup>CD25<sup>+</sup> Treg cells prolonged the survival of C3H grafts significantly longer than B6-prestimulated CD4<sup>+</sup>CD25<sup>+</sup> T cells (MST = 36 vs 23 d,  $p = 0.017$ ).

#### 4. Notes

1. Ab-coated dishes should be covered with plain medium until they are used for panning.
2. To prevent cell aggregation, it is recommended to use MACS buffer containing 2 mM EDTA.
3. BALB/c may reject C3H grafts faster than B6 grafts.

#### Acknowledgments

The authors thank Dr. Zoltan Fehervari for critical reading of the manuscript, and Drs. T. Takahashi and T. Nomura for development of procedures. This work was supported by grants-in-aids from the Ministry of Education, Science, Sports, and Culture, the Ministry of Human Welfare, and Japan Science and Technology Agency.

#### References

1. Sakaguchi, S., Sakaguchi, N., Shimizu, J., et al. (2001) Immunologic tolerance maintained by CD25<sup>+</sup> CD4<sup>+</sup> regulatory T cells: their common role in controlling autoimmunity, tumor immunity and transplantation tolerance. *Immunol. Rev.* **182**, 18–32.
2. Maloy, K. J. and Powrie, F. (2001) Regulatory T cells in the control of immune pathology. *Nat. Immunol.* **2**, 816–822.
3. Shevach, E. M. (2002) CD4<sup>+</sup> CD25<sup>+</sup> suppressor T cells: more questions than answers. *Nat. Rev. Immunol.* **2**, 389–400.
4. Sakaguchi, S., Sakaguchi, N., Asano, M., Itoh, M., and Toda, M. (1995) Immunologic self-tolerance maintained by activated T cells expressing IL-2 receptor alpha-chains (CD25). Breakdown of a single mechanism of self-tolerance causes various autoimmune diseases. *J. Immunol.* **155**, 1151–1164.
5. Asano, M., Toda, M., Sakaguchi, N., and Sakaguchi, S. (1996) Autoimmune disease as a consequence of developmental abnormality of a T cell subpopulation. *J. Exp. Med.* **184**, 387–396.
6. Suri-Payer, E., Amar, A. Z., Thornton, A. M., and Shevach, E. M. (1998) CD4<sup>+</sup>CD25<sup>+</sup> T cells inhibit both the induction and effector function of autoreactive T cells and represent a unique lineage of immunoregulatory cells. *J. Immunol.* **160**, 1212–1218.
7. Shimizu, J., Yamazaki, S., and Sakaguchi, S. (1999) Induction of tumor immunity by removing CD25<sup>+</sup>CD4<sup>+</sup> T cells: a common basis between tumor immunity and autoimmunity. *J. Immunol.* **163**, 5211–5218.
8. Suttmuller, R. P., van Duivenvoorde, L. M., van Elsas, A., et al. (2001) Synergism of cytotoxic T lymphocyte-associated antigen 4 blockade and depletion of CD25<sup>+</sup> regulatory T cells in antitumor therapy reveals alternative pathways for suppression of autoreactive cytotoxic T lymphocyte responses. *J. Exp. Med.* **194**, 823–832.

9. Itoh, M., Takahashi, T., Sakaguchi, N., et al. (1999) Thymus and autoimmunity: production of CD25<sup>+</sup>CD4<sup>+</sup> naturally anergic and suppressive T cells as a key function of the thymus in maintaining immunologic self-tolerance. *J. Immunol.* **162**, 5317–5326.
10. Takahashi, T., Kuniyasu, Y., Toda, M., et al. (1998) Immunologic self-tolerance maintained by CD25<sup>+</sup>CD4<sup>+</sup> naturally anergic and suppressive T cells: induction of autoimmune disease by breaking their anergic/suppressive state. *Int. Immunol.* **10**, 1969–1980.
11. Thornton, A. M. and Shevach, E. M. (1998) CD4<sup>+</sup>CD25<sup>+</sup> immunoregulatory T cells suppress polyclonal T cell activation *in vitro* by inhibiting interleukin 2 production. *J. Exp. Med.* **188**, 287–296.
12. Thornton, A. M. and Shevach, E. M. (2000) Suppressor effector function of CD4<sup>+</sup>CD25<sup>+</sup> immunoregulatory T cells is antigen nonspecific. *J. Immunol.* **164**, 183–190.
13. Salomon, B., Lenschow, D. J., Rhee, L., et al. (2000) B7/CD28 costimulation is essential for the homeostasis of the CD4<sup>+</sup>CD25<sup>+</sup> immunoregulatory T cells that control autoimmune diabetes. *Immunity* **12**, 431–440.
14. Takahashi, T., Tagami, T., Yamazaki, S., et al. (2000) Immunologic self-tolerance maintained by CD25<sup>+</sup>CD4<sup>+</sup> regulatory T cells constitutively expressing cytotoxic T lymphocyte-associated antigen 4. *J. Exp. Med.* **192**, 303–310.
15. Read, S., Malmstrom, V., and Powrie, F. (2000) Cytotoxic T lymphocyte-associated antigen 4 plays an essential role in the function of CD25<sup>+</sup>CD4<sup>+</sup> regulatory cells that control intestinal inflammation. *J. Exp. Med.* **192**, 295–302.
16. Shimizu, J., Yamazaki, S., Takahashi, T., Ishida, Y., and Sakaguchi, S. (2002) Stimulation of CD25<sup>+</sup>CD4<sup>+</sup> regulatory T cells through GITR breaks immunological self-tolerance. *Nat. Immunol.* **3**, 135–142.
17. McHugh, R. S., Whitters, M. J., Piccirillo, C. A., et al. (2002) CD4<sup>+</sup>CD25<sup>+</sup> immunoregulatory T cells: gene expression analysis reveals a functional role for the glucocorticoid-induced TNF receptor. *Immunity* **16**, 311–323.
18. Lehmann, J., Huehn, J., de la Rosa, M., et al. (2002) Expression of the integrin alpha Ebeta 7 identifies unique subsets of CD25<sup>+</sup> as well as CD25<sup>-</sup> regulatory T cells. *Proc. Natl. Acad. Sci. USA* **99**, 13,031–13,036.
19. Caramalho, I., Lopes-Carvalho, T., Ostler, D., Zelenay, S., Haury, M., and Demengeot, J. (2003) Regulatory T cells selectively express toll-like receptors and are activated by lipopolysaccharide. *J. Exp. Med.* **197**, 403–411.
20. Hori, S., Nomura, T., and Sakaguchi, S. (2003) Control of regulatory T cell development by the transcription factor Foxp3. *Science* **299**, 1057–1061.
21. Khattri, R., Cox, T., Yasayko, S. A., and Ramsdell, F. (2003) An essential role for Scurfin in CD4<sup>+</sup>CD25<sup>+</sup> T regulatory cells. *Nat. Immunol.* **4**, 337–342.
22. Fontenot, J. D., Gavin, M. A., and Rudensky, A. Y. (2003) Foxp3 programs the development and function of CD4<sup>+</sup>CD25<sup>+</sup> regulatory T cells. *Nat. Immunol.* **4**, 330–336.
23. Walker, L. S., Chodos, A., Eggena, M., Dooms, H., and Abbas, A. K. (2003) Antigen-dependent proliferation of CD4<sup>+</sup>CD25<sup>+</sup> regulatory T cells *in vivo*. *J. Exp. Med.* **198**, 249–258.



24. Klein, L., Khazaie, K., and von Boehmer, H. (2003) *In vivo* dynamics of antigen-specific regulatory T cells not predicted from behavior *in vitro*. *Proc. Natl. Acad. Sci. USA* **100**, 8886–8891.
25. Yamazaki, S., Iyoda, T., Tarbell, K., et al. (2003) Direct expansion of functional CD25<sup>+</sup>CD4<sup>+</sup> regulatory T cells by antigen-processing dendritic cells. *J. Exp. Med.* **198**, 235–247.
26. Annacker, O., Pimenta-Araujo, R., Burlen-Defranoux, O., Barbosa, T. C., Cumano, A., and Bandeira, A. (2001) CD25<sup>+</sup>CD4<sup>+</sup> T cells regulate the expansion of peripheral CD4 T cells through the production of IL-10. *J. Immunol.* **166**, 3008–3018.
27. Gavin, M. A., Clarke, S. R., Negrou, E., Gallegos, A., and Rudensky, A. (2002) Homeostasis and anergy of CD4<sup>+</sup>CD25<sup>+</sup> suppressor T cells *in vivo*. *Nat. Immunol.* **3**, 33–41.
28. Fisson, S., Darrasse-Jeze, G., Litvinova, E., et al. (2003) Continuous activation of autoreactive CD4<sup>+</sup> CD25<sup>+</sup> regulatory T cells in the steady state. *J. Exp. Med.* **198**, 737–746.
29. Sakaguchi, S., Hori, S., Fukui, Y., Sasazuki, T., Sakaguchi, N., and Takahashi, T. (2003) Thymic generation and selection of CD25<sup>+</sup>CD4<sup>+</sup> regulatory T cells: implications of their broad repertoire and high self-reactivity for the maintenance of immunological self-tolerance. *Novartis Found. Symp.* **252**, 6–16.
30. Nishimura, E., Sakihama, T., Setoguchi, R., Tanaka, K., and Sakaguchi, S. (2004) Induction of antigen-specific immunologic tolerance by *in vivo* and *in vitro* antigen-specific expansion of naturally arising Foxp3<sup>+</sup> CD25<sup>+</sup>CD4<sup>+</sup> regulatory T cells. *Int. Immunol.* **16**, 1189–1201.
31. Godfrey, W. R., Ge, Y. G., Spoden, D. J., et al. (2004) *In vitro*-expanded human CD4(+)CD25(+) T-regulatory cells can markedly inhibit allogeneic dendritic cell-stimulated MLR cultures. *Blood* **104**, 453–461.
32. Hoffmann, P., Eder, R., Kunz-Schughart, L. A., Andreesen, R., and Edinger, M. (2004) Large-scale *in vitro* expansion of polyclonal human CD4(+)CD25high regulatory T cells. *Blood* **104**, 895–903.
33. Hoffmann, P., Ermann, J., Edinger, M., Fathman, C. G., and Strober, S. (2002) Donor-type CD4(+)CD25(+) regulatory T cells suppress lethal acute graft-versus-host disease after allogeneic bone marrow transplantation. *J. Exp. Med.* **196**, 389–399.
34. Cohen, J. L., Trenado, A., Vasey, D., Klatzmann, D., and Salomon, B. L. (2002) CD4(+)CD25(+) immunoregulatory T Cells: new therapeutics for graft-versus-host disease. *J. Exp. Med.* **196**, 401–406.

## Modulation of the Immune Response Using Dendritic Cell–Derived Exosomes

Nicole R. Bianco, Seon-Hee Kim, Adrian E. Morelli,  
and Paul D. Robbins

### Summary

Initial studies in our laboratory were focused on the use of dendritic cells (DC) genetically modified to express Th2-derived cytokines (i.e., interleukin [IL]-4 and IL-10) or apoptotic proteins (i.e., Fas Ligand [FasL]) to reduce inflammation in a mouse model of experimentally induced arthritis. Exosomes are nano-sized vesicles (40–100 nm diameter) released by different cell types, including DC, that contain many of the proteins thought to be involved in regulating the immune response. We have demonstrated that exosomes derived from immature DC treated with immunomodulatory cytokines (i.e., IL-10, IL-4) are able to inhibit inflammation in a murine footpad model of delayed-type hypersensitivity (DTH) and reduce the severity of established collagen-induced arthritis (CIA). In fact, the exosomes were as therapeutic as the parental DC. Because purified DC-derived exosomes are very stable vesicles, they may be a better approach for future treatment of arthritis and other autoimmune disorders than the more unstable DC. In this chapter we detail a protocol for preparing the exosomes produced by murine bone marrow–derived DC. We also review methods to assess the purity and concentration of purified exosomes, by using electron microscopy, Western blot analysis, and flow cytometry. Finally, we describe methods to assess the function of exosomes *in vitro*, using the mixed leukocytes reaction, and *in vivo* by means of DTH and an experimental model of CIA.

**Key Words:** Rheumatoid arthritis; exosomes; autoimmune disease; dendritic cells; collagen-induced arthritis; delayed-type hypersensitivity.

### 1. Introduction

#### 1.1. Discovery of Exosomes

Exosomes are membrane-bound nanovesicles (50–100 nm diameter) generated by reverse budding of the limiting membrane of multivesicular late endosomes. Exosomes were first described in the 1980s, originating from

differentiating red blood cells (1). Because exosomes are generated in the late endosomal compartment by inverse budding, they carry many membrane-associated proteins. Exosomes have also been shown to be released by various cells of hematopoietic origin (B cells, T cells, DC, mast cells, and platelets) and tumor cells (2,3). Initially, exosomes were considered to be cellular “garbage bags,” removing unwanted proteins from cells with a low content of lysosomes, such as the transferrin receptor from differentiating reticulocytes (4). It is now believed that exosomes may serve many functions, depending on the cell type and stage of maturity of the originating cell.

### 1.2. Immunologic Effects of Exosomes

Exosomes originating from immune cells, such as B cells, T cells, DC, and mast cells, are thought to play a role in communicating immuno-regulatory signals to other immune cells in either an immuno-stimulating or suppressive manner. Indeed, exosomes derived from immune cells express regulatory molecules to carry out this function, including major histocompatibility complex class I and II molecules, B7-1, B7-2, as well as various targeting and adhesion molecules that may dock exosomes to acceptor cells (3).

In murine models, exosomes can be immunostimulatory or suppressive, depending on the state of maturation and cell type from which they derive. Peptide-pulsed DC-derived exosomes are able to elicit a potent antitumor immune response in mice (5,6) and have recently been tested in phase I human trials (7,8). Tumor cell-derived exosomes carrying tumor antigens also have been demonstrated to have antitumor effects in mice (9). *Toxoplasma gondii* antigen-pulsed DC2.4 cell line-derived exosomes have also been shown to be able to trigger humorally mediated immunity to the *T. gondii* parasite (10).

However, several reports have shown that exosomes may also exert immunosuppressive functions. Small exosome-like vesicles (termed tolerosomes) produced by rat intestinal epithelial cells cultured in the presence of interferon- $\gamma$  and the model antigen ovalbumin (digested) were able to induce antigen-specific tolerance after injection into untreated mice (11). Allogeneic exosomes from immature bone marrow-derived DC delayed rejection of heart allografts in rats (12). Furthermore, T cells and tumor cells are able to generate exosome-like vesicles expressing Fas ligand (FasL), which induce apoptosis of T cells that would otherwise counteract tumor growth (13–16). FasL containing vesicles have been found in the first trimester syncytiotrophoblast and may be responsible for immune privilege in the placenta (17).

We have shown that both DC and exosomes derived from immature DC pretreated with interleukin (IL)-10 produce anti-inflammatory exosomes that suppress the onset of murine collagen-induced arthritis (CIA) and reduce the

severity of established arthritis (**18**). In fact, exosomes were as effective as the parental DC. Moreover, exosomes from DC transduced with recombinant adenovirus encoding FasL (**19**) or IL-4 (unpublished data) produce exosomes able to suppress inflammation in a murine model of delayed type hypersensitivity and partially reverse established CIA. Because exosomes are more stable in vitro than DC, they may be a better approach for future treatment of arthritis and other autoimmune disorders.

In this chapter, we first detail a protocol for preparing the exosomes from murine bone marrow-derived DC and methods to assess the purity and concentration of exosomes using electron microscopy, Western blot and FACS analysis for exosome-associated proteins. Finally, we describe methods to assess the function of exosomes in vitro (mixed leukocyte reaction [MLR]), and in vivo by means of delayed-type hypersensitivity (DTH) and the mouse model CIA.

## **2. Materials**

### **2.1. Preparation of Exosomes Released by Dendritic Cells**

#### *2.1.1. DC Generation*

1. ACK cell lysing buffer (Mediatech, Herdon, VA).
2. Nycoprep 1.077 (NycoMed, Roskilde, Denmark).
3. RPMI-1640 medium (Mediatech).
4. RPMI-1640 complete medium: RPMI-1640 medium supplemented with 10% fetal calf serum (FCS) (heat-inactivated and filtered), 2 mM L-glutamine, 1% of nonessential amino acids, 50  $\mu$ M 2-mercaptoethanol, 100 U/mL penicillin, and 100  $\mu$ g/mL streptomycin.
5. Mouse recombinant granulocyte-macrophage colony-stimulating factor (GM-CSF) (Endogen, Rockford, IL).
6. Mouse recombinant IL-4 (Endogen, Rockford, IL).
7. Hanks' balanced salt solution (HBSS) (Mediatech).

#### *2.1.2. Exosome Isolation*

1. Phosphate-buffered saline (PBS).
2. Beckman SW-41 Ultracentrifuge rotor.
3. Bio-Rad protein assay kit and bovine serum albumin (BSA) to act as a standard.
4. Microtiter 96-well plates.

### **2.2. Visualization of Exosomes Using Electron Microscopy**

1. Formvar/carbon coated EM grid.
2. Neutral 1% aqueous phosphotungstic acid or 1% uranylacetate.
3. Transmission electron microscope (JEOL-1210 computer controlled high contrast 120 kv transmission electron microscope).

### **2.3. In Vitro Characterization of Exosomes**

#### *2.3.1. Western Blot Analysis*

1. 5X protein loading sample buffer: 1 g SDS, 5 mg bromophenol blue, 5 mL glycerol, 2.5 mL Tris-HCl, pH 6.8, 2.8 mL 2-mercaptoethanol.
2. Nitrocellulose or polyvinylidene fluoride (PVDF).
3. Methanol (MeOH).
4. 10X SDS running buffer: 144 g glycine, 30.2 g Tris, 10 g SDS in 1 L ultrapure H<sub>2</sub>O. 1X SDS running buffer: 100 mL 10X buffer, 900 mL ultrapure H<sub>2</sub>O.
5. 10X semidry transfer buffer (no MeOH): 116.4 g Tris, 58.6 g glycine, 1.0 g SDS in 1 L ultrapure H<sub>2</sub>O. 1X semidry transfer buffer: 100 mL 10X buffer, 700 mL H<sub>2</sub>O, 200 mL MeOH.
6. Semidry transfer apparatus (Bio-Rad; Hercules, CA).
7. Amido Black Staining Solution (Sigma Chemical Co., St. Louis, MO).
8. PBS-Tween-20 (PBS-T): PBS plus 0.1% Tween-20.
9. Nonfat dry milk.
10. BSA.
11. Primary and horseradish peroxidase-conjugated secondary antibodies.
12. Western blot developing reagents of choice.

#### *2.3.2. FACS Analysis*

1. 4- $\mu$ m Latex beads (Interfacial Dynamics).
2. MES buffer: dissolve 1.33 g MES in 200 mL deionized H<sub>2</sub>O, heat to 50°C, adjust pH to 6.0 with NaOH, then bring the volume to 250 mL with dH<sub>2</sub>O when the solution has cooled.
3. PBS.
4. Storage buffer: PBS, 0.1% sodium azide, 0.1% glycine.
5. Staining buffer: PBS, 1% heat inactivated FCS, 0.1% (w/v) sodium azide, adjust pH to 7.4–7.6. Store at 4°C.
6. BSA.
7. Fixative: PBS, 4% (w/v) paraformaldehyde, adjust pH to 7.4–7.6.
8. Monoclonal antibodies (MAb) of choice.

### **2.4. In Vitro and In Vivo Functional Testing of Exosomes**

#### *2.4.1. MLR*

1. Splenic T cells from BALB/c mice.
2. Antigen-presenting cells, including DC from BALB/c or C57Bl/6 mice.
3. Round-bottomed 96-well plates.
4. <sup>3</sup>H-thymidine.
5. Microplate  $\beta$  counter.

#### *2.4.2. Mouse DTH*

1. C57Bl/6 mice.
2. Antigen (keyhole limpet hemocyanin [KLH] or ovalbumin [OVA]) emulsified 1:1 in complete Freund's adjuvant (CFA).

3. Antigen (KLH or OVA) in PBS (20  $\mu\text{g/paw}$ ) for boost injection.
4. Spring-loaded caliper (Dyer, Lancaster, PA).

#### 2.4.3. Mouse CIA

1. DBA/1 lacJ (H-2<sup>d</sup>) mice.
2. Bovine type II collagen (Chondrex, Redmond, WA) in 0.05 M acetic acid at a concentration of 2 mg/mL.
3. Incomplete Freund's adjuvant.
4. Lipopolysaccharide (Sigma).
5. Spring-loaded caliper (Dyer).

### 3. Methods

#### 3.1. Preparation of Exosomes From Bone Marrow–Derived DC

##### 3.1.1. DC Generation From Bone Marrow Cells

The following method for bone marrow DC generation has been adapted from Son et al. (20).

1. Sacrifice the mice in a CO<sub>2</sub> chamber. Bone marrow from 10 mice will yield approx 10  $\mu\text{g}$  of exosomes.
2. Swab the mice with 70% EtOH.
3. Disinfect the scissors and forceps using 70% EtOH.
4. Make a transverse incision across the abdomen and deflect the skin to expose the entire hind limb.
5. Dissect the femur and tibia bilaterally by cutting the joints and removing as much muscle as possible. Place the bones in a 50-mL sterile conical tube containing sterile HBSS.
6. Remove the HBSS and rinse the bones with 30 mL of HBSS.
7. Place the bones in a 10-cm diameter Petri dish containing approx 15 mL of RPMI.
8. Using sterile gauze, remove the muscle, separate the bones and place them in a new 10-cm Petri dish containing approx 15 mL of RPMI.
9. Carefully remove the tips of the bones and flush out the bone marrow, using a 21-gauge needle and a 10-mL syringe filled with RPMI, into a 50-mL tube containing RPMI.
10. Centrifuge at 500g for 7 min at room temperature (RT).
11. Remove the supernatant and resuspend in 2–3 mL of ACK cell lysing buffer per two mice (to lyse the contaminating erythrocytes). Gently homogenize using an 18-gauge needle.
12. Allow to stand for 5 min.
13. Add 2 vol of complete medium.
14. Centrifuge at 500g for 7 min at RT.
15. Remove the supernatant: the pellet should appear white.
16. Resuspend in 8 mL of RPMI and transfer to a new tube overlaying 4 mL of Nycoprep, taking care not to mix the layers.
17. Spin at 600g for 20 min at RT.

18. Remove the cells at the interface and transfer to a new 15-mL tube and add 5 mL of HBSS.
19. Spin the cells at 500g for 7 min. While centrifuging, pipet 2 mL of complete medium into 24-well cell culture plates.
20. Resuspend the cells in 48 mL of complete medium and pipet 2 mL into each well from **step 19** to give 4 mL total/well (approx  $10^6$  cells/well).
21. Incubate the cells at 37°C, 5% CO<sub>2</sub> overnight.
22. Harvest the nonadherent cells and transfer to 50-mL tubes. Discard the adherent macrophages.
23. Spin at 500g for 7 min, aspirate supernatant, and resuspend each tube in 24 mL of medium containing 50 µL of stock GM-CSF (10 µg/mL) and 50 µL of stock IL-4 (20 µg/mL) (1000 IU/mL of each in final concentration).
24. Add 2 mL of medium per well plus 2 mL of cells.
25. Culture at 37°C for 4 d.
26. Harvest semiadherent DC and replat in fresh medium containing GM-CSF and IL-4. Alternatively, perform infection or treat with recombinant protein (*see Notes 1–3*).
27. Harvest the cells and exosomes 2–3 d later.

### 3.1.2. Exosome Isolation

The method for exosome isolation has been adapted from They et al. (21). Collected culture supernatants are serially centrifuged at 300g for 10 min, 1200g for 20 min, and 10,000g for 30 min. The supernatant from the final spin is ultracentrifuged (Beckman SW-41) at 100,000g for 1–2 h to pellet the exosomes. The exosome pellet is washed in saline, centrifuged at 100,000g for 1–2 h, and resuspended in 100–200 µL of PBS. **Figure 1** shows a schematic diagram of the isolation protocol (*see Notes 4 and 5*). The amount of protein in the exosome preparation is assessed by the Bradford assay using the microtiter plate protocol (Bio-Rad, Hercules, CA). For short-term storage, the exosomes are kept at 4°C to preserve the membrane integrity. For long-term storage, and when membrane integrity is not an issue (i.e., Western blotting), the exosomes are kept at –80°C.

### 3.2. Visualization of Exosomes Using Electron Microscopy

Exosomes (10 µL) purified by differential ultracentrifugation and resuspended in PBS are loaded on a Formvar/carbon coated grid for 1 min, negatively stained with 10 µL neutral 1% aqueous phosphotungstic acid or 1% uranylacetate for 1 min and viewed using a JEM-1011 computer controlled high contrast 80 kV transmission electron microscope. Exosomes are typically 50–120 nm in diameter and appear “saucer” shaped. **Figure 2** shows an electron micrograph of exosomes secreted from unmodified DC.

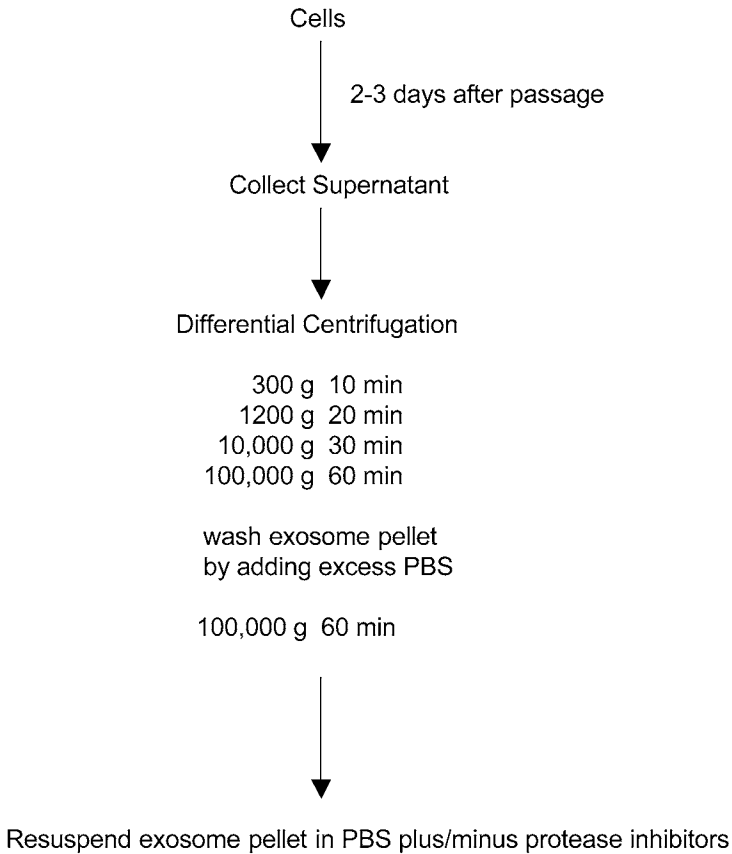


Fig. 1. Exosome purification scheme.

### 3.3. *In Vitro* Characterization of Exosomes

#### 3.3.1. Western Blot Analysis

For Western blot, exosomes (3–10  $\mu\text{g}$ ) are separated by 12 or 15% sodium dodecyl sulfate-polyacrylamide gels, semidry transferred onto PVDF and detected by Western blotting using an enhanced chemiluminescence detection kit. Exosomal proteins for which we routinely blot include Hsc70, CD71, and major histocompatibility complex class II.

The basic protocol is as follows:

1. Dilute the exosomes in 5X sodium dodecyl sulfate sample buffer.
2. Boil the samples for 5 min at 95°C and load onto a sodium dodecyl sulfate-polyacrylamide gels.



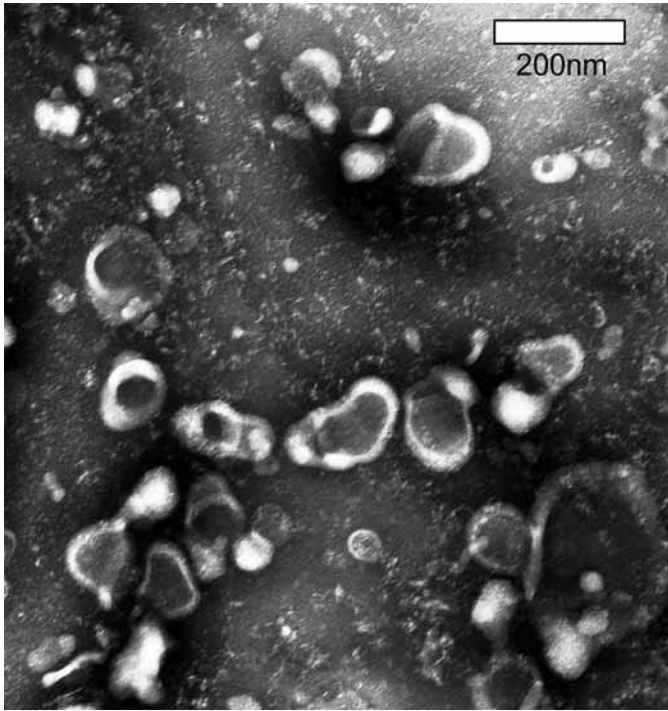


Fig. 2. Electron micrograph of DC-derived exosomes.

3. After the gel has finished running, set up the semidry transfer following the manufacturer's protocol.
4. After transferring, check for the transfer of proteins by staining the membrane with Amido Black. Destain the membrane by washing in MeOH for  $3 \times 5$  min. Wash the membrane in PBS-T for 5 min.
5. Block the membrane for 1 h or overnight in 5% dry milk in PBS-T.
6. Wash the membrane in PBS-T for  $3 \times 5$  min.
7. Incubate the membrane in primary MAb (in 1% BSA/PBS-T) for 2 h or overnight using the supplier's dilution recommendations.
8. Wash the membrane in PBS-T for  $3 \times 1$  min, then  $3 \times 5$  min.
9. Incubate the membrane in secondary antibody labeled with horseradish peroxidase (in 5% milk/PBS-T) at a dilution of 1:5000 for 1 h.
10. Wash the membrane in PBS-T for  $3 \times 1$  min, once for 15 min, then  $3 \times 5$  min.
11. Detect proteins using chemiluminescence kit of choice and develop on autoradiography film.

### 3.3.2. FACS Analysis

For flow cytometry, exosomes are required to be attached to latex beads that have been precoated with an antibody that recognizes markers exposed on the exosome surface. Then the exosome-latex bead complexes are labeled with

fluorochrome-conjugated MAb. This method is necessary because of the small size of the exosomes (*see Note 6*).

1. Use 2.5 mL of 4- $\mu$ m latex beads (4% solids) and wash with 10 mL of MES buffer.
2. Centrifuge the beads at 3000g for 20 min.
3. Repeat the washing and centrifugation steps.
4. Resuspend the beads in 5 mL of MES buffer.
5. Add 250  $\mu$ L of beads (5 mg) to 250  $\mu$ L of BSA in MES buffer (1 mg/mL) and 60  $\mu$ g of antibody that will be used to attach the exosomes.
6. Incubate overnight at RT, rocking slowly.
7. Centrifuge at 3000g for 20 min.
8. Remove the supernatant and resuspend in 1 mL of PBS.
9. Repeat **steps 7 and 8**.
10. Centrifuge at 3000g for 20 min.
11. Remove the supernatant and resuspend in 500  $\mu$ L of storage buffer.
12. To set up the experiment, distribute 15  $\mu$ L of labeled beads into the desired number of microfuge tubes.
13. Add 50–100  $\mu$ g of exosomes and make up the volume to 500  $\mu$ L. Alternatively, a master mix can be made of beads and exosomes, then distributed into FACS tubes at **step 16**.
14. Incubate for 2–4 h at 4°C, rocking slowly.
15. Centrifuge at 700g in a microcentrifuge for 5 min.
16. Remove the supernatant and resuspend in 100  $\mu$ L of cold HBSS or staining buffer, then distribute the beads to FACS tubes.
17. Block each tube with 10  $\mu$ L of normal goat serum for 10 min on ice.
18. Add 1–2  $\mu$ L of labeled antibody (e.g., FITC or PE). Incubate for 30–45 min on ice. Cover the tubes, as the fluorophores are light sensitive.
19. To wash away excess MAb, add 1 mL of cold HBSS or staining buffer to each tube. Centrifuge the tubes for 5 min at 700g.
20. Aspirate the supernatant and resuspend in 200–400  $\mu$ L of staining buffer. If not analyzing immediately, resuspend in 200  $\mu$ L of cold 4% paraformaldehyde.
21. Analyse by FACS.

### **3.4. In Vitro and In Vivo Functional Testing of Exosomes**

#### **3.4.1. MLR**

To test the ability of DC-derived exosomes to suppress T-cell proliferation, the effect of adding DC-derived exosomes to a MLR is tested. T cells are purified from the spleens of BALB/c mice for in vitro micro-culture in round-bottomed 96-well plates. In each well,  $5 \times 10^4$  splenic T cells are seeded with C57Bl/6 derived DC plus increasing concentrations of exosomes (0–2  $\mu$ g/mL) at a ratio of 10:1. On day 5 of culture, 1  $\mu$ Ci of  $^3$ H-thymidine is added to each well 16 h prior to harvest. Radioactive labeling of proliferating T cells is measured on a microplate beta counter (Wallac, Turku, Finland).

### 3.4.2. Mouse DTH

To investigate the antiinflammatory effect of DC-derived exosomes *in vivo*, a DTH model in C57Bl/6 mice is used. C57Bl/6 mice are sensitized by injecting 100  $\mu\text{g}$  of antigen (KLH or OVA) emulsified 1:1 in CFA at a single dorsal site. Two weeks later, one hind footpad of the immunized mouse is injected with 1  $\mu\text{g}$  of exosomes (in 50  $\mu\text{L}$  of PBS), 12–24 h before challenging with antigen. The contra-lateral footpad receives an equal volume of PBS as an injection control. Mice are then challenged in both footpads by injecting 20  $\mu\text{g}$  of antigen dissolved in 20  $\mu\text{L}$  of PBS. Footpad swelling is measured with a spring-loaded caliper at 24, 48, and 72 h postinjection. Results are expressed as the difference in swelling ( $\times 0.01$  mm), before and after antigen boost injection.

### 3.4.3. Mouse CIA

Similar pathologies to human rheumatoid arthritis can be induced in the DBA/1 lacJ (H-2<sup>q</sup>) strain of mice with injection of bovine type II collagen. Bovine type II collagen in 0.05 *M* acetic acid at a concentration of 2 mg/mL is emulsified in an equal volume of CFA and injected into tail base of the mouse. On d 21, the mice receive an intradermal boost injection of type II collagen in incomplete Freund's adjuvant. To examine the ability of DC-derived exosomes to prevent CIA, the mice receive injections of exosomes at d 28, before the time of disease onset. For the treatment of established disease studies, mice are synchronized into disease onset with 20  $\mu\text{g}$  of lipopolysaccharide *i.p.*, and then injected *i.v.* with 1  $\mu\text{g}$  of exosomes (in 500  $\mu\text{L}$  of PBS) 4 d later (day 32) after disease onset. The mice are then monitored by means of an established macroscopic system ranging from 0 to 4: 0, normal; 1, detectable arthritis with erythema; 2, significant swelling and redness; 3, severe swelling and redness from joint to digit; and 4, maximal swelling and deformity with ankylosis. In addition, thickness of each of the four paws may be measured with the caliper. The average macroscopic score is expressed as a cumulative value for all paws, with a maximum possible score of 16 per mouse.

## 4. Notes

1. For recombinant adenoviral infection,  $10^6$  DC are mixed with  $5 \times 10^9$  viral particles in a total volume of 1 mL of serum-free media. After incubation for 24 h, DC are washed intensively three times with HBSS and incubated for a further 48 h. On day 8, culture supernatant is collected for exosome purification and collection of the infected DC.
2. For treatment with recombinant protein, the cells are incubated with the protein for 24 h. The cells are then washed and the exosomes collected 48 h later.

3. As serum contains exosome-like vesicles, it is recommended that the DC are cultured in medium with FCS that has been depleted of contaminating vesicles and protein aggregates by ultracentrifugation at 100,000g for 1 h. This is especially necessary if the exosomes are to be used for protein sequencing by mass spectrometry.
4. The following ultracentrifugation protocol adapted from Wubbolts et al. (22) also works very well. Collected culture supernatants are serially centrifuged at 200g for 10 min, twice at 500g for 10 min, once at 2000g for 15 min and once at 10,000g for 30 min. The supernatant from the final spin is ultra-centrifuged (SW-41) at 100,000g for 1 h to pellet the exosomes. The exosome pellet is washed in saline, centrifuged at 100,000g for 1 h, and resuspended in PBS.
5. If the exosomes are to be used for protein characterization, they are resuspended in PBS plus a protease inhibitor cocktail.
6. 4.5- $\mu$ m Dynabeads (25  $\mu$ L, Dynal, Lake Success, NY) that are coated with H-2A<sup>b</sup> MAb or CD11b MAb may also be used instead of latex beads. Beads coated with exosomes are then labeled with the phycoerythrin-labeled MAb of interest.

## Acknowledgments

The authors would like to thank William Shufesky for assistance with the FACS protocol for exosomes. We also thank Dr. Simon Watkins and Ana Lopez for technical assistance with electron microscopy. This work was supported by National Institutes of Health grants AR-6-2225, DK44935 and U19 AI56374 (to P.D.R.), and RO1 HL077545 and RO1 HL075512 (to A.E.M).

## References

1. Pan, B. T. and Johnstone, R. M. (1983) Fate of the transferrin receptor during maturation of sheep reticulocytes in vitro: selective externalization of the receptor. *Cell* **33**, 967–978.
2. Denzer, K., Kleijmeer, M. J., Heijnen, H. F., Stoorvogel, W., and Geuze, H. J. (2000) Exosome: from internal vesicle of the multivesicular body to intercellular signaling device. *J. Cell Sci.* **113**, 3365–3374.
3. Thery, C., Zitvogel, L., and Amigorena, S. (2002) Exosomes: composition, biogenesis and function. *Nat. Rev. Immunol.* **2**, 569–579.
4. Johnstone, R. M., Adam, M., Hammond, J. R., Orr, L., and Turbide, C. (1987) Vesicle formation during reticulocyte maturation. Association of plasma membrane activities with released vesicles (exosomes). *J. Biol. Chem.* **262**, 9412–9420.
5. Zitvogel, L., Regnault, A., Lozier, A., et al. (1998) Eradication of established murine tumors using a novel cell-free vaccine: dendritic cell-derived exosomes. *Nat. Med.* **4**, 594–600.
6. Chaput, N., Scharztz, N. E., Andre, F., et al. (2004) Exosomes as potent cell-free peptide-based vaccine. II. Exosomes in CpG adjuvants efficiently prime naive Tc1 lymphocytes leading to tumor rejection. *J. Immunol.* **172**, 2137–2146.

7. Morse, M. A., Garst, J., Osada, T., et al. (2005) A phase I study of exosome immunotherapy in patients with advanced non-small cell lung cancer. *J. Transl. Med.* **3**, 9.
8. Escudier, B., Dorval, T., Chaput, N., et al. (2005) Vaccination of metastatic melanoma patients with autologous dendritic cell (DC) derived-exosomes: results of the first phase I clinical trial. *J. Transl. Med.* **3**, 10.
9. Altieri, S. L., Khan, A. N., and Tomasi, T. B. (2004) Exosomes from plasmacytoma cells as a tumor vaccine. *J. Immunother.* **27**, 282–288.
10. Aline, F., Bout, D., Amigorena, S., Roingeard, P., and Dimier-Poisson, I. (2004) *Toxoplasma gondii* antigen-pulsed-dendritic cell-derived exosomes induce a protective immune response against *T. gondii* infection. *Infect. Immun.* **72**, 4127–4137.
11. Karlsson, M., Lundin, S., Dahlgren, U., Kahu, H., Pettersson, I., and Telemo, E. (2001) “Tolerosomes” are produced by intestinal epithelial cells. *Eur. J. Immunol.* **31**, 2892–2900.
12. Peche, H., Heslan, M., Usal, C., Amigorena, S., and Cuturi, M. C. (2003) Presentation of donor major histocompatibility complex antigens by bone marrow dendritic cell-derived exosomes modulates allograft rejection. *Transplantation* **76**, 1503–1510.
13. Andreola, G., Rivoltini, L., Castelli, C., et al. (2002) Induction of lymphocyte apoptosis by tumor cell secretion of FasL-bearing microvesicles. *J. Exp. Med.* **195**, 1303–1316.
14. Martinez-Lorenzo, M. J., Anel, A., Gamen, S., et al. (1999) Activated human T cells release bioactive Fas ligand and APO2 ligand in microvesicles. *J. Immunol.* **163**, 1274–1281.
15. Abrahams, V. M., Straszewski, S. L., Kamsteeg, M., et al. (2003) Epithelial ovarian cancer cells secrete functional Fas ligand. *Cancer Res.* **63**, 5573–5581.
16. Abusamra, A. J., Zhong, Z., Zheng, X., et al. (2005) Tumor exosomes expressing Fas ligand mediate CD8+ T-cell apoptosis. *Blood Cells Mol. Dis.* **35**, 169–173.
17. Frangmyr, L., Baranov, V., Nagaeva, O., Stendahl, U., Kjellberg, L., and Mincheva-Nilsson, L. (2005) Cytoplasmic microvesicular form of Fas ligand in human early placenta: switching the tissue immune privilege hypothesis from cellular to vesicular level. *Mol. Hum. Reprod.* **11**, 35–41.
18. Kim, S. H., Lechman, E. R., Bianco, N., et al. (2005) Exosomes derived from IL-10-treated dendritic cells can suppress inflammation and collagen-induced arthritis. *J. Immunol.* **174**, 6440–6448.
19. Hee Kim, S., Bianco, N., Menon, R., et al. (2005) Exosomes derived from genetically modified DC expressing FasL are anti-inflammatory and immunosuppressive. *Mol. Ther.* **13**, 289–300.
20. Son, Y. I., Egawa, S., Tatsumi, T., Redlinger, R. E., Jr., Kalinski, P., and Kanto, T. (2002) A novel bulk-culture method for generating mature dendritic cells from mouse bone marrow cells. *J. Immunol. Methods* **262**, 145–157.

21. Thery, C., Boussac, M., Veron, P., et al. (2001) Proteomic analysis of dendritic cell-derived exosomes: a secreted subcellular compartment distinct from apoptotic vesicles. *J. Immunol.* **166**, 7309–7318.
22. Wubbolts, R., Leckie, R. S., Veenhuizen, P. T., et al. (2003) Proteomic and biochemical analyses of human B cell-derived exosomes. Potential implications for their function and multivesicular body formation. *J. Biol. Chem.* **278**, 10,963–10,972.



## Breaking Self-Tolerance to Tumor-Associated Antigens by In Vivo Manipulation of Dendritic Cells

Ines Mende and Edgar G. Engleman

### Summary

Dendritic cells (DC) are extremely potent antigen-presenting cells, which can prime both naïve CD4<sup>+</sup> and CD8<sup>+</sup> T lymphocytes. In their immature state, DC continuously sample and process antigens from the surrounding environment, but only mature DC express sufficient levels of costimulatory molecules to activate naïve T cells. DC present in tumors are functionally immature owing to the immunosuppressive actions of tumor-derived factors and regulatory T cells, and such immature DC promote immune tolerance to the tumor. Recent studies from animal models suggest that Toll-like receptor (TLR) agonists such as CpG can reverse the tolerogenic state of tumoral DC. Strategies that allow DC to gain access to both tumor antigens and TLR agonists, *in situ*, can overcome tumor tolerance leading to the induction of potent systemic antitumor immunity.

**Key Words:** Dendritic cells; vaccination; Flt3-ligand; toll-like receptor ligand; tumor-associated antigens.

### 1. Introduction

Dendritic cells (DC) are potent antigen-presenting cells, which play an important role in the initiation of primary T-cell responses (1). DC reside as immature cells in peripheral tissues where they continuously sample and process antigens from the environment. Upon activation, they express a variety of costimulatory molecules as well as high levels of major histocompatibility complex (MHC) class I and II molecules, and migrate to the local lymph nodes where they present their processed antigens to naïve T cells, thereby initiating a cognate immune response (2). If these properties could be harnessed in patients with tumors, antitumor immunity should be readily attainable. Unfortunately, tumors typically contain relatively few DC and those that are



present are often tolerogenic (3–5), as tumor-secreted factors, such as interleukin-10 or transforming growth factor- $\beta$ , or the presence of T-regulatory cells can prevent their proper activation (6,7). Reversal of tumor tolerance requires activation of tumor DC, which can occur if their Toll-like receptors (TLR) come into contact with agonistic TLR ligands (8,9). TLR ligands are comprised of a wide range of molecules that are typically found in pathogenic bacteria and viruses but not mammals. Once bound to these ligands the TLRs initiate a signaling cascade in DC that leads to upregulation of costimulatory molecules and secretion of inflammatory cytokines (10).

Thus, reversal of tumor tolerance requires that adequate numbers of DC be exposed to tumor antigens and that the antigen-loaded DC be activated by an appropriate stimulus. Initially, investigators sought to take advantage of the properties of DC by isolating DC precursors from the blood of individual patients, loading the cells *in vitro* with one or more tumor associated antigens and returning them to the patients by intravenous or subcutaneous injection (11–13). Although vaccination of cancer patients with such *ex vivo* antigen pulsed DC has shown promise in some trials, this approach has proven extremely difficult to standardize and overall clinical efficacy has been disappointing (14). We describe here two different methods to induce antitumor immunity by *in vivo* manipulation of DC. Both methods have been successfully used in mouse models to treat weakly immunogenic tumors (15–17). The first method uses Flt3-ligand (Flt3-L), a DC growth factor (18), to bring a large number of immature DC to an accessible site, followed by injection into that site of a mixture of tumor antigen and TLR agonist to induce DC activation (15,17). The second approach involves administration of a DC attracting chemokine and a TLR agonist directly into tumors to recruit and activate DC intratumorally where there is already an abundance of available tumor antigens (16). This strategy avoids the need to identify, produce and administer tumor antigens.

## 2. Materials

### 2.1. Administration of Tumor-Associated Antigen and CpG to Flt3-L Treated Animals

#### 2.1.1. Flt3-L and Vaccine Preparation

1. Recombinant human Flt3-ligand (Peprotech): reconstitute in sterile PBS and keep at 4°C for up to 1 wk. Aliquots of reconstituted Flt3-ligand may be stored at –70°C for several months prior to use but repetitive freezing and thawing should be avoided.
2. Phosphorothioate-stabilized Oligonucleotides (synthesized by Oligos Etc. Inc., Wilsonville, OR):  
Stimulating CpG 1826: TCCATGACGTTTCCTGACGTT  
Control oligonucleotide: TCCAGGACTTTCCTCAGGTT

Oligonucleotides are reconstituted in sterile water (30 mg/mL) and aliquots can be stored at  $-70^{\circ}\text{C}$ . Prior to in vivo use, CpG should be diluted in sterile PBS to a working concentration (see **Note 1**).

3. Tumor-associated antigen TRP2<sub>180–188</sub> (SVYDFVWL, produced by Sigma-Genosys with a purity >95% as determined by HPLC). TRP2 peptide should be diluted in DMSO at a concentration of at least 50 mg/mL to avoid high concentrations of DMSO in the final vaccine and stored at  $-20^{\circ}\text{C}$  prior to use.
4. Injection material: 1-mL syringe, 27.5-gauge needle.
5. Animals: male C57Bl/6 mice, 6–8 wk old (Jackson Laboratories) (see **Note 2**).
6. Ear punch.

### 2.1.2. Tumor Inoculation

1. B16 tumor cells (ATCC).
2. Culture medium: RPMI 1640 medium, 10% fetal bovine serum (FBS), 100 IU/mL penicillin, 100  $\mu\text{g}/\text{mL}$  streptomycin, 10 mM glutamine. RPMI 1640 medium and all supplements are obtained from Invitrogen Life Technologies. FBS (Invitrogen) should be heat inactivated for 20 min at  $56^{\circ}\text{C}$  prior to use.
3. Freezing medium: 50% culture medium, 40% FBS, 10% DMSO.
4. 10X Trypsin/EDTA (Invitrogen, stored at  $-20^{\circ}\text{C}$  prior to use). 1X Solution is prepared by dilution in PBS just before use.
5. Injection material: 1-mL syringe, 27.5-gauge needle, or 0.5-mL tuberculin syringe with attached needle.
6. Hair trimmer.
7. Caliper.

### 2.2. Recruitment and Activation of Tumoral DC

1. Recombinant murine CCL20 (Peprotech Inc., Rocky Hill, NJ). Reconstitute in PBS and store aliquots at  $-80^{\circ}\text{C}$ . Working aliquots can be stored at  $4^{\circ}\text{C}$  for up to 1 wk.
2. CpG and control oligonucleotides (see **Subheading 2.1**). The working concentration of CpG is higher than that used in the prior method, as CpG is administered intratumorally instead of subcutaneously. A final concentration of CpG of 2.67 mg/mL (corresponding to 80  $\mu\text{g}$  CpG per injection volume) should be prepared in sterile PBS.
3. C57Bl/6 mice, B16 melanoma cells, hair trimmer, ear punch, injection material.

### 2.3. In Vivo Depletion of Lymphocyte Subsets

1. CD4<sup>+</sup> T-cell depletion: CD4 monoclonal antibody (MAb) (clone GK 1.5) or CD4<sup>-/-</sup> mice (Jackson Laboratory).
2. CD8<sup>+</sup> T-cell depletion: CD8 MAb (clone 2.43) or CD8<sup>-/-</sup> mice (Jackson Laboratory).
3. Natural killer (NK) cell depletion: rabbit anti-asialo-GM1 serum (Wako Chemicals USA Inc., Virginia). Control rabbit serum (Sigma-Aldrich, St. Louis, MO).

### 3. Methods

Two strategies are described for *in vivo* manipulation of DC to induce anti-tumor immunity against the weakly immunogenic tumor, B16 melanoma. Both methods have been successfully tested in at least two different tumor models and can be easily adapted to other tumor models. The first approach, which uses Flt3-L to expand DC *in vivo* before vaccinating animals with a mixture of tumor-associated antigen and TLR9 agonist, has been shown to reverse tumor tolerance and induce antitumor immunity even when the immunogen is a self-antigen (see **Tables 1** and **2**). A key consideration when adapting this strategy to other tumor models is the choice of antigen which should contain at least one immunodominant CD8<sup>+</sup> T-cell epitope (see **Note 3**) expressed on the tumor cells. Many such tumor-associated antigens have been identified for use in MHC identical mouse strains (**19**). However, because humans are genetically diverse, multiple epitopes and probably multiple antigens are likely to be required for a broadly effective vaccine. Vaccination with a single, well defined tumor associated antigen might lead to tumor escape via downregulation of antigen expression, whereas vaccination with whole tumor extracts or nucleic acid might lead to auto-immunity because most tumor antigens are self antigens expressed by normal tissues (**19**).

The second approach utilizes a DC attracting chemokine to recruit DC into tumors where they can acquire a potentially unlimited range of tumor associated antigens, thus avoiding the need for identification, production, and delivery of such antigens or their genes. Intratumoral injection of an appropriate TLR agonist induces upregulation of costimulatory molecules on tumoral and tumor-draining lymph node DC. The combination of DC recruitment to tumors and DC activation ensures that sufficient levels of tumor-derived antigens are presented to T cells in a stimulatory manner, leading to induction of potent anti-tumor immunity. The amount of tumor protection, which can be achieved by this method compared to controls, is summarized in **Table 3**. Although data derived from vaccination approaches in animal models have limited capacity to predict the value of a therapeutic strategy for human cancer, it is useful to test and optimize new strategies in a tumor preventive setting, before evaluation as a therapeutic model, as established tumors are extremely difficult to eradicate.

#### **3.1. Expanding DC *In Vivo* With Flt3-L Followed by Administration of a Tumor-Associated Antigen and TLR Agonist**

##### **3.1.1. Preparation and Use of Flt3-L**

1. Expansion of DC with Flt3-L:
  - a. Flt3-L is reconstituted in sterile PBS at 50 µg/mL. Fill syringe with Flt3-L, expel any air bubbles and inject 200 µL into the peritoneum of 6- to 8-wk-old

**Table 1**  
**Overview of the Animal Models in Which the Flt3-L/Antigen/CpG Combination Strategy has Been Successfully Used for Tumor Therapy**

Tumor cell line	Tumor dose	Tumor antigen	Mouse strain	Relevant MHC	Immunodominant CTL epitope	Reference
B16-OVA (MO5)	$1 \times 10^4$	Ovalbumin	C57Bl/6	H2 <sup>b</sup>	SIINFEKL (H-2K <sup>b</sup> )	<a href="#">15</a>
B16	$1 \times 10^4$ – $1 \times 10^5$	TRP2 <sub>180–188</sub>	C57Bl/6	H2 <sup>b</sup>	TRP2 <sub>180–188</sub> (H-2K <sup>b</sup> )	<a href="#">17</a>
CT26	$1 \times 10^6$	AH1 peptide (SPSYVYHQF)	Balb/c	H2 <sup>d</sup>	AH1 (SPSYVYHQF) (H-2L <sup>d</sup> )	<a href="#">17</a>
MC38.CEA	$2 \times 10^6$	CEA	CEA-tg mice	H2 <sup>b</sup>	Not identified	<a href="#">17</a>

**Table 2**  
**Therapeutic Effects of Flt3-L + Antigen + CpG on Survival of Tumor-Bearing Mice Compared to Control Treatments**

Flt3-ligand therapy		Percent survival following tumor therapy					Reference
Tumor antigen	Tumor cells	Flt3-L + CpG + antigen	Flt3-L + CpG	PBS + CpG + antigen	Flt3-L + antigen	PBS	
TRP2	B16	80%	0%	0%	–	0%	<a href="#">17</a>
OVA	B16-OVA	60%	20%	0%	20%	–	<a href="#">15</a>
AH1	CT26	100%	20%	0%	–	0%	<a href="#">17</a>

**Table 3**  
**Therapeutic Effects of Intratumoral CCL20 Injections + CpG on Survival of B16-Bearing Mice Compared to Control Treatments**

Tumor cells	CCL20 injections		CCL20 transduction		Reference
	Therapy	Percent tumor-free after 30 d	Therapy	Percent survival (100 d)	
B16	i.t. CCL20 + 5 × CPG	50%	CCL20 + 5 × CPG	40%	<i>16</i>
	i.t. CCL20 + 5 × ODN	20%	CCL20 + 5 × ODN	0%	<i>16</i>
	PBS	0%	Mock + 5 × CPG	0%	<i>16</i>
CT26	i.t. CCL20	20%	CCL20	100%	<i>16</i>
	PBS	5%	PBS	0%	<i>16</i>

animals (five per treatment group). Mice receiving the same volume of PBS should be used as controls. Each mouse should be individually marked in the ear, so that it is later possible to correlate tumor growth and induction of immunity with vaccine efficacy.

- b. In vivo expansion of DC by Flt3-L requires the continuous presence of the growth factor for at least 1 wk. Therefore, mice should be injected with 200  $\mu$ L of Flt3-L (10  $\mu$ g) once a day for a period of 7–10 d.
2. Preparation of antigen and DC activator:
  - a. Each mouse in the vaccination group should receive 300  $\mu$ g of the antigen TRP2 (*see Note 3*) and 30  $\mu$ g CpG subcutaneously (s.c.) the day after the last Flt3-L injection. CpG (or control oligonucleotide) and tumor antigen should be mixed and diluted to their final concentration of 300  $\mu$ g/mL CpG and 3 mg/mL TRP2 peptide in sterile PBS directly before use. It is important to inject a mixture of tumor antigen and TLR-agonist rather than injecting them separately, as CpG should activate the same DC that process the antigen for presentation to T cells.
  - b. Mix gently by inverting the tubes.
  - c. Fill a 1-mL syringe attached to a 27.5-gauge needle with antigen/CpG mixture (no air bubbles should be present) and inject 100  $\mu$ L subcutaneously into the left flank.

### 3.1.2. Tumor Challenge

1. Maintenance of the B16 melanoma: B16 cells are maintained in RPMI 1640 supplemented with 10% FBS, 5 mM glutamine, penicillin, and streptomycin. B16 cells grow in an adherent fashion in tissue culture flasks and need to be passaged at a 1:10 ratio approximately twice per week (*see Notes 4 and 5*). As B16 is

relatively unstable and tumorigenicity may change during culture, it is best to freeze cells on a regular basis. Such cells are best used for tumor experiments one or two passages after thawing.

2. Preparation of tumor cells for injection: B16 cells should be used when the cells are in exponential growth phase. Optimal tumor dose load may vary between  $1 \times 10^4$  and  $5 \times 10^5$  cells depending on the experiment and culture conditions, and should be determined in preliminary experiments. For tumor prevention experiments, a tumor inoculation of  $1 \times 10^5$  B16 cells represents a good starting point.
  - a. Aspirate medium from tissue culture flask with B16 cells (<50% density).
  - b. Wash once with PBS to remove FBS.
  - c. Add 3 mL 1X trypsin solution to the flask, incubate for 5 min at 37°C or until the cells start to detach from the flask.
  - d. Add 10 mL of culture medium to inactivate the trypsin, dislodge cells from flask by pipetting, and transfer cells into 50-mL centrifuge vial. Wash cells once with culture medium.
  - e. Resuspend the cells in ice-cold sterile PBS and filter through a 40- $\mu$ m nylon mesh to remove any aggregates.
  - f. Determine viable cell counts and dilute the cells with sterile PBS to a final concentration of  $1 \times 10^6$  B16 cells/mL of PBS. The cells should be kept on ice during transfer to the animal facility.
3. Injection of B16 melanoma cells:
  - a. The right flank of mice should be shaved prior to tumor inoculation to facilitate injection and monitoring of tumor growth.
  - b. All experimental groups should be inoculated identically. Therefore, great care should be taken that the syringe is filled with a homogenous cell suspension and that no air bubbles are present. The cells should be mixed just before filling of the syringe by inverting the tube several times and should be mixed between injections by carefully inverting the syringe. B16 cell suspensions tend to become more concentrated near the plunger. Therefore, the last 50–100  $\mu$ L should be discarded.
  - c. Each mouse should be injected s.c. with 100  $\mu$ L of B16 cell suspension into the shaved part of the right flank. A defined swelling/bleb should be visible after correct injection at this site.
4. Monitoring of tumor growth:
  - a. Once the tumor becomes visible, tumor growth should be monitored three times a week. As s.c. B16 tumors are easily palpable, the tumor diameter can be directly measured using a caliper. Either tumor area or tumor size can be used to monitor tumor growth. The tumor area is calculated as the product of two perpendicular diameters multiplied by 0.8 and tumor size represents the product of the largest diameter multiplied by 0.52 and the square of the smallest diameter.
  - b. Another way of determining the efficacy of the vaccine is to compare survival of the mice. All mice whose tumors reach a certain diameter (usually 20 mm) or show signs of distress should be euthanized.

### **3.2. Vaccination of B16 Melanoma-Bearing Mice With a Mixture of TRP2 Peptide and CpG Following DC Expansion With Flt3-L**

1. For evaluation of antitumor activity, mice receive a s.c. injection of  $1 \times 10^4$  B16 cells in 100  $\mu$ L PBS into the right flank as described in **Subheading 3.2.3**. Because of the aggressive growth of B16 tumors it is necessary to reduce the number of tumor cells to  $1 \times 10^4$  cells to allow the vaccine sufficient time to induce an antitumor immune response.
2. Flt3-L treatment is begun 3 d after tumor inoculation. Ten micrograms of Flt3-L (50  $\mu$ g/mL in PBS) per mouse is administered daily over a course of 9 d by intraperitoneal (i.p.) injection (similar to **Subheading 3.2.2**). At day 12 after tumor inoculation (or 1 d after the last Flt3-L injection), mice receive a single injection of a solution containing 30  $\mu$ g CpG and 300  $\mu$ g TRP2 peptide s.c. into the left flank. Use of contralateral injection sites ensures that differences in tumor growth are due to induction of systemic immune responses rather than local inflammation (*see Note 5*).
3. Tumor growth should be measured by determining the perpendicular diameters with a caliper three times a week.

### **3.3. Recruiting DC to B16 Tumors With CCL20 Chemokine Followed by Intratumoral Injection of CpG**

1. Inoculate three groups of male C57Bl/6 mice with  $5 \times 10^4$  B16 cells s.c. into the right flank (tumor dose may need to be adapted depending on the particular clone of B16 used). The injection area should be shaved before tumor inoculation to mark the injection site.
2. Recruitment of DC is induced by intratumoral injections of CCL20 for a period of 3 wk starting 1 d after tumor challenge (*see Note 7*). At the time of the first CCL20 injection, the tumor is not yet visible. Therefore, it is critical to mark the area of tumor inoculation. The recombinant CCL20 protein is diluted in PBS to a final concentration of 3.3  $\mu$ g/mL and 30  $\mu$ L of this solution should be administered directly into the tumor. It is best to use small syringes such as a tuberculin syringe with low retention volume for this purpose.
3. Tumor growth should be monitored at least twice a week. As repeated injections may induce local inflammation at the injection site, tumor-bearing mice receiving intratumoral PBS injection should serve as control. Induction of systemic immunity may also be evaluated by rechallenge of mice with  $5 \times 10^4$  B16 tumor cells in the opposite flank.
4. In contrast to more immunogenic tumors such as CT26, increasing intratumoral DC numbers in B16 tumors is not sufficient to induce systemic antitumor immunity. In this case, the DC need to receive external activation signals to overcome inhibitory signals provided by the tumor. For activation of recruited DC, inject mice with 80  $\mu$ g CpG (or control oligonucleotide) in 30  $\mu$ L of PBS into the tumor on day 7 after tumor inoculation. This procedure should be repeated every 3 d for a total of five injections (d 7, 10, 13, 16, and 19).



### 3.4. Assessing the Role of Lymphocyte Subsets in Vaccine-Induced Antitumor Activity

The role of individual lymphocyte subsets in the development of antitumor immunity and tumor regression can be assessed by *in vivo* depletion of the cells of interest such as CD4<sup>+</sup> and CD8<sup>+</sup> T cells or NK cells. This can be achieved either by the use of gene-deficient mouse models, derived from the same strain used for tumor experiments, or by injection of high doses of antibodies directed against the specific cell subset.

1. To study the role of CD4<sup>+</sup> T cells and CD8<sup>+</sup> T cells in either of the described vaccination protocols, CD4<sup>-/-</sup> or CD8<sup>-/-</sup> mice (both in the C57Bl/6 background) and wild type C57Bl/6 mice, which serve as controls, are challenged with B16 cells and vaccinated as described in the protocols above.
2. If other tumor models are used for which no gene-deficient mice are available, CD4<sup>+</sup> and CD8<sup>+</sup> T cells may be depleted by *i.p.* injections of 200–500  $\mu$ g in 500  $\mu$ L PBS of purified CD4 MAb (clone GK 1.5) or CD8 MAb (clone 2.43) or control rat MAb starting on the day before vaccination and repeated on day 1 and day 3 after vaccination to achieve complete depletion. Thereafter, antibodies should be administered once weekly to ensure continuous depletion (*see Note 8*).
3. NK cell contribution to tumor protection may be assessed by *i.p.* injection of 20  $\mu$ L anti-asialo GM1 or control serum starting the day before vaccination. Complete depletion of NK cells can be achieved if treatment is repeated about every 4 d throughout the experiment.

## 4. Notes

1. CpG oligonucleotide 1826 activates both murine B cells and DC via TLR9. CpG 1826 is not the only TLR9 ligand with stimulating capacity. There are a variety of CpG sequences with varying potential to activate dendritic cells, B cells, or NK cells (20). Thus, the optimal stimulating sequence needs to be determined for each vaccination strategy. For purposes of applying these approaches in humans, it is important to be aware that TLR9 in humans is not present in conventional DC but only in plasmacytoid DC and B cells. In addition, a different CpG sequence is needed to interact with human TLR9.
2. It is important that mice in all vaccination groups are of the same sex and about the same age to reduce the variables influencing the results. In our experience, male mice show less variability in response than female mice and are, therefore, preferred, although female mice have the advantage that it is easier to randomize the experiment after tumor injection.
3. The Flt3-L + antigen + CpG combination therapy can be adapted for evaluation in a variety of tumor models and can even reverse tolerance against self-antigens. All tumor antigens should be tested for potential endotoxin contamination before use and further purified if necessary. Commercially available tests (e.g., Gel clot assay, Cambrex, Inc.) can easily be performed by following the manufacturer's instructions.

4. Tumor cell cultures are susceptible to mycoplasma contamination. Therefore, all cell lines obtained from other sources should be initially tested for mycoplasma contamination by commercially available tests. Signs of mycoplasma contamination may include slow or no growth.
5. Culture conditions may have a major impact on the tumorigenicity of cell lines and should not be altered once the optimal tumor dose is established. FBS represents a critical factor and different serum batches should be tested for their influence on tumor cell growth in case it is necessary to switch serum batches during the study.
6. For all tumor experiments, it is necessary to include appropriate control groups of mice, e.g., PBS injections instead of Flt3-L, control oligonucleotides instead of CpG and Flt3-L treatment + CpG without antigen.
7. The ability of CCL20 to recruit DC into the tumor is significantly enhanced if CCL20 is continuously provided in the tumor environment. Therefore, it may be preferable to transduce tumor cells with CCL20 cDNA and use these CCL20-secreting tumor cells in certain experiments.
8. Depletion of cell subsets in the blood should be confirmed by flow cytometric analysis using MAb directed against epitopes different from those recognized by the depleting MAb.

## Acknowledgments

This work was supported by grants from the National Heart Lung and Blood Institute (HL57443), National Institute of Allergy and Infectious Diseases (AI060019), and National Institutes of Health (EB005824).

## References

1. Banchereau, J. and Steinman, R. M. (1998) Dendritic cells and the control of immunity. *Nature* **392**, 245–252.
2. Banchereau, J., Briere, F., Caux, C., et al. (2000) Immunobiology of dendritic cells. *Annu. Rev. Immunol.* **18**, 767–811.
3. Gabrilovich, D., Ishida, T., Oyama, T., et al. (1998) Vascular endothelial growth factor inhibits the development of dendritic cells and dramatically affects the differentiation of multiple hematopoietic lineages in vivo. *Blood* **92**, 4150–4166.
4. Bell, D., Chomarat, P., Broyles, D., et al. (1999) In breast carcinoma tissue, immature dendritic cells reside within the tumor, whereas mature dendritic cells are located in peritumoral areas. *J. Exp. Med.* **190**, 1417–1426.
5. Vermi, W., Bonecchi, R., Facchetti, F., et al. (2003) Recruitment of immature plasmacytoid dendritic cells (plasmacytoid monocytes) and myeloid dendritic cells in primary cutaneous melanomas. *J. Pathol.* **200**, 255–268.
6. Engleman, E. G., Brody, J., and Soares, L. (2004) Using signaling pathways to overcome immune tolerance to tumors. *Sci. STKE* **2004**, 28.
7. Zou, W. (2005) Immunosuppressive networks in the tumour environment and their therapeutic relevance. *Nat. Rev. Cancer* **5**, 263–274.

8. Pasare, C. and Medzhitov, R. (2003) Toll pathway-dependent blockade of CD4+CD25+ T cell-mediated suppression by dendritic cells. *Science* **299**, 1033–1036.
9. Yang, Y., Huang, C. T., Huang, X., and Pardoll, D. M. (2004) Persistent Toll-like receptor signals are required for reversal of regulatory T cell-mediated CD8 tolerance. *Nat. Immunol.* **5**, 508–515.
10. Medzhitov, R. (2001) Toll-like receptors and innate immunity. *Nat. Rev. Immunol.* **1**, 135–145.
11. Hsu, F. J., Benike, C., Fagnoni, F., et al. (1996) Vaccination of patients with B-cell lymphoma using autologous antigen-pulsed dendritic cells. *Nat. Med.* **2**, 52–58.
12. Nestle, F. O., Alijagic, S., Gilliet, M., et al. (1998) Vaccination of melanoma patients with peptide- or tumor lysate-pulsed dendritic cells. *Nat. Med.* **4**, 328–332.
13. Fong, L., Hou, Y., Rivas, A., et al. (2001) Altered peptide ligand vaccination with Flt3 ligand expanded dendritic cells for tumor immunotherapy. *Proc. Natl. Acad. Sci. USA* **98**, 8809–8814.
14. Fong, L. and Engleman, E. G. (2000) Dendritic cells in cancer immunotherapy. *Annu. Rev. Immunol.* **18**, 245–273.
15. Merad, M., Sugie, T., Engleman, E. G., and Fong, L. (2002) In vivo manipulation of dendritic cells to induce therapeutic immunity. *Blood* **99**, 1676–1682.
16. Furumoto, K., Soares, L., Engleman, E. G., and Merad, M. (2004) Induction of potent antitumor immunity by in situ targeting of intratumoral DCs. *J. Clin. Invest.* **113**, 774–783.
17. Okano, F., Merad, M., Furumoto, K., and Engleman, E. G. (2005) In vivo manipulation of dendritic cells overcomes tolerance to unmodified tumor-associated self antigens and induces potent antitumor immunity. *J. Immunol.* **174**, 2645–2652.
18. Maraskovsky, E., Brasel, K., Teepe, M., et al. (1996) Dramatic increase in the numbers of functionally mature dendritic cells in Flt3 ligand-treated mice: multiple dendritic cell subpopulations identified. *J. Exp. Med.* **184**, 1953–1962.
19. Gilboa, E. (1999) The makings of a tumor rejection antigen. *Immunity* **11**, 263–270.
20. Krieg, A. M. (2002) CpG motifs in bacterial DNA and their immune effects. *Annu. Rev. Immunol.* **20**, 709–760.

---

# Index

## A

- Activation induced cell death (AICD), 418
- Adenovirus, 445
- Adhesion molecules, 409
- Adjuvant, 32, 411, 432
  - complete Freund's, 313, 315, 318, 411, 446
  - incomplete Freund's, 278, 315, 410
- Adjuvant arthritis, 280
- Affymetrix chips, 219, 221
- Allograft rejection, 337
  - direct pathway of alloantigen recognition, 338
  - indirect pathway of alloantigen recognition, 338
- Alloxan, 288
- Anchor enzyme, 226
  - cleavage of cDNA, 229, 235
- Androgen blockade, 379
- Anergy
  - in B cell tolerance, 10
  - in T cell tolerance, 31, 167, 216, 272
  - of Treg cells, 84
- Antigen processing, 26, 271, 274, 279
  - by TEC, 108, 279
  - compartments associated with, 108
  - Western blot analysis of, 111–112
- Apoptosis
  - apoptotic cells in cross presentation, 33
  - during thymic development, 134
  - in induction of clonal deletion, 186
  - rescue from, 171
- APECED, 36
- Asparagine endopeptidase (AEP), 277

## Autoimmune disease

- etiology of, 271–283
- spontaneous, 285–311

Autoimmune regulator (AIRE), 2, 31, 108, 131, 141, 294, 298, 377

## B

- BAFF, in B cell tolerance, 10
- BB rat, 409
- B cells
  - as APC, 12
  - apoptosis, 11
  - depletion, 11
  - in hyperacute rejection, 12
  - tolerance, 9–12
- B cell receptor (BCR)
  - editing, 10
  - somatic hypermutation, 10
- Bcl-2, 301
- Bcl-2-interacting mediator of cell death (BIM), 2
- Blastocyst, 74
- Bone marrow, 407
  - as a source of CD34<sup>+</sup> cells, 11
  - enrichment of CD11c<sup>+</sup> cells from, 50–51
  - in B cell development, 9
  - transplantation, 166, 391–403, 432
- Bone morphogenetic proteins, 147–148

## C

- Cancer immunotherapy, 281
- Carboxyfluorescein diacetate succinimidyl ester (CFSE), 258, 316, 356
- labeling of cells with, 367, 371

- use in assessing T cell proliferation in vitro, 320
    - use in monitoring CTL function in vivo, 365–376
  - CD4<sup>+</sup>CD25<sup>+</sup> T cells *see* Regulatory T cells
  - CD4<sup>+</sup>CD45<sup>high</sup> T cells, 328
    - purification of, 329, 330–331
  - CD8<sup>+</sup>CD28<sup>-</sup> T cells *see* CD8<sup>+</sup> regulatory T cells
  - CD8<sup>+</sup> regulatory T cells, 7
  - CD34<sup>+</sup> progenitor cells, 29, 198
  - Cell tracker blue, 266
  - Cell tracker orange, 258
  - Central nervous system (CNS), 313, 411
  - Chemokines
    - in dendritic cell migration/recruitment, 28, 465
    - in thymocyte migration, 130
    - in type 1 diabetes, 299–300
  - Chimera, chick-quail, 133, 139
  - Cholera toxin, 216, 217
  - Clonal deletion, 31, 83, 107, 163, 167, 171, 185, 198, 225, 254, 271, 272, 274, 294, 295, 347, 365, 377, 391, 392
    - analysis of in FTOC, 179–182
    - escape from, 276, 279, 281
    - in mixed chimerism, 13
  - Clonal exhaustion, in mixed chimerism, 13
  - Clonal expansion, 200, 365
  - Collagen
    - type I, 253
    - type II, 410, 452
  - Collagen-induced arthritis, 443
  - Common myeloid progenitor, 29, 48
  - Common lymphoid progenitor, 29, 48
  - Complement, 314
  - Concanavalin A, 166
  - Co-receptor, 409
    - blockade, 417
  - Co-stimulation, 409
    - B7-CD28 pathway, 14, 366, 392
    - blockade, 14, 391–403, 417, 418, 419
    - CD40-CD154 pathway, 3, 392
    - control by Treg, 36
    - inducible co-stimulator ligand (ICOSL), 60
    - in pathogenesis of type 1 diabetes, 292–294
  - Coxsackie virus, 288
  - C-peptide, 348
  - Crohn's disease, 327
  - Cross presentation of antigen, 3, 30
  - Cyclophosphamide
    - in establishing mixed chimerism, 13
    - in induction of type 1 diabetes, 289
  - Cyclosporine A, 418
  - Cytokeratin *see* Keratin
  - Cytosine-poly-guanine oligodeoxynucleotide (CpG)
    - in dendritic cell maturation, 8
  - Cytotoxic T lymphocyte (CTL), 365
  - Cytotoxic T lymphocyte antigen (CTLA) 4
    - expression by Treg, 432
    - in Treg function, 5
- D**
- Decoy receptor 3 (DCR3), 293
  - Dectin-1, 409
  - Delayed type hypersensitivity (DTH), 337, 443
  - Demyelination, 313
  - Dendritic cell
    - CD8 $\alpha$ <sup>+</sup> dendritic cells, 30, 48
    - DC1, 28
    - DC2, 28
    - differentiation from bone marrow, 218, 228, 253, 443
    - differentiation from ES cells, 67–68, 229
    - gene expression profiling of, 215–224

- in RTOC, 186, 195
- interferon  $\alpha$ -producing dendritic cells (IDC), 28
- regulatory properties, 34
- licensed, 33
- maturation, 26–27
  - in response to:
    - CD40L, 26
    - LPS, 26, 68–69
    - necrotic cells, 33
    - NKT cells, 33
    - TLR agonists, 33
    - TNF $\alpha$ , 216
- mucosal, 27
- myeloid, 3, 216
- plasmacytoid, 3
  - involvement in tolerance, 4
- regulatory, 3, 34
  - differentiated DC (diffDC), 34
- semi-mature, 216
- subsets, 26–30
- thymic, 129, 163, 165, 167, 198, 254, 348
- tolerogenic, 168
  - interaction with Treg, 8–9, 216
- tumor-derived, 460
- vaccination, 38
- 2-Deoxyguanosine (2-dGuo), 187
  - in preparation of alymphoid fetal thymi, 189–190, 347
- Determinant
  - cryptic, 274, 280, 281, 292
  - dominant, 280, 313, 460
  - spreading, 279, 280
  - subdominant, 274, 280, 281
- Dexamethasone
  - in inhibition of dendritic cell maturation, 8, 33
- Diabetes
  - induction of, 344–345
  - type 1, 285–311, 409
    - adoptive transfer of, 289
    - pathogenesis of, 287
- DiGeorge syndrome, 142
- Donor specific transfusion (DST), 407, 418, 419
  - in induction of dominant tolerance, 414
- E**
- E-cadherin
  - role in adhesion of Langerhan's cells, 28
- Embryoid bodies (EB), 60
  - cystic, 70
  - simple, 70
- Embryonic stem (ES) cells, 59, 73
  - cloning of, 65–66
  - differentiation to EB, 61–62, 66–67
  - from NOD mice, 291
  - genetic modification of, 61, 64–65
  - maintenance of, 61
  - passage of, 63
- Endocytosis
  - receptor mediated, 26
- Endocytic receptors
  - DC-SIGN, 33
- Endosome, late, 443
- Epitope *see* Determinant
- Experimental autoimmune
  - encephalomyelitis (EAE), 3, 275–276, 281, 411
  - immunotherapy of, 313–326, 405
  - induction by active immunization, 315–316, 318
- Induction by adoptive transfer of T cells, 317, 321–322
- Exosomes, 30, 443–455
  - affect on MLR, 451
  - affect on DTH, 452
  - affect on CIA, 452
  - characterization of, 446–447, 449–451
  - preparation from DC, 445, 447–448
  - visualization by electron microscopy, 445, 448
- Extracellular matrix (ECM), 253

in thymus, 129  
receptors for, 129  
Eya1, 143–144

**F**

Fas, 2  
in pancreatic  $\beta$  cell destruction, 293  
in SLE, 411  
Fas-ligand, 443, 445  
Feeder cells *see* Primary embryonic fibroblasts  
Fetal thymus organ culture (FTOC), 49, 50, 53–54, 171–184, 380  
staining, 51  
Fibroblast, 166, 229  
primary embryonic, 74–76  
preparation, 60–61, 62–63  
Fibroblast growth factors, 148–149  
FGF 7, 139  
FGF 8, 142  
FGF 10, 139, 142  
Flagellin, 216  
Flt3-L  
in B cell development, 74  
in DC recruitment, 458  
in DC expansion *in vivo*, 460–463  
in T cell development, 78  
Foxp3, 3, 36, 83, 84, 298, 314, 408, 432  
Foxn1, 134, 145  
role in thymic epithelial development, 145–147  
FTY720, 419

**G**

Gastritis, 285  
Gene expression signatures, 244  
Genetic modification  
of dendritic cells, 59  
of embryonic stem cells, 64–65  
Glutamic acid decarboxylase (GAD), 285, 295  
Goblet cells, 328  
Graft-vs-host disease (GVHD), 3, 31, 84, 381, 432

risk factor in mixed chimerism, 13  
Graft-vs-leukemia (GVL) reaction, 166  
Granulocyte-macrophage colony stimulating factor, 48, 52, 55, 257, 445  
in directed differentiation of ES cells, 62, 68, 70  
Growth hormone, 379

**H**

H2-DM, 107  
as a marker of endosomes in TEC, 115–117  
isolation of H2-DM<sup>+</sup> compartments, 117–118  
H-2M, 279  
Heat shock protein (hsp) 65, 280  
*Helicobacter* spp, 333  
Hemolytic anemia, 285  
Hemangioblast, 73  
Hematopoietic cell chimerism *see* Mixed chimerism  
Hematopoietic progenitors *see* Hematopoietic stem cell  
Hematopoietic stem cell, 73, 163, 253  
transplantation, 381  
Hen eggwhite lysozyme (HEL), 274  
Heterologous immunity, 418  
HIV, 166, 379  
Homeostatic T cell proliferation, 199, 377, 378, 386, 432  
Hoxa3, 142–143

**I**

IA-2, 285, 295  
Imidazoquinolines, 216  
Immune privilege, 444  
Immunodeficiency, 145  
Immunodominance, 272–275  
Immunological ignorance, 272  
Immunological memory, 33, 215  
memory T cells, 378, 384–385, 418, 419  
Immunological synapse, 409

- Indoleamine 2,3-dioxygenase, 60  
   in tryptophan catabolism, 34  
 Inflammatory bowel disease, 298, 327–335  
   induction of, 331–333  
   monitoring of, 331–333  
 Inflammatory stimuli, 215  
 Insulin, 285, 295  
 Insulin-like growth factor (IGF)-1, 379  
 Insulinitis, 285  
   detection of, 287–288  
 Interferon  $\alpha$  *see* Type I interferon  
 Interferon  
   type I, 4  
     in generation of Tr1 cells, 85  
   type II  
     in NKT cell function, 6  
 Interferon  $\gamma$  *see* Type II Interferon  
 Interleukin 1 $\beta$  (IL-1 $\beta$ )  
   in dendritic cell stimulation, 217  
 Interleukin 2 (IL-2)  
   in generation of CD4<sup>+</sup>CD25<sup>+</sup> Treg, 298, 431  
   in pathogenesis of type 1 diabetes, 292  
 Interleukin 3 (IL-3)  
   in directed differentiation of ES cells, 62, 68, 70  
 Interleukin 4 (IL-4)  
   in NKT cell function, 6  
   in semi-maturation of DC, 216  
   in generation of bone marrow derived DC, 257  
 Interleukin 6 (IL-6)  
   intrathymic production of, 380  
 Interleukin 7 (IL-7)  
   in B cell development, 74  
   in T cell development, 78, 129–130  
   secretion by TEC, 129, 380  
 Interleukin 10 (IL-10)  
   in inhibition of dendritic cell maturation, 8  
   in modulation of dendritic cell function, 228  
   in pathogenesis of type 1 diabetes, 292  
   in NKT cell function, 6  
   in regulatory dendritic cell function, 34  
   in Treg function, 5, 36, 80  
   tumor derived, 458  
 Interleukin 12 (IL-12), 366  
   secreted by dendritic cells, 27  
 Interleukin 13 (IL-13)  
   in NKT cell function, 6  
 Intravital two photon imaging, 355–363  
 IPEX syndrome, 36  
 Islets of Langerhans, 337, 351  
   isolation of, 342–343  
   transplantation under the kidney capsule, 343–344
- J**
- Jugular vein  
 cannulation of, 358–359
- K**
- Keratin, 129  
 keratin 5, 109, 135–137  
 keratin 8, 109, 135–137, 380  
 Keratinocyte, 166  
 Kidney capsule  
 as a site of transplantation, 164, 339, 347–353
- L**
- Langerhans cell, 28, 48  
*Leishmania mexicana* promastigote, 217  
 Leukemia inhibitory factor (LIF)  
 in the maintenance of pluripotency, 65  
 Linked suppression, 406, 415–416  
 Lipopolysaccharide (LPS), 49, 216, 217  
 Lymph node, 254, 457  
 inguinal, 356  
 intravital T cell imaging in, 355–363



- popliteal, 356, 358, 362  
 exposure of, 359–361
- Lymphocytic choriomeningitis virus (LCMV), 172, 418  
 derived peptide, 173
- Lympho-epithelial cross-talk, 139  
 role of Foxn1, 146
- Lymphopenia, 35, 200, 377, 386, 419
- Lymphoproliferative autoimmune syndrome, 5
- Lymphotoxin  $\beta$  (LT $\beta$ ), 141
- Lysosome, 444
- M**
- Macrophage, 278, 285  
 in pathogenesis of EAE, 313  
 thymic, 129  
 depletion of, 188, 191
- Macrophage colony stimulating factor (M-CSF), 49, 52, 74
- Macropinocytosis, 26
- Magnetic resonance imaging (MRI), 348
- Marginal zone, 28
- Mass spectrometry, 16
- Mast cell, 444
- Matrix  
 3-dimensional, 163, 164  
 3-dimensional collagen matrices, 253–269
- M-cells, 28
- Mesenchymal cells, 125, 129  
 in formation of the thymic capsule, 131  
 secretion of growth factors, 139
- Mesoderm, 73, 80
- Microarray, 215–224
- Microbial associated molecular patterns (MAMPs), 216
- Microchimerism, 13
- Mitosis, 199
- Mixed chimerism, 12–13, 31, 391–403, 414, 419  
 detection of, 396–397
- Mixed leukocyte reaction (MLR), 166, 431, 434, 443
- Monocytes, 26  
 differentiation of dendritic cells from, 29
- Mouse lysozyme, 277–278
- Multiple sclerosis, 313, 411
- Mycophenolate mofetil, 400, 419  
 in inhibition of dendritic cell maturation, 8
- Mycoplasma, 467
- Myelin basic protein (MBP), 274, 275, 276, 277, 411  
 encephalitogenic peptides from, 315  
 Golli-MBP, 275
- Myeloablative conditioning, 391
- N**
- Natural Killer T (NKT) cells, 6, 84  
 role in type 1 diabetes, 6, 286, 297
- Negative selection *see* Clonal deletion
- Neomycin resistance gene, 65
- Neural crest cells (NCC), 133, 138  
 role of Pax3 in survival and migration, 144
- Noggin, 147–148
- Non-myeloablative conditioning, 391
- Non-obese diabetic (NOD) mouse, 84, 279, 285–311, 339, 345, 408, 409, 411, 417
- Notch  
 in thymocyte maturation, 130, 186  
 ligands  
 Delta-like 1, 73–74, 130  
 Delta-like 4, 130  
 Jagged 1 and 2, 130
- Nude* mouse, 134, 348
- O**
- Oncostatin M, 380
- Oophoritis, 285
- OP9 bone marrow stromal cell line, 73  
 OP9-DL1, 74, 75–77, 186

**P**

- Pancreatic  $\beta$  cells, 286
  - Pannus formation, 411
  - Parathyroid, 131
    - GCM2 expression by, 131, 145
  - Parkinson's disease, 339
  - Pax1, 143
  - Pax3, 144
  - Pax9, 143
  - PD-1 ligand, 146
  - Peptidoglycan, 216
  - Peripheral blood mononuclear cells (PBMC), 86, 165
    - AC133<sup>+</sup> PBMC, 165
  - Pertussis toxin, 216, 217, 315, 319, 321
  - Pluripotency, 59, 65
  - Phagocytosis, 26
  - Pharyngeal region
    - pharyngeal arches, 131–133
      - role of Tbx1 in patterning, 142
    - pharyngeal clefts, 131–132
    - pharyngeal pouches, 131–132
  - Phytohemagglutinin (PHA), 165, 166
  - Placenta, 444
  - Pneumocystis carinii*, 333
  - Positive selection, 74, 146, 164, 166, 171, 185–186, 198, 254, 347, 378
    - analysis of in FTOC, 178–179
    - of CD4<sup>+</sup>CD25<sup>+</sup> Treg, 35, 295
  - Positron emission tomography (PET), 348
  - Pre-immunocyte, 47
    - enrichment from bone marrow, 49
  - Prostaglandins, 3, 216, 217
  - Prostatitis, 285
  - Proteomics, 15–16
- Q**
- Qa-1
    - in function of CD8<sup>+</sup> regulatory T cells, 7

**R**

- Rapamycin, 400, 419
    - in inhibition of dendritic cell maturation, 8
  - Rat insulin gene promoter, 291
  - Reaggregate thymus organ cultures (RTOC), 74, 130, 185–196
  - Recent thymic emigrants, 197, 207, 384
  - Regulatory T cell (Treg), 2, 59, 215, 225, 313, 405, 457
    - adaptive Treg
      - expansion of, 418
    - CD4<sup>+</sup>CD25<sup>+</sup> Treg, 35–37, 416
    - in prevention of autoimmunity, 84, 286
    - in prevention of IBD, 327
    - in prevention of type 1 diabetes, 297–299
    - naturally occurring Treg, 4, 83, 225, 229, 431
      - adoptive transfer of, 431–441
      - cloning of, 89–90
      - cytokine production by, 91
      - expansion of, 89–90, 405
      - ex vivo stimulation of, 437
      - in vitro stimulation of, 435–437
      - isolation of, 86–89
      - phenotypic analysis of, 90–91
      - suppressive activity of, 91–92
    - positive selection of, 35–36, 168, 377
  - Reticulocyte, 444
  - Retinoic acid, 149–150
  - Rheumatoid arthritis, 409, 410–411, 452
- S**
- Serial analysis of gene expression (SAGE), 225–251
  - Sequestration
    - intramolecular, 271, 272–273
    - of self-antigen, 272
  - Severe combined immune deficiency (SCID) mice, 327

- use for generation of “humanized” mice, 15
- Sialoadenitis, 285
- Six1, 143–144
- Sonic hedgehog (Shh), 150
- Stem cell factor (SCF), 129
- Streptozotocin, 288, 339
- Superantigen, 295, 395, 400
- Syncytiotrophoblast, 444
- Systemic lupus erythematosus (SLE), 411
  - role of interferon  $\gamma$ , 16
- T**
- Tacrolimus, 418
- Tagging enzyme, 226
  - release of SAGE tags, 230, 236
- Tbx1, 141–142
- T cell receptor (TCR)
  - $\alpha\beta$ TCR, 165, 185
  - $\gamma\delta$ TCR, 165
  - affinity, 273
  - editing, 31
  - excision circles (TREC), 163, 197–213, 378
    - as an estimate of thymic function, 200–201, 384
    - detection of, 202–203
    - generation of, 198–199
  - hypervariable regions, 198
- Tetramethylrhodamine-dextran, 362
- Tetramer
  - of MHC class I peptide complexes, 374
- T helper 1 (Th1) cells
  - in type 1 diabetes, 296–297
- T helper 2 (Th2) cells, 443
  - in type 1 diabetes, 296–297
- T helper 3 (Th3) cells, 37
- Thymectomy, 35
- Thymic aplasia, 138
- Thymic atrophy *see* Thymus involution
- Thymic epithelial cells (TEC), 107, 125, 171, 198, 348, 379
  - cortical (cTEC), 107, 127, 378
    - in positive selection of Treg, 35
  - endodermal origin, 133–134
  - establishment of TEC lines, 113–115
  - expression of FgfR2IIIb, 139
  - in positive selection, 186
  - keratin expression by, 115, 129
  - medullary (mTEC), 107, 127, 163, 278
    - AIRE expression by, 31, 108, 131, 141, 279, 377
  - phenotype, 128
  - progenitors, 134–135
  - subcapsular/subtrabecular, 127
  - tolerogenicity of, 167
- Thymic nurse cells, 128, 378
- Thymocytes
  - CD4<sup>+</sup>CD8<sup>-</sup> cells, 50, 164, 166, 198
    - isolation, 51
    - TN1 cells (CD44<sup>+</sup>CD25<sup>-</sup>), 135
    - TN2 cells (CD44<sup>+</sup>CD25<sup>+</sup>), 79
  - CD4<sup>+</sup>CD8<sup>+</sup> (DP) cells, 127, 165, 166, 173, 185, 198, 380
    - isolation from neonatal thymus, 191–192
  - CD4<sup>+</sup>CD8<sup>-</sup> (SP) cells, 127, 164, 165, 166, 172, 173, 198, 380
  - CD4<sup>+</sup>CD8<sup>+</sup> (SP) cells, 127, 164, 165, 166, 172, 173, 198, 380
- Thymopoiesis, 197, 198, 377, 378, 379, 380, 381–385, 386
- Thymus
  - accessory, 138
  - cortex, 125, 138
  - corticomedullary junction, 127, 129, 146
  - in development of Treg, 4
  - involution, 166, 200, 377–390
  - medulla, 31, 125, 138
  - microenvironment, 73, 163, 185
  - organogenesis, 125–162
  - structure, 126
- Thyroiditis, 285
- Tissue engineering, 164

- Tolerance
- Central tolerance *see* Clonal deletion
  - dominant tolerance, 59, 405–429
    - confirmation of, 415–417
  - infectious, 405, 406, 416
  - peripheral, 225, 294, 347
  - transplantation, 337–346, 391–403, 405, 434–435
- Tolerosome, 444
- Toll-like receptors (TLR), 457, 458
- expression by  $\beta$  cells, 299
  - expression by Treg, 432
  - in B cell activation, 10
  - in dendritic cell activation, 216
- Total body irradiation (TBI), 391, 395–396
- Toxoplasma gondii*, 444
- Transcriptome, 246
- Transferrin receptor, 444
- Transplantation
- heart, 337, 408, 444
  - islet, 337, 340–341, 342–344, 408
  - kidney, 337, 408
  - liver, 408
  - neuronal, 339
  - skin, 337, 338–339, 340, 341–342, 408
- Transporter associated with antigen processing (TAP)-1, 171, 174
- T regulatory 1 (Tr1) cells, 6, 37, 83, 225, 229
- alloantigen specific, 94–96
    - cloning of, 96–97
  - cytokine production by, 99
  - induction of, 93–94
  - phenotype of, 99
  - role in inflammatory bowel disease, 6, 85
  - role in airway hyperreactivity, 85
  - role in allograft rejection, 85
  - suppressive function of, 100–102
- Transforming growth factor (TGF)  $\beta$
- in generation of CD4<sup>+</sup>CD25<sup>+</sup> Treg, 298
  - in induction of Foxp3 expression, 299
  - in NKT cell function, 6
  - in Treg function, 5, 36, 84
  - in pathogenesis of type 1 diabetes, 292
  - tumor derived, 458
- Treg *see* Regulatory T cell
- Tumor-associated antigen
- breaking of tolerance to, 457–468
- Tumor necrosis factor  $\alpha$  (TNF $\alpha$ ), 3, 130
- in semi-maturation of dendritic cells, 216
  - in pathogenesis of type 1 diabetes, 292
- U**
- Ulcerative colitis, 327
- V**
- Vaccination
- to tumor associated antigens, 38
- V(D)J recombination
- in B cell receptor gene rearrangement, 9
- Velocity
- of cells in 3D-matrices, 253, 261, 265
- Vitamin D3 (1 $\alpha$ ,25-dihydroxyvitamin D3)
- in inhibition of dendritic cell function, 8, 33
  - in modulation of dendritic cell function, 229
- W**
- Wnt family, 151
- X**
- Xenoantigens, 167
- Xenograft, 406
- Z**
- ZAP70, 2, 409
- Zyosan, 216, 217



Series Editor: John M. Walker

# Immunological Tolerance

## Methods and Protocols

Edited by

**Paul J. Fairchild***Sir William Dunn School of Pathology, University of Oxford, Oxford, UK*

*Immunological Tolerance: Methods and Protocols* provides a comprehensive guide to the techniques currently used for culturing and characterizing the cell types responsible for imposing self-tolerance and the experimental models employed to study their function both *in vitro* and *in vivo*. The volume is divided into easy to follow sections. The first section is an introduction to immunological tolerance, while the second section discusses the generation and culture of thymic epithelial cells, regulatory T cells and dendritic cells. The next section describes protocols for studying tolerance *in vitro* while another section explores the study of tolerance *in vivo*. The final section reviews both proven and novel strategies for the induction of tolerance through mixed chimerism, the adoptive transfer of regulatory T cells, or the administration of biologicals. With meticulous analysis of novel approaches, *Immunological Tolerance: Methods and Protocols* provides a thorough guide to the field of immunological tolerance.

### FEATURES

- Provides up-to-date reviews of the literature on essential topics in immunological tolerance
- Methods for the generation and culture of critical cell types and approaches to characterization
- Describes protocols for the study of tolerance both *in vitro* and *in vivo*
- Provides insights into novel techniques for tolerance induction

### CONTENTS

Frontiers of Immunological Tolerance. **Part I** Cell Types Contributing to Immunological Tolerance. Balancing Tolerance and Immunity: *The Role of Dendritic Cell and T Cell Subsets*. Differentiation of Dendritic Cell Subsets from Mouse Bone Marrow. Genetic Modification of Dendritic Cells Through the Directed Differentiation of Embryonic Stem Cells. Generation of Immunocompetent T Cells from Embryonic Stem Cells. Isolation, Expansion, and Characterization of Human Natural and Adaptive Regulatory T Cells. Derivation, Culture, and Characterization of Thymic Epithelial Cell Lines. **Part II** The Study of Immunological Tolerance *In Vitro*. Thymus Organogenesis and Development of the Thymic Stroma. Generation of a Tissue-Engineered Thymic Organoid. Studying T-Cell Repertoire Selection Using Fetal Thymus Organ Cultures. Investigating Central Tolerance with Reaggregate Thymus Organ Cultures. Estimating Thymic Function Through Quantification of T-Cell Receptor Excision Circles. Gene Expression Profiling of Dendritic Cells by Microarray. SAGE Analysis of Cell Types Involved in Tolerance Induction. Analyzing the Physicodynamics of Immune Cells in a Three-Dimensional Collagen Matrix. **Part III** The Study of Immunological Tolerance *In Vivo*. Etiology of Autoimmune Disease: *How T Cells Escape*

*Self-Tolerance*. Animal Models of Spontaneous Autoimmune Disease: *Type 1 Diabetes in the Nonobese Diabetic Mouse*. Antigen-Based Therapy and Immune Regulation in Experimental Autoimmune Encephalomyelitis. Induction and Regulation of Inflammatory Bowel Disease in Immunodeficient Mice by Distinct CD4<sup>+</sup> T-Cell Subsets. *In Vivo* Models for the Study of Transplantation Tolerance. Ectopic Transplantation of Tissues Under the Kidney Capsule. Intravital Two-Photon Imaging of T-Cell Priming and Tolerance in the Lymph Node. Tracing Tolerance and Immunity *In Vivo* by CFSE-Labeling of Administered Cells. **Part IV** Methods for Inducing and Breaking Immunological Tolerance. Thymic Involution: *Implications for Self-Tolerance*. Inducing Mixed Chimerism and Transplantation Tolerance Through Allogeneic Bone Marrow Transplantation with Costimulation Blockade. Induction of Dominant Tolerance Using Monoclonal Antibodies. Induction of Tolerance by Adoptive Transfer of Treg Cells. Modulation of the Immune Response Using Dendritic Cell-Derived Exosomes. Breaking Self-Tolerance to Tumor-Associated Antigens by *In Vivo* Manipulation of Dendritic Cells. Index.

Methods in Molecular Biology™ • 380  
 IMMUNOLOGICAL TOLERANCE  
 METHODS AND PROTOCOLS  
 ISBN: 978-1-58829-652-8  
 E-ISBN: 978-1-59745-395-0  
 ISSN: 1064-3745  
[humanapress.com](http://humanapress.com)

